MAR 15 1982 Conf-810833

429-E

E1.10:810833

ORIGINAL

Proceedings of the Mechanical, Magnetic and Underground Energy Storage 1981 Annual Contractors' Review

COMPLETED
407

August 24—26, 1981
Washington, D.C.

Prepared for:
U.S. Department of Energy
Assistant Secretary,
Conservation and Renewable Energy
Division of Energy Storage
Under Contract No. W-7405-ENG-36

Published February 1982

DISCLAIMER

"This report was prepared as an account of work sponsored by an agency of the United States Government. Neither the United States Government nor any agency thereof, nor any of their employees, makes any warranty, express or implied, or assumes any legal liability or responsibility for the accuracy, completeness, or usefulness of any information, apparatus, product, or process disclosed, or represents that its use would not infringe privately owned rights. Reference herein to any specific commercial product, process, or service by trade name, trademark, manufacturer, or otherwise, does not necessarily constitute or imply its endorsement, recommendation, or favoring by the United States Government or any agency thereof. The views and opinions of authors expressed herein do not necessarily state or reflect those of the United States Government or any agency thereof."

This report has been reproduced directly from the best available copy.

Available from the National Technical Information Service, U. S. Department of Commerce, Springfield, Virginia 22161.

Price: Printed Copy A17
Microfiche A01

Codes are used for pricing all publications. The code is determined by the number of pages in the publication. Information pertaining to the pricing codes can be found in the current issues of the following publications, which are generally available in most libraries: *Energy Research Abstracts, (ERA); Government Reports Announcements* and Index (*GRA* and I); *Scientific and Technical Abstract Reports (STAR);* and publication, NTIS-PR-360 available from (NTIS) at the above address.

Conf-810833

Proceedings of the Mechanical, Magnetic and Underground Energy Storage 1981 Annual Contractors' Review

August 24—26, 1981
Washington, D.C.

Prepared by:
MCC Associates, Inc.
Silver Spring, Md. 20910

For:
Los Alamos National Laboratory
Los Alamos, New Mexico 87545
Under Contract No. W-7405-ENG-36

Prepared for:
U.S. Department of Energy
Assistant Secretary,
Conservation and Renewable Energy
Division of Energy Storage
Washington, D.C. 20585

Published February 1982

INTRODUCTION

The Mechanical, Magnetic, and Underground Energy Storage Programs of the Division of Physical and Chemical Energy Storage of the Department of Energy (DOE) are developing reliable, efficient and economic energy storage technologies to support other DOE end-use divisions in their energy substitution and energy-savings missions. The technologies being developed will contribute to the reliability of renewable energy systems such as solar and wind energy. By load leveling and reduction of seasonal peak load they will reduce capital and operating expense in conventional systems and accelerate load shifting to coal, nuclear, or solar thermal electric systems. The mechanical storage technologies, applicable to vehicle shaft power, will contribute to fuel savings in individual vehicles and mass transport systems.

Implementation of the Mechanical, Magnetic and Underground Energy Storage Programs under the direction of Saul Strauch has been assigned to lead laboratories and universities. These lead assignments and program elements for FY 1981 were as follows:

UNDERGROUND ENERGY STORAGE PROGRAM

Lead Laboratory: Pacific Northwest Laboratory

Seasonal Thermal Energy Storage (STES)
James E. Minor, Program Manager

The goals of the STES Program are to demonstrate the economic storage and retrieval of energy on a seasonal basis, using heat or cold available during a surplus period to reduce peak period demand; reduce electric utilities peaking problems; and contribute to the establishment of favorable economics for solar heating and cooling systems.

Seasonal storage in aquifers will be evaluated in the Aquifer Thermal Energy Storage (ATES) Program. A parallel Technical Support Program will provide data on aquifer behavior, data from field tests and economic and mathematic modeling data. Previous work on earth storage, and work under the International Energy Agency on pond, lakes, tanks, and constructed caverns will be evaluated and additional field tests or research recommended, if appropriate.

Compressed Air Energy Storage (CAES)
Landis D. Kannberg, Program Manager

The goals of the CAES Program are to develop design and stability criteria for long-term operation of underground reservoirs used for CAES in order to accelerate the commercialization of the concept; and to develop and assess second-generation technologies for CAES that require little or no supplementary firing by petroleum fuels in order to eliminate the dependence of CAES on these fuels.

SUPERCONDUCTING MAGNETIC ENERGY STORAGE PROGRAM (SMES)

Technical Consultant: Francis Bitter National Magnet Laboratory (MIT)

Lead Laboratory: Los Alamos National Laboratory
John D. Rogers, Program Manager

The goals of the SMES Program are to design, fabricate, and place into operation a 30MJ Superconducting Magnetic Energy Storage Unit for line stabilization on an interstate high voltage power line by 1983.

MECHANICAL ENERGY STORAGE PROGRAM

Lead Laboratory: Lawrence Livermore National Laboratory
T. M. Barlow, Program Manager

The goals of the MEST Program are to develop, demonstrate, and evaluate mechanical energy storage technology for vehicular and fixed-base applications and to carry out the research, development and demonstration activities in a manner that maximizes the commercialization potential of the technology.

The sixth Thermal and Chemical Storage Annual Contractors' Review Meeting was held on September 14-16, 1981, at the Tysons Corner Marriott in Vienna, VA. This report is a compilation of papers presented and represents the proceedings of this meeting. Project overviews and contractor reports contained herein were prepared by the responsible individual/organization and no technical editing has been performed by DOE.

This year's review was organized by Oak Ridge National Laboratory with the arrangements made by MCC Associates, Inc. We wish to extend our appreciation to all program participants whose enthusiastic involvement made the meeting successful. Special thanks is extended to Marianne McCarthy of MCC Associates whose efforts made the meeting proceed in an orderly fashion. A very special note of appreciation is offered to our banquet speaker, Ezra Heitowit, of the House Committee on Science and Technology, who enlarged our understanding of Congressional Perspectives on Energy Research and Development.

James H. Swisher, Director
Division of Energy Storage
Technology
Office of Energy Systems Research
U.S. Department of Energy
Forrestal Building, CE-141
1000 Independence Avenue
Washington, DC 20585

James F. Martin, General Chairman
Thermal and Chemical Storage
Annual Contractors' Review
Meeting
Oak Ridge National Laboratory
P.O. Box Y, Bldg. 9204-1, MS-3
Oak Ridge, TN 37830

John D. Rogers, Conference Chairman, LANL, greets the Banquet Speaker, Dr. Edward Hammel

Dr. James H. Swisher, Director, Office of Physical and Chemical Energy Systems, and John D. Rogers, LANL.

Review Committee member Dr. Henry A. Scarton, RPI (center), and other participants listen to a presentation

Anthony Coppa, of General Electric, delivers his presentation on "Flywheel Housing Design-Concept Development"

Drs. Chin Fu Tsang (Lawrence Berkeley Laboratory) and Allan I. Michaels (Argonne National Laboratory) chat during a break.

John R. Raymond and Jay Eliason (Pacific Northwest Laboratory), and Dr. Satish Kulkarni listen to a paper on Mechanical Energy Storage.

MECHANICAL, MAGNETIC, and UNDERGROUND ENERGY STORAGE 1981 ANNUAL CONTRACTORS' REVIEW

Washington, D.C.
August 24-26, 1981

INTRODUCTION . . . i

PHOTOGRAPHS . . . iii

TABLE OF CONTENTS . . . v

COMPRESSED AIR ENERGY STORAGE (CAES) PROGRAM

COMPRESSED AIR ENERGY STORAGE TECHNOLOGY PROGRAM OVERVIEW
L. D. Kannberg (Pacific Northwest Laboratory) 3

AN OVERVIEW OF THE SECOND GENERATION COMPRESSED AIR ENERGY STORAGE STUDIES
Frank R. Zaloudek (Pacific Northwest Laboratory) 9

ADIABATIC CAES USING HARD ROCK CAVERNS
Michael J. Hobson (Acres American Incorporated) 14

ASSESSMENT OF PRINCIPAL SUBSYSTEMS, EQUIPMENT ITEMS AND COMPONENTS OF SECOND-GENERATION COMPRESSED AIR ENERGY STORAGE (CAES) SYSTEMS
David L. Chiang and Cordell K. Jee (ENTEC Research Associates, Inc.) 20

THERMOMECHANICAL SCREENING OF THERMAL ENERGY STORAGE MATERIALS FOR COMPRESSED AIR ENERGY STORAGE
Lynn Marksberry (FluiDyne Engineering Corporation) 25

ECONOMIC ASSESSMENT COMPRESSED AIR ENERGY STORAGE (CAES) SYSTEMS
R. W. Reilly and D. R. Brown (Pacific Northwest Laboratory) 31

RESERVOIR STABILITY STUDIES
T. J. Doherty (Pacific Northwest Laboratory) 39

SALT EXPERIMENTAL STUDIES FOR CAES
Robert L. Thoms and Richard M. Gehle (Louisiana State University) 46

NUMERICAL AND LABORATORY STUDIES OF CAES RESERVOIRS IN THE SYKESVILLE GNEISS
Arlo F. Fossum and Terje Brandshaug (RE/SPEC Inc.) 53

NUMERICAL AND EXPERIMENTAL ANALYSES OF THE POROUS MEDIUM RESERVOIR AT PITTSFIELD, ILLINOIS
L. E. Wiles, R. L. Erikson, R. D. Allen, and T. J. Doherty
(Pacific Northwest Laboratory) 59

COMPRESSED AIR ENERGY STORAGE AQUIFER FIELD TEST CONCEPTUAL DESIGN, CONSTRUCTION AND OPERATION
John A. Istvan (PB-KBB Inc.) 69

MAGNETIC ENERGY STORAGE PROGRAM

MAGNETIC ENERGY STORAGE PROGRAM OVERVIEW AND INTERNATIONAL ACTIVITIES
M. O. Hoenig (Massachusetts Institute of Technology) 77

30 MJ SUPERCONDUCTING MAGNETIC ENERGY STORAGE FOR BPA TRANSMISSION LINE STABILIZER
R. I. Schermer (Los Alamos National Laboratory) 81

DESIGN AND FABRICATION OF THE BONNEVILLE POWER ADMINISTRATION'S 30-MJ SUPERCONDUCTING ENERGY STORAGE COIL FOR LONG-DISTANCE TRANSMISSION LINE STABILIZATION
J. R. Purcell and S. C. Burnett (General Atomic Company)
R. Schermer (Los Alamos Scientific Laboratory) 87

COMPUTER-AUTOMATED CONTROLS FOR SUPERCONDUCTING MAGNETIC ENERGY STORAGE
Alphonse L. Criscuolo (Los Alamos National Laboratory) 92

SEASONAL THERMAL ENERGY STORAGE (STES) PROGRAM

SEASONAL THERMAL ENERGY STORAGE PROGRAM
James E. Minor (Pacific Northwest Laboratory) 99

AQUIFER THERMAL ENERGY STORAGE (ATES) PROGRAM MANAGEMENT
John R. Raymond (Pacific Northwest Laboratory) 103

BETHEL, ALASKA AQUIFER THERMAL ENERGY STORAGE PROJECT
Jack Cherne (TRW) 104

CONCEPTUAL DESIGN OF ATES SYSTEM DEMONSTRATION - STATE UNIVERSITY OF NEW YORK STONY BROOK CAMPUS, LONG ISLAND
William V. Skinner and Donald J. Supkow (Dames & Moore) 109

THE UNIVERSITY OF MINNESOTA AQUIFER THERMAL ENERGY STORAGE PROJECT
M. Walton (University of Minnesota) 119

SEASONAL STORAGE TECHNOLOGY PROGRAM
Jay R. Eliason (Pacific Northwest Laboratory) 127

LEGAL AND REGULATORY ISSUES AFFECTING THE AQUIFER THERMAL ENERGY STORAGE CONCEPT
Paul L. Hendrickson (Pacific Northwest Laboratory) 130

ECONOMIC ASSESSMENT AQUIFER THERMAL ENERGY STORAGE (ATES) SYSTEMS
R. W. Reilly, D. R. Brown, and H. D Huber (Pacific Northwest Laboratory) 131

ENVIRONMENTAL ASSESSMENT
George E. Wukelic (Pacific Northwest Laboratory) 139

FIELD TEST FACILITY
David A. Myers (Pacific Northwest Laboratory) 140

MOBILE, ALABAMA FIELD TEST FACILITY
Fred J. Molz, Joel G. Melville, A. David Parr (Auburn University) 141

COMPENDIA OF EXISTING INFORMATION TASK
Leigh S. Prater (Pacific Northwest Laboratory) 149

SEASONAL THERMAL ENERGY STORAGE TECHNOLOGY INFORMATION SYSTEM
Victor E. Hampel (Lawrence Livermore Laboratory) 150

PUBLICATION OF THE SEASONAL THERMAL ENERGY STORAGE (STES) NEWSLETTER
Chin Fu Tsang (Lawrence Berkeley Laboratory) 151

REGIONAL ASSESSMENT OF AQUIFERS FOR THERMAL ENERGY STORAGE
Dorothy B. Stoffel (Century West Engineering) 152

LIBRARY DEVELOPMENT AND SURVEY OF REINJECTION EXPERIENCE
Charles H. Lee, Mike Snyder, and Glenda Casper (Midwest Research Institute) 159

PHYSICOCHEMICAL ANALYSIS OF AQUIFER MATERIALS AND GROUND-WATER FLUIDS FROM STES FIELD TEST FACILITIES
Stephen C. Blair (Pacific Northwest Laboratory) .166

PREMEABILITY CREEP/COMPACTION STUDIES ON SANDSTONES
C. Cooley (Terra Tek, Inc.) and J. A. Stottlemyre (Pacific Northwest Laboratory) . . 167

AQUIFER THERMAL ENERGY STORAGE - GENERIC LABORATORY STUDY OF OTTAWA SILICA SAND AND MASSILLON SANDSTONE AND DEVELOPMENT OF LABORATORY CORE TESTING APPARATUS AND FIELD INJECTABILITY APPARATUS
P. Eric Peterson, L. B. Owen and C. H. Cooley (Terra Tek, Inc.)
J. A. Stottlemyre (Pacific Northwest Laboratory) 168

GEOCHEMICAL MODELING OF THE EFFECTS OF TEMPERATURE ON MINERAL PRECIPITATES AND GROUND-WATER QUALITY AT A STES SITE
J. A. Stottlemyre and E. A. Jenne (Pacific Northwest Laboratory) 176

NUMERICAL SIMULATION
Charles T. Kincaid (Pacific Northwest Laboratory) 177

NUMERICAL SIMULATION - CFEST CODE DEVELOPMENT
Sumant K. Gupta and Charles T. Kincaid (George Maddox & Associates) 178

SUMMARY OF SIMULATION TECHNIQUES FOR AQUIFER THERMAL ENERGY STORAGE (ATES)
James W. Mercer, Charles R. Faust and William J. Miller (GeoTrans, Inc.)
F. J. Pearson, Jr. (Intera Environmental Consultants, Inc.) 183

NUMERICAL SIMULATION--SITE SIMULATION
Chin Fu Tsang (Lawrence Berkeley Laboratory) 195

HYDROLOGIC STUDIES SUPPORT
J. W. Crosby, III and Vernon Ichimura (Washington State University) 203

STUDY OF COUPLED ENERGY AND MASS TRANSPORT IN GEOLOGIC MEDIA
Stuart Childs (Oregon State University) 204

NONAQUIFER STES CONCEPTS
Donald E. Blahnik (Pacific Northwest Laboratory) 205

MECHANICAL ENERGY STORAGE PROGRAM

DEVELOPMENT OF MECHANICAL ENERGY STORAGE (MEST) TECHNOLOGY
Thomas M. Barlow (Lawrence Livermore National Laboratory) 217

ASSESSMENT OF TAXICAB FLEET OPERATION IN NEW YORK CITY
Milton C. Krupka and Sydney V. Jackson (Los Alamos National Laboratory) 225

ASSESSMENT OF FLYWHEEL SYSTEM BENEFITS IN SELECTED VEHICLE APPLICATIONS
L. H. Kubo and L. Forrest (The Aerospace Corporation) 231

HEAT ENGINE/FLYWHEEL VEHICLE DRIVE DESIGN RESULTS AND ANALYSIS, PHASE I
I. Kalns (Eaton Corporation) 241

CONTROL-STRATEGY STUDY FOR A HEAT-ENGINE/FLYWHEEL/CONTINUOUSLY-VARIABLE-TRANSMISSION VEHICLE
Andrew A. Frank and Norman H. Beachley (University of Wisconsin) 248

REGENERATIVE BRAKING THROUGH ELASTOMERIC ENERGY STORAGE
L. O. Hoppie and G. C. Nowell (Eaton Corporation) .256

URBAN TRANSIT BUS PROPULSION WITH A PRACTICAL COMPOSITE FLYWHEEL
L. J. Lawson (Garrett-AiResearch) 266

MECHANICAL ENERGY STORAGE APPLICATION STUDIES
David B. Eisenhaure, Tim E. Bliamptis, and Bruce G. Johnson
(The Charles Stark Draper Laboratory, Inc.) 275

ADVANCED FLYWHEEL STORAGE SYSTEM
Philip O. Jarvinen (Massachusetts Institute of Technology) 282

FLYWHEEL ROTOR AND CONTAINMENT TECHNOLOGY DEVELOPMENT
S. V. Kulkarni (Lawrence Livermore National Laboratory) 290

APPROACH FOR MANUFACTURING COST/DESIGN TRADE-STUDIES FOR FLYWHEELS
B. Noton (Battelle-Columbus) 303

FLYWHEEL ROTOR DYNAMICS: WHIRLING OF COMPOSITE-MATERIAL FLYWHEEL SYSTEMS
C. W. Bert and G. Ramanujam (University of Oklahoma) 310

COMPOSITE FLYWHEEL DURABILITY AND LIFE EXPECTANCY: TEST PROGRAM
K. L. Reifsnider, S. V. Kulkarni, and D. M. Boyd
(Lawrence Livermore National Laboratory) 318

ROTOR TESTING IN FY 1981
R. S. Steele, Jr. and E. F. Babelay, Jr. (Union Carbide Corporation) 329

FIBER COMPOSITE MATERIALS TESTING
H. Thomas Hahn and W. K. Chin (Washington University) 337

FIBER COMPOSITE MATERIALS FATIGUE STUDIES
J. C. Duke, Jr., R. Stiffler, and K. L. Reifsnider
(Virginia Polytechnic Institute and State University) 344

LONG TERM CREEP CHARACTERISTICS OF COMPOSITE FLYWHEEL MATERIALS
F. F. Ling and S. J. Calabrese (Rensselaer Polytechnic Institute) 352

FLYWHEEL HOUSING DESIGN-CONCEPT DEVELOPMENT
A. Coppa (General Electric) 359

COMPOSITE FLYWHEEL BURST CONTAINMENT
Alan D. Sapowith and William E. Handy (Avco Systems Division) 369

CIRCULAR WEAVE FLYWHEEL MATERIALS EVALUATION AND COMPOSITE FLYWHEEL BURST CONTAINMENT
Alan D. Sapowith and William E. Handy (Avco Systems Division) 375

AGENDA 380

LIST OF ATTENDEES 384

COMPRESSED AIR ENERGY STORAGE PROGRAM

BLANK PAGE

PROJECT SUMMARY

Program Title: Compressed Air Energy Storage Technology Program

Program Manager: L. D. Kannberg

Organization: Pacific Northwest Laboratory
Richland, Washington 99352
Phone: (509) 375-6161, ext 319

Program Goals: Develop design and stability criteria for long-term operation of underground reservoirs used for compressed air energy storage (CAES) in order to accelerate the commercialization of the concept. Develop and assess second-generation technologies for CAES that require little or no supplementary firing by petroleum fuels in order to eliminate the dependence of CAES on these fuels.

Program Status: The Reservoir Stability Criteria Studies are progressing satisfactorily. Preliminary stability criteria for the three major types of storage reservoirs have been formulated. Generic numerical studies are complete. Most generic laboratory studies are complete. An aquifer field study site was selected, explored, and leased. Site development activities including drilling of the injection/withdrawal well and monitoring wells were conducted.

In Second-Generation Technologies, studies have been directed at screening the major advanced technologies: thermal energy storage, fluidized bed combustion, and coal gasification and the initiation of thermal storage bed material testing. The screening was completed in early FY-1981. A decision was made to concentrate resources in thermal storage stability testing supporting development of adiabatic CAES. A study evaluating equipment for advanced CAES concepts was completed.

Contract Number: DE-AC06-76RLO 1830

Contract Period: FY-1981

Funding Level: $2,725,000

Funding Source: U.S. Department of Energy

COMPRESSED AIR ENERGY STORAGE TECHNOLOGY PROGRAM OVERVIEW

L.D. Kannberg
Pacific Northwest Laboratory*
Richland, Washington 99352

ABSTRACT

Energy storage is a key element in the electric utility industry strategy for shifting energy consumption from oil to coal, nuclear and renewable energy sources. The U.S. Department of Energy (DOE) Compressed Air Energy Storage (CAES) Technology Program is directed at developing a new technology designed to reduce the consumption of oil in the generation of electric power. The program has two major elements: Reservoir Stability Studies and Second-Generation Concepts Studies. The Reservoir Stability Studies are aimed at developing stability criteria for long-term operation of large underground reservoirs used for compressed air storage. The Second-Generation Concepts Studies are aimed at developing new concepts that will require little or no petroleum fuels for operation.

In this overview, the program efforts during FY-1981 are outlined and major accomplishments towards the objectives of the program are identified.

INTRODUCTION

Compressed air energy storage (CAES) is a technique for supplying electric power to meet peak load requirements of electric utility systems. It incorporates a modified state-of-the-art gas turbine and an underground reservoir---an aquifer, a salt cavity or a mined hard rock cavern. The compressor and turbine sections of the gas turbine are alternately coupled to a motor/generator. During nighttime and weekend off-peak periods, low-cost power from base load plants using coal or nuclear fuels, would be used to drive motors to compress air which would be stored in the underground cavern. During the subsequent daytime peak-load periods the compressed air would be withdrawn from storage, mixed with fuel, burned and expanded through the turbines to generate peak power. This concept reduces the consumption of premium fuels by more than 60 percent for conventional CAES systems. Some advanced CAES concepts would not require petroleum fuels at all.

Studies have shown that the CAES concept is technically feasible and, for utilities with a proper power generation mix, economically viable. CAES systems offer several advantages over conventional systems used by utilities for meeting peak load requirements. CAES plants are not limited to the same degree of siting difficulties faced by conventional pumped hydro plants. Finally, a well designed CAES plant should have a smaller adverse impact on the environment than either a conventional peaking plant or a pumped hydroelectric storage facility.

In view of the potential benefits that the concept offers, DOE has undertaken a comprehensive program in order to accelerate commercialization of the technology. The Pacific Northwest Laboratory (PNL) was selected by DOE as the lead laboratory for the CAES Technology Program. As such, PNL is responsible for assisting the DOE in program responsibilities for planning, budgeting, contracting, managing, reporting and disseminating information. Under subcontract to PNL are a number of companies, universities and consultants that are responsible for various research tasks within the program. This report presents an overview of the CAES program activities by PNL and its subcontractors during FY-1981.

PROGRAM OBJECTIVES

The CAES Technology Program has evolved into two research and development elements and a supporting effort on environmental concerns. Recognizing that long term reservoir stability is a key issue to successful implementation of CAES technology, the Reservoir Stability Studies element has had the major emphasis in the early phases of the program. Recognizing also that the petroleum fuel requirements of conventional CAES systems may be an obstacle to large scale acceptance of the concept, the Second-Generation Concepts Studies element has been established and will dominate the research and development activity during the latter phases of the program.

---

*Operated for the U.S. Department of Energy by Pacific Northwest Laboratory under prime contract no. DE-AC06-76RLO 1830.

The objectives of the program are as follows:

- Reservoir Stability Studies - Establish stability criteria for large underground air reservoirs (in salt domes, hard rock, and porous rock formations) that may be used for air storage in utility applications.

- Second-Generation Concepts Studies - Develop advanced CAES technologies that would eliminate the dependence of CAES systems on petroleum fuels.

PROGRAM STRUCTURE

The structure of the CAES Technology Program represents continuation of tasks initiated since FY-1977. It also includes several major new items initiated during FY-1981. The latter includes activities in field studies and material testing for thermal energy storage for various advanced CAES systems.

In the Reservoir Stability Studies, four phases of activity for each of the three major types of storage reservoirs (aquifers, salt cavities, and hard rock caverns) have been either completed or are in effect. These phases are as follows:

- Phase 1 - State-of-the-art surveys (Preliminary stability criteria)
- Phase 2 - Numerical studies (Interim stability criteria)
- Phase 3 - Laboratory studies (Interim stability criteria)
- Phase 4 - Field studies (Final stability criteria)

This approach was dictated by the need to make optimal use of knowledge available from related disciplines and to provide the technical information to the DOE/Electric Power Research Institute (EPRI) Demonstration Program in a rapid manner. Phase 1 was completed in FY-1979. The bulk of Phases 2 and 3 were completed during FY-1981. Phase 4 activities for aquifer reservoirs were initiated during FY-1980.

In the Second-Generation Concepts studies, three concepts have been evaluated:

- CAES/FBC - Coal-fired fluidized bed combustion integrated with CAES
- CAES/TES - Thermal energy storage integrated with CAES
- CAES/CG - Coal gasifiers integrated with CAES

The feasibility of the three concepts were compared with conventional CAES plants and with other types of energy storage for electric utilities in a screening study. In addition, a study was commissioned and completed to evaluate system and component requirements for second-generation CAES concepts. This task identified equipment development which may be required to promote the feasible advanced CAES concepts to demonstration.

The CAES Technology Program is also committed to identifying the impacts that this new technology may have on the environment. A program element on environmental concerns is an integral part of the overall program. Activities in this area are coordinated with the Division of Environmental Control Technologies. This topic will not be addressed in this paper.

A work structure outline for the CAES Technology Program is shown in Fig. 1.

FUNCTIONAL ORGANIZATION

PNL leads this program and is performing the required program management, planning and research support in the area of porous rock studies. Under subcontract to PNL, in Reservoir Stability Studies, Re/Spec Inc. provided support in the numerical and experimental studies of the behavior of hard rock caverns; Louisiana State University (LSU) supplied experimental support in the study of the behavior of salt cavities; Serata Geomechanics supplied numerical support in the study of the behavior of salt cavities. PNL has performed much of the numerical and laboratory studies for CAES in porous rock. PB-KBB Inc. was selected in FY-1981 to design, construct and operate a field test of CAES in aquifers investigating the effects of CAES operating conditions and the potential for thermal storage in a porous rock aquifer. Acres American Inc. established the feasibility of integrating thermal energy storage with CAES. This led to the screening studies of second generation CAES concepts and the decision to perform CAES thermal materials research at FluiDyne Inc. and PNL.

The program functional organization is shown in Fig. 2. Major accomplishments reached by PNL and its subcontractors during FY-1981 are described in the next section.

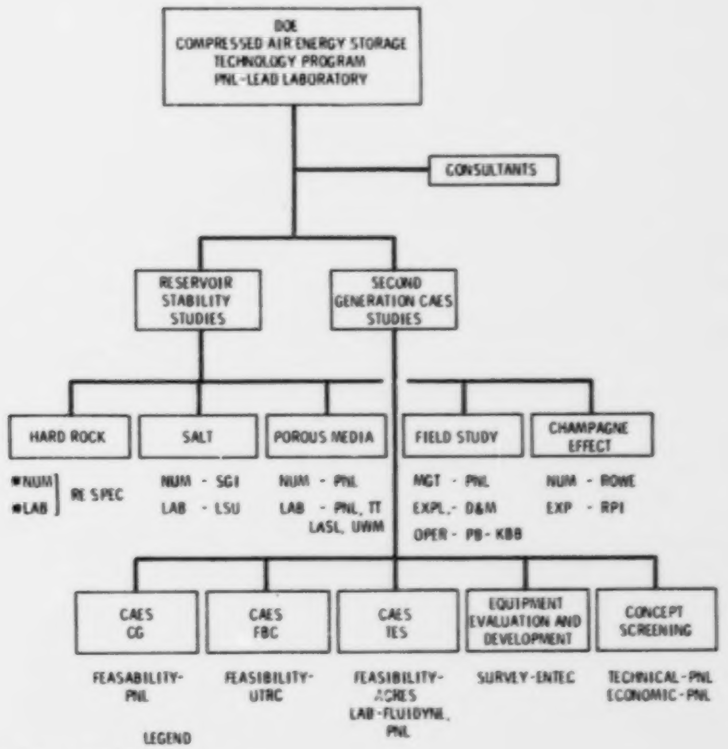
DOE
COMPRESSED AIR ENERGY STORAGE
TECHNOLOGY PROGRAM
PNL-LEAD LABORATORY
CONSULTANTS
RESERVOIR STABILITY STUDIES
SECOND GENERATION CAES STUDIES
HARD ROCK
SALT
POROUS MEDIA
FIELD STUDY
CHAMPAGNE EFFECT
*NUM
*LAB
RE SPEC
NUM - SGI
LAB - LSU
NUM - PNL
LAB - PNL, TT
LASL, UWM
MGT - PNL
EXPL.- D&M
OPER - PB - KBB
NUM - ROWE
EXP - RPI
CAES CG
CAES FBC
CAES TES
EQUIPMENT EVALUATION AND DEVELOPMENT
CONCEPT SCREENING
FEASABILITY-
PNL
FEASIBILITY-
UTRC
FEASIBILITY-
ACRES
LAB-FLUIDYNE,
PNL
SURVEY-ENTEC
TECHNICAL-PNL
ECONOMIC-PNL

LEGEND

RE SPEC - RE SPEC INC.
SGI - SERATA GEOMECHANICS INC.
LSU - LOUISIANA STATE UNIVERSITY
TT - TERRA TEK INC.
LASL - LOS ALAMOS SCIENTIFIC LABORATORY
UWM - UNIVERSITY OF WISCONSIN-MILWAUKEE
D&M - DAMES & MOORE
PB-KBB - PB-KBB INC.
ROWE - ROWE AND ASSOCIATES
RPI - RENSSELAER POLYTECHNIC INSTITUTE
UTRC - UNITED TECHNOLOGIES RESEARCH CENTER
ACRES - ACRES AMERICAN INC.
FLUIDYNE - FLUIDYNE ENGINEERING CORP.
ENTEC - ENTEC RESEARCH ASSOCIATES
PNL - PACIFIC NORTHWEST LABORATORY

Fig. 1. Compressed Air Energy Storage Technology Program Work Structure Outline

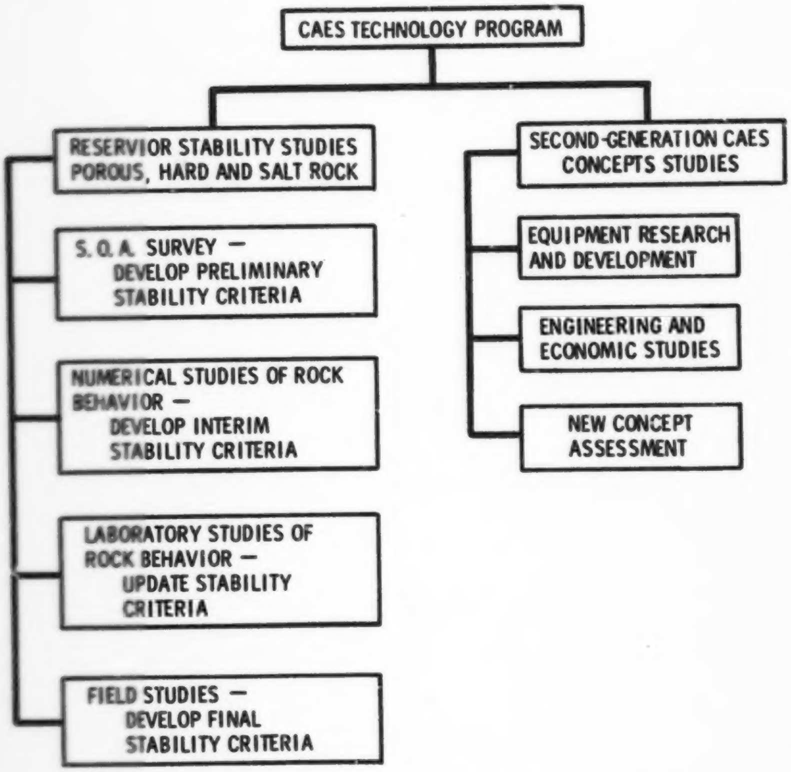
CAES TECHNOLOGY PROGRAM
RESERVIOR STABILITY STUDIES POROUS, HARD AND SALT ROCK
S. O. A. SURVEY — DEVELOP PRELIMINARY STABILITY CRITERIA
NUMERICAL STUDIES OF ROCK BEHAVIOR — DEVELOP INTERIM STABILITY CRITERIA
LABORATORY STUDIES OF ROCK BEHAVIOR — UPDATE STABILITY CRITERIA
FIELD STUDIES — DEVELOP FINAL STABILITY CRITERIA
SECOND-GENERATION CAES CONCEPTS STUDIES
EQUIPMENT RESEARCH AND DEVELOPMENT
ENGINEERING AND ECONOMIC STUDIES
NEW CONCEPT ASSESSMENT

Fig. 2. Compressed Air Energy Storage Program Functional Organization

PROGRAM ACCOMPLISHMENTS

The accomplishments of FY-1981 were highlighted by major advances in the porous rock field study, completion of the salt and hard rock numerical studies, and hard rock laboratory studies, and the screening and prioritization of selected advanced CAES concepts. There were also several setbacks in the program. Substantial budget reductions in March forced the cancellation of a major new initiative in development of two-stage, high head, reversible pump/turbines for Underground Pumped Hydroelectric Storage (UPH). It was also necessary to postpone a study of solar-augmented, adiabatic CAES. The dramatic flooding of the Jefferson Island salt mine caused a substantial loss of equipment used by Louisiana State University for CAES testing in that mine, and necessitated the relocation of CAES testing to the Cote Blanche mine. Field studies using salt cavities and an experimental thermal energy storage test facility are still postponed indefinitely because of budget limitations.

RESERVOIR STABILITY STUDIES

During FY-1981, efforts concentrated on completion of numerical modeling studies, continuation of laboratory studies and initiation of field studies through site exploration and confirmation. Accomplishments during FY-1981 included the following:

- Completed all generic structural and fluid flow numerical studies of porous media, hard rock and salt reservoirs.

- Relocated in-mine CAES tests for salt in Louisiana and completed substantial cyclic thermal and mechanical laboratory testing of salt.

- Completed all numerical laboratory studies of hard rock subject to CAES cyclic mechanical, thermal and chemical loading, and evaluated the design developed for the Potomac Electric Power Company (PEPCO) study of CAES in hard rock.

- Completed laboratory studies of structural behavior for porous rock response to cyclic ventilation and initiated combined effects testing of porous rocks in the PNL flow facility.
- Explored and confirmed a site near Pittsfield, Illinois, for the aquifer field test studies.
- Awarded, via competitive RFP, a contract for design, construction and operation of the field test facility in Pittsfield, Illinois. The injection/withdrawal well and monitoring wells for that testing facility were drilled and cased.

SECOND-GENERATION CONCEPTS STUDIES

The major milestones, accomplishments and activities in the Second-Generation Concepts Studies during FY-1981 were as follows:

- Completed a conceptual design of an adiabatic CAES (ACAES) plant using hard rock caverns for air storage.
- Completed a technical and economic assessment of fluidized bed augmented compressed air energy storage systems and system load following capability.
- Completed a screening study of second-generation CAES concepts.
- Initiated detailed thermomechanical and thermochemical testing of candidate thermal energy storage materials for hybrid and adiabatic CAES.
- Completed a study determining the availability of turbomachinery and ancillary components for second-generation CAES concepts.

More detailed descriptions of the activities and accomplishments are given in the papers presented on specific tasks in the CAES program.

PROJECT SUMMARY

Project Title: Second Generation CAES Studies

Principal Investigators:
M.J. Hobson, Acres American Inc.
C. Jee, Entec Research Associates
D.G. DeCoursin, FluiDyne Eng. Corp.
R.W. Reilly, PNL
K.R. Wheeler, PNL
F.R. Zaloudek, PNL (Project Manager)

Organization:
Pacific Northwest Laboratory (PNL)
Operated by Battelle Memorial Institute
Richland, WA 99352

Project Goals: Develop Second Generation CAES concepts that have minimal or no dependence on petroleum fuels

Project Status: A major engineering and economic study of adiabatic CAES (ACAES) was completed by Acres American Inc. in early FY-1981. With the completion of this study, detailed engineering feasibility and power cost information is now available on the four CAES concepts originally identified as being potentially attractive for utility energy storage application. The other identified concepts included Hybrid CAES, CAES/FBC and CAES/CG.

Economic studies were performed at PNL to place the economic data on these concepts on the same basis to allow comparisons. It was found that ACAES was the most economically attractive of the Second Generation concepts considered and more attractive than conventional CAES under most conditions. ACAES was also more economically attractive than many non-CAES technologies including storage batteries, combustion turbines and the advanced combined cycle under many conditions.

The technological status of these concepts was independently assessed by ENTEC Research Associates. From the results, it was concluded that ACAES and Hybrid CAES were closest to commercialization. It was estimated that only 3 to 5 years of development would be required to start detailed design of a utility installation.

The results of the economics and technology studies were assessed in a PNL study along with utility acceptance factors. It was concluded that, at this time, the ACAES concept appears most attractive for early commercialization. It was recommended that CAES program equipment development activities emphasize ACAES requirements; namely thermal energy storage (TES) materials identification and turbomachinery development.

Two related subtasks were initiated to address the identification of TES materials for ACAES. FluiDyne Engineering Corp. was awarded a subcontract to examine the performance and durability of candidate TES materials under thermal-mechanical ratcheting conditions expected during thermal cycling. PNL initiated work to define the resistance of these materials to thermal-chemical failure mechanisms. The results on the first group of materials will be available in early FY-1982.

Contract Number: DE-AC06-76RLO 1830

Contract Period: October 1, 1980 to September 30, 1981

Funding Level: $116,000

Funding Source: U.S. Department of Energy

AN OVERVIEW OF THE SECOND GENERATION COMPRESSED AIR ENERGY STORAGE STUDIES

Frank R. Zaloudek
Pacific Northwest Laboratory*
PO Box 999
Richland, Washington

INTRODUCTION

The overall objective of the Compressed Air Energy Storage (CAES) Technology Program is to develop compressed air energy storage systems to meet the peak load requirements of the electric utility industry.

Studies have shown that CAES is technically feasible and, with a proper utility power generation mix, is economically viable. CAES systems offer several advantages over conventional systems used by utilities for meeting peaking load requirements. The principal advantage is to reduce utility dependence on petroleum fuels. Replacement of current gas turbines by conventional CAES plants could result in annual savings of 100,000,000 barrels of oil or more. Other advantages include lesser siting problems and smaller environmental impacts than other storage systems.

The Second Generation CAES Studies were initiated as part of the CAES Technology Program to assess and develop new CAES concepts that require little or no supplementary firing by petroleum fuels. These concepts could further reduce or completely eliminate the dependence of CAES on potentially scarce petroleum fuels.

The purpose of this paper is to summarize the progress of the Second Generation CAES Studies towards project goals during FY-1981 and to summarize the present status of the project.

SECOND GENERATION CAES STUDIES IN PRIOR YEARS

Activities in prior years have included the preliminary screening of a number of new concepts which utilize reduced quantities of petroleum fuels or coal for supplementary firing. This screening resulted in the identification of several concepts that appeared technologically and economically viable. These concepts included the following:

- adiabatic CAES (ACAES)
- hybrid CAES
- coal-fired CAES utilizing a fluidized bed combustion system (CAES/FBC)
- CAES system integrated into a coal gasification plant (CAES/CG).

Conceptual design and economic studies were undertaken to obtain realistic information to base decisions on which of these should be considered for further development. The studies of ACAES and CAES/FBC were funded by Pacific Northwest Laboratory (PNL). The CAES/FBC study was completed; the ACAES study was still underway at the end of FY-1980. The remainder of the concepts were funded by Electric Power Research Institute (EPRI) and are essentially complete.

In addition, two additional concepts were identified in later screening studies as being potentially viable:

- solar assisted CAES (Solar/CAES)
- CAES directly coupled to a coal-fired steam plant (CAES/DCS).

However, conceptual design and economic analyses of these concepts to define their technological and economic feasibility have not as yet been undertaken.

---

*Operated for the U.S. Department of Energy by Battelle Memorial Institute under prime contract DE-AC06-76RLO 1830.

RESULTS OF FY-1981 SECOND GENERATION CAES STUDIES

Major FY-1981 activities were directed towards completion of the engineering and economic study of the ACAES concept, assessing the relative merits of the ACAES, Hybrid CAES, CAES/FBC and CAES/CG concepts, and the development of recommendations on the direction of developmental activities.

Conceptual Design and Economic Studies of Adiabatic CAES

In the adiabatic CAES cycle no fuel is consumed. The heat of compression is stored during the charging cycle instead of discarding it as in a conventional CAES plant. This stored heat is used during the discharge cycle to heat the compressed air withdrawn from storage before it is expanded in the turbine. The adiabatic CAES concept can be used with any type of storage reservoir, mined hard rock caverns, solution-mined caverns in salt, or aquifers.

Acres American, Inc. completed a conceptual design study and economic analysis of an adiabatic CAES plant using a water-compensated hard rock cavern for high pressure air storage. It was based on the earlier DOE/EPRI/Potomac Electric Power Company (PEPCO) 920-MW conventional CAES plant design prepared by Acres for a site in Maryland.

During charging, grid power is used to drive a compressor which compresses air to 1215 psi for storage in a mined hard rock cavern air storage reservoir. When the air emerges from the low pressure compressor, its temperature and pressure are 870°F and 225 psi. Instead of cooling the air in intercoolers as in a conventional CAES cycle, the air flows through a thermal energy storage (TES) unit where the heat of compression is stored. The cooled air is then further compressed in the high pressure compressor to 850°F and 1215 psi. The additional heat of compression is stored in a second, high pressure TES unit. The compressed air is then stored at a temperature below 125°F in the storage reservoir. The Acres study considered only air storage in mined hard rock caverns. However, solution mined salt caverns or aquifers could also be used.

During discharge, the motor/generator is uncoupled from the compressors and coupled to the turbines. Air from the reservoir is heated to 830°F in the high pressure TES and expanded in the high pressure turbine to 240 psi and 440°F. It is reheated to 865°F in the low pressure TES and further expanded in the low pressure turbine.

Based on a charging plant heat rate of 10,000 Btu/kWh, it was predicted that the round trip heat rate would be 14,800 Btu/kWh and the total cycle efficiency, 23%. The plant would require 12 hours of charging to produce 10 hours of operation in the discharge mode.

It was concluded that the plant configuration developed in the study did not contain any design or equipment availability problems that would preclude construction of a plant in the near future. However, a number of areas were identified where additional engineering attention would have to be directed before detailed design could proceed. These areas included:

- thermal energy storage (TES) materials properties and behavior
- high temperature air shafts
- valves
- turbomachinery

The economic analysis of 1990 levelized busbar energy costs indicated that ACAES had a significant advantage over the combustion turbine and was competitive with oil-fired CAES. Typical levelized busbar energy costs predicted were 225, 391 and 261 mills/kWh for ACAES, combustion turbine and oil-fired CAES respectively for 20% capacity factor.

Economic Studies

The conceptual design and economic analyses of the ACAES, hybrid CAES, CAES/FBC and CAES/CG concepts contained detailed information on the power costs for each option. However, comparisons of power costs between concepts were very difficult because of differing site-related factors and system design parameters. To enable direct comparisons, an effort was funded at PNL to reanalyze these costs and to put them on the same engineering and economic bases. The details of this analysis are presented in a later paper.

The principal result of this analysis was that ACAES appears to have the greatest potential for low cost energy of the second generation concepts examined. The busbar power costs for ACAES were found to be significantly lower (> .2) and high cost charging power (25 mill/kWh) where the power costs for all systems tended to converge. ACAES was also found to have significant power cost advantage over conventional CAES when low cost charging power (10 mill/kWh) is available. However, with high cost charging power (25 mill/kWh), ACAES loses its power cost advantage over conventional CAES.

Comparisons of ACAES power costs with non-CAES technologies were also made. It was found that ACAES has a significant power cost advantage over combustion turbines and the advanced combined cycle except at high charging power costs where the advanced combined cycle shows some advantages. In all cases, ACAES had lower power costs over storage batteries; however, there is some question over the accuracy of some assumptions used in this analysis. Comparisons of the power costs between a 1000-MW ACAES plant and a 2000-MW UPH plant showed a disadvantage for ACAES. However, the power costs for UPH will probably increase significantly for smaller plants. Therefore, UPH may lose some of its power cost advantage in a comparison between equivalent sized plants. This problem remains to be resolved.

Equipment Status

Since the commercial availability of equipment and components for the second generation concepts under consideration is a key matter in determining the future direction of the CAES Technology Program, a study was funded with ENTEC Research Associates to independently reassess the capability of industry to supply this equipment in a time frame consistent with the CAES Program commercialization goals.

After a review of the second generation CAES design studies, ENTEC focussed their attention to the following principal areas of concern:

- turbomachinery
- high pressure and temperature alloy valves
- piping and expansion joints
- concrete vessels for TES containment
- cycling coal gasifiers.

The results of the ENTEC study appeared to be less optimistic, although not inconsistent with the conclusions of the conceptual design studies. From these results, it was concluded that ACAES and hybrid CAES are closest to technological readiness of the second generation concepts considered. Either type plant could be made ready for detailed design with only 3 to 5 years of developmental activities. Principal areas of development include turbomachinery, TES materials identification and high pressure valves. The CAES/PFBC cycle appears to require substantially more R&D to bring it to a stage of technological readiness than either hybrid or ACAES designs. A cycling CAES/CG plant does not appear feasible in the near future.

Second Generation Concepts Assessments

A study was performed at PNL to integrate the information presented in the conceptual design studies, economic analyses and equipment availability studies and to develop recommendations regarding concepts which should receive further developmental attention. This study was restricted to the ACAES, hybrid CAES, and cycling versions of CAES/FBC and CAES/CG concepts. It covered consideration of technological readiness, economics and utility acceptability. It was concluded that ACAES appears to be the most attractive concept for early commercialization and should receive principal developmental attention in the CAES Technology Program developmental efforts. Development activities should include TES materials evaluation and turbomachinery engineering.

Developmental Activities

Experimental activities were undertaken in FY-1981 to evaluate the principal candidate TES materials for ACAES and hybrid CAES systems. Materials receiving attention include Taconite pellets and crushed granite. Supplementary funding is being received from EPRI to extend consideration to Denstone and cast iron spheres. Since the simulation of all conditions present in a CAES TES bed would be prohibitively expensive, the investigation was divided into two parts, each considering one of the principal hypothesized failure mechanisms for TES materials.

An investigation of thermal-mechanical ratcheting was funded at FluiDyne Engineering Corporation. In this investigation, candidate TES materials will be thermal cycled at atmospheric pressure in a 2 ft diameter, 15 ft high test column. Hydraulic cylinders will be used to simulate the mechanical forces exerted by a 65 ft high prototype TES bed. Measurements will be made of thermal and hydraulic performance, comminution and particulate elutriation. Testing is expected to be initiated in late FY-1981 or early FY-1982.

A study of thermal-chemical failure mechanisms is underway at PNL. In this study, the corrosion potential of TES materials will be examined statistically in an autoclave under combined conditions of high stress, high temperature and in the presence of water contaminated by air pollutants. Exposed samples will be microscopically examined to determine the progress of surface and internal cracking, comminution and intergranular corrosion. The results will be used to estimate service life of these materials. Samples are presently being exposed in the autoclave, and results are expected by the end of FY-1981.

FUTURE PROGRAM DIRECTIONS

It is expected that in coming years, increasing emphasis in the Second Generation CAES Studies will be placed on CAES materials and equipment development. Studies of TES materials and CAES reliability initiated in FY-1981 will be continued into FY-1982. Proposals and recommendations regarding turbomachinery development are presently being considered and evaluated. One interesting informal proposal received involves the investigation of convertible compressor/turbines for CAES applications. Such equipment is not far from present state-of-the-art and could have a substantial impact on the cost and complexity of CAES plants. Pending availability of funding, the engineering and economics analysis of the Solar/CAES, DCS/CAES and ACAES with aquifer air and heat storage will be completed and the relative advantages of these concepts over competing peaking power options will be assessed.

PROJECT SUMMARY

Project Title:	Conceptual Design of Adiabatic CAES in Hard Rock
Principal Investigator:	M. J. Hobson
Organization:	Acres American Incorporated Columbia, Maryland 21044
Project Goals:	Determine near-term technical and economic feasibility of adiabatic CAES with hard rock cavern storage.
Project Status:	The project has been completed, and the final report has been submitted. The study was performed under five project tasks Task I involved technology review, storage material cost/performance assessment and analysis of the Thermal Energy Storage (TES) system. A sensible heat pebble bed approach was selected and several candidate storage materials were identified. Task II involved technology review, development of a turbomachinery configuration identification of performance, cost and future potential for development of more efficient plant equipment. Task III involved cycle optimization based upon real machinery limitations and estimation of performance over the operating range. Task IV involved development of a 4-unit conceptual plant design based upon the site used for the recent PEPCO CAES/UPH study. Task V involved estimation of plant construction and operating costs and development of comparative energy production costs.
Contact Number:	DE-AC06-76RLO 1830, Subcontract B-82284-A-E
Contract Period:	December 1979 - December 1980
Funding Level:	$268,441
Funding Source:	U. S. Department of Energy through Battelle-Pacific Northwest Laboratory

ADIABATIC CAES USING HARD ROCK CAVERNS

Michael J. Hobson
Acres American Incorporated
Thermal Energy Division
Columbia, Maryland

ABSTRACT

A conceptual design for an adiabatic (no fuel) compressed air energy storage (CAES) plant was developed utilizing a water-compensated cavern mined in hard rock. Estimates of capital and operating costs were compared with oil-fired CAES and combustion turbines. Projections of future total annual costs suggest that adiabatic CAES has potential for energy storage in electric utility systems. Areas requiring further development are identified for establishment of a system worthy of utility acceptance.

INTRODUCTION

The principle of adiabatic CAES is based on storing the heat of compression during the charging mode and returning this heat to the air released from storage in the generation mode. Adiabatic CAES was first studied in an Electric Power Research Institute (EPRI) funded effort performed by Central Electricity Generating Board (CEGB) in 1978 [1]. The findings indicated that fuel topping was preferable in the short term but high temperature (1200 to 1500°F) adiabatic cycles should be pursued in the long term.

In 1977 Department of Energy (DOE), EPRI and Potomac Electric Power Company (PEPCO) funded a comprehensive preliminary engineering study [2] of an oil-fired CAES plant and an underground pumped hydro plant designed to operate on the PEPCO system. The 924 MW CAES plant configuration and the site selected for it was utilized as a basis for the adiabatic (no fuel) CAES conceptual design so as to make cost comparisons as accurate as possible. This work was supported by the U.S. Department of Energy under Subcontract No. B-82284-A-E [3] through Pacific Northwest Laboratory, operated for DOE by Battelle Memorial Institute.

THE ADIABATIC CAES CYCLE

The PEPCO oil-fired CAES site was selected for the high quality of rock at depth. Construction cost studies indicated that the most economic air storage pressure was in the 1000 psig range. The stored air pressure is held sensibly constant by water compensation through a water column from the cavern to a surface reservoir.

Surveys for adiabatic CAES of available turbomachinery and computerized analysis of feasible cycles showed that a two-stage cycle with a storage pressure of 1250 psig provided the best compromise of operational efficiency and capital cost at that site.

The optimum performance criteria for the cycle were calculated using data from existing Dresser Clark product lines modified to operate at as high a top temperature as possible without extensive redesign. Figure 1 shows a simplied form of the cycle developed.

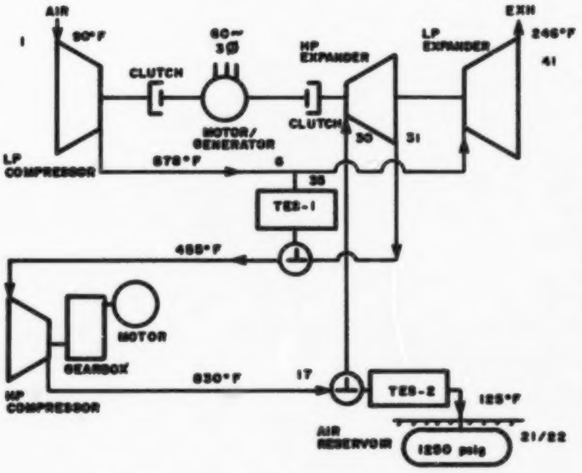

Figure 1. Adiabatic CAES Cycle.

THERMAL STORAGE

Large quantities of heat are required to be stored during adiabatic CAES operation--3,379 Btu per kWh generated--and the thermal energy storage (TES) system design requires to be capable of storing the heat for many hours with negligible losses. The critical performance parameters of TES are:

- low pressure loss (dp)
- low end temperature difference (T_e).

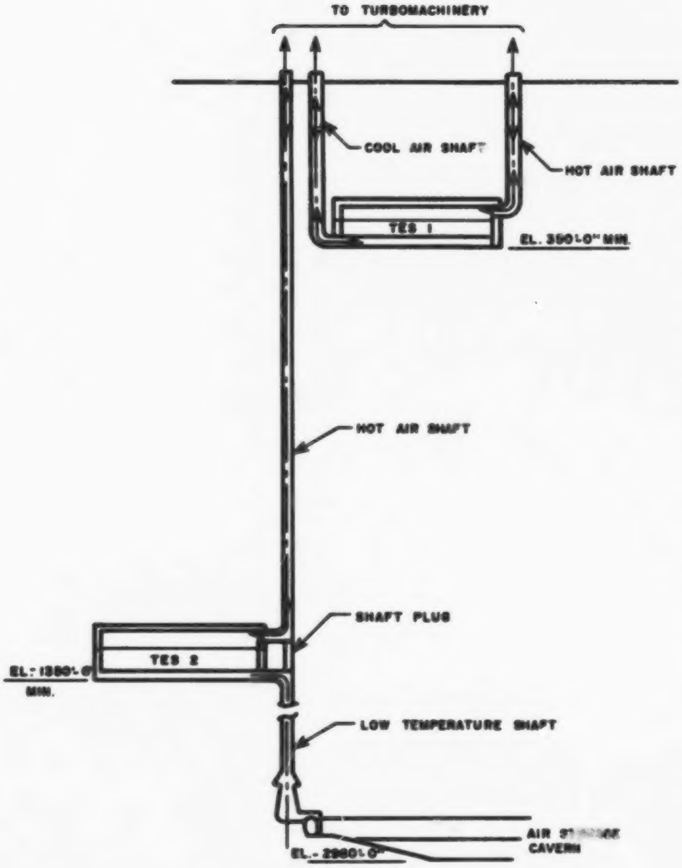
TO TURBOMACHINERY
COOL AIR SHAFT
HOT AIR SHAFT
TES 1
EL. 350'-0" MIN.
HOT AIR SHAFT
SHAFT PLUG
TES 2
EL.-1300'-0"
MIN.
LOW TEMPERATURE SHAFT
AIR ST
CAVERN
EL.-2900'-0"

Figure 2. TES Underground Pressure Containment

End temperature difference is the TES average charging temperature minus the TES average discharging temperature. It embodies all heat losses in the TES system and significantly affects plant efficiency and output.

Valuable assistance was provided by MIT and CEGB in the selection of the thermal storage system, design of the concept and the prediction of operational characteristics. Figure 2 shows the underground TES pressure containment configuration selected. The only TES system capable of meeting these criteria was a pebble bed sensible heat system similar to those utilized in solar heat storage and wind tunnel installations. Iron ore pellets appear to provide the most practical media, but certain rock types and purpose made products such as Denstone™ may be economically superior.

The pebble bed material is contained in a series of vertical cylindrical steel tanks located in a cavern. Air is directed through the beds by distribution ducts to ensure even flow as shown in Figure 3, a cross section through one of the tanks. Figure 4 is an elevation on one TES composed of several tanks.

The TES is externally insulated to contain heat. The rock containment is protected from overheating by a measured flow of cooling air which is depressurized in a two stage expander at the surface to supply plant power.

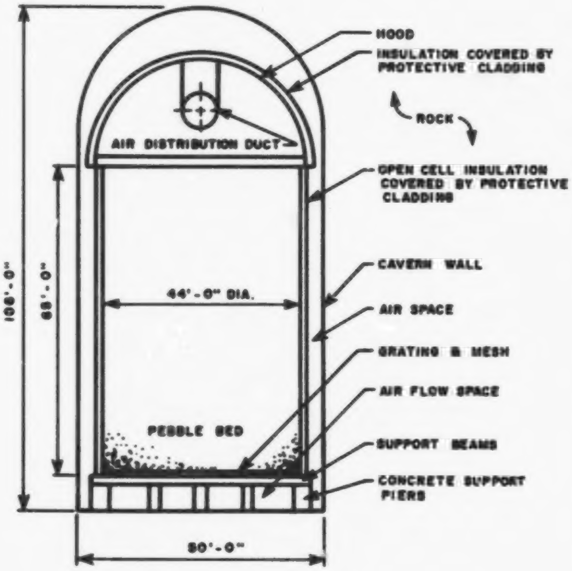
HOOD
INSULATION COVERED BY PROTECTIVE CLADDING
ROCK
AIR DISTRIBUTION DUCT
OPEN CELL INSULATION COVERED BY PROTECTIVE CLADDING
CAVERN WALL
AIR SPACE
GRATING & MESH
AIR FLOW SPACE
SUPPORT BEAMS
CONCRETE SUPPORT PIERS
PEBBLE BED
44'-0" DIA.
108'-0"
65'-0"
50'-0"

Figure 3. Typical TES Section

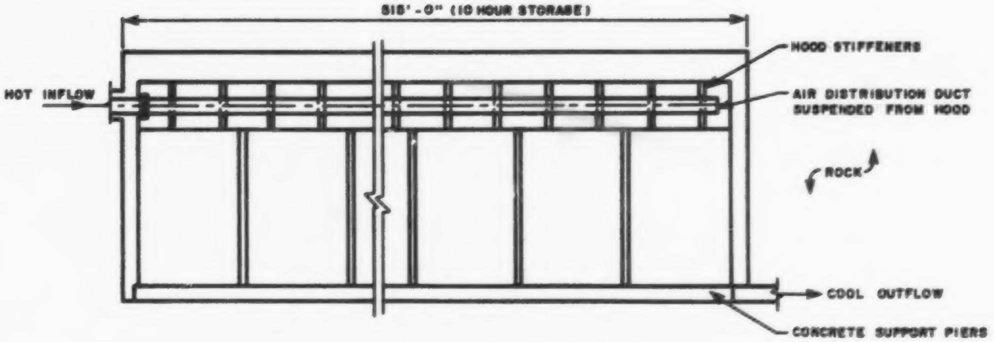
515'-0" (10 HOUR STORAGE)
HOOD STIFFENERS
HOT INFLOW
AIR DISTRIBUTION DUCT SUSPENDED FROM HOOD
ROCK
COOL OUTFLOW
CONCRETE SUPPORT PIERS

Figure 4. Typical TES Elevation

PLANT PERFORMANCE

Electric utilities are reluctant to consider generation systems that are inflexible or have operational constraints. For this reason, care was exercised in development of a plant design that would respond satisfactorily to variable charging and generation rates.

Figure 5 is a computer printout for the plant design point. The off-design performance calculations show 3 percent less generation at 75 percent turbine flow and 7 percent less at 50 percent flow.

```
COMPONENT NO.    1        2        3        4        5        6        7        8        9       10       11
COMP. NAME     INLET    COMPR    PIPE     COMPR    PIPE     VALVE    PIPE     HEATX    PIPE     VALVE    PIPE

FLOW, LB/S    2600.0   2600.0   2600.0   2600.0   2600.0   2600.0   2600.0   2600.0   2600.0   2600.0   2600.0
TEMP, F         90.0    494.6    494.6    877.9    877.9    877.9    877.9    455.0    455.0    455.0    455.0
PRES, PSIA      14.2     78.0     77.8    221.3    220.7    220.7    221.2    216.2    214.1    214.1    213.7
H, BTU/LB      131.5    229.5    229.8    327.5    327.5    327.5    327.5    119.6    219.6    219.6    219.6

COMPONENT NO.   12       13       14       15       16       17       18       19       20       21
COMP. NAME     PIPE     HEATX    COMPR    PIPE     COMPR    PIPE     VALVE    PIPE     HEATX    PIPE

FLOW, LB/S    2600.0   2600.0   2600.0   2600.0   2600.0   2600.0   2600.0   2600.0   2600.0   2600.0
TEMP, F        455.0    236.0    461.4    461.4    830.0    830.0    830.0    830.0    125.0    125.0
PRES, PSIA     210.2    206.2    453.5    452.5   1216.3   1201.3   1201.2   1201.5   1209.5   1263.0
H, BTU/LB      219.6    165.6    220.9    220.9    315.4    315.4    315.4    315.4    133.7    133.5

                                                GENERATION

COMPONENT NO.   22       23       24       25       26       27       28       29       30       31       32
COMP. NAME     CAVRN    HEATX    PIPE     HEATX    PIPE     VALVE    PIPE     PIPE     VALVE    TURBN    PIPE

FLOW, LB/S    3120.0   3120.0   3120.0   3120.0   3120.0   3120.0   3120.0   3120.0   3120.0   3120.0   3120.0
TEMP, F        125.0    100.0    100.0    805.0    805.0    805.0    805.0    805.0    805.0    437.9    437.9
PRES, PSIA    1263.0   1263.0   1188.4   1184.4   1148.4   1148.3   1125.7   1125.2   1110.6    237.9    237.5
H, BTU/LB      133.5    126.9    127.3    308.8    308.8    308.8    308.9    308.9    308.9    215.3    215.3

COMPONENT NO.   33       34       35       36       37       38       39       40       41
COMP. NAME     VALVE    PIPE     HEATX    PIPE     VALVE    PIPE     PIPE     VALVE    TURBN

FLOW, LB/S    3120.0   3120.0   3120.0   3120.0   3120.0   3120.0   3120.0   3120.0   3120.0
TEMP, F        437.9    437.9    862.0    862.0    862.0    862.0    862.0    860.0    237.6
PRES, PSIA     237.5    238.5    233.5    232.3    232.3    231.5    231.0    229.0     15.2
H, BTU/LB      215.3    215.3    323.3    323.3    323.3    323.3    323.3    323.3    166.9

 COMPRESSOR POWER, MW       MOISTURE REMOVED, LB/S          TURBINE POWER, MW         FUEL CONSUMPTION, LB/S
     1         276.61               1          0.00            1         300.26              1          0.00
     2         274.76               2          0.00            2         501.93              2          0.00
     3         156.07               3          0.00            3           0.00              3          0.00
     4         266.36               4          0.00            4           0.00              4          0.00
 TOTAL         973.79       TOTAL              0.00         TOTAL        802.20         TOTAL           0.00

                                     SUMMARY:   DAILY   STORAGE CYCLE

ELECTRIC ENERGY RATIO (KWHR IN/KWHR OUT) =  1.477        COMPRESSION TIME/GENERATION TIME =         1.22
SPECIFIC FUEL CONSUMPTION, BTU/KWHR =         0.0        AIR FLOW TO STORAGE CAVERN, LB/S =       2600.0
"ROUNDTRIP" HEAT RATE, BTU/KWHR =         14773.7        AIR FLOW FROM STORAGE CAVERN, LB/S =     3120.0
HEATING VALUE OF FUEL, BTU/LB =               0.0        STORAGE PRESSURE, PSIA =                 1263.0
AIR STORED, M LB/DAY =                     93,600        COMPRESSION TIME, HRS =                   10.00
AIR LEAKAGE, MM LB/DAY =                    1.310

________

NOTE:  For state point numbers see Figure 1.
```

Figure 5. Adiabatic CAES Plant Thermodynamic Analysis - Design Point

A measure of an energy storage plant efficiency is the Electric Energy Ratio (EER)--input energy divided by output energy. EER for a pumped hydro plant is about 1.35 compared to 1.48 for this adiabatic CAES conceptual design. Improvement in EER would be possible if (a) the equipment train top temperature could be raised and (b) pressure losses could be reduced. This could be achieved by selecting a single-stage cycle with a greater pressure ratio, however, considerable turbomachinery development is required before such equipment is available.

CAPITAL AND OPERATING COSTS

Adiabatic-CAES in Hard Rock - 10 Hr. Storage

20. LAND AND RIGHTS	$ 16,496,000
21. GENERATION/COMPRESSION SYSTEM	230,249,000
22. COMPRESSED AIR STORAGE	64,410,000
23. THERMAL ENERGY STORAGE - IRON ORE FILL	59,749,000
25. ELECTRIC PLANT EQUIPMENT	67,094,000
26. GENERAL PLANT FACILITIES	10,572,000
DIRECT COST COST/KW	$ 448,570,000 $561
23. THERMAL ENERGY STORAGE - ROCK FILL	56,065,000
23. THERMAL ENERGY STORAGE - DENSTONE FILL	108,556,000
23. THERMAL ENERGY STORAGE - CAST IRON FILL	222,804,000

JULY 1980 DOLLARS

Table 1. Capital Cost Estimate 800 MW Plant

Drawings were prepared to show the plant layout and system arrangement. Estimates of capital cost for the plant were based on the detailed costs prepared for the oil-fired PEPCO CAES plant together with equipment prices assembled by Dresser Clark. TES costs were based on four alternative media, iron ore pellets, granulated rock, Denstone™ and cast iron, as shown in Table 1. The installed cost per kW of $561 with iron ore pellet fill compares with a direct cost of approximately $411 for an equivalent oil-fired CAES plant.

The operating costs for the plant were based on a plant staff complement of 68 and estimated to be $2.64/kW-yr for fixed and 0.19 mils/kWh for data, the levelized busbar cost of generated electricity was calculated for a range of plant capacity factors. The results are shown in Table 2.

1990 Levelized Busbar Cost (Mills/kWh)
(EPRI 1978 Technical Assessment Guide)

Capacity Factor (percent)	Oil-Fired CAES[a] (10-hour storage)	Adiabatic CAES[b] Iron Oxide Fill (10 - hour storage)	Adiabatic CAES[b] Denstone Fill (10-hour storage)	Adiabatic CAES[b] Cast Iron Fill (10-hour storage)	Combustion Turbine[c]
10	369.9	378.2	410.6	492.3	446.4
15	297.6	276.0	297.6	351.8	409.6
20	261.4	224.9	241.1	281.7	391.2
25	238.6	194.2	207.2	239.7	380.0

(a) 924 MW output, 30-year life, Commencing 1990.

(b) 800 MW output, 30-year life, Commencing 1990.

(c) 50 MW output, 30-year life, 300 $/kW capital cost (1990), 2.0 mills/kWh variable O & M, 140 mills/kW-yr fixed O & M, 12,000 Btu/kWh heat rate (1980 dollars).

Table 2. Comparison of Oil-Fired CAES, Adiabatic CAES, and Combustion Turbines

The results indicate that except for the most costly TES fill material (cast iron), adiabatic CAES appears to be significantly more economic that oil-fired CAES and combustion turbines.

These results cannot be considered conclusive because of the many factors that influence the calculation of levelized energy cost, particularly the cost of charging energy and the escalation rate of fuel oil and off-peak power. However, the findings suggest that adiabatic CAES deserves a more detailed examination.

AREAS REQUIRING FURTHER DEVELOPMENT

The TES system performance and reliability can affect adiabatic CAES more acutely than any other component. Only relatively small systems have been operated to date. A program to establish design parameters is required, therefore, to allow engineers to specify TES systems with confidence.

The turbomachinery selected for the study was specified as modified off-the-shelf technology. If more advanced components are considered, the cycle performance could be improved and hopefully costs could be reduced.

It was recognized that TES media loss would occur, causing carryover of particulate and blade erosion. Air cleaning devices were therefore included in the piping system. However, considerable research is proceeding on PFB particulate cleanup, and also the expander gas path can be equipped with stumbling steps to increase blade life, although at the cost of about 2 percent in efficiency. Refinement of the TES systems and turbomachinery design should include development of applicable air quality criteria and an appropriate particulate control solution.

The thrust of all adiabatic CAES system development should be directed towards electric utility acceptance. Involvement of the industry in development projects will ensure compliance with utility criteria and more accurate projection of costs.

CONCLUSION

Adiabatic CAES appears to be a competetive large-scale electric energy storage system, particularly in capacities between 200 to 1000 MW. A program of development is now required to advance the concept towards acceptance by electric utilities for peaking and load leveling service.

REFERENCES

1. Glendenning, I., P. E. Chew, R. Grant, R. Glanville and M. H. Hoye. Technical and Economic Assessment of Advanced Compressed Air Storage (ACAS) Concepts, EPRI EM-1289, prepared for Electric Power Research Institute by Central Elecricity Generating Board, RP 1083-1, December 1979.

2. Rasmussen, J. E., P. E. Schaub. Preliminary Design Study of Underground Pumped Hydro and Compressed Air Energy Storage in Hard Rock, prepared by PEPCO and Acres American Incorporated under DOE Contract EC-77-C-01-5047 and EPRI Research Project 1081-1, 1977 - 1980.

3. Hobson, M. J., S. Bahadur, C. L. Driggs, D. C. James, P. E. Chew, R. Kohanski, J. L. Nash-Webber. Conceptual Design and Engineering Studies of Adiabatic CAES With Thermal Storage, prepared for Battelle Pacific Northwest Laboratory by Acres American Incorporated, Columbia, MD, March 1981.

PROJECT SUMMARY

Project Title: A Line-By-Line Assessment of the Principal Subsystems, Equipment Items and Components of Second-Generation Compressed Air Energy Storage (CAES) Systems

Principal Investigator: David L. Chiang

Organization: ENTEC Research Associates, Inc.
451 Hungerford Drive, Suite 609
Rockville, Maryland 20850

Project Goals: Evaluate the present and potential future availability of principal systems, equipment and components to meet the performance requirements of second-generation CAES plants in commercial utility usage as peaking plants. Potential problems regarding availability and performance shall be identified and research requirements defined.

Project Status: The assessment project has been completed and the technical report is in the final stages of preparation.

To ensure that all key equipment, subsystems and components were identified, a review of four second-generation CAES concepts was conducted. The concepts included: CAES/coal-fired fluidized bed combustor, CAES/coal gasification, adiabatic CAES/hardrock air storage reservoir, and the hybrid CAES/thermal energy storage.

A thorough examination was performed to determine each vendor's capability to design, as well as their capacity to manufacture, CAES equipment in a timely manner. To effectively determine commercial availability, each vendor's capability was surveyed and examined by analyzing catalogs, conducting a direct contact survey, and conducting a number of on-site interviews.

Based on the analysis of catalogs and the results of the surveys, major problem areas and equipment constraints relevant to CAES equipment availability were identified.

A survey of CAES-related equipment R&D was conducted on other energy projects within the Department of Energy and industry. A data base on equipment constraints was obtained. These constraints were compared with the information obtained from the vendors surveyed.

Contract Number: DE-AC06-76RLO 1830, subcontract B-B5453-A-L

Contract Period: October 8, 1980 through September 30, 1981

Funding Level: $63,000

Funding Source: U.S. Department of Energy through Battelle-Pacific Northwest Laboratories

ASSESSMENT OF PRINCIPAL SUBSYSTEMS, EQUIPMENT ITEMS AND COMPONENTS OF SECOND-GENERATION COMPRESSED AIR ENERGY STORAGE (CAES) SYSTEMS

David L. Chiang Cordell K. Jee
ENTEC Research Associates, Inc.
451 Hungerford Drive, Suite 609
Rockville, Maryland 20850
(301) 424-1745

ABSTRACT

Several candidate Compressed Air Energy Storage (CAES) technologies were evaluated in this study and included the adiabatic CAES with hardrock air storage reservoir (ACAES/hardrock), the CAES with fluidized bed combustor (CAES/FBC), CAES with coal gasification (CAES/CG), and the hybrid CAES with thermal energy storage (hybrid CAES/TES). The specific subsystems, equipment and components evaluated for each technology were as follows:

- Turbomachinery design, manufacturing or operating shortfalls which may limit the early commercialization of CAES application.
- The availability of high pressure and temperature, large diameter alloy valves, control valves, pipes, and fittings.
- The availability of high efficiency filtration equipment to minimize potential damages to the turbomachinery.
- The current design and manufacturing limit on power transmission gears.
- Methods to contain thermal expansion of the well casing.

INTRODUCTION

The U.S. Department of Energy is sponsoring a program to accelerate the demonstration and commercialization of energy storage concepts in the advanced CAES category. Based on past and current technical and economic analyses, the application of these concepts or technologies by the electric utilities could save more than one million barrels of oil (equivalent) per day.

There are, however, major technical and manufacturing barriers preventing widespread industry adoption of this technology. This study was initiated to identify and clarify these barriers and recommend possible courses of action to be taken. Specifically, the assessment performed in the study addresses the following salient issues:

- Are the uppermost operating requirements of CAES systems within industry technical and manufacturing state-of-the-art?
- What is the lead time required to upgrade/redesign currently available equipment for CAES application?
- What influencing factors will synchronize industry's developmental efforts with DOE's commercialization time-frame for CAES application?
- What research and development activities, if any, should DOE undertake to stimulate the early commercialization of this application?

TURBOMACHINERY AVAILABILITY

A survey of turbomachinery vendors was conducted and reponses from senior-level representatives of these vendors were far from being uniform or consistent. However, several key issues became apparent as a result of the survey. They include the following:

- No manufacturers have turbomachinery trains operating under similar conditions to CAES/FBC and adiabatic CAES systems; but most turbomachinery manufacturers surveyed are confident that compressors, expanders and gears can be manufactured to the operating requirement of CAES/FBC and adiabatic CAES applications.

- The estimated developmental/scale-up timeframe ranges from 2-5 years from the date of order. A detailed technical investigation, analysis, and in some cases, a prototype developmental program will be required to upgrade/modify current designs for CAES application.

- Strong market indications (either firm orders which will allow the company to write-off developmental cost on the first machine, or strong economic indications that CAES is financially attractive to utilities) will be necessary to stimulate a more active interest on the part of manufacturers to direct resources to upgrading their components for CAES applications.

- From the perspective of depth of technical research required, adiabatic CAES technical issues are more readily identifiable with possible solutions than the CAES/FBC. In the case of CAES/FBC the potential "showstopper" is the development required for the gas turbine and the associated coal-fired fluidized bed system.

VALVE INDUSTRY READINESS

A survey of the valve industry's capabilities to supply large diameter (48" to 96"), high pressure and temperature valves indicate that the valve industry is currently capable of supplying valves in quantity up to 60" diameter for the pressure and temperature ranges required for adiabatic compressed air energy storage (ACAES) systems. Sizes up to 120" diameter have been supplied to refineries for fluid catalytic cracking service; however, the continuing functional ability of these larger valves requires considerable scheduled maintenance for reliable service. All manufacturers surveyed are confident that 60" diameter and larger valves meeting ACAES operating requirements can be met, but it will take a minimum of two years of design modification and testing before a fully functional valve can be manufactured.

PIPING AND EXPANSION JOINT INDUSTRY READINESS

Piping and thermal expansion of aboveground piping and well casing were examined after completing the survey of nine manufacturers. The major conclusions drawn from this examination are as follows:

- Pipes operating under ACAES conditions are readily available; however, large diameter pipes (greater than 90") will be designed and manufactured under ASME pressure vessel code Session VIII, Division I, rather than piping codes specified under ANSI B31.3. The code variance will not affect pipe availability although it will have an impact on its costs.

- Thermal expansion of the well casing is routinely handled by the oil and gas industry when the wells operate at temperatures less than 650°F. Temperatures greater than 650°F will require significant amounts of developmental work in both cement material and cementing practices.

- Aboveground piping stresses due to thermal expansion can be contained by the proper application of currently available expansion joints and the use of expansion loops.

CYCLIC COAL GASIFICATION FEASIBILITY

An integrated coal gasification and CAES system was recently conceived as an attractive alternative for generating utility peak-load power. A number of gasification/CAES system configurations have been investigated by several power equipment manufacturers and architect-engineering firms and a feasibility analysis was performed. The results of the analysis indicated the following:

- It is unlikely that an integrated coal gasification/CAES plant can be operated in a daily cyclic operation such that the coal gasification plant will be shut down and be maintain in a "hot" standby condition. This is made based on the projected longer response time and potential operating problems resulting from frequent shut down and startup. These operational problems may include the thermal stress on material, formation of undesirable liquid products, and excess corrosion and embrittlements in a coal gasifier environment.

- It is technically feasible to operate the coal gasification process at partial load (approximately 50%) without adversely affecting the performance of a process. However, the feasibility of such operation hinges on further economic advantages and possible use of fuel gas during off-peak periods.

CONCRETE PRESSURE VESSEL

An assessment of the prestressed concrete thermal energy storage (TES) pressure vessel used in a conceptual design of an A-5 hybrid advanced compressed air storage (ACAS) plant reveals that no major problems exist regarding the availability of the concrete and the construction as well as the operation of the vessel. Methods and techniques have been developed, material standards have been established, and logistic problems have been resolved as a result of experience in the nuclear power industry. Reactor containment vessels of nuclear power plants are similar to the TES prestressed concrete pressure vessels and the following factors apply:

- Size of Structure - the overall size of a nuclear reactor containment vessel is approximately 210 feet high by 150 feet in diameter. The wall thickness of the vessel is 4.5 feet for the side walls and 3.5 feet for the dome, which has a radius of 70 feet. Thus, the inside diameter of the vessel is approximately 140 feet and the volume is approximately 2,600,000 cubic feet.

- Structural Characteristics - the vessel is designed and constructed to withstand a light aircraft impact, an earthquake of a magnitude of 6 (Richter Scale) and a reactor accident resulting from equipment failures, loss of coolant (LOCA), and other malfunctions.

- Construction - procedures and material standards have been well defined and documented by the U.S. Nuclear Regulatory Commission. At various stages of constructing the containment vessel, tests are conducted to assure safety and integrity. Vendors have experienced no problems conforming to the stringent standards and supplying the material.

POTENTIAL R&D AREAS

In general, major technical issues will ultimately be resolved by industry if market forces are sufficiently favorable to justify directing internal resources to resolving design/manufacturing issues in a timely manner. Although the market issue is the overriding concern of all the firms surveyed, a key technical issue cited as requiring resolution is in the turbomachinery area, specifically compressors and their component parts as shown in the table below.

Major Issues Perceived by Compressor Manufacturers

Technical/Market Issues	Company Surveyed A	B	C	D	E	F	G	H
Material		●	O	O	◓	O	NC	◓
Seals		◓	O	O	◓	O	NC	O
Blading		●	◓	◓	◓	◓	NC	◓
Systems		●	O	NC	O	NC	NC	◓
Erosion		●	●	●	●	●	NC	●
Gears/Clutch		◓	◓	◓	◓	◓	NC	◓
Manufacturing		◓	◓	◓	◓	◓	NC	◓

● = Major barrier (potential "showstopper")
◓ = Needs further investigation
O = Not a critical issue
NC = No comment

Other R&D areas include the resolution of thermal stresses expected on large diameter valves operating at elevated temperatures and pressures. Most manufacturers are limited by the number of research and design personnel they are willing to commit to conducting studies in this area. Increases in both size and pressure-temperature ratings will be major undertakings for CAES systems, requiring extensive analysis, drawings, tooling and testing.

For the cyclic coal gasification/CAES combination, two key areas were identified for further R&D investigations. These areas include investigations of potential hybrid coal gasification and steam production systems and investigations of reliability of operating coal gasifiers at reduced load conditions.

REFERENCES

1. Acres American Incorporated. Conceptual Design and Engineering Studies of Adiabatic CAES with Thermal Energy Storage. Subcontract No. B-82284-A-E, Contract No. EY-76-C-06-1830, U.S. Department of Energy through Battelle-PNL. September 1980.

2. United Technologies Research Center. Parametric Performance Evaluation and Technical Assessment of Adiabatic Compressed Air Energy Storage Systems. Prepared for Electric Power Research Institute, Final Report on Project 1199-1. EPRI EM-1188. October 1979.

3. United Technologies Research Center. Technical and Economic Assessment of Fluidized Bed Augmented Compressed Air Energy Storage System. Subcontract No. B-51299-A-L, U.S. Department of Energy through Battelle-PNL. UTRC R80-954490-20. June 1980.

4. United Technologies Research Center. Concept Screening of Coal Gasification CAES Systems. Prepared for Electric Power Research Institute, Final Report on Project 1199-1. EPRI EM-1077. May 1979.

5. Central Electricity Generating Board. Technical and Economic Assessment of Advanced Compressed Air Storage (ACAS) Concepts. Prepared for Electric Power Research Institute, Final Report on Project 1083-1. EPRI EM-1289. December 1979.

6. E. J. Sosnowicz. Report of Interviews with European Equipment Manufacturers for MSS/CAES Plant Application. United Engineering & Constructors Inc. October 13, 1978 to October 27, 1978.

7. D. W. Hatcher, C. B. Tolliver. Survey of Industrial Coal Conversion Equipment Capabilities: Mechanical Piping Connectors and Expansion Joints. Oak Ridge National Laboratory, Contract No. W-7405-eng-26. ORNL/TM-6586. June 1979.

8. W. R. Williams, J. R. Horton, W. R. Reed, W. F. Boudreau. Survey of Industrial Coal Conversion Equipment Capabilities: Equipment Operating Experience, Prices, and Development Program. Oak Ridge National Laboratory, Contract No. W-7405-eng-26. ORNL/TM-6587. January 1980.

9. W. R. Williams, J. R. Horton, W. F. Boudreau, M. Siman-Tov. Survey of Industrial Coal Conversion Equipment Capabilities: Rotating Equipment. Oak Ridge National Laboratory, Contract No. W-7405-eng-26. ORNL/TM-6074. April 1978.

10. J. T. McCabe, F. E. Kramberger, B. R. Hao, D. Dubis, S. E. Carson. An Assessment of Synthane Mechanical Equipment. Mechanical Technology Inorporated, Contract No. AC01-77ET10622, U.S. Department of Energy. MTI-79TRS. May 1980.

PROJECT SUMMARY

Project Title:	Thermomechanical Screening of Thermal Energy Storage Materials for Compressed Air Energy Storage
Project Manager:	David G. DeCoursin
Organization:	FluiDyne Engineering Corporation 5900 Olson Memorial Highway Mineapolis, Minnesota 55422
Project Goals:	Determine the thermal, hydraulic and mechanical performance of beds of specified TES media. Measure and characterize comminution and particulate elutriation of these beds. Provide design data for full-scale beds at proposed Adiabatic CAES (ACAES) system design condition.
Project Status:	Major tasks completed to date include test facility design, hardware procurement, and component fabrication. Installation is in progress and will be completed in August 1981. Documentation completed and transmitted include the Preliminary Test Plan, the Quality Assurance Plan, and Monthly Progress Reports to date. The Facility checkout will be completed by October 1, 1981 and tests of two materials for 100 cycles each will be completed by February 1982.
Subcontract Number.	B-B5473-A-L
Prime Contract Number:	DE-AC06-76RLO 1830
Contract Period:	March 12, 1981 through March 12, 1982
Funding Level:	$250,000
Funding Source:	U.S. Department of Energy

THERMOMECHANICAL SCREENING OF THERMAL ENERGY STORAGE MATERIALS FOR COMPRESSED AIR ENERGY STORAGE

Lynn Marksberry
FluiDyne Eningeering Corporation
Minneapolis, Minnesota

SUMMARY

A facility has been designed and is being assembled to perform thermomechanical screening of TES bed materials for Compressed Air Energy Storage (CAES) power plants. Candidate storage media will be thermally cycled between 100 and 900 F to determine the effect of thermal racheting on degradation of the storage media and on performance of the beds. These data will provide a basis on which to select media and design the thermal store for commercial plants.

INTRODUCTION

Thermal energy storage is required for adiabatic and hybrid CAES. The method of storage will be sensible heat in large pebble beds. Thermal store configuration and operating requirements are described in Refs. 1, 2 and 3. The most severe operating conditions involve daily cycling between approximately 311 K (100 F) and 756 K (900 F) at high pressure, about 8.3 MPa (1200 psi). Under these conditions, the storage media (pebbles) will be subjected to thermomechanical and thermochemical effects which could degrade performance of the bed and create dust which could erode the turbine blades.

Thermomechanical effects are caused by the dead weight loads on the pebbles (bed heights to 19.8 m (65 ft) are being considered) and by the stresses created by alternate expansion and contraction of the bed during each thermal cycle. Pebbles are especially prone to dusting and breakage under such conditions because of the point-to-point contact. Small dust particles that are elutriated from the bed may cause erosion of the turbine. Large particles from fracture of pebbles will tend to plug regions of the bed and thereby reduce its overall performance as a heat exchanger.

Thermochemical effects are caused by condensation of water vapor in the bed. The condensate will be acidic and may corrode the pebbles (whether metal or ceramic). Corrosion could lead to dusting of the corrosion film (e.g., rust on metal balls) or a reduction in strength and subsequent breakage.

Cost and life are important considerations in the selection of the storage media (i.e., material configuration, and properties). System studies (Refs. 1,2, and 3) have identified media with costs ranging from roughly \$9.11/Mton (\$10/ton to over \$9.11 Mton (\$1000/ton). PNL has established a program of screening tests to evaluate various storage media with the ultimate objective of identifying one or more low cost materials with satisfactory performance. The thermomechanical tests are being done by FluiDyne; the thermochemical tests are being done by PNL.

STORAGE MEDIA

The lowest cost pebble bed material is on-site rock waste from excavating the CAES and TES caverns. The first problem with rock waste is its highly irregular shape and jagged edges. The irregular shapes result in a high flow resistance packing. The jagged edges will be prone to fracture and the generation of particulates. The second problem is variability in mineral constituency of rock, giving anisotropic properties which could lead to excessive fracturing of the media.

On site rock waste could be improved by tumbling, washing, and screening operations which would add to cost. An alternative is naturally occurring rock having a more favorable shape such as stream pebbles and perhaps having better composition.

The next level with respect to cost is the use of "fired" materials which provide a uniform quality and spherical shape. The lowest cost candidate is iron ore pellets used as feedstock for the steel industry. The cost is \$44-55 per Mton (\$40-\$50 per ton) point-of-origin, and CAES-TES quantities are miniscule in comparison to annual production rates. A small operation produces 1 million tons per year and a single large plant in the Minnesota iron range produces over 15 million tons per year, compared with 45,000 Mton (50,000 tons) required for a 1000 MW CAES plant. The information on Fig. 1 (Ref. 3) shows that iron ore pellets are available throughout the U.S. They are produced to fairly uniform properties with frequent quality control.

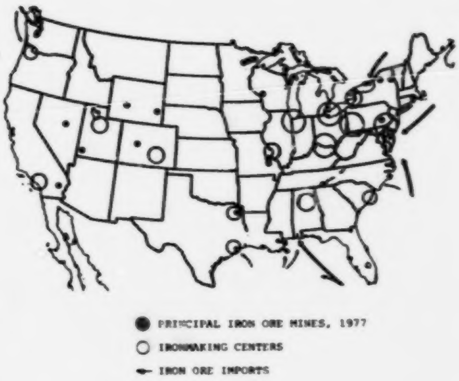

FIG. 1 SOURCE OF IRON ORE
Ref. Iron Ore - Mineral Commodity Profiles
MCP-3 May 1978 USDI

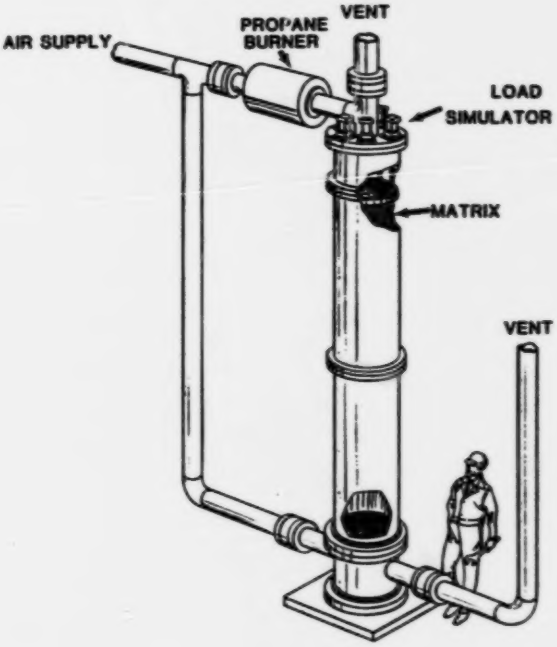

FIG. 2 SKETCH OF HEATER

A higher cost option is fireclay pellets such as Denstone (produced by the Norton Refractories Company). In contrast to iron ore, they are produced in small quanties as compared with CAES needs. This offers the opportunity for tailoring the properties to the specific needs of CAES.

Better quality fired pellets are available at higher cost. The cost increases rapidly with improvement of the shape and the thermomechanical properties.

The use of metal balls has also been studied. The cost is comparable to the high quality ceramic spheres mentioned above. The higher cost is, in part, offset the properties differences between metals and ceramics. Metals are superior in energy storage density, resistant to fracture, and more closely match the thermal expansion of the containment vessel. They are, however, subject to corrosion. Cast iron balls produced for grinding media are being considered.

Current plans are to test Denstone and iron ore pellets first, then cast iron and rock (types and shapes not yet defined).

TEST FACILITY

The test facility has been designed to simulate the most critical features of full-scale operation; these are the temperaturing cycling conditions and dead weight load. Budgetary restrictions imposed two limits: operation at atmospheric pressure and reduced bed size. Operation at full pressure is not needed to create the thermomechanical conditions and therefore this restriction is not significant. However, simulation of dead weight is critical and therefore, a method of loading the bed will be used.

The heater vessel is shown in Fig. 2 and a process schematic is shown in Fig. 3. The vessel is 0.91 m (3 ft) diameter and 6.1 m (20 ft) high. It is designed to accommodate a 4.6 m (15 ft) high test matrix. An upper and lower grate-and-screen assembly enclose the test matrix. The upper grate is connected to a hydraulically driven load simulator that is designed to exert up to 454 KN (100,000 lbf) at the top of the matrix in order to simulate the full-scale dead weight load.

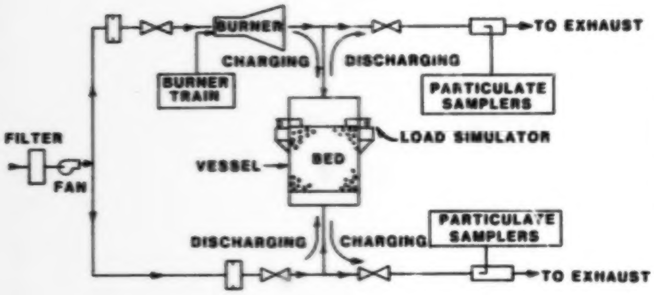

FIG. 3 PROCESS SCHEMATIC

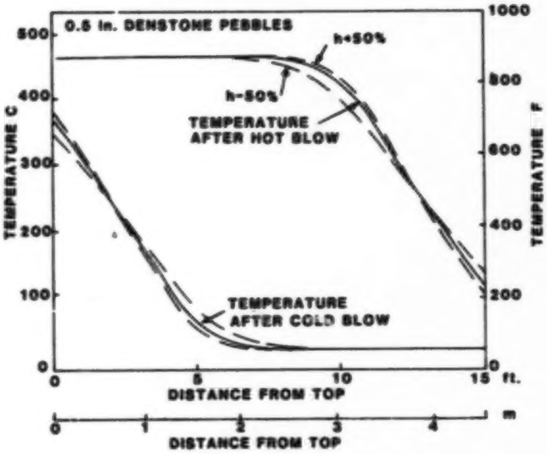

FIG. 4 TEMPERATURE WAVE - DENSTONE

The vessel is instrumented at approximately 30 cm (1 ft) intervals with pebble temperature, fluid temperature and fluid pressure sensors. Velocity distribution across the top of the bed will measured to determine uniformity and detect bypass flow. These measurements will provide the thermal and hydraulic matrix performance data.

Strain gages and vessel wall temperature sensors are placed on the vessel circumference on approximately the mid-point of the vessel. This instrumentation has been selected to detect any manifestation of the racheting phenomena. A hot wall containment design concept is simulated in that the test vessel is externally insulated.

Air is drawn into the system through a fabric filter by a fan. During the charging cycle, air flows through a flow metering station and a temperature controlled burner. The hot air 756 K (900 F) enters the upper plenum and flows down through the matrix to the lower plenum and out a discharge line. During the discharge cycle, the filtered cool air goes through a flow metering station to the lower vessel plenum. The air flows upward through the plenum and out a discharge line. Cycling time will be approximately 4 hours. Continuous operation is planned with operators in attendance only during the day shift, five days per week. Preliminary calculations of the temperature wave for test beds of the primary candidates (Denstone, iron ore, cast iron) are presented in Figs. 4 through 6. Note in Fig. 5 the small effect of a 50% change in heat transfer coefficient.

Flow data is required for the heat and mass balance and to establish the hydraulic condition of the matrix. Particulate measurements will be made at two sampling stations on each of the discharge lines. One station will provide a time averaged rate by periodically weighing accumulation on a filter. The other will provide size distribution by classifying the particulate in four size ranges. Relative bed motion will be obtained by a position indicator on the hydraulic rams.

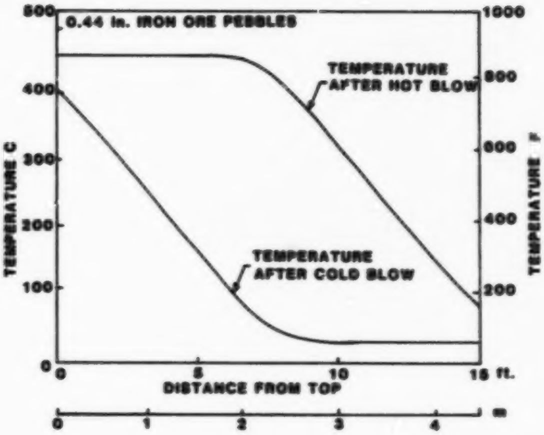

FIG. 5 TEMPERATURE WAVE - IRON ORE

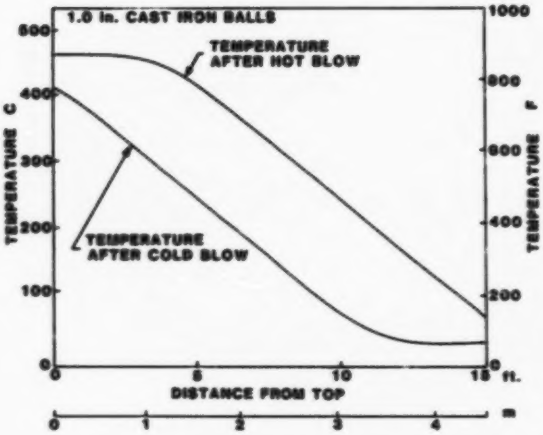

FIG. 6 TEMPERATURE WAVE - CAST IRON

Ancillary equipment including fans, fabric filter, exhaust stack, and controls are available from a concurrent Department of Energy test program concerned with development of high temperature air heaters for the MHD power cycle. These items will be shared between the two programs. Much of the instrumentation, all of the computer based data acquisition system, and the support facilities are provided by FluiDyne. This equipment is used to support MHD testing, three fired fluidized bed combustors, emission test rigs, and extensive aerodynamic test facilities (see Figure 7).

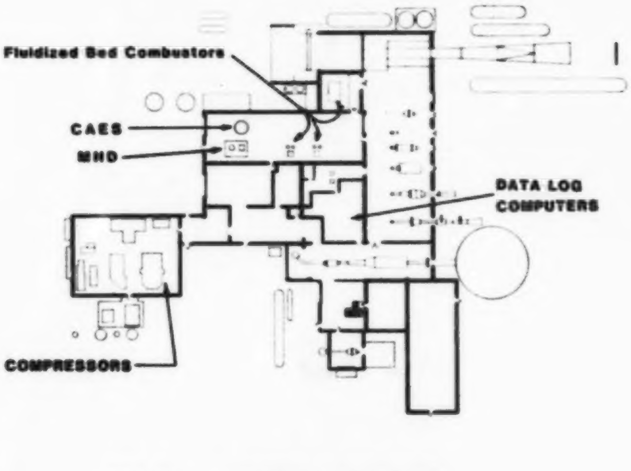

FIG 7. FLUIDYNE LABORATORY

Each batch of pebbles will be inspected and certain measurements will be made before and after the thermal cycling tests. Visual inspection and bulk density measurements will indicate the degree and type of pebble breakage. Two tests used for quality control purposes in the production of iron ore pellets will be made to give a relative ranking of the different materials and the effect of thermal cycling. These tests are ASTM E-279 Tumble Test and ASTM E-382 Compression Strength test. In addition, cold flow pressure gradient measurements of each bed will be made before and after thermal cycling. These various data will reveal changes caused by thermal cycling and will contribute to relative ranking of the materials.

A summary of the degree of full-scale simulation provided by the test facility is given in the following table.

Property Factor	Simulation
Strength	Yes
Hardness	Yes
Shape	Yes
Press/Depress	No
Corrosion	No
Temperature Factor	
Temperature Change	Yes
Temperature Gradient	Yes
Number of Heat/Cool Cycles	Yes
Containment Expansion*	Yes
Thermal Stress	Yes
Containment Factor	
Bed Height	Yes
Bed Diameter	No
Wall Smoothness*	Yes
Wall Particulates*	Yes

*For metal containment

The major factor that is not simulated is corrosion. Work on corrosion is being done at PNL.

PROJECT STATUS

The project is on schedule and installation will be completed early August 1981. This will be followed by shakedown and the first test (Denstone) is expected to begin about October 1, 1981. The Denstone material is on hand and iron ore pellets have been ordered. Tests of these two materials should be completed by the end of the year.

REFERENCES

1. Conceptual Design and Engineering Studies of Adiabatic CAES with Thermal Energy Storage, Final Report, Subcontract No. B-82284-A-E, Contract No. E4-76-C-06-1830, U.S. Department of Energy through Battelle Pacific Northwest Laboratory, Acres American Incorporated, Contractor

2. I. Glendenning, P.E. Chew, R. Grand, R. Glanviyle, Matt. Moye, Technical and Economic Assessment of Advanced Compressed Air Storage (ACAS) Concepts, Final Report, EPRI EM-1289, Project 1081-1, Funded by Electric Power Research Institute, Central Electricity Generating Board, Contractor

3. Preliminary Design and Cost ACAS A-5 Hybrid, Final Review Meeting, December 1980, United Engineers and Constructors, Contractor

4. F.L. Klinger, Iron Ore - Mineral Commodity Profiles, MCP-13, May 1978, Bureau of Mines, Unites States Department of the Interior.

ACKNOWLEDGEMENT

This work was supported by the U.S. Department of Energy under Subcontract B-B5473-A-L, through Pacific Northwest Laboratory, operated for DOE by Battelle Memorial Institute. In addition, major test facility components procured under DOE Contract No. DE-AC01-80ET15602 are being made available for use on this project.

PROJECT SUMMARY

Project Title:	Economic Assessment Support for the Compressed Air Energy Storage Program
Principal Investigator:	Raymond W. Reilly
Organization:	Compressed Air Energy Storage (CAES Program, Pacific Northwest Laboratory, Richland, Washington 99352 (509) 376-4359
Project Goals (FY81):	Provide a comparative economic analysis of Second Generation CAES technologies. Investigate the feasibility of conducting a CAES reliability study that includes reliability estimates for the compressed air storage medium.
Project Status:	The economic performances of second generation CAES technologies (CAES coupled to fluidized bed combustors, to coal gasification units, and to thermal energy storage devices) were compared to conventional CAES and to gas turbines during FY81. The input data were taken from A&E design estimates. Designs were normalized to the same technical and economic assumptions, and busbar estimates were prepared for each technology. The results were integrated into a comparative report on the second generation technologies produced by the Program Office. A literature search was conducted and specialists in underground construction were contacted to determine the availability of reliability data for CAES storage media. The information was also characterized and a modeling approach was recommended. The final report on this investigation is now being prepared.
Contract Number:	DE-AC06-76RLO 1830
Contract Period:	Continuing
Funding Level:	$40,000
Funding Source:	U.S. Department of Energy

ECONOMIC ASSESSMENT COMPRESSED AIR ENERGY STORAGE (CAES) SYSTEMS

R. W. Reilly/D. R. Brown
Compressed Air Energy Storage Technology Program
Pacific Northwest Laboratory
P.O. Box 999
Richland, Washington 99352
(509) 376-4359; FTS: 444-4359

I. ABSTRACT

This paper describes the economic assessment program undertaken in support of the Compressed Air Energy Storage (CAES) Technology Program during FY81. The work was performed at Pacific Northwest Laboratory for the U.S. Department of Energy. The effort comprised two major activities: 1) a comparative economic analysis of second generation CAES technologies, and 2) a low-level study of the feasibility of conducting a CAES reliability investigation. The final reports from both efforts are now in preparation.

II. COMPARATIVE ECONOMIC ANALYSIS

INTRODUCTION

The intent of the economic comparisons was to identify the second generation CAES technologies that have the greatest potential for cost-effective energy storage and that should be pursued further. The technologies under evaluation include CAES coupled to fluidized bed combustors, coal gasification units, and thermal storage devices. Comparisons are also made against conventional CAES, Underground Pumped Hydro, and oil-fired technologies.

The economic analysis is composed of two parts: 1) development of comparable cost estimates for the technologies, and 2) estimation of the cost of producing (storing) electricity from these technologies. Comparisons are made under a range of financial and utilization scenarios. All technologies are assumed to be of the same maturity and reliability, although only conventional CAES is a demonstrated technology.

CAPITAL COST ESTIMATES

General Approach

The best cost/performance data for economic comparison of these technologies exist in A&E design efforts developed for EPRI, DOE, and individual utilities. However, direct comparison of CAES technologies using the results of these studies is difficult, since they were based upon different economic and site assumptions. This comparison normalizes each of the design studies to a common set of cost and design assumptions, thus enabling economic comparisons between them under a consistent set of financial assumptions.

During the normalization process, the basic engineering design developed by the A&E firm was not altered, so as to minimize the introduction of error. Rather, the balance-of-plant items (such as land cost, switchyard size, and cooling systems) were standardized, ensuring that the economic comparisons reflect differences in the technologies, rather than differences in the cost of ancillary systems.

The PEPCO conventional CAES design was selected as the standard for normalizing the balance-of-plant estimates. It had been the basis for the CAES/FBC and adiabatic CAES balance of plant estimates (in the source documents), and the same design assumptions had been used for the UPHS study.

Normalization Procedure

The major components of the normalization procedure are outlined below:

1. All cost estimates were converted to midyear 1979 price levels.

2. All labor and supply costs were normalized to a site on the northeast coast of the U.S.

3. All turbomachinery costs in the design studies were converted to single-plant cost estimates. In the FBC study the low pressure turbomachinery cost estimate was based upon a production run of 50.

UTRC provided a cost estimate based upon an equivalent situation for this normalization study. This adjustment added $60 million to the CAES/FBC plant cost estimate contained in the original document.

4. The MSS Mississippi plant designs, based upon out-of-doors turbomachinery, were adjusted to include costs for turbomachinery buildings, based upon the costs found in the PEPCO conventional CAES design.

5. Switchyards were normalized to breaker-and-a-half designs based upon costs supplied by the Bonneville Power Administration. The number of transmission lines servicing the plants was adjusted according to plant size. One line was assumed intercepted for the 220 MW_e hybrid and conventional plants and two lines for the remainder of the 800-1000 MW_e installations.

6. All cooling cost estimates were normalized (on a $\$/kW_t$-rejected basis) to wet cooling, using mechanical draft wet cooling towers.

7. All optional cost items unique to a particular design study were eliminated from the cost estimates.

8. The hybrid cost estimate was adjusted to include two TES filter systems and a TES bypass (cost information provided by UE&C). The adiabatic CAES plant design includes filter systems, but not a TES bypass.

9. After the direct cost estimates were made, indirect costs were applied to all of the estimates on a consistent basis. Fifteen percent of direct cost was allowed for the Architect/Engineer and construction management fee. Contingency was applied on a differential basis to reflect the relative uncertainties: 15% of direct cost was allowed for turbomachinery, cavern construction, thermal energy storage, fluidized bed combustors and coal gasification units; 5% was allowed for the remainder of the capital cost estimate, including land, switchyard, and balance of plant items.

10. Interest during construction (IDC) and escalation during construction (EDC) were included in the estimation of busbar cost. The assumption made is that the cost-payout curve is S-shaped, skewed towards the end of construction, with half of total cash flow at 60% of construction period.

Normalized Capital Cost Estimates

The capital cost estimates that resulted from the normalization process are listed in Table 1. Information on the oil-fired combustion turbine and combined cycle plants was taken from the EPRI Technical Assessment Guide (1979). The cost and performance specifications are for advanced units expected to be available in 1985.

As indicated by the table, the MSS Conventional CAES design is estimated to cost almost exactly the same amount as the PEPCO conventional CAES design on a per-kilowatt basis, despite the fact that they are different sizes (220 MW_e vs. 924 MW_e). This equivalence exists because the MSS cavern is formed by solution mining in a salt deposit, whereas the PEPCO cavern is formed by more expensive hard-rock mining. This advantage in cavern cost appears to compensate for the economies of scale garnered by the PEPCO plant. Since the two plants have much the same cost, Electric Energy Ratio (EER), and Fuel Heat Rate, the PEPCO design serves as the Conventional CAES concept for the balance of the analysis.

BUSBAR COST ESTIMATES

Methodology for Comparative Analysis

The economic performance of the normalized plant designs was compared using the levelizing methodology presented in the (EPRI) Technical Assessment Guide (1979). Life-cycle costs were determined for a set of base-case economic assumptions, and then some of these assumptions were varied to investigate the relative busbar costs under alternative scenarios. All busbar estimates were made over a range of capacity factors (0.075-0.250). Two compression energy costs (10 mills/kWh and 25 mills/kWh) were selected to investigate the effect of variation in charging cost.

Technical Parameters and the Cost of Operation

The technical parameters (heat rate, EER, storage capacity, etc.) and operating costs for the technologies are included in Table 2.

TABLE 1: CAPITAL COST SUMMARY FOR CAES TECHNOLOGIES
($1,000,000 at July 1979 Price Levels)

	PEPCO Conv	MSS Conv	Adiabatic	Hybrid	FBC
Land Purchase, Site Preparation and Construction Facilities	10.4	3.5	10.4	3.5	8.3
Generation/Compression	172.3	41.4	196.5	43.2	173.8
Compressed Air Storage	51.1	9.6	50.1	15.1	58.3
Thermal Energy Storage	-0-	-0-	52.8	19.6	-0-
Air Reheat Equipment	4.0	1.2	-0-	1.1	196.5
Electric Plant Equipment	50.0	10.8	49.9	10.8	42.0
General Plant Facilities	34.1	10.1	24.4	9.0	36.1
TOTAL DIRECT COSTS	321.9	76.6	384.1	102.3	515.0
Contingency	38.4	8.9	49.1	11.5	68.6
A/E and Construction Management	48.3	11.5	57.6	15.3	77.2
TOTAL INDIRECT COST	86.7	20.4	106.8	26.8	145.8
TOTAL CAPITAL COST (less EDC and IDC)	408.6	97.0	490.9	129.2	660.8
$/kW	443	441	614	587	742

NOTE: Detailed cost breakdowns have not been developed for CAES/CG.

TABLE 2: SYSTEM DESCRIPTIONS

	Conv	Adiab	Hybrid	FBC	CG	UPHS	Combustion Turbine	Oil-Fired Combined Cycle
Capital Cost ($/kW)	443	614	587	742	654	706	254	390
Construction Time (yr)	5	6.25	5.5	7.75	6.25	8	1	2
Power Output (MW_e)	924	800	220	891.2	862.2	1000	200	600
Storage (hours)	8.3	8.3	8	8.8	8.8	10	---	---
Fuel Heat Rate (Btu/kWh)	4250	-0-	2660	4437	4500	-0-	10,300	7,300
EER (kWh-in/kWh-out)	0.75	1.48	1.038	0.897	0.739	1.32	-0-	-0-
Fixed O&M ($1,000,000/yr)	3.47	2.91	0.43	7.0	13.0	3.0	0.05	2.8
Variable O&M (mills/kWh)	0.25	0.25	0.6	3.0	4.8	-0-	2.84	1.16
Life (years)	30	30	30	30	30	50	30	30

Base-Case Results

The assumptions employed in the base case are listed in Table 3. The results of the base-case analysis are depicted in Figure 1 (comparison of the CAES technologies), Figure 2 (comparison against oil-fired combined cycle and combustion turbine plants), and Figure 3 (a 50-year comparison against UPHS).

The base case represents a situation where fuel oil costs escalate at only a moderate rate (8%/yr) with respect to coal (7%) and compression energy (7%) costs. The results in Figure 1 indicate that, in general, adiabatic CAES generates lowest cost power at the low charging energy cost, whereas conventional

TABLE 3: BASE CASE ASSUMPTIONS

PARAMETER	VALUE	UNITS	PARAMETER	VALUE	UNITS
Discount Rate	10	%/yr	Energy Prices		
Fixed Charge Rate	18	%/yr	(July 1979 price level)		
Inflation Rate	6	%/yr	Fuel Oil	5.24	$/MBtu
Escalation Rates			Coal	1.86	$/MBtu
Fuel Oil	8	%/yr	Compression Energy	10, 25	mills/kWh
Coal	7	%/yr			
Compression Energy	7	%/yr	System Lifetime	30	years
Construction	6	%/yr	Start Plant Operation	1990	
O&M	6	%/yr			
			Base Year for Cost Estimates	July 1979	

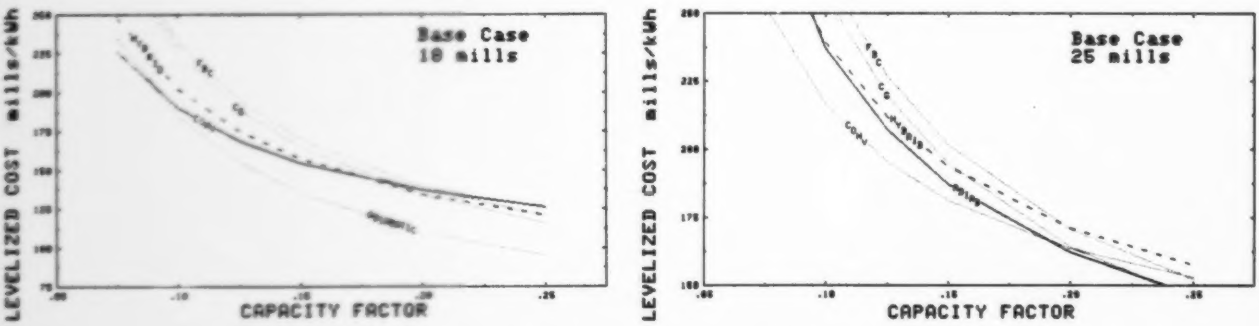

Figure 1. Comparison Under Base Case Conditions

CAES is least expensive at high charging energy costs. The other CAES concepts (hybrid, CAES/FBC, and CAES/CG) become competitive only at the high capacity factors for the high compression energy cost situation.

In Figure 2 conventional and adiabatic CAES are compared against oil-burning peaking (combustion turbine) and intermediate load (combined cycle) technologies. At the low compression energy cost, the CAES technologies are distinctly less expensive than the oil-fired units. At the high compression energy cost, CAES technologies are more economic than the combustion turbine, but the oil-fired combined cycle plant generates less costly energy than either of the CAES technologies.

In Figure 3, the two CAES Units are compared against a 1000 MW_e underground pumped hydro storage plant. Since the UPHS plant has an expected lifetime of 50 years, the levelized costs of both conventional and adiabatic CAES were recalculated based upon that same lifetime. The turbomachinery for both plants and the TES fill were assumed to be replaced after 25 years of operation. At 10 mills/kWh charging cost, UPHS is slightly more economic than adiabatic CAES, and considerably more economic than conventional CAES. At the higher 25 mills/kWh charging cost, UPHS has a greater advantage over adiabatic CAES (due to its lower EER), but conventional CAES has become more competitive, even becoming the least expensive of the three at low capacity factors.

If we were to compare economic performance at the 2000 MW_e plant size, the relationships between the three technologies would shift dramatically. Neither adiabatic CAES nor conventional CAES would gain significant economies of scale by doubling plant size, whereas the per-kilowatt capital cost of UPHS would decrease by about 23%.

High Oil-Price Escalation Rate

If we assume all of the original base-case parameters, but escalate fuel oil prices at 10% per year (3% over coal and compression energy), then adiabatic CAES is most cost-effective under almost all circumstances investigated (see Figure 4). At the low compression energy cost adiabatic CAES is considerably more economic than the other CAES technologies and the oil-fired generation plants. At the higher

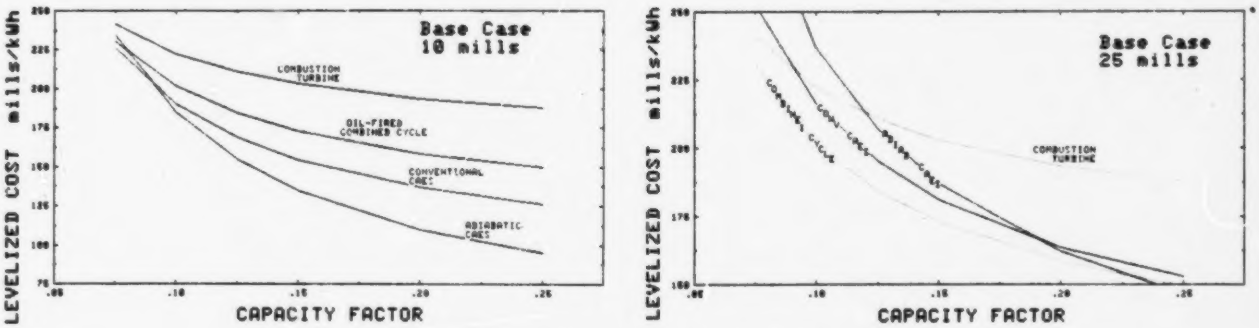

Figure 2. Comparison Under Base Case Conditions

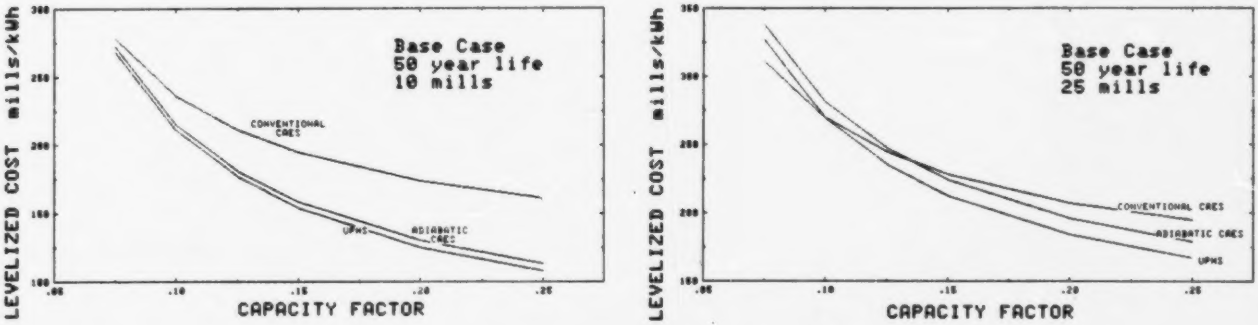

Figure 3. Comparison Under Base Case Conditions

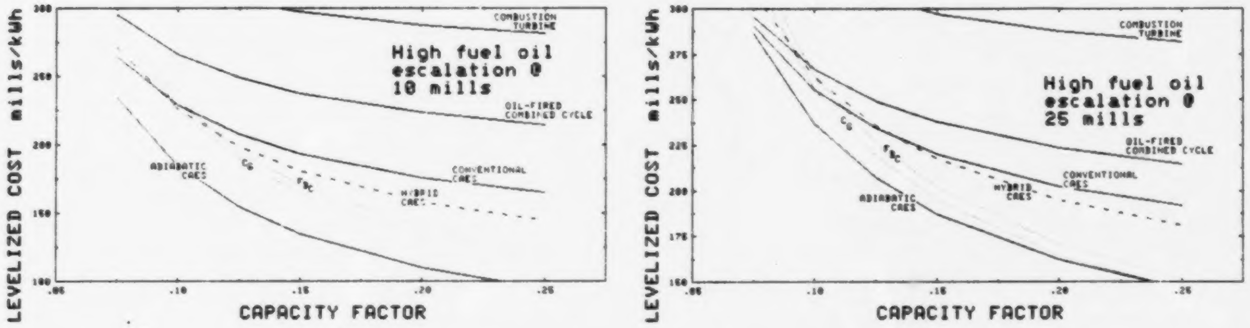

Figure 4. Comparison Under High Fuel Oil Escalation Rate

compression energy cost, coal gasification and fluidized bed combustion approach the economic performance of adiabatic CAES. The relationship between adiabatic CAES and UPHS remains unchanged from the base case, since neither of them burn fuel oil.

Municipal Financing

The cost of capital and fixed charge rate employed in the analysis thus far are those suggested by EPRI in the Technical Assessment Guide (1979) for analysis of future generation technologies. These rates represent a typical financial structure for a private utility. The effect of a municipal utility financing structure on the economic performance of the CAES technologies is assessed in Figure 5. The cost of capital is 8% and the fixed charge rate is 12%; all other assumptions are the same as in the base case. Such an assumption favors the more highly capital intensive technologies, and this effect

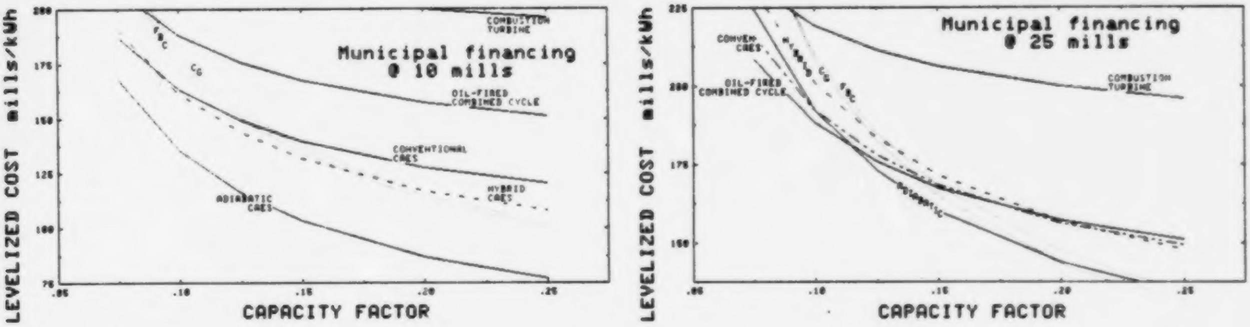

Figure 5. Comparison Under Municipal Financing

is evident in the results. At the low compression energy cost adiabatic CAES exhibits considerable advantage over its closes competitors; at the higher compression energy cost, adiabatic CAES maintains a small advantage over its competitors, except below about 12% capacity factor, where the oil-fired combined cycle plant is least expensive.

DISCUSSION

In the brief analyses developed here, it appears that adiabatic CAES has the greatest potential for cost-effective energy storage. Adiabatic CAES is the most cost effective CAES technology in:

- most situations at low compression energy costs
- high compression energy cost with high fuel-oil price escalation
- high compression energy cost with municipal financing.

The only situation in which another CAES technology appears to be more cost effective is under the assumptions of minimal fuel oil price escalation and high compression energy cost. In this situation conventional CAES proves more economic than adiabatic CAES, but oil-fired combined cycle is more cost effective than all of the CAES technologies.

The economic comparisons made in this paper are based upon two important assumptions. The first is that the CAES technologies would be used in the same manner by a utility system, which will generally not be the case. Because of system restrictions on availability of charging power, some CAES technologies would be used more intensively than others. The conventional CAES plant (with an EER of only 0.75) could be used to a significantly larger degree than the adiabatic CAES plant (with its EER of 1.48). And, because of this greater utilization, the per-kWh cost of operation to the utility may be greater with adiabatic CAES than with conventional CAES, despite the fact that adiabatic appears less expensive to operate in these comparisons.

The second assumption is that the cost/performance information employed in this paper is equally good for all of the technologies. Conventional CAES is the only demonstrated CAES technology, and the cost estimates prepared for it should be very good. The hybrid and adiabatic CAES technologies have equally detailed cost information, but these technologies are unproven, and it is possible that cost estimates understate the capital investment necessary for a working system. CAES/FBC and CAES/CG are only rough cost estimates, and there is a greater probability that the capital cost estimates are inaccurate.

III. CAES RELIABILITY INVESTIGATION

During FY81 a small-scale study was made into the feasibility of performing a CAES reliability investigation. The investigation comprised three sections: 1) recommendations for model development, 2) evaluation of reliability data availability for above ground components, and 3) evaluation of data availability for below-ground structures and equipment.

The results of the investigation indicate that a Markov model should be developed that has the capability to: 1) model CAES systems with multiple compression/generation units, 2) model fractional loss of capacity, 3) model daily and weekly cycles, 4) model operation under a variety of demand curves, and 5) monitor the amount of energy stored in the cavern.

The investigation into above ground equipment reliability data indicates that usable data are available, but they need to be modified to reflect differences in environment and duty cycle.

The investigation into below-ground reliability data found a dearth of centralized cavern reliability data. Reliability data is available on a case by case basis from some similar industries, but collection and integration of the data would be costly.

REFERENCES

Hybrid CAES	Preliminary Engineering Design Cost of Advanced Compressed Air Storage (ACAS) A-5 Hybrid, United Engineers and Constructors, January 1981.
Adiabatic CAES	Conceptual Design and Engineering Studies of Adiabatic CAES with Thermal Energy Storage, ACRES American Incorporated, March 1981.
Fluidized-Bed Combustion/CAES	Technical and Economic Assessment of Fluidized Bed Augmented Compressed Air Energy Storage, United Technologies Research Center, January 1980.
Coal Gasification CAES	Concept Screening of Coal Gasification Systems, United Technologies Research Center, May 1979.
Oil-Fired Combustion Turbines	Technical Assessment Guide, Electric Power Research Institute, July 1979.
Underground Pumped Hydro Storage	Preliminary Design Study of Underground Pumped Hydro and Compressed Air Energy Storage in Hard Rock, Volume XI Plant Design - UPH, Acres American Incorporated, July 1980.
Conventional CAES	Preliminary Design Study of Underground Pumped Hydro and Compressed Air Energy Storage in Hard Rock, Volume XII Plant Design - CAES, Acres American Incorporated, June 1980.
	Preliminary Engineering Design and Cost of Advanced Compressed Air Storage (ACAS) A-5 Hybrid, United Engineers and Constructors, January 1981.

PROJECT SUMMARY

Project Title:	Reservoir Stability Studies
Principal Investigator:	T. J. Doherty
Organization:	Pacific Northwest Laboratory PO Box 999 Richland, Washington 99352 Phone: (509) 375-6161, x 320
Project Goals:	Develop criteria for long term stability of underground compressed air energy storage (CAES) reservoirs for utility applications through literature, numerical, experimental and field studies as required.
Project Status:	Preliminary stability criteria were completed and used as a basis for initiation of numerical and experimental studies to address CAES specific needs. Reservoir types examined included compensated hard rock, solution-mined salt caverns, and anticlinal porous media structures. Numerical model development and generic experimental work were carried to completion by FY-1981. These studies identified specific experimental needs including in-mine evaluations of salt cyclic response, and a site specific geotechnical design evaluation for a hard rock cavern. Porous media studies identified the need for combined effects laboratory studies and a field test involving air injection into an aquifer structure. Salt reservoir study this year included coordinated laboratory and in-mine evaluations of salt response to cyclic loading directed to finalization of salt stability criteria in early FY-1982. Hard rock cavern response prediction methods were corroborated by an applied numerical and experimental evaluation of the Potomac Electric Power Company (PEPCO) demonstration project geotechnical design and site materials. The porous media segment of the program completed design and construction of the porous media flow facility, initiated numerical and experimental operations and integrated it into a support function for the field activities initiated during FY-1980. The aquifer field test completed its exploration, leasing and permitting phases, and a construction and operations contractor was selected and the major field study contract placed. Construction of the field test surface facilities and major procurements have been initiated. The injection withdrawal well is installed and completed and drilling and subsurface instrumentation activities are continuing. Air injection is scheduled for mid FY-1982.
Contract Number:	DE-AC06-76RLO 1830
Contract Period:	October 1980 to September 1981
Funding Level:	$1,722,000
Funding Source:	U.S. Department of Energy

RESERVOIR STABILITY STUDIES

T. J. Doherty
Pacific Northwest Laboratory*
Richland, Washington 99352

ABSTRACT

The objective of the reservoir stability studies project is to develop stability criteria for large underground reservoirs in salt domes, hard rock caverns, and porous rock structures for air storage in utility applications. Because reservoir stability was deemed crucial to commercialization of compressed air energy storage (CAES) systems this project has received major emphasis in the early phases of the overall CAES program. A long term plan, including state-of-the-art assessment, numerical model development and experimental studies culminating in field research, as necessary, was formulated. This plan, initiated in 1977, has been completed during FY-1981 to the stage of specific experimental studies and field research.

Activities within this project during FY-1981 have included completion of site specific geotechnical design evaluations using methodologies developed to assess hard rock cavern stability, implementation of in-mine research to evaluate numerical and laboratory study conclusions on the response of domal salt, and preparation of integrated laboratory and field study facilities to assess developed predictive methods and determine in situ response of a porous media reservoir to air injection. The major activity in the project has been the field study component of the porous media studies. Accomplishments there have included completion of exploration, permitting and leasing, operation contractor selection and negotiation, and initiation of procurement and construction for an FY-1982 test initiation. A major program milestone, drilling of the injection withdrawal well for this test, was completed ahead of schedule.

INTRODUCTION

The unique aspect of the compressed air energy storage concept is the use of subsurface geology as an economical large-scale pressurized air storage element. For a nominal design, air at pressures between 4 MPa (40 bar) and 8 MPa (80 bar) is stored in the underground reservoirs and cycled on a daily basis. Three broad classes of rock have been identified as candidate hosts for CAES reservoirs: hard rock, porous rock, and salt.

The type of host rock is an important factor in the choice of modes for CAES operation. Excavation costs in hard rock dictate that CAES operations utilize a compensated storage system. Operation of a compensated system requires relatively low storage temperatures (less than $\sim100^{\circ}C$) to avoid boiling and large vapor plumes when warm water reaches the surface. Basic concerns for compensated hard rock caverns center on the rock mechanics aspects of cavern shape and layout, air leakage and the response of the rock surfaces to cyclic loadings and wetting-drying.

Storage in salt (primarily domal) can be either compensated or uncompensated, although uncompensated is more acceptable because of brine storage problems at the surface and concerns about control of solution, precipitation and erosion of the salt. The only operational CAES peaking power plant, at Huntorf in West Germany, uses an uncompensated salt cavity. Compressed air energy storage in salt is also generally restricted to lower temperature, less than $80^{\circ}C$ at this point, because creep closure of the cavern is greatly accelerated at higher temperatures. Good operational experience to date at Huntorf insures feasibility of storage in solution-mined salt caverns. Differences between American and German domal salts and the mechanics of long term cyclic salt performance with respect to development of useful monitoring systems structure the research needs for domal salt reservoirs.

Compressed air energy storage in porous media operates in a damped, compensated mode. It is uncompensated for short cycle times, but the longer term approach to equilibrium with a specific discovery pressure in the storage system is a compensated response. No major structural problems have been identified with storage of air in porous media at less than $150^{\circ}C$. Storage of the heat of compression within the rock formation is being investigated for temperatures to $300^{\circ}C$ through numerical, experimental and field evaluations in order to utilize the formation for thermal energy storage. This could reduce fuel use in the cycle and positively affect system economics. Temperature and geochemical effects could restrict air storage temperatures to levels that would not allow sufficient energy recovery to be feasible. Establishment of the upper temperature limit for stable reservoir operation will determine the thermodynamic cycle efficiency and thus, the feasibility. Experience with storage of natural gas and oil in such underground reservoirs has accumulated for nearly 50 years. In most instances, this storage has involved seasonal cycling of gas and oil with low mass flow rates and at low temperatures relative to potential CAES reservoir operation. Compressed air energy storage reservoirs will be subjected to daily cycling of air with attendant temperature, pressure, and humidity fluctuations. The CAES reservoirs must remain stable and operational under these conditions over periods of 30 to 50 years. Thus, while previous gas storage experience is valuable, little data exist for specific CAES operating conditions.

---

*Operated for the U.S. Department of Energy by Battelle Memorial Institute under prime contract no. DE-AC06-76RLO 1830.

The resolution of the above issues could substantially improve the commercial viability of CAES. The Reservoir Stability Studies were established to resolve those issues.

PROJECT DESCRIPTION AND OBJECTIVES

The purpose of the Reservoir Stability Studies is to establish criteria for long-term stability of underground CAES reservoirs. These criteria are intended to be guidelines and reference sources that utilities and architect-engineering firms may use to evaluate reservoir stability at candidate CAES sites. The criteria are quantitative where possible, qualitative where necessary, and provide a focal point for CAES relevant geotechnical knowledge, whether developed through specific research or available from petroleum, mining or other geotechnical practices using rock materials.

Early in the program a plan was formulated for fulfilling the project purpose of establishing reservoir stability criteria. It was recognized that a significant amount of research would be required because of the unusual and unique operating conditions and rock behavior encountered in each type of CAES reservoir. The plan contained four major activities for CAES in each rock type.

- State-of-the-Art Survey: To establish preliminary reservoir stability criteria and identify areas requiring research and development.
- Numerical Modeling: To parametrically evaluate the response and stability of CAES reservoirs under a wide variety of CAES operating and geotechnical conditions. These results will be used to guide activities in other phases of the program.
- Laboratory Testing: To examine issues not presently amenable or appropriate to numerical modeling; provide data for use in numerical models; and investigate fundamental rock mechanics, thermal/fluid, and geochemical phenomena as appropriate to CAES.
- Field Studies: To corroborate numerical modeling and laboratory analyses in order to provide accurate estimates of reservoir response to CAES conditions; to examine geotechnical issues not amenable to evaluation with numerical modeling or laboratory testing; and to verify the existing reservoir stability criteria and amend them as necessary.

The sequence of carrying out the four elements of the plan is illustrated in Fig. 1. Three parallel activities, one each for domal salt, hard rock, and porous media were required to adequately address the three unique geological conditions. Work was initiated by state-of-the-art surveys, proceeding to numerical model development and application. Coordinated generic laboratory evaluations leading to specific experimental studies began during the numerical work. Preliminary stability criteria were assembled from state-of-the-art assessment and early study. These criteria are successively refined and completed throughout the process, and finalized at the culmination of the study sequence. The results from each level of study structure and focus following efforts and may identify the need for in situ validation of the criteria and the developed methodologies through a field study. This plan was designed to fulfill the purpose of the Reservoir Stability Studies and to interface with other CAES-related activities being carried on by the U.S. Department of Energy (DOE), Electric Power Research Institute (EPRI), and private concerns. Special efforts were made to schedule activities to coordinate with the DOE/EPRI and utility-sponsored CAES Demonstration Studies.

The project organization, as it has evolved based on the research needs, is indicated in Fig. 2. Based on the above described plan, study elements have been structured for each reservoir type. The fourth element is a field study of porous media, which is coordinated with and follows after the numerical and experimental studies within the porous media element. Hard rock and salt elements do not have formal field study elements as operational experience, budget constraints or the site specific nature of a field evaluation preclude them within the scope of research activity.

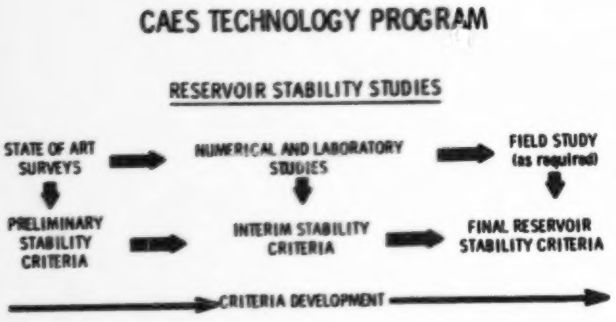
CAES TECHNOLOGY PROGRAM
RESERVOIR STABILITY STUDIES
STATE OF ART SURVEYS
NUMERICAL AND LABORATORY STUDIES
FIELD STUDY (as required)
PRELIMINARY STABILITY CRITERIA
INTERIM STABILITY CRITERIA
FINAL RESERVOIR STABILITY CRITERIA
CRITERIA DEVELOPMENT

Fig. 1. Reservoir Stability Plan of Action

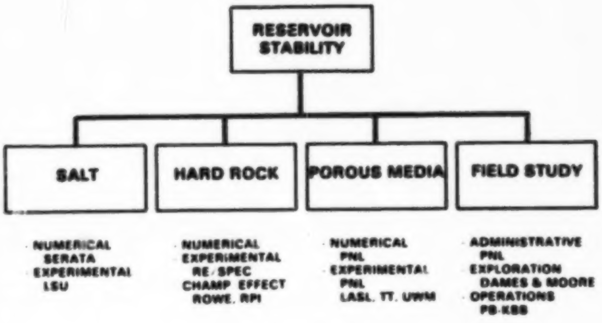
RESERVOIR STABILITY
SALT
HARD ROCK
POROUS MEDIA
FIELD STUDY
· NUMERICAL
SERATA
· EXPERIMENTAL
LSU
· NUMERICAL
· EXPERIMENTAL
RE/SPEC
CHAMP EFFECT
ROWE, RPI
· NUMERICAL
PNL
· EXPERIMENTAL
PNL
LASL, TT, UWM
· ADMINISTRATIVE
PNL
· EXPLORATION
DAMES & MOORE
· OPERATIONS
PB-KBB

Fig. 2. Reservoir Stability Project Structure

Table 1 lists the project elements and the participants who have contributed to the project to date.

Project accomplishments in prior years have included publication of preliminary stability criteria upon completion of the state-of-the-art element and completion of numerical model development activities and preliminary laboratory evaluation for all three reservoir types. Focused experimental studies in salt and the need for a porous media field study were identified based on this work.

This timely progress defined the specific objectives of the Reservoir Stability Studies for this reporting period, which were:

- Complete investigative numerical and laboratory studies in hard rock, porous rock, and salt and develop interim or final reservoir stability criteria for specific reservoir types as applicable
- Initiate integrated experimental and field studies of porous media to demonstrate proof of principle in situ and to validate reservoir stability criteria.

In association with the above objectives a major director-controlled milestone was established for the Reservoir Stability Studies. This milestone was for completion of drilling of the injection/withdrawal well for the porous media field study. It was selected to insure significant progress of the field study activity from the exploration and permitting phase to the construction and operation phase.

PROGRESS AND ACCOMPLISHMENTS

The three activity areas within the Reservoir Stability Project all made significant movement towards completion during FY-1981. All assigned tasks were completed essentially according to plan or are on schedule to that end. Brief summaries of work accomplished during this reporting period are outlined below, with topic areas defined by reservoir type.

Hard Rock Caverns

Major concerns related to compensated CAES in hard rock include 1) determination of rock properties and behavior under cyclic thermal, pore liquid saturation, and mechanical loading conditions, 2) determination of the effect of local rock failure on cavern stability, 3) evaluation of the relative value of rock structural improvement methods, and 4) determination of the impact of fracture networks on global air leakage. Studies to address these issues were completed this year with progress summarized below.

Re/Spec Inc. is the lead contractor in hard rock cavern studies. Their tasks during this fiscal year, after completion of all generic numerical and experimental studies, along with associated methodology development, were to carry out a confirmatory evaluation of the Acres American design for hard rock CAES caverns performed for Potomac Electric Power Company (PEPCO) under the demonstration programs. Revision and updating of the stability criteria are planned for completion by the end of the year.

TABLE 1. Reservoir Stability Studies Participants

Title	Contractor	Status
• Update of Preliminary Stability Criteria	PNL	On Schedule
Porous Media Studies		
• Numerical Studies of Porous Rock Reservoirs	PNL	On Schedule
• Laboratory Studies of Porous Media		
– Aquifer Field Test Support	PNL	On Schedule
– Porous Media Flow Facility	PNL	Operational
– Porous Rock Ventilation Studies	University Wisconsin-Milwaukee	Complete
– Thermomechanical Properties of Reservoir Rock	Los Alamos Scientific Laboratory	Complete
– Geochemical Response of Porous Media	Terra Tek	Complete
• Field Studies of Aquifer Reservoir		
– Legal, Regulatory, and PNL Support	PNL	On Schedule
– Site Acquisition and Qualification Contractors	(Many)	Complete
– Exploration Geological Control	Dames & Moore	Complete
– Design, Construction and Operation	PB-KBB	On Schedule
– Field Study Environmental Support	PNL/EV	On Schedule
Salt Studies		
• Numerical Studies of CAES Salt Caverns	Serata Geomechanics	Complete
• Laboratory and In Situ Studies of Domal Rock Salt	Louisiana St. Univ.	Late due to Jeff. Is. flooding
Hard Rock Studies		
• Numerical Studies of CAES Hard Rock Caverns	Re/Spec	Complete
• Laboratory Studies of Hard Rock	Re/Spec	Complete
• Champagne Effect Studies		
– Numerical	Rowe & Associates	On Schedule
– Laboratory	Rensselaer Polytechnic Institute	On Schedule

In the numerical studies, models were developed with capability to structurally characterize a rock mass and to simulate excavation processes and cyclic thermoelastic and pressure loading typical of CAES. They could also account for water compensation. It was found that multiple caverns could be located in competent rock at 750 m without cavern collapse. Substantial strength reductions due to local rock failure or thermal shock do not alter this conclusion. Air leakage was found to be affected by stress ratio but was predictable and insignificant for most conditions. A review of European experience supported these conclusions. The evaluation of the PEPCO design concluded that the shape, support system, and stability of the cavern will be sufficient for CAES operations, and the design results in favorable fatigue response.

Laboratory studies indicated that strength reductions can be expected in the tensile and compressive strength of rock masses subjected to a CAES cavern environment. The percentage loss of failure strength of the rock decreases with increasing mean stress, and most of the damage will be caused in the first few cycles, indicating that a rock mass would shake down quickly to stable behavior. It has also been demonstrated that foliated and/or jointed rock masses require special attention and assessment of strength requirements and strength values become quite site specific. The PEPCO Sykesville gneiss, a rock having highly anisotropic strength, was found to be stable under CAES conditions for the PEPCO design. Publication of finalized hard rock stability criteria will conclude the technical feasibility studies of hard rock caverns. The conclusion of these studies is that stable caverns for air storage can be excavated and utilized for air storage within the practice of good 'state of the art' geotechnical engineering.

Salt Cavern Reservoirs

Major concerns related to CAES in underground salt caverns include 1) evaluation of long-term salt response to cyclic mechanical and thermal loads, 2) resolution of the difference in the response of varying types of salt to CAES loadings, and 3) determination of the potential for surficial air penetration of the cavern wall.

Numerical modeling of salt was completed during the reporting period with validation of the numerical model. Elevated temperature and boundary deterioration due to air penetration were the critical parameters analyzed. The numerical work completed early this fiscal year included benchmark calibration for elevated temperature effects. The series of thermal and thermomechanical analyses evaluated cavern response, and response of the Louisiana State University in-mine slant borehole tests. Elevated temperature to 200°F were found to alter response but not significantly affect long-term stability. Air penetration was assessed as a local stability problem that would not affect general long-term stability. This numerical work related to salt caverns was completed although the recision plans reduced the total planned work load. Final reports have been prepared for publication.

Laboratory studies of salt response to CAES conditions included coordinated laboratory-scale and in-mine, bench-scale testing. Triaxial cyclic thermal and mechanical testing is being performed on salt specimens from several Louisiana salt mines, the Huntorf site in West Germany, and Kansas and Nevada bedded salt. Cyclic mechanical loading results in strain cycling that is very small in response to cyclic stress having a larger range, but much greater strain is exhibited during elevated temperature portions of thermal cycling. Acoustic emission patterns appear to trace cyclic strain very closely, showing potential as a technique for in-situ monitoring of salt cavern stability. Tests in boreholes in the floor of the Jefferson Island salt mine were initiated during FY-1980, but this facility was lost during a mine flooding accident early in FY-1981. Slant boreholes in pillars of the Cote Blanche mine were prepared for testing to replace the lost facility and are now operational. There was minimal impact on early FY-1982 completion of this task.

The draft of the salt reservoir stability criteria is undergoing final revision. Technical research activities related to criteria preparation will all be complete early in FY-1982. It is concluded that salt is a capable and proven geological medium for air storage.

Porous Media Studies and Field Study

Although natural gas has been stored in porous rock formations for more than 50 years, and the conditions required for natural gas storage are similar, CAES systems require daily cycling, as compared to annual cycling for natural gas. Further, air has at least twice the viscosity of natural gas, and air storage may have economic advantages if it can be stored at elevated temperatures within the porous matrix. These requirements outline the following concerns related to CAES porous media reservoir stability:

- low frequency fatigue caused by cyclic pressure, temperature, and humidity conditions on porous media and caprock
- reservoir material properties at nonambient conditions
- effects of reservoir morphology, anisotropy, and inhomogeneity
- response of wellbore casing and cementation materials
- wellbore desaturation and air-water interface movement
- the potential for geochemical reactions
- the generation and transport of fine particulate matter.

These concerns all relate to 1) the performance of CAES wells in aquifers over the range of operating and geophysical conditions, 2) the geochemical stability of typical CAES porous rock and caprock, and 3) the structural stability of porous rock and caprock.

A series of studies directed at addressing these concerns were formulated early in the program. These numerical and experimental studies resulted in quantification of and in many cases, resolution of these issues. However, many of the results of the work indicated a need for validation of the numerical and experimental methods in situ, through performance of a proof of principle field test. During the previous period a plan to perform this test was formulated and approved and a site located through a selection process. Also, at this time, all planned numerical model development was completed, generic and separate effects laboratory study finished.

Numerical work during this reporting period was limited to utilization of developed models to assist in planning and design of the field test based on the selected site data. Prediction of the performance of the air injection and cycling field test flow and thermal response is presently under way. Included are bubble development analyses, water coning assessments, thermal response determinations, and desaturation predictions.

Porous media laboratory studies eliminated several unknowns as major CAES concerns for aquifer storage. It was shown that porous rock exposed to CAES conditions remained a viable storage medium for long periods of time even at over 150°C. Although some increase in friability was observed for high-temperature humid-air atmospheres, lack of confinement limits the applicability of test results for CAES reservoirs. Exposure of numerous types of porous rock to dry air ventilation at modest temperatures and pressures showed little impact on rock properties. Structural testing of caprock materials at elevated temperatures pointed to strength increase with increasing temperature when some dessication was allowed, as near a wellbore. Data scatter was severe however and results, though positive, were inconclusive. These interim testing activities were completed early in the year, and all porous media field study experimental support activities were concentrated at PNL. A flow facility for porous rock desaturation and cyclic ventilation with moist air was designed and constructed and is presently operational in support of field activities. This facility has triaxial capability over a range of temperatures to simulate in situ stress and temperature conditions and allows full flow control of adjustable air and water vapor mixtures. This allows the combined effects of stress, temperature, flow and moisture to be evaluated simultaneously under time varying conditions to closely simulate the CAES environment, and is a unique experimental capability unavailable elsewhere.

The aquifer field test, the field study component of the porous media studies, has progressed from the planning and site selection stages, which were completed at the end of FY-1980 to facility construction in preparation for air injection testing, scheduled for FY-1982. Early in 1981, site exploration and confirmation activities including drilling and environmental evaluations were completed. The exploration phase provided the data base for the permitting process and the specific geological data required to design the test facilities, perform predictive studies, and implement the lease options for the test term. This phase was culminated with an environmental feasibility report and submission of an application to the Illinois Environmental Protection Agency for a construction permit. In parallel with this exploration and permitting process, an RFP was issued for construction and operation of the field test, proposals were received and contractor selection carried out. PB-KBB Inc. of Houston, Texas, was awarded this operations and construction contract. While negotiations were carried out to value engineer and refine the final contract, PNL interfaced with the Illinois Environmental Protection Agency (IEPA) on permit questions, and the design and construct phase of the field test was initiated with PB-KBB through an interim letter contract. The site lease was signed in May, the construction permit was issued in early June, and contract negotiations with PB-KBB were completed and the contractor then mobilized for the summer drilling program.

The first well, the injection/withdrawal well, finished drilling on June 29. This satisfied the major director-controlled milestone in the reservoir stability study slightly ahead of schedule. Activity under way presently includes monitoring well field drilling, surface system design and procurement, and subsurface instrumentation preparation. Work is on schedule and within budget.

A summary of accomplishments during FY-1981 to date, listed below, indicate good performance with respect to the project plan for the year.

- Hard rock numerical and experimental evaluation of PEPCO design complete
- Champagne effect studies implemented and coordinated with Electric Power Research Institute (EPRI) activity
- Salt numerical model evaluation complete
- Salt in-mine facility operational
- Porous media numerical evaluation of field study initiated
- Porous media flow facility operational
- Field study exploration phase complete
- Field study operations contract awarded and signed
- Field study Illinois Environmental Protection Agency construction permit received
- Field study injection/withdrawal well completed
- Field study monitoring well field under construction
- Surface equipment procurements initiated and instrumentation plans complete.

Project primary objectives for the coming funding period will be to finalize hard rock and salt stability criteria, completing the geotechnical study phases of those studies, and to initiate air injection testing for the aquifer field test in conjunction with the required technical support functions.

PROJECT SUMMARY

Project Title:	Laboratory Tests of Salt Specimens Subjected to Loadings and Environmental Conditions Appropriate to a Compressed Air Energy Storage Reservoir.
Principal Investigator:	Robert L. Thoms
Organization:	Institute for Environmental Studies Louisiana State University Baton Rouge, Louisiana 70803
Project Goals:	Perform tests on rock salt under compressed air energy storage (CAES) conditions, and develop a data base for long-term effects of cyclic loads on rock salt. Incorporate the data base into operating criteria for CAES reservoirs in salt formations.
Project Status:	The project is in a late phase of data collection in the laboratory and in the Cote Blanche salt mine in south Louisiana. Data are being compiled and figures prepared for reporting. In situ tests in the Cote Blanche mine at -1370 ft (417.6 m) currently are in progress at natural background temperatures (92°F). Tests at elevated temperatures are planned for cyclic air pressure application. Results indicate laboratory and in situ test data for cyclic loads on rock salt from different sources are similar in a general sense. For quantitative comparison laboratory tests on Cote Blanche salt specimens also will be performed for this study.
Contract Number:	Subcontract B-67966-A-H
Contract Period:	1 October 1978 through 30 September 1981
Funding Level:	$433,896
Funding Source:	U.S. Department of Energy through Battelle Memorial Institute, Pacific Northwest Laboratory.

SALT EXPERIMENTAL STUDIES FOR CAES

Robert L. Thoms Richard M. Gehle
Louisiana State University
Baton Rouge, Louisiana

ABSTRACT

Tests of rock salt are described for long-term effects of compressed air energy storage. Results from an in situ test in the Cote Blanche mine in south Louisiana are described and compared to laboratory test data. Results indicate similar general behavior from both types of tests, and additional work is in progress to provide a basis for quantitative comparisons.

INTRODUCTION

Objectives of these studies are: (1) to establish a data base, from a test program, on the long-term effect on rock salt caverns of compressed air energy storage (CAES) associated loads; and (2) to formulate stability criteria for CAES reservoirs in salt formations.

General considerations for CAES associated loads can be indicated with reference to Fig. 1 which depicts loading phases for noncompensated salt caverns. A noncompensated cavern at depth is stressed primarily by the "effective overburden", i.e., as displayed in reference (1), the difference (g-p) in geostatic stress (g) and cavern pressure (p). The geostatic stress depends on depth and overburden density; and cavern pressure is operator controlled via liquid (brine during cavern construction by solution mining) "head" or gas (air) pressure following cavern construction.

A fundamental criteria for geostorage in salt caverns is that the effective overburden shall always be positive i.e., (g-p)>0; otherwise the neighboring rock formation at certain control points, e.g., the casing "seat" or "shoe", may be in tension. In practice this is handled by limiting cavern pressure, p, by an empirical criterion based on operating experience.

Long-term effects of large positive values of effective overburden, augmented by cyclic air pressure and temperature, are of major concern for noncompensated CAES caverns in salt. The most severe effects will be realized if deep caverns are utilized with relatively low cavern pressures.

This study has consisted to date mainly of generalized laboratory testing of salt under simulated CAES load conditions. Two test phases have been employed: (1) studies in the Louisiana State University (LSU) laboratories and (2) in situ studies in salt mines in south Louisiana. Limited numerical modeling has been employed in both phases for planning appropriate tests.

Results presented previously include: (1) rock salt displays good endurance to long-term cyclic load effects; (2) acoustic emissions appear feasible for monitoring CAES caverns in salt; (3) permeability of rock salt is strongly affected generally by degree of disturbance, both in situ and in laboratory specimens; and (4) rock salt displays long-term creep, but over short-terms, approximately linear displacement response to cyclic loads.

Current and recent work now will be presented for the two phases of this study in the order, (1) in situ mine tests, and (2) laboratory tests at LSU.

IN SITU MINE TESTS

In situ mine tests had been initiated in the Jefferson Island (JI) mine in 1980 and were reported during the 1980 Mechanical, Magnetic, and Underground Energy Storage Contractors' Review Meeting for the Department of Energy (DOE) on November 11, 1980. Ironically, only 9 days later on November 20, the JI mine was flooded and the in situ CAES test site was lost. Dr. Thoms, Mr. Richard Gehle, and a student worker, Robert Kayser, were in the mine at the time and were safely evacuated. However, they were forced to abandon underground the portable acoustic emissions (AE) equipment which had been obtained for the CAES study.

Another in situ CAES test site was kindly made available in the Cote Blanche mine operated by Domtar, Ltd., of Canada. The Cote Blanche mine also is conveniently located in south Louisiana; and an instrument "shack" and test holes were promptly emplaced there such that in situ CAES testing was underway again by around mid April, 1981.

Figure 2 depicts schematically the state of stress around a typical test hole at the in situ site in the Cote Blanche mine. The indicated overburden stress state (crossed lines) corresponds to results for principal stresses and axes from a plane strain, nonlinear finite element analysis of the site at a depth of 1370 ft (418 m). The background for this analysis is included in reference (2). The shaded zone around the lower portion of the test hole indicates magnitude of air pressure applied within the hole during a test performed on May 7, 1981. The latter stress state is axisymmetric, and hence cannot be compared directly to the plane strain state for the initial overburden stresses; nevertheless, a sense of relative stress magnitudes from the two depicted stress states can be obtained.

Figures 3(a,b) depict data obtained from an in situ test performed on May 7, 1981. Applied internal hole pressure and corresponding resulting diametrical hole displacement and acoustic emissions are indicated by the recorded traces. A hole "caliper" developed for the in situ test phase was first calibrated in the LSU laboratory and then installed in the "number 1" test hole at the site. The test schedule included four stages: (1) hole pressurization (increased from atmospheric pressure value), (2) holding constant pressure for some time interval, (3) applying cyclic air pressure in the hole, and (4) depressurization (decreased to atmospheric pressure value).

Figure 3(a) displays data corresponding to hole pressurization, stage (1), of the test. With reference to Fig. 3(a) it appears that the hole diameter initially increased with monotonically increasing values of applied air pressure (as anticipated). However, the diametrical displacement rate decreased as the magnitude of air pressure approached a constant value; and then reversed in sign (hole diameter decreased) after some time under the constant pressure condition. Thereafter the hole continued to close (not shown). This implies creep closure due to overburden dominated effects of the applied test hole pressure relatively soon. With reference to Fig. 2, this should not be surprising, since the effective overburden (g-p) can be anticipated to be relatively large around the test hole. The creep closure effect could be countered by increasing hole pressure p, however safety considerations limit test hole pressures to around 400 psi (2.76 mPa). Thus, estimates indicate values of effective overburden around the test holes in the Cote Blanche mine result in creep closure conditions more severe than for "typical" noncompensated operational CAES caverns.

Figure 3(b) depicts data corresponding to cyclic pressurization, stage (3), of the test of May 7. Note that the pressure trace in Fig. 3(b) has been "offset" from the trace of Fig. 3(a). The short-term diametrical response of the test hole obviously tracks the applied cyclic pressure in an approximately linear trend. The displayed in situ short-term response of rock salt to cyclic loads thus corroborates behavior of laboratory specimens subjected to cyclic loads as presented in previous reports from this study. The "band width" of diametrical displacement amplitudes with time apparently is affected in the long-term by creep closure. This in situ cyclic response also is consistent with rock salt specimen behavior in laboratory tests.

An acoustic emissions (AE) trace is evident in Figs. 3. The recordings indicate "frequency counting", which was not found to be as useful as more processed measures of AE for indicating salt response. Thus a portable replacement AE unit similar to the one lost in the J.I. flood was reordered.

Plans are well along to place heaters in the test holes. These will be used to simulate cyclic thermal loads associated with CAES operations. Laboratory tests, as noted in the following section of this report, indicate a strong sensitivity of salt creep to increased temperatures. This has been well known for some time and reported by other workers, for example in reference (3), for constant load creep tests. Results from in situ tests for cyclic thermal loads will be particularly interesting.

Other work planned for in situ tests includes performing "effective" permeability borehole tests. Currently materials have been ordered to fabricate a second version of a "straddle packer" for in situ permeability measurements along boreholes in the salt mine. An earlier version was fabricated and tested in the Cote Blanche mine; however, leaks developed between the inflatable packers and the walls of the borehole, thus making the test ineffective. Sandia Corporation personnel (Mr. R. Beasley) have been very helpful in furnishing information as described in reference (4) on a successful saddle packer designed and used by their workers for permeability measurements downhole in bedded salt deposits of the Southwestern U.S.

LABORATORY TESTS

For laboratory tests at LSU rock salt specimens are subjected to loading conditions based on operating effects on CAES caverns in salt formations.

A matrix of tests was developed and has been used in testing salt from at least four different sources. Salt has been obtained from a number of sources for CAES related tests, with the most generous supply made available through the Strategic Petroleum Reserve (SPR) of the Department of Energy (DOE), and arranged by Sandia Corporation.

Figure 4 depicts typical laboratory test data for a sample of Bryan Mound dome salt. The specimen was subjected to triaxial compression (Von Karman type cell) during a three stage test ranging through stress conditions: (1) constant (conventional creep); (2) cyclic, for both lateral and axial stresses; and (3) cyclic, at elevated temperatures.

Figure 4 indicates that rock salt under the given test conditions was more affected by increased temperature than by cyclic load effects. This is an extension of findings by previous investigators relative to the dominating effort of elevated temperature for stability of openings in rock salt.

Elevated temperatures in CAES cavern walls will be a result of injection of hot air during the charging portion of a typical CAES cycle. Air has relatively little heat capacity and heat transfer to the cavern walls may be attenuated by an insulating layer of "condensate" (brine). Rock salt itself transfers heat readily, hence natural background formation temperatures probably will dominate the cavern walls. This implies that temperature surveys should be included in well loggings for potential CAES caverns in salt. In the laboratory, constant elevated temperatures, as contrasted to applied cyclic elevated temperatures, should be adequate to represent CAES effects.

Permeability tests performed in the laboratory were consistent with results reported by other workers. Generally permeability decreased rapidly with only a limited number of cyclic loads for triaxial compression tests. Uniaxial and triaxial extension tests could not be readily modified to carry out permeability tests.

After collecting rock salt specimens firsthand from the Jefferson Island mine for permeability tests, it became apparent that the degree of disturbance of specimens dominated subsequent "permeability" characteristics in the laboratory. This was also true in the mine, where qualitative tests indicated rock salt in disturbed zones displayed "induced" permeability. Thus, emphasis on permeability measurements has been shifted mainly to in situ borehole tests in undisturbed zones in mines.

CONCLUSIONS

Comparison of laboratory and in situ test data for rock salt indicate similar general behavior under cyclic loading conditions. Laboratory tests indicate generally that rock salt displays more creep sensitivity to elevated temperatures than to cyclic loads typical of CAES environments. For quantitative comparisons of laboratory and in situ data cores from the Cote Blanche mine must be taken and specimens tested in the LSU laboratory. This is planned for the completion phase of the in situ tests for CAES effects on rock salt.

ACKNOWLEDGEMENTS

Appreciation is expressed to Domtar, Ltd., for permitting in situ CAES tests to be performed in the Cote Blanche mine in south Louisiana. Mr. Bill Caughlin, plant manager, and Mr. Gary Bucien, mine engineer, were most helpful in their support of this work.

This work was supported by the U.S. Department of Energy under Subcontract No. B-67966-A-H, Laboratory Testing of Salt Specimens for Long-Term Effects of Compressed Air Energy Storage, through Pacific Northwest Laboratory, operated for DOE by Battelle Memorial Institute.

REFERENCES

1. Thoms, R. L., M. Nathany, and R. Gehle, Low-Frequency Cyclic Loading Effects on Rocksalt, Proceedings International Symposium on Subsurface Space for Environmental Protection, Low-Cost Storage and Energy Savings, June, 1980, ROCKSTORE 80, Vol. 2, pg. 755, Stockholm, Sweden.

2. Gehle, R. M., Finite Element Analysis of Slow, Time Dependent, Rock-Salt Deformations, Thesis Submitted in Partial Fulfillment of the Requirements for the Degree of Master of Science in the Department of Engineering Science, Louisiana State University, May, 1980.

3. Lomenick, T. F., Accelerated Deformation of Rock Salt at Elevated Temperature and Pressure and its Implications for High Level Radioactive Waste Disposal, Thesis Submitted for Partial Fulfillment of the Requirements for the Degree of Doctor of Philosophy, University of Tennessee, March, 1968.

4. Peterson, E. W., P. L. Lagus, R. D. Broce, and K. Lie, Systems Science and Software, In Situ Permeability Testing of Rock Salt, SAND 81-7073, Prepared for Sandia National Laboratories under Contract to the United States Department of Energy, Albuquerque, New Mexico, April, 1981.

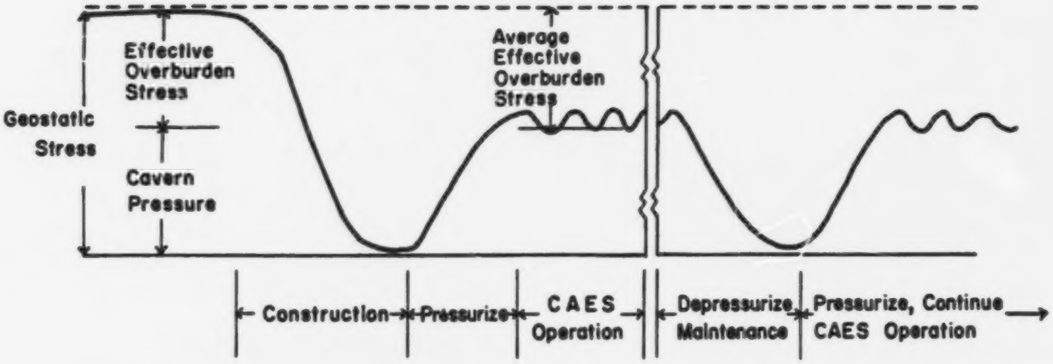
Effective
Overburden
Stress
Geostatic
Stress
Cavern
Pressure
Average
Effective
Overburden
Stress
Construction
Pressurize
CAES
Operation
Depressurize
Maintenance
Pressurize, Continue
CAES Operation

Fig. I. CAES CAVERN LOADING PHASE

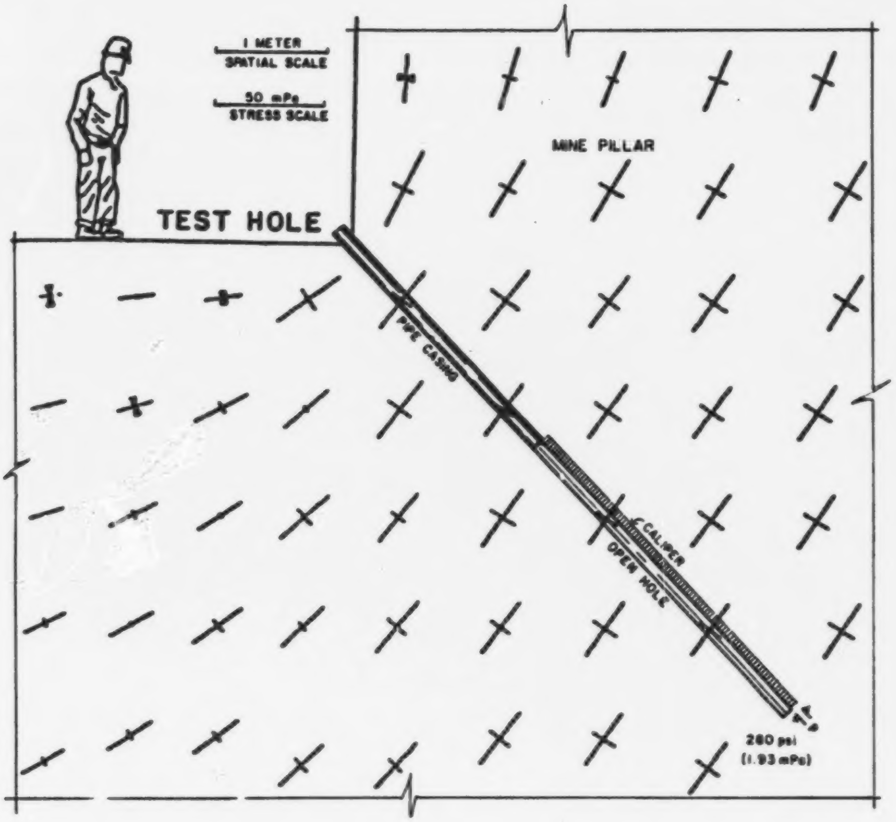
I METER
SPATIAL SCALE
50 mPa
STRESS SCALE
TEST HOLE
MINE PILLAR
PIPE CASING
CALIPER
OPEN HOLE
280 psi
(1.93 mPa)

Fig. 2. Stress Conditions for In Situ Test Site, - 1370 ft. (417.6 m).

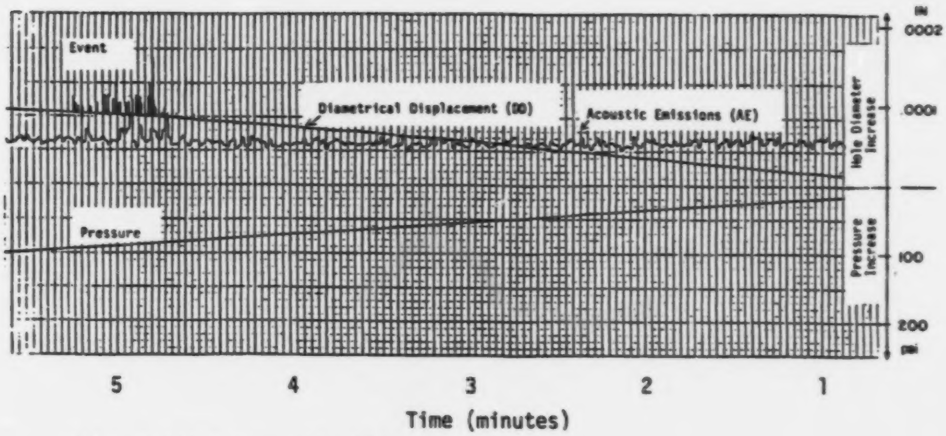

(a). Initial Pressurization

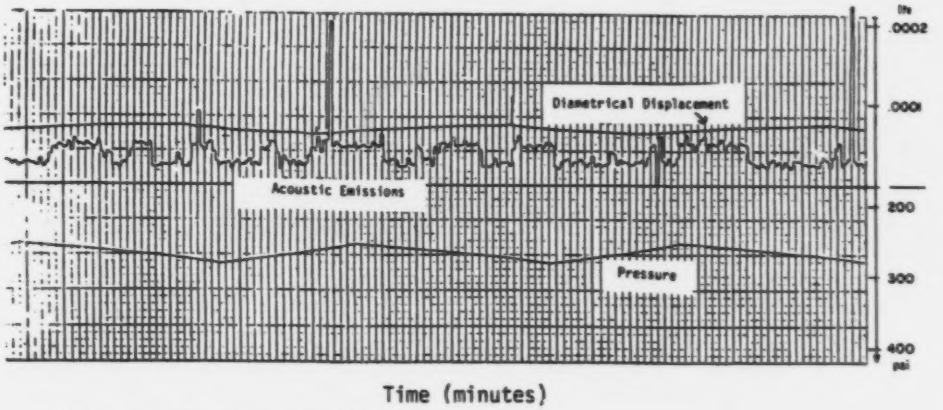

(b). Cyclic Pressurization

Fig. 3. In Situ CAES Test in Cote Blanche Mine. May 7, 1981

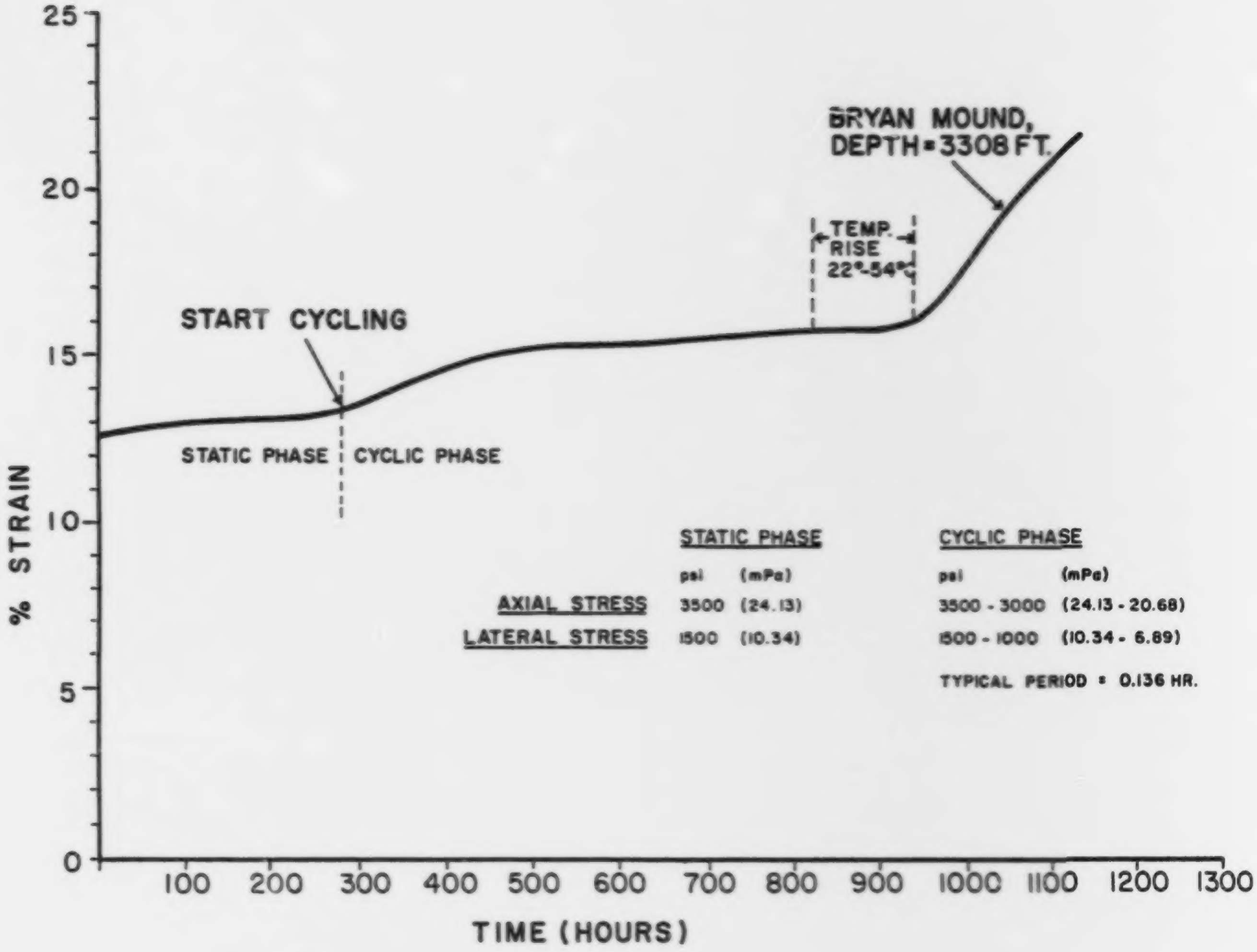

	STATIC PHASE		CYCLIC PHASE	
	psi	(mPa)	psi	(mPa)
AXIAL STRESS	3500	(24.13)	3500 - 3000	(24.13 - 20.68)
LATERAL STRESS	1500	(10.34)	1500 - 1000	(10.34 - 6.89)

TYPICAL PERIOD = 0.136 HR.

Fig. 4. Laboratory Test Data

NUMERICAL AND LABORATORY STUDIES OF CAES RESERVOIRS IN THE SYKESVILLE GNEISS

Arlo F. Fossum Terje Brandshaug
RE/SPEC Inc.
Rapid City, South Dakota

ABSTRACT

Numerical and Laboratory Studies of Reservoirs in the Sykesville Gneiss were performed to assess cavern stability and necessary artificial support requirements. These studies indicate that stability of the caverns could be maintained with minimal support.

INTRODUCTION

The compressed air energy storage (CAES) concept, in which mined caverns in hard rock are used to store compressed air for use in electric utility load-leveling operations, has been the subject of a number of research studies in the past several years (1-7). For the most part, these studies have been generic in the sense that a site specific rock and location were not investigated. Numerical models were developed and used to predict the behavior of compensated CAES caverns and a methodology was established for the development of stability criteria. Rock properties were obtained from laboratory investigations of the response of generic rock specimens to loading conditions typifying those of an operating CAES cavern.

In this paper site specific results are presented from a stability analysis of the ACRES American Design of the Potomac/Electric Power Company (PEPCO) CAES System in which laboratory determined properties of the site rock, Sykesville Gneiss, are used in the numerical calculations.

PROGRAM DESCRIPTION

The program consisted of the following two major phases:

PHASE I. Laboratory Testing

Core of Sykesville Gneiss drilled at depth were obtained from ACRES American Inc. A geological description was made of this rock including its mineralogical composition.

Tests were conducted on prepared specimens at room and elevated temperatures with dry and saturated moisture conditions. These tests included indirect tensile tests, anisotropic triaxial compression tests and thermally cycled fatigue tests. The tests were designed to determine the amount of strength reduction caused by the non-ambient conditions associated with CAES.

PHASE II. Numerical Modeling

Numerical simulations were made for the construction and operation of the PEPCO caverns with the use of the numerical procedures developed in a previous study (7). The PEPCO system considered in this study consisted of an array of four caverns located at a depth of 700 meters in Sykesville Gneiss. The cavern height was 27 meters with a width of 18.3 meters. The coefficient of lateral earth stress was assumed to be equal to 1.8 and the extraction ratio was 25 percent.

Elastic stresses were determined for the four PEPCO caverns following initial excavation. This information was then related to case history data for determination of artificial support requirements (8). Thermal and thermoelastic operational analyses were made to determine the cyclic stresses around the caverns.

RESULTS

The Sykesville Gneiss used in this study was obtained from an area approximately three miles wide by 25 miles long extending in a northerly direction from Wheaton to Eldersburg, Maryland. This area is underlain by the Sykesville formation of early Paleozoic time. The specimens were uniform with 50 percent Quartz, 30 percent Mascovite, 15 percent Biotite, and small amounts of Chlorite, Pyrite, Garnet, and Maguetite.

RSI-PUBL. NO. 81-07

From the standpoint of stability of a CAES cavern, the major concern, with a foliated metamorphic rock such as the Sykesville Gneiss, arises from the foliation itself. Foliation planes can cause the strength, elasticity, and thermal properties of the rock to be anisotropic and rather variable. In addition, weathering of such rocks can be accelerated along planes of foliation by the pressure of easily altered metamorphic minerals.

A suite of tests was performed at ambient conditions to provide a baseline for comparison of tests conducted at non-ambient conditions. The baseline tests included indirect tension tests and triaxial compression tests. The indirect tension tests were performed on a Tinius-Olsen apparatus. The specimen length (25 mm) was approximately half of the specimen diameter (47 mm). The specimen is placed in a machine so that diametral compression is applied between the platens of the machine. The loading rate was controlled so that failure occurred within 5-15 min.

For the triaxial compression tests, the field core of the Sykesville Gneiss had to be subcored at different angles to the foliation. The dimensions of these specimens included diameters of 22 mm and lengths of 45 mm. To perform a triaxial compression experiment, the specimen is placed between the platens of a testing machine and jacketed with an impermeable membrane. This assembly is placed in a pressure vessel and the annulus is filled with silicone oil. The pressure vessel is sealed at both ends and placed in the main frame of the testing apparatus. Hydrostatic pressure is applied directly following vessel assembly. Axial stress is then applied and monitored with a load cell placed directly in line with the loading column. A load-hold procedure is used that produces an axial specimen stress rate of 5.75×10^{-2} MPa Sec^{-1} until the specimen fails.

Baseline Test Results

The sample mean and standard deviation of tensile strength obtained from six indirect tension tests in which the load was normal to the planes of foliation was 5.30 MPa and 0.78 MPa, respectively.

Figure 1 shows the results of the triaxial compression tests in the form of linear Mohr failure envelopes for specimens subcored such that the angle of foliation to the longitudinal axis existed at 0°, 30°, 45°, 60°, and 90°. The results obtained at 0° and 90° are essentially equivalent. The influence of foliation on strength can be seen clearly as the angle of foliation varies. Because the diameter of the subcore is only 0.022 m, the strength of the Sykesville Gneiss obtained from these tests is likely to be an upper estimate.

All of the tests performed on specimens with foliation angels of 30°, 45°, and 60° resulted in failure along the planes of foliation. Failure was through the foliation for the tests conducted on specimens with foliation angles of 0° and 90°.

Non-Ambient Test Results

Influence of Moisture

The two extreme values of moisture content in the rock specimens were obtained either by submerging the specimens in water at moderate pressure (0.7 MPa) or desicator-drying them over calcium chloride, $CaCl_2$. The specimens were weighed periodically until equilibrium was achieved.

The sample mean and standard deviation of tensile strength obtained from 6 indirect tension tests on saturated specimens in which the load was normal to the planes of foliation was 4.37 MPa and 1.37 MPa, respectively. From small sampling theory, student's t distribution can be used to test the significance of the differences in mean values of tensile strength between the dry and saturated results. It was determined that the null hypothesis (no difference between means) could be rejected at a 0.20 level of significance. Thus, the conclusion is made that the difference in mean tensile strength between the wet and dry specimens is probably significant although judgment could be "reserved".

Results of the triaxial compression tests on saturated specimens of the Sykesville Gneiss with an angle of foliation of 30° to the longitudinal axis showed that the differences in the intercepts and slopes with the dry tests were negligible. Thus, it is concluded that the shear strengths of these rocks are probably not affected by moisture.

Influence of Temperature

Specimens tested at temperatures to 100°C showed no reduction in either indirect tensile strength or unconfined compressive strength. Triaxial compression tests were not conducted above room temperature.

Influence of Thermal Shock

During the operation of a CAES cavern, the host rock will be subjected to rather sudden changes in temperature along the cavern wall as the compensating water rises and falls in the cavern corresponding to the daily charge and discharge operations. To simulate these conditions in the laboratory, a relatively severe test was conducted in which the specimens of rock were heated to different temperatures and then quenched in cold water. One and ten thermal cycles were completed at 0°-50°C, 0-100°C, and 0°-150°C. The specimens were then tested for reductions in the tensile and shear strength. It was found that the null hypothesis for the mean tensile strengths between these tests and the baseline tests could be rejected at a level of significance of 0.05. Thus, it is concluded that this cycle of thermal shock is probably significant.

An interesting fact is that there is no statistically significant differences between the mean tensile strengths of specimens cycled at the higher temperatures and those cycled at 0°-50°C. In addition, the number of thermal cycles after the first did not influence the tensile strengths of the specimens. Thus, it is concluded that most of the damage from thermal shock occurs in the first cycle and that a significant reduction in tensile strength can be expected. The percentage reduction in tensile strength was 36 percent.

Similar results were found for the triaxial compression tests on specimens with angles of foliation of 30°. Figure 2 illustrates the results in the form of linear Mohr failure of envelopes. As was the case for the indirect tensile strengths, the shear strengths did not vary significantly between the first and tenth thermal cycle. Also, there were no significant differences between the shear strengths of specimens cycled between 0°-50°C, 0°-100°C, or 0°-150°C. The angle of internal friction appears to have increased while the cohesion appears to have decreased. Thus, the percentage drop in shear strength decreases with increasing confining pressure over the range of interest to CAES caverns. At zero confining pressure the decrease in shear strength is on the order of 50 percent while at a confining pressure of 20 MPa the shear strength is reduced by about 25 percent.

Numerical Modeling Results

Laboratory data of the Sykesville Gneiss was used in the numerical simulation models of the PEPCO caverns. Elastic stresses were determined for the four PEPCO caverns following initial excavation. These data were then related to case history data for determination of artificial support requirements (8). Based on a quality classification of the Sykesville Gneiss with the Geomechanics rating system (9) that gave a most likely value of 80, and on case history studies, Figure 3 was developed that suggests that the cavern walls do not need any form of artificial support, while the roof will need light support.

A failure analysis was performed with a linear Mohr-Coulomb criterion for foliated rock. Figure 4 shows that failure along foliation planes was limited to a small region in the cavern roof and floor (outer cavern).

Thermoelastic analyses of the operation of the caverns resulted in no tensile stresses along the cavern walls. Thus, the cavern walls are subjected to cyclic compression - compression stress states. This type of stress state is the most favorable type of cyclic stress state from the standpoint of avoiding fatigue failure.

CONCLUSIONS

The testing program demonstrated that the planes of foliation have a pronounced effect on the shear strength of Sykesville Gneiss. When the direction of the major principal stress is oriented at 30° to 50° from the foliation plane, the shear strength can be reduced by as much as 50 percent as compared to that for orientation of 0° and 90°. The loss of tensile strength experienced by specimens subjected to the simulated CAES conditions is not a major concern since this strength is generally quite low to begin with. For design purposes, it would be wise to assume that the host rock has zero tensile strength.

The loss of cohesion because of thermal shock is significant (50 percent) and appears to occur after one thermal cycle. The cohesive strength of a rock is its shear strength with zero normal stress acting on the failure plane. Even at the wall of a cavern, however, the normal stress acting on potential shear failure planes will be relatively high. The percentage loss of shear strength of the rock decreases with increasing normal stress. Numerical analyses have shown that even with reduced properties, stability of the PEPCO caverns should be maintained with minimal artificial support requirements both before and during CAES operation.

ACKNOWLEDGMENT

This work was supported by the U.S. Department of Energy under Subcontract No. B-49407-A-H Prime Contract DE-AC06-76RLO 1830 with Pacific Northwest Laboratory operated by Battelle Memorial Institute.

REFERENCES

1. P. F. Gnirk, A. F. Fossum: On the Formulation of Stability and Design Criteria for Compressed Air Energy Storage in Hard Rock Caverns, Proceedings of the 14th Intersociety Energy Conversion Engineering Conference, Boston, Massachusetts, Aug. 5-10, 1979, v. 1, pp. 429-440.

2. A. F. Fossum: Laboratory Testing of Hard Rock Specimens for Compensated CAES Caverns, Proceedings of the 1979 Mechanical and Magnetic Energy Storage Contractors' Review Meeting, U. S. Department of Energy, Division of Energy Storage Systems, Washington, D.C., Aug. 1979, pp. 119-127.

3. P. F. Gnirk, A. F. Fossum: Synopsis of Stability and Design Criteria for CAES and UPHS in Hard Rock Caverns, ROCKSTORE 80 -- SUBSURFACE SPACE, International Symposium for Environmental Protection, Low-Cost Storage and Energy Savings, Stockholm, June 23-27, 1980, pp. 615-222.

4. A. F. Fossum: Laboratory Studies of Hard Rock for CAES, Proceedings of the 1980 Mechanical and Magnetic Energy Storage Contractors' Review Meeting, U. S. Department of Energy, Division of Energy Storage Systems, Washington, D.C., pp. 214-219.

5. P. F. Gnirk, T. Brandshaug, G. D. Callahan, J. L. Ratigan: Numerical Studies of Compensated CAES Caverns in Hard Rock, Proceedings of the 1979 Mechanical and Magnetic Energy Storage Contractors' Review Meeting, U. S. Department of Energy, Division of Energy Storage Systems, Washington, D. C., August 1979, pp. 106-117.

6. T. Brandshaug: Thermomechanical Assessment of Compensated CAES Caverns in Hard Rock, Proceedings of the 21st U.S. Symposium on Rock Mechanics, Rolla, Missouri, May 28-30, 1980, pp. 163-174.

7. T. Brandshaug, A. F. Fossum: Numerical Studies of CAES Caverns in Hard Rock Proceedings of the 1980 Mechanical and Magnetic Energy Storage Contractors' Review Meeting, U. S. Department of Energy, Division of Energy Storage Systems, Washington, D.C., pp. 207-212.

8. E. Hoek, The Role of Modeling in the Design of Nuclear Waste Repositories: The Design Engineer's Viewpoint, LLL/ONWI Workshop on Thermomechanical Modeling for Hardrock Waste Repository, Berkeley, 1979.

9. Z. T. Bieniawski: Geomechanics Classification of Rock Masses and Its Application in Tunnelling, Proc. Third International Congress on Rock Mechanics. ISRM, Denver, Vol. 11A, 1974, pp. 27-32.

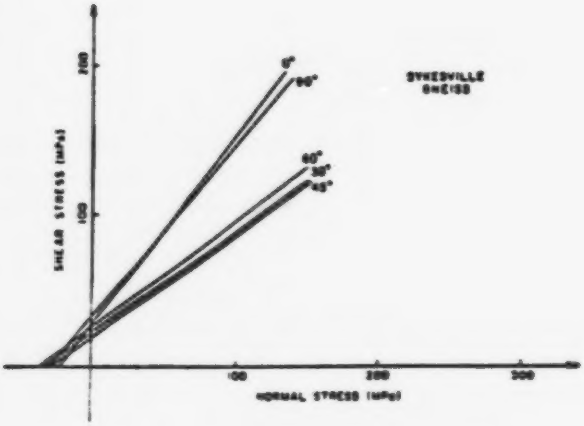

Figure 1. Linear Mohr Failure Envelopes for Different Angles of Foliation.

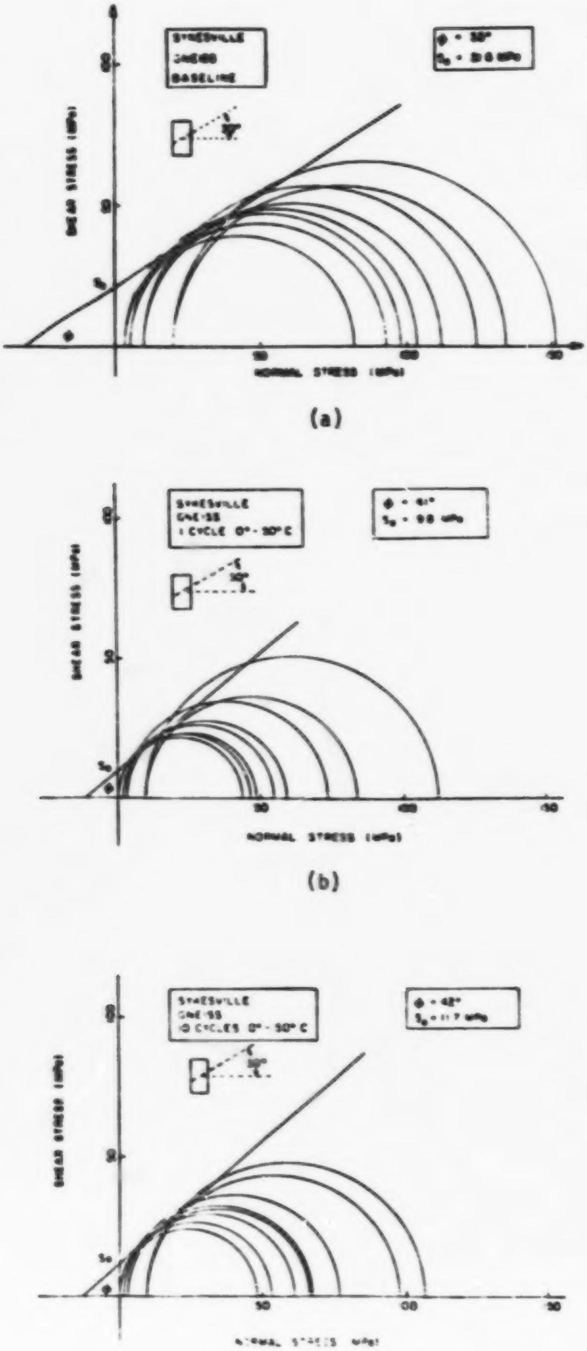

Figure 2. Linear Mohr Failure Envelopes for (a) Ambient Conditions, (b) One Thermal Cycle, (c) 10 Thermal Cycles.

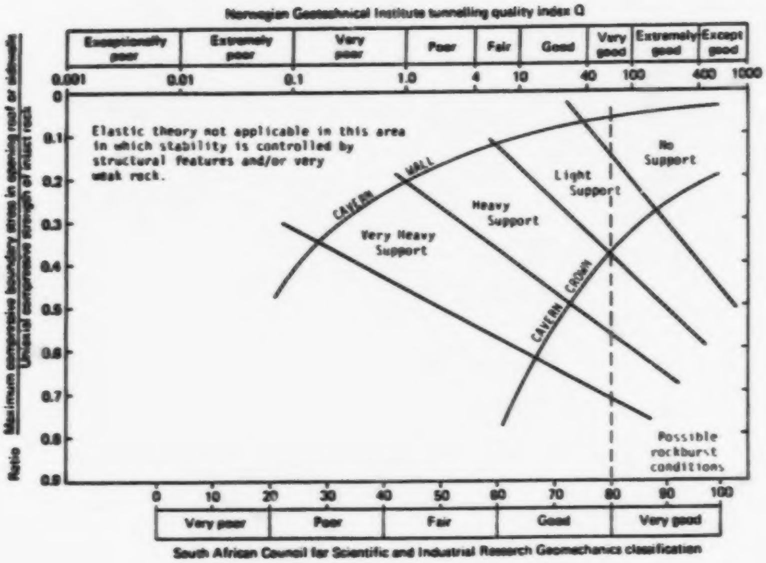

Figure 3. Guide to Required Artificial Support of the PEPCO Caverns.

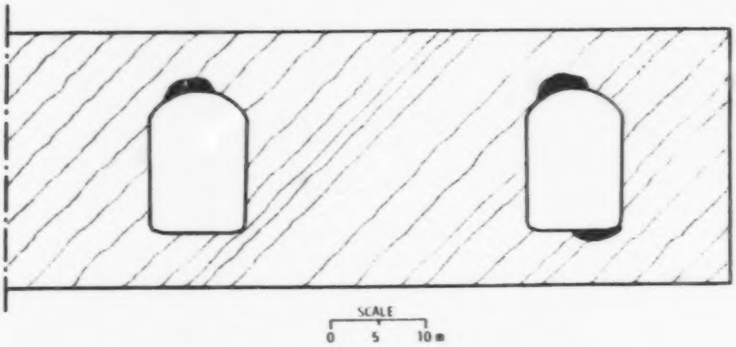

Figure 4. Failure Zones Around the PEPCO Caverns After Initial Excavation.

PROJECT SUMMARY

Project Title:	Fluid/Thermal Analysis for Porous Media Reservoirs
Principal Investigator:	L.E. Wiles
Organization:	Pacific Northwest Laboratory PO Box 999 Richland, Washington 99352 Phone: (509) 375-2049
Project Goals:	Modify existing models to be capable of analyzing the thermohydraulic performance of the demonstration site reservoir. Use the models to analyze the demonstration site reservoir and to support the design of the facility.
Project Status:	Bubble development and water coning studies have been done for the demonstration site reservoir. Modifications are underway to adapt the thermal model to the site specific conditions. Specific plans to use the dehydration model have not been made.
Contract Number:	DE-AC06-76RLO 1830
Contract Period:	FY-1981
Funding Level:	$45,000
Funding Source:	U.S. Department of Energy

PROJECT SUMMARY

Project Title:	Porous Media Experimental Studies
Principal Investigator:	R. L. Erikson
Organization:	Pacific Northwest Laboratory PO Box 999 Richland, Washington 99352 Phone: (509) 376-8627
Project Goals:	To investigate potential physical and chemical property alterations of reservoir sandstone under CAES conditions simulated in the CAES porous media flow facility. Generate ancillary laboratory data in support of the CAES Pittsfield field site.
Project Status:	The CAES porous media flow facility has been constructed and the system acceptance testing completed. Initial experiments designed to investigate the permeability of triaxially loaded sandstone to hot air have been initiated. Compatibility testing of St. Peter sandstone and ground water from the Pittsfield site at elevated temperature and pressure is in progress. Future experimentation on the St. Peter sandstone conducted in the CAES flow facility will involve: 1) air permeability and fatigue testing under cyclic conditions; and 2) investigation of desaturation rates and mechanisms.
Contract Number:	DE-AC06-76RLO 1830
Contract Period:	FY-1981
Funding Level:	$155K
Funding Source:	U.S. Department of Energy

NUMERICAL AND EXPERIMENTAL ANALYSES OF THE POROUS MEDIUM RESERVOIR AT PITTSFIELD, ILLINOIS

L.E. Wiles, R.L. Erikson, R.D. Allen and T.J. Doherty
Pacific Northwest Laboratory*
PO Box 999
Richland, Washington

ABSTRACT

Numerical and experimental predictions of the St. Peter sandstone reservoir behavior at Pittsfield, Illinois, are being conducted. These analyses are based upon field and laboratory determinations of structural dimensions and physical properties and upon operating CAES design conditions. Numerical modeling addresses bubble development, water coning, thermal development and reservoir dehydration. Air injection rate is calculated as a function of time. The advance of the 50% saturation front during bubble development is depicted in depth versus radius curves for time periods up to 60 days. Experimental analysis embraces ground water chemistry, permeability and dehydration. Permeability of the St. Peter is highly variable due to vertical changes in lithology and variable friability. The new CAES porous media flow facility simulates field conditions of air flow rate, confining pressure, desaturation profile and dynamic stress.

INTRODUCTION

Pacific Northwest Laboratory (PNL) is conducting a field study on an aquifer air storage system, utilizing the St. Peter sandstone. This porous media reservoir is overlain by 90 meters (295 ft) of relatively impervious dolomitic and limestone caprock formations and laterally contained within a second order dome, one of several known minor folded structures associated with the Pittsfield anticline. Exploration activities have defined the geometry of the structure, permeability and porosity of the St. Peter sandstone, hydrostatic discovery pressure and threshold pressure of the caprock. Preparations for field experimentation require definition of parameters such as injection pressure, air temperature, bubble radius, and time. Numerical and laboratory studies are being coordinated with field developments to provide bases for establishing or modifying field parameters. For example, numerical modeling of the specific reservoir enables prediction of bubble development time. Also, experiments on St. Peter specimens are quantifying permeability and dehydration characteristics under simulated CAES conditions. Continued parallel studies during the field experiment will probably result in modifications of modeling assumptions and laboratory parameters which will improve the accuracy of both numerical and experimental predictions.

NUMERICAL ANALYSIS

Numerical models, which were developed at PNL to predict thermohydraulic performance of compressed air energy storage (CAES) in aquifers, have been applied to the specific reservoir properties at Pittsfield to predict reservoir response. This modeling influences the design of tests and selection of equipment specifications.

Reservoir Description

The reservoir geometry, physical properties and operating conditions used in the demonstration site modeling are listed in Table 1. The domal trap has been assumed to be axisymmetric. The caprock is assumed to overlie the domed reservoir as an impermeable right circular cone with slope of 0.0125. The modeled region has a radius of 800 m (2624 ft) and a closure of 10 m (33 ft) (corresponding to the caprock slope). At its center the reservoir bed is 68 m (223 ft) thick. An impermeable horizontal basement rock is assumed. The outer boundary of the reservoir is assumed to be connected to a hydrostatic sink at a radius of 10,000 m (6.21 mi.) to permit outflow (and inflow) of aquifer water.

Relative permeabilities of the reservoir rock to air and water are plotted as functions of water saturation in Fig. 1. Capillary pressure as a function of water saturation is plotted in Fig. 2.

---

*Operated for the U.S. Department of Energy by Battelle Memorial Institute under prime contract no. DE-AC06-76RLO 1830.

TABLE 1. Reservoir Characteristics

Geometry	
Depth to uppermost reservoir bed	200 m (656 ft)
Vertical thickness at apex	68 m (223 ft)
Effective diameter of air storage zone	1600 m (5248 ft)
Wellbore diameter	0.1 m (4 in.)
Producing length	3 m (9.84 ft)
Reservoir closure	10 m (33 ft)
Physical Properties	
Porosity	20%
Permeability (horizontal and vertical)	700 md
Thermal conductivity	0.015 cal/cm sec°C
Specific heat	0.22
Specific gravity	2.12
Operating Conditions	
Nominal pressure	1.014 MPa (147 psi)
Air flow rate (injection)	35.42 SM^{3}m (1250 SCFm) (max)
Air pressure (compressor outlet)	2.07 MPa (300 psi) (max)
Air injection temperature range	50-200°C (122-392°F)

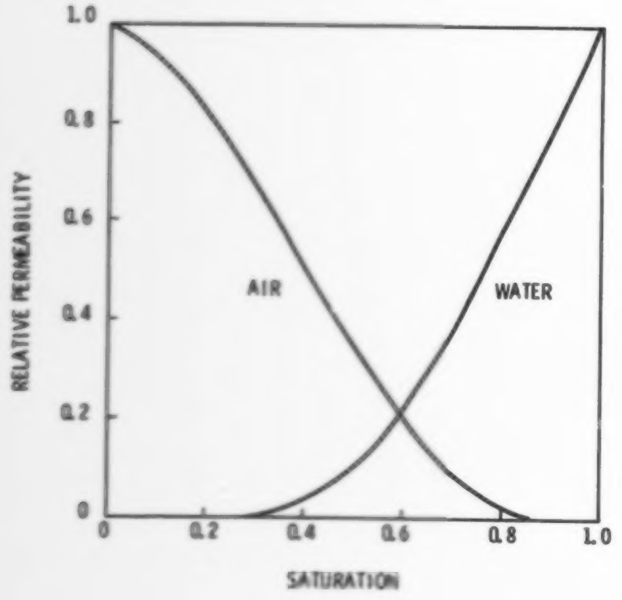

Fig. 1. Reference Relative Permeability Functions

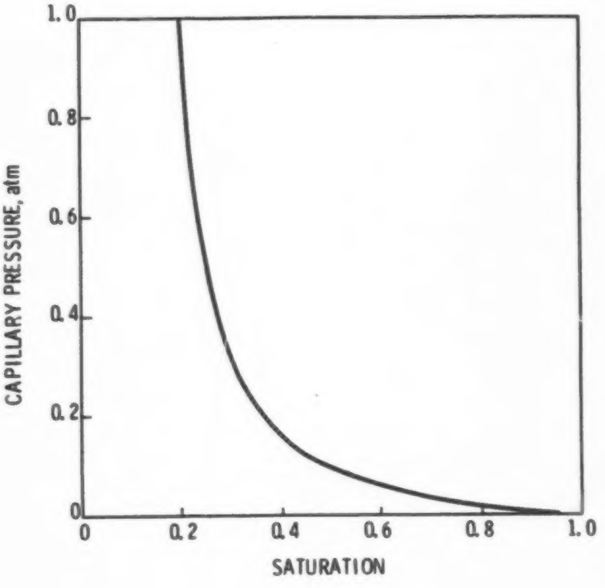

Fig. 2. Reference Capillary Pressure Function

Bubble Development

Bubble development calculations are described by Wiles and McCann(1). The model is two-dimensional (cylindrical), two-phase (air-water), isothermal, and includes both capillary pressure and relative permeability. The time-dependent pressure ramp shown in Fig. 3 defines the bottom-hole pressure for the bubble development simulation. The wellbore pressure remains constant unless the compressor flow limit of 35.42 SM^3m (1250 SCFm) is exceeded. The gradual increase in pressure from 1.014 to 1.898 MPa (147 to 275 psi) simulates a pressure function that may be necessary to reduce the possibility of fracturing of the reservoir rock. Computationally, bubble development begins with displacement of the water standing in the wellbore. The mass of wellbore water is about 600 kg (1323 lb) based on a water column 115 m (377 ft) deep and a wellbore radius of 10 cm (3.94 in). Water injection requires about four hours based upon the linear bottom hole pressure ramp shown in Fig. 3. After the wellbore is voided, air is injected continuously throughout the bubble development phase.

The air injection rate variation over a 60 day period is shown in Fig. 4. The rate is limited by the imposed bottom hole pressure maximum of 1.898 MPa (275 psi) which is reached after 24 hours of injection. The model predicts that the air injection rate decreases by up to 8% over the next 36 hours. The rate then increases at a declining rate over the balance of the injection period. The behavior of the injection flow rate curve may be determined by a combination of at least two participating effects. Physically, at the top of the pressure ramp an equilibration between imposed pressure and gravitational and capillary forces takes place. This effects a decline in the downward thrust of the bubble, leaving only the radial component to accommodate further bubble growth. This may contribute to the temporary decline in the injection rate. Numerically, the results may be affected by the grid spacing.

The advance of the "50% saturation front" is shown in Fig. 5. This value was chosen for display because it represents significant displacement of water and significant mobilities of both air and water. The bubble growth is initially both downward and radial. The downward growth slows appreciably as hydrostatic and capillary forces approach the bubble pressure. At this point the radial growth rate increases. After 60 days the air injection was terminated and a "closed in" period of 30 days was computed. The bubble underwent appreciable flattening of the lower 50% saturation front. The

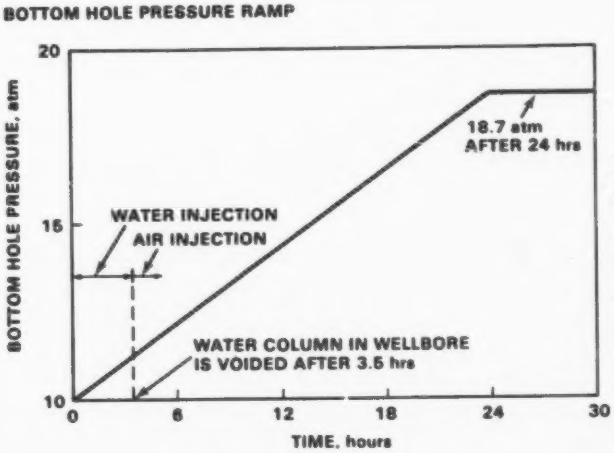

Fig. 3. Initial Reservoir Pressure Loading Ramp for Bubble Development

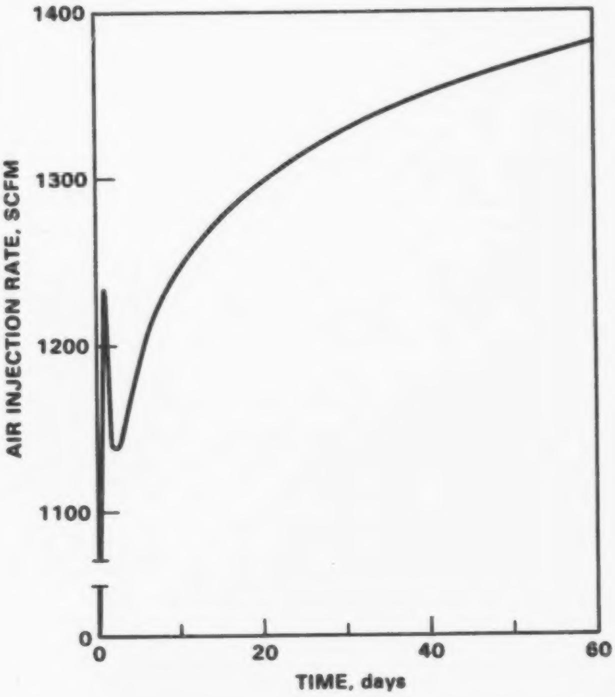

Fig. 4. Volume Flow Rate versus Time for 275 psi Constant Pressure Air Injection

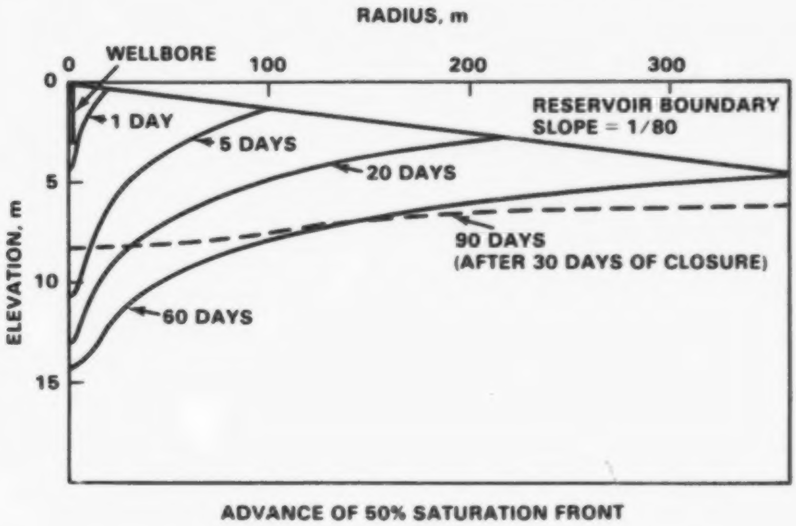

Fig. 5. Lines of Constant Saturation versus Radius for Different Time Periods during Bubble Development

rate of pressure equilibration is dominated by the capillary transition zone and the flow resistance between aquifer water and the hydrostatic sink. A radius-to-sink less than the assumed 10,000 m (6.21 mi.) would lessen this resistance. This would increase both the bubble growth rate and the pressure equilibration rate.

Water Coning

Upward conical migration of ground water during air withdrawal may occur in CAES reservoirs in which water underlies the air storage zone. This hydrological condition exists at the Pittsfield site. Water coning involves the intrusion of water into the wellbore or near-wellbore region. The water movement responds to pressure gradients created during the reservoir discharge cycle. Potential adverse effects include decreased air flow rate for a given pressure drop, geochemical instability near the wellbore, wellbore corrosion, and damage to surface equipment associated with water production.

Water coning is not likely to create problems within a full scale reservoir(1). In particular, water coning should be significantly easier to avoid in reservoirs that are characterized as edge-water drive. The Pittsfield experimental site, however, has a useful closure limit of only about 10 m (32.8 ft) and the entire air storage zone will be underlaid by water. However, the possible presence of lower permeability layers below the wellbore would inhibit water coning. Evidence from the experimental studies suggests the presence of stratified layers of lower vertical permeability within the St. Peter formation. The design of thermal air cycling experiments can be influenced by the water coning potential, e.g., reduced withdrawal rate and period would tend to inhibit water coning. Specific studies in this area are continuing.

A water coning simulation has been done using the bubble development solution as a starting point for cyclic operation. The results suggest that water buildup may occur around the wellbore for two reasons. One, the buildup can be induced by operational conditions. If the injection and withdrawal cycles are of the same duration, then the air flow rates must be equal to preserve the bubble mass. Since the bubble pressure is relatively low (11 to 12 atm) at the Pittsfield site then the air density around the wellbore during extraction can be much less than the air density during injection. To achieve equal mass flow rates the pressure gradient during extraction will be greater than that during injection. As a result, net water buildup will occur. Second, when water rises towards the wellbore it is supplied from a region of high liquid mobility. Subsequent water drainage from the wellbore region is based on low liquid mobility. Thus, there is a tendency for the water to be trapped, thereby resulting in a water buildup. Both of these phenomenon may be virtually eliminated by judicial selection of the duration of the withdrawal cycle relative to the injection cycle. This matter is presently being evaluated using the available computational tools.

Thermal Development

One purpose of the Pittsfield experiment is to evaluate reservoir behavior at elevated temperature. In this analysis, the length of the injection/withdrawal cycle moderately affects the radius of thermal penetration into the reservoir.(3) The presently planned test program will involve air cycling for 16 months. The initial baseline cycling will use air at 50°C (122°F) over a 4 month period and will approximate isothermal injection. Subsequent tests will inject air at 100°C (212°F), 150°C (302°F) and 200°C (392°F), each over a four month period. Numerical results will show radial temperature profiles in the wellbore region for 4 to 8 hour cycles. The calculations will use a two-dimensional (cylindrical) and single phase (air) model described by Wiles.(3) Dehydration processes near the wellbore or cyclic movement of water into and out of the wellbore (due to water coning) would inhibit thermal development.

Reservoir Dehydration

The humidity of withdrawn air was predicted using a one-dimensional (radial), two-phase (air-water) model(4). Water transport was limited to the vapor phase. During injection of undersaturated air at elevated temperature, the air will become saturated as it passes through residual water in the heated region near the wellbore. As the air mass moves outward it cools and water is condensed. This mechanism produces a dehydrated region around the wellbore.

During withdrawal the air gains heat and moisture as it moves toward the wellbore. When air enters the dehydrated zone, it continues to gain heat but not moisture. Therefore, this code predicts that extracted air is, in general, undersaturated at reservoir conditions for reservoirs charged with heated air.

EXPERIMENTAL ANALYSIS

The goal of this study is to obtain and interpret experimental data on the response of geologic materials to high temperature CAES in aquifers. Experimental evaluation of the Pittsfield reservoir materials has been the specific objective of all experimental work during this reporting period. The recently completed CAES porous media flow facility has begun to contribute significantly to this work.

St. Peter Ground Water Analysis

Cation concentrations were determined by inductively coupled plasma spectroscopy and major anion concentrations were measured by ion chromatrography. The water was obtained from the test well designated Yakley No. 7. Ground water chemistry is presented in Table 2. Ground water analysis will continue as necessary during drilling and testing at PNL and also under the auspices of PB-KBB Inc., the operations contractor.

Permeability of St. Peter Sandstone

The permeability of St. Peter sandstone to nitrogen gas was measured on core samples taken from borehole Yakley No. 1 at room temperature and pressure. Samples were prepared to allow gas passage both parallel and perpendicular to bedding planes. The data for permeability as a function of depth are shown in Fig. 6. Average permeabilities parallel and perpendicular to the bedding were 576 and 695 md, respectively. The considerable scatter in the data is attributed to the variable degree of cementation and friability of the sandstone. The amount of data is not sufficient to demonstrate anisotropy of permeability with respect to bedding orientation. The measured porosities of samples recovered from between 216 and 224 m (707 and 735 ft) were from 12 to 18 percent.

CAES Porous Media Flow Facility Experiments

The major thrust in the experimental program during FY-1981 has been the final design and construction of the CAES porous media flow facility and the successful acceptance testing of this system. Experiments in past years have incompletely simulated CAES aquifer field conditions of compressed air flow rate, confining pressure, desaturation profile, dynamic stress, etc. The flow facility allows experimental design to embrace physical property measurements at realistic pressures and temperatures under dynamic conditions of air flow. For example, reservoir rock will be characterized with respect to: 1) permeability under confined pressure, 2) stress-strain behavior, 3) rates of desaturation, and 4) cyclic fatigue.

TABLE 2. Chemical Composition of Ground Water from St. Peter Formation

Constituents	Concentrations (mg/ℓ)
Al^{+++}	0.10
As*	0.07
B^{+++}	1.76
Ba^{++}	0.04
Ca^{++}	137.00
K^{+}	25.00
Li^{+}	0.53
Mg^{++}	63.77
Na^{+}	959.00
Si^{++++}	3.20
Sr^{+}	5.09
Mn*	0.10
U*	0.40
$SO_4^{=}$	714.00
F^{-}	3.00
Cl^{-}	1925.00

---

*All valence states

Note: The following elements were not detected: Ag, Cd, Co, Cr, Cu, Fe, Mo, Ni, P, Pb, Sb, Se, Sn, Th, Ti, Tl, Zn, Zr

The permeability of triaxially loaded St. Peter sandstone to hot air has been measured. The test sample was recovered from the 210 m (689 ft) depth in borehole Yakley No. 1. This is a very competent part of the formation, with a permeability in the lower range for the St. Peter. The experimental parameters were: 1) sample and air temperatures 22°C (72°F) and 93°C (200°F), 2) confining pressures (hydrostatic) of 8.28 MPa (1200 psi) and 17.25 MPa (2500 psi), and 3) pore air pressure of 1.898 MPa (275 psi). These values were chosen to simulate future field test conditions within the Pittsfield reservoir.

The results of 67 measurements are summarized in Fig. 7. Permeability of the sandstone was measured perpendicular to the bedding by adjusting values of the air flow rate and pressure drop across the core. The data ranges shown in Fig. 7 represent ± one standard deviation from the mean at each test temperature. At 22°C (72°F) 29 measurements were averaged and evaluated whereas at 93°C (200°F) 38 measurements were averaged and evaluated. Increasing the confining pressure to 17.25 MPa (2500 psi) had no effect on the measured permeabilities. This demonstrates that the 8.28 MPa (1200 psi) confining pressure was adequate to prevent spurious air flow between the specimen and its jacket. The permeability results at 22°C (72°F) obtained in the flow facility are consistent with the population of "least permeabilities" measured with zero confining pressure and 1 atmosphere pore pressure (Fig. 7). Although the data in Fig. 7 show permeability decreasing with temperature by almost 60 md from 22°C (72°F) to 93°C (200°F), more experimentation is necessary (and underway) to quantify the significance of this response. Samples from other depths and well locations require study before this quantitative behavior can be established.

A dehydration curve for St. Peter sandstone is shown in Fig. 8. The experimental parameters were as follows: 1) sample origin-borehole Yakley No. 1, depth 210 m (689 ft), 2) confining pressure 8.28 MPa (1200 psi), 3) pore pressure 1.898 MPa (275 psi), 4) sample temperature 93°C (200°F). Dry air at an absolute humidity of 0.01% and a flow rate of 3 to 4 cm^3/sec was injected into the sample. Moisture removal from the rock was monitored by measuring the effluent air humidity. The high initial rate of moisture removal gradually decreased as the outlet air humidity approached the inlet air humidity. A portion of the residual water may not be removable under these conditions because of isolation in blind pores and high capillary forces.

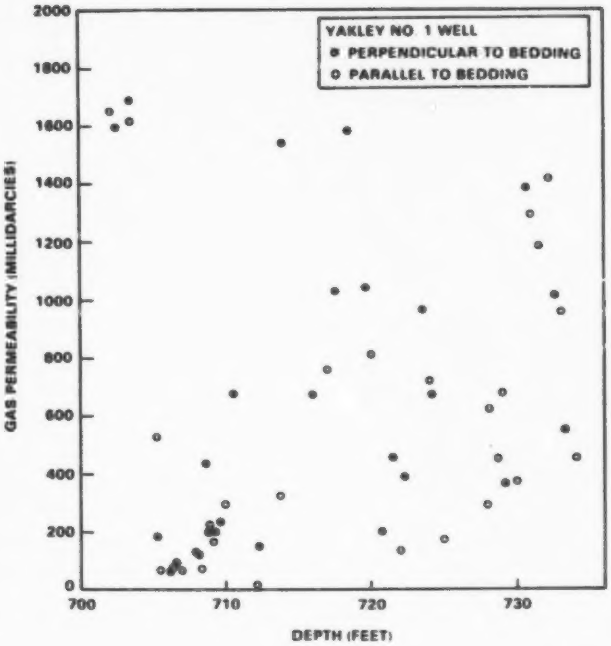

Fig. 6. Data for Permeability as a Function of Depth

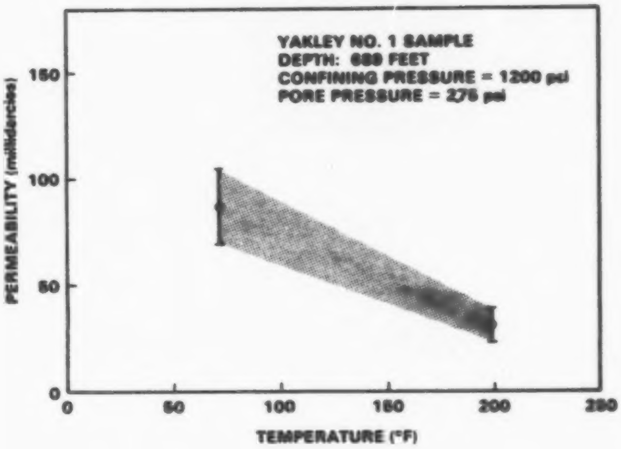

Fig. 7. Permeability versus Temperature Measurements for Yakley No. 1 Sample

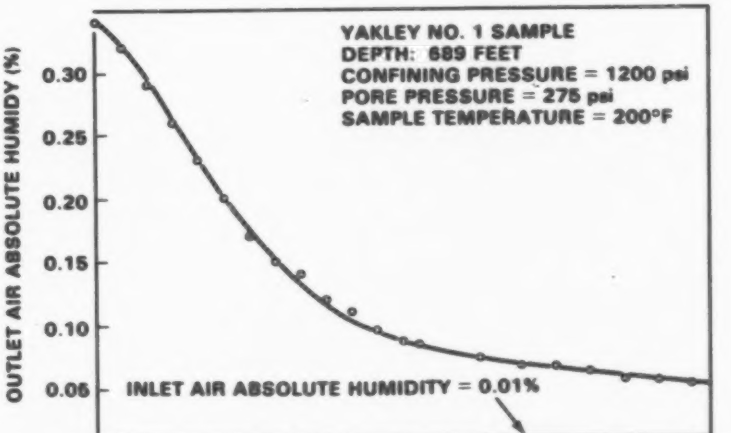

Fig. 8. Dehydration Curve for St. Peter Sandstone

Planned experiments on the St. Peter sandstone will detail 1) air permeability and fatigue under cyclic CAES conditions and 2) various rates and mechanisms of desaturation. This specialized work will be coordinated with standard reservoir testing on Pittsfield core by PB-KBB Inc. The combined data will provide an expanded data base for modeling predictions and field test evaluation.

FUTURE WORK

From the standpoint of numerical modeling, an important aspect of the field test program will be to evaluate the predictive accuracy of models. Testing of assumptions and evaluation of certain sensitive parameters based upon field experience could enhance model accuracy. The areas of particular interest are bubble development, water coning, thermal development, cyclic pressure response and reservoir dehydration. Site specific variations in geologic environment such as permeability variations and structural or stratigraphic non-uniformities will test the generalizations. The field test values are necessary to formulate rational and economical numerical tools.

Future experiments in the porous media flow facility will determine detailed response of the St. Peter sandstone to temperatures, pressures and humidities in the presence of confining pressures, all selected to represent probable field study combinations of these parameters. Properties measured will include permeability, Young's modulus, compressibility, coefficient of thermal expansion, cyclic fatigue, thermal spalling and desaturation.

Future directions in both numerical modeling and laboratory experimentation will be influenced by reservoir findings at the Pittsfield site. Continuous interpretation of field results generated by the PB-KBB Inc. team through its liaison with PNL will enable timely shifts in program emphasis.

REFERENCES

1. L. E. Wiles and R. A. McCann, Water Coning in Porous Media Reservoirs for Compressed Air Energy Storage, PNL-3470, Pacific Northwest Laboratory, Richland, WA, June 1981.

2. D. L. Katz, M. R. Tele, K. H. Coats, M. L. Katz, S. C. Jones and M.C. Miller, Movement of Underground Water in Contact with Natural Gas, The American Gas Association, New York, 1963, p. 129.

3. L. E. Wiles, Numerical Analysis of Temperature and Flow Effects in a Dry, Two-Dimensional, Porous Media Reservoir Used for Compressed Air Energy Storage, PNL-3047, Pacific Northwest Laboratory, Richland, WA, October 1979.

4. L. E. Wiles, The Effects of Water on Compressed Air Energy Storage in Porous Rock Reservoirs, PNL-2869, Pacific Northwest Laboratory, Richland, WA, March 1979.

BEST DOCUMENT AVAILABLE

PROJECT SUMMARY

Project Title:	Compressed Air Energy Storage (CAES) Aquifer Field Test - Conceptual Design, Construction and Operation
Principal Investigator:	John A. Istvan
Organization:	PB-KBB Inc. Subsurface Systems and Technology Houston, Texas 77024
Project Goals:	Field evaluation of a typical aquifer for storing and cycling compressed air under conditions similar to those which would be obtained in a full scale CAES operation. Determine the effect of varying injection temperature from ambient to 200°C. Preliminary laboratory reservoir stability and simulation criteria will be modified based upon actual field data. Post injection core testing will determine the permanent effect of air injection on the formation.
Project Status:	Well field design is completed and seven wells are being drilled: One injection/withdrawal well, two close-in instrument wells and four sampling/logging wells. Design of surface injection package has been completed and bids for construction are being evaluated. Cores are being analyzed and data transmitted to Battelle for modeling and simulation of bubble development and withdrawal cycling. Instrumentation package is being finalized as to temperature and pressure equipment, type of psychrometers, installation procedures, and data collection equipment on the surface, such as gauges and recorders.
Contract Number:	B-82313-A-L
Contract Period:	January 20, 1981 through July 1, 1983
Funding Level:	$2.2MM
Funding Source:	U.S. Department of Energy through Pacific Northwest Laboratory, operated by Battelle Memorial Institute.

COMPRESSED AIR ENERGY STORAGE AQUIFER FIELD TEST
CONCEPTUAL DESIGN, CONSTRUCTION AND OPERATION

John A. Istvan
PB-KBB Inc.
Subsurface Systems and Technology
Houston, Texas

ABSTRACT

The field experiment under development near Pittsfield, Pike County, Illinois is discussed with regard to site characterization, Illinois Environmental Protection Agency permitting, specific numerical modeling, injection/withdrawal well construction, monitoring and sampling/logging well field layout, surface plant design, and project status.

INTRODUCTION

The Pacific Northwest Laboratory, operated for the U.S. Department of Energy by Battelle Memorial Institute, entered into a contract with PB-KBB Inc. of Houston, Texas, on January 20, 1981 to design, procure, construct and install all components necessary to conduct a field experiment involving injection of compressed air into a shallow confined sandstone aquifer. The contract also includes all aspects of drilling, well completion, surface equipment installation, monitoring device installation, air injection, reservoir monitoring and pre-test/post-test reservoir rock and caprock evaluation and site restoration.

The final product of this endeavor is to include the following: 1) demonstration of injection, storage and recovery of compressed air; 2) evaluation of numerical modeling and laboratory conclusions about CAES behavior in aquifers; and 3) evaluation and modification of preliminary reservoir stability criteria. Simultaneous activities in field experimentation, numerical modeling and laboratory testing are expected to have synergistic effects upon resolution of particular criteria.

This project is to be carried out in a rural portion of Pike County, Illinois. The area is characterized by gently rolling pastureland, lightly wooded tracts and intermittent streams. Economic activities within the near region include farming, cattle and hog raising, and light manufacturing. The compressed air energy storage experiment will not impose deleterious effects upon either the economic regime or natural habitat of the area.

SITE SELECTION AND CHARACTERIZATION

To store compressed air by water displacement, a trap consisting of an impermeable caprock formation overlying a permeable water-bearing formation is necessary to prevent vertical air leakage.(1) The boundary between impermeable and permeable beds must be convex upward to prevent horizontal leakage. Such a structure may be a closed anticline, dome or lens. (Figure 1)

Site screening and selection involved establishing geologic criteria for the overlying caprock and the sandstone reservoir. These criteria were chosen to enable injection of an air bubble, and subsequent air cycling by injection and withdrawal at various temperatures, over a period of one to two years. Structure and lithology were sought to safisfy the following field design characteristics:

- depth to reservoir: 200 m (656 ft)
- radius of reservoir: 100 m (328 ft)
- thickness of reservoir: > 10 m (32.8 ft)
- reservoir pore volume: up to 10^6 m^3 (1.307 x 10^6 yd^3)
- reservoir permeability: > 300 md
- vertical closure: > 10 m (32.8 ft)
- caprock thickness: > 6 m (19.7 ft)
- caprock threshold pressure: > 1380 kPa (200 psi)
- lithology: impermeable carbonate or shale over pure sandstone
- ground water discovery pressure: 1.035 kPa (150 psi) or higher
- ground water gradient: negligible and no communication with potable aquifers.

Eleven potential sites (2) were identified in Illinois on the basis of prior drilling activities. These sites were chosen for screening on the basis of generally favorable stratigraphy, structure, and accessibility. After screening, the Pittsfield anticline in Pike County which trends WNW for about 30 km, was the leading candidate site.

Site characterization used techniques which have been successfully applied to proving natural gas reservoirs. These consist of drilling; visual and geophysical logging; mineralogical analysis; measurements of permeability, porosity and threshold pressure; seismic reflection/refraction prospecting; and hydrology analysis with respect to discovery pressure, ground water gradient, and water chemistry. An extensive confirmatory drilling and seismic program (2) was conducted to verify the presence of a suitable second order dome within the larger Pittsfield anticline. This dome is about 1200 m in diameter and somewhat dumbbellshaped with a larger lobe toward the south. The dip of this structure averages near 1 degree.

The Ordovician St. Peter sandstone, a blanket formation covering hundreds of square kilometers, is the candidate compressed air reservoir bed. Its porosity is typically 15-20% and its laboratory permeability is generally more than 300 md. Ground water within the St. Peter is confined by a head of about 122 m which corresponds to a discovery pressure of 1.195 MPa. Three successive impervious carbonate formations overlie the St. Peter, i.e., the Joachim dolomite, the Platteville dolomite and the Galena limestone. Their combined thickness is 160 m. Extensive core analyses indicate the caprock sequence is more than sufficient to retain air at more than 1.20 MPa. (Figure 2)

A 160-acre drilling and facility installation lease on the land overlying the eastern one-half of the dome was negotiated with Mr. Elmer Yakley. All surface and subsurface operations will be conducted within this area. The CAES injection facility will be located on about five acres. The western one-half of the dome underlies property owned by Mrs. Bertha Mumford. An air storage lease has been negotiated with her for the 160 acres over that portion of the structure. Air storage options are available within a two mile radius.

ILLINOIS ENVIRONMENTAL PROTECTION AGENCY (IEPA) PERMITS

Pacific Northwest Laboratory prepared a comprehensive application to the IEPA for a Construction Permit to drill and complete the injection well. This application included a thorough feasibility study which was supported by a geologic/hydrologic exploration report prepared by Dames and Moore of Park Ridge, Illinois. (2)

Initial application was made on March 9, 1981. After answering two requests for additional data, approval of the "Form A" application was granted on June 8, 1981.

Constraints on the project are as follows:

- Wells are to be installed as proposed in the application.
- I/W well depth shall not exceed 700 ft. (213 m)
- Drilling permits are to be obtained from the Department of Mines and Minerals prior to installing wells.
- IEPA is to be advised 10 days prior to commencing drilling of the I/W well.
- A well completion report is to be submitted for the I/W well.
- Construction and completion of facilities will be certified by an Illinois registered P.E. to confirm completion according to approved plans and documents.

IEPA requested that they be advised when drilling would be under way so that they could observe procedures. During completion of the injection/withdrawal (I/W) well, members of IEPA inspected the site and approved the installation.

Before air injection commences, an Operation Permit (Form B) must be obtained. That application requires a thorough well completion report including discussion of hydrogeology, injection equipment, and monitoring procedures. This application is being prepared.

NUMERICAL MODELING

Numerical models developed at PNL enable simulations of air injection and cycling within the environment of a porous medium reservoir. These models are being applied to parametrically evaluate the significance of specific reservoir properties. Results from this modeling will have considerable influence on the design of field tests and on some specifications for injection and monitoring equipment. Reservoir properties incorporated into the models include dimensions, physical properties and operating conditions. The areas being addressed include bubble development, water coning, thermal development, and reservoir dehydration. This work is reported in detail by Wiles et al. (3)

As new field and laboratory data are acquired, these will be transmitted to the CAES Program Office for use in concurrent numerical modeling, i.e., to adjust programs so that they reflect properties and processes identified in the field.

INJECTION/WITHDRAWAL WELL

A surface hole of 12.5 inches (31.75 cm) diameter was drilled to a depth of 60 ft. (18m). The lowest 2 ft. (61 cm) penetrated bed rock. Ten and 3/4" (27.3 cm) diameter casing was installed and cemented back to the surface. On the next day, the shoe was drilled out and the hole was then drilled to its core point at 639 ft. (195 m) using air and foam. From 639 ft. (195 m) to 669 ft.(204m) (9.15 m) of core was obtained. This core represents vuggy Joachim dolomite, greenish "transition" sandstone at the top of the St. Peter, and clean white St. Peter sandstone below the transition zone.

Gamma-ray/neutron, density, resistivity, dipmeter and deviation logs were run to enable correlation of the stratigraphy with exploratory holes Yakley No. 1, Yakley No. 7 and Mumford No. 3.

New oil field casing was installed to 664 ft. (202.4 m) depth. This installation had the following specifications: seven in. (17.8 mm), K-55, long thread and coupling, 23 lb/ft, Bakerloced, properly torqued and Gatorhawk externally tested with a friction reducer in the test fluid, in the slips for one minute and in tension for one minute before being run into the hole. Casing was cemented in tension with 175 SX of Class A with 35% silica flour and 2% $CaCl_2$.

The well will be gravel packed and instrumented as shown. (Figure 3). Instrumentation will not be installed until just prior to injection to minimize calibration problems. This package will enable continuous monitoring and recording of temperature, pressure and humidity. Injection pressure will be not more than 2.07 MPa (300 psi). Volume injection rate will not exceed 35.4 SCMm (1250 SCFm). Relative humidity of injected air will be about 5% or less. The temperature of injection will vary from ambient to 200°C (392°F).

INSTRUMENTATION WELLS

Two or more close-in wells will be drilled at about 3 m (9.84 ft) and 6 m (19.68 ft) from the I/W well. These wells will be instrumented with thermistors, piezometers and thermocouple psychrometers to enable continuous detection and recording of temperature, pressure and humidity. These wells will be surveyed so that exact locations of the sensing heads will be known. These wells will permit accurate following of early bubble growth, desaturation and thermal growth within the reservoir. Close-in wells will also measure fluctuations in physical properties during air cycling at ambient and higher temperatures. (Figure 4)

SAMPLING AND LOGGING WELLS

Four wells which permit water sampling, geophysical logging and wireline monitoring were drilled at different directions and radii from the I/W well. All are located on the eastern half of the air storage dome in an array that takes advantage of structure symmetry demonstrated in previous exploration. These wells will allow tracking of the bubble as it develops. Fluid in the wells can either be pushed through the St. Peter by the encroaching air bubble or raised to the surface with an oil field plunger (rabbit). Temperature, pressure and relative saturation can be measured through a lubricator by wireline methods. (Figure 5) Lynes, Inc. temperature and pressure detecting devices and Wescor thermocouple psychrometers will be used. Energy Resource Management of Cannon Beach, Oregon will calibrate and install the instrumentation.

SURFACE PLANT

The surface plant will use a skid-mounted injection facility consisting of an air compressor, booster, dehydrator, heater, and all piping and instrumentation necessary to meet injection requirements. The plant will provide for steady-state injection and cyclic injection and withdrawal to simulate the operations of one well within a full-scale CAES plant. The injection/withdrawal frequency will be from two to four cycles per day based on final numerical modeling of the reservoir/plant capability. In no case will the injection pressure exceed 60% of the integrated caprock threshold pressure. Measurements of temperature, pressure, mass flow rate and humidity will be continuously recorded. A bypass test section with sampling manifold will enable particulate sampling by filter during withdrawal of air from the reservoir. (Figure 6)

PROJECT STATUS

Geologic exploration was completed in February 1981, with the identification of a second order dome at a depth of about 197 m (645 ft) west of Pittsfield, Illinois. (1) Land leasing, I/W well permitting, I/W well drilling and completion, and sampling/logging well drilling are complete. Site development now under way includes surface plant layout, road access and PNL is arranging for utility connections. Numerical modeling is being based on geologic, geometric and operating parameters - all specific for this experiment-to provide quantitative inputs to field design decisions. Laboratory examinations of reservoir and caprock specimens are continuing. The final design procurement initiation of the compressor plant, monitoring well field and instrumentation, and ancillary equipment is on schedule. Completion of the installation, injection of the air bubble, and initial air cycling experiments are scheduled for FY-1982.

REFERENCES

1. R.D. Allen, L.D. Kannberg, and T.J. Doherty, "Aquifer Field Test for Compressed Air Energy Storage", *Proceedings of the 16th Intersociety Energy Conversion Engineering Conference*, Atlanta, GA, August 9-14, 1981.

2. J.S. Trapp and T.E. Jensen, *Geologic and Hydrologic Input to Feasibility Study for Battelle Pacific Northwest Laboratories*, D&M Job No. 09781-002-07, Dames and Moore, Park Ridge, IL, March 6, 1981.

3. L.E. Wiles, R.L. Erikson, R.D. Allen and T.J. Doherty, "Numerical and Experimental Analyses of the Porous Medium Reservoir at Pittsfield, Illinois", presented at the 1981 Annual Contractors Review Meeting, Washington, D.C., August 24-26, 1981.

BLANK PAGE

MAGNETIC ENERGY STORAGE PROGRAM

BLANK PAGE

PROJECT SUMMARY

Project Title: Magnetic Energy Storage Program Overview

Principal Investigator: Mitchell O. Hoenig

Organization:
Francis Bitter National Magnet Laboratory
Massachusetts Institute of Technology
167 Albany Street NW16-176
Cambridge, Massachusetts 02139

Project Goals: MIT's role has been that of DOE's SMES Program monitor and adviser to DOE.

Accomplishments: Preparation of request for proposal and quotation (RFP/Q) for a 10,000 MWh diurnal SMES system. The document was completed in March 1981.

Review of overall SMES Programs, including technology at LASL, University of Wisconsin as well as work by O. Mawardi on the concept of a force compensating SMES coil.

Preparation of a final report, in view of the termination of our contract. This work is in process.

Contract Number: DE-AC02-80ET26502

Contract Period: 1 September 1980 through 31 August 1981

Funding Level: $80,000

Funding Source: U.S. Department of Energy, Division of Energy Storage

MAGNETIC ENERGY STORAGE PROGRAM OVERVIEW

Mitchell O. Hoenig
Francis Bitter National Magnet Laboratory
Massachusetts Institute of Technology
167 Albany Street
Cambridge, Massachusetts 02139

INTRODUCTION

MIT's role during the current fiscal year has been limited to that of technical monitor and advisor to DOE.

DOE POSITION ON SMES

DOE's position on diurnal SMES as of March 1, 1981 was as follows:

(1) Generate and support a major scoping study of a large SMES system. This was to be done by an industrial firm in response to an RFP/RFQ to be prepared by MIT.

(2) Reach a decision whether or not to proceed with SMES before the end of 1983. The decision was to be reached following a review of the industrial scoping study.

(3) Proceed to build a 0.5 to 50 MWh demonstration SMES plant or relegate SMES to long range programming.

The RFP/RFQ documentation for the scoping study was completed in March 1981 by MIT and was approved by DOE for preliminary issue to potential bidders. The RFP/RFQ was never formally issued due to lack of DOE funding. A new scoping study, funded by EPRI is however due to be initiated before the end of CY1981. A new RFP/RFQ was prepared and issued by EPRI in June 1981, in collaboration with DOE.

The scoping study will be performed by one of six bidding teams, to be selected shortly and should be completed by July 1, 1983.

MIT POSITION ON SMES

Our participation as technical monitors and consultants to DOE will terminate with the completion of our current contract on August 31, 1981.

We have drawn the following conclusions as the result of our participation in the program.

(1) LASL's program to build a 30 MJ SMES unit for electric utility transmission line stabilization on the Bonneville Power Administration system[1] should be given top priority. Its successful operation will be a major input to the DOE decision whether or not to proceed with the diurnal SMES demonstration plant.

(2) The University of Wisconsin (UW) has demonstrated state-of-the-art technology which will be needed for a large SMES system. New and innovation concepts, materials and fabrication techniques are needed in addition to UW's achievements. These must be brought to a practical technological level, before they can be evaluated economically and integrated into a master plan.

(3) Innovation concepts are needed in the following technological areas.

(a) Conductor

The UW monolithic conductor[2] is insufficiently flexible for field installation in a deep SMES. We believe a flexible cable more in line with the LASL-30 MJ conductor should be developed and tested on the basis of 50 kA, 1.8 K and 1 atm operation.

(b) Cryostat and Cryogenics

The UW cryostat and He II concept[3] relies on a large reservoir of helium. On the basis of a low aspect ratio SMES coil this could represent 10 to 50 million liters of helium II inventory. An integral cryostat in the form of a tight casing around the cable, manufactured above ground, looks like a solution to the problem. This again calls for hardware development and testing. Problems of heat transfer and protection must be answered.

(c) Protection

The concept of a 1 to 10 GWh SMES coil with a common vacuum chamber would require an expensive and cumbersome protection resistor. The alternative which appeals to us is a set of perhaps ten separate concentric coils, each designed to store 11.1% of total energy, with each in a separate vacuum chamber. The coils would be closely coupled magnetically. If any one of the ten coils would lose vacuum, lose helium or show signs of a quench, it would be switched to discharge to a small, series connected external resistor. Most of its energy would then be induced magnetically into the other nine coils which would remain in service. This concept should not only be studied further, but should in our opinion be at least computer simulated. If such a concept is feasible , it would offer the following advantages: (i) reduced concern about the possibility of a quench, (ii) ability for utility use of the facility to continue indefinitely on the basis of 90% capacity, (iii) repair if necessary at a convenient time, and (iv) use of a considerably smaller protection circuit.

(4) Consolidation of DOE's and possibly EPRI's effort on the basis of long term planning with industry. A technical SMES board of directors with a small technical staff and authority over developmental programs is suggested.

(5) The question of environmental shielding should be resolved as soon as possible. The cost of shielding a low aspect ratio 10 GWH coil system is such as to make this type of design uneconomical.

1980-81 ACCOMPLISHMENTS

Progress on the LASL - 30 MJ SMES system will be described by R. Schermer (LASL) and J. Purcell (GAC) in subsequent papers. While limited by funding constraints, the program has maintained its momentum and should meet its objectives within the next two years.

Work at the University of Wisconsin has been greatly disturbed by funding constraints at DOE. Progress has been made in areas of superfluid helium technology and conductor development. Unfortunately their representatives are not participating in this conference.

In Japan work is progressing at JAERI and ETL/Tsukuba. Potential objectives have been described in the literature.[4] At JAERI subsize 10 kA prototype pool boiling cables, made by Mitsubishi and Toshiba have been tested successfully. L. Dresner of ORNL, USA is collaborating at JAERI in the design of force cooled cabled conductors. Several companies are participating in a design study of a 100 MJ, 2 m diameter, 50 kA, 8 T pulsed energy storage coil for fusion. At Tsukuba a 100 kJ, approximately 2 m diameter toroidal, diurnal SMES coil has become operational. Work is proceeding on a 1 MWh toroidal SMES storage coil to be completed in 1985. This coil would have an overall diameter of 20.8 m.

The most significant technological advancements have been made by the French CEA laboratories in superfluid helium technology,[5] where this coolant will be used in the recently funded Torr Supra tokamak on a scale which includes six 2 m diameter toroidal superconducting coils.

REFERENCES

1. R.I. Schermer, "30-MJ Superconducting Magnetic Energy Storage for BPA Transmission Line Stabilizer," Proc. Mech., Magnetic, and Underground Energy Storage 1980 Annual Contractors Review Meeting, CONF-801128, pp. 256-262.

2. S.W. Van Sciver, K.S. Haw, K.T. Harting, G.F. McIntosh and W.C. Young, "Conductor and Structural Component Studies for Diurnal Energy Storage," Proc. Mech., Mag., and Underground Energy Storage 1980 Annual Contractors Review Meeting, CONF-801128, pp. 280-286.

3. Y.M. Eyssa and R.W. Boom, "Diurnal Superconductive Energy Storage System Design," Proc. Mech. Mag. and Underground Energy Storage 1980 Annual Contractors Review Meeting, CONF-801128, pp. 271-278.

4. J.D. Rogers, "Magnetic Energy Storage," IEEE Trans. on Magnetics MAG-17, No. 1, January 1981, pp. 330-335.

5. G. Claudet and P. Seyfert "He II Thermodynamics and Phase Transition Dynamics," 1981 Cryogenic Engineering Conference, August 10 - 14, 1981, San Diego, California, paper KA-3.

PROJECT SUMMARY

Project Title: Superconducting Magnetic Energy Storage (SMES)

Principal Investigator: John D. Rogers

Organization: University of California
Los Alamos National Laboratory
Los Alamos, NM 87545
(505) 667-5427; FTS 843-5427

Project Goals: The goals of the SMES program are two-fold. These are to design, fabricate, and place into operation a 30 MJ, 10 MW SMES unit for electric utility transmission line stabilization on the Bonneville Power Administration (BPA) system by 1983. The second goal is to design and have constructed a SMES unit up to 10 MWh size. This unit will be a completely engineered prototype of an electric utility diurnal load leveling system. A superconducting fault current limiter for utility application, based upon SMES technology, fusion program technology, and a variation of a Westinghouse Electric Corp. circuit concept, is being spun-off from the program for evaluation and development.

Project Status: The engineering of the BPA SMES transmission line stabilization system is in an advanced state. All large hardware items are complete or delivered except the nonconducting dewar. The 30 MJ coil was completed by General Atomic Co. (GA). The design of the seismic coil interface to the dewar mounting is complete and an order was placed with GA for the coil mounting to be made. The converter was delivered to Los Alamos and is undergoing tests with computer control. The transformers that connect between the power transmission line and the converter have been delivered to the BPA Tacoma Substation. The heat rejection unit is being operated in conjunction with testing of the converter. The gas recovery unit was delivered and successfully operated after repair of one of the Corblin compressors. The trailer mounted refrigerator was repaired by the manufacturer for damage incurred during shipping and has been returned to Los Alamos for testing and operation. The hardware procurement for the control and data acquisition system is complete. Software for the control system is 60% complete. An environmental evaluation for installation of the unit at the BPA Tacoma Substation was finished.

Contract Number: W-7405-ENG-36

Contract Period: Continuing

Funding Level: $1,550,000 FY81

Funding Source: Department of Energy, Division of Physical and Chemical Energy Storage and Division of Electrical Energy Systems.

This summary covers papers of the following
authors: Schermer, Criscuolo and Purcell.

30 MJ SUPERCONDUCTING MAGNETIC ENERGY STORAGE FOR BPA TRANSMISSION LINE STABILIZER

R. I. Schermer
Los Alamos National Laboratory of the
University of California
Los Alamos, New Mexico 87545

ABSTRACT

The Bonneville Power Administration operates the transmission system that joins the Pacific Northwest and southern California. A 30 MJ (8.4 kWh) Superconducting Magnetic Energy Storge (SMES) unit with a 10 MW converter can provide system damping for low frequency oscillations. The unit is scheduled to operate in 1982. Progress during FY 81 is described. The coil is complete. All major components of the electrical and cryogenic systems have been received and testing has begun. Computer control hardware is in place and software development is proceeding. Support system components and dewar lid are being fabricated and foundation design is complete. A contract for dewar fabrication is being negotiated.

INTRODUCTION AND SUMMARY

The Pacific Northwest and southern California are part of the Western U.S. Power System and are connected by two 500 kV, ac-power transmission lines, collectively referred to as the Pacific AC Intertie and one ± 400 kV dc-transmission line, the Pacific HVDC Intertie. These transmission lines are operated by the Bonneville Power Administration (BPA).

The stability of the Western Power System is affected by the relative weakness of the tie provided by the 905-mile-long Pacific AC Intertie. Studies made before energization of the Pacific AC Intertie showed that negatively damped oscillations with a frequency of about 20 cpm were likely to occur, and in 1974 negatively damped oscillations with a frequency of 21 cpm (0.35 Hz) were observed. Subsequent to these instabilities, BPA installed equipment on the HVDC Intertie to modulate power flow between the interties, damping the oscillations, and increasing the stability limit of the Pacific AC Intertie from about 2100 MW to 2500 MW, whenever the HVDC Intertie is operating. However, the availability of the HVDC Intertie is 89.5%, and the southern terminal was down for six months at one time as a result of earthquake damage. A back up stabilizing system could be used. Late in 1975, representatives of BPA and the Los Alamos National Laboratory developed the concept of installing a small SMES unit for the purpose of providing system damping similar to that now available through modulation of the interties. The design parameters of the unit to be installed at the Tacoma Substation are summarized in Table 1.

Several descriptions of the project have appeared previously,[1,2,3,4] and should be consulted for details. This report will concentrate principally on the work done in FY 81.

TABLE 1

DESIGN PARAMETERS OF THE 30-MJ SYSTEM STABILIZING SMES UNIT

Maximum power capability, MW	10
Operating frequency, Hz	0.35
Energy interchange, MJ	9.1
Maximum stored energy, MJ	30.0
Coil current at full charge, kA	4.9
Maximum coil terminal voltage, kV	2.18
Coil operating temperature, K	4.5
Coil lifetime, cycles	$>10^7$
Heat load at 4.5 K, W	<150
Coil diameter, m	3.0

Figure 1 is an isometric view of the 30 MJ system components in their planned arrangement. At the upper left of the figure is the ac-dc converter flanked by two, 6 MVA, transformers. The right half of the figure is occupied by the cryogenic system -- refrigerator, heat rejection subsystem, gas recovery subsystem, liquid nitrogen supply, and gaseous helium supply with each subsystem housed in its own trailer. Not shown is the control trailer, located immediately behind the cryogenic system trailers, that houses the mini-computers which permit the system to run unattended. All of the above subsystems have been assembled at Los Alamos for test under computer control prior to final assembly at Tacoma. The coil and nonconducting dewar will be shipped directly to Tacoma without a test at Los Alamos.

In the center of Fig. 1 is the coil, contained within its fiber-reinforced plastic liquid helium vessel. The coil is complete and is waiting at General Atomic to be attached to the seismic mounting elements and the dewar lid. Dewar procurement has been delayed by contract placement difficulties; the dewar is the critical path item.

SITE PREPARATION

All the cryogenic, electrical and control equipment has been placed in location at Los Alamos, with all necessary interconnecting plumbing and electric power, control and signal cables. All of the interconnecting hardware will be usable at Tacoma without modification.

Foundation plans have been transmitted to BPA but no work has begun at the Tacoma Substation.

COIL CONSTRUCTION

Conductor qualification tests were described at the 1980 Annual Contractors' Review.[4] New England Electric Wire delivered finished conductor to General Atomic (GA) on a timely basis over the last five months of 1980, with the last spool of conductor arriving on schedule in January, 1981. GA completed coil winding in March, 1981, and coil assembly in July, 1981, both dates slightly ahead of schedule. Construction was performed at a cost of approximately $950,000, which was $180,000 under the contract price. Coil details are given in the following paper by J. Purcell.[5]

COIL SUPPORT

Support of the superconducting coil against seismic loads was described previously.[4] The support system is shown in Fig. 2. In FY 81 the details of the support system were defined, and the interaction of the support elements with the rest of the 30 MJ system was examined. This detailing process, which involved several iterations of design and computer analysis, is complete.

Fabrication drawings for all the support elements were prepared at Los Alamos. These elements will be procured and installed by GA under an extension of the coil construction contract. All elements are currently being fabricated.

A major component of the support system is the stainless steel dewar lid, which is also a complex interface for the coil electric and cryogenic systems. Lid design at Los Alamos extended into the late spring of 1981. Based on competitive bidding, a contract for lid fabrication has been

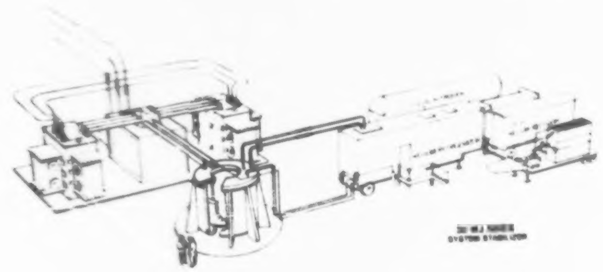

Fig. 1. Isometric view of 30-MJ system layout.

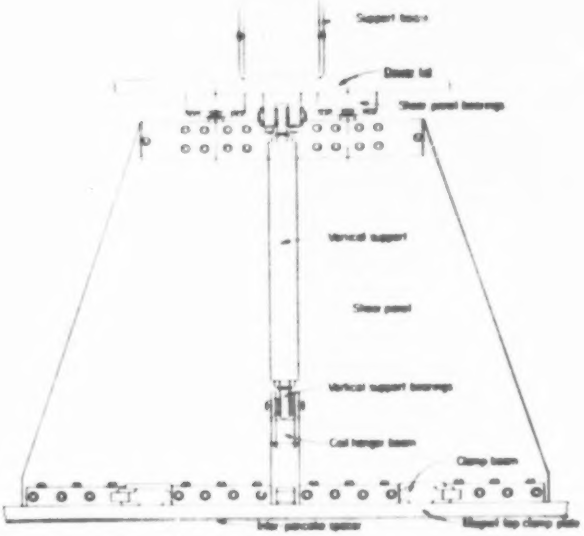

Fig. 2. 60-degree segment of coil support system. View along radius from coil o.d.

placed with Monarch Machine of Los Angeles, CA, at a cost of $41,000. Current scheduling calls for the lid to be completed in October 1981 and to be shipped to GA to facilitate alignment and assembly of the support components. The lid will then be shipped to the dewar vendor -- approximately in February, 1982 -- to be used in the dewar acceptance test and also as a template for the dewar flange bolt holes. Finally, the lid will be returned to GA where it will be permanently mounted to the coil supports. The coil will be shipped to Tacoma with the supports and lid attached.

The lid is suspended by bolts from six stainless steel support beams (Fig. 1), which span the gap between the inner and outer concrete pillars. Fabrication drawings have been prepared by Los Alamos for these beams and an RFQ has been issued for them.

Design of the concrete pillars and foundation for the coil and dewar was performed by a Civil Engineering group at the Los Alamos National Laboratory. At their request, BPA performed a soil test at the proposed coil location in their Tacoma, WA, substation. This test shows a 10 ft. thick surface layer of sand and gravel, underlaid with 5 ft. of peat, resting on a base of sand and gravel. Because of the measured high compressibility of the peat, an unsupported foundation would settle approximately 10 in., which would be unacceptable if the structure tilted so that the support pillars were no longer vertical. A decision was made to use pilings under the foundation to eliminate the settling. Structural drawings were prepared and transmitted to BPA. Preliminary estimate of the foundation cost is $50,000.

DEWAR

Bids were received from five prospective vendors for construction of the fiber reinforced plastic dewar. Out of several options presented we selected, on the basis of price and technical merit, a system with an epoxy/glass fabric liquid helium vessel and a polyester/chopped glass room temperature vessel. The epoxy vessel will be fabricated by wet, hand layup over a specially constructed wood and plaster mold and cured at approximately 150° F using hot air in a plastic bag. The polyester vessel will be formed by chopper gun spray over a second mold, after which the two vessels will be permanently bonded together to form the vacuum seal. Materials and fabrication techniques were developed by consultants to the prospective vendor in the course of fabricating numerous dewars that were approximately the required diameter, 3 m, but smaller in height.

Technical evaluation of the bids was performed in January 1981 and a prospective vendor selected. Great difficulty was experienced in actually placing the contract, however; and the process is still not complete at this writing. All of the bids which were considered technically and economically feasible were from small companies, with no permanent work force, supplies or equipment, and record keeping and accounting practices not up to government standards. The process of auditing and qualifying the prospective vendor has been long and tedious. The dewar is clearly the critical path item for the project, even with a promised delivery date of seven months after award of contract.

ELECTRICAL SYSTEM

The 10 MJ converter was installed and electrically connected to an existing 3.25 MVA transformer unit. Damage that occurred to the converter when it was delivered was found to be limited to the sheet metal cabinet and had no effect on the electrical circuitry. Two bent doors had to be replaced. An 800 kW liquid cooled load dump was designed and built to be used as a resistive load for the converter. The heat rejection system was connected to the load dump. Ethylene glycol is being used as the coolant in the closed cycle loop. Load tests were performed at different current levels up to the rated current of 5000 A. The current distribution in the eight parallel connected SCRs of each bridge leg shows too wide a spread. This problem is being investigated. The converter has been controlled manually from the computer control panel to our full satisfaction. Different fault conditions have been simulated and the converter logic has responded properly.

One of the two 6 MVA power transformers was damaged during shipment and had to be repaired at the supplier's plant. The rebuilt transformer was tested at the plant, was accepted by Los Alamos personnel, and was then shipped to Tacoma. Both power transformers are now at the Tacoma site awaiting the arrival of the other system components.

There was significant progress in the design and installation of the control, instrumentation, and data acquisition system. Software development work for the three DEC PDP-11-23 microcomputers concentrated on supervisory control and on the subprograms for starting and running the converter and the heat rejection system. The converter control programs have been completed and checked including the signal paths from and to the converter. An accompanying paper[6] explains in more detail the work performed in the control, instrumentation, and data acquisition system.

CRYOGENICS

All the components of the cryogenic system are mounted on trailers, as seen in Fig. 1, to be portable. The refrigerator trailer, containing the Koch Model 2800 helium liquefier/refrigerator and its associated piping and controls, was originally received from Helix Corporation (predecessor to Koch) in September, 1980. Initial testing revealed serious internal damage to the liquefier cold box caused by improper packaging during shipment. Rather than simply returning the cold box, the entire trailer was returned to the vendor. This permitted a minor modification to be performed on the compressor, a step necessitated by field experience acquired since the original compressor order was placed. Simultaneously, the trailer frame was straightened and braced. Problems with various water cooling systems in the trailer, caused by contamination of unknown origin, increased both the time and cost of the repairs. The trailer was tested after repair and was returned to Los Alamos in early July, 1981. Because of the delay, a major milestone, testing the complete cryogenic system under computer control, has been shifted from August, 1981 to December, 1981.

The gas recovery system was mounted in its trailer and successfully tested. After considerable effort was put into the design of proper shock mountings for the Corblin compressors, it was found that the compressors operated satisfactorily when bolted directly to the trailer frame after it was reinforced. During the trailer checkout phase one of the compressors seized due to a failure of the lubrication system. The faulty compressor was repaired successfully using parts from a spare compressor, and steps will be taken to prevent a recurrence of the problem.

The heat rejection system mounting was completed. The system was tested by using it to cool the load resistor, during converter checkout, at power loads up to 700 kW. It should easily handle the 300 kW cooling load from the refrigerator compressors.

Numerous small jobs still remain to be done on the gas recovery and heat rejection trailers. Plumbing must be stenciled for proper identification, the plethora keys for safety interlocks must be combined in a more rational fashion, and operating instructions must be written.

Pending receipt of the refrigerator trailer, the test dewar instrumentation was checked using a CTi 1400 refrigerator that was available at Los Alamos. Simultaneously, data were obtained on coolant flow patterns inside this test dewar which models the 30 MJ coil and nonconducting dewar during cooldown from room temperature to 4 K. The 30 MJ dewar has an unusual shape for a large system--that of an open-mouthed vessel. Most previous superconducting coil systems sealed the coil within a metal helium vessel with only small connections to the outside. The open area above the 30 MJ coil acts as a large source of heat into the liquid helium, which can be readily accommodated during operation but creates difficulties in the temperature region between 4 and 10 K. A backup plan for cooling the 30 MJ coil has, therefore, been developed. The Model 2800 refrigerator will cool the system to as far below 10 K as possible. Liquid helium will then be transferred directly into the system from a waiting storage dewar; 500 to 1000 ℓ of liquid should be adequate. With this boost past the troublesome temperature interval, the Model 2800 will then proceed to fill the vessel with liquid.

REFERENCES

1. H. J. Boenig, J. C. Bronson, D. B. Colyer, W. V. Hassenzahl, J. D. Rogers, and R. I. Schermer, June 1978, "A Proposed 30-MJ Superconducting Magnetic Energy Storage Unit for Stabilizing an Electric Transmission System," Los Alamos Scientific Laboratory report LA-7312P.

2. J. D. Rogers, H. J. Boenig, J. C. Bronson, D. B. Colyer, W. V. Hassenzahl, R. D. Turner, and R. I. Schermer, Jan. 1979, "30-MJ SMES Unit for Stabilizing an Electric Transmission System," IEEE Trans. on Magnetics, Vol. MAG-15, Jan. 1979, pp. 820-823.

3. R. I. Schermer, Dec. 1979, "The Stabilization Unit for Bonneville Power Administration," Proc. 1979 Mech. and Magnetic Energy Storage Contractors' Review Meeting, CONF-790854, pp. 10-19.

4. R. I. Schermer, Nov. 1980, "30-MJ Superconducting Magnetic Energy Storage for BPA Transmission Line Stabilizer," Proc. 1980 Mech. and Magnetics Energy Storage Contractors' Review Meeting, CONF-801128, pp. 255-262.

5. J. Purcell, "30-MJ Superconducting Coil Fabrication," Proc. Mech. Magnetic, and Underground Energy Storage 1981 Annual Contractors' Review.

6. A. S. Criscuolo, "Computer Automated Controls for Superconducting Magnetic Energy Storage," Proc. Mech. Magnetic, and Underground Energy Storage 1981 Annual Contractors' Review Meeting.

DESIGN AND FABRICATION OF THE BONNEVILLE POWER ADMINISTRATION'S 30-MJ SUPERCONDUCTING ENERGY STORAGE COIL FOR LONG-DISTANCE TRANSMISSION LINE STABILIZATION*

J. R. Purcell and S. C. Burnett
General Atomic Company, San Diego, California
and
R. Schermer
Los Alamos Scientific Laboratory, Los Alamos, New Mexico

INTRODUCTION

Electric power systems that have major load and generation centers separated by long distances may experience low-frequency power oscillations. Such instabilities have occurred on the 3800-MW Pacific AC Intertie that connects the Southern California load to the hydroelectric power source of the Pacific Northwest, some 900 miles distant. A separate, almost parallel, dc-transmission line also connects these areas. The Bonneville Power Administration, which operates this system, has overcome the instability by using a system of controls and circuitry for transferring power between the HVDC and HVAC lines. The maximum possible power modulation on the HVDC Intertie is ±40 MW, which can stabilize the HVAC Intertie from about 2100 MW to 2500 MW whenever the HVDC is operating. The HVDC does not operate continuously, however, so other line stabilization methods were explored.

Studies by Los Alamos Scientific Laboratory and the Bonneville Power Administration have shown that a 30-MJ (8.4-kWh) superconducting magnetic energy storage (SMES) unit with a 10-MW converter could provide similar damping capabilities. Construction of the magnet has recently been completed at General Atomic Company in San Diego, California. Figure 1 shows an artist's concept of the coil installation, including the mobile refrigeration system to provide the coil with the required supply of liquid helium.

---

*Work supported by Los Alamos Scientific Laboratory, Contract 4X49-6722H-1.

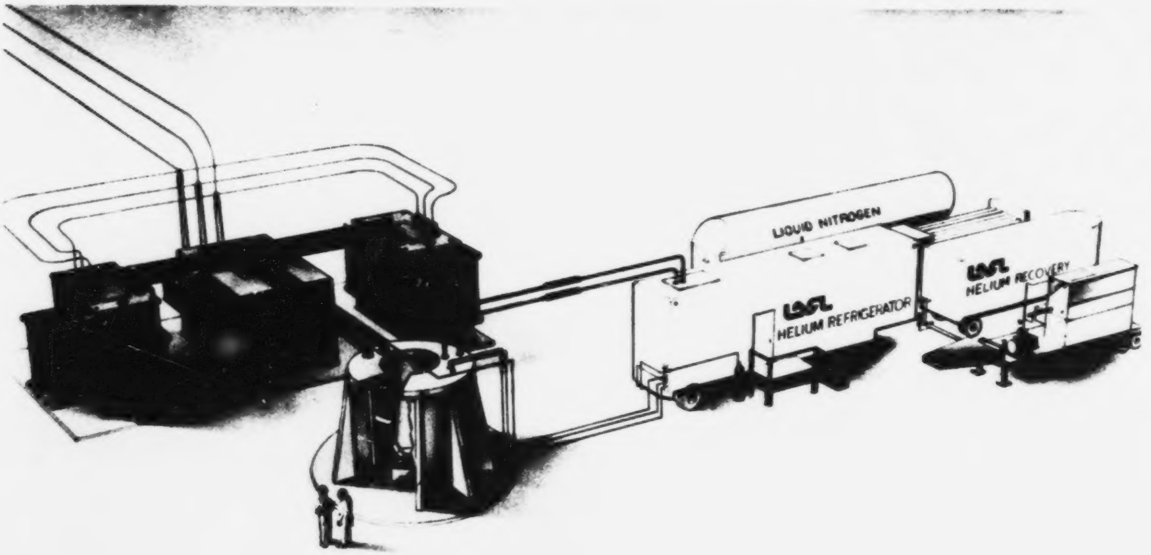

Fig. 1. 30-MJ SMES system stabilizer.

MAGNET OPERATION

Normal Operation

During normal operation the coil will be charged to 4470 A, storing 25 MJ. When required by the power line, the coil will discharge 5 MJ into the line or take 5 MJ additional charging energy. The energy storage coil is coupled to the power line via a 10-MW, ±2-kV power supply-inverter. The frequency of the power line oscillations to be damped is 0.35 Hz. The coil normally will be operated unattended with only daily inspections. The refrigerator will be computer controlled, and an alarm system will alert remote personnel in the event of a malfunction.

Abnormal Operating Conditions

The coil is cryogenically stabilized, and any normal region will quickly shrink to zero. Protection of the coil is necessary, however, in the event of external malfunctions. A fast-acting dump switch, together with the 1-ohm dump resistor, will prevent damage to the coil in case of a power supply runaway.

The coil is designed also to be self-protecting from its own stored energy, should low liquid helium level or a total loss of liquid helium occur and the low helium level sensors fail. After disconnection of the 10-MW power supply, the heat generated by "normal" or non-superconducting operation will be dissipated harmlessly throughout the coil owing to the large copper volume of the conductor.

DESIGN FEATURES

Design of the coil is relatively simple except that great care was taken to minimize the pulse field losses because the coil cycles at a 0.3-Hz rate. In addition, the design life of 10^8 cycles dictates modest design stresses in the mechanical structure.

The magnet is a superconducting solenoid. It consists of 20 individual coils, each wound in the double pancake fashion, stacked on top of each other and held together by 48 aluminum tie rods. The basic design parameters are listed in Table 1.

Each of the 20 coils consists of an inner support ring (a filament-wound fiberglass-epoxy composite), a conductor, a stainless steel support strap, an interturn insulator, and interlayer spacer plates.

The conductor configuration is shown in Fig. 2. One composite niobium-titanium/copper superconductor strand is surrounded by six copper wires to form an 81.7-A subcable. Six of these first-level subcables are twisted around one insulated copper cable to form the second-level cable. Ten second-level cables are twisted into the final conductor.

The coil is natural convection, immersion cooled at 4.5 K in liquid helium. The conductor is designed to facilitate intimate contact between coolant and copper strands. Channels, grooves, and vent holes are provided in all plastic components to aid natural convection and removal of gases from inside the coil.

FABRICATION

Winding of the pancakes and assembly of the solenoid proceeded in a straightforward manner. Figure 3 shows an isometric view of the pancake composition, and Fig. 4 shows the pancake winding.

The stainless steel support strap is anchored to the inner support ring with several fasteners and interwound with the conductor to carry the hoop stresses and axial loads. Strap tension during coil winding is held to 500 kg. This tension gives a preload sufficient to prevent the coil from lifting off the bobbin when energized.

An insulator strip, also providing coolant passages, is wound into the coil at both sides of the conductor (see Fig. 3).

A plastic ramp inserted at the circumference guides the conductor to the outside of the coil. The stainless steel strip is tied to itself, and winding tension is maintained by an adjusting screw. Plastic insulation is provided between the two parts of the tensioning clamp to avoid a closed loop. The voltage drop across this connection is 8.75 V.

TABLE 1
BASIC PARAMETERS OF 30-MJ COIL

STORED ENERGY, PEAK	30 MJ
PEAK CURRENT	4900 A
PEAK MAGNETIC FIELD	2.85 TESLA
PULSE FREQUENCY	0.35 HERTZ
PULSE AMPLITUDE	4000 A to 4900 A (20–30 MJ)
DESIGN OPERATING LIFE	10 YEARS
DESIGN CYCLES	10^8
NOMINAL POWER	8.5 MW
PEAK POWER	10 MW
PEAK EMERGENCY DISCHARGE VOLTAGE	7 kV
HEAT LOAD	~50 W
AMPERE–TURNS	4.51×10^6
COIL TYPE	SUPERCONDUCTING SOLENOID
ORIENTATION	VERTICAL AXIS
COOLING	LIQUID HELIUM BATH, 4.5 K (NOMINAL)
CONDUCTOR:	
MATERIAL	NbTi/COPPER
CONFIGURATION	RUTHERFORD CABLE
COIL CONFIGURATION	DOUBLE PANCAKE MODULES (20)
NUMBER OF LAYERS	40
NUMBER OF TURNS PER LAYER	23
WINDING I.D.	107.4 in.
WINDING O.D.	129.0 in.
COIL HEIGHT	47.7 in.
TOTAL WEIGHT	37,800 lb

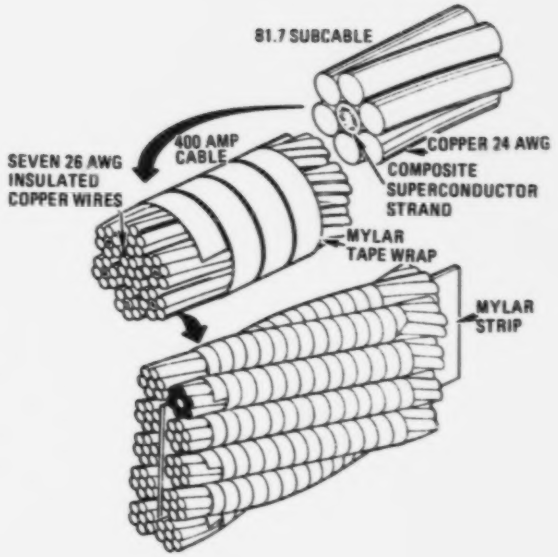
81.7 SUBCABLE
400 AMP CABLE
COPPER 24 AWG
COMPOSITE SUPERCONDUCTOR STRAND
SEVEN 26 AWG INSULATED COPPER WIRES
MYLAR TAPE WRAP
MYLAR STRIP

Fig. 2. Buildup of 4900-A conductor for 30-MJ coil.

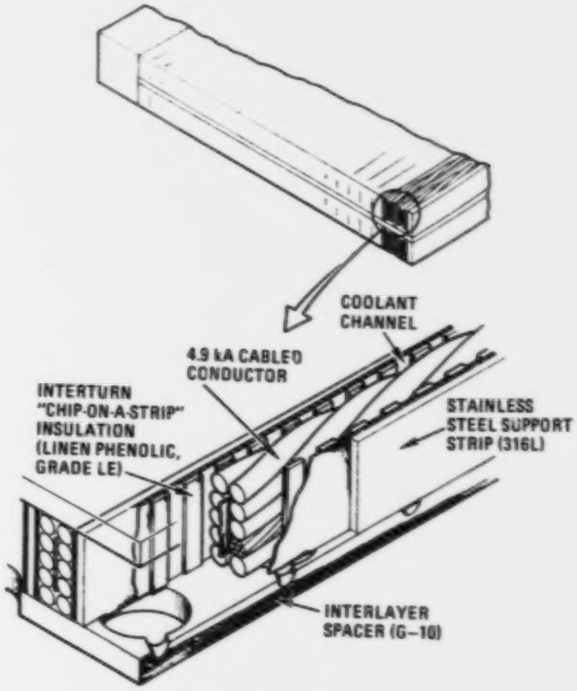
COOLANT CHANNEL
4.9 kA CABLED CONDUCTOR
INTERTURN "CHIP-ON-A-STRIP" INSULATION (LINEN PHENOLIC, GRADE LE)
STAINLESS STEEL SUPPORT STRIP (316L)
INTERLAYER SPACER (G–10)

Fig. 3. Isometric view of pancake assembly.

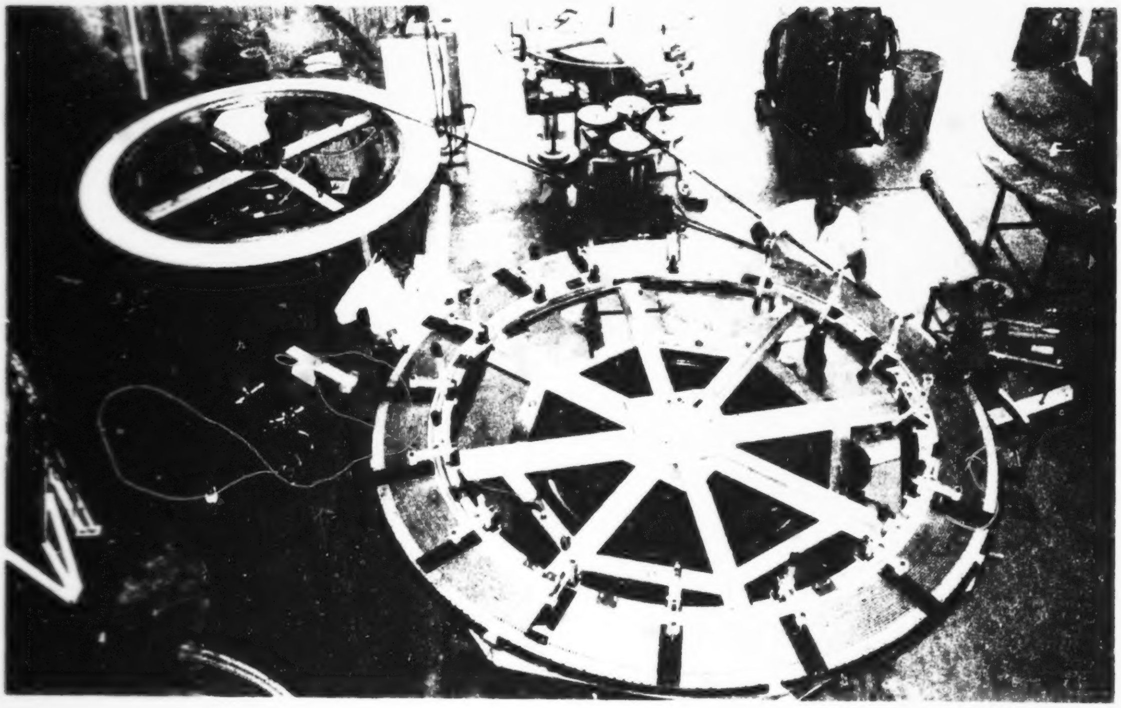

Fig. [illegible]. Shop-winding of an upper pancake.

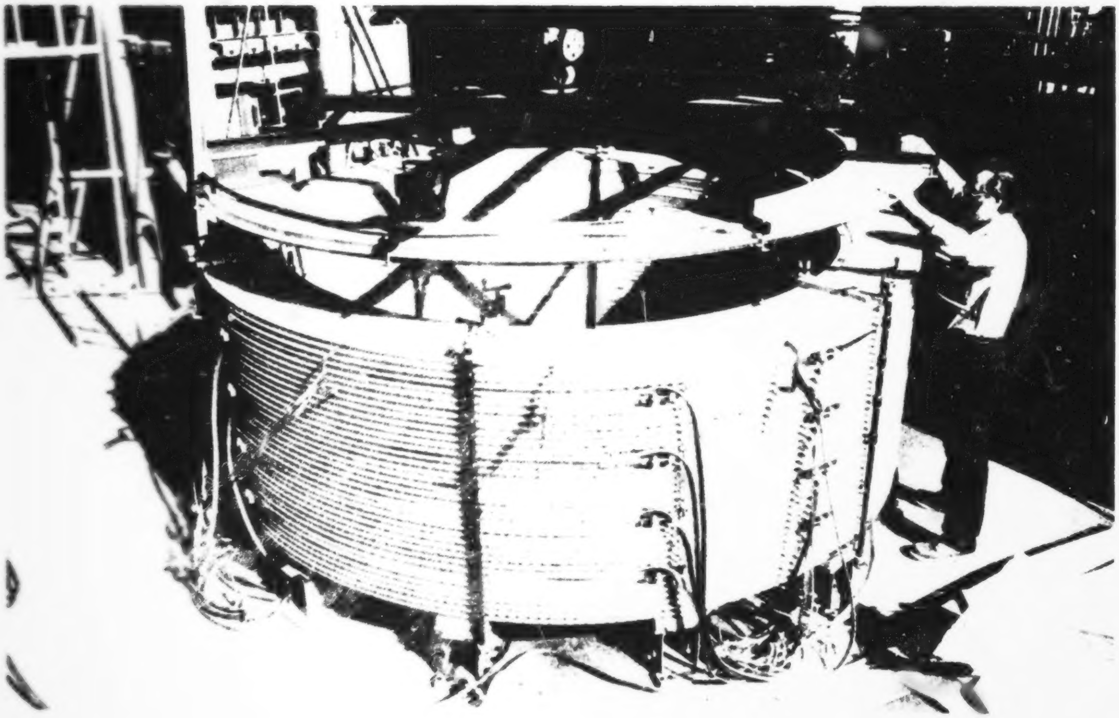

Fig. [illegible]. A [illegible] of [illegible] pancake being stacked on the [illegible] solenoid stack.

There is no splice between the top and bottom layers of each double pancake. A perforated and grooved interlayer spacer plate is inserted between the top and bottom layers of each coil and also between the coils.

The magnet is assembled using 20 of the above-described double coil subassemblies stacked and aligned. Figure 5 shows a double pancake being placed on the solenoid stack. The solenoid is held together by 48 aluminum tie rods. Each pair of tie rods connects an upper and lower plastic clamping beam, which provide the clamping forces to hold the magnet together. A stack of Belleville washers at the upper end of each tie rod provides elasticity in the system to avoid overstressing the tie rods during cooldown and operation. This is necessary because the tie rods are thermally insulated from the coil and cool down first. In addition to the vertical clamping devices, spiral pins are driven through adjacent inner support rings to provide shear resistance during the design base earthquake. Installed in the cryostat, the magnet is supported by six hanger beam assemblies, which are designed so that any three can carry the full weight of the magnet.

The electrical connection between each of the 20 double pancake coils is made in a staggered pattern around the outside of the coil. A 15.2-cm portion of the cable is straightened out, and each individual subcable is soldered to an individual subcable of the next coil with a 7.6-cm overlap. All ten connections are insulated from each other and clamped down on a splice plate.

The lead-in and lead-out connections are made in a similar way on top of the magnet. The lead entering the bottom coil is brought down the outside, well supported and clamped with an extra copper bar for additional stability in case of low helium level within the dewar.

PROGRAM STATUS

The 30-MJ magnet is now complete. The fabrication process was finished ahead of schedule and was considerably under estimated cost. This is largely attributable to the fabrication economies that resulted from designing with efficiency of manufacturing as a major design goal.

The magnet will be installed at the northern end of the Bonneville Power Administration Intertie in 1982. Initial testing will be carried out at the site of application. The coil will represent a first commercial application of superconductivity. It is expected that other power grids will also want to take advantage of the advances afforded by this technology.

COMPUTER-AUTOMATED CONTROLS FOR SUPERCONDUCTING MAGNETIC ENERGY STORAGE

Alphonse L. Criscuolo
Los Alamos National Laboratory
Los Alamos, New Mexico 87545

ABSTRACT

A computer-automated control system that allows unmanned operation of the Superconducting Magnetic Energy Storage (SMES) system has been designed and almost completely installed at Los Alamos National Laboratory. In addition to unmanned operation, the computer offers continual monitoring and recording of all the important SMES signals, operator guidance in starting up and maintaining SMES, emergency shutdown control, and high-speed data acquisition for failure diagnosis. The major components of the computer-automated control system are two slave computers that perform the data acquisition and a master computer that performs the control.

INTRODUCTION

The Superconducting Magnetic Energy Storage (SMES) system will function as a lossless stabilizer for the ac electrical power intertie between the Pacific Northwest and Southern California. Potentially hazardous, low-frequency power oscillations occurring on this intertie will be dampened by exchanging energy, in the proper phase, between the intertie and the superconducting coil.

An automatic Control and Data Acquisition (CDA) system is required to provide SMES efficient, reliable, unattended operation at an unmanned site and to provide data for evaluating system performance in real-time and off-line.

The SMES system must operate in an uncttended mode because the installation site, Tacoma Substation, is manned only four hours per day. The SMES system is comprised of several complicated subsystems from many different contractors. Each subsystem interacts with the other subsystems, although the subsystems do not provide communication interfaces to one another to allow anticipation of these interactions. The CDA will supply these interfaces.

This system is the first attempt at stabilizing an ac power network using superconducting technology.[1,2] Therefore, it is necessary that sufficient data from SMES is recorded to permit evaluating the system's performance. This same data should make it possible to pinpoint failures and minimize the repair time.

This paper describes the major subsystems of SMES in some detail from a control point of view, describes the CDA system configuration, discusses the benefits to SMES of the CDA system, and states the status of the CDA system.

SMES SYSTEM DESCRIPTION

Functionally, SMES may be organized into three major subsystems, (1) energy transfer and storage, (2) cryogenics, and (3) control and data acquisition. However, for the purpose of identifying units of hardware and their interfaces, 12 subsystems are identified in Fig. 1. The function of each of these will be described briefly.

The ac-dc converter and superconducting coil are the two subsystems that provide transfer and storage, respectively, of energy. The 12-MW converter accepts 13.8-kV ac voltage from the intertie and transforms it to a dc voltage ranging from 0 to 2.5 kV, which is applied to the coil. The coil stores the energy removed from the intertie in its magnetic field and may conduct up to 4.9 kA. The magnetic energy can be returned to the intertie by operating the converter in the regenerative mode.

The cryogenic function of SMES is satisfied by the dewar, refrigerator, gas recovery, liquid nitrogen, and heat rejection subsystems. The cryogenic subsystems maintain the extremely cold environment required to cause the coil to become superconducting. The dewar contains the liquid helium in which the coil is submerged and is designed to reduce the heat transferred to the coil from the outside environment. The refrigerator replenishes the liquid helium lost in the dewar due to heat gain from the coil leads and the environment. The gas recovery system removes the gaseous helium from the dewar and supplies helium to the refrigerator during peak demands. The heat rejection system removes heat from the various compressors in the refrigerator, vacuum, and gas recovery systems.

The control and data acquisition functions are satisfied by three computers, the Bonneville Power Administration (BPA) interface electronics, an uninterruptable power supply, and an electronic protection subsystem. Automatic control of SMES is provided by one of the three computers. The two other computers acquire and store data from SMES. The BPA interface provides for SMES power set-points transmitted by microwave from BPA's central control facility. This interface also passes status information to and from BPA's supervisory control and data acquisition system. The uninterruptable power supply provides clean power to the computers and instrumentation and avoids start-up delays encountered during power dropouts. The electronic protection system is a hardwired interlock system that acts in parallel with the computer to shut down SMES in an emergency.

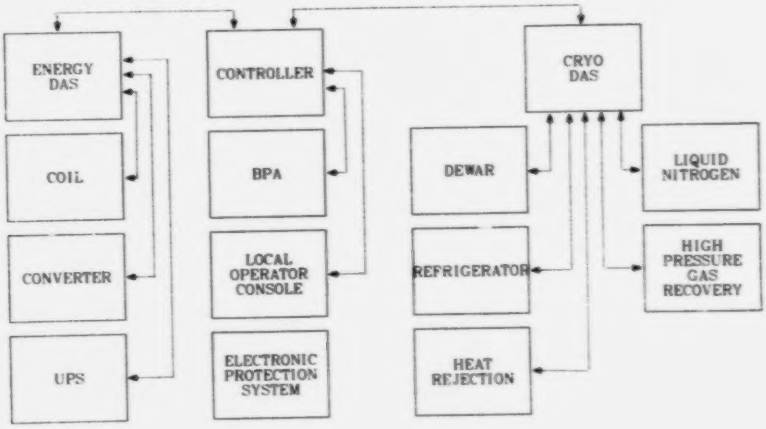

Fig. 1. Control and Data Acquisition System Block Diagram.

CONTROL AND DATA ACQUISITION CONFIGURATION

The configuration of the CDA system is illustrated in Fig. 1. The Uninterruptable Power Supply (UPS) and those systems serving the energy transfer/storage function are interfaced to one data acquisition computer (Energy DAS slave) while those systems serving the cryogenic functions are interfaced to another data acquisition computer (Cryo DAS slave). The Controller (master) is interfaced to the BPA intertie, the local operator, and each of the slave computers.

This configuration of three computers sharing the control and data acquisition tasks, known as distributed processing,[3] was chosen to accommodate the high data rates required to operate the ac-dc converter and the possibly large physical separation between each slave computer and the master computer.

Removing the SMES system control tasks and the peripheral management tasks from the slave computers allows them to acquire data at their fastest possible rate. This permitted implementation of the EDAS and CDAS with standard commercial hardware while satisfying the data rates needed for SMES.

In the early stage of SMES design, there was a real possibility that the master computer would be located approximately 400 ft. from the other SMES subsystems. If the data acquisition function had been in the master, a significant cost would have been incurred to cable the SMES signals to the master and the noise on these signals would have increased. The distributed processing is a solution to these problems.

The SMES system demands a variety of resources from the master and slave computers to satisfy the control and data acquisition requirements. These resources are illustrated for the master and slaves in Figs. 2 and 3, respectively.

The Q-Bus is a set of signals that conform to an electrical and mechanical specification allowing the central processing unit (CPU) of the computer to communicate with the many other resources required to make the computer useful. A large number of manufacturers supply functional hardware which can communicate with the Q-Bus, thus providing a flexible and relatively inexpensive computer. Each of the computers has the physical space to accommodate functions which may be required in the future.

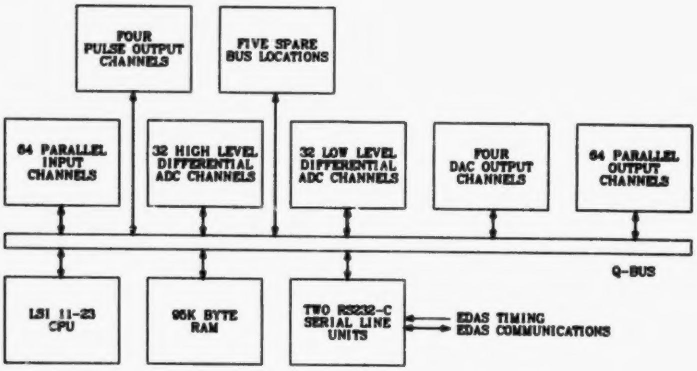
FOUR PULSE OUTPUT CHANNELS
FIVE SPARE BUS LOCATIONS
64 PARALLEL INPUT CHANNELS
32 HIGH LEVEL DIFFERENTIAL ADC CHANNELS
32 LOW LEVEL DIFFERENTIAL ADC CHANNELS
FOUR DAC OUTPUT CHANNELS
64 PARALLEL OUTPUT CHANNELS
Q-BUS
LSI 11-23 CPU
96K BYTE RAM
TWO RS232-C SERIAL LINE UNITS
EDAS TIMING
EDAS COMMUNICATIONS

Fig. 2. Master Computer Resources.

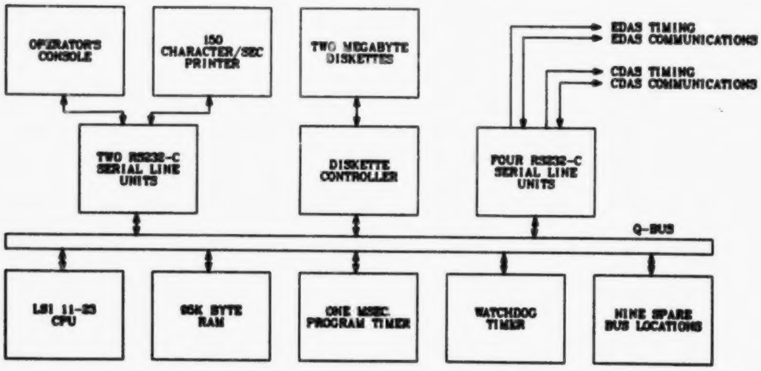
OPERATOR'S CONSOLE
150 CHARACTER/SEC PRINTER
TWO MEGABYTE DISKETTES
EDAS TIMING
EDAS COMMUNICATIONS
CDAS TIMING
CDAS COMMUNICATIONS
TWO RS232-C SERIAL LINE UNITS
DISKETTE CONTROLLER
FOUR RS232-C SERIAL LINE UNITS
Q-BUS
LSI 11-23 CPU
96K BYTE RAM
ONE MSEC PROGRAM TIMER
WATCHDOG TIMER
NINE SPARE BUS LOCATIONS

Fig. 3. Slave Computer Resources.

BENEFITS OF CDA TO SMES

The primary reasons for an automatic control system in SMES are to permit unmanned operation and data recording. These needs may be satisfied by a variety of control system implementations. The computer-based implementation offers several benefits unavailable from other types of control systems. These assets fall into the categories of control, recording, maintenance, and operator interaction.

A major advantage of a computer-based control system is the flexibility of designing the control sequence. It is not necessary to have detailed control sequences designed before procuring and installing a significant portion of the control system. It is necessary that a reasonable estimate be made of the fastest response time required by a subsystem and the number of signals to be monitored or controlled. As each subsystem becomes clearly defined, the control sequence for the subsystem may be designed, coded, and tested; sometimes even in the absence of the subsystem hardware, thereby minimizing problems when integrating the subsystem with the controller. Generally, if the subsystem operation changes, no hardware changes are required in the controller and, depending on the extent of the change, only a minor effort is necessary to change the control sequence.

Another aspect of the control flexibility is the ease with which the system performance may be tuned. Within the master computer is a table, the run-time data base, containing the important characteristics of each signal in the SMES system. The operator may change the performance of a subsystem by adjusting the value of setpoints in this table. The control sequence is not being modified, only the setpoint at which an action is to be initiated is being modified.

The method of recording data with the computer offers the advantages of the data being in a format that is convenient for analysis, the recording media has a large capacity that is easily transported and stored, and the data may be saved or discarded as a function of the events occurring in the SMES system.

All acquired data in the SMES system is converted to binary form for recording in the computer memory and on the magnetic diskettes. This form allows immediate evaluation of the data by the master and slave computers for control and display and is in a form readable by many other BPA or DOE computers. The diskettes containing the long-term performance data (days to weeks) are small, light, and reasonably rugged. This is superior to recording on paper or analog tape, each of which would require many man hours to analyze.

Each of the slave computers has the capability of recording transient data. This data is important when a failure occurs in the SMES system. Each signal in the SMES system is recorded at a rate appropriate for that signal. For example, the vacuum diffusion pump oil temperature is sampled once every 10 s while the ac-dc converter output voltage is measured 200/s. There are effectively 2000 transient data recordings/s. If these were all saved on the diskette, it would become full in approximately five minutes. Instead, this data is stored in a portion of the slave computer memory in such a manner that if the data has been stored for more than 15 s, it is discarded and that memory location is reused for new transient data. If a SMES system failure does occur, the transient data for the 15 s prior to, and after, the failure is retained in this portion of the slave memory. The master computer can then request the data and store it on the diskette. Compare this with a high-speed x-y recorder or magnetic tape that is continuously recording this data so a failure may be analyzed.

The computer can facilitate isolating failures and maintaining the SMES system. Presently, whenever a subsystem has a fault, it is identified to the operator by the printer and a video display. In many cases, the fault is isolated down to a subassembly level, such as a pump or fan. The BPA will be notified by the master computer when a critical fault has occurred so an operator may be dispatched. A log of the faults will be available to the operator on the printer. Preventive maintenance may be done by monitoring trends in certain parameters to indicate a component is wearing out. For example, an increase in a compressor crankcase oil temperature could indicate that a bearing or cooling water pump is wearing out.

An advantage which may seem paradoxical in an unmanned system is the interaction permitted by the computer between the operator and the SMES system. The system will become unattended only when it becomes operational in Tacoma, Washington. Before that time, many hours will be spent by various personnel to make the SMES system operate efficiently.

There are approximately 350 signals required to monitor or control the SMES system. One alternative is to connect these signals to switches, knobs, meters, and lamps at some central location. It would require a highly trained person to start the system and diagnose a system fault.

Another alternative is to program the start sequence, running sequence, and monitoring sequence into the computers. The computer can guide a relatively unskilled person through the start-up procedure. The computer can then watch the SMES signals and present only alarm signals to the operator. The operator may still request a display of any SMES signal whenever desired by typing a command to the master computer. The signals may be processed by the computer to display various kinds of information to the operator and the form of the display may be changed to emphasize or clarify the data being presented.

Referring again to the run-time data base, an operator may tune the system from a central point by typing new entries into the data base. This procedure would be preferable to walking out to the gas recovery trailer, unscrewing a panel, and adjusting a screw (probably more than once) to change the inlet pressure that turns on the compressor.

STATUS OF THE SMES CDA

The Control and Data Acquisition subsystem of the SMES system is at an advanced state of installation. Approximately $60,000 has been expended on hardware that is presently in place. A little over two man-years of design are in the CDA, including six months in the software.

The hardware providing the functions shown in Figs. 2 and 3 has been installed in a computer room established in a trailer. The complete cabling has been fabricated and a major portion of it is installed. The central junction box, containing electronics to make the subsystem signals compatible with the computers, is in place. Nearly all this hardware has been tested and is operating satisfactorily.

The control sequence for the ac-dc converter has been designed and coded; the hardware is presently being checked. The control sequences for the High Pressure Gas Recovery and Heat Rejection subsystems have been designed.

All software for the data acquisition, interprocessor communications, and operator interaction has been designed, coded, and tested on the hardware.

The significant tasks to be addressed in the near future are the design of high voltage isolation amplifiers for obtaining signals from the coil, the control of the helium refrigerator, and the design of the BPA interface.

REFERENCES

1. H. J. Boenig, J. C. Bronson, D. B. Colyer, W. V. Hassenzahl, J. D. Rogers, and R. I. Schermer, June 1978, "A Proposed 30-MJ Superconducting Magnetic Energy Storage Unit for Stabilizing an Electric Transmission System," Los Alamos Scientific Laboratory report LA-7312P.

2. J. D. Rogers, H. J. Boenig, J. C. Bronson, D. B. Colyer, W. V. Hassenzahl, R. D. Turner, and R. I. Schermer, Jan. 1979, "30-MJ SMES Unit for Stabilizing an Electric Transmission System," IEEE Trans. on Magnetics, Vol. MAG-15, January 1979, pp. 820-823.

3. M. J. Seamons, A. L. Criscuolo, June 1981, "Microcomputer Control for the Superconducting Magnetic Energy Storage System," 24th Midwest Symposium on Circuits and Systems, University of New Mexico, Albuquerque, New Mexico.

SEASONAL THERMAL ENERGY STORAGE PROGRAM

BLANK PAGE

PROJECT SUMMARY

Project Title: Seasonal Thermal Energy Storage Program

Principal INvestigator: James E. Minor

Organization:

Pacific Northwest Laboratory
P.O. Box 999
Richland, Washington 99352
(509) 375-2548

Project Goals: Develop the technology for economic storage and retrieval of energy on a seasonal basis, using heat now wasted or heat or cold available during a surplus period to reduce peak period demand; reduce electric utility peaking problems; and contribute to the establishment of favorable economics for solar heating and cooling systems.

Development of the technology for seasonal storage in aquifers is proceeding in the Aquifer Thermal Energy Storage (ATES) program. The Seasonal Storage Technology program will provide detailed evaluation of aquifer behaviour including data from field tests, economic and mathematical modeling data. Methods of seasonal storage being developed by a number of other countries (earth, ponds, lakes, constructed caverns and others) will be evaluated for application in the United States and essential improvements to selected technologies will be undertaken.

Project Status: In the Aquifer Thermal Energy Storage Program, conceptual design studies including aquifer characterization, were in progress at three sites. Well fields for aquifer characterization were completed at all sites, and chill tests conducted at Stony Brook, New York. Demonstration activities at Minnesota are being converted to high temperature field tests.

Eight tasks in the Seasonal Storage Technology Program are in progress. Contracted work in each of these tasks is discussed individually. The Mobile test site has been converted to a true doublet. A test cycle at 59°C has been completed and a test cycle at 90°C has been initiated.

Nonaquifer methods of seasonal storage are being evaluated. An international conference on seasonal thermal energy storage has been organized, and abstracts from 13 countries accepted.

Contract Number: DE-AC06-76RLO 1830

Contract Period: Continuing

Funding: FY 1981 $5,800 BO/$5,200 BA

Funding Source: U.S. Department of Energy, Office of Energy Systems Research

SEASONAL THERMAL ENERGY STORAGE PROGRAM

James E. Minor
Pacific Northwest Laboratory
Richland, Washington 99352

INTRODUCTION

The Pacific Northwest Laboratory (PNL) manages the Seasonal Thermal Energy Storage (STES) Program for the DOE Office of Energy Systems Research. The Seasonal Thermal Energy Storage Program Office within PNL has set program gaols and developed a Multi-Year Program Plan to meet those goals. A matrix of external contracts has been placed. The research and development work of the STES program is being performed by industry, universities, other DOE laboratories, and PNL.

PROGRAM INCENTIVES

Seasonal storage of thermal energy can be utilized, in the near term, to provide a significant contribution to improved efficiency in the use of existing thermal energy sources and in the use of renewable energy. This contribution will encourage a shift from the use of imported and costly petroleum fuels to more abundant and available energy sources such as coal and nuclear power. Thermal energy storage, when incorporated in energy supply and distribution systems, will support the economic and reliable use of renewable, intermittent energy sources such as solar or winter chill. Thermal storage will also contribute to the off-plant distribution and use of waste heat from industry and utility sources.

The STES program is designed to provide the technology for storage and retrieval of energy on a seasonal basis, using heat or cold available from waste sources, renewable energy, or conventional sources during a surplus period to reduce peak period demand, reduce electric utility load problems, and contribute to the establishment of favorable economics for district heating and cooling systems. The primary current thrust of the STES program is toward utilization of ground water systems (aquifers) for thermal energy storage.

During the last decade, the storage of thermal energy in aquifers has received considerable attention. The benefits of storing large quantities of thermal energy on a seasonal basis have been identified, including: (a) the benefit of using energy storage to provide reliable end use of renewable energy sources such as solar, particularily to balance the load/demand unbalance between summer and winter; (b) the cost effectiveness of utilizing heat now wasted in electrical generation plants; (c) the beneficial use of industrial waste heat; and (d) the use of winter chill to provide summer cooling for buildings. Seasonal aquifer storage should make substantial contribution to the satisfaction of those needs. Recent studies and field experiments have reported that energy recovery rates in excess of 70 per cent can be achieved.

Aquifers are available in or near the most centers of population. However, at some sites where energy storage is needed, no suitable, accessible aquifer will be available. A range of seasonal thermal energy storage techniques using natural lakes or ponds, or constructed storage are being evaluated in other countries. These methods are being evaluated to determine which candidates have the widest geographic application and lend themselves most efficiently to the provision of economic storage where aquifer availability or aquifer use restrictions make aquifer storage impractical.

PROGRAM IMPLEMENTATION

The STES Program organization provides for two major subprograms -- the Aquifer Thermal Energy Storage (ATES) Program and the Seasonal Storage Technology (SST) Program. Seasonal storage in aquifers was to be evaluated in the ATES Demonstration. The conceptual design studies that were in progress at three sites are now being phased out, while retaining one site for high temperature aquifer field studies and transferring the technical information gained on chill storage to the New York State ERDA and the State University of New York.

At Bethel, Alaska, the retrieval of waste heat from a diesel electric utility has been studied by TRW. A plan was developed for defining the geologic structure at the site; determining whether a usable aquifer was available; and characterizing that aquifer. Three observation wells, a supply well, and an injection well were successfully drilled through 400 feet of permafrost, and an aquifer producing good quality water was identified at 600 feet. Work on this project was terminated before non-isothermal aquifer tests could be conducted.

At the Stony Brook Campus of the University of New York, Dames and Moore is studying the use of a cooling tower in the winter to chill aquifer water for use in summer cooling. A well doublet was completed together with observation wells; and a chill test conducted using a compressor to chill the ground water. This work was partially funded by the New York State ERDA, and information from this study was evaluated by the State of New York to determine whether an operating chill storage system will be developed at Stony Brook.

At the St. Paul campus of the University of Minnesota, the storage of water at 150°C is being studied. The energy source to be used initially is the St. Paul campus coal fired heating plant. After obtaining required permits, a well field suitable for a series of short cycle tests was planned and core holes, observation wells, and a supply and injection well completed. A series of short cycle tests utilizing injection temperatures ranging from 100-150°C have been initiated. Work at this site will be continued as a series of longer cycles, high temperature field tests.

The Seasonal Storage Technology program is designed to provide the base technology and environmental information essential to the ultimate beneficial use of aquifer energy storage and to evaluate nonaquifer methods of seasonal thermal energy storage and select that method or methods which would provide optimum availability of storage by aquifer and nonaquifer methods.

The program is organized around the following tasks:

Legal/Institutional Assessment
Economic Assessment
Environmental Assessment
Field Test Facilities
Compenida
Laboratory Analysis
Numerical Simulation
Nonaquifer STES Concepts

Activities in each of those tasks are covered in individual papers.

The field test activities conducted by Auburn University are continuing. The well field has been redesigned as a true doublet, and all necessary additional supply and observation wells completed. A cycle of injection, storage and recovery of water heated to 59°C was completed. In previous tests mixing waters from different sources, recurrent difficulties were encountered in injecting the heated water. In this cycle with the true doublet, no injection problems were encountered.

Data from the injection portion of the cycle were utilized by Lawrence Berkeley Laboratory using CCC code to predict recovery chaaracteristics. Good correlation was obtained between predicted and experimental recovery data.

In the environmental area, a programmatic environmental assessment for the ATES program was completed and published at DOE/EA-0131.

The current field tests at 50-90°C conducted by Auburn University are to be supplemented by field tests at the University of Minnesota in the 100-150°C range.

Information available on current work in progress on seasonal thermal energy storage in other countries will be substantially increased by an International Conference planned for October, 1981. Abstracts have been accepted from 13 countries. Methods of storage to be presented include:

Aquifer
Earth
Ponds/Lakes
Constructed Aquifer
Rock
Cavern
Thermochemical
Tanks

REPORTS PUBLISHED DURING FY 1981

Blahnik, D.E., 1980. "Preliminary Survey and Evaluation of Nonaquifer Thermal Energy Storage Concepts for Seasonal Storage," Pacific Northwest Laboratory, Battelle, Richland, WA. PNL-3625.

Century West Engineering, 1981. "Regional Assessment of Aquifer for Thermal Energy Storage," Prepared for Pacific Northwest Laboratory, Battelle, Richland, WA. Volume 1-3.

Doughty, C., G. Hellstrom, C.F. Tsang, J. Claesson, 1981. "A Study of ATES Thermal Behavior Using a Steady Flow Model," Lawrence Berkeley Laboratory, Berkeley, CA. LBL-11029.

BEST DOCUMENT AVAILABLE

Eliason, J.R., 1981. "Waste Heat and Chill Storage in Aquifer Systems," Pacific Northwest Laboratory, Battelle, Richland, WA. PNL-SA-9164.

Fox, Kenneth, 1981. "The Aquifer Thermal Energy Storage Demonstration Program," Pacific Northwest Laboratory, Battelle, Richland, WA. PNL-SA-9136.

Hendrickson, P.L., 1981. "Legal and Regulatory Issues Affecting the Aquifer Thermal Energy Storage Concept," Pacific Northwest Laboratory, Battelle, Richland, WA. PNL-3437, REV. 1.

Hendrickson, P.L., 1980. "Legal and Regulatory Issues Affecting the Aquifer Thermal Energy Storage Concept," Pacific Northwest Laboratory, Battelle, Richland, WA. PNL-3437.

Ichimura, V.I., 1980. "Annual Report for Hydrologic Studies Support, INTERCOMP Code Conversion," Geological Engineering Section, Washington State University, College of Engineering Research Report. 80/15-44.

Mercer, J.W., C.R. Faust, W.J. Miller, F.J. Pearson, Jr., "Review of Simulation Techniques for Aquifer Thermal Energy Storage (ATES)," Prepared for Pacific Northwest Laboratory, Battelle, Richland, WA. PNL-3769.

Meyer, C.F. and W. Hausz, 1980. "Guidelines for Conceptual Design and Evaluation of Aquifer Thermal Energy Storage Systems," G.E. Tempo, Santa Barbara, CA. GE80TMP-44. PNL-3581.

Minor, J.E., 1981. "Seasonal Thermal Energy Storage Program Progress Report: January 1980 - December 1980," Pacific Northwest Laboratory, Battelle, Richland, WA. PNL-3746.

Parr, A.D., F.J. Molz, J.G. Melville, 1981. "Aquifer Testing for Thermal Energy Storage," Presented at the John Ferris Symposium, Spring Meeting of American Geophysical Union, Washington, D.C.

Prater, L.S., G. Casper, R.A. Kawin, 1981. "Bibliography of the Seasonal Thermal Energy Storage Library," Pacific Northwest Laboratory, Battelle, Richland, WA. PNL-3645.

Prater, L.S., J.R. Eliason and V.E. Hampel, 1981. "The Seasonal Thermal Energy Storage Technology Information System," Pacific Northwest Laboratory, Battelle, Richland, WA. PNL-SA-8800.

Stottlemyre, J.A., C.H. Cooley, G.J. Banik, 1981. "Temperature Sensitivity of Ottawa Sand and Massilden Sandstone Intrinsic Permeabilities," Presented at the 22nd Rock Mechanics Symposium, Cambridge, Mass.

Wukelic, G.E., D.L. Lee, 1981. "Environmental Assessment: Aquifer Thermal Energy Storage Program." DOE/EA-0131.

PROJECT SUMMARY

Project Title: Aquifer Thermal Energy Storage (ATES) Program Management

Principal Investigator: John R. Raymond

Organization:
Pacific Northwest Laboratory
P.O. Box 999
Richland, Washington 99352
(509) 375-2601

Project Goals: The initial goal of this program was to establish conceptual design contracts with the maximum number of potential demonstration contractors. After these contracts were in place, the principal task in Phase I was the characterization of the aquifers for conceptual designs, develop the functional design criteria for the above ground portions, and complete the conceptual designs and proposals for Phase II work.

From the Phase II proposals submitted at the end of Phase I it was intended to establish the maximum number of Phase II contracts allowed by funding and technical considerations. During Phase II design, construction, startup, and operation of the aquifer demonstrations would be implemented to demonstrate aquifer storage feasibility (economic, technical, environmental and institutional) in operating demonstrations.

Project Status: During this reporting period, work continued on the three Phase I (implementation of aquifer characterization and conceptual design) ATES Demonstration Projects:

Site	Prime Contractor	Energy Source	Storage Temperature	User Application
Bethel, Alaska	TRW Inc.	Diesel-Electric Utility	<105°C	District Heating
State Univ. of New York Campus, New York	Dames & Moore	Winter Chill	4°C	District Cooling
Univ. of Minnesota St. Paul Campus, Minnesota	Univ. of Minnesota	University Heating Plant	150°C	District Heating

Planning documentation was completed for the three projects, and in addition, documentation of the Functional Design Criteria was completed. Also, the required permits were obtained for test drilling to characterize site geohydrology. Aquifer characterization was in an advanced status at all three project sites, with most of the test and production well drilling and analysis completed.

Due to the reduced level of funding available for the Seasonal Thermal Energy Storage Program, the ATES Demonstration Projects are being phased out. The Bethel and Stony Brook Projects will be terminated at the end of FY-1981; and the Minnesota Project will be converted to a high-temperature ATES field test facility.

Contract Number: DE-AC06-76RLO 1830

Contract Period: FY-1979 through FY-1981

Funding Level: $3382K, FY-1981, B/O

Funding Source: U.S. Department of Energy, Office of Energy Systems Research

PROJECT SUMMARY

Project Title: Bethel, Alaska, Aquifer Thermal Energy Storage Demonstration Project

Principal Investigator: Jack M. Cherne

Organization:
TRW
One Space Park
Redondo Beach, California 90278
(213) 535-4321

Project Goals: The first goal was to identify and characterize a viable aquifer. Concurrently, a conceptual design for an ATES system would be developed, including an energy source, thermal transport, storage aquifer and users. During the study, the economic viability of the conceptual system would be established, and the institutional and environmental concerns for future development will be identified. The products of Phase I would be a complete conceptual design for Phase II and a plan for a Phase II program.

Project Status: Work continued during this reporting period on tasks established in FY-1980. All management, environmental, institutional, and aquifer characterization plans were completed.

Three test wells were drilled and analyses made for subsurface characterization. The wells were completed as observation wells for monitoring future pumping tests and thermal/tracer injection tests. Doublet (one injection well and one supply well) wells were completed for the thermal/tracer injection test and preliminary tests were made which indicated the presence of an aquifer that may be suitable for the demonstration project.

The amount and availability of waste heat from the Bethel Utility generators were defined, and energy requirements of candidate users were determined. Designs of the surface and subsurface systems for the Phase I tests were completed.

Drilling costs were much higher than anticipated for the Bethel Project. The increased costs required that work be suspended while a comprehensive economic and technical assessment of the project was made. TRW was issued a Stop Work Order on December 10, 1980. Program funding recisions in FY-1981 and expected budget reduction for the STES Program in FY-1982, necessitated termination of the Bethel ATES Demonstration Project at the close of FY-1981.

Contract Number: DE-AC06-76RLO 1830, Subcontract B-68264-A-G

Contract Period: May 1, 1980 through September 30, 1981

Funding Level: $1,292,657 for FY-1981

Funding Source: U.S. Department of Energy through Pacific Northwest Laboratory

BETHEL, ALASKA
AQUIFER THERMAL ENERGY STORAGE PROJECT

Jack Cherne
Manager, ATES Project
TRW Energy Systems
One Space Park
Redondo Beach, CA 90278

ABSTRACT

TRW Energy Systems Group, under contract to Battelle, Pacific Northwest Laboratory, was developing the conceptual design of a seasonal thermal energy storage system in Bethel, Alaska, using an aquifer for storage. The system would use a diesel electric generating plant as the source of the thermal energy, an aquifer beneath the property of the utility, and an energy transport system to take the energy from the utility, store it in the aquifer, and provide it to the city for space heating and hot water of the local hospital, municipal buildings, schools and residences.

This paper describes the progress made this year in characterizing the aquifer and the development of a system design criteria for use in the conceptual design.

INTRODUCTION

The prospective Aquifer Thermal Energy Storage System project is located in the Town of Bethel, Alaska. Bethel, 450 miles west of Anchorage, on the Kuskokwim River, in the Yukon-Kuskokwin River delta and is at 30 feet above sea level. Bethel has a population of 4,000 and is the regional center for trade, transportation, administration, health care and education for the 80,000 square mile, 20,000 population of southwestern Alaska.

Bethel, like many isolated communities in Alaska, uses diesel generators for electric power. Hot water and space heating was normally supplied by oil fired units. The plan was that waste heat from the deisel power plants would be stored in the aquifer and used on a seasonal basis in a district heating system for many of the buildings in the community. The town of Bethel is well suited for this demonstration for the following reasons:

- Source of surplus heat is available
- Seasonal variation of surplus heat in summer and deficit in winter
- Rising costs of fossil fuel in region
- Expectation of finding a useable aquifer is strong
- A preliminary economic analysis indicates system would produce energy to users at one-third present cost.

The Phase I of the project included site analysis, well drilling, aquifer characterization, conceptual design of the system and preparation for a Phase II design and implementation of the design. Work continued on the tasks initiated last fiscal year (FY-1980).

The Management Plan, Aquifer Characterization Plan and Environmental/Institutional Plans were completed. These documents form the baseline for the project.

Most of the work accomplished during this reporting period was in Test Site Development. This task consisted of the following elements:

- Procurement and transport of materials and equipment
- Design of the hot water test system
- Site preparation, and well drilling
- Test system construction
- Drilling and completing the wells
- System design criteria.

Procurement and Transport of Materials and Equipment

The key facet in the procurement of materials and equipment was the short time between the project start and the planned start of drilling. Some of the constraints included the various transportation difficulties to Bethel. The last barge from Seattle leaves on September 6. A number of items required a fairly long lead time. These included:

- down hole pump
- heat exchangers
- booster pumps, and
- aquifer instrumentation.

Early design decisions were made on the selection of these items so that the procurement lead time could match the most economical transportation mode.

The most critical transportation problem concerned the drill rig and well casing. The two methods of bringing this equipment to Bethel are by barge or by air, both from Anchorage. Selection of the drilling contractor was not made in time to use the barge. In any event, demobilization of the drill rig back to Anchorage was always an air operation due to the scheduled time (winter). Drill rig transport by air has become a common practice in Alaska due to the extensive drilling on the north slope.

Design of the Hot Water Test System

The aquifer characterization experiments require the injection of hot water into a well. The water will be extracted from a production well and heated by waste heat from the diesel generators of the Bethel Utility Corporation (BUC). Two systems, one for pumping, heating and distributing the water, the other for conditioning and distributing the electric power for the water pumps and the instruments, were designed. These systems are described below.

The Water Supply System

The function of this system is to pipe water from the extraction well to the injection well through heat exchangers during the hot water tests, and by-pass the heat exchangers during isothermal tests. The heat necessary to raise the water temperature by up to 100°F is extracted from the coolant of the diesel generator units of the BUC. The water will be pumped from the extraction well at the rate of 200 gpm by a down hole pump and will flow through the tubes of two heat exchangers, connected in parallel, prior to reaching the injection well.

The flow rate of the aquifer water will be controlled to a constant value of 200 gpm; thus, the water temperature at the injection well will vary as a function of the power output of the utility.

Rhodamine dye stored in a 100 gallon tank will be injected into the hot water through a calibrated capillary and the dye concentration at the injection well will be measured.

The Power Supply System

The BUC produces power at 2400 Volts alternating current (Vac) and distributes power at 208 Vac whereas the instrumentation system on the wells and the heating strips (required to prevent freezing of the wells) require 110 Vac while the 200 gpm, 25 horsepower down hole pump and the 1000 gpm, 25 horsepower pump are best driven by 460 Vac motors. Accordingly, the electrical system specification was issued for bid. As a result of discussions with prospective bidders and the utility personnel, the bid request was modified to include an overhead electrical distribution system, as well as a ground based network. The distribution system evolved into two distinct networks. These are a 460 V, 3 phase, 60 Hz, 3 wire, 40 kva and a 208 V/120 V, 3 phase/1 phase, 60 Hz, 4 wire, 32.5 kva.

The 460 Vac system supplies the production well pump (W2) and the circulation pump for the heat exchanger. The 460 voltage level was chosen to adequately supply the motor inrush and operating currents without incurring undue losses, costs and wire size penalty.

The 120 Vac/208 Vac network is basically a Y connected system. Line to neutral voltage is used to power the instrumentation and heater systems. Both systems are metered for electrical energy output and are suitably protected by fused disconnects, breakers and grounding.

During operation, each pump is powered via an independent supply line and a pump control panel thus allowing full flexibility of operation, i.e., single pump, dual operation or programmed. Each well is supplied by an individual 45A, 120 Vac, single phase line. These lines originate at the central TRW control panel which is equipped with dedicated circuit breakers. A permanently connected 15A utility outlet and a 30A fused disconnect are provided at each wellhead. The fused disconnect will be used to de-energize the heaters during sensitive measurements and data collection periods.

Instrumentation

In Aquifer Characterization Planning, the instrumentation requirements were defined. In this task the details of the instrumentation system were selected, the elements of the system procured and shipped to the site.

The Aquifer Characterization instrumentation program comprises temperature, pressure, flow and strain measurements. Thermocouple connectors are provided at each well head for the type T thermocouples. The temperature will be measured using a Fluke 2190A digital thermometer, a Fluke Y2001 thermocouple selector and a Fluke Y2009 battery pack. The temperatures will be manually recorded at least once a day during the test program. The temperature from W-1, the injection well, will be continuously recorded on the Fluke Datalogger.

Hydrostatic pressure in the observation well will be sensed using Sensotec pressure transducers equipped with 0-5 V amplifers. A Fluke Datalogger will automatically record these pressures at a predetermined interval. The data will also be transcribed on a Techtran 817 data cassette. Production well pressure at the 200 ft level and atmospheric pressure will be sensed and recorded using Paroscientific DIGIQUARTZ pressure transducers, and pressure computers feeding a Hewlett Packard 150B printer.

Flow will be sensed with an Electronic Flo-Meters Inc. type F-3-500 flowmeter and Type DC-16 instrument. Data will be recorded on the Fluke 2240B Datalogger.

Sinco model 52621 vibrating wire strain gages on the casings of the water wells will have connectors terminating at the injection and production well heads. A Sinco portable readout will be used to display the change in strain directly and these readings will be manually recorded.

Stationary data acquisition equipment will be powered through an Elgar 6006B 110 Vac line conditioner. Portable equipment will be battery powered.

Drilling and Completing the Wells

Mobilization of the drilling equipment and materials was completed by September 20, 1980 and drilling started on Observation Well O-1.

Drilling of this first well was a learning experience for all concerned. The driller, who was the most highly recommended water well driller in Alaska, was used to punching a hole down to an aquifer without regard to performing the tests required by this program. Difficulties were experienced obtaining core samples with the wire line hammer available (9-in. throw). A heavier, longer throw (36-in.) hammer had to be flown in from Anchorage. Finally a drill rod subassembly was machined in order to get split spoon samples on the drill rod.

Drilling of the second observation well went much smoother and a usable gamma log was obtained, indicating two possible aquifer locations; one at 530-590 ft level and another between 700 and 800 ft. At this point a joint decision between TRW, Harding & Lawson and PNL was made to drill the withdrawal well, W-1 next, in order that a pumping test could be run to determine the most suitable aquifer. W-1 was drilled without significant incident and a 300 gpm pump installed. Initial tests showed excellent conditions with approximately 40 ft drawdown at maximum pump capacity. An additional pumping test was conducted with the lower aquifer zone plugged off. This test confirmed that most of the water was contributed from the zone at the 530-590 ft level. Subsequently, the remaining wells, O-3 and W-2, were drilled to a depth of 620 ft rather than 800 ft in recognition of the upper zone as being the productive one. All observation wells were instrumented in accordance with the plan in order to collect data during the isothermal and energy injection tests which will follow.

System Design Criteria

The development of design criteria was initiated by establishing contacts with the Bethel people responsible for producing the thermal energy that will be the source for the district heating project and those who will be managing and using the heat. The information obtained in these contacts fall into three categories:

- Availability of waste heat from the utility
- Physical requirements for the distribution system, and
- Energy requirements and existing heating plant of potential users.

BEST DOCUMENT AVAILABLE

Waste Heat from the Diesel Generator Units

The Bethel Utility Corporation has four General Motors Diesel (GMD) S16-EMD-2100 generator units installed to date. Each is rated at 2100 kW or 3070 hp. Heat can be extracted from the engine cooling water and from exhaust gas streams.

The engine cooling water flow rate is 850 gpm; each of the radiators is rated at 500 gpm and can extract up to 6.45×10^6 BTU/hr. The coolant leaves the engine at 180 to 185°F. The heat removed is proportional to the energy output, according to information obtained from GMD. Some of the design criteria, such as the acceptable flowrate variations in the distribution loop, the design value and the seasonal adjustment in the supply temperature, will depend on the design concept for control of waste heat utilization.

The District Heating Distribution System

Practical experience with Utiliduct domestic water and sewer system serves to eliminate some previously considered options. The City of Bethel Facilities has operated an underground water distribution system before that system was destroyed by freezing during a prolonged power outage due to fire at the BUC. The replacement piping was installed above ground in the Utiliduct, and this system, which was much cheaper to install, is easier to maintain and operate. The City recommended that TRW consider above ground insulated steel piping with Victaulic fittings supported on mud sills. Mud sills are more versatile and cheaper than pipes. The heat losses should not be excessive since the losses in the 1.5 mile long domestic water loop result in 0.5 to 1°F temperature drop in the water flowing at 50°F and a rate of 350 gpm. PVC is not usable; it is subject to creasing in cold weather, gets torn up by snowmobiles and damaged by vandalism.

Automatic equipment (i.e., controls, motorized valves) is not appropriate because of power fluctuations and outages, and because of a tendency of the operators to neglect inspections and maintenance when manual operation is not required. Each pump must have a spare in place, plumbed in since maintenance in winter is too difficult.

Energy Requirements and Existing Heating Plants of Candidate Users

Potential users for the District heating system are:

Bethel Hospital
Municipal Building Complex
Kuskokwim Community College
Kilbuck Elementary School
Domestic Water Heating System (the Utiliduct)
Bethel High School
Bethel Heights Housing Complex

The new Bethel Hospital is the prime candidate for utilizing heat from the utility. It is located near the utility and its new heating plant uses 180°F water for space heating and 140 and 110°F for hot water. TRW obtained a set of drawings of the heating plant and is now in position to examine the several ways of integrating the hot water from BUC into this plant. Since the needs of a hospital to maintain space and water temperatures are critical to the well being of the patients, the oil fired water heaters will have to be able to operate with and without the district heating and will have to be maintained and periodically exercised.

The new hospital would provide the ATES demonstration project with particularly favorable conditions: a large user, modern plant, proximity to the utility and to the aquifer, and high fuel costs. It appears that a suitable demonstration would be possible using the hospital only.

Project Status

Drilling costs were much higher than anticipated for the Bethel Project. The uncertainties of water and stratigraphy precluded a fixed price or unit price contract for drilling and the qualified drillers would only do the work on a per diem basis. The time required and complications encountered resulted in drilling costs of over $850,000, whereas less than $400,000 had been planned. Similar problems were encountered in estimating the cost of site preparation and mechanical work in this remote area of Alaska and this caused further cost overruns. This situation required that work be suspended while a comprehensive economic and technical assessment of the project is made. TRW was issued a Stop Work Order on December 10, 1980. The recision of program funding in FY-1981 and expected budget reduction for the STES Program in FY-1982 necessitated termination of the Bethel ATES Demonstration Project at the close of FY-1981.

PROJECT SUMMARY

Project Title: Conceptual Design of Aquifer Thermal Energy Storage System Demonstration - State University of New York, Stony Brook Campus, Long Island.

Principal Investigator: William V. Skinner/Donald J. Supkow

Organization:
Dames & Moore
6 Commerce Drive
Cranford, New Jersey 07016

Project Goals: To develop a conceptual design for a cost effective system to store seasonally sufficient chill energy in an aquifer to provide 12×10^6 ton-hours of summer air conditioning for the Stony Brook West Campus.

Project Status: The source needs and transport criteria reports are complete. Aquifer studies are complete and the Aquifer Characterization Report is in preparation.

ATES system cost estimates are being prepared for two separate applications; the first is limited to two buildings and the second is for the entire west campus.

Aquifer characterization field studies are complete. After obtaining baseline measurements a doublet test was performed wherein 18,000,000 gallons of water was chilled to 41.5°F, successfully injected, stored and recovered from the Upper Magothy Aquifer. Reinjection of the recovered water into a smaller well presented difficulties. This problem is currently under study but at present it is believed to be surmountable.

Thermal recovery efficiency is 65% based upon total chill BTU's recovered at 100 percent water recovery. Thermal recovery efficiency is 37% based upon quantity of chilled BTU's recovered from water having less than a 4°F temperature rise above injection temperature. The 3.5°F cutoff occurred after 42% of the injected water was recovered.

As a result of funding restraints, the project goals for the feasibility study have been reduced. The detailed economic evaluation and conceptual design tasks have been eliminated. Current goals are completion of the aquifer characterization report and preparation of preliminary estimated costs for two alternative ATES schemes (limited and full scale) for SUNY to consider in long range financial planning.

BEST DOCUMENT AVAILABLE

CONCEPTUAL DESIGN OF ATES SYSTEM DEMONSTRATION - STATE UNIVERSTIY OF NEW YORK STONY BROOK CAMPUS, LONG ISLAND

William V. Skinner Donald J. Supkow

Dames & Moore
6 Commerce Drive
Cranford, New Jersey

ABSTRACT

To provide for design of an aquifer thermal energy storage (ATES) system, it is necessary to determine if the aquifer characteristics are compatible with the user's air conditioning criteria. The Stony Brook West Campus seasonal air conditioning requirement is 12 x 10^6 ton-hrs. based upon a survey of individual building requirements and historical operational data. To meet this demand, transfer and storage of two billion gallons of water at a peak flow rate of 24,000 GPM will be required. The maximum temperature rise which can be accepted from the storage medium during chill recovery is less than 4°F. A doublet test facility was installed on site to test aquifer performance during a carefully monitored injection/storage/recovery cycle wherein 18 million gallons of water was chilled, stored and recovered to determine first cycle field efficiency. The results indicate a first cycle efficiency of 37 percent with a 3.5°F rise. It is expected the efficiency would improve with additional cycles.

INTRODUCTION

The basic function of an aquifer in an ATES system is to provide a storage and transmission medium for thermal energy using ground water as the energy transport fluid. To determine whether the Upper Magothy aquifer can adequately serve this function, it was characterized by evaluation of those hydraulic and thermal parameters which are significant in terms of their affects upon the storage capacity and efficiency of the ATES system. ATES demand criteria were established on the basis of maximum load requirements for conceptual alternative designs. Although the Upper Magothy Aquifer lacks the ideal stratigraphic conception of an aquifer confined by well defined upper and lower aquicludes, the thinly bedded silts/sand/clays characteristic of this aquifer served to confine chilled water within the injection zone reasonably well.

Findings indicate that it is feasible to store sufficient chill energy in the Upper Magothy Aquifer to meet the demand criteria for the "central plant option". A smaller alternative system is being considered as an intermediate step to provide an operating history in advance of final designs for the central plant option.

Because of USDOE funding recissions in March of 1981, Dames & Moore was advised to suspend all tasks except those necessary for completion of the Aquifer Characterization Report. As a consequence, a portion of one above ground and one below ground task remains incomplete, and all the coupling tasks were suspended before any significant work began. However, SUNY has requested and NYSERDA has agreed to fund a limited amount of the suspended coupling work to enable preparation of preliminary cost estimates for two ATES systems: 1) a central plant option and 2) a reduced scale application to two large buildings. Program continuance will depend upon the projected cost effectiveness of the ATES options and SUNY's ability to provide capital funds for any type of system improvements.

AQUIFER CHARACTERIZATION PROGRAM DESCRIPTION

A test site for aquifer evaluation was selected near the Engineering Heavy Laboratory, incorporating an existing 12-inch well and a 150 ton mechanical chiller formerly used for air conditioning. A well doublet system consisting of the existing 12-inch well (PI-1), a new 6-inch well (PI-2), and nine specially constructed observation wells (TPMW-1 through -9) provided the means for measurement of parameters selected for aquifer characterization (Figure 1).

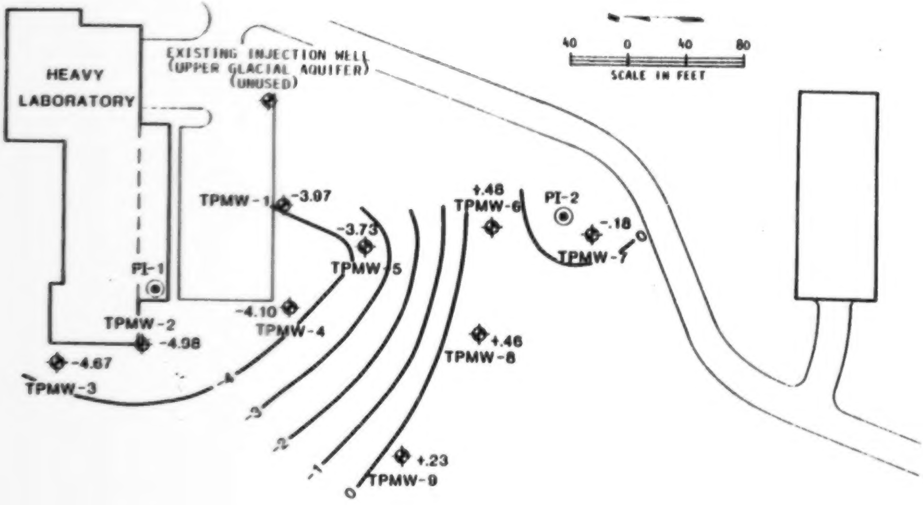
HEAVY LABORATORY
EXISTING INJECTION WELL (UPPER GLACIAL AQUIFER) (UNUSED)
40 0 40 80
SCALE IN FEET
TPMW-1 -3.97
-3.73
TPMW-5
+.48 TPMW-6
PI-2
-.18
TPMW-7
0
PI-1
-4.10
TPMW-4
TPMW-2 -4.98
-4.87
TPMW-3
-4
-3
-2
-1
0
+.46 TPMW-8
+.23 TPMW-9

FIGURE 1

Plan of Doublet Test Facility
Temperature change (°C) at 325 ft. depth resulting from injection of chilled water is illustrated.

Pumping tests and water level measurements were made to determine the aquifer hydraulic properties of permeability, storage coefficient, ground water flow directions and velocity. Field and laboratory tests were performed on soil samples to determine thermal conductivity, heat capacity, porosity, permeability and composition (Table 1). Ground water samples were collected and analyzed for appropriate chemical parameters (Table 2) before and during the doublet test. Data obtained during the doublet test indicated an increase in copper content in water leaving the mechanical chiller. This is being evaluated.

TABLE 1

AQUIFER CHARACTERISTICS

1.	Permeability (based upon 100 ft.)	136 ft/day - 385 ft/day
2.	Thickness (effective)	100 ft.
3.	Transmissivity (range)	10,200 - 28,000 gpd/ft.
4.	Storage Coefficient	$5.16x10^{-4}$ - $1.76x10^{-3}$
5.	Hydraulic Gradient (avg.)	$8.64x10^{-3}$
6.	Range of hydraulic gradient	$1.65x10^{-2}$ - $7.78x10^{-4}$
7.	Porosity	35%
8.	Ground water approach velocity (range)	6.46 ft/day - 86.3 ft/day
9.	Thermal Conductivity	7.0 x 10^{-3} Cal/°C/cm
10.	Heat Capacity	.636 - .655 C/cc/o_C

TABLE 2

CHEMICAL ANALYSIS RESULTS (mg/l)

Obtained during 48-hr. Pumping Test before start of Doublet Test

Total Dissolved Solids	28
Free Carbon Dioxide	6
Total Alkalinity	10
Silicate	0.82
Ammonia	<0.06
Nitrite	<0.01
Nitrate	0.10
Phosphate	<0.01
Sulfate	6
Chloride	5
Calcium	0.87
Chromium	<0.010
Copper	<0.010
Iron	<0.017
Lead	<0.050
Magnesium	0.59
Manganese	<0.007
Mercury	<0.001
Potassium	0.43
Sodium	3.66
Bicarbonate Alkalinity	10
Carbonate Alkalinity	0

Temperature measurements were made throughout the duration of the test with a thermister, at 5-foot intervals at depths of between 200 ft. and 400 ft., in the nine thermal stilling wells. The temperature of the pumped water was monitored continuously on a chart recorder. Water flow in the doublet system was monitored with a turbine totalizing and indicating meter.

A well doublet test was conducted by pumping 18 x 10^6 gallons of water at a rate of 300 GPM from Well PI-2, chilling it from its ambient temperature of about 51°F to about 41.5°F with the mechanical chiller (to simulate winter chilling by cooling tower) and injecting the chilled water in PI-1. Following the end of chill injection, the system was left idle for 48 days. Following the idle period, chilled water was recovered from storage by pumping PI-1 over a 76-day period.

A numerical model was used to simulate the test conditions and to predict aquifer response to chill storage and recovery.

RESULTS

The transmissivity was found to be variable throughout the site. This was indicated by the piezometric surface contour map, the baseline thermal measurements, and the varied response of water levels in the observation wells during a pumping test conducted prior to the doublet test. Table 1 presents a summary of aquifer characteristics in the doublet test area. Similar characteristics would be expected in the campus area tentatively selected for the demonstration.

Based upon the occurrence of interbedded sand and clay and/or silt in the injection zone, it was expected the average hydraulic conductivity would be much greater in the horizontal direction than in the vertical direction at any given well location, thereby indicating significant hydraulic anisotropy. As a result of detailed temperature measurements within time and space, the movement of the thermal plume through the injection zone was well defined (Figure 2). Successive temperature profiles in Well TPMW-2 illustrate how the inhomogenieties caused by a silt/clay zone in the aquifer result in two chill plumes, which eventually merged as time progressed. Temperature changes at 325 ft. depth (center of injection zone) resulting from the injection of 18 x 10^6 gallons of chilled water into PI-1 are illustrated in Figure 1. The chill front is not a sharp boundary but is a zone of increasing temperature extending radially away from the injection well. The elongation of the temperature change contours in the direction of PI-2 may be caused by inhomogenieties in the aquifer and the increased gradient toward PI-2.

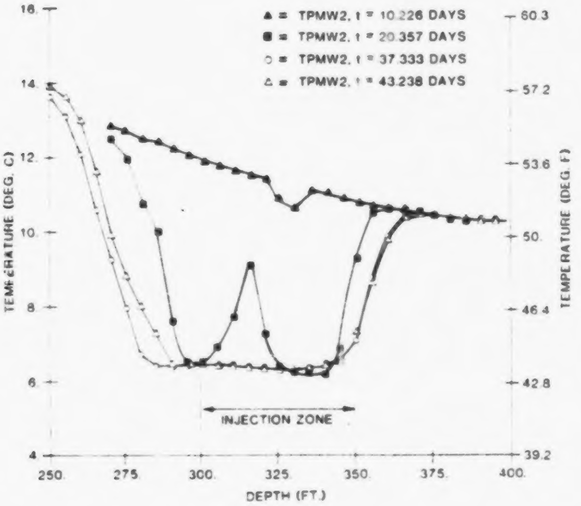

FIGURE 2

Consecutive Profiles of Temperature vs Depth for Observation Well TPMW-2. Note influence of less permeable layer at 320 ft. Minimum temperature of 43°F in aquifer injection zone is evident as is the migration of the chill plume above 300 ft.

In Figure 3 is a cross section along the line of observation wells TPMW-3 through -7 at a depth of 200 ft. to 400 ft. which illustrates temperature changes from baseline conditions to the end of chill injection (same time period covered by the map in Figure 1).

The clay/silt layer at a depth of 350 feet formed an effective barrier to downward movement of chilled water. However, the thinly interbedded clay/silt layers above 300 feet were a less effective barrier to the vertical upward movement of chilled water, especially in the vicinity of Well TPMW-2.

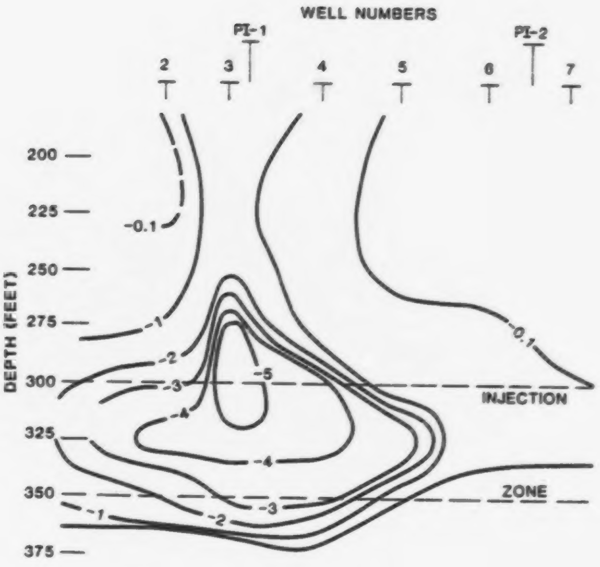

FIGURE 3

Vertical Section Along Line of Observation Wells
Illustrating Temperature Change as a Result of
Injection.
(Note rise in chill plume through aquitard.)

During the 48-day storage portion of the test, the temperature of the injected chilled water increased about 0.5°F. Very little movement of stored chill because of regional ground water flow was detected.

At the start of the chill recovery portion of the doublet test, the pumping rate from PI-1 was limited to 100 GPM because of clogging problems in the injection well PI-2. The test was operated at this rate until a decision was made to increase the chill recovery pumping rate to 300 GPM and waste the water which could not be returned to the aquifer by injection into PI-2.

In comparing Figures 1 and 3 (ΔT to end of injection cycle) with Figures 4 and 5 (ΔT to end of recovery cycle) it is apparent that a simple contraction of the chill storage zone depicted in Figure 1 did not occur. The chill plume did not reverse directions along the same flow paths when PI-1 was changed from an injection to a pumping mode. The vector shift could be due to one or more of the following factors: 1) permeability differences throughout the site, 2) regional ground water gradient causing drift of the chill plume, and 3) injection rate in PI-2 was less than the pumping rate of PI-1 for the chill recovery cycle (note that pumping and injection rates were equal during the chill injection cycle).

Whereas chilled water was injected into PI-1 at a constant temperature of 41.5°F (5°C) during the entire chill injection cycle, the temperature of water pumped from PI-1 during the chill recovery cycle increased in proportion to the volume of water recovered.

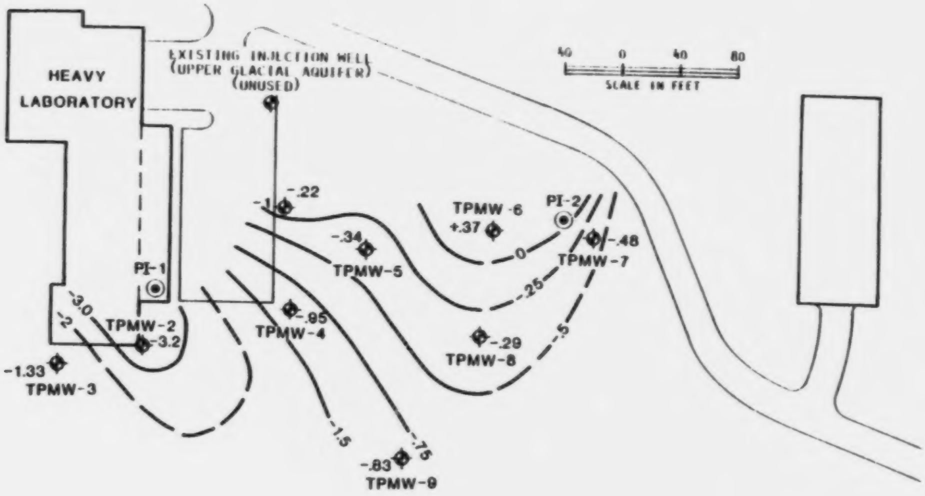
HEAVY LABORATORY
EXISTING INJECTION WELL (UPPER GLACIAL AQUIFER) (UNUSED)
40 0 40 80
SCALE IN FEET
-1
-.22
TPMW-6
+.37
PI-2
-.48
TPMW-7
-.34
TPMW-5
-0
-.25
-.5
PI-1
-3.0
-2
TPMW-2
-3.2
-1.33
TPMW-3
-.95
TPMW-4
-.29
TPMW-8
-1.5
-.75
-.83
TPMW-9

FIGURE 4

Plan of Temperature Change (°C) at 325 ft. Depth Illustrating Residual Chill Near End of Recovery

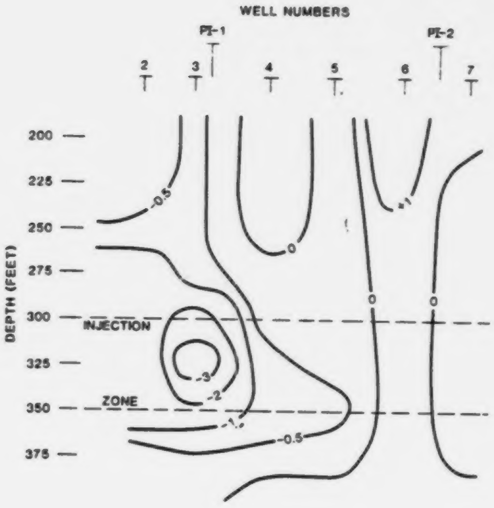

FIGURE 5

Vertical Section Along Line of Observation Wells Illustrating Temperature Change (Temp. °C) from Beginning of Test (Baseline) to Near End of Recovery

The rate of temperature rise during chill recovery was predicted on the basis of the computer model which was developed to simulate the aquifer performance during the doublet test. Several different predictive runs were made using various assumed conditions. For the case of no regional ground water flow, the simulated production curve (see Figure 6) matched the actual recovery temperature reasonably well for the early portion of the recovery cycle.

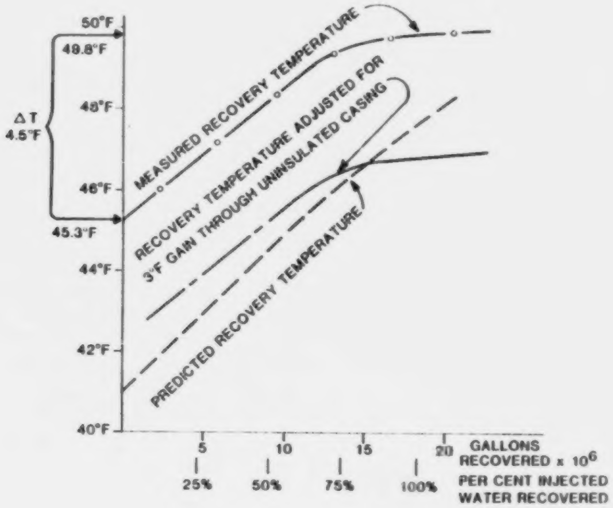

FIGURE 6

Recovery Curves of Temperature vs Volume Recovered

Although chilled water was injected at a temperature of 41.5°F the minimum temperature in storage near the injection well was 43°F indicating a 1.5° rise from heat gain in transit partially by heat conducted through the well casing from the warm Upper Glacial Aquifer and partially by friction in passing through the static turbine blades of the pump through which the water was injected. This heat gain was also observed during the recovery cycle. These two sources of extraneous heat can be eliminated by appropriate well design, consequently we have adjusted the temperature recovery curve to reflect no significant heat gain during transit in calculating the chill recovery efficiency of the system.

The real temperature recovery curve, after adjustment for the extraneous heat gains discussed above, is also illustrated in Figure 6. Both chill recovery curves are based on recovered volume vs temperature.

To calculate total chill recovery efficiency where total volume recovered = total volume injected:

$$\text{Total Efficiency} = \frac{\text{Total Energy Recovered in one injection volume}}{\text{Total Energy Injected}} \times 100$$

On a practical basis, the recovered chill energy cannot be used in an air conditioning system if it is above a certain critical "cutoff" temperature. As the chilled water is recovered from the aquifer by pumping, the temperature is expected to rise in conformance with the recovery curve (Figure 7) as recovery progresses.

The equation for this efficiency is:

$$\frac{\text{useable chill BTU's recovered}}{\text{total chill BTU's injected}} \times 100$$

where total BTU's injected is (T ambient - T injection) X total volume injected in gals. x 8.5 $\frac{\text{lb}}{\text{gal}} \times 1 \frac{\text{BTU}}{\text{lb}/{}^\circ\text{F}}$

and where useable chill BTU's recovered is (T ambient - integrated average T of recovered water) X total volume recovered in gals. X 8.5 $\frac{\text{lb}}{\text{gal}} \times 1 \frac{\text{BTU}}{\text{lb}/{}^\circ\text{F}}$

For example, from Figure 6 we see that at a cutoff temperature of 43°F, 2×10^6 gallons of water was pumped, for 44°F, 5×10^6 gallons, etc. Using these figures, we can calculate a curve for efficiency as a function of cutoff temperature (see Figure 7).

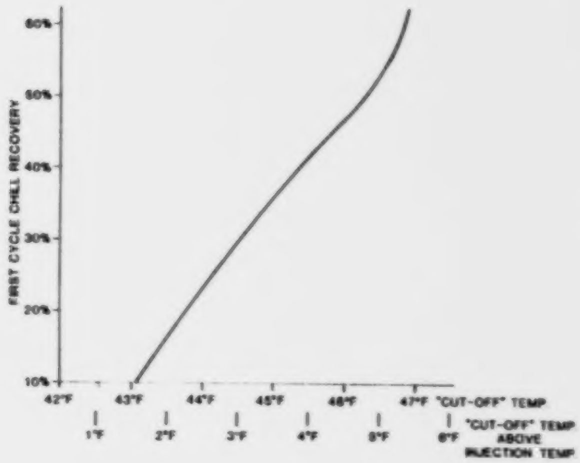

FIGURE 7

Curve Illustrating First Cycle Recovery as a Function of Cutoff Temperature

With the upper scale on Figure 7, the efficiency can be read as a function of cutoff temperature expressed as degrees Farenheit above injection temperature. From this curve, efficiency evaluation for various combinations of injection temperature and recovery cutoff temperature can be made. This assumes that average chill losses in the aquifer will be about 0.5°F during the chill storage period between chill injection and recovery.

The experiment ran for only one cycle of chill injection and recovery. Chill loss is proportional to the temperature difference between the aquifer storage zone and the adjacent aquiclude. As the adjacent aquicludes become chilled during each cycle, it is reasonable to expect that chill losses within the aquifer will be reduced on succeeding cycles thereby increasing the recovery efficiency on succeeding cycles.

CONCLUSIONS

Based on the results to date of the Stony Brook ATES experiment as outlined herein, the following conclusions have been reached:

1. Chill energy can be successfully stored in and recovered from the test aquifer.
2. The hydraulic and thermal properties can be successfully modeled to predict the recovery temperature of the injected cold water.
3. For maximum chill energy recovery from the aquifer, the above ground system should be designed to utilize as high a cutoff temperature as possible.
4. Materials other than copper, such as stainless steel, may have to be used to avoid aquifer contamination by reinjected water.
5. Well capacity will have to be overdesigned to accommodate injection well capacity.
6. Injection and recovery wells will require insulation to avoid heat gains from overlying warm aquifers.
7. Injected chill water should be through drop pipes designed and operated to reduce friction loss and heat gain and prevent introduction of air.

PROJECT SUMMARY

Project Title:	Aquifer Thermal Energy Storage Project at the University of Minnesota	
Principal Investigators:	Warren E. Soderberg, J.C. O'Gara, and Matt Walton	
Organization:	University of Minnesota 319 - 15th Ave. S.E. Minneapolis, Minnesota 55455	Minnesota Geological Survey 1633 Eustis St. St. Paul, Minnesota 55108
Project Goals:	The project goal is to construct a test facility with a nominal 5-megawatt thermal power input/output capacity, perform a series of test cycles at temperatures up to 150°C (300°F), and acquire the basic hydrological, hydrogeochemical, and hydrogeothermal data needed to design a full-scale application of the ATES concept to a major regional bedrock aquifer.	
Project Status:	Eight monitor wells have been constructed and instrumented with thermocouples. Pressure transducers have not yet arrived; they will be installed after calibration. The water supply well has been drilled and the screen is being placed. Drilling has started on the heat injection well. Well completion is expected in October 1981. Surface connections between well sites and to the University heating plant have been made. The heat exchanger and heat discharge system have been installed. Pumps are ready for installation, and the control system is in place. Computer models have been run on the basis of preliminary values for hydrologic and thermal properties. Laboratory investigation and computer modeling of the chemical equilibria and kinetics of water-rock reactions are in progress. Test cycles are expected to begin in November 1981.	
Contract Number:	DE-AC06-76RLO 1830, Subcontract B-97601-A-C	
Contract Period	May 1980 through May 31 1982	
Funding Level:	$1,900,000	
Funding Source:	U.S. Department of Energy through Battelle Pacific Northwest Laboratories	

THE UNIVERSITY OF MINNESOTA AQUIFER THERMAL ENERGY STORAGE PROJECT

Matt Walton
University of Minnesota, Minnesota Geological Survey
St. Paul, Minnesota

ABSTRACT

Construction of an ATES test facility in a major regional aquifer is scheduled for completion in October 1981, at the University of Minnesota, St. Paul campus. The pumping well doublet designed for injection and withdrawal of hot water at up to 300 gpm and 150°C (300°F) has a nominal maximum thermal power input/output of 5 megawatts. Eight monitor wells are instrumented with thermocouples and pressure transducers. Delays and cost overruns have resulted from well construction problems in weak sandstone and fractured dolomite. Laboratory investigations and computer modeling of the fluid dynamics, and thermal and chemical properties of the system are in progress.

INTRODUCTION

The conceptual design of the University of Minnesota Aquifer Thermal Energy Storage (ATES) project was described in detail in the Proceedings of the 1980 Contractors' Review (Battelle PNL 1980). It will be briefly summarized here.

The project entails the construction of a test facility with a nominal 5-megawatt thermal power input/output capacity to provide the basic hydrogeological, hydrogeochemical and hydrogeothermal parameters needed to design a full-scale application of the ATES concept to a major regional bedrock aquifer. The test facility is designed to inject and withdraw hot water at the rate of 300 gpm at a maximum temperature of 150°C with an operating temperature differential, or delta T, of 66°C.

HYDROGEOLOGIC SETTING

The Twin Cities metropolitan area is underlain by a stratified sequence of lower Paleozoic sedimentary formations consisting of porous sandstone and fractured dolomite beds grouped into four major regional aquifers separated and confined by relatively impervious shale formations or zones. These bedrock formations are overlain by as much as several hundred feet of glacial drift, commonly 50 feet to 150 feet thick. The Twin Cities are near the center of a broad, shallow, multiple-aquifer artesian basin in the Paleozoic strata. In the center of the basin the Paleozoic section is well over 1,000 feet thick. The Mount Simon-Hinckley aquifer, which is the lowermost at a depth of about 1,000 feet, is tapped by some large industrial and municipal wells. The Franconia-Ironton-Galesville aquifer is little used near the center of the basin because it has comparatively low hydraulic conductivity. The Prairie du Chien-Jordan aquifer is a major metropolitan area and regional water source. The St. Peter aquifer is used mainly by suburban domestic wells.

The Franconia-Ironton-Galesville (FIG) aquifer was chosen for the Minnesota ATES test. In the University campus area (Fig. 1) the aquifer is about 200 feet thick. The top is at a depth of 560 feet to 600 feet below the surface (altitude 348 feet). The static water level is at an altitude of about 770 feet, providing a head of about 422 feet above the top of the formation. Thus the aquifer is at sufficient depth and has sufficient head to make high temperature pressurized hot water storage possible. There are no competing uses of the aquifer that affect the University area. The hydraulic conductivity, though known to be relatively low, was judged to be adequate for the yields needed, and lower conductivity tends to mitigate the thermal stratification problem of hot water storage. Finally, the overlying and underlying shale formations provide tight confinement.

TEST FACILITY DESIGN

To achieve the goals of the initial phase of the test program and to provide data needed to obtain long-term variances from state rules preventing ground-water reinjection, it was considered essential to obtain data on at least three and preferably four or five cycles of heat injection, storage and withdrawal, starting with water at 100°C and increasing the temperature of injection to 150°C in two steps. Given the effective time constraints on the program, this established a 24-day test cycle of injection, storage and withdrawal as the basic unit for the initial program. This cycle, together with the thickness and porosity of the aquifer, determined the dimensions and configuration of the test facility.

The test array, now under construction, consists of two pumping wells 240 meters (790 feet) apart with an array of monitor wells designed to measure pressure and temperature within the aquifer, the confining beds and the overlying and underlying aquifer (Fig. 2). Monitor wells at a radius of 7

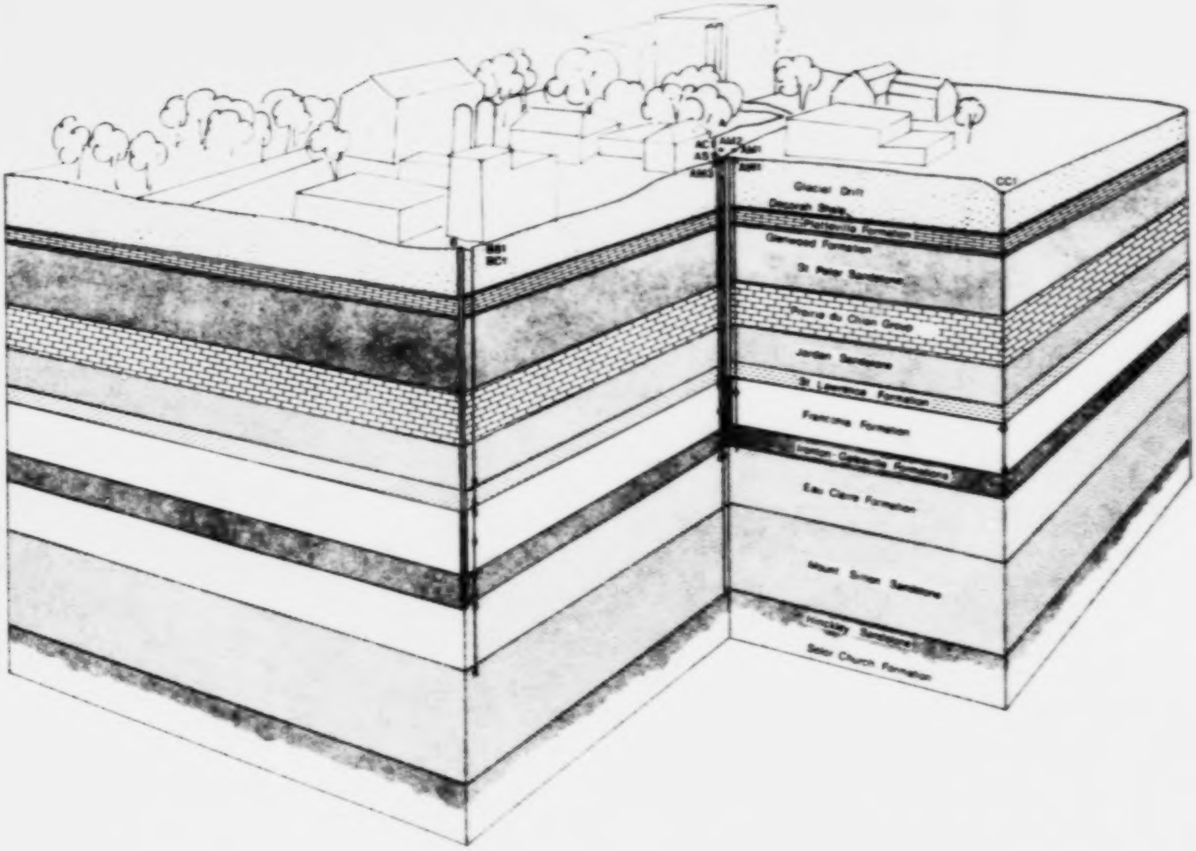
AC1
AS1
AM2
AM1
CC1
BS1
BC1
Glacial Drift
Decorah Shale
Platteville Formation
Glenwood Formation
St Peter Sandstone
Prairie du Chien Group
Jordan Sandstone
St Lawrence Formation
Franconia Formation
Ironton-Galesville Sandstone
Eau Claire Formation
Mount Simon Sandstone
Hinckley Sandstone
Solor Church Formation

Figure 1. Block diagram of the ATES site, University of Minnesota, St. Paul.

meters (23 feet) are located to measure the passage of a thermal front or thermocline about half way through an 8-day heat injection period. Near the end of the 8-day heat injection the thermocline will influence monitor wells 14 meters (46 feet) out.

It was recognized from the start that this design called for very tight spacing of the monitor network. However, because the thickness and porosity of the aquifer are given, the only ways to increase the radius of the network and still measure the effects of heat injection are to increase either the rate of water injection or the duration of the test cycle in proportion to the square of the desired increase in network radius, with a corresponding increase in water volume and heat demand. We feel that 300 gpm is a practical limit to the injection rate in a single well in the FIG aquifer, and thus the dimensions of the network were established.

CONSTRUCTION

During the past year we have been engaged in the construction of the test facility. At the same time we have been conducting analytical and experimental work on the properties of the rock, the chemistry of water in the aquifer system, rock and water interactions at various temperatures and pressures, and developing hydraulic, thermal and chemical equilibrium and mass transport models. All of the monitor wells have been completed (Fig. 3), the pumping well at site B is being completed, and drilling of the primary heat injection well at site A is imminent. Connections for the pumping wells at sites A and B have been made through an existing utility tunnel, and the steam line, heat exchanger, auxiliary pumps, controls and heat discharge system have been installed. Upon completion and hydraulic testing of the pumping wells, the test facility will be ready to begin operation. This elusive date is now estimated to be some time in October.

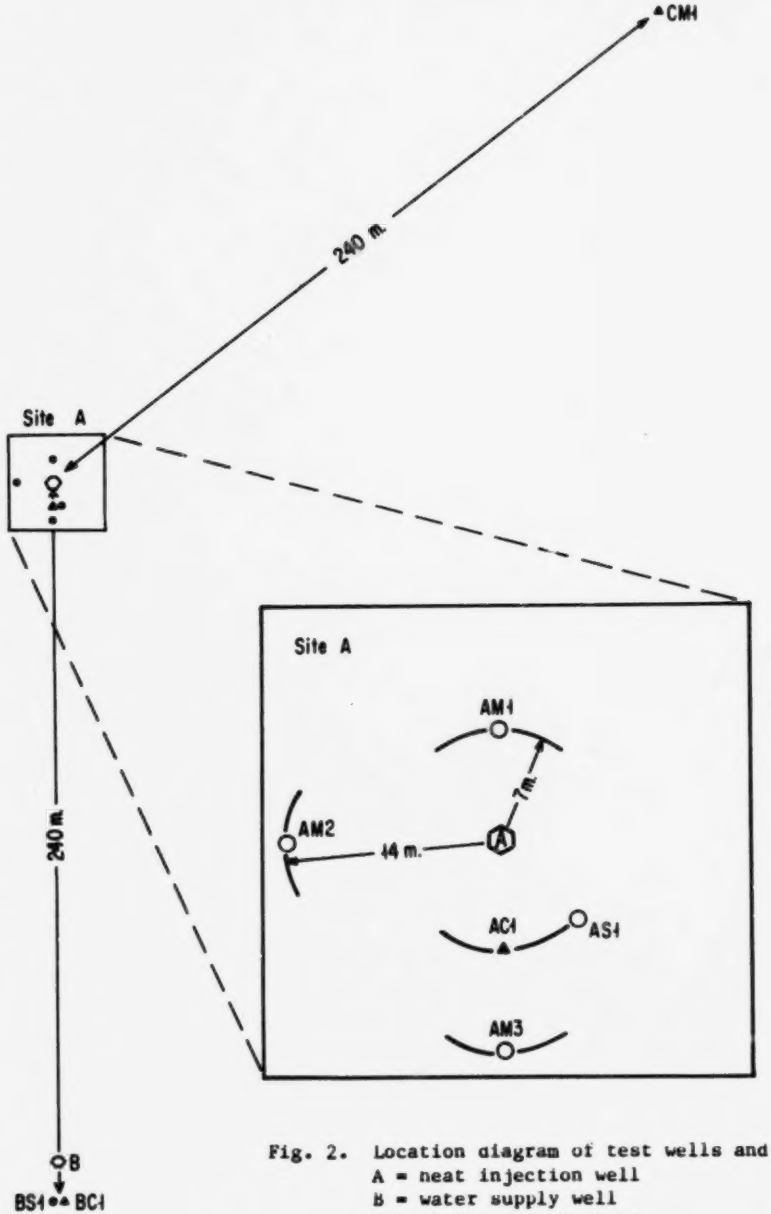

Fig. 2. Location diagram of test wells and monitor wells.
A = heat injection well
B = water supply well
AC1, BC1 = core borings
AS1, BS1 = supplemental monitor wells for AC1 and BC1
AM1, AM2, AM3, CM1 = monitor wells

CONSTRUCTION PROBLEMS

The construction of this test facility has entailed significant cost overruns, design modifications and delays, resulting directly from difficulties with drilling and well construction, mainly in the weak, friable, almost unconsolidated sands of the St. Peter and Jordan sandstone formations and the highly fractured and fissured dolomite in the Prairie du Chien Group beds. Essentially all of the problems that are associated with drilling in weak, running and caving ground have been encountered, resulting in slow progress and high casing and grouting costs. We have no reason to think that the rock formations at the site are unusually fragile in comparison with the rest of the basin, in which thousands of wells have been completed, and our drilling is being done by experienced contractors. Our drilling problems remain a source of bafflement and frustration, but the job is getting done.

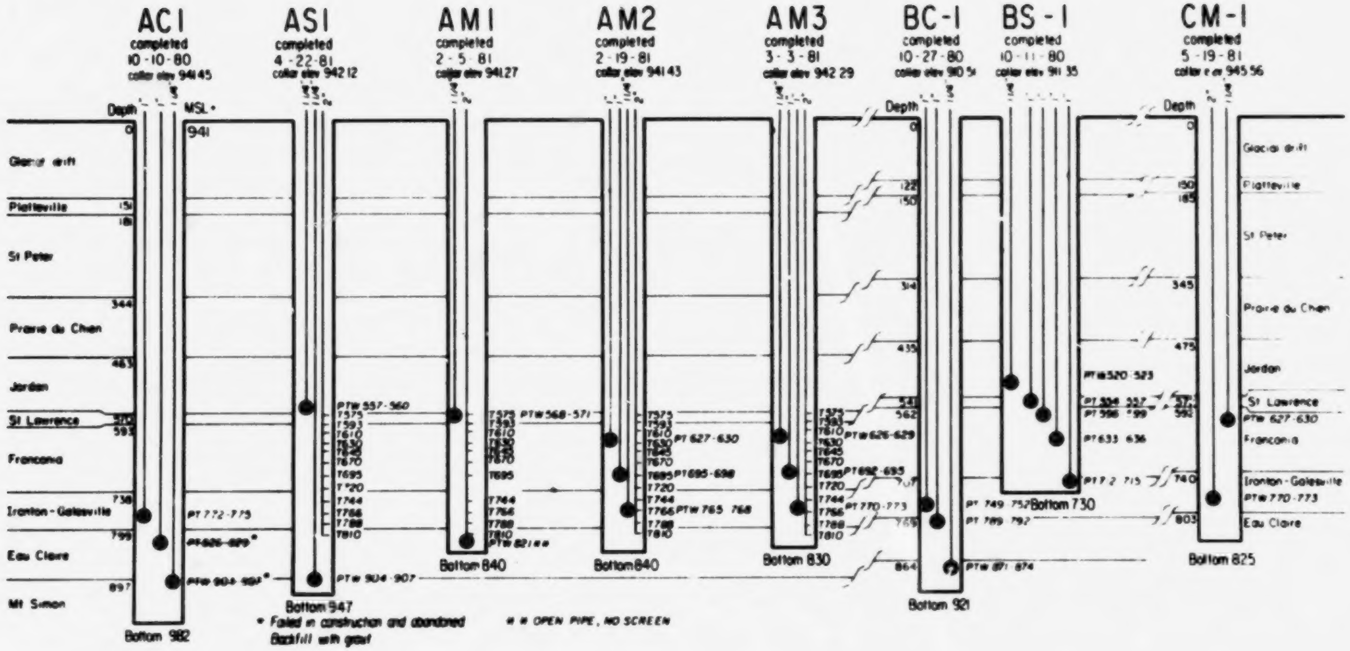
ACI
completed
10-10-80
collar elev 941.45
ASI
completed
4-22-81
collar elev 942.12
AMI
completed
2-5-81
collar elev 941.27
AM2
completed
2-19-81
collar elev 941.43
AM3
completed
3-3-81
collar elev 942.29
BC-I
completed
10-27-80
collar elev 910.5
BS-I
completed
10-11-80
collar elev 911.35
CM-I
completed
5-19-81
collar elev 945.56
Depth
MSL
0
941
Glacial drift
Platteville
151
181
St Peter
344
Prairie du Chien
463
Jordan
St Lawrence
570
593
Franconia
738
Ironton - Galesville
799
Eau Claire
897
Mt Simon
PT 772-775
PT 826-829*
PTW 904-907*
Bottom 982
PTW 557-560
T575
T593
T610
T630
T645
T670
T695
T720
T744
T766
T788
T810
PTW 904-907
Bottom 947
* Failed in construction and abandoned
Backfill with grout
PTW 568-571
PTW 821**
Bottom 840
** OPEN PIPE, NO SCREEN
PT 627-630
PT 695-698
PTW 765-768
Bottom 840
PTW 626-629
PT 692-695
PT 770-773
Bottom 830
Depth
0
122
150
314
435
541
562
864
PT 749-752
PT 789-792
PTW 871-874
Bottom 921
PTW 520-523
PT 534-537
PT 596-599
PT 633-636
PT 712-715
Bottom 730
Depth
0
150
185
345
475
592
740
803
Glacial drift
Platteville
St Peter
Prairie du Chien
Jordan
St Lawrence
PTW 627-630
Franconia
Ironton - Galesville
PTW 770-773
Eau Claire
Bottom 825

Fig. 3. Monitor well instrumentation as of 11 August 1981.
PT = Screen location for pressure and temperature measurements; numbers = depth in feet.
PTW = Screen location for pressure, temperature, and water samples; numbers = depth in feet.
T = Thermocouple location in closed casing; numbers = depth in feet.

Some additional impact on costs may have flowed from the fact that the Department of Health and Pollution Control Agency variance needed to re-inject heated water was contested for somewhat obscure reasons by an environmentalist organization. Possibly for this reason our state inspection and construction requirements have been, to say the least, stringent.

The principal functional problem resulting from drilling difficulties stems from significant deviations from straight and vertical alignment in the monitor wells. Information currently available on hole alignment is given in Table 1.

Table 1. Deviations of drill holes from vertical

Hole	Depth, ft	Survey Method	Deviation from Vertical
AC1	982	*PLT	(?) greater than hole diameter
AS1	904	†DHM	20.17 ft S.22°40'E.
AH1	840	DHM PLT	(instrument failed) (?) greater than hole diameter
AH2	840	DHM	21.28 ft S.6°35'E.
AH3	830	DHM	27.47 ft S.67°38'E.
BC1	921	PLT	(?) greater than hole diameter
BS1	730	Interference with well B	about 30 ft northward
CH1	743	DHM	not significant
Site B well	777	PLT	2.67 ft S.32°W.

*PLT = Plumb line triangulation
†DHM = Downhole magnetic

Extreme care was taken in drilling the site B pumping well. A deflection of only 2.67 feet in 777 feet was measured by plumb line triangulation, which is within the American Water Well Association (AWWA) code. The other wells are grossly out of alignment. Deviations in the monitor wells are comparable in magnitude to the carefully planned spacing between wells in our initial monitor network. This will result in an irregular pattern of instrument stations, rather than a rational geometrical array. Analysis of this problem awaits completion of well A and final downhole gyroscopic surveying of all holes. Some impairment of our network seems inevitable, and our modeling program will need modification.

The magnitude of the deviations in borehole alignment has been a surprise to us. The absolute error in location of an instrument station in a crooked hole will increase with depth. This means, from the practical standpoint, that deep, thick aquifers need large monitor networks to offset drilling errors. Such networks entail a corresponding increase in volume of water injected and thus an increase in the duration of the test cycle. We believe we can still get useful results from the short-cycle tests we have planned, but the need to follow up with an expanded monitor network and a long-cycle test program seems evident.

CURRENT INVESTIGATIONS

Investigations have gone forward during the construction of the test facility in a number of categories:

1. Downhole studies
    a. geophysical logging of holes as completed

   - b. inflatable straddle packer testing of hydraulic properties of zones within the aquifer and confining beds
   - c. periodic static water-level measurements in holes following completion
   - d. water sample collection and analysis

2. Studies of cores and samples
   - a. detailed logging of cores from holes AC-1 and BC-1
   - b. petrographic description and analysis of thin sections and samples from cores
   - c. preparation of core samples for porosity and permeability tests

3. Hydrogeochemical research
   - a. design and construction of two small-diameter (1 inch) submersible pumps to extract water samples from monitor well piezometer tubes
   - b. chemical analysis of aquifer rock and water samples by atomic absorption spectrophotometry and other methods
   - c. experiments on the kinetics of rock dissolution in water at atmospheric pressure and acquisition of pressure reactors to study dissolution up to 150°C and corresponding vapor pressure
   - d. theoretical studies of the effects of variation in pressure and temperature on equilibrium constants
   - e. development of an auxiliary computer program DELH and data files to adapt the program MINEQL to high-temperature computations in order to compute chemical equilibria of minerals in hot water

4. Instrumentation and data processing
   - a. calibration, installation and testing of thermocouples in monitor wells at site A
   - b. connection of instrumentation at site A into data logger and system debugging
   - c. completion of data manipulation and reduction program and documentation of its use

5. Hydrologic and hydrothermal modeling
   - a. preparation of radial flow and thermal energy transport models for calibration with field test data
   - b. sensitivity of temperature to thermal conductivity, rock heat capacity, porosity and dispersivity
   - c. sensitivity of pressure to hydraulic conductivity
   - d. sensitivity of anisotropic flow to variation in vertical hydraulic conductivity
   - e. maximum head changes at site A during injection and withdrawal, based on preliminary estimates of hydraulic parameters
   - f. positions of 200°F, 150°F and 100°F temperature fronts during a 24-day test cycle, based on preliminary estimates of hydraulic parameters
   - g. variation of water temperature with time during various heat injection and recovery cycles with calculated percent heat recovery at end of each cycle

Some investigative activities have been discontinued, at least for the time being, due to the overrun in well construction cost. These include the development of hot water technology related to heat exchange, assessment of system economic and energy aspects and conceptual studies of future applications. However, studies of biological activity in the water and the ground have been designed and will be implemented when the hot water test cycles begin.

SUMMARY OF RESULTS TO DATE

To summarize very briefly the results of the ongoing investigations to date: The aquifer comprises three main zones, an upper zone about 45 feet thick of fine dolomitic sandstone and fine sandy dolomite with varying amounts of glauconite and feldspar and a hydraulic conductivity of about 2 feet per day, a middle zone 80 feet thick of silty to shaly rock with a hydraulic conductivity of about 0.1 foot per day, and a lower zone 50 feet thick of fine to coarse quartz arenite with a hydraulic conductivity of about 4 feet per day. Hot water injected into this aquifer will produce an asymmetrical thermal front, probably roughly approximated by the results of preliminary computer modeling shown in Figure 4. The chemical effect of hot water injection will be the precipitation of $CaCO_3$ and the solution of silica with a net decline in Ca concentration and net increase in dissolved Mg, CO_3 and $Si(OH)_4$. The effects on small amounts of iron and complex minerals such as glauconite in the rock have not yet been investigated. Total dissolved solids will probably increase from about 200 ppm by a factor of 2 or 3. The net effect does not appear to be threatening to the operation of the system. Modeling water temperature and heat recovery shows considerable variation in storage function depending on the duration of injection, storage and recovery periods. Modeling results for 24-day cycles are shown in Figure 5, and for an annual cycle in Figure 6. The annual cycle shows heat recovery increasing from 73 percent the first year to 84 percent in the fifth year, suggesting that useful results are possible, but it is noteworthy that heat recovery requires twice the pumping rate of heat injection to obtain this favorable result.

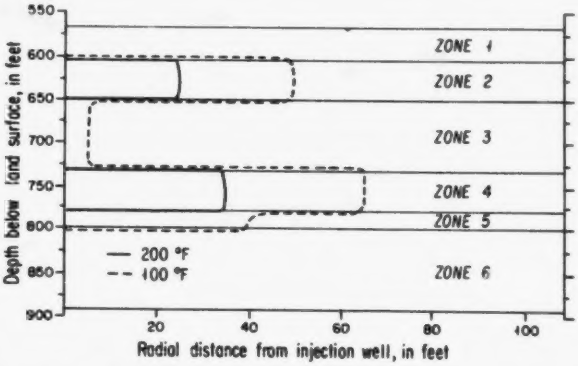

Fig. 4. Position of 200°F and 100°F temperature fronts after 8 days of injecting 300°F water at a rate of 300 gpm. Hydrologic zonation and thermal properties identical to those described in USGS-ATES Technical Progress Report for October 1 to December 31, 1980.

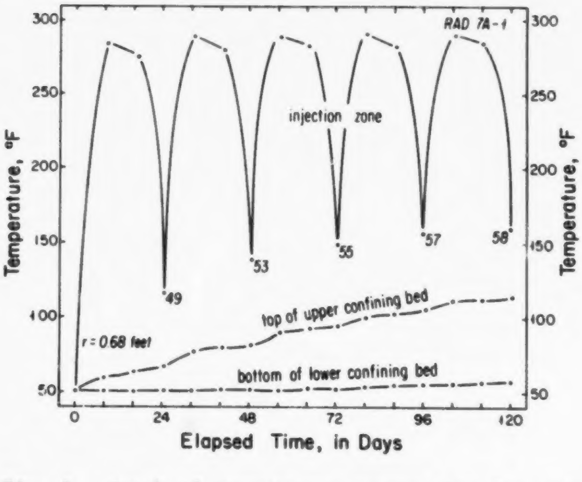

Fig. 5. Graph of temperature versus time for injection zone and upper confining bed during five 24-day cycles (8 days injection, storage and withdrawal cycle). The injection/withdrawal rate is 300 gpm and the injection temperature is 300°F.

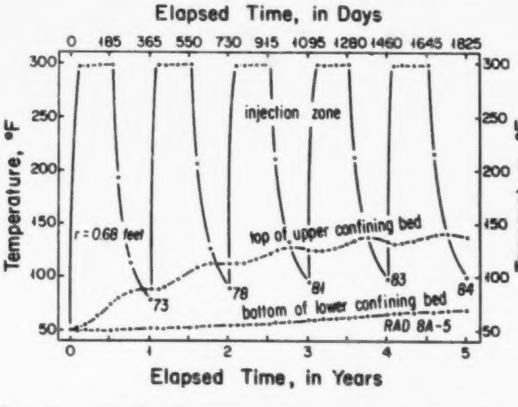

Fig. 6. Graph of temperature versus time for injection zone and upper and lower confining beds during five 1-year cycles (6 months injection at 300 gpm and 6 months withdrawal at 600 gpm) and percentage of heat recovery at the end of each withdrawal period. The injection temperature is 300°F.

PROJECT SUMMARY

Project Title: Seasonal Storage Technology Program Management

Principal Investigator: Jay R. Eliason

Organization:
Pacific Northwest Laboratory
P.O. Box 999
Richland, Washington 99352
(509) 375-2582

Project Goals: The Seasonal Storage Technology Program is designed to conduct research and development studies required to provide a sound technical base for the commercialzation of seasonal thermal energy storage concepts.

Project Status: The Seasonal Storage Technology Program has been organized into the following tasks: Legal/Institutional Assessment; Economic Assessment; Environmental Assessment; Field Test Facilities; Compendia; Physicochemical Analysis; Numerical Simulation; and Nonaquifer STES Concepts. The first seven tasks are initially emphasizing development of technical support for the ATES concept. Progress for individual tasks is identified in separate project summaries.

A Consultant Review Team which provides a technical review of the program has been established to provide an independent overview of program activities. Recommendations made by the Consultant Review Team provide guidance for planning and conducting the program. The Consultant Review Team at this time is composed of the following individuals: Stanley N. Davis, Professor, Department of Hydrology and Water Research, University of Arizona; Robert D. MacNish, Chief, Arizona District, U.S. Geological Survey; Donald Langmuir, Professor, Department of Chemistry and Geochemistry, Colorado School of Mines; Howard E. Lowitt, Energetics Incorporated; David L. Schreiber, CRT Coordinator, Consulting Hydraulic Engineer; and John F. Spencer, Assistant Director, Washington State Department of Ecology.

Contract Number: DE-AC06-76RLO 1830

Contract Period: Continuing

Funding Level: $1,763,800, FY 1981, B/O

Funding Source: U.S. Department of Energy, Office of Energy Systems Research

SEASONAL STORAGE TECHNOLOGY PROGRAM

Jay R. Eliason
Pacific Northwest Laboratory
P.O. Box 999
Richland, Washington 99352

INTRODUCTION

The Seasonal Storage Technology Program is designed to conduct research and development studies required to provide a sound technical base for commercialization of seasonal thermal energy storage concepts. Initial activities of this task are an effort primarily directed toward support of the Aquifer Thermal Energy Storage concept. Long-range task goals include investigation and evaluation of other seasonal thermal energy storage concepts which may be considered for future emphasis.

During FY 1981 the program structure developed in FY 1980 was continued. Subcontracts have been placed with industrial contractors, universities, national laboratories, government agencies and private consultants to obtain qualified expertise in all research areas.

APPROACH

The Seasonal Storage Technology Program has been organized to provide near-term support to the ATES Demonstration Program and long-range investigation and evaluation of other seasonal thermal energy storage concepts. The program has been organized into the following tasks and task leaders have been assigned:

Legal/Institutional Assessment - Paul L. Hendrickson
Economic Assessment - Raymond W. Reilly
Environmental Assessment - George E. Wukelic
Field Test Facilities - David A. Myers
Compendia - Leigh S. Prater
Physicochemical Analysis - Steven C. Blair
Numerical Simulation - Charles T. Kincaid
Nonaquifer STES Concepts - Donald E. Blahnik

These tasks and task leaders will continue as the basic program framework into FY 1982.

Also the Consultant Review Team, which provides a technical review of the program, provided an independent overview of program activities in January 1981. Recommendations made by the Consultant Review Team was composed of the following individuals: Stanley N. Davis, Professor, Department of Hydrology and Water Research, University of Arizona; Robert D. MacNish, Chief, Arizona District, U.S. Geological Survey; Donald Langmuir, Professor, Department of Chemistry and Geochemistry, Colorado School of Mines; Howard E. Lowitt. Energetics Incorporated; David L. Schreiber, CRT Coordinator, Consulting Hydraulic Engineer; and John F. Spencer, Assistant Director, Washington State Department of Ecology.

Project summary sheets describing each task activity will be included in these proceedings. These descriptions will include reference to subcontractor activities which are being conducted and in many cases are also described in separate papers in the proceedings.

The following objectives have been developed to provide an overview of specific task activities:

Legal/Institutional Assessment - to conduct comprehensive reviews of legal and institutional requirements relevant to STES concept commercialization.

Economic Assessment - to develop methodology for accurate economic assessment of STES concepts and to apply these methodologies to specific data sets developed for economic evaluation.

Environmental Assessment - to assist in determining and meeting evnironmental documentation requirements and defining environmental research and monitoring needs to support commercialization of STES concepts.

Field Test Facilities - to perform field tests of STES concepts and provide background data and experience for concept evaluations.

Compendia - to collect, summarize, and trasmit STES related information and to develop and maintain key data in an interactive data base.

Physicochemical Analysis - to investigate materials chemical and physical response to incremental temperature and pressure changes imposed by thermal energy storage.

Numerical Simulation - to develop numerical simulation codes for assessment of STES concepts and application of these codes in support of field tests.

Nonaquifer STES Concepts - to evaluate proposed STES systems other than aquifer storage including analysis of operating characteristics, applications, thermal effectiveness, and economics.

STATUS

The Seasonal Storage Technology Program has directly involved eleven industrial contractors, six universities, two government agencies outside of DOE, several private consultants and three of the DOE national laboratories outside of PNL. Activities planned for FY 1982 will continue this diversified involvement of external support to this PNL coordinated program.

Within PNL commitments have been obtained to maintain the management and support staff required to continue the planned program activities. The following papers by each task leader will provide the detailed breakdown of contracting activities.

PROJECT SUMMARY

Project Title:	Legal and Regulatory Issues Affecting the Aquifer Thermal Energy Storage Concept
Principal Investigator:	Paul L. Hendrickson
Organization:	Battelle Pacific Northwest Laboratory P.O. Box 999 Richland, WA 99352
Project Goals:	Investigate and document significant legal and regulatory issues that can effect the implementation of a test or commercial ATES project in the U.S.
Project Status:	An initial report, PNL-3437, was issued in October 1980. An updated and expanded version of the report will be issued in October 1981 under the number PNL-3437 REV.1. Issues in four categories have been considered in the research: regulatory and permit requirements prior to start-up, issues related to potential areas and theories for liability from an ATES operation, and institutional and financial issues applicable to heat or chill delivery. The regulatory and permit analysis focuses on federal requirements, although state requirements are also considered.
Contract Number:	DE-AC06-76RLO 1830
Contract Period:	October 1, 1980 - September 30, 1981
Funding Level:	$39,000
Funding Source:	U.S. Department of Energy

PROJECT SUMMARY

Project Title: Economic Assessment of Seasonal Thermal Energy Storage (STES) Technologies

Principal Investigator: Raymond W. Reilly

Organization:
Pacific Northwest Laboratory
P.O. Box 999
Richland, Washington 99352
(509) 376-4359 (FTS: 444-4359)

Project Goals: Develop a computer code suitable for economic analysis of aquifer thermal energy storage (ATES) systems. Estimate the cost of ATES heat storage under a wide range of geologic, technical, and economic conditions.

Project Status: During FY 81 AQUASTOR, a techno-economic computer code for estimating the cost of aquifer thermal energy storage, was completed. It is presently being documented and will be made available to the general public in March, 1982.

The code was subsequently employed to estimate the cost of aquifer heat storage under a wide range of technical and economic conditions. The final report on this investigation is now being prepared.

Contract Number: DE-AC06-76RLO 1830

Contract Period: Continuing

Funding Level: $80,000

Funding Source: U.S. Department of Energy

ECONOMIC ASSESSMENT AQUIFER THERMAL ENERGY STORAGE (ATES) SYSTEMS

R.W. Reilly/D.R. Brown/H.D. Huber
Seasonal Thermal Energy Storage (STES) Program
Pacific Northwest Laboratory
P.O. Box 999
Richland, Washington 99352
509-376-4359 (FTS: 444-4359)

INTRODUCTION

This paper describes the economic assessment program undertaken in support of the Seasonal Thermal Energy Storage (STES) Program during FY 81. The effort comprised two major activities: 1) completion and checkout of AQUASTOR, a computer code for estimating the cost of seasonal thermal energy storage in aquifers, and 2) systematic investigation of the cost of heat storage in aquifers.

AQUASTOR development is complete, and a user's manual will be prepared during the first part of FY 82. The code will be made available for public use in March, 1981 through the Argonne Code Center and the DOE Technical Information System.

During the latter part of the fiscal year, AQUASTOR was employed in a systematic investigation of the cost of heat storage from a seasonal heat source. Technical and economic assumptions were varied in parametric analyses to provide estimates of the cost of ATES energy delivery under a range of potential conditions. The key results from this investigation are presented here and in a final report now under preparation.

This work was performed in support of the Seasonal Thermal Energy Storage (STES) Program at the Pacific Northwest Laboratory (PNL), DOE's lead laboratory for seasonal thermal energy storage research. Funding was provided by the Office of Energy Systems Research, U.S. Department of Energy.

THE AQUASTOR CODE

The major tool employed in the investigation of ATES economics is AQUASTOR, a computer code developed at PNL specifically for evaluation of the economics of heating and cooling using energy supplied by ATES. AQUASTOR provides the capability to evaluate the impact of varying technical and economic conditions upon the cost of heating/cooling using ATES-supplied energy. It consists of two major parts. The supply submodel calculates the unit costs of energy production by simulating the exploration, development, and operation of an ATES system, and the transmission of this energy to a distribution center. The distribution submodel calculates the unit cost of delivered energy by simulating the development and operation of district and/or point demand heating (cooling) systems.

AQUASTOR can simulate nearly any financial and tax structure by varying the rates of return on equity and debt, the debt-equity ratio, tax rates, investment credits, and depreciation schedules. Both municipal utility and private ownership can be simulated. The supply submodel and the distribution submodel may have the same or different financial structures. The code reports levelized costs in constant dollars, allowing inputs for inflation and four different escalation rates (purchased thermal energy, electricity, O&M, and capital expenditures).

The code calculates the cost of energy delivery by actually designing thermal collection and delivery systems and simulating cash flows over the lifetime of the system. The selection of piping, insulation, pumps, and other capital items is optimized, based upon capital, operation, and maintenance costs.

AQUASTOR does not attempt to simulate fluid or thermal flow within the aquifer. Rather, it captures the relevant aquifer characteristics in three input parameters: fluid recovery fraction, thermal storage efficiency, and discovery aquifer temperature. The fluid recovery fraction is simply the ratio of the water recovered from the storage well field to the previously injected water. It can vary from a fractional value to greater than one, depending upon the nature of the aquifer being simulated, the temperature differential between the injected water and the in-situ water, and system response to temperature degradation. (Some users may shut down when the temperature of the water starts to degrade; others may be able to continue operation by increasing the flow rates, or by employing supplemental energy sources.) The thermal storage efficiency is similarly the ratio of energy recovered to energy injected, both defined with respect to the discovery water temperature. Defining storage efficiency in this manner isolates aquifer storage efficiency from the characteristics of the above-ground equipment. The storage and supply wellfields may have different thermal efficiency factors; they will almost certainly have different fluid recovery factors, one being the reciprocal of the other.

The code operates on an average-year performance basis. In an actual ATES development, aquifer efficiency is expected to rise dramatically over the first several years of operation as the aquifer is conditioned to the temperature of storage by lost thermal energy, and it is expected to approximate a steady state afterwards. In the present configuration of AQUASTOR, only the steady state situation is modelled.

HEAT STORAGE ESTIMATES

SYSTEM DESCRIPTION

The cost of storing heat in an ATES system from a seasonal heat source was estimated, using the AQUASTOR code. The system modelled is depicted in Figure 1. The ATES installation consists of a pair of well fields (in the same aquifer), two heat exchangers, and transmission piping that connects the four elements. During the storage operation, groundwater is withdrawn from the supply (or low temperature) wellfield and is circulated through a heat exchanger to collect thermal energy from the heat source. It is then transmitted to the storage (or high temperature) wellfield, where it is pumped into the aquifer until needed. During the recovery cycle, the storage well field is pumped, and the hot water is circulated through a second heat exchanger to transfer the heat to the user.

GENERAL APPROACH

Nine base case configurations were generated in order to cover a range of potential conditions. These consisted of three source temperatures (325F/163C, 250F/121C, and 175F/79C) at three different system sizes (3 MW, 10 MW, and 50 MW peak demand). These configurations were used as the base for parametric analysis to determine the importance of various economic and technical factors to the cost of ATES energy. The technical and economic assumptions employed in the base cases are presented below:

Economic Assumptions	
System Startup	January, 1990
System Lifetime	30 years
Base Year for Costs	January, 1980
Inflation Rates	
General Inflation	6%/year
O&M Expense	6%/year
Capital Equipment	6%/year
Electricity	7%/year
Thermal Energy	7%/year
Cost Information	
Electricity	$.05/kWh
Thermal Energy	$2.00/MBtu
Exploration Costs	$100K-400K/site
Well Drilling/Casing	$100/foot
Financing Information	
Mode	municipal
Interest Rate	10%/year
Technical Assumptions	
Energy Source	
Availability	120 days
Temperatures	325 F (150 C) 250 F (121 C) 175 F (79 C)
Return Temperature	90 F - 100 F
Load Description	
Peak Demand	3, 10, & 50 MW
Load Factor	25%
Reject Temperature	100 F (38 C)
Aquifer/Wellfield	
Well Depth	400 feet
Well Spacing	25 acres
Maximum Well Flow Rate	150,000 lb/hr

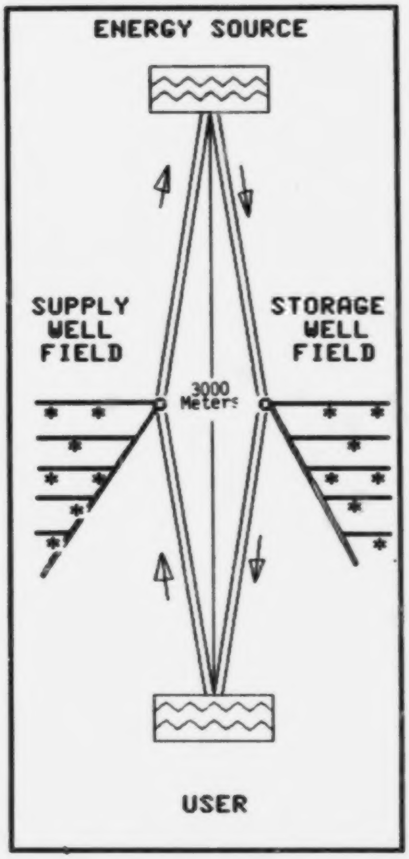

Figure 1: System Configuration

Thermal Efficiency	
Storage Aquifer	70% @ 175 F 63% @ 250 F 60% @ 325 F
Supply Aquifer	85%
Fluid Recovery Factor	
Storage Aquifer	90%
Supply Aquifer	112%
Fluid Transport	
Pipe	carbon steel
Insulation	calc. silicate
Construction	above ground
Source-User distance	3000m one way

The cost estimates presented here are levelized costs expressed in January, 1980 constant dollars. They represent only energy purchase and storage costs, since they do not include distribution and end-use equipment. By investigating a point demand as a load, two purposes are accomplished: 1) emphasis is placed upon the economics of energy storage parameters, rather than upon the dominating economic effect of a large distribution system, and 2) costs can be estimated for potential point-demand users -- large commercial and industrial users with existing distribution systems such as airports, major office complexes, and factories.

The capital budget for each of the systems investigated include exploratory and development costs for the aquifer system, and purchase and installation of all hardware (including the user heat exchanger). The operating costs provide for all pumping energy (including both sides of both heat exchangers), system maintenance, financing, and administrative costs.

BASE CASE RESULTS

The results of the base case analysis are presented in Figure 2, which shows how the cost of ATES storage varies with system size at three source temperatures. ATES is highly dependent upon economies of scale for cost-effective implementation: the cost curve is fairly flat beyond 8 MW, and tends to rise steeply for system sizes below 5 MW.

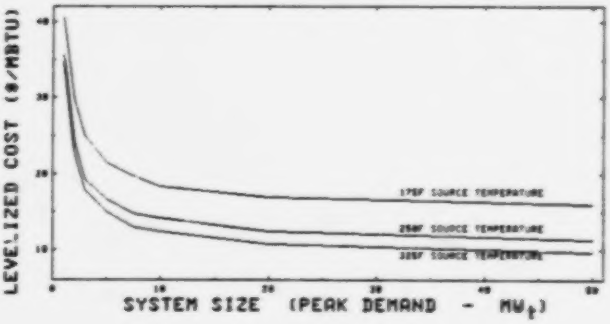

Figure 2: Cost versus System Size

Figure 3 depicts a component breakdown of levelized cost of ATES energy supply for the 10 MW base case at 325 F source temperature. The levelized costs of purchased thermal energy is $5.41 (or 44% of the total costs), despite the purchase price being only $2.00/MBTU. This difference reflects the effect of price escalation and thermal losses in the aquifer and pipelines. Electricity constitutes only about 5% of the total levelized costs: the cost of pumping energy is rather insignificant at a 400' well depth. Operations and maintenance constitutes 24% of the total levelized cost and capital equipment accounts for the remaining 27%. Of course, if a distribution system were included in the cost estimates, the capital fraction would be far higher.

For comparison purposes, if hot water were supplied by an electric boiler (@ $.05/kWh and 7% escalation), the levelized cost of energy would be $18.90/MBTU. An equivalent oil-fired system (@ $6.00/MBTU escalating at 8%) would result in a levelized cost of $14.03/MBTU.

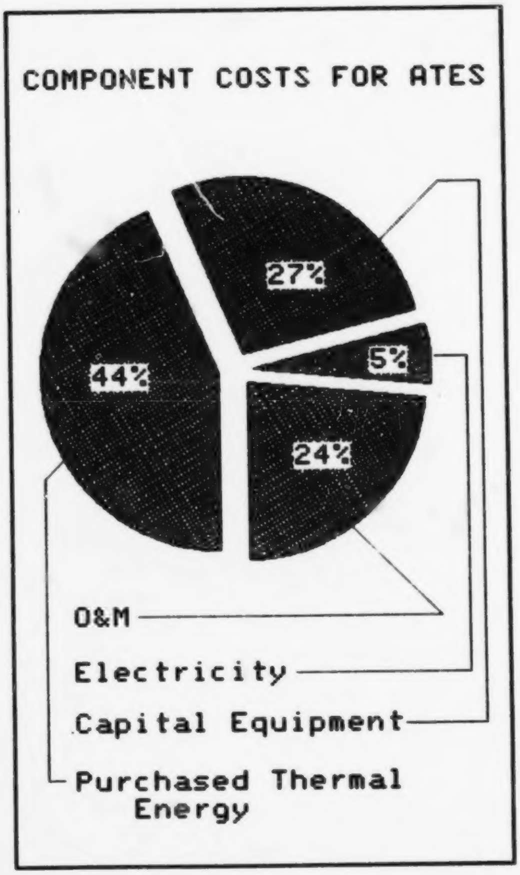

Figure 3: Component Cost Breakdown for ATES

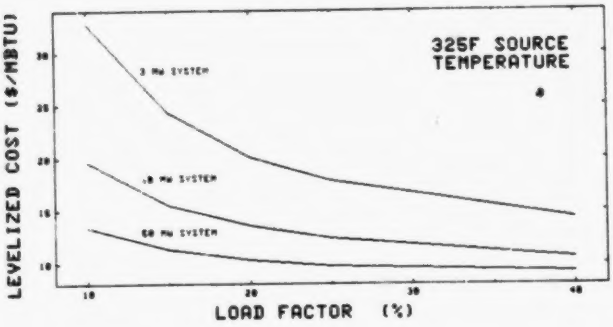

Figure 4: Cost versus Load Factor

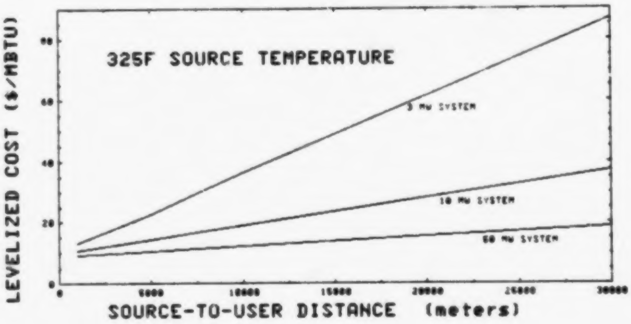

Figure 5: Cost versus Transmission Distance

PARAMETRIC ANALYSES

Parametric analyses were conducted to investigate the effects of technical and economic factors upon the cost of ATES operation. Only the results for the 325F source temperature systems are reproduced here (at each of three system sizes: 3 MW, 10 MW, and 50 MW).

SUPPLY/DEMAND PARAMETERS

Load Factor

The effect of load factor on system economics is depicted in Figure 4. The load factor is defined as the ratio of average annual hourly demand to peak hourly demand. In this analysis, a greater load factor is equivalent to a larger total amount of stored energy, since peak demand is maintained constant. The base case load factor is 25%, about equal to that for a city in a moderately cool climate. The effect of load factor on system economics is not so pronounced as might be expected, since capital equipment represents only 27% of total levelized cost. If an extensive distribution system were modelled as part of this investigation, then the load factor would have greater impact.

Transmission Distance

The cost of ATES heating is dependent upon the transmission distance between the four components of the system. In the base case, each of the four legs was modelled at 1500 meters, giving a source-to-user separation of 3000 meters, and a total pipeline length of 6000 meters, (about 4 miles). In the analysis of source-user separation (Figure 5), we see that the relationship between transmission distance and levelized cost is essentially linear. It is evident from the three curves presented that there are considerable economies of scale in pipeline construction, and that feasible transport distance is a function of system size. Transport distance, especially for small systems, must be minimized for economic ATES implementation.

Source Availability

One of the major capital components of an ATES system is well construction. The number of wells required is determined by the maximum flow rate required either into or out of the aquifer. This maximum flow rate is, in turn, determined by either the peak demand of the user (user-controlled), or the peak storage flow (source-controlled). Figure 6 denotes the relationship of source availability and levelized cost. In the base case, the energy was assumed to be available continuously for 120 days per year. The range investigated here is 30-180 days (at 24 hours per day). For source availabilities above 104 days, the number of wells is controlled by demand parameters, and so the curve is relatively flat, reflecting only decreasing heat exchanger and pipe sizes. At availabilities less than 104 days, the number of wells is dependent upon supply availability, and the total cost changes more quickly.

WELL PARAMETERS

Well Cost

The effect of well cost on levelized cost is investigated in Figure 7. Well cost includes drilling and casing, but not the cost of pumps. The relationship is linear and rather flat, since wells constitute only a portion of the total capital cost, which is itself only 27% of total levelized cost. In the base case, wells were estimated to cost $100/foot, or $40,000 per well.

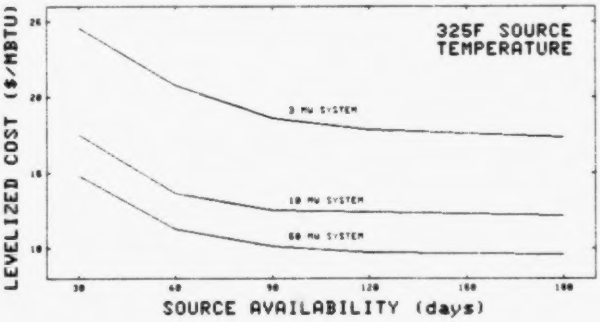

Figure 6: Cost versus Source Availability

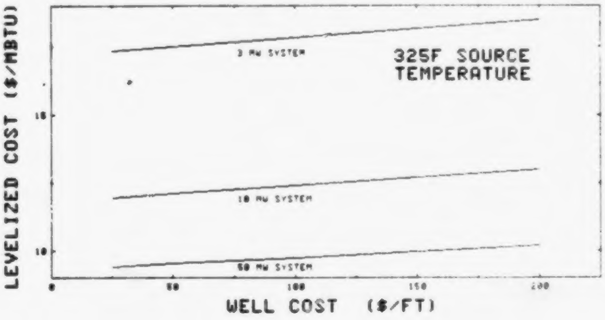

Figure 7: Cost versus Well Cost

Average Well Life

The effect of well life on levelized cost is similar to that of well cost, since as well life decreases, the total cost of wells rises. As indicated by the curves (Figure 8), there is not much effect on levelized cost until the average well life drops below 5 years.

Well Depth

The effect of well depth upon levelized cost is more pronounced than that of well cost, since a deeper well requires increased pump size and greater pumping power in addition to greater well drilling and casing expense (Figure 9). In the base case, 400-foot wells were assumed. If we increase the required well depth to 1500 feet, then we get a significant increase in storage cost.

Well Flow Rate

The relationship between maximum well flow rate and levelized cost is a step function, since cost does not increase with reduced well flow rate until another pair of wells is required by the system (Figure 10). An additional well adds not only drilling costs, but also an additional pump and manifolding required to connect the well over its 25 acre spacing. In the base case a maximum well flow rate of 150,000 was assumed, not large for water wells or geothermal wells, but probably reasonable for the aquifer transmissivities that will be required for economic aquifer thermal efficiencies.

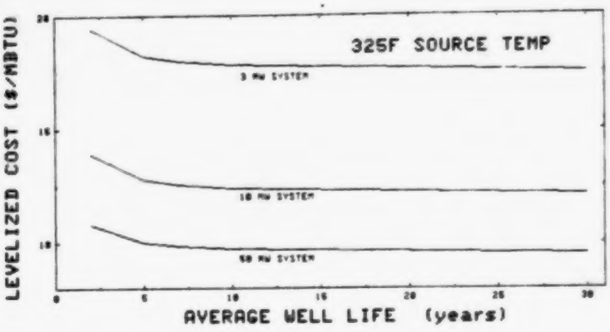

Figure 8: Cost versus Average Well Life

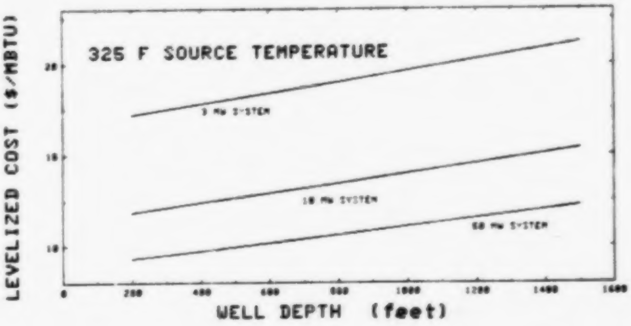

Figure 9: Cost versus Well Depth

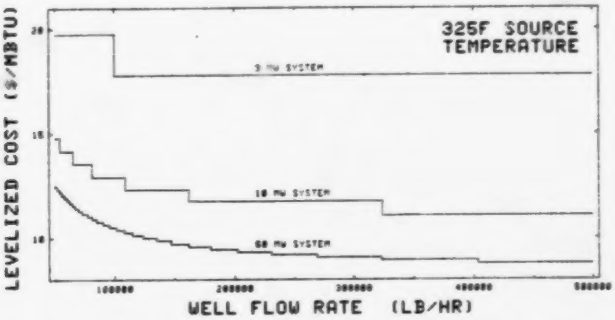

Figure 10: Cost versus Well Flow Rate

Fluid Recovery Factor

The fluid recovery factor is defined as the ratio of water recovered from the storage aquifer to that previously injected into the aquifer. The base case assumed 90% recovery. In Figure 11, the effect of different fluid recovery factors is investigated, down to 50%. As fluid recovery factor is decreased the aquifer thermal efficiency was reduced in order to maintain the same average temperature of water recovered from the aquifer. (At a 50% fluid recovery factor, for instance, the fractions of thermal energy recovered from the storage aquifer are 34% @ 325 F, 35% @ 250 F, and 39% @ 175 F.) Hence, the graph above represents the change in levelized cost with decreases in overall aquifer performance.

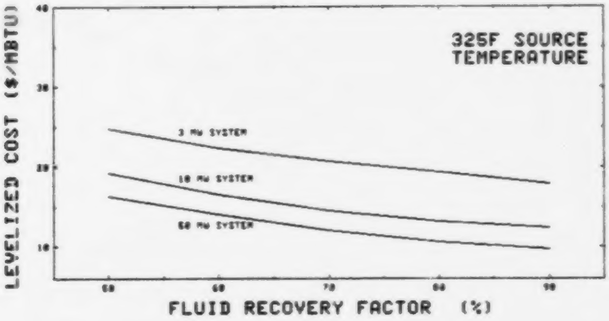

Figure 11: Cost versus Fluid Recovery Factor

ECONOMIC PARAMETERS

Cost of Electricity

The levelized cost of energy is rather insensitive to electrical cost in this simulation (Figure 12), since pumping energy is such a small portion (5%) of total levelized cost.

Cost of Purchased Thermal Energy

The cost of purchased energy is critical to the cost-effective use of ATES systems, since its cost is magnified by system thermal losses. As indicated by Figure 13, the cost of ATES rises quickly with increasing cost of purchased thermal energy.

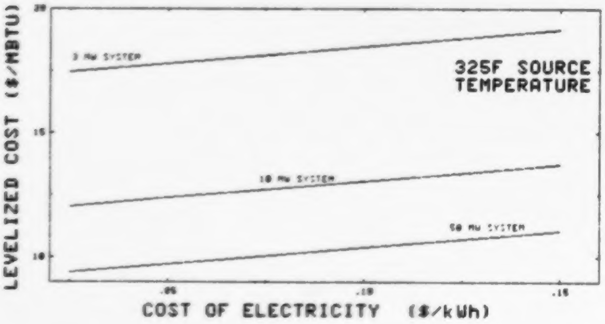

Figure 12: Cost versus Electrical Cost

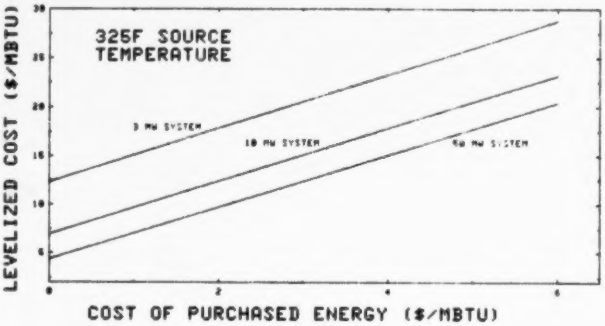

Figure 13: Cost versus Cost of Thermal Energy

Cost of Capital

The effect of financing mode is investigated in Figure 14. Both municiple (100% bond, no taxes) and private financing (after-tax rate at 50% bond/50% equity) are investigated. The cost of capital is important to the levelized cost in this simulation. Its effect on levelized cost would be far greater if a distribution system were included as part of the ATES system.

ELIMINATION OF USER HEAT EXCHANGER

Under certain conditions, elimination of user heat exchanger may be feasible, allowing aquifer water to be transferred directly to the end user. The economic effect of this system modification is shown in Figure 15.

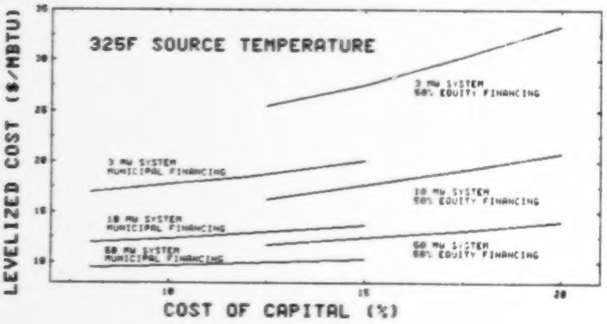

Figure 14: Cost versus Cost of Financing

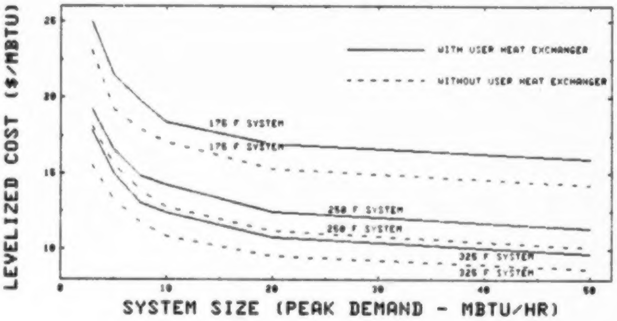

Figure 15: Effect of No User Heat Exchanger

SUMMARY

Several technical and economic factors control the economic performance of ATES systems. Costs are prohibitive for systems of small size, long transmission distances, and expensive purchased thermal energy. High temperature sources are preferred over low temperature sources, but these may be more scarce, and there will be more competition for higher quality energy. ATES appears to be cost-competitive with oil-fired and electric hot water systems under a broad range of potential situations.

PROJECT SUMMARY

Project Title: Environmental Assessment

Principal Investigator: George E. Wukelic

Organization:
Pacific Northwest Laboratory
P.O. Box 999
Richland, Washington 99352
(509) 376-5860 (FTS: 444-5860)

Project Goals: Ensure the environmental acceptability of promising STES concepts prior to their implementation.

Project Status: All environmentally-related activities within the STES Program are coordinated under this task. Current emphasis is on aquifer thermal energy storage (ATES) activities and includes:

(1) Environmental documentation support to ensure compliance with the National Environmental Policy Act (NEPA).

(2) Environmental research assistance to determine the significance and magnitude of potential environmental effects.

During FY 81, a programmatic environmental assessment for the Aquifer Thermal Energy Storage Program was finalized (DOE/EA-0131) and is scheduled for publication and distribution during the last quarter of FY 81. Although the ATES Program has been recently redirected, the environmental assessment adequately covers the revised program and the finding of no significant impact is still applicable.

Also during FY 81, this task successfully coordinated all environmentally-related activities and requirements associated with the aquifer characterization studies in progress in Bethel, Alaska; Stony Brook, NY; and Minneapolis, MN. Emphasis during FY 82 will be in support of these requirements as they relate to activities at field test facilities in Mobile, Alabama, and Minneapolis, Minnesota.

Contract Number: DE-AC06-76RLO 1830

Contract Period: Continuing

Funding Level: $50,000 FY 1981 B/O

Funding Source: U.S. Department of Energy, Office of Energy Systems Research

PROJECT SUMMARY

Project Title:	Field Test Facility
Principle Investigator:	David A. Myers
Organization:	Pacific Northwest Laboratory P.O. Box 999 Richland, WA 99352 (509) 375-2462
Project Goals:	To test and demonstrate the storage of thermally altered ground water in aquifer systems.
Project Status:	A major contract has been continued with Auburn University to operate a field test facility near Mobile, Alabama. An initial cycle has been run with an average injection temperature of $57.5^{o}C$ ($135^{o}F$), with a volume of 25.8×10^3 m^3 (6.8×10^6 gallons). The test was shortened due to technical difficulties with the water heating system. A second cycle of injection/storage/recovery has been started, with injection temperatures near $90^{o}C$. Negotiations are underway to ascertain the feasibility of converting the University of Minnesota ATES Program to a Field Test Facility. Adaptation of the ATES site to a test facility will require the installation and instrumentation of an additional 4 monitoring wells. Projected tests include 60 day injection, storage and recovery periods at $150^{o}C$ ($300^{o}F$). Injected volume is projected to be 64 to 98×10^3 m^3 (17 to 25×10^6 gallons).
Contract Number:	DE-AC06-76RLO 1830
Contract Period:	Continuing
Funding Level:	48K, FY 1981
Funding Source:	U.S. Department of Energy, Office of Energy Systems Research

PROJECT SUMMARY

Project Title: Thermal Energy Storage in Confined Aquifers Using the Doublet Well Configuration

Principal Investigators: Fred J. Molz, Joel G. Melville, A. David Parr

Organization: Civil Engineering Department
Auburn University
Auburn, Alabama 36849

Project Goals: Conduct doublet field experiments in aquifer thermal energy storage. Three injection-storage-recovery cycles are planned to evaluate the doublet configuration and measure thermal efficiency for injection temperatures of 60°C, 90°C, and 125°C.

Project Status: Preliminary aquifer testing and analysis have been completed. These hydrodynamical data are necessary for application of predictive numerical models and for fundamental understanding of experimental results.

The first experimental cycle has been completed. The average injection temperature was 58.5°C. The volume of water injected was 6.87×10^6 gallons. Based on an equal recovery volume, the energy recovery was 55.3%.

To distinguish hydrodynamic and hydrothermal behavior, a tracer, sodium bromide, was injected with the hot water. Results of the tracer study indicated very small dispersion, but significant convection of the injected water.

The second, 90°C, cycle is underway. Injection will continue through the summer.

Contract Number: Subcontract No. B-67770-A-0
Prime Contract DE-AC06-76RLO 1830

Contract Period: 03/26/80 through 12/31/82

Funding Level: $1,087,000.

Funding Source: U.S. Department of Energy through Battelle Pacific Northwest Laboratories

BEST DOCUMENT AVAILABLE

MOBILE, ALABAMA FIELD TEST FACILITY

Fred J. Molz Joel G. Melville A. David Parr
Civil Engineering Department
Auburn University
Auburn, Alabama 36849

ABSTRACT

During recent years, study of the possibility of using aquifers for seasonal thermal energy storage in the form of heated water has accelerated. Since 1976, Auburn University has conducted two sets of storage experiments in a confined aquifer near Mobile, Alabama. The present paper discusses the preparation for a third set of experiments and results to date of the first injection-storage-recovery cycle utilizing a supply and injection well in the same aquifer. Among other things, such a configuration should minimize geochemical problems experienced during previous studies.

Prior to the first injection, a series of well tests was performed. Then water was heated from 20°C to 58.5°C and an injection rate of $45 m^3/hr$ was easily maintained at an injection pressure of $2.0 \times 10^4 Nm^{-2}$ (3 psi). Previous experiments often required $1.45 \times 10^5 Nm^{-2}$ (21 psi) to maintain an injection rate of $22.7 m^3/hr$ due to swelling and dispersion of formation clays. This problem was eliminated in the present study.

The volume injected in the experiment was $26 \times 10^3 m^3$ (6.87×10^6 gallons). After a storage time of one month, recovery of an equal volume yielded an energy recovery of 55.3%. Sodium bromide tracer studies indicated very small dispersion, but significant convection of the warm, buoyant water. A second injection cycle at 90°C is underway.

INTRODUCTION

During recent years, study of the possibility of using aquifers for seasonal thermal energy storage (STES) in the form of heated water has accelerated (refs. 1, 2, 3, 4, 5, 6, 7, 8). In addition, there are experiments recently completed or presently underway in Denmark, France, Germany, Switzerland and Sweden. Much current information can be obtained by consulting the various issues of the STES Newsletter (Dr. Chin Fu Tsang, Editor, Earth Sciences Division, Lawrence Berkeley Laboratory, Berkeley, CA 94720).

Beginning in 1976, Auburn University conducted two sets of thermal energy storage experiments in a confined aquifer near Mobile, Alabama. Past results are reported in the above references as well as in proceedings of the IECEC (refs. 9, 10).

Clogging of the injection-production well during injection was an important negative result of the Mobile experiments. The present writers (ref. 3), and others have suggested that using water from the storage aquifer as supply water for the boiler or other heating system would minimize clogging problems. Drilling the supply well and the injection-production well in the same formation leads to what is often called the doublet configuration. If aquifer storage of thermal energy becomes feasible on a commercial scale, it seems likely that a system based on the doublet configuration will offer distinct advantages. Therefore, there is a real need to study this concept experimentally so that potential advantages and disadvantages can be identified clearly before major amounts of money are invested in the concept. This paper will discuss the preparation for a third set of experiments and the results to date of the first injection-storage-recovery cycle utilizing a supply and injection well placed in the same aquifer.

DESCRIPTION OF EXPERIMENTS

In order to test a doublet supply-injection well configuration, a third round of experiments consisting of three injection-storage-recovery cycles were started in early 1981 at the Mobile site. A schematic of the doublet system is shown in Fig. 1. The injection and supply wells fully penetrate the confined aquifer and are separated by 244 m (800 ft).

Fig. 2 shows the location of the supply well, injection well and boiler with respect to the 28 observation wells used to measure temperature, hydraulic head and tracer concentration. The different types of observation wells are indicated on the figure.

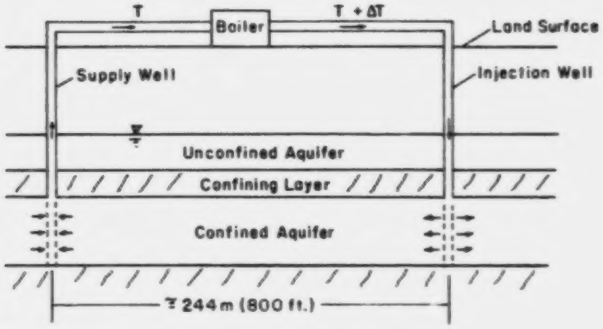

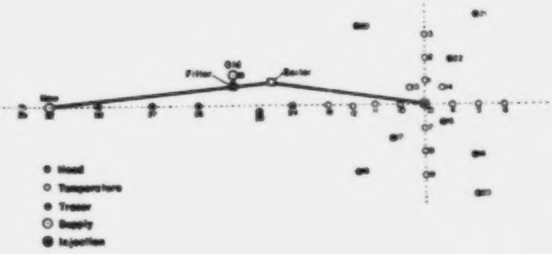

Fig. 1. Diagram of the "doublet" supply-injection well configuration used in the third set of aquifer storage experiments now being performed near Mobile, Alabama.

Fig. 2. Top view of the complete well field that has been constructed at the Mobile site. Water is obtained from the new supply well, heated by the boiler and injected into well I2. Water recovered from I2 after storage is injected back into S2 for later use.

Observation wells that are used to measure temperature in the storage formation are constructed as shown in Fig. 3. Thermistors are used to measure temperature at six locations in each well. Two thermistors are installed at each location to provide a backup array. The wells are backfilled with sand in order to minimize unrepresentative thermal convection within the well bores. Temperature is measured also in the upper and lower aquitards. One well is screened in each of these formations and temperature is measured at two locations in each well. The observation wells that are used to measure hydraulic head are constructed similar to the temperature wells but, of course, are not backfilled with sand.

A tracer experiment was performed during the first cycle to compare the movements of solute and heat in the aquifer. A chemical feed system was used to inject sodium-bromide into the hot water pipeline throughout the first injection. Water samples were obtained from wells 15, 17, and 22 so that tracer concentration could be recorded as a function of time.

Hot water pumped from the injection well during the recovery phase of each cycle will be returned to the confined aquifer through the supply well in order to minimize the amount of energy needed to heat water for subsequent injections. This procedure may create clogging problems, however, since the concentration of clay particles in the pumped water may tend to increase with repeated cycles. In order to control clogging and to maintain acceptable injection rates, a rapid sand filtering system was installed. The filtering system can either be used or bypassed during injection and recovery phases.

The planned injection temperatures for the second and third cycles, which are yet to be completed, are 90°C and 125°C respectively. These temperatures are higher than those utilized in any other experiments to date and should yield valuable information concerning the potentially important effect of buoyancy-induced vertical convection. This effect tends to change the shape of the thermal storage zone from that of a cylinder to that of a cone with its narrow portion concentric to the bottom of the injection well.

PRE-INJECTION AQUIFER TESTING

Because the data collected in the present experiments are serving as the basis for rather extensive mathematical modeling studies, more than the usual attempt was made to determine accurate hydraulic properties of the storage aquifer and aquitards. These properties included both vertical and horizontal permeability of the storage aquifer, storativity, and vertical permeability of the upper and lower aquitards. Thermodynamic properties such as thermal conductivity and heat capacity are important also and were measured in previous studies (ref. 3).

The horizontal to vertical permeability ratio (anisotropy ratio) is an important parameter because it is a major factor in determining the degree of buoyancy-induced convection mentioned previously. This parameter was measured using the pumping test well configuration shown in Fig. 4 along with the analysis procedure developed by Weeks (ref. 11). Water was pumped from a well screened in the bottom three meters of the confined aquifer while drawdowns were observed in three observation wells screened in the top three meters. Pumping continued for 12 hours at a constant rate of 9.5 liters per second. Analysis of the resulting data indicated an anisotropy ratio of 6.7 with a horizontal permeability of 53.6 m/day and a storage coefficient of 0.00049. Each observation well yielded a value for horizontal permeability which differed from the mean value of 53.6 by less than 2 percent.

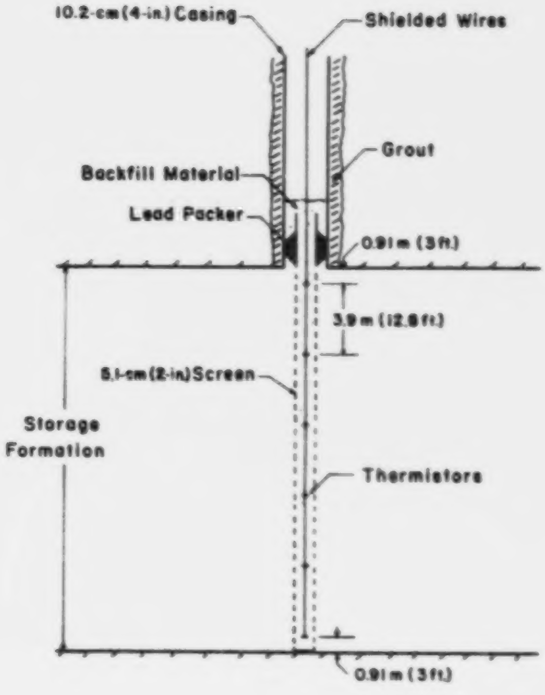
10.2-cm (4-in.) Casing
Shielded Wires
Grout
Backfill Material
Lead Packer
0.91 m (3 ft.)
3.9 m (12.8 ft.)
5.1-cm (2-in) Screen
Storage Formation
Thermistors
0.91 m (3 ft.)

Fig. 3. Diagram showing the details of the construction of a temperature-monitoring observation well.

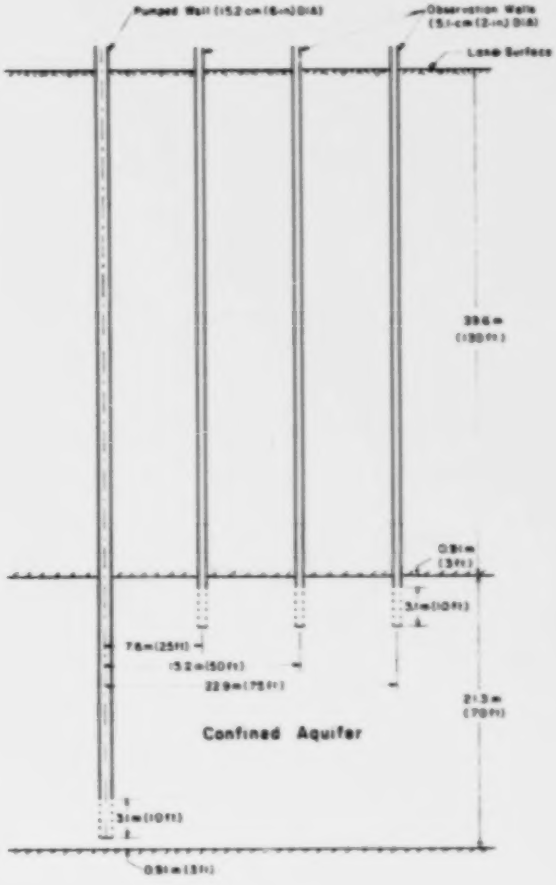
Pumped Well (15.2-cm (6-in) DIA)
Observation Wells (5.1-cm (2-in) DIA)
Land Surface
39.6 m (130 ft)
0.91 m (3 ft)
3.1 m (10 ft)
7.6 m (25 ft)
15.2 m (50 ft)
22.9 m (75 ft)
21.3 m (70 ft)
Confined Aquifer
3.1 m (10 ft)
0.91 m (3 ft)

Fig. 4. Diagram showing the test well configuration used to measure both the horizontal and vertical permeability in the storage aquifer.

The degree of confinement of a potential storage aquifer is determined by the vertical permeability of the upper and lower aquitards. These hydraulic parameters, as well as an independent measure of the horizontal storage aquifer permeability, were determined using a leaky aquifer pumping test analysis developed by Neuman and Witherspoon (ref. 12). A fully-penetrating pumping well was installed in the storage aquifer along with a fully-penetrating observation well. In addition, two aquitard observation wells were installed -- one in the upper confining layer and one in the lower as shown in Fig. 5. A 99-hour pumping test at the rate of 6.9 liters/sec yielded a horizontal permeability of 53.4 m/day which was nearly identical to the value obtained from the partially penetrating test. Data was also obtained which ultimately will allow computation of the vertical aquitard permeability. However, an independent value for the compressibility of the aquitard clay must be obtained through a conventional consolidation test which will be underway shortly.

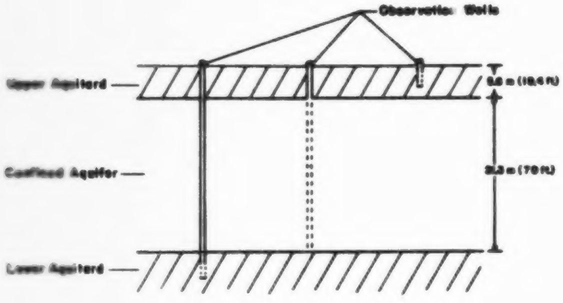

Fig. 5. Observation well configuration for the leaky-aquifer pumping test. All three wells are located at a radial distance of 15 meters from the pumped well.

RESULTS OF FIRST CYCLE

Shown in Fig. 6(a) is the cumulative injection volume as a function of time. The horizontal line segments represent shut-down periods due mostly to mechanical problems. During operational periods the average injection rate (slope of line) was very close to 45 m^3/hr. Recovery pumping rates are shown in Fig. 6(b).

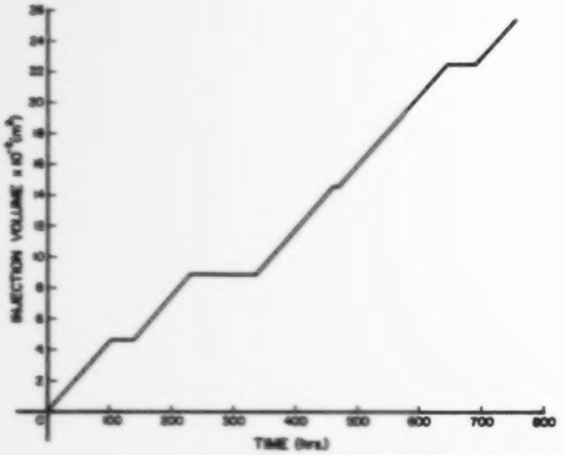

Fig. 6(a). Plot of cumulative injection volume versus time for the first of three planned injections.

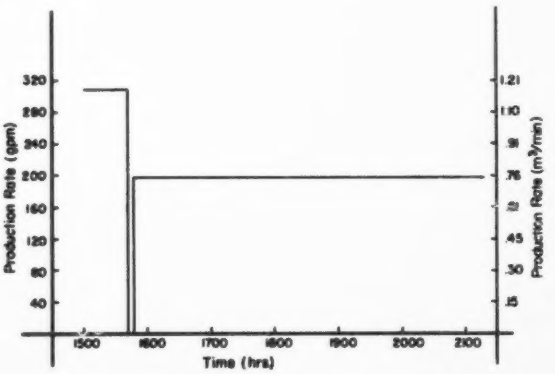

Fig. 6(b). Recovery well pumping for the first experimental cycle.

Shown in Fig. 7(a) is the injection temperature history. This was maintained at a fairly constant value, although there was a drop-off in average temperature of approximately 5°C during the 756 hour injection period due to increasing malfunction of the boiler. Over the entire 756 hour period, the average injection temperature was approximately 58.5°C.

Fig. 7(b) shows the constant decline of temperature at the recovery well. Some heat loss occurred during the storage phase (755 hours) and constant decline of temperature during recovery indicates that increasing amounts of cool water are pumped from the injection well, probably from near the bottom of the well. Tracer data at the recovery well support the idea that significant convection occurred during the test.

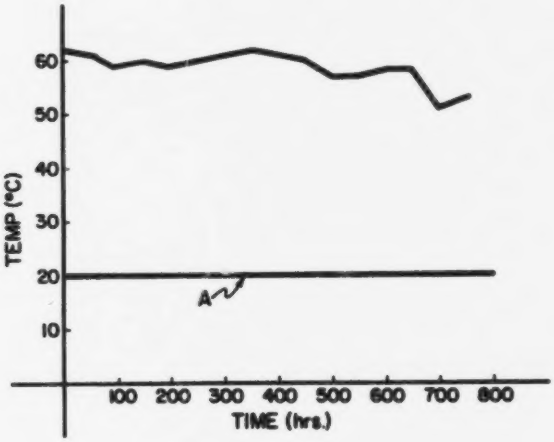

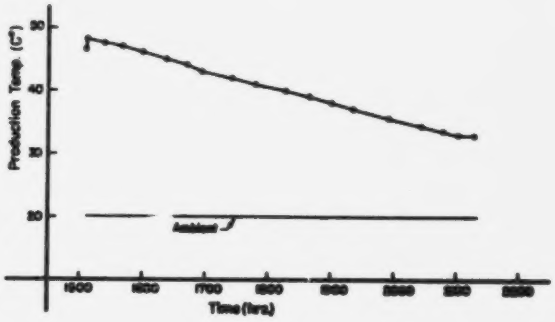

Fig. 7(a). Plot of injection temperature versus time for the first injection. The horizontal line marked "A" represents the ambient ground water temperature in the storage aquifer.

Fig. 7(b). Recovery well temperature. The horizontal line "A" is the ambient ground water temperature. The energy recovery was 55.3%.

The most notable result during the first cycle was the absence of injection well clogging due to clay particle swelling, dispersion and migration. During previous experiments, this phenomenon was identified as the major technical problem (refs. 4, 5). Shown in Fig. 8 is the specific capacity history of the second cycle injection described by Molz et al. (ref. 5). Regular backwashing was required in order to maintain an acceptable injection rate. Backwashing was initiated whenever the injection pressure reached 1.45×10^5 Nm^{-2} (21 psi). This is to be contrasted with the present experiment which operated with an injection pressure of 2.0×10^4 Nm^{-2} (3 psi) and a specific capacity virtually constant at 59×10^{-4} $m^3/sec/m$ which is almost seven times higher than the average obtainable from Figure 8.

Study of data obtained from previous experiments (ref. 4) led to the conclusion that the clogging effect was initiated by osmotic swelling of the formation clays (ref. 13). This phenomenon occurs when clay platelets in equilibrium with ground water having a relatively high ion concentration comes in contact with water having a relatively low ion concentration. Such a situation occurred in previous experiments at the Mobile site when relatively pure supply water from a shallow aquifer was heated and injected into a deeper storage aquifer. In the present experiments supply water was obtained directly from the storage aquifer and NaBr was added which increased the Na concentration by about 5 mg/l. Thus, the water injected had a slightly higher cation concentration than the native ground water, which is probably the main reason why clogging was not observed.

Shown in Fig. 9 is the normalized break-through curve for the Br tracer which was mixed with the injection water at a concentration of approximately 11 mg/l. This data was obtained early in the experiment at well #15 which is located 15.25 m from the injection well. Data analysis based on the radial dispersion equation (ref. 14) indicated a relatively low dispersivity of approximately 0.1 m. This estimate will be refined as further tracer data become available. Samples were taken near the center of the aquifer where permeability is relatively high, and this could lead to a low estimate for dispersivity.

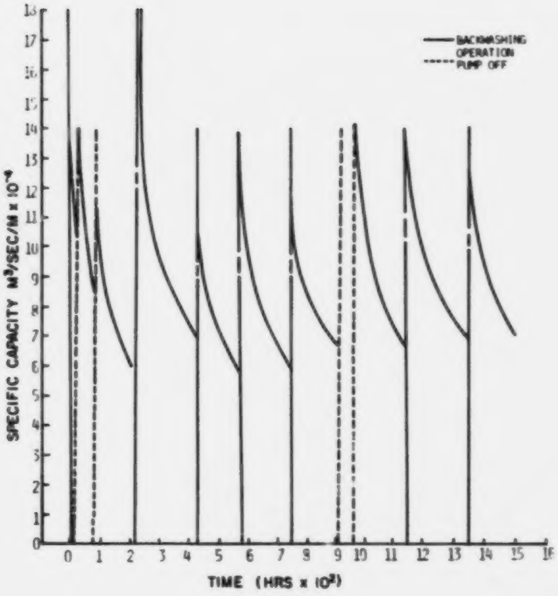

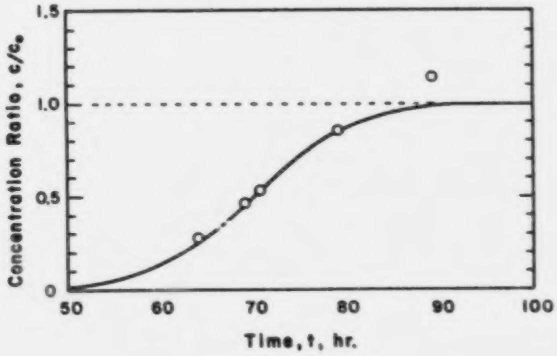

Fig. 8. Injection well specific capacity during a previous study (ref. 5) when clay swelling and dispersion was causing clogging in the injection well.

Fig. 9. Normalized tracer concentration versus time in well #15 which is located 15 meters from the injection well. Breakthrough occurred between 60 and 80 hours after injection began, and C_0, the tracer concentration in the injected water, was approximately 11 mg/l.

CONCLUSIONS

At the present time, firm conclusions about most aspects of the experiment are not possible because the study is still underway. However, the average hydraulic properties of the storage aquifer are relatively well defined and the dispersivity appears to be approximately 0.1 m.

The major conclusion to date is that use of the doublet configuration (supply and injection well in the same aquifer) was a major step toward elimination of the clogging problem observed during previous studies at the Mobile site. The addition of NaBr tracer to the injection water could also have contributed to elimination of what was the most troublesome technical problem during previous studies.

Sodium bromide tracer data from the first cycle indicate small dispersivity but significant convection of the warm injected water which reduces thermal efficiency of the aquifer storage technique if recovery pumping draws water from the entire thickness of the confined aquifer.

ACKNOWLEDGEMENTS

This work was supported by the U.S. Department of Energy through a subcontract awarded by the Battelle Pacific Northwest Laboratories (Subcontract B-67770-A-0.

REFERENCES

1. D. Werner and W. Kley, Problems of Heat Storage in Aquifers. Journal of Hydrology, 34, 1977, 35-43.

2. B. Mathey. Development and Resorption of a Thermal Disturbance in a Phreatic Aquifer with Natural Convection. Journal of Hydrology, 34, 1977, 315-333.

3. F. J. Molz, J. C. Warman and T. E. Jones. Aquifer Storage of Heated Water: Part I -- A Field Experiment. Ground Water, 16, 1978, 234-241.

4. F. J. Molz, A. D. Parr, P. F. Andersen, V. D. Lucido and J. C. Warman. Thermal Energy Storage in a Confined Aquifer: Experimental Results. Water Resources Research, 15, 1979, 1509-1514.

5. F. J. Molz, A. D. Parr and P. F. Andersen. Thermal Energy Storage in a Confined Aquifer: Second Cycle. Water Resources Research, 17, 1981, 641-645.

6. S. S. Papadopulos and S. P. Larson. Aquifer Storage of Heated Water: Part II -- Numerical Simulation of Field Results. Ground Water, 16, 1978, 242-248.

7. T. Yokoyama, H. Umemiya, T. Teraoka, H. Watanabe, K. Katsuragi and K. Kasahara. Seasonal Thermal Storage in Aquifer for Utilization. Bulletin, Japanese Society of Mechanical Engineers, 23, 1980, 1646-1654.

8. C. F. Tsang, T. Buscheck and C. Doughty. Aquifer Thermal Energy Storage -- A Numerical Simulation of Auburn University Field Experiments. Water Resources Research, 17, 1981, 647-658.

9. F. J. Molz, A. D. Parr and P. F. Andersen. Thermal Energy Storage in Aquifers: Experimental Study. Proceedings of the 14th Intersociety Energy Conversion Engineering Conference, American Chemical Society, Volume I, 1979, 534-537.

10. C. F. Tsang, F. J. Molz and A. D. Parr. Experimental and Theoretical Studies of Thermal Energy Storage in Aquifers. Proceedings of the 15th Intersociety Energy Conversion Engineering Conference, American Chemical Society, Volume 2, 1980, 1244-1248.

11. E. P. Weeks. Determining the Ratio of Horizontal to Vertical Permeability by Aquifer-Test Analysis. Water Resources Research, 5, 1969, 196-214.

12. S. P. Neuman and P. A. Witherspoon. Field Determination of the Hydraulic Properties of Leaky Multiple Aquifer Systems. Water Resources Research, 8, 1972, 1284-1298.

13. H. van Olphen. An Introduction to Clay Colloid Chemistry. John Wiley. New York, 1963.

14. S. K. Gupta, R. E. Batta and R. N. Pandey. Calculating Hydrodynamic Dispersion Coefficients, Journal of Hydrology, 47, 1980, 369-372.

PROJECT SUMMARY

Project Title: Compendia of Existing Information Task

Principal Investigator: Leigh S. Prater

Organization: Pacific Northwest Laboratory
P.O. Box 999
Richland, Washington 99352
(509) 375-2660 (FTS: 444-7511, Ext. 2660)

Project Goals: Collect, summarize, and transmit information related to Seasonal Thermal Energy Storage (STES).

Project Status: The STES Library was established in FY 1979, and it now contains over 1900 documents on topics related to thermal energy storage. During FY 1981, the STES Library was used by researchers from many countries, including the United States, Sweden, Israel, Canada, France, and Germany. Bibliographic information from the STES Library has been entered into a computerized information system called the STES Technology Information System (STES-TIS). This system provides the capability to conduct customized, on-line searches of the STES Library.

The STES Technology Information System was created with the assistance of Lawrence Livermore Laboratory. The STES-TIS is designed to provide a centralized, on-line source of information to assist with development of STES technologies. The STES-TIS contains four types of resources: administrative, bibliographic, computational, and communications.

A document containing regional aquifer assessments was completed in FY 1981. This document, prepared by Century West Engineering, gives a qualitative assessment of the ATES potential of major U.S. aquifers.

The STES Newsletter, which contains brief reports about thermal energy storage projects around the world, is being published on a quarterly basis by Lawrence Berkeley Laboratory. The STES Newsletter currently reaches individuals and organizations in 22 countries.

Contract Number: DE-AC06-76RLO 1830

Contract Period: Continuing

Funding Level: $68,500

Funding Source: U.S. Department of Energy, Office of Energy Systems Research

PROJECT SUMMARY

Project Title: Seasonal Thermal Energy Storage Technology Information System

Principal Investigator: Viktor E. Hampel

Organization: Lawrence Livermore Laboratory
P.O. Box 808
Livermore, California 94550
(415) 422-4357 (FTS: 532-4357)

Project Goals: Establish a comprehensive, computer-based information system for the Seasonal Thermal Energy Storage (STES) Program.

Project Status: The STES Technology Information System (STES-TIS) was established in FY 1980, and development of the system continued through FY 1981. The STES-TIS is a subset of the Technology Information System developed at Lawrence Livermore Laboratory. The system is designed to provide a centralized, on-line source of information to assist with the development of STES technologies.

The STES-TIS provides the capability to store and manipulate various types of data files. In general, the STES-TIS contains four types of resources: administrative, bibliographic, computational, and communications. The administrative resources include files containing task descriptions, weekly highlights, a quarterly newsletter, and conference information. The bibliographic resources consist of various data files related to the STES Library. The computational resources provide automated access to various computers on which the economic and hydrologic models developed for the STES Program can be run. The communications resources include electronic mail, conferencing, and the capability to link with or write to the terminal of another user.

A user's manual for the STES-TIS was printed and distributed in FY 1981. The STES Program staff and contractor personnel were also trained in the use of the system.

Contract Number: DE-AC06-76RLO 1830, Subcontract B-97602-A-0

Contract Period: May 15, 1980 through September 30, 1981

Funding Level: $256,700

Funding Source: U.S. Department of Energy through Pacific Northwest Laboratory

PROJECT SUMMARY

Project Title:	Publication of the Seasonal Thermal Energy Storage (STES) Newsletter
Principal Investigator:	Chin Fu Tsang
Organization:	Earth Sciences Division Lawrence Berkeley Laboratory Berkeley, CA 94720 (415) 486-5782
Project Goals:	To promote national and international cooperation and technical information exchange by organizing, soliciting, editing, and publishing a quarterly International STES Newsletter.
Project Status:	The International STES quarterly Newsletter is published as scheduled. Much enthusiasm both in the United States and abroad is apparent from the many contributions to and requests for this publication. Thus, the Newsletter is fulfilling its role as a focal point for international information exchange, discussion of ideas, and for establishing an atmosphere of cooperation internationally and within the U.S. Currently the Newsletter is distributed to researchers and project managers in 23 countries.
Contract Number:	B-B2497-A-O
Contract Period:	October 1, 1980 through September 30, 1981
Funding Level:	$30,000
Funding Source:	U.S. Department of Energy through Pacific Northwest Laboratory

BEST DOCUMENT AVAILABLE

PROJECT SUMMARY

Project Title:	Regional Assessment of Aquifers for Thermal Energy Storage
Principal Investigator:	Dorothy B. Stoffel
Organization:	Century West Engineering North 1010 Washington Spokane, Washington (509) 326-4227
Project Goals:	Qualitatively describe the Aquifer Thermal Energy Storage (ATES) potential of major aquifers throughout the United States.
Project Status:	Existing hydrogeologic data were collected for major aquifers in each of the twelve ground-water regions that comprise the United States. For the purposes of the study, a major aquifer was defined as one which has significant areal extent and which can sustain well yields of at least 50 gallons per minute. On the basis of the hydrogeologic data collected, each major aquifer was characterized and then evaluated for its ATES potential. The results of the study have been compiled. This compilation contains, for each region, a discussion of the hydrogeologic framework, evaluations of major aquifers, and a tabulation of the hydrogeologic data upon which the evaluations were based. Also included is an estimation of the ATES potential of each of the twelve regions. The regions which generally have the best potential for ATES development are: Western Mountain Ranges region, Alluvial Basins region, High Plains region, Glaciated Central region, Unglaciated Central region, Unglaciated Appalachians region, Glaciated Appalachians region, and Coastal Plain region. The regions which generally have the lowest potential for ATES development are: Columbia Lava Plateau region, Colorado Plateau region, Hawaii, and Alaska. These evaluations are regional in scale and do not eliminate the possibility that small, local aquifers may be suitable for ATES; nor do they guarantee that the regional aquifers will be uniformly suitable or unsuitable over their extent.
Contract Number:	DE-AC06-76RLO 1830, Subcontract B-93966-A-O
Contract Period:	March 29, 1980 through September 22, 1980; final report received June, 1981
Funding Level:	$38,317
Funding Source:	U.S. Department of Energy through Pacific Northwest Laboratory

REGIONAL ASSESSMENT OF AQUIFERS FOR THERMAL ENERGY STORAGE

Dorothy B. Stoffel
Century West Engineering
North 1010 Washington
Spokane, WA 99201

ABSTRACT

Implementation of the Aquifer Thermal Energy Storage (ATES) concept depends upon the availability of suitable aquifers. A study of major United States aquifers has been conducted to qualitatively assess the potential of these aquifers for ATES development.

Existing hydrogeologic data from approximately 700 sources have been collected and stored on computer for all major aquifers in each of the twelve ground-water regions that comprise the United States. Limiting guidelines for hydrogeologic properties were established in order to evaluate each aquifer's potential for ATES development. The hydrogeologic data collected for each aquifer were compared with these limiting guidelines and the ATES potential of each aquifer was established.

The results of the study have been compiled. The compilation contains for each region, a discussion of the hydrogeologic framework, evaluations of major aquifers, and a tabulation of the hydrogeologic data upon which the evaluations were based. Also included is an estimation of the ATES potential of each of the twelve regions.

The geologic environments which contain aquifers best suited for ATES development are those which contain regionally extensive, well-sorted sands or sandstones with interbedded silts, clays, or shales. The geologic environments which have limited regional ATES potential are those that contain aquifers in which the ground-water movement is controlled by secondary porosity or affected by rapid facies changes.

The regions of the United States which have high potential for ATES development are: the mid-continent, the coastal plain, and the area of continental glaciation. Regions which have low potential for ATES development are: the mountain ranges, the alluvial basins; Colorado plateau, Columbia lava plateau, Hawaii, and Alaska. These evaluations are regional in scale and do not eliminate the possibility that small, local aquifers may be suitable for ATES, nor do they guarantee that the regional aquifers will be uniformly suitable or unsuitable throughout their extent.

INTRODUCTION

The work presented within this report is a part of the Seasonal Thermal Energy Storage (STES) Program, which is managed by the Pacific Northwest Laboratory for the United States Department of Energy (DOE). The objective of the STES program is to conduct research and development studies required to provide a sound technical base for the implementation of STES concepts. Potential storage media include aquifers, lakes, ponds, and earth. Storage of thermal energy in aquifers has been chosen for initial development under the STES Program.

The purpose of this study is to collect and summarize hydrogeologic data and to qualitatively describe the ATES potential of all major aquifers throughout the United States. For the purpose of this study, the United States has been broken into the following twelve ground-water regions: 1) western mountain ranges, 2) alluvial basins, 3) Columbia lava plateau, 4) Colorado plateau, 5) high plains, 6) glaciated central lowland, 7) unglaciated central region, 8) unglaciated Applachians, 9) glaciated Applachians, 10) Atlantic and Gulf coastal plain, 11) Hawaii, and 12) Alaska (Figure 1).

The regional scope of this project involves the accumulation, tabulation, and review of existing hydrogeologic data for the major aquifers of the twelve ground-water regions in order to establish the ATES potential of each aquifer, as well as the overall ATES potential of each region. For this study, a major aquifer is defined as one which has significant areal extent and which can sustain typical well yields of at least 50 gallons per minute (gpm).

The initial phase of the project involved a literature search for references which describe the general hydrologic framework of a region, and references which provide specific hydrologic information which would indicate an aquifer's potential for ATES. The most available and applicable publications from each state and from the United States Geological Survey were reviewed. A bibliography for each region was developed to document all publications reviewed. Approximately 700 publications were reviewed and are contained in the bibliography.

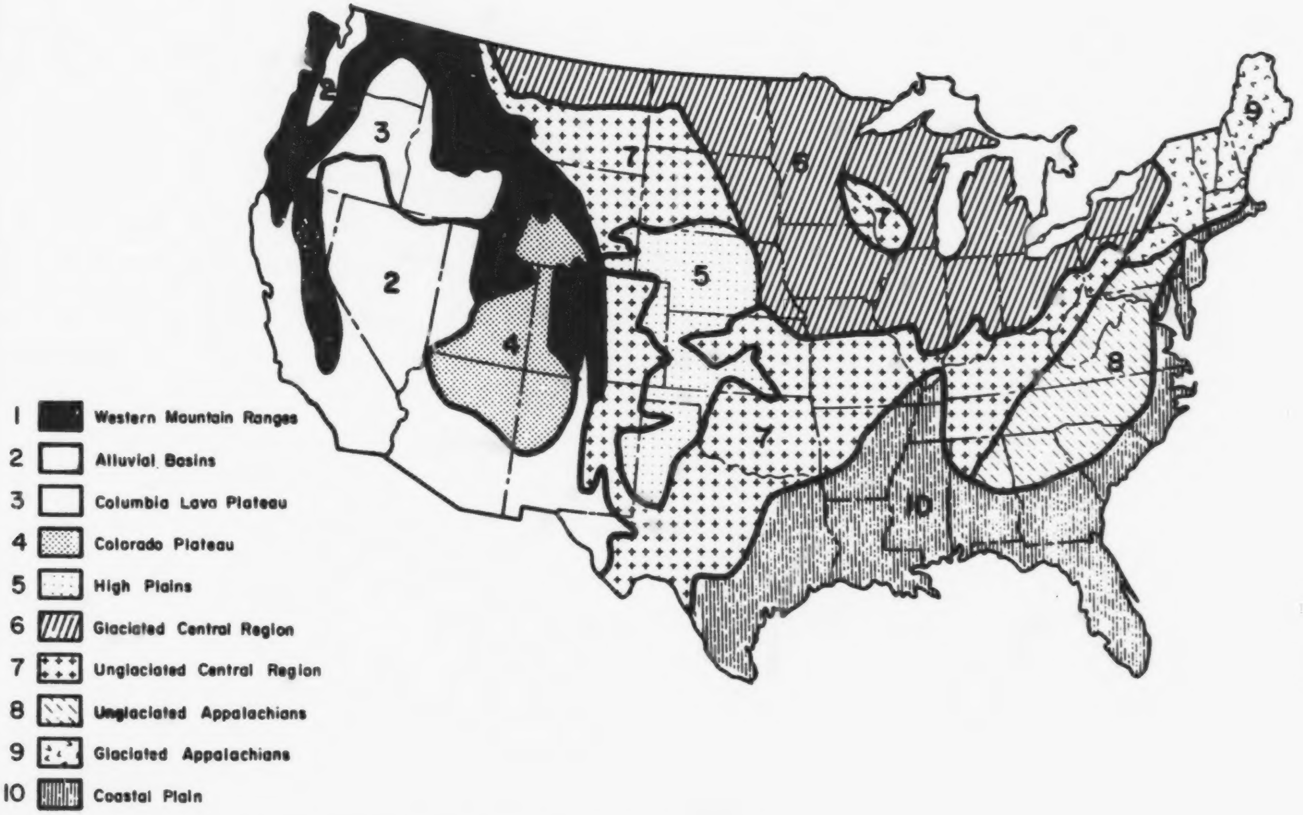
1 Western Mountain Ranges
2 Alluvial Basins
3 Columbia Lava Plateau
4 Colorado Plateau
5 High Plains
6 Glaciated Central Region
7 Unglaciated Central Region
8 Unglaciated Appalachians
9 Glaciated Appalachians
10 Coastal Plain
1
2
3
4
5
6
7
8
9
10

MAJOR GROUND-WATER REGIONS OF THE UNITED STATES, EXCEPTING ALASKA AND HAWAII

Source: Johnson 1966, page 48

FIGURE 1

A computer program was developed and utilized for aquifer data storage and tabulation. The data are stored and tabulated by aquifer and listed under the region in which the aquifer exists. Data that are acccumulated and stored pertain to hydraulic properties, geometry, geologic characteristics, thermal characteristics, and water quality information for each aquifer. In addition to citing all available data in the literature, the program averages values when more than one reference cites data for a specific aquifer characteristic. All data have a reference number which is keyed to a numbered reference in the bibliography. This identifies the data source so that additional information may be obtained for future use.

Prior to beginning actual data analysis and aquifer evaluation, it was necessary to establish limiting guidelines for aquifer parameters and properties. Limiting guidelines were developed for each of the three different types of storage.

- low temperature (greater than 60°C, less than 95°C),
- high temperature (greater than 95°C, less than 150°C), and
- chill (greater than 0°C, less than 10°C).

The limiting guidelines, represented in Figures 2 and 3, are separated by small yield system (50 gpm to 500 gpm) versus large yield system (greater than 500 gpm).

Additional factors evaluated in the limiting guidelines but not listed on Figures 2 and 3 were: degree of confinement, homogeneity versus heterogeneity, isotropy versus anisotropy, porosity, hydraulic gradient, and flow velocity. The guidelines used were flexible and serve as a means of tentatively evaluating an aquifer's potential for ATES. The use of these guidelines does not necessarily preclude an aquifer from future development of its ATES potential. These general guidelines are to be adjusted in light of site-specific information obtained from ATES testing facilities.

* Values near 20,000 for Transmissivity are desirable

		CHILL			LOW TEMPERATURE			HIGH TEMPERATURE		
AQUIFER CHARACTERISTICS	UNITS	UNSUITABLE	MARGINAL	SUITABLE	UNSUITABLE	MARGINAL	SUITABLE	UNSUITABLE	MARGINAL	SUITABLE
Depth	Feet	< 20	—	> 20	< 20	—	> 20	< 20	—	Sufficient Hydrostatic Pressure
Thickness	Feet	< 20	>20 <25	>25 <100	< 20	>20 <25	>25 < 100	< 20	>20 <25	>25 <100
Typical Well Yield	gpm	< 50	—	>50 <500	< 50	—	>50 <500	< 50	—	>50 <500
Transmissivity	gpd/ft	<1000 or >20,000	—	>1000 or <20,000 *	< 1000 or > 20,000	—	>1000 or < 20,000 *	<1000 or >20,000	—	>1000 or < 20,000 *
Porosity	%	< 5	>5 <15	> 15	< 5	>5 <15	> 15	< 5	>5 <15	> 15
Thermal Conductivity	BTU/ft.-Hr.-F°	<.50	—	.50 - 2.0	< .50	4.1 - 8.0	.50 - 2.0	> 8.0	4.1 - 8.0	2.1 - 4.0

Fig. 2. Small System Limiting Guidelines

* Values near 20,000 for Transmissivity are desirable

		CHILL			LOW TEMPERATURE			HIGH TEMPERATURE		
AQUIFER CHARACTERISTICS	UNITS	UNSUITABLE	MARGINAL	SUITABLE	UNSUITABLE	MARGINAL	SUITABLE	UNSUITABLE	MARGINAL	SUITABLE
Depth	Feet	< 20	—	> 20	< 20	—	> 20	< 20	—	Sufficient Hydrostatic Pressure
Thickness	Feet	<100	—	≥100	< 100	—	≥100	<100	—	≥ 100
Typical Well Yield	gpm	< 500	—	>500	<500	—	> 500	< 500	—	> 500
Transmissivity	gpd/ft	<1000	—	> 1000 *	< 1000	—	>1000 *	< 1000	—	>1000 *
Porosity	%	< 5	>5 <15	> 15	< 5	>5 <15	> 15	< 5	>5 < 15	> 15
Thermal Conductivity	BTU/ft - Hr - F°	<.50	2.1-4.0	.50 - 2.0	< .50	2.1 - 4.0	.50 - 2.0	> 8.0	4.1 - 8.0	2.1 - 4.0

Fig. 3. Large System Limiting Guidelines

During the development of the limiting guidelines, two geologic characteristics of an aquifer were recognized as the major limits to an aquifer's regional suitability for ATES. The two properties are secondary porosity and rapid facies changes. Aquifers with secondary porosities have limited ATES potential owing to the random and unpredictable volumes of stored water in these aquifers. Aquifers developed in geologic environments with rapid facies changes are eliminated from regional consideration for ATES potential owing to rapid changes in the hydraulic properties over the areal extent of the aquifer. During the course of this study it was found that these two physical characteristics alone provided the most significant limitations to a specific aquifer and to a region's ATES potential.

Because of the regional scope of this study, only regional aquifers were considered for ATES potential, and only the most recent and available literature was reviewed. Small, local aquifers are not covered by this project, but may have potential for ATES. Furthermore, the regional aquifers which are identified as generally suitable for ATES may be unsuitable for ATES at specific localities while aquifers which are identified as generally unsuitable for ATES may be suitable for ATES at specific localities. The purpose of this regional study is to determine aquifers which appear to have the greatest potential for ATES and should not preclude site-specific studies.

Hydrologic and Geologic Model

Scrutiny of the limiting guidelines established for aquifer evaluation reveals an ideal hydrologic model for aquifers which are most suitable for ATES. When comparing the model with the real world the geologic environments which have aquifers most suitable for ATES are those which contain thick, regionally extensive, well-sorted sands or sandstones that are interbedded with impermeable silts, clays, or shales. Ideal sands or sandstones have low hydraulic gradients and flow velocities which are possible with a small dip angle. Figure 4 is a generalized geologic cross section depicting a geologic environment that is suitable for ATES development.

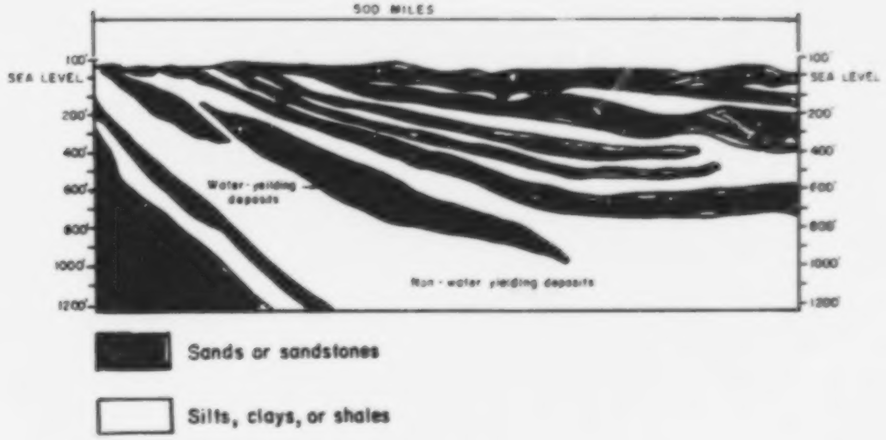

Fig. 4. Generalized Geologic Cross Section of an Environment Suitable for ATES Development

Examination of the general geology of the United States reveals the following three major geologic environments which approximate the ideal model: 1) Paleozoic marine sedimentary rocks of the mid-continent area, 2) Cretaceous and Tertiary sedimentary units of the coastal plain, and 3) Pleistocene outwash and fine-grained units in areas of continental glaciation.

Regional ATES Potential

After all major aquifers were evaluated for their ATES potential, each of the twelve ground-water regions were evaluated for the overall regional potential for ATES. Figure 5 lists the ground-water regions, indicates the regional potential for ATES, and provides an explanation for why regions were rated as having high or low potential. Generally it was determined that regions with aquifers composed of thick, regionally extensive, well-sorted sands or sandstones have high potential for ATES. Regions containing aquifers which have secondary porosities and/or aquifers associated with geologic environments that have rapid facies changes have low potential for ATES.

Conclusions

There is a direct correlation between aquifer suitability for ATES and geologic environment. Based upon the limiting guidelines established for aquifer evaluation for ATES potential, it was determined that the geologic environments which contain aquifers most suitable for ATES development are those that contain regionally extensive sands or sandstones with interbedded silts, clays, or shales. These environments approximate the hydrologic model for ideal aquifer thermal energy storage and retrieval. Geologic environments with limited regional ATES potential are those that contain aquifers with secondary porosities or aquifers associated with geologic units that have rapid facies changes.

The regions of the United States which have high potential for ATES development are: the mid-continent, the coastal plain, and the area of continental glaciation. The regions of the United States which have low potential for ATES development are: the mountain ranges, the alluvial basins, Colorado plateau, Columbia lava plateau, Hawaii, and Alaska.

REGION	ATES POTENTIAL	REMARKS
WESTERN MOUNTAIN RANGES	LOW	MOST AQUIFERS HAVE SECONDARY POROSITIES OR ASSOCIATED WITH GEOLOGIC UNITS THAT HAVE RAPID FACIES CHANGES
ALLUVIAL BASINS	LOW	MOST AQUIFERS ASSOCIATED WITH GEOLOGIC UNITS THAT HAVE RAPID FACIES CHANGES
COLUMBIA LAVA PLATEAU	LOW	MOST AQUIFERS HAVE SECONDARY POROSITIES
COLORADO PLATEAU	LOW	MOST AQUIFERS HAVE SECONDARY POROSITIES OR ASSOCIATED WITH GEOLOGIC UNITS THAT HAVE RAPID FACIES CHANGES
HIGH PLAINS	HIGH	PALEOZOIC SEDIMENTARY ROCKS HAVE HIGH POTENTIAL
GLACIATED CENTRAL LOWLAND	HIGH	PALEOZOIC SEDIMENTARY ROCKS AND PLEISTOCENE UNITS HAVE HIGH POTENTIAL
UNGLACIATED CENTRAL REGION	HIGH	PALEOZOIC SEDIMENTARY ROCKS HAVE HIGH POTENTIAL
UNGLACIATED APPALACHIANS	LOW	MOST AQUIFERS HAVE SECONDARY POROSITIES
GLACIATED APPALACHIANS	HIGH	PLEISTOCENE UNITS HAVE HIGH POTENTIAL
ATLANTIC AND GULF COASTAL PLAIN	HIGH	CRETACEOUS AND TERTIARY SEDIMENTARY UNITS HAVE HIGH POTENTIAL
HAWAII	LOW	MOST AQUIFERS HAVE SECONDARY POROSITIES
ALASKA	LOW	LACK OF SUFFICIENT HYDROGEOLOGIC DATA TO ADEQUATELY ASSESS REGION'S ATES POTENTIAL

Fig. 5. ATES Potential of Each Ground Water Region

PROJECT SUMMARY

Project Title: Maintenance and Development of the Seasonal Thermal Energy Storage (STES) Library

Principal Investigator: Charles H. Lee

Organization:
Midwest Research Institute
425 Volker Boulevard
Kansas City, Missouri 64110

Project Goals: Perform activities necessary for maintenance and development of the STES Library, including technical abstracting and assignment of keywords.

Project Status: Maintenance and development of the STES Library continued during FY 1981. The library now contains over 1900 documents on topics related to thermal energy storage.

During FY 1981, bibliographic data from the STES Library were entered into a computerized information system called the STES Technology Information System (STES-TIS). Each library article is represented by a citation in the bibliographic data files of the STES-TIS. Customized, on-line literature searches can be conducted.

Keywords have been assigned to the library articles. These keywords will be added to the bibliographic data files to improve the capability to conduct customized literature searches.

Researchers from many countries, including the United States, Sweden, Israel, Canada, France, and Germany, used the STES Library during FY 1981.

Improvements made during FY 1981 have resulted in a more useful, efficient library.

Contract Number: DE-AC06-76RLO 1830, Subcontract B-97521-A-O

Contract Period: August 5, 1981 through September 30, 1981

Funding Level: $91,516

Funding Source: U.S. Department of Energy through the Pacific Northwest Laboratory

LIBRARY DEVELOPMENT AND SURVEY OF REINJECTION EXPERIENCE

Charles H. Lee
Mike Snyder
Glenda Casper
Midwest Research Institute
425 Volker Boulevard
Kansas City, MO 64110

ABSTRACT

This presentation is in two parts: Part I-Survey of Reinjection Experience; and Part II-Library Development. Part I identifies and documents 45 sites which have experience in ground-water reinjection for cooling applications. The selection of sites was based on geographic location and availability of information. Information on the cooling system, well log, and water quality data was collected for each site. An analysis was made for each site based on this information. Many problems associated with reinjection can be avoided if the system is carefully designed and maintained.

Part II of this presentation describes maintenance and development of the Seasonal Thermal Energy Storage (STES) Library. Since August 1980, Midwest Research Institute (MRI) has assisted the Pacific Northwest Laboratory (PNL) with operation of the STES Library. The library currently contains approximately 2,000 documents related to thermal energy storage. Key information for each document, including author, title, date, publisher, abstract, identification number, and keywords has been entered in a computerized information system. Improvements made during the past year have resulted in a more useful and efficient library operation.

PART I. SURVEY OF REINJECTION EXPERIENCE

A. INTRODUCTION

Understanding the problems associated with the reinjection of ground water is an important element in the successful use of aquifers for seasonal thermal energy storage. However, experience with the reinjection of heated water is not well documented in the literature. To fill in these gaps in the published data, MRI conducted a study to identify and document sites having information on ground-water reinjection. Our primary emphasis was on the reinjection of heated ground water from cooling applications.

B. METHODOLOGY

Our approach was, first, to identify as many sites as possible and, then, to concentrate efforts at each site on identifying (a) how ground water was being used in the system and (b) the types of associated reinjection problems. The information that we collected includes the cooling system concepts, ground-water flow rates, injection temperatures, well logs, and water quality data.

We divided the continental United States into five geographic regions: north, south, east, west, and central. An effort was made to obtain as diverse aquifer types within each region as possible. We used both telephone and mail as survey tools. Initial contacts were by telephone to identify potential sites; then survey forms were sent to those sources that seemed to have the most information. The response to the mail survey was slow and sometimes required several follow-up calls. However, the rate of success using this survey approach was high. We were able to obtain information on 45 sites.

C. RESULTS

The information on each site was collected from a number of sources: well drillers, consulting engineering firms, state regulatory agencies, equipment manufacturers and distributors, the National Water Well Association, state geological surveys, and local public works water quality labs. In general, the best sources turned out to be the well drillers and the site maintenance superintendents. The information obtained on each site was compiled and analyzed, the site described briefly, and cooling and reinjection problems characterized. The end result of this study was the establishment of a data base of reinjection experience (both successful and unsuccessful) based on a variety of sites around the country with different hydrogeologic characteristics and cooling systems. These sites, their basic characteristics, and major operating problems are identified in Table 1.

TABLE 1

DOCUMENTED SITES

Site	State	Aquifer	Reinjection Rate (gpm)	Reinjection Temp. (°F)	Comments
		NORTH			
1. C.F. Industries, Aurora	NE	Sand and gravel	150, 2 wells	60	Minor plugging problems
2. U.S. Meat Animal Research Center, Clay Center	NE	Sand and gravel	2,000, 2 wells	68	No problems
3. Private residence, Lake Poinsett	SD	Sand and gravel	8	64	New site
4. Idaho State University, Pocatello	ID	Sand and gravel	572	64	No problems
5. Southdale Shopping Center, Edina	MN	Sand and gravel		83	Plugging problems, reinjection discontinued
6. Artistic Woven Labels, Holdrege	NE	Sand	240	67	Minor plugging problems
7. Private residence, Idaho Falls	ID	Shale	-	75	Do not reinject
		SOUTH			
8. Lido Regency Condominium, Sarasota	FL	Limestone	350	90-100	Thermal problems
9. Beach Terrace Condominium, Sarasota	FL	Limestone	Not known	85	No problems
10. Manatee Junior College, Bradenton	FL	Limestone	1,250	95	Thermal problems
11. Florida State University, Tallahassee	FL	Limestone	Many wells	-	Thermal problems in the past
12. George Smith, Inc., Round Rock	TX	Limestone	7	84	Needs additional reinjection well
13. Hercules, Inc., Savannah	GA	Limestone	820	92	Declining water table
14. General Services Administration, Savannah	GA	Limestone	1,000	80	No problems
15. Private residence, Indian Land	SC	Shale	8	92	No problems
		EAST			
16. Edinboro State College, Edinboro	PA	Sand and gravel	50-100	60	No problems
17. General Electric Co., Johnson City	NY	Sand and gravel	125	95	No major problems
18. Long Island Lighting Co., Hicksville	NY	Sand and gravel	500	64	Thermal problems
19. We're Associates, Inc., Lake Success	NY	Sand and gravel	1,500-2,000, 3 wells	65	No problems
20. Lever Management, Garden City	NY	Sand and gravel	400, 2 wells	70	No problems
21. Intown Motor Lodge (old Frederick Hotel), Endicott	NY	Shale	50 est.	70-75	Bad fouling problems, reinjection discontinued

TABLE 1 (continued)

	Site	State	Aquifer	Reinjection Rate (gpm)	Reinjection Temp. (°F)	Comments
			WEST			
22.	Utah Technical College, Orem	UT	Sand and gravel	1,500	68	No problems
23.	Sandia Savings (Sims Building), Albuquerque	NM	Sand and gravel	500	88	No problems
24.	Gig Harbor High School, Gig Harbor	WA	Sand and gravel	75	105	Potential fouling problems
25.	New Mexico Junior College, Hobbs	NM	Sand and gravel	950	78	Thermal problems
26.	Valcris, Inc., Turlock	CA	Sand and gravel	450-600	83	No problems
27.	Turlock Refrigerating Co., Turlock	CA	Sand and gravel	1,500 est.	80-85	Discontinued due to state regulations
28.	Shell Development Co., Salida	CA	Sand and gravel	Not available	95	Thermal problems, reinjection discontinued
29.	Brewster High School, Brewster	WA	Sand and gravel	64	-	No problems
30.	Roswell High School, Roswell	NM	Sand and gravel	Not available	95	Plugging problems
31.	Monterrey School, Roswell	NM	Sand and gravel	Not available	95	Plugging problems
32.	Sierra Middle School, Roswell	NM	Shale and limestone	Not available	95	Plugging problems
33.	Goddard High School, Roswell	NM	Limestone	Not available	95	Plugging problems
			CENTRAL			
34.	Private residence, Troy	OH	Sand and gravel	8	62	Plugging problems
35.	Westover Retirement Residence, Hamilton	OH	Sand and gravel	60, 3 wells	75-95	Thermal and plugging problems
36.	OK Elementary School, Wichita	KS	Sand and gravel	70, 2 wells	85	No problems
37.	Cleveland Elementary School, Wichita	KS	Sand and gravel	200	-	Ground-water level too high
38.	Aviation Education Center, Wichita	KS	Sand and gravel	Not available	95	High ground-water level
39.	Certified Bakers, Wichita	KS	Sand and gravel	60-70, 2 wells	65	Plugging problems; reinjection discontinued
40.	University of Friends Church, Wichita	KS	Sand and gravel	50-60 est.	85	No problems
41.	American Telephone and Telegraph Co., Norway	IL	Sandstone	400	80	No problems
42.	Private residence, Bellevue	OH	Limestone	10	62	No problems
43.	Private residence, Bellevue	OH	Limestone	10	62	Thermal intermixing problem
44.	Rich Township High School, Olympia Fields	IL	Limestone	1,500, 2 wells	70	No reinjection problems
45.	Commonwealth Edison-Unmanned Station, Goodings Grove	IL	Dolomite	860	94	Bad fouling problems

In the course of identifying and documenting reinjection sites for the study, information was compiled on the type of cooling applications for which ground water was being used. The simplest of systems used ground water for direct cooling. In one such system, ground water is passed through a shell and tube heat exchanger where it cools a liquid. If the ground water is cold enough, the liquid could be chilled water from the cooling system. Another direct cooling method is the use of a water-to-air heat exchanger or "fan and coil" system. Air is cooled by passing it over coils chilled by ground water. Schematics of direct cooling systems are shown in Fig. 1.

In some systems, the ground water serves two functions: it pre-cools the air before the air passes over the air conditioning coil, and it condenses the refrigerant in a chiller or condenser. Fig. 2 shows such a system.

Figs. 3 and 4 show how ground water is used in chillers. In both the water-to-water and water-to-air cooling systems, ground water is used for condensing. The circulating water is used as a heat source or sink depending on the season.

The major operating problems could be broadly categorized as plugging problems and thermal pollution problems. Plugging is caused by iron fouling due to the oxidation of ferrous iron and its precipitation as ferric hydroxide. Iron-using bacteria could also cause plugging problems by becoming so abundant they clog well screens or aquifer openings with slimy sludge. It is also possible for reduced manganese to oxidize, precipitate, and cause plugging problems.

Recommended levels of iron and manganese for relatively trouble-free well operation are 0.3 and 0.03 ppm, respectively. Even fairly high levels of these elements in ground water can be handled if the water is not exposed to oxygen and if wells are regularly rehabilitated. Very hard water can cause scaling problems in a cooling system and occasionally in a reinjection well. Annual maintenance can solve this problem, however.

A number of sites had thermal pollution problems resulting from reinjection practices. In fact, several sites had discontinued ground-water usage because temperatures were too high. Some sites were forced to discontinue reinjection because of the implementation of stricter state injection standards which the site could not meet economically. In other states, reinjection of cooling water was prohibited or discouraged.

D. CONCLUSION

Reinjection of heated ground water is a relatively new practice; the successful, older sites are not more than 25 years old. The body of information on reinjection is still small, but it is growing rapidly. Information collected from sites such as the 45 sites documented in this study can help to minimize reinjection problems by assisting with proper system design.

PART II. LIBRARY DEVELOPMENT

A. INTRODUCTION

The use of aquifers for Seasonal Thermal Energy Storage (STES) is a promising new technology for the conservation of energy. The STES Library has been established to serve as an information center for the collection, organization, and distribution of information related to STES. Although the STES Library contains documents pertinent to various types of seasonal thermal energy storage, the primary emphasis is on aquifer thermal energy storage. At the present time, the STES Library contains approximately 2,000 documents.

B. DESCRIPTION OF THE STES LIBRARY

1. Facilities

The STES Library is located at the Pacific Northwest Laboratory (PNL). Since August 1980, MRI has been assisting PNL with maintenance and development of the STES Library. The library is staffed with a full-time librarian from MRI. The library contains a Hewlett-Packard terminal system, including a terminal, printer and plotter. This system is used for remote access to various computers.

BEST DO[illegible] AVAILABLE

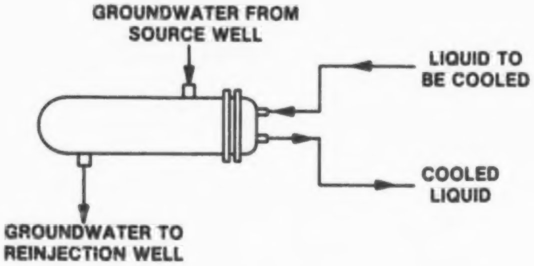
GROUNDWATER FROM SOURCE WELL
LIQUID TO BE COOLED
COOLED LIQUID
GROUNDWATER TO REINJECTION WELL

(A) SHELL AND TUBE HEAT EXCHANGER

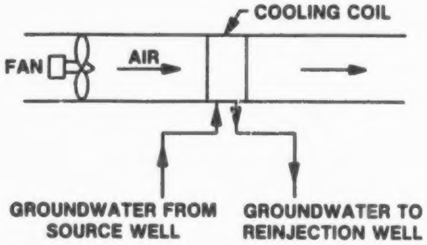
COOLING COIL
FAN
AIR
GROUNDWATER FROM SOURCE WELL
GROUNDWATER TO REINJECTION WELL

(B) WATER TO AIR HEAT EXCHANGER

Fig. 1. Ground Water for Direct Cooling

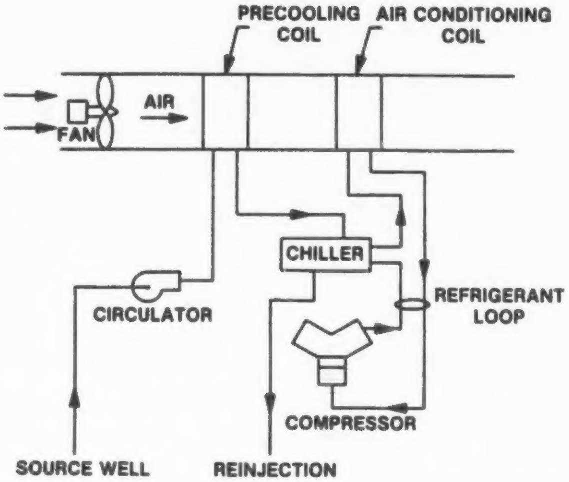
PRECOOLING COIL
AIR CONDITIONING COIL
AIR
FAN
CHILLER
CIRCULATOR
REFRIGERANT LOOP
COMPRESSOR
SOURCE WELL
REINJECTION

Fig. 2. Ground Water for Precooling and Condensing

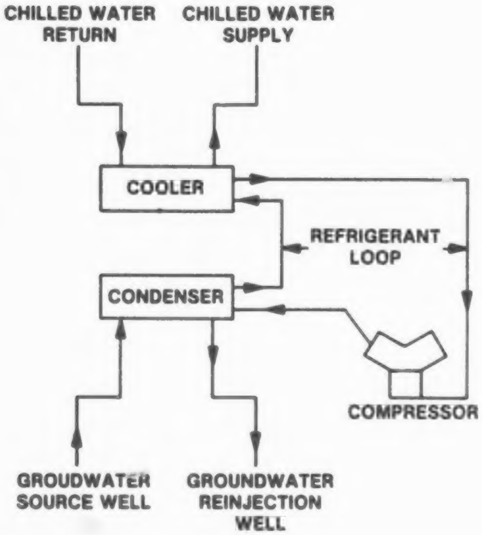
CHILLED WATER RETURN
CHILLED WATER SUPPLY
COOLER
REFRIGERANT LOOP
CONDENSER
COMPRESSOR
GROUDWATER SOURCE WELL
GROUNDWATER REINJECTION WELL

Fig. 3. Ground Water Condensing for a Chilled Water System

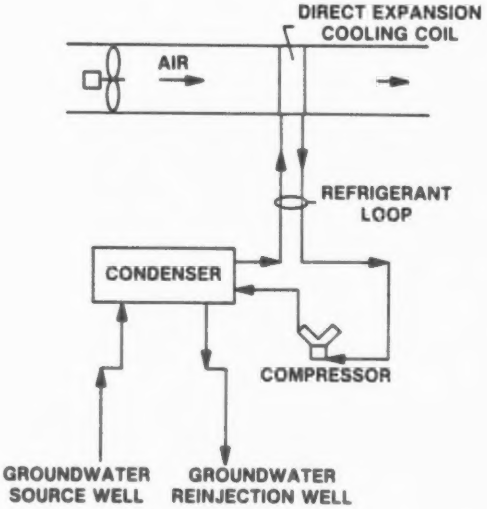
DIRECT EXPANSION COOLING COIL
AIR
REFRIGERANT LOOP
CONDENSER
COMPRESSOR
GROUNDWATER SOURCE WELL
GROUNDWATER REINJECTION WELL

Fig. 4. Ground Water Condensing for a Direct Expansion System

2. STES Technology Information System

Bibliographic information from the STES Library has been entered into the STES Technology Information System (STES-TIS), which is being developed with assistance from Lawrence Livermore Laboratory. The STES-TIS is a comprehensive, computer-based information system which provides the capability to store and manipulate various types of data files, including the bibliographic data file. Each library article is represented by a citation in the bibliographic data file. Each citation contains seven fields: abstract, identification number, author, title, reference, date, and keywords. Except for the abstract, most of these fields have been filled. We have attempted to verify the information contained in the bibliographic data file and to locate information that was previously missing.

MRI has established a system for assigning keywords to library articles. This system contains 38 categories and 82 descriptors. During FY-1981, each document was reviewed, and keywords were identified and entered into the bibliographic data file. Documents can now be accessed by keyword(s), word(s) or phrase(s) contained in the abstract or title, by author, publisher, document number, or combinations of these.

Approximately 400 abstracts have been entered into the information system. A major effort is needed to complete entry of abstracts into the system.

3. Acquisition process

New documents are continually being identified and procured for the STES Library. These documents are identified through periodic literature searches and through direct requests from PNL staff. The literature searches are completed through DIALOG Information Retrieval Service from Lockheed Information Systems. Data bases used in DIALOG include NTIS, COMPENDEX, GEOREF, ENERGYLINE, ENVIROLINE, SCISEARCH, and CA SEARCH. The listings obtained as a result of the literature searches are reviewed, and documents needed for the STES Library are ordered. When a new item is received, it is given an identification number and keywords are established for it. Bibliographic information for the new item is then entered into the STES-TIS.

C. CIRCULATION

Periodically an annotated listing of new documents in the STES Library is produced and distributed to the STES staff. This allows the staff to request the new documents they wish to review. New documents covering a specific STES topic are automatically routed to personnel working in that area.

Customized searching of the library can be done in the STES-TIS by any authorized user or by the STES librarian. Nearly 60 searches were completed by the librarian this fiscal year. Many requests originated from researchers outside PNL, including researchers from France, India, Japan, and Canada. Information packets, including STES Program documents, printouts of customized searches, and copies of non-copyrighted documents were prepared in response to requests for information.

D. CONCLUSION

The availability and the accessibility of information are of great importance to modern research. The STES Library has proven to be an effective means of transmitting information needed by researchers in the field of energy storage. Improvements made during FY-1981 have resulted in a more useful and efficient library operation.

PROJECT SUMMARY

Project Title: Physicochemical Analysis of Aquifer Materials and Ground-Water Fluids from STES Field Test Facilities

Principal Investigator: Stephen C. Blair

Organization:
Pacific Northwest Laboratory
Water and Land Resources Department
Richland, WA 99352

Project Goals: Use laboratory scale and field test data to determine how the physical and chemical properties of an aquifer system may change under conditions imposed by a STES facility.

Project Status: This project is only partially completed. Laboratory testing equipment (termed the Aquifer Properties Test Facility or APTF) has been developed and constructed at Terra Tek, Inc. Starting in early FY-1982 the APTF will be used to perform laboratory scale tests on reservoir materials and associated ground water. Initial tests will include measurements of sample permeability and creep/compaction as well as chemical monitoring of pore fluid as it is circulated through a sample: all measurements will be conducted under simulated, STES operating conditions, e.g. time varying temperature, stress and flow rate.

A contract has been awarded to Terra Tek, Inc., to develop a mobile, inline, injectivity-impairment test stand. This equipment is designed to permit evaluation of injection well longevity as a function of injection water quality and reservoir injection parameters. Completion of the equipment is scheduled for August 1981.

Contract Number: DE-AC06-76RLO 1830

Contract Period: Continuing

Funding Level: $156,900, FY-1981, B/O

Funding Source: U.S. Department of Energy through Pacific Northwest Laboratory

PROJECT SUMMARY

Project Title: Permeability Creep/Compaction Studies on Sandstones

Principal Investigator: C. Cooley, J. A. Stottlemyre

Organization:
Terra Tek, Inc.
Salt Lake City, Utah

Pacific Northwest Laboratory
Water and Land Resources Department
Richland, WA 99352
(509) 376-8639 (FTS: 444-8639)

Project Goals: Determine the effects of temperature on permeability of sand and sandstone to water.

Project Status: Data in the literature indicates that the permeability of sands and sandstone decrease significantly with temperature increase from 20°C to 150°C. Numerous experiments were conducted at PNL and Terra Tek to address these potential problems. Important results include: 1) the permeability of Massillon sandstone and Ottawa sand to deionized, deaerated, prefiltered water are not particularly temperature sensitive if apparatus contamination (metal colloid) is eliminated; 2) temperature-induced bulk sample compaction and expansion of grains into pore space results in less than 0.5 percent loss in porosity; 3) published distilled water viscosity/temperature relationships are adequate; and 4) particles (fines) internal to the rock cores are preferentially mobilized at temperature, but do not seem to perturb the permeability in short laboratory cores.

Contract Number: B-96462

Contract Period: January 15, 1980 through November 30, 1980

Funding Level: $108,007

Funding Source: U.S. Department of Energy through Pacific Northwest Laboratory

PROJECT SUMMARY

Project Title: Aquifer Thermal Energy - Generic Laboratory Study of Ottawa Silica Sand and Massillon Sandstone

and

Development of Laboratory Core Testing Appartus and Field Injectability Apparatus

Principal Investigator: P. Eric Peterson, J. A. Stottlemyre, L. B. Owen and C. H. Cooley

Organization:
Terra Tek, Incorporated
University of Utah Research Park
420 Wakara Way
Salt Lake City, Utah 84108

Project Goals: Three major goals are to be met in this project: 1) To complete a laboratory scale program to provide baseline data for permeability impairment and compressibility of two generic reservoir materials; 2) To design and construct a laboratory core testing apparatus capable of subjecting rock specimens to ATES in-situ stresses and temperatures while measuring permeability and volume strain; and 3) To design and construct a field injectability apparatus capable of on-site analysis of interaction of ATES water with the ATES reservoir. This apparatus uses membrane filters or rock specimens as analogs for the ATES reservoir.

Project Status: Results from the laboratory scale testing program have identified two mechanisms of permeability reduction in Ottawa Silica Sand and in Massillon sandstone.

Permeability degradation in Ottawa silica sand and Massillon sandstone occurred because of metal corrosion product contamination from the experimental appartus flow loop. Two modifications of the test apparatus have been made which control this source of permeability degradation. First, brass and aluminum components were removed and replaced with stainless steel thereby reducing the quantity of corrosion products. Second, the pore fluid was filtered before introduction to the specimen. A second and minor source of permeability degradation for these materials is the thermally induced mobilization of small internal particles. These particles plug the flow channels in the specimens and decrease their permeability. Though this degradation mechanism has only a small effect in the laboratory specimens, it could have a major effect in a large reservoir.

These permeability degradation mechanisms apply to Ottawa silica sand and to Massillon sandstone, the two materials studied in our program. Other degradation mechanisms are possible with other types of geological materials. Site specific geological materials should be tested to accurately assess any ATES site.

The laboratory core testing apparatus has been built and is currently undergoing acceptance testing. The apparatus is able to generate confining pressures to 103 MPa, at flow rates to 6.2 ml/second, and temperature to 100°C. Measurements of specimen permeability and volume strain are possible at in-situ conditions.

The field injectability apparatus has been built and will undergo acceptance tests late in 1981.

	Laboratory Core Testing Program	Core Testing Apparatus	Injectability Apparatus
Contract Number:	B-B2405--0	P.O. #78992	B-2684 AD
Contract Period:	12/80-6/81	6/80-6/81	4/81-8/81
Funding Level:	$45,300	$235,000	$59,928

Funding Source: Department of Energy through Battelle, Pacific Northwest Laboratory

AQUIFER THERMAL ENERGY STORAGE - GENERIC LABORATORY STUDY OF OTTAWA SILICA SAND AND MASSILLON SANDSTONE and DEVELOPMENT OF LABORATORY CORE TESTING APPARATUS AND FIELD INJECTABILITY APPARATUS

P. Eric Peterson, J. A. Stottlemyre*, L. B. Owen and C. H. Cooley
Terra Tek, Inc., Salt Lake City, Utah
*Battelle PNL, Richland, Washington

ABSTRACT

Laboratory tests were performed to quantify the effects of temperature upon the permeability of Massillon sandstone and Ottawa silica sand. The resulting data have revealed two permeability impairment mechanisms: 1) contaminant plugging resulting from the corrosions of components in the experimental apparatus, and 2) particulate plugging traceable to fines within the specimens. Additionally, a core testing apparatus and field injectability apparatus have been designed and built for use by Battelle PNL. The features and uses of both apparatus are described in this paper.

INTRODUCTION

Terra Tek, under subcontract to Battelle PNL, is performing three tasks which aid the assesment of Aquifer Thermal Energy Storage (ATES) concepts. The three tasks are: 1) The laboratory measurement of permeability, at elevated temperature, of Massillon sandstone and Ottawa silica sand, 2) The design and construction of a laboratory core testing apparatus for use by Battelle PNL, and 3) The design and construction of a field injectability apparatus.

The purpose of these tasks is to help in the understanding of aquifer and water quality response to the injection and production of hot water. Reservoir permeability, stresses, and porosity may change dramatically as the reservoir temperature and pressure vascillates with injection and production. The laboratory core testing has simulated these stresses and temperatures while measuring critical properties of the test specimen. The core testing apparatus being built for Battelle will likewise be capable of subjecting core samples to the stresses and temperatures typical to ATES while measuring pertinent core properties. The field injectability apparatus is able to quanitatively assess the permeability impairment potential of ATES site water using core samples and filter analogs.

This paper will discuss each of the three tasks.

TESTING PROGRAM

Two possible ATES reservoir materials, Massillon sandstone and Ottawa silica sand, are being characterized through laboratory testing. The current focus of these tests is to obtain baseline data relating specimen permeability to temperature. Measurements of sample compaction, and water quality are made to help in understanding possible changes in permeability at elevated temperature. Also being investigated are the effects of thermal cycling, and pore fluid composition on permeability. Testing is performed under in-situ pressures at temperatures of 25°C and 150°C.

Procedure

The experiments on sieved (.09 to .11 mm) Ottawa silica sand and on Massillon sandstone were performed using similar techniques. In all cases the specimens were brought to the in-situ stress state, at which time flow was established at 25°C and maintained constant while permeabilities and strain were measured. The specimen and pore fluid temperature were then increased to 150°C. Stress state and flow were held constant at 150°C while measurements were taken. The sample and pore fluid were then returned to 25°C and steady state measurements of permeability and strain taken.

Results

The early results of these tests showed a significant degradation of permeability at 150°C as compared to 25°C. This degradation was evident in both Massillon sandstone as well as Ottawa silica sand. See Figures 1 and 2 for plots of permeability versus temperature for these two materials.

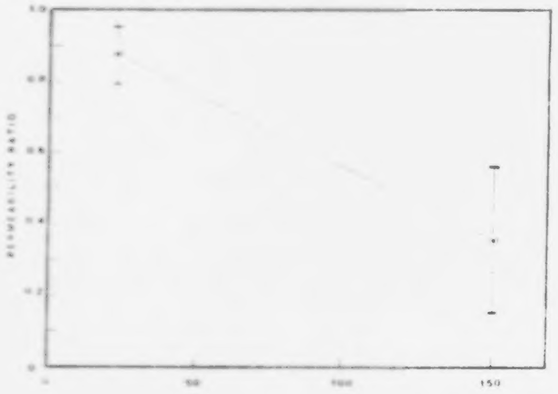

Figure 1. Permeability versus Temperature for Massillon Sandstone

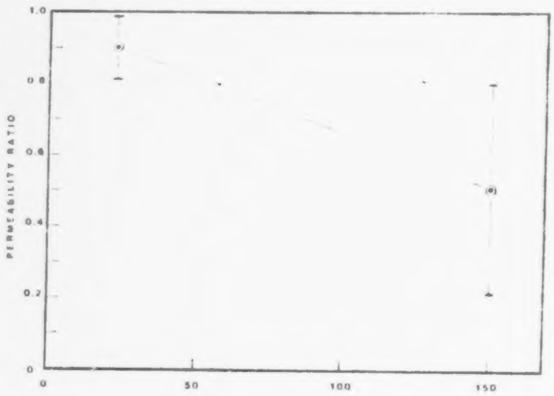

Figure 2. Permeability versus Temperature for Ottawa Silica Sand

Filtering the pore fluid before introduction to the samples helped reduce the magnitude of the permeability degradation which was shown to be caused by particulate contamination from the metals in the apparatus flow loop[1]. These contaminating particulates were primarily metal oxides and hydroxides originating from brass, aluminum, and stainless steel used in the apparatus.

Replacing the brass and aluminum components with stainless steel reduced the particulate load in the pore fluid. This modification, coupled with 0.45 μm filtration of the pore fluid before the sample, controlled this mechanism of permeability degradation.

After these modifications a small but measurable permeability degradation was still observed in both rock types. Testing was then carried out on specimens of Ottawa silica sand that were washed to remove small particulates. Test results from these washed samples showed a lesser permeability degradation suggesting particulate plugging as an impairment mechanism.

Tests using 2% $CaCl_2$ brine as the pore fluid showed a similar degree of degradation in both rock types. Therefore, salinity induced clay swelling or mobilization is not a likely degradation mechanism in these materials[1].

Current Testing

Current experimental work with Ottawa silica sand and Massillon sandstone is focused on investigating the effects of thermal cycling. Here the specimens are subjected to several cycles of heating and cooling while permeability and strain are measured. The thermal cycles have minimums and maximums of 25°C and 150°C while stress state and flow are held constant.

Figure 3 shows preliminary data for permeability as a function of thermal cycling. No dramatic reduction of permeability is observed. Figure 4 shows sample strain, corrected for apparatus and quartz expansion, over several temperature cycles. There is less than 0.25% permanent compaction during the first cycle for either material, subsequent cycles showed no permanent compaction.

Testing of sand packs to evaluate possible well completion designs will occur late in 1981. Tests will be performed under conditions similar to the preceding temperature effect tests.

Conclusions

A major mechanism contributing to permeability degradation in Massillon sandstone and Ottawa silica sand was contamination from the experimental apparatus. Filtering the pore fluid immediately before introduction to the sample and minimizing corroding components in the apparatus

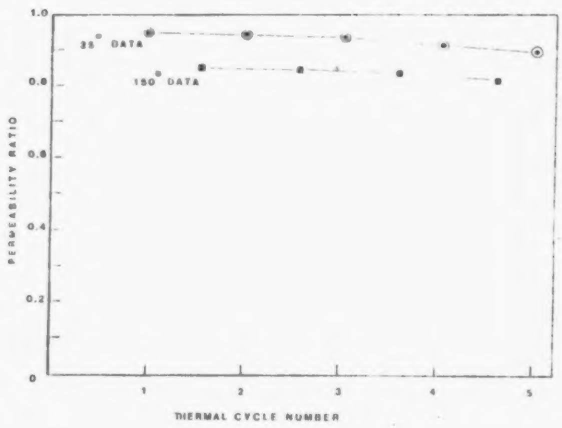

Figure 3. Permeability versus Cycle.

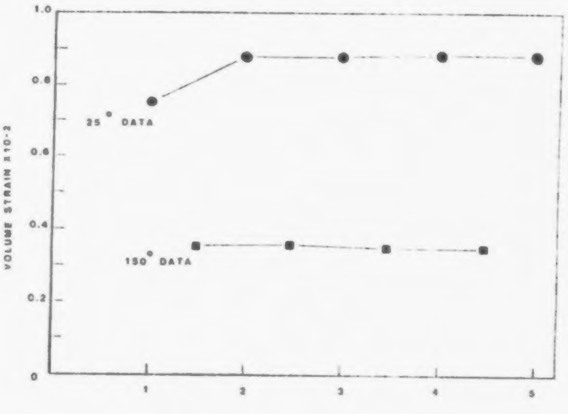

Figure 4. Strain versus Cycle.

eliminated this cause of degradation. Since it has been shown that metal contamination results in the permeability reduction of aquifer material, permeability field equipment should be corrosion resistant and particle load in ATES injection fluids must be closely controlled.

A minor cause of permeability degradation is plugging by small internal particulates. Though this has a small effect in the laboratory on core size samples, it may have a large effect in an aquifer where fines from a large area migrate to a comparatively smaller area around the wellbore.

Thermal cycling in laboratory specimens seems to have little cumulative effect upon permeability and volume strains are recoverable after the first cycle.

The two materials investigated in our experiments are possible reservoir rock types, but are not necessarily typical aquifer materials. The response of each aquifer to injection of hot fluids will be unique. The response of each reservoir depends upon many variables, some of which are: the composition and quantity of internal particulates, the actual in-situ stress state, the geochemical composition of the reservoir material, and the injection fluid. Therefore, to reliably assess the performance of an ATES reservoir, testing for each site is necessary.

LABORATORY CORE TESTING APPARATUS

To reliably quantify potential reservoir impairing mechanisms, it is necessary to subject test specimens to in-situ like stresses and temperatures. Terra Tek has designed and built for Battelle P.N.L. a laboratory core testing facility which is able to reproduce these in-situ conditions. With this apparatus control of confining stress, pore fluid pressure, temperature, and flow rate is possible concomitant with measurement of specimen permeability and strain. Figure 5 shows this core testing apparatus.

Many of the design features incorporated in this apparatus are outgrowths of experience gained in the laboratory core testing program. The use of titanium components in the permeability flow loop, as well as the use of upstream filters, was made evident from the early laboratory core testing program.

The core testing apparatus can subject specimens to the following conditions:

Hydrostatic Stress	103 MPa
Axial Stress (2" Diameter Sample)	200 MPa
Pore Fluid Pressure	103 MPa
Pore Fluid Types	Gas to light brine
Pore Fluid Flow Rate	0.1 ml/sec to 16 ml/sec
Pore Fluid Sampling	Via pressurized bomb
Temperature	200°C maximum
Temperature Cycle	150°C amplitude
Filtering	0.45 μm upstream/downstream

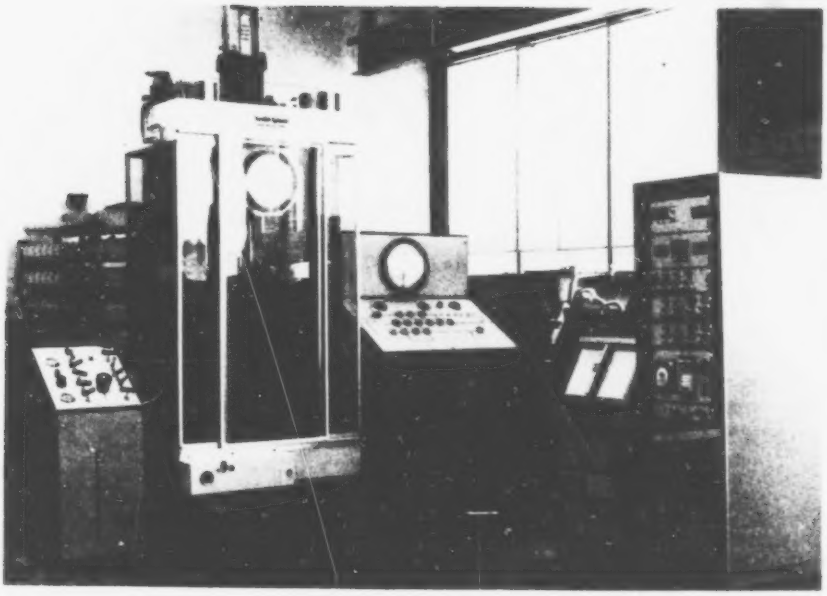

Figure 5. Core Testing Apparatus.

This system features a four post load frame rated at 500 kips and elastic constant of 15 x 10^7 lbs/in. It utilizes a servo-controlled 100 kip upper actuator for sample loading, and a lower, auxiliary actuator, for elevation of the lower vessel closure. A 6 inch I.D., 32 inch long triaxial test vessel rated for 15 ksi @ 200°C is attached to the upper crosshead. Figure 6 shows a schematic of the axial loading system.

A separate module featuring a 15 ksi air driven pump and 15 ksi regulator controls the confining pressure inside the vessel. Figure 7 shows a schematic of the confining pressure system. Heating of the sample (to 200°C) is accomplished by an internal immersion heater controlled by a microprocessor. In-vessel instrumentation allows measurement of sample axial load, axial and transverse strain and strain rate, measurement and control of sample temperature.

Figure 6. Schematic of Axial Loading System.

Figure 7. Schematic of Confining Pressure System.

The system also features a permeability module. (See flow schematic.) Flow rate is controlled with a servo-controlled intensifier. Flow rates from 0.1 ml/sec to 16 ml/sec are possible. The working fluid (light brine) may be heated to temperatures as high as 200°C. Temperature deviation within the flow loop is less than ±5°C. Instrumentation includes a turbine flow meter, upstream and downstream absolute pressure transducers, a sample differential pressure transducer, flow fluid temperature probes and an analog, backup pressure gage. The system design rating is 15 ksi at 100°C. Figure 8 shows a schematic of the pore fluid flow loop.

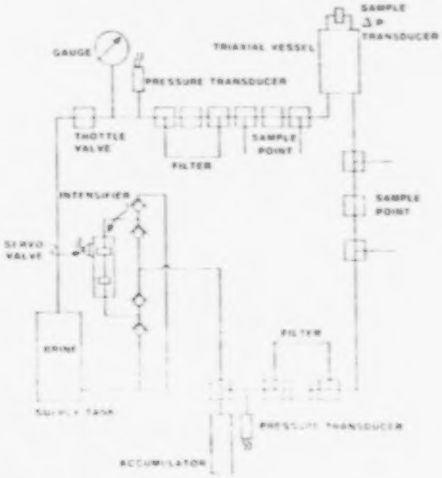

Figure 8. Flow Loop Schematic.

The entire system is controlled from an electronics control console which, features a sixteen channel analog output. This output may be concurrently fed to a furnished X-Y-Y' recorder and an optional computer. System control accuracies range from ±2% of full scale for confining pressure to ±.1% of full scale for sample axial load.

Field Injectability Apparatus

The change in permeability of a core sample or a membrane filter (with the appropriate pore size distribution) to injected water is a rapid and simple method of establishing injectability. Membrane filtration data provide an indication of the impairment potential of injected water resulting from scale formation or deposition of suspended solids. Core tests provide similar data and are also useful in establishing whether detrimental water-rock interactions are significant.

Terra Tek has designed and fabricated a field test apparatus for evaluating the injectability of ATES waters. A flow schematic of the apparatus is shown in Figure 9. The semi-automatic system has provisions for conducting two simultaneous tests to provide evaluation of the injectability of waters before and after passage through ATES heaters.

The field injectability apparatus has the following specifications:

Apparatus Capabilities:	A. Simultaneous operation of either two membrane filter test loops or two core test loops or one membrane filter and one core testing loop. B. Particle size determinations using three in-series membrane filters.
Design Pressure:	7 MPa
Design Temperature:	150°C (200°C with inclusion of heat exchangers upstream of flowmeters)

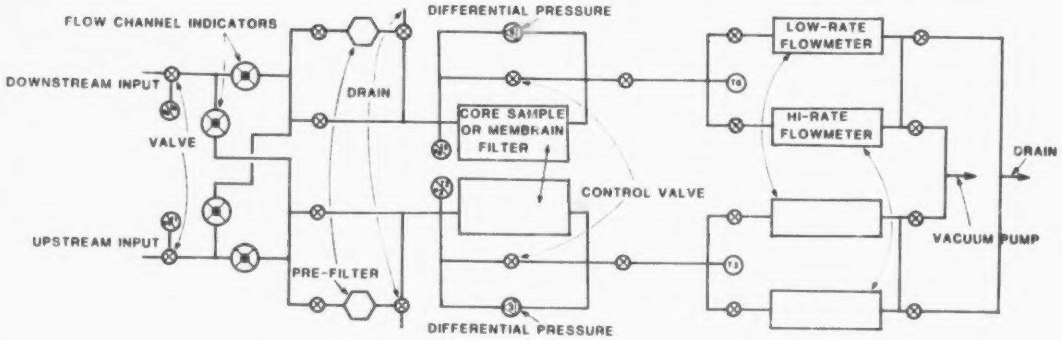
FLOW CHANNEL INDICATORS
DOWNSTREAM INPUT
VALVE
UPSTREAM INPUT
DRAIN
PRE-FILTER
DIFFERENTIAL PRESSURE
CORE SAMPLE OR MEMBRAIN FILTER
CONTROL VALVE
DIFFERENTIAL PRESSURE
LOW-RATE FLOWMETER
HI-RATE FLOWMETER
DRAIN
VACUUM PUMP

Figure 9. Field Injectability Apparatus Flow System Schematic.

Materials of Construction:
Flowmeter Bodies - 316 Stainless Steel
Pressure Transducer Bodies - 300 Series Stainless Steel
Valves & Fittings - 316 Stainless Steel
Tubing - Inconel 600

Control Modes:
Automatic valve selection for flow options
Automatic core/membrane filter temperature control
Manual flow rate control

Date Display/ Acquisition: Digital displays and automated data acquisition via a four channel thermal printer.

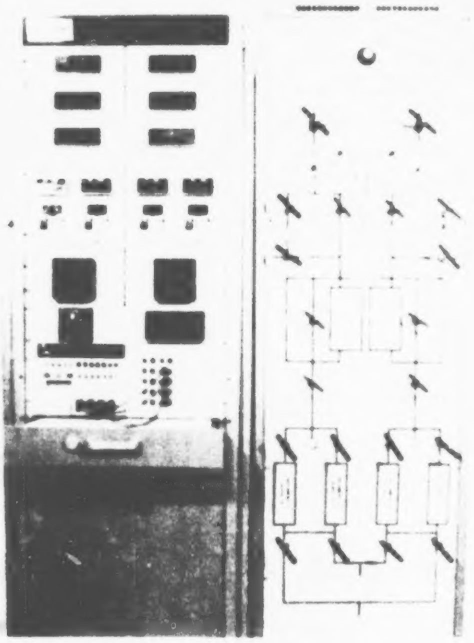

Figure 10. Completed Field Injectability Apparatus. The electronics rack (left) houses flow, presure, and temperature measuring devices and a four channel thermal printer for data acquisition. The flow system (right) can be operated at either constant flow or constant pressure. Core samples and membrane filters are maintained at the appropriate temperature by thermostated heating jackets.

The injectability test frame is connected, as a bypass system, to the main ATES flowline via an electrically-controlled manifold that permits simultaneous testing of input and output streams from the ATES heat exchangers. Injectability tests may be carried out at either constant differential pressure or constant flow. Coarse and fine control valves are used to initially set and maintain differential pressure or constant flow. Cumulative flow and instantaneous flow rate are obtained via turbine flowmeters and their associated output devices. A four channel thermal printer is used to record all data. The system is equipped with high pressure cartridge filters to permit prefiltration of water prior to passage through the membrane filter or core sample. The latter capability is used to establish the benefit to be derived from pre-injection treatment systems, if the injectability of raw effluent is low.

An auxiliary vacuum system is employed to quickly de-gas the test system prior to a run in order to eliminate entrained air that might adversely affect permeability measurements. The vacuum system is also used to bleed residual fluid from the system after each run. Temperature controllers and clam-shell heating jackets are used to maintain epoxy-mounted core samples and membrane filters at constant temperature.

As shown in Figure 10 the flow system is mounted on a single test frame that includes a small integral bench. A separate instrument rack is used to house the electronic readout and control devices. The design of the test apparatus permits locating the equipment in either permanent enclosures (i.e., buildings, large trailers, etc.) or in small trucks or vans.

REFERENCES

1. J.A. Stottlemyre, Investigating Air/Water/Rock Interactions in a CAES Porous Rock Reservoir. Mechanical, Magnetic, and Underground Energy Storage 1980 Annual Contractors' Review, Washington, D.C., November 10-13, 1980. U.S. Department of Energy.

PROJECT SUMMARY

Project Title: Geochemical Modeling of the Effects of Temperature on Mineral Precipitates and Ground-Water Quality at a STES Site

Principal Investigator: J. A. Stottlemyre, E. A. Jenne

Organization:
Pacific Northwest Laboratory
Water and Land Resources Department
Richland, WA 99352

Project Goals: Compare FTF-generated data and computer-simulation data concerning the effects of temperature on mineral precipitates and ground-water quality. Emphasis will be on evaluating geochemical modeling capabilities.

Project Status: This project is only partially completed.

The computer model WATEQ4 has been installed on the Boeing Univac computer and the model is now operational. Input data for the model are now being collected and data requirements for five common aquifer minerals are now 60% complete.

A draft paper has been completed which discusses the application of geochemical modeling to the STES Program.

Contract Number: DE-AC06-76RLO 1830

Contract Period: Continuing

Funding Level: ∿$10K

Funding Source: U.S. Department of Energy through Pacific Northwest Laboratory

JECT SUMMARY

Project Title: Numerical Simulation

Principal Investigator: Charles T. Kincaid

Organization:

Battelle, Pacific Northwest Laboratory
P.O. Box 999
Richland, WA 99352
(509) 375-2867 (FTS: 444-7511 ext. 2867)

Project Goals: Provide technical support in the form of numerical simulation techniques capable of assessing the performance and impacts of aquifer thermal energy storage (ATES).

Within PNL this subtask is to establish a responsive, internal capability for the simulation of ATES facilities. Externally we are utilizing the best available technology to advance the state-of-the-art and provide the necessary analysis capabilities for the engineering community.

Project Status: An independent, responsive simulation modeling capability has been developed through the joint efforts of internal staff and an external contractor. This multi-dimensional code, Coupled Fluid, Energy, and Solute Transport (CFEST), employs a finite element method in solution of the three conservation equations. A substantial effort has been made to produce a user oriented analysis package. Modifications to the analysis package have been the responsibility of the contractor, Dr. S. K. Gupta. Development of auxiliary programs has been primarily the responsibility of PNL personnel. The Galerkin finite element code is presently complimented by interactive input/output and automatic mesh generation packages. A data processing package (FILTER) has also been produced.

Considerable time and effort has been devoted to administering the various contracts under the numerical simulation subtask. These contracts include efforts by Lawrence Berkeley Laboratory, Oregon State University, Washington State University, GeoTrans, Inc., and George Maddox & Associates. Of particular interest are publications prepared by the last two. Final editing and publication has just been completed for the GeoTrans authored report entitled, "Review of Simulation Techniques for Aquifer Thermal Energy Storage (ATES)". A draft of the documentation for the CFEST code, prepared by Dr. S. K. Gupta and PNL staff, is presently being reviewed. Publication of this document will depend upon supplementary funding for final editing and printing.

Contract Number: DE-AC06-76RLO 1830

Contract Period: Continuing

Funding Level: $80,000 FY-1981

Funding Source: U.S. Department of Energy, Office of Energy Systems Research

PROJECT SUMMARY

Project Title: Numerical Simulation - CFEST Code Development

Principal Investigator: Sumant K. Gupta

Organization:

George Maddox & Associates
West 601 Mallon - Suite 2
Spokane, WA 99201
(509) 326-7515

1301 Maple Lane
West Richland, WA 99352
(509) 967-2640

Project Goals: Extend the current ground-water analysis capability of the FE3DGW (finite element three-dimensional ground-water) code to include energy and conservative solute transport. Verify the analysis through the use of published solutions to simplified analyses, and more complex hypothetical problems. Validate the simulative ability of the new code through the analysis of completed experiments conducted by Auburn University.

Project Status: The Coupled Flow, Energy, and Solute Transport (CFEST) multidimensional finite element code extended from FE3DGW was further improved during the year to streamline the input data needs. Supportive programs for interactive input data preparation were developed to reduce labor time, andd the input format errors. For doublet system application, interactive grid generation programs were developed which uses minimum specific site related information to generate the grid files. Code to develop grid based on a steady state analytical solution of isothermal flow potentials and streamlines was also prepared.

CFEST was verified against published analytical solutions. CFEST is currently being applied to the Auburn field experiment. A draft of the code's documentation has been prepared. It will be finalized once the Auburn simulations are completed.

Contract Number: DE-AC06-76RLO 1830, Consultant Agreement B-29028-A-L

Contract Period: October 1, 1980 through September 30, 1981

Funding Level: $78,000

Funding Source: U.S. Department of Energy through Pacific Northwest Laboratory

NUMERICAL SIMULATION - CFEST CODE DEVELOPMENT

Sumant K. Gupta
George Maddox & Associates
1301 Maple Lane
West Richland, WA 99352

Charles T. Kincaid
Paul R. Meyer
Lance W. Vail
Pacific Northwest Laboratory
P.O. Box 999
Richland, WA 99352

ABSTRACT

This paper is a review of progress in the development, verification and validation of a numerical simulation code analyzing energy storage and recovery in the aquifer environment. A standard Galerkin weighted residual approach has been applied to fluid, energy, and solute transport. The resulting finite element code has been tested against published solutions and field observations. A draft of code documentation has been prepared.

INTRODUCTION

The STES Program, directed by Battelle's Pacific Northwest Laboratory (PNL) for the Department of Energy (DOE), has the overall objective of developing the necessary technical support for seasonal thermal energy storage. The most viable application of the STES concept is to the aquifer environment. This is primarily due to the heat storage capacity of water and the large volumes of water which can be stored in the aquifer environment. For the efficient management of this program, an independent predictive computation capability must be available and responsive to programmatic needs.

Research concerning geothermal reservoirs and their numerical simulation has yielded models applicable to similar situations as found in aquifer thermal energy storage (ATES). While being developed for deep confined media and high temperatures, the physical and energy phenomena of these models are the same as those required for ATES. Therefore, the physical-mathematical relationships to be employed in the analysis of ATES have been taken directly from earlier research (references 1, 2, and 3).

Towards supplying the STES Program with an independent, responsive numerical simulation capability George Maddox & Associates have been retained to build upon known ground-water simulation codes to produce a coupled analysis of fluid flow and energy transport within a confined aquifer. During the 1980 fiscal year, major modifications were made to the FE3DGW (finite element three-dimensional ground-water) code (reference 4). Energy and conservative solute transport were added to the existing ground-water analysis package. Both transport processes are modeled by the convection-dispersion equation. Efforts during FY-1981 have focused upon verification, validation, and documentation of the resulting analysis package. The present code can be employed in the analysis of coupled fluid, energy and solute transport (CFEST) within the confined aquifer environment.

CFEST CODE DESCRIPTION

A draft of CFEST code documentation has been prepared. Due to funding uncertainty and limitation, items of higher priority have not permitted effort to be expended upon final editing and publication of this material. Best estimates are that it will be published in the first quarter of FY-1982. A brief summary of the CFEST code's mathematical formulation, assumptions, and features is presented in the following paragraphs.

The governing partial differential equations describing the responses of fluid, energy, and solute within an aquifer are based upon equations of conservation. These equations of mass, energy, and solute conservation are coupled through fluid density which is a function of pressure, temperature and solute concentration. To reduce truncation and roundoff errors, the change in dependent variables are simulated rather than their true value. A consistent solution to each of the three equations is sought via a cyclical implicit scheme.

Assumptions used in the development of the mathematical models and fundamental to their use include:

1. The flow is transient and laminar (Darcian).
2. The permeability and coordinate axes are collinear.
3. Fluid density is a function of pressure, temperature and solute concentration.
4. Fluid viscosity is a function of temperature and concentration.

5. The injection fluid is miscible with the resident aquifer fluids.

6. Aquifer properties (i.e. porosity, permeability, thickness and elevation) vary spatially. Variations in thickness can be continuous while material properties are assumed piecewise constant.

7. Hydrodynamic dispersion is a function of fluid velocity.

8. Boundary conditions permit natural water movement in the aquifer, heat losses/gains to adjacent formations, and the location of injection, production and observation wells anywhere within the system.

9. The porous medium and fluid are compressible.

10. The fluid and porous media are in thermal equilibrium.

11. Rock density and all heat capacities remain constant.

The above stated assumptions do not differ markedly from those of competitive codes. They are virtually the same as those for the INTERCOMP code. Lawrence Berkeley Laboratory's CCC (consolidation-convection-conduction) code differs primarily in its use of a temperature dependent heat capacity (constant volume). These codes employ finite difference and integrated finite difference methodologies, respectively, rather than the finite element method employed for CFEST.

The CFEST analysis package includes a variety of features which make it applicable to the STES study of confined aquifers. In addition to three-dimensional analyses, it can model vertical, horizontal, and axisymmetric two-dimensional flows. Dirichlet and Neumann boundary conditions are admissible. Virtually all combinations of the three conservation equations can be solved. Thus, one performs only the necessary analysis when only fluid and energy are of interest. Several auxiliary programs have been developed for the CFEST package. They include programs for (1) interactive input generation, (2) automatic grid generation, and (3) interactive plotting of results.

CFEST VERIFICATION AND VALIDATION

During FY-1980, CFEST was verified with analytical solutions of flow and conservative solute transport. Fiscal year 1981 activities have included verifying CFEST with an analytical solution of convective heat transport in porous media and validating CFEST with data from the 1978 Mobile field experiment.

Avdonin (reference 5) developed an analytical solution of one-dimensional convective heat transport within a confined aquifer with conductive heat transport through overburden and underburden. Fig. 1 shows a comparison of Avdonin's solution with CFEST's numerical solution.

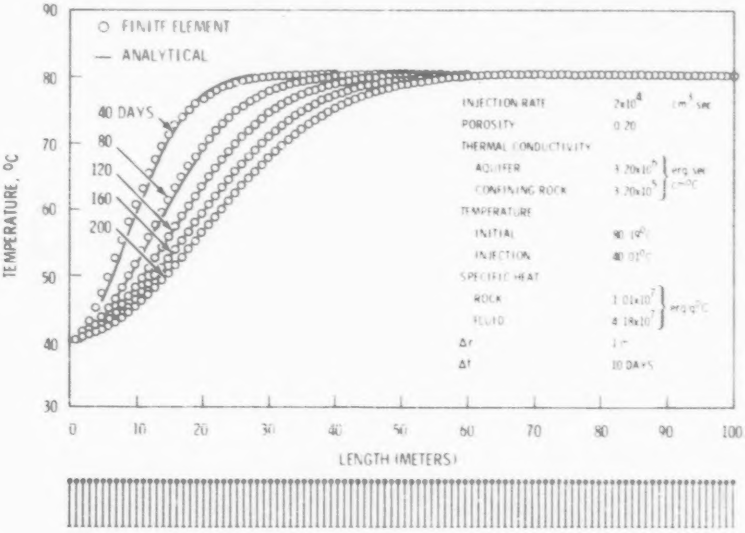

Fig. 1. Comparison of CFEST Results with Avdonin's Analytic Solution

Auburn University conducted field experiments in 1978 at a site 32 km north of Mobile, Alabama. A single well was used to inject and recover heated water. Water was injected at an average temperature of 55°C and an average flow rate of 7.9 kg/sec for 79 days. After a 51 day storage period, water was pumped at an average rate of 15.7 kg/sec for 41 days. Data from the experiment was used as the basis for validating CFEST.

An axisymmetric grid was developed for the simulation. Aquifer parameters established in earlier studies were used (reference 6). The hydraulic driving stresses were assumed constant in time for each of the phases; injection, storage, and production. The injected fluid was assumed to have a constant temperature.

Thermal contour plots of the simulated results at the end of injection, end of storage and end of production phase are shown in Figs. 2, 3, and 4, respectively. Selected observed temperatures are also shown. The plots show general agreement with the observed values. It is believed that differences between observed and simulated values can be attributed to aquifer nonhomogeneity.

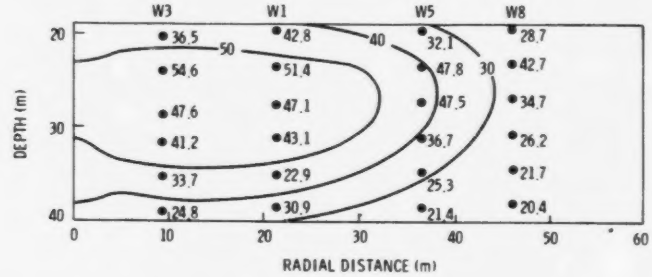

Fig. 2. Comparison of Observed Temperatures and Simulated Contours at End of Injection Period

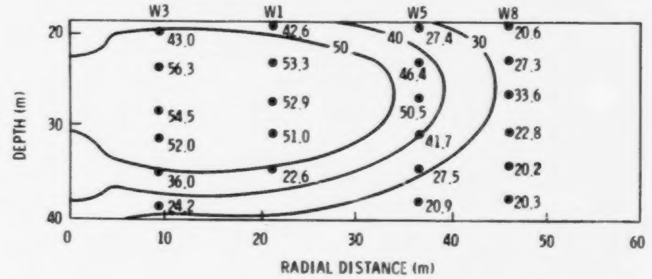

Fig. 3. Comparison of Observed Temperatures and Simulated Contours at End of Storage Period

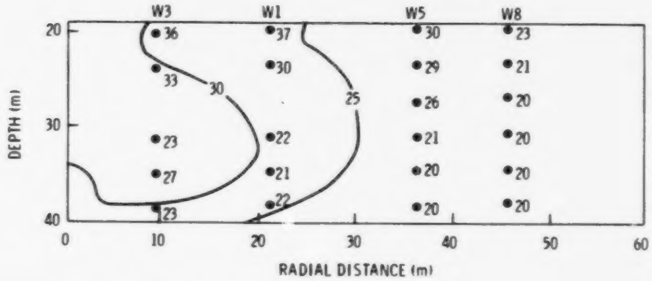

Fig. 4. Comparison of Observed Temperatures and Simulated Contours at End of Production Period

The simulated and observed temperatures of recovered water are shown in Fig. 5. These temperatures yield a recovery ratio of 0.67 based on equal volumes of injected and recovered water. The observed recovery ratio of 0.66 indicates good agreement.

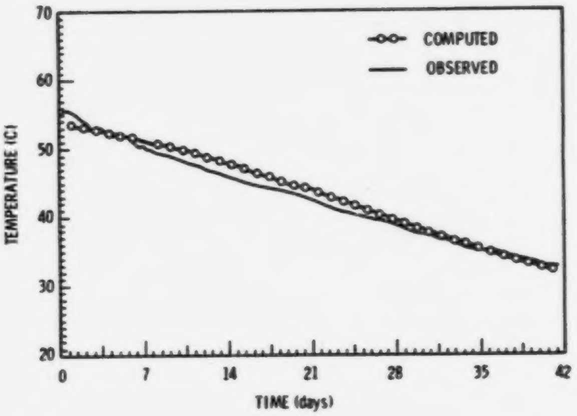

Fig. 5. Comparison of Observed and Simulated Temperatures at Production Well from Beginning of Production Period

REFERENCES

1. A Model for Calculating Effects of Liquid Waste Disposal in Deep Saline Aquifer. June 1976. Intercomp Resource Development and Engineering, Inc., PB-256903.

2. M. J. Lippmann, C. F. Tsang, and P. A. Witherspoon. April 1977. Analysis of the Response of Geothermal Reservoirs Under Injection and Production Procedures. Society of Petroleum Engineers, SPE 6537.

3. M. L. Sorey. 1978. Numerical Modeling of Liquid Geothermal Systems. Geological Survey Professional Paper 1044-D, U.S. Gov. Printing Office, Washington, D.C.

4. S. K. Gupta, C. R. Cole, and F. W. Bond. September 1979. Methodology for Release Consequences Analysis - Part III, Finite-Element Three-Diomensional Ground-Water (FE3DGW) Flow Model. PNL-2939, Pacific Northwest Laboratory.

5. N. A. Avdonin. 1964. "Some Formulas for Calculating the Temperature Field of a Formation During Thermal Injection." Nef'i Gaz. Vol. 7, No. 3, pp. 37-41.

6. C. F. Tsang, T. Buscheck, and C. Doughty. June 1981. "Aquifer Thermal Energy Storage: A Numerical Simulation of Auburn University Field Experiments." Water Resources Research. 17(3):647-658.

PROJECT SUMMARY

Project Title: Review of Simulation Techniques for Aquifer Thermal Energy Storage (ATES)

Principal Investigator: James W. Mercer

Organization:
GeoTrans, Inc.
P.O. Box 2550
Reston, VA 22090

Project Goals: To review and evaluate state-of-the-art simulation techniques and applications relevant to the analysis of Aquifer Thermal Energy Storage.

Project Status: The project and the final report have been completed.

The analysis of ATES systems will rely on the results from mathematical and geochemical models. These models describe important processes active in ATES including ground-water flow, heat transport (heat flow), solute transport (movement of contaminants), and geochemical reactions.

In general, available models of the saturated ground-water environment are adequate to address most concerns associated with ATES; that is, design, operation and environmental assessment. However, basic data deficiencies limit the application of geochemical reaction and biological kinetic models for ATES, and deficiencies exist in the coupled transport of fluid and energy within unsaturated sediments overlying unconfined aquifers.

Assuming that models are applied appropriately, the primary limitation on model calculations is the data base used to construct the model. Numerical transport models are limited by the uncertainty of subsurface data and the lack of long-term historical data for calibration. Geochemical models are limited by the lack of thermodynamic data for the temperature ranges applicable to ATES. Model applications undertaken with data collection activities on ATES sites should provide the most important contributions to the understanding and utilization of ATES. Therefore, the primary conclusion of this review is that model application to field sites in conjunction with data collection activities is essential to the development of this technology.

Contract Number: DE-AC06-76RLO 1830, B-B2424-A-O

Contract Period: November 1980 to March 1981

Funding Level: $38,000

Funding Source: U.S. Department of Energy through Pacific Northwest Laboratory

SUMMARY OF SIMULATION TECHNIQUES FOR AQUIFER THERMAL ENERGY STORAGE (ATES)

James W. Mercer
Charles R. Faust
William J. Miller
GeoTrans, Inc.
P.O. Box 2550
Reston, VA 22090

F. J. Pearson, Jr.
Intera Environmental Consultants, Inc.
11999 Katy Freeway
Suite 610
Houston, TX 77079

ABSTRACT

The analysis of aquifer thermal energy storage (ATES) systems will rely on the results from mathematical and geochemical models. These models describe important processes active in ATES including ground-water flow, heat transport, solute transport, and geochemical reactions. In general, available models of the saturated ground-water environment are adequate to address most concerns associated with ATES. A review of model applications to ATES shows that the major emphasis has been on generic sensitivity analysis and site characterization.

INTRODUCTION

During the last decade, the storage of thermal energy in aquifers has received considerable attention as a means to conserve and more efficiently use energy supplies. Since the geologic environment provides the storage container for the heated or chilled water, a thorough analysis of the hydrologic transport and thermal/chemical interactions in the geologic media used for storage is essential to a complete assessment of any ATES project. Because the analysis deals with a complex thermal/chemical problem, it inevitably involves models and simulation. Models provide the framework to incorporate all the processes that will be active in an ATES project, thereby permitting analysis and prediction of ATES behavior.

The variety and complexity of mathematical models (usually partial differential equations) used in ATES applications are numerous. This is possible because of significant advances in digital computers. This proliferation of mathematical models is often bewildering to the hydrologist who is trying to keep up with the research literature. Although the number of model types is large, only a few basic processes are considered. This is somewhat ironic since the large number of "different" models is the result of various simplifying assumptions used to reduce a general set of equations to some solvable form. Fortunately, if one keeps in mind the fundamental processes being simulated, then different or simplified forms of equations are less confusing.

Models used for ATES studies may be divided into three general categories: (1) analytical, (2) numerical, and (3) geochemical. Analytical models are based on exact mathematical solutions to transport processes and are used where data and simplified assumptions permit. Numerical models for transport processes are based on equation approximations and matrix solution techniques. They are more general than analytical models, and are used for more complicated problems when supporting data permits. Geochemical models, on the other hand, are based on the solution to a set of chemical reaction and related equations. In general, geochemical models calculate the nature of chemical reactions, but not whether the reaction actually will occur or its rate of occurrence. Because of this lack of rate information, geochemical models are usually not incorporated directly into the analytical or numerical models.

ANALYTICAL SOLUTIONS

For ATES applications the two major concerns are ground-water flow and heat transport. The analytical solutions used to describe ground-water flow all assume isothermal conditions. Likewise, the heat transport solutions generally assume a very simple and known flow field.

The number of solutions for ground-water flow is substantial and many references already exist (see, for example, Walton (1970), Kruseman and DeRidder (1976), and Hantush (1964)). Analytical solutions for ground-water flow are used in two primary ways. They are most commonly used in the analysis of aquifer tests to determine transmissive and storage properties of the aquifer. They can also be used to predict water level changes for idealized aquifer conditions.

There are also a number of analytical solutions for various simplified forms of the solute transport equation. Examples of such solutions may be found in Ogata and Banks (1961) and Codell and Schreiber (1979). The solute transport equation is similar in form to the heat transport equation, and a solution to one can be easily modified to be a solution to the other.

Analytical solutions are also available for analyzing aquifer tests in fractured media for a variety of aquifer conditions—confined, unconfined, quasi-steady-state leakage and unsteady leakage. Stretslova-Adams (1978) reviews and evaluates many of these solutions. Only one analytical solution for fractured media is presented in this section, that by Gringarten et al. (1975).

The analytical solutions available for analyzing heat transport are listed in Table 1. The first solution is for flow only; all others include both flow and heat transport. Also included in Table 1 are the major assumptions and possible usage of the solutions.

TABLE 1. Summary of Analytical Solutions

Reference	Problem	Major Assumptions	Usage
Davis & DeWeist (1966)	steady ground-water flow among wells	uniform hydrologic properties	evaluating well spacing and patterns
		porous medium	determining ground-water flow field for heat transport solutions
Lauwerier (1955)	linear heat transport	convection in the receiving formation	same as those given for Avdonin solution
		conductive heat loss to confining units	
Gringarten et al. (1975)	linear heat transport	convection in receiving medium	evaluating heat transport in fractured or fissured media
		Conduction in confining bed	
		finite thickness for confining bed	
Avdonin (1964)	linear heat transport	conduction and convection in receiving formation	test for numerical models
	radial heat transport	conductive heat loss to confining units	estimating position of thermal front
		single well (radial)	estimating heat losses to confining layers
Carslaw & Jaeger (1959)	one-dimensional heat conduction	one-dimensional heat conduction	couple with numerical model to compute heat losses to confining layers
Gringarten & Sauty (1975)	heat flow between well doublet	convection in the receiving formation	estimate well spacing
		conductive heat loss to confining units	estimate production temperatures after breakthrough
		two wells	
Hellstrom et al. (1979), Claesson (1980)	tilting of interface due to density differences	interface separating two fluids of different density	estimate tilting of thermal front

NUMERICAL SOLUTIONS

Numerical models provide the most general tool for the quantitative analysis of ATES applications. They are not subject to many of the restrictive assumptions required for analytical solutions. In spite of the flexibility of numerical models, their mathematical basis is actually less sophisticated than that of the analytical methods.

To develop a numerical model of a physical system (in our case, an aquifer), it is first necessary to understand how that system behaves. This understanding takes the form of laws and concepts. As presented, these concepts and laws are then translated into mathematical expressions, usually partial differential equations, with boundary and initial conditions. Numerical methods provide a means for solving these equations in their most general form.

Numerical solution normally involves approximating continuous partial differential equations with a finite number of equations at discrete points in time and space. Thus, the region and time period of interest are divided in some fashion, resulting in an equation or set of equations for each subregion and time step. These discrete equations are combined to form a system of algebraic equations that must be solved for each time step. Finite-difference and finite-element methods are the major numerical techniques used in ground-water applications. The important components and steps of model development for the two alternative methods are shown in Fig. 1.

Comprehensive reviews on models used in geothermal applications have been presented by Cheng (1978), Pinder (1979) and Mercer and Faust (1979). In addition to these references, Tsang et al. (1980a) present a review on ATES that also contains numerical models.

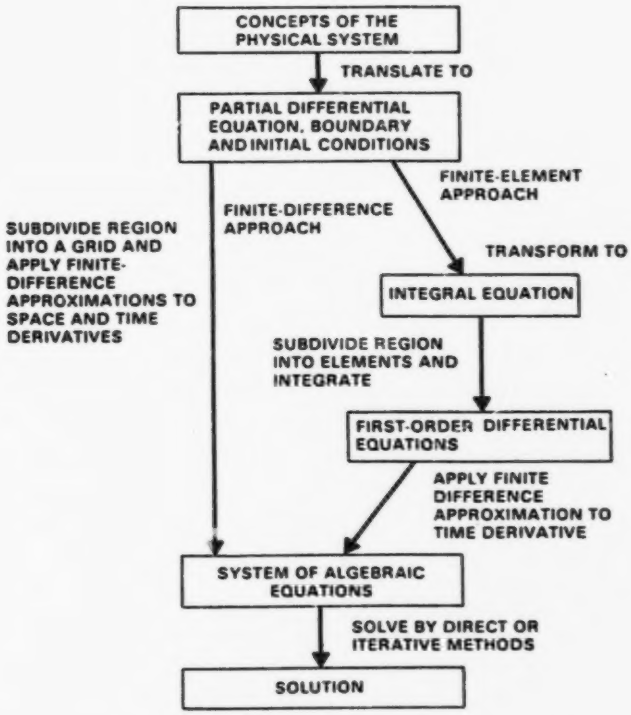
CONCEPTS OF THE PHYSICAL SYSTEM
TRANSLATE TO
PARTIAL DIFFERENTIAL EQUATION, BOUNDARY AND INITIAL CONDITIONS
FINITE-ELEMENT APPROACH
FINITE-DIFFERENCE APPROACH
SUBDIVIDE REGION INTO A GRID AND APPLY FINITE-DIFFERENCE APPROXIMATIONS TO SPACE AND TIME DERIVATIVES
TRANSFORM TO
INTEGRAL EQUATION
SUBDIVIDE REGION INTO ELEMENTS AND INTEGRATE
FIRST-ORDER DIFFERENTIAL EQUATIONS
APPLY FINITE DIFFERENCE APPROXIMATION TO TIME DERIVATIVE
SYSTEM OF ALGEBRAIC EQUATIONS
SOLVE BY DIRECT OR ITERATIVE METHODS
SOLUTION

Fig. 1. Generalized Model Development by Finite-Difference and Finite Element Methods (from Faust and Mercer 1980)

Table 2, extended from Tsang et al. (1980a), summarizes current modeling studies in ATES. This table is by no means complete, but does indicate the level of effort for numerical modeling of heat transport. These models were selected because they represent a fairly complete sampling of available codes. In addition to using approximating techniques such as finite difference, integrated finite difference and finite element, the codes treat heat flow as well as consolidation, solute transport and two-phase flow.

TABLE 2. Modeling Studies in Aquifer Thermal Energy Storage (extended from Tsang et al. 1980a)

Research Institute	Project
Royal Institute of Technology Stockholm, Sweden (Pinder et al. 1980; Voss et al. 1981)	One- and two dimensional finite element model
Lund University, Sweden (Hellström 1978; Claesson et al. 1978)	Two-dimensional, doublet, semi-analytical model; two-dimensional finite-difference program developed to study storage in eskers
Technical University of Denmark, Denmark (Qvale 1978; Reffstrup 1979)	One- and two-dimensional finite element models; study of using compensation wells for countering regional flow
University of Neuchâtel, Switzerland (Mathey 1977; Mathey and Manjos 1978)	Two- and three-dimensional finite element models
Institut de Production d'Energie de l'École Polytechnique Fédérale de Lausanne, Switzerland (Joos 1978)	Three-dimensional finite element model
École des Mines de Paris, France (deMarsily 1978)	Two-dimensional, radial, finite-difference model; two- and three-dimensional finite element models
Bureau des Recherches Géologiques et Minieres (BRGM), France (Gringarten et al. 1977)	Layered two-dimensional finite-difference model
Yamagata University, Japan (Yokoyama et al. 1980)	Two-dimensional finite-difference model
U.S. Geologial Survey, United States Papadopulos and Larson 1978)	SWIP model, based on a finite-difference scheme, used to model the Auburn experiment
U.S. Geological Survey, United States (Faust and Mercer 1979)	Three-dimensional finite-difference model
Lawrence Berkeley Laboratory, United States (Mangold et al. 1980)	Two- and three-dimensional integrated finite-difference model
Texas A&M University, United States (Grubaugh and Reddell 1980)	Three-dimensional finite element model
Dames & Moore, United States (Huyakorn, written comm. 1980)	Two- and three-dimensional finite element models
University of Kansas, United Statees (Willhite et al. 1974)	Three-dimensional finite-difference model
Pacific Northwest Laboratories, United States (Gupta et al. 1980)	Two- and three-dimensional finite element model

GEOCHEMICAL MODELS

ATES requires an understanding of (1) the local or site-specific aquifer characteristics, (2) the economics of the heat producers and consumers, (3) the pumping and well bore equipment, and (4) chemical compatibilities between the injected liquid and the inplace liquid, the aquifer solid matrix, and any surrounding confining units. It has been shown that flow and transport models can be valuable tools for evaluating some of these aspects. In this section, we review some geochemical models presently available which can help evaluate chemical problems associated with ATES.

The geochemical models discussed in this section have a different purpose from the thermal and fluid flow models discussed earlier. The state of the geochemist's art has not yet reached the point where it is possible to calculate the reactions which will occur in any given mixture of waters or between any water and its aquifer. The principles of thermodynamics enable one to calculate the tendency of reactions to occur as a system tends toward a state of equilibrium, but data and a theoretical framework are not yet available to predict how fast these reactions will actually take place. The models described here are used to calculate the nature of chemical reactions which could occur for any given ATES scheme but they do not attempt to predict whether the reaction actually will occur and how fast. They are nonetheless very important to the evaluation of potential ATES schemes, for it is important to be certain that, for example, the water to be injected will not have a tendency to precipitate an aquifer-clogging solid upon mixing with the formation water or to react with the formation itself so as to produce a solution capable of corroding the surface equipment when it is pumped back. Two types of models are commonly used by geochemists. These types are here termed, aqueous solution models and geochemical reaction models.

Aqueous solution models provide the methodology by which measured chemical compositions of solutions are transformed into such thermodynamically significant quantities as free ion activities. For example, the quantity important to determining whether a calcium-bearing mineral dissolves or precipitates is the thermodynamic activity of the free calcium ion in solution. What is measured in the chemical analysis of the solution is merely the concentration of the total calcium in solution. Models which permit the calculation of activites from concentrations are called aqueous solution or speciation models.

Geochemical reaction models describe the chemical reactions which result from, for example, mixing two solutions, addition of solids to a solution, and temperature changes to a solution or to a system of solids and a solution. These reactions are described in terms of the masses of elements which are transferred between solid phases and the solution or from one solid to another. Changes in solution chemistry from such a model are needed to determine the changes in solution density and viscosity which will affect the flow in the system. Changes in solid masses are related to changes in the volume in the system and have a potential to affect the aquifer porosity and permeability. Two types of geochemical reaction models are mass transfer and reaction path models.

A partial summary of geochemical models is given in Table 3. The models summarized are capable of predicting a number of chemical phenomena which may be important to ATES. Such phenomena include the effects of (1) changing temperature and pressure on the equilibrium position of possible reactions, (2) mixing injected and formation waters, and (3) injected water on formation mineral solubilities and formation water gas solubilities.

TABLE 3. Partial Summary of Geochemical Models

Reference	Model	Aqueous Sp	Gases	Temperature Range°C	Pressure Range Bars
Kharaka & Barnes (1973)	SOLMNEQ	181	3	0-300	1-1000
Plummer et al. (1976)	WATEQF	105	3	0-100	1
Ball et al. (1979)	WATEQ2	220	3	0-100	1
Nordstrom et al. (1979)	GEOCHEM	2000	2	25	1
Nordstrom et al (1979)	MINEQL/ REDEQL2	*	*	25	1
Wolery (1979)	EQ3	140	8	0-300	to steam saturation or 500 bars

* depends on data base.

APPLICATIONS OF TRANSPORT MODELS

REVIEW OF FIELD APPLICATIONS

In addition to discussing available models, it is appropriate to summarize actual examples and site-specific factors associated with ATES. Such a summary is listed in Table 4, which is extended from that given in Tsang et al. (1980a). Also, three on-going demonstration field studies are in progress. These demonstration projects are located at Minneapolis-St. Paul, Minnesota, Stony Brook, New York, and Bethel, Alaska. All of these studies, except the Minnesota project, have utilized or will utilize unconsolidated sediments as storage mediums. The Minnesota project will utilize a cemented sandstone sequence; the geologic conditions of the Alaska project have not been reported.

Besides the projects summarized, a number of other field projects have been or are currently being conducted in a variety of countries, for which little or no data are available. For example, Sauty et al. (1978) mentioned two 1974 injection/production projects without interim storage at Neuilly and Noisy, France. Also, the Lawrence Berkeley Laboratory ATES Newsletters have mentioned studies in Germany and China. The German field tests were performed at Munsterlander Bucht, West Germany in 1978 and 1979 (ATES Newsletter, September 1979) and additional pilot studies were planned to utilize an aquifer in the vicinity of the Munich-Grosshadern Hospital in late 1980 or 1981 (ATES Newsletter, June 1980). Chinese projects occurred at Shanghai and Beijing. They entailed producing cool aquifer water for industrial use and reinjecting the spent warm water after treatment. These projects were primarily meant to combat land subsidence (ATES Newsletter, May 1979 and June 1980).

TABLE 4. Data from ATES Field Experiments (extended and modified from Tsang et al. 1980a)

	Ambient Ground-Water Temp (°C)	Mean Injection Temp (°C)	Amount Injected (m^3)	Injection Period (days)	Storage Period (days)	Amount Withdrawn (m^3)	Energy Recovery Ratio	Comments
Krefeld, Germany (1974)	∿10.0	45.0	430	64				Water-table aquifer 3.35 m thick
Neuchâtel, Switzerland (1974)	11.0	51.0	494	9	∿122	16,370	40	Water-table aquifer, large buoyance convection
Mobile, Ala USA								Confined aquifer, injection well clogging
(1976)	20.0	36.4	7,688	17	44	14,260	69	
(1978-1979)	20.0	55.0	54,784	79	53	55,345	66	
		55.4	58,000	63	63	66,400	76	
Bonnaud, France (1976-1977)	12.0	40.0	1,400	20	122	3,000	30	Confined aquifer, large thermal dispersion
Gard, France (1977-1978)	14.0	33.5	20,200	88	42 32	17,000	18.5	Water-table aquifer
Yamagata Basin, Japan								Leaky confined aquifer, doublet wells too close together
(Summer 1977)	16.0	23.7	8,843	64	96	9,930	40	
(Winter 1978)	18.3	5.3	9,430	∿90		11,200	40	
(Summer 1978	14.0							
College Station, Texas, USA								Water-table aquifer
(1978-1979)	21.0	8.9	31,800	∿92	∿60	∿9,688	23	
(1979-1980)		∿5.0	∿8,138				31	

Finally, Voss (1980) and Voss (1981) have reported an ATES project in Stidsvig, Sweden. This project entailed the storage of industrial waste heat in an esker in southern Sweden and the use of mathematical models to evaluate the aquifer hydraulics and the subsequent heat transport analysis.

SITE-SPECIFIC CONSIDERATIONS

The utilization of models in an ATES project will be application dependent. A major factor affecting the modeling approach will be the aquifer character. An ideal aquifer for ATES is difficult to define due to the many physical factors that must be considered. For example, a thin aquifer is more suitable for minimizing the tilting of a thermal front; however, a thin aquifer will probably have greater heat losses. Table 5 provides a summary of some of the desirable characteristics of an ATES site, and circumstances that are favorable and unfavorable. In all cases, a low natural gradient is desirable.

TABLE 5. Desirable Characteristics of an ATES Project and Corresponding Favorable and Unfavorable Aquifer Conditions

Desired Character	Favorable Condition	Unfavorable Condition
Lack of thermal tilting	Thin aquifer, low vertical permeability, moderate horizontal permeability	Thick aquifer, high vertical permeability
Low heat loss to confining beds	Thick aquifer	Thin aquifer
Low pumping and injection costs	High horizontal permeability	Low horizontal permeability
Rapid heat exchange between fluid and rock	High porosity, fine grains, homogeneous conditions	Heterogenous conditions
Low heat loss to surface	Deep confined aquifer	Shallow water-table aquifer
Minimum thermal dispersion	Homogeneous aquifer	Highly heterogenous aquifer
Lack of regional flow	Low regional hydraulic head gradient (i.e., low pore water velocity)	High regional hydraulic head gradient (i.e., high pore water velocity)

The governing equations for fluid flow, heat transport, and solute transport include many parameters. In general, these parameters represent physical properties of the fluid or aquifer rock. Assuming that models are applied appropriately, the primary limitation on model calculations is the data base used to construct the model. For ground-water flow important parameters are:

fluid: ρ .... density, (ML^{-3})

μ .... dynamic viscosity, ($ML^{-1}t^{-1}$)

β_T .... coefficient of thermal expansion, (T^{-1})

β_p .... coefficient of fluid compressibility, ($ML^{-1}t^{-2}$)

rock: $\bar{k}$ .... intrinsic permeability tensor, (L^2)

ϕ .... porosity, (dimensionless)

α .... intergranular vertical compressibility, ($M^{-1}LT^2$)

Additional properties requirred for heat transport include:

fluid: c_p .... heat capacity at constant pressure, $(L^2t^{-2}T^{-1})$

rock: c_{pr} ... heat capacity at constant pressure, $(L^2t^{-2}T^{-1})$

$\bar{\bar{K}}_m^*$ .... medium conduction/dispersion tensor, $(MLt^{-3}T^{-1})$

And for solute transport:

rock: $\bar{\bar{D}}$ .... dispersion tensor, (L^2t^{-1})

For the most general case, all of the above parameters are considered functions of temperature and pressure. For temperature variations found in ATES, this dependence is small and many of the parameters may be treated as constants. For projects involving temperature variations of 50°C, the dependence on temperature should be included for at least the fluid properties.

CONCLUSIONS AND RECOMMENDATIONS

It should be emphasized that aquifers are highly site-specific in their characteristics. While certain features may be generalized, the number of relevant parameters required to characterize a specific aquifer for ATES is large and unique (Hooper and Angus 1979, Volumes 1 and 2). For this reason, many of the conclusions must be qualitative and the general modeling results presented in an illustrative manner.

To use and model an aquifer as a storage medium requires more detailed knowledge of the aquifer's characteristics than conventional uses of aquifers for water supply. This required information is not generally obtained for conventional applications, but it can be determined to the required degree of detail by currently available methods (Hooper and Angus 1979, Volumes 1 and 2).

Models have been successfully used in ATES for both field studies and generic studies. Most of the basic physical processes active in ATES can be adequately represented in a model. These include fluid flow, heat conduction and convection, consolidation, solute transport, and two-phase flow. For field studies, models have been demonstrated as effective for preliminary feasibility modeling, conceptualization, and field data collection. A conclusive demonstration of predictive analysis is yet to be performed. Generic studies have been helpful in determining what factors and parameters most strongly affect recovery. For example, it has been demonstrated that the recovery factor increases with additional storage cycles.

It is evident that the solution of problems related to ATES usually requires an understanding of the coupled behavior of interacting physical and chemical processes. This understanding, in general, is best obtained by careful analysis of the processes in the field and laboratory. Once this is accomplished, the conceptual models of these processes can be translated into mathematical models that are suitable for predictive purposes. It seems that mathematical models, both analytical and numerical, are sufficiently powerful to solve many ATES applicatons. Unfortunately, the conceptual basis of some of these mathematical models appears to need reinforcement. This is especially true for incorporating chemical and biological reactions into models. Even if the mathematical models were known to be correct, the essential parameters describing field conditions are often unavailable.

As indicated in this review, there are many models available that consider a wide range of applications. Therefore, it appears that little additional model development is necessary unless and until available codes are applied to complete and representative data sets from typical ATES facilities. One question that has not been addressed adequately by modeling and field studies concerns economics. Limited economic studies have been conducted, but, in general, do not depend on detailed aquifer modeling results. A modeling approach to this problem is to combine an economic model with a reservoir model. Such an approach has been taken for geothermal development by Maddock et al. (1979). Similar work for ATES should complement field demonstration projects that are completed to production.

Mathematical models will continue to play an important role in the design, operation, and environmental assessment of aquifer thermal energy storage. These models span the range from the very simple to the very complex. The major conclusions and recommendations concerning these models and their applications to ATES may be summarized as:

- Model application to field sites in conjunction with data collection activities is highly recommended to confirm the adequacy of the assumptions fundamental to currently available codes.

- There is little need for additional development of aquifer simulation models until the capabilities of the available models have been applied to and validated against the entire range of potential ATES applications.
- While geochemical and biological models are available, their thermodynamic and reaction rate data bases for application to the temperature range of ATES must be developed and documented.
- The physics of nonisothermal unsaturated flow should be investigated and available models validated against laboratory or field studies before the potential of unconfined aquifers for ATES can be estimated.
- The optimization of well field design (e.g., multiple wells) should be studied under constraints of gradient control, flow rates, energy recovery efficiency, and energy recovery quality.
- A potentially useful management tool lies in the combination of reservoir and economic models to provide a design and operational scenario which is optimal in an economic sense.
- Fractured aquifers, in general, are not favorable for ATES, and development of models for this type of media is not warranted for the ATES program.
- ATES is mainly concerned with near-well performance and environmental effects away from the well; both of these problems can be addressed by present technology.
- Transport models are generally complex and difficult to use, requiring the user to be highly trained in order to avoid misuse.
- Costs associated with modeling may be divided into computer costs and mantime costs. In general, mantime expenses are much greater than computer expenses.
- ATES applications require a considerable amount of detailed field data.
- The adequacy of the field data will be the major factor controlling the credibility of any analysis and prediction.

REFERENCES

1. Avdonin, N. A. 1964. "Some Formulas for Calculating the Temperature Field of a Stratum Subject to Thermal Injection." Nefti'i Gaz. 3:37-41.

2. Ball, J. W., E. A. Jenne, and D. K. Nordstrom. 1979. "WATEQ2-A Computerized Chemical Model for Trace and Major Element Speciation and Mineral Equilibria of Natural Waters." In Chemical Modeling in Aqueous Systems, pp. 815-835. E. A. Jenne, ed. American Chemical Society Symposium Series 83, Washington, D.C.

3. Carslaw, H. S. and J. C. Jaeger. 1959. Conduction of Heat in Solids. Oxford Press. Clarendon, Great Britain, p. 510.

4. Cheng, P. 1978. "Heat Transfer in Geothermal Systems." Advances in Heat Transfer, 14:1-105.

5. Claesson, J. 1980. Tilting Rate of a Wide Thermal Front. Notice 1980/4, Department of Mathematical Physics, Lund Institute of Technology, Lund, Sweden.

6. Claesson, J., et al. 1978. Theoretical Analysis and Computer Simulation of Solid-Fluid Heat Storage Systems in the Ground; Extractions of Earth Heat. Interim report, part I and II, Department of Mathematical Physics and Building Science, Lund Institute of Technology, Lund, Sweden.

7. Codell, R. B. and D. L. Schreiber. 1979. NRC Models for Evaluating the Transport of Radionuclides in Groundwater. In Management of Low-Level Radioactive Waste. Vol. 2, pp. 1193-1212, M. W. Carter et al., ed.

8. Davis, S. N. and R. J. M. DeWiest. 1966. Hydrogeology. John Wiley and Sons, Inc., New York, New York, p. 463.

9. de Marsily, G. 1978. "Peut-ou Stocker de l'Energie dans le Sol?" Annales des Mines. 1978(4):11-24.

10. Faust, C. R. and J. W. Mercer. 1979. "Geothermal Reservoir Simulation 2. Numerical Solution Techniques for Liquid- and Vapor-Dominated Hydrothermal Systems." Water Resources Research. 15(1):31-46.

11. Faust, C. R. and J. W. Mercer. 1980. "Ground-water Modeling: Recent Developments." Ground-Water. 18(6):569-577.

12. Gringarten, A. C. and J. P. Sauty. 1975. "A Theoretical Study of Heat Extraction for Aquifers with Uniform Regional Flow." Journal of Geophysical Research. 80(35):4956-4962.

13. Gringarten, A. C. et al. 1975. "Theory of Heat Extraction from Fractured Hot Dry Rock." Journal of Geophysical Research. 80(8):1120-1124.

14. Gringarten, A.C. et al. 1977. Etude Theorique du Stockage d'Eau Chaude par Puits Unique Aquifere en l'Absence d'Ecoulement Regional (Programme Esther). Paper RS-576, in Resume des Principaux Resultats Scientifiques et Techniques du Service Geologique National Pour 1977: Orleans, France, Service Bulleting of the Bureau de Recherches Geologiques et Minieres.

15. Grubaugh, E. K. and D. L. Reddell. 1980. Heat Transport in Ground-Water Systems: Volume 1 - Finite Element Model. TR-104, Volume 1. Texas Water Resources Institute, Texas A&M University.

16. Gupta, S. K. et al. 1980. Description and Applications of the FE3DGW CFEST Three-Dimensional Finite-Element Models. Presented at the Lawrence Berkeley Laboratory Workshop on "Modeling Thermal-Hydrological Flow in Fractured Rock Mass." February 19-20, Berkeley, California.

17. Hantush, M. S. 1964. "Hydraulics of Wells." In Advances in Hydroscience. pp. 281-432. V. T. Chow, ed., Academic Press, New York, New York.

18. Hellström, G. 1978. Aquifer Storage Projects in Sweden. LBL-8431, Proceedings, Thermal Energy Storage in Aquifers Workshop, Lawrence Berkeley Laboratory, Berkeley, California.

19. Hellström, G. et al. 1979. Heat Storage in Aquifers. Buoyancy Flow and Thermal Stratification Problems. Lund Institute of Technology, Lund, Sweden.

20. Hooper and Angus Associates Ltd. 1979. Study to Examine the Technical and Economic Feasibility of Using Aquifers as a Chilled Water Source or Storage Medium for Building Air Conditioning Systems - Vol. I. Toronto, Canada.

21. Hooper and Angus Associates Ltd. 1979. Study to Examine the Technical and Economic Feasibility of Using Aquifers as a Chilled Water Source or Storage Medium for Building Air Conditioning Systems - Vol. II. Toronto, Canada.

22. Joos, B. 1978. "Tests de Sensibilite du Programme Diffusion-Transport." In Rapports Scientifiques et Techniques sur le Comportement des Nappes Southerraines, Vol. 6. Institute de Production d'Energie, Centre d'Hydrogeologie de l'Universite de Neuchtel, Lussanne, Switzerland.

23. Kharaka, Y. K. and I. Barnes. 1973. SOLMNEQ: Solution-Mineral Equilibrium Calculations. 215-899, Survey Computer Contribution.

24. Kruseman, G. P. and N. A. DeRidder. 1976. Analysis and Evaluation of Pumping Test Data. International Institute for Land Reclamation and Improvement Bulletin 11, Wageningen, The Netherlands.

25. Lauwerier, H. A. 1955. "The Transport of Heat in an Oil Layer Caused by the Injection of a Hot Fluid." Appl. Sci. Res. Ser. A, 5(2-3):145-150

26. Maddock, T. III, et al. 1979. Management Model for Electrical Power Production from a Hot-Water Geothermal Reservoir. University of Arizona Technical Report No. 34.

27. Mangold, D. C. et al. 1980. CCC User's Manual - Versions II (Draft). LBL-10909, Lawrence Berkeley Laboratory, University of California, Berkeley, California.

28. Mathey, B. 1977. "Development and Resorption of a Thermal Disturbance in a Phreatic Aquifer with Natural Convection." Journal of Hydrology. 34:315-333.

29. Mathey, B. and A. Menjos. 1978. Underground Heat Storage: Choice of a Geometry and Efficiency. In Proceedings, Thermal Energy Storage in Aquifers Workshop, Lawrence Berkeley Laboratory, LBL-8431, Berkeley, California.

30. Mercer J. W. and C. R. Faust. 1979. "A Review of Numerical Simulation of Hydrothermal Systems." Hydrological Sciences. Bulletin 24, 3, 9:335-343.

31. Nordstrom, D. K. et al. 1979. "A Comparison of Computerized Chemical Models for Equilibrium Calculations in Aqueous Systems." pp. 857-892. E. A. Jenne, ed. Chemical Modeling in Aqueous Systems: American Chemical Society Symposium Series 93.

32. Ogata, A. and R. Banks. 1961. A Solution of the Differential Equation of Longitudinal Dispersion in Porous Media. U.S. Geological Survey Professional Paper 411-A, p. 7.

33. Papadopulos, S. S. and S. P. Larson. 1978. "Aquifer Storage of Heated Water: Part II - Numerical Simulation of Field Results." Ground Water. 16(4):242-248.

34. Pinder, G. F. 1979. State-of-the-Art Review of Geothermal Reservoir Modeling. LBL-9093-GSRMP-S-UC-66a, Lawrence Berkeley Laboratory, University of California.

35. Pinder, G. F. et al. 1980. GAFETTA - A Galerkin Assymmetric Finite Element Thermal Transport Aquifer Model. Report 80 08, Department of Water Resources Engineering, Royal Institute of Technology, Stockholm, Sweden.

36. Plummer, L. M. et al. 1976. WATEQF-A Fortran IV Version of WATEQ, a Computer Program for Calculating Chemical Equilibrium of Natural Water. U.S. Geological Survey Water-Resources Investigations 76-13. (Revised and Reprinted December 1978).

37. Qvale, E. B. 1978. The Danish Seasonal Aquifer Warm-Water Storage Program. In Proceedings, Thermal Energy Storage in Aquifers Workshop. LBL-8431, Lawrence Berkeley Laboratory, Berkeley, California.

38. Sauty, J. P. et al. 1978. The Effect of Thermal Dispersion on Injection of Hot Water in Aquifers. LBL-8883, Lawrence Berkeley Laboratory, Univ. of California Second Invitational Well-Testing Symposium Proceedings, Berkeley, California.

39. Streltsova-Adams, T. D. 1978. Fluid Flow in Naturally Fractured Reservoirs. Second Invitational Well-Testing Symposium Proceedings, October 25-27, Berkeley, California.

40. Tsang, C. F. et al. 1980a. Aquifer Thermal Energy Storage - A Survey. Lawrence Berkeley Laboratory, University of California, Berkeley, California.

41. Voss, C. 1980. Notes from an International Seminar on Heat Storage in Aquifers, April 15-16, 1980. Lund-MPh-80/13, Lund Institute of Technology, Lund, Sweden.

42. Voss, C. et al. 1981. Simulation of Low Temperature Seasonal Energy Storage in a Shallow Glaciofluvial Aquifer. Report 8011, Swedish Board for Energy Source Development, Royal Institute of Technology, Stockholm, Sweden.

43. Walton, W. C. 1970. Groundwater Resource Evaluation. McGraw-Hill Book Co., New York, New York. p. 664.

44. Willhite, G. P. et al. 1974. Disposal of Heated Water Through Ground-Water Systems: Volume 1 - Technical and Economic Feasibility. The Kansas Water Resources Research Institute, University of Kansas.

45. Wolery, T. J. 1979. Calculation of Chemical Equilibrium Between Aqueous Solution and Minerals: The EQ3/6 Software Package. UCRL-52658, Lawrence Livermore Laboratory, Livermore, California.

46. Yokoyama, T. et al. 1980. "Seasonal Thermal Storage in Aquifer for Utilization." Bulletin of the JSME. 23(184):1646-1654.

PROJECT SUMMARY

Project Title: Mathematical Studies in Aquifer Thermal Energy Storage

Principal Investigator: Chin Fu Tsang

Organization:
Earth Sciences Division
Lawrence Berkeley Laboratory
Berkeley, CA 94720
(415) 486-5782

Project Goals: To perform ATES generic studies, carry out field-specific planning and simulation studies, and improve modeling techniques.

Project Status: During this fiscal year, work has been completed on the study of the dependence of the energy recovery factor and the recovery temperature as a function of aquifer properties, storage period, partial and full penetration, storage volume and temperature. The general conclusion is that with a proper selection of an aquifer and a carefully designed system, a good recovery can be realized. A report has been completed summarizing these results.

For the purpose of technical or economic optimization, site characterization studies have been carried out with the objective of estimating energy recovery factor for a wide range of aquifer and storage conditions.

In sites where buoyancy flow may be neglected, dimensionless parameter groups have been derived and type curves have been plotted to quickly obtain energy recovery factors and production temperatures for different conditions. In sites where buoyancy flow cannot be neglected, a semi-empirical method has been developed which reproduces the results of a realistic numerical model (CCC) over a wide range of parameters.

Much progress has also been made in predicting the results of field experiments by Auburn University at Mobile, Alabama. Calculations were able to predict to within about 5%, the experimental value of the energy recovery factor and the production temperature. Studies of these results disclosed a discrepancy between calculated and observed rate of decrease of production temperatures which may be due to thermal dispersion and nonisothermal transient wellbore effects. Work has been initiated to study these, since an understanding of the discrepancy is important in ensuring a satisfactory prediction for further field cases.

Improvement of our numerical model CCC to handle saturated-unsaturated flow is continued at a low level. We expect to finish the coding and initial debugging before the end of this fiscal year.

Contract Number: B-10470-A-0, B-10472-A-0, B-10473-A-0

Contract Period: October 1, 1980 through September 30, 1981

Funding Level: $128,000

Funding Source: U.S. Department of Energy through Pacific Northwest Laboratory

NUMERICAL SIMULATION--SITE SIMULATION

Chin Fu Tsang
Earth Sciences Division
Lawrence Berkeley Laboratory
University of California
Berkeley, CA 94720

ABSTRACT

The Seasonal Thermal Energy Storage (STES) Program at Lawrence Berkeley Laboratory during 1981 consists of four lines of work: (1) to solicit, review, organize, and edit appropriate articles for a quarterly international STES Newsletter; (2) to perform Aquifer Thermal Energy Storage (ATES) generic studies; (3) to carry out site-specific planning and simulation studies; and (4) to improve modeling techniques. These four tasks form a well-balanced program of work to stimulate interest and information exchange in this field to provide technical support to field projects, and to develop techniques that may be useful for industrial applications of this concept. The present paper reviews our site-specific studies during 1981.

INTRODUCTION

Lawrence Berkeley Laboratory (LBL) began working on seasonal thermal energy storage in aquifers in 1976. Initial studies included comprehensive generic calculations based on a numerical model to calculate the coupled heat and fluid flow in a three-dimensional, complex geometry aquifer system. Proof-of-concept calculations were made for a number of hypothetical situations, the result of which have been published in a series of papers (see references 1-3).

In 1978 LBL organized and hosted the First International Workshop on Aquifer Thermal Energy Storage (ATES). Active workers from nine countries participated in this workshop and their contributions were published in the workshop proceedings (reference 4). Since the workshop, a periodic newsletter (reference 5) has kept researchers abreast of the current status of various projects worldwide. Many of these projects are reviewed in two survey papers published in 1979 (references 6 and 7) and an update survey to be published in 1981 (reference 8).

The LBL 1981 ATES project includes four main tasks: (a) to solicit, review, organize, and edit appropriate articles for a quarterly international STES Newsletter; (b) to perform ATES generic studies; (c) to carry out site-specific planning and simulation studies; and (d) to improve modeling techniques. Of particular note among these is the STES Newsletter which is published quarterly with distribution to over 350 researchers, developers, and program managers in 23 countries.

This paper concentrates on our site-related studies during 1981: site characterization for optimal storage conditions, and prediction and simulation of the Mobile field experiments.

SITE CHARACTERIZATION

The purpose of our ATES site-characterization studies is to develop some general parameters or procedures whereby, for a given site, the energy recovery factor may be predicted readily for a wide range of operating conditions. This provides the basic results needed for technical or economic optimization of the ATES system. Here, the energy recovery factor is defined as the energy recovered divided by energy stored for the same amount of water injected into and produced from the aquifer. Energy is measured with reference to ambient aquifer temperature energy.

Two ATES site characterization schemes have been developed at LBL during the past year, the first neglecting buoyancy flow, the second including it.

The first study (reference 9) considers the thermal behavior of an ATES system with steady radial fluid flow around a single injection/production well. Buoyancy flow is neglected and the aquifer is confined above and below by impermeable layers. Neglecting buoyancy flow may be a reasonable assumption for cases with low aquifer permeability, short storage cycle length, or small temperature difference between injected and ambient water. A criterion (reference 10) exists which may be used to determine if buoyancy flow is negligible for a given case. However, conclusions from this study may still be applicable in a relative sense for cases in which buoyancy flow is significant.

With the above assumptions, the thermal behavior of the system can be described in terms of the following four dimensionless parameter groups:

$$Pe = \frac{QC_w}{2\pi\lambda_a H} ; \qquad Q = \frac{C_a^2 H^2}{C_c \lambda_c t_i} ; \qquad Bi = \frac{\lambda_a C_a}{\lambda_c C_c} ; \qquad \frac{C_a}{C_c}$$

where Q is the flowrate; H is the aquifer thickness; λ_a and λ_c are the aquifer and aquitard thermal conductivities; C_w, C_a, and C_c are the water, aquifer, and aquitard volumetric heat capacities, and t_i is the injection time period.

A simple steady flow model has been used to calculate recovery factors and temperatures as a function of these parameters. Some of the results are shown in Figs. 1 and 2.

Fig. 1 shows the calculated energy recovery factor as a function of Pe and Λ numbers for the first cycle. Results for subsequent cycles have also been calculated. Note that the large initial increase in recovery factor is followed by a more gradual increase as Pe and Λ are increased.

Fig. 2 displays the temperature of water extracted during the production period of the first and fifth cycles for different values of Pe and Λ. For values of Pe larger than 200, production temperature shows little dependence on Pe.

Various other factors have also been considered such as thermal dispersion effects, dependence on cycle periods, the influence of a finite-thickness caprock, and long-term behavior. Table 1 displays the application to the Mobile (reference 11) and Bonnaud (reference 12) experiments. In this table, ε is the calculated energy recovery factor and ε_{exp} is the experimentally observed value. For the Auburn case, two calculations were made: (a) assuming that the well penetrates the full thickness of the aquifer, and (b) correcting for the fact that experimentally the well was open to only 9 m out of the 21 m thickness of the aquifer. The comparisons are very encouraging.

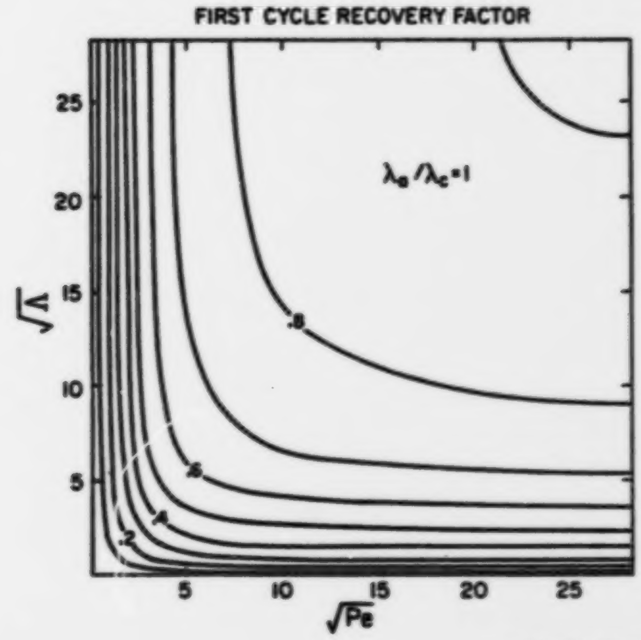

XBL 8012-6516

Fig. 1. Recovery factor as a function of $\sqrt{Pe}$ and $\sqrt{\Lambda}$ for the first cycle, when $\lambda_a/\lambda_c = 1$.

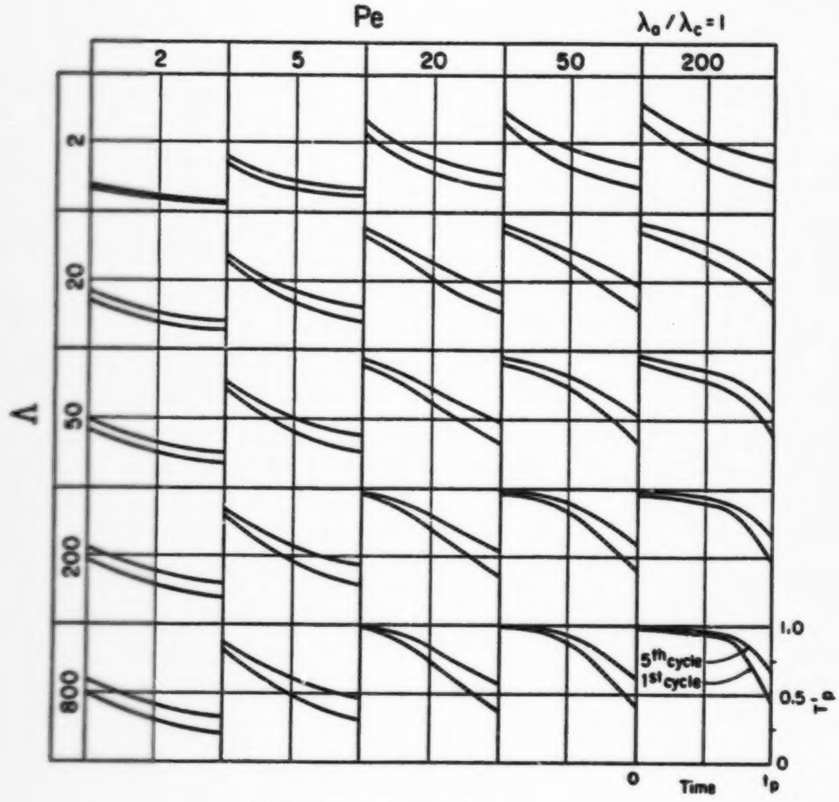

PRODUCTION TEMPERATURE

XBL 8012-6582C

Fig. 2. First and Fifth Cycle Production Temperatures Versus Time for a Range of Pe and Λ when $\lambda_a/\lambda_c = 1$.

Table 1.

	$\sqrt{Pe}$	$\sqrt{\lambda}$	ε	ε_{exp}
Mobile (first cycle)				
(a)	8.8	9.0	0.71	0.66
(b)	10.1	6.8	0.68	
Bonnaud (fourth cycle)	3.9	5.0	0.63	0.677

To investigate the effect of thermal front tilting caused by buoyancy flow, a second study (reference 13) has been carried out. Calculations have been conducted over a wide range of aquifer permeabilities and injection temperatures using the numerical model CCC, which takes into account the temperature-dependent parameters and the buoyancy flow process. In each case, an energy balance was kept for various times, separating radial diffusive losses in the aquifer and the vertical losses to the confining layer. A study of these results shows that over a wide range of conditions, the radial and vertical heat losses can be decoupled. Thus the energy recovery factor epsilon may be expressed as the product of two factors, $\varepsilon = E_a \cdot E_c$, where E_a is the energy recovery factor when the aquifer is insulated from the confining layers above and below, and E_c is the energy recovery factor when the only heat loss is that due to vertical conduction diffused into the upper and lower confining layers.

The decoupling of radial and vertical heat losses reduces the number of parameter groups required to describe the system to three: Pe, Λ, and Bi. However, the thermal front tilting influences both the radial and vertical losses, since the tilting modifies the area over which heat conduction occurs. An empirical shape factor based on the thermal front angle of tilt is introduced to modify the parameter groups. Thus E_a depends on the modified Pe number, Pe*, while E_c depends on Λ* and Bi*.

E_c as a function of Λ* and Bi* is calculated from a one-dimensional heat conduction problem in which heat diffuses from aquifer to aquitard. E_a as a function of Pe* is calculated from vertically insulated cases of ATES cycles. Hence, using values of Pe*, Λ* and Bi* obtained from field input data, E_c and E_a may be determined and combined to form epsilon. Although not mathematically rigorous, the method has been shown to yield accurate predictions for a wide range of conditions when compared with CCC-simulated results.

SIMULATION OF THE MOBILE EXPERIMENTS

While the first cycle of the 1981 series of experiments was being carried out by Auburn University at Mobile, Alabama, LBL performed a numerical simulation based on the field operating conditions to predict the outcome of the experiment before its conclusion. The goal was to test our understanding of the aquifer storage problem and to verify our numerical model CCC.

Details of the Mobile experiment are described elsewhere in this volume. The basic idea is that water at approximately 55 to 60°C is injected over a period of one month into an aquifer approximately 21 m thick and with a permeability of about 63 darcys. It is then stored for one month and subsequently produced. The injected water is obtained from a supply well perforated in the same aquifer 240 m away from the injection/production well. LBL was provided with the basic geological, well test, injection flowrate, and injection temperature data.

The simulation method was similar to that used by LBL to model the 1979-1980 Auburn experiment (reference 14). The well test data and geological information were studied and analyzed to obtain reservoir parameters and their range of uncertainty. Our results generally confirmed the analyses done by Auburn University. The parameters used in our numerical simulation are listed in Table 2. Since the supply well is 240 m from the injection/storage well, radial calculation mesh would be adequate. Based on the injection flowrates and temperatures provided, we employed the numerical model CCC to calculate production temperature and energy recovery factor for a given production flow rate schedule. The result is presented as curve A in Fig. 3, where the experimental result is also plotted. The experimental results were made known to us after we completed and presented our results. The predicted energy recovery factor is 0.62 compared to the experimental value of 0.56. This agreement is satisfactory.

Table 2. Parameters Used in Numerical Simulation

Thermal conductivity:	Aquifer	2.29 J/m.s.°C
	Aquitard	2.56 J/m.s.°C
Heat capacity of rock		1.81×10^6 J/m^3.°C
Aquifer horizontal permeability		63 darcys
Aquifer vertical to horizontal permeability ratio		1:7
Aquitard to aquifer permeability ratio		10^{-5}
Porosity:	Aquifer	0.25
	Aquitard	0.35
Storativity:	Aquifer	6×10^{-4}
	Aquitard	9×10^{-2}

Subsequent to comparing our predictions with the experimental results, we made a series of parameter sensitivity studies. Several sets of calculations were made, including:

1. Mesh variation. Results are found to be nearly mesh-independent.
2. An arbitrary increase of aquifer permeability from 63 darcys to 94 darcys. The calculated recovery factor is reduced from 0.62 to 0.55. The production temperature is shown as curve B in Fig. 3.
3. Two-layered-permeability aquifer system, in which the upper layer is 1.5 times as permeable as the lower but with an average of 63 darcys corresponding to the field value. The recovery factor is calculated to be 0.60.
4. Three-layered-permeability aquifer system, in which the middle layer is 1.5 times as permeable as the upper and lower layers while keeping the average at the field value of 63 darcys. The recovery factor is calculated to be 0.62; production temperature is displayed as curve C in Fig. 3.
5. Simulation of a large thermal dispersion effect. We followed Sauty (reference 15) who approximated this effect by using an effective thermal conductivity value. A value ten times the normal value was used. Based on an approximate relationship developed by Doughty et al. (reference 9), this corresponds to a dispersion length of 3 m. The energy recovery factor is calculated to be 0.57; production temperature is shown as curve D in Fig. 3.

Several additional parameter-sensitivity calculations were made. It was found that although the recovery factor can be made to reproduce the experimental data, the time rate of decrease of calculated production temperature for many alternative cases is always faster than the experimental value. After these studies, we came to the preliminary conclusion that this production-temperature discrepancy may be due to either thermal dispersion or nonisothermal, transient wellbore effects. Efforts have been initiated to study both processes. Understanding the cause of this discrepancy is important for further prediction calculations. Although the comparison of experiment and calculation may be considered satisfactory, we want to be sure that the discrepancy will not increase with changes in storage temperature or other conditions.

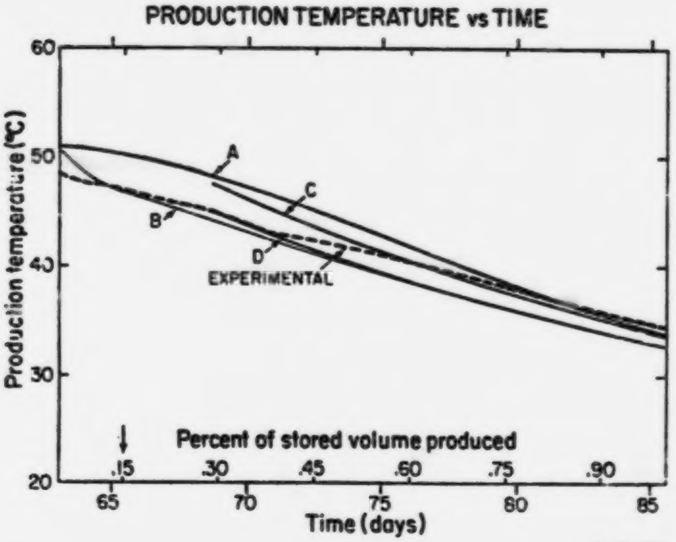

Fig. 3. 1981 Mobile Experiment First Cycle Production Temperature as a Function of time. Curve A shows the basic numerical simulation result, while curves B, C, and D show parameter study results described in the text.

SUMMARY AND CONCLUSIONS

In this paper we have concentrated on reporting the results of only one of our four tasks under the STES Program, the site-related studies. Considerable progress has been made in site characterization for optimization. In sites where buoyancy flow may be neglected, dimensionless parameter groups have been derived and type curves have been plotted to quickly obtain energy recovery factors and production temperatures for different conditions. In sites where buoyancy flow cannot be neglected, a semi-empirical method has been developed which reproduces the results of a realistic numerical model (CCC) over a wide range of parameters.

Much progress has also been made in predicting the results of field experiments by Auburn University at Mobile, Alabama. Calculations were able to predict, to within about 5%, the experimental value of the energy recovery factor and the production temperature (see Fig. 3). Studies of these results disclosed a discrepancy between calculated and observed rate of decrease of production temperatures which may be due to thermal dispersion and nonisothermal transient wellbore effects. Work has been initiated to study these, since an understanding of the discrepancy is important in ensuring a satisfactory prediction for further field cases.

ACKNOWLEDGEMENTS

Continued cooperation and assistance from C. Doughty and T. A. Buscheck are much appreciated. This work was supported by the Assistant Secretary of Conservation and Solar Energy, Office of Advanced Conservation Technology, Division of Thermal and Mechanical Storage Systems of the U.S. Department of Energy under Contract W-7405-ENG-48. This report represents work performed within the STES Program managed by Pacific Northwest Laboratory.

REFERENCES

1. C. F. Tsang, M. J. Lippmann, and P. A. Witherspoon. Numerical Modeling of Cyclic Storage of Hot Water in Aquifers. Symposium on Use of Aquifer Systems for Cyclic Storage of Water. Fall Annual Meeting of the American Geophysical Union, San Francisco. 1976.

2. C. F. Tsang, M. J. Lippmann, and P. A. Witherspoon. Underground Aquifer Storage of Hot Water from Solar Energy Collectors. Proceedings of International Solar Energy Congress, New Delhi, India, January 16-21, 1978.

3. C. F. Tsang, T. Buscheck, D. Mangold, and M. J. Lippmann. Mathematical Modeling of Thermal Energy Storage in Aquifers. Proceedings of Aquifer Thermal Energy Storage Workshop, Lawrence Berkeley Laboratory, Berkeley, California, May 10-12, 1978. LBL-8431.

4. Proceedings of Aquifer Thermal Energy Storage Workshop, Lawrence Berkeley Laboratory, Berkeley, California, May 10-12, 1978. LBL-8431.

5. STES Newsletter, a quarterly review of seasonal thermal energy storage, Chin Fu Tsang, editor, published by Lawrence Berkeley Laboratory, Berkeley, California 94720.

6. C. F. Tsang. A Review of Current Aquifer Thermal Energy Storage Projects. Invided paper at the International Assembly on Energy Storage, Dubrovnik, Yugoslavia, May 27-June 1, 1979. LBL-9834.

7. C. F. Tsang and D. Hopkins. Aquifer Thermal Energy Storage--A Survey. Invited paper at Symposium on Recent Trends in Hydrogeology, Berkeley, California, February 8-9, 1979, to be published as a Special Paper of the Geologiccal Society of America.

8. C. F. Tsang. A Survey of Recent International Activities in Aquifer Thermal Energy Storage. Invited paper, National Conference on Solar Energy, August 4-7, 1981, Montreal, Canada.

9. C. Doughty, G. Hellstrom, C. F. Tsang, and J. Claesson. A Study of ATES Thermal Behavior Using a Steady Flow Model, LBL-11029, January 1981. Submitted to Water Resources Research.

10. G. Hellstrom, C. F. Tsang, and J. Claesson. Heat Storage in Aquifers: Buoyancy Flow and Thermal Stratification Problems. LBL-11059. To be submitted to Journal of Geophysical Research.

11. F. J. Molz, A. D. Parr, and F. P. Andersen. Thermal Energy Storage in a Confined Aquifer--Second Cycle. Journal of Water Resources Research, vol. 17, no. 3, June 1981.

12. A. Menjoz and J. P. Sauty. Stockage de calories en aquifere par convection forcee a partir d'un puits unique. Presented at 7eme Symposium International sur les Transferts de Chaleur et de Mass en Milieu Poreux, Toulouse, France, August 26-28, 1980.

13. T. A. Buscheck and C. F. Tsang. Characterization of Heat Storage in Confined Aquifers and its Application to the Auburn Field Experiments. Proceedings of Second World Congress of Chemical Engineering, October 4-9, 1981, Montreal, Canada.

14. C. F. Tsang, T. Buscheck, and C. Doughty. Aquifer Thermal Energy Storage--A Numerical Simulation of Auburn University Field Experiments. Water Resources Research, vol. 17, no. 3, June 1981.

15. J. P. Sauty, A. C. Gringarten, and P. A. Landel. The Effect of Thermal Dispersion on Injection of Hot Water in Aquifers. Proceedings of Second Invitational Well Testing Symposium, October 25-27, 1978, Berkeley, California.

PROJECT SUMMARY

Project Title: Hydrologic Studies Support

Principal Investigator: J. W. Crosby III, Vernon Ichimura

Organization:
Washington State University
Geological Engineering
Pullman, WA 99164
(509) 335-8546

Project Goals: Alter the Intera Deep Well Disposal Model (DWDM) code to make it compatible with IBM computers without losing the accuracy apparent in runs made on CDC computers.

In addition to the basic comparison of old and new codes, an analysis will be made of the Mobile, Alabama test facility's two experiments performed between March 1978 and April 1979. Comparison of computed results will be made with data from the experiments.

Project Status: Of the two stated project goals, the first has been completed and the latter is in the final documentation stage.

Solutions computed by the Washington State University (WSU) version of INTERCOMP have been compared to several published solutions of isothermal and nonisothermal problems. The Avdonin, and Gringarten & Sauty nonisothermal solutions were used to test the energy transport capabilities of the INTERCOMP code. Comparisons were very good in both cases.

Several additional options have been created for use in thermal energy storage problems. They include:

1) Restart capability
2) Manual block size input
3) Spatially variable initial temperature distribution
4) Regional variation in hydraulic parameters
5) Print options for Darcy velocity and hydraulic cconductivity.

Numerical simulation of the Auburn University experiments (performed in 1978 and 1979) have been completed and compare very favorably with the published work from Lawrence Berkeley Laboratory (LBL). Coarse and fine grid simulations have been completed. For the coarse grid, recovery efficiencies for the two injection/storage/recovery cycles are reported as 65 and 75%. These compare well with the observed values of 66 and 76%, respectively. Discrepancies exist in the absolute energy injected and recovered as computed by the INTERCOMP and LBL analyses. Resolution of this discrepancy will involve assessing the merits of employing heat capacity of constant volume or constant pressure. A first draft of the final report is scheduled to be completed in July.

Contract Number: DE-AC06-76RLO 1830, DE-AM06-76RLO2221, Task Agreement No. DE-AT06-79RL10119, Modification No. A003

Contract Period: September 26, 1979 through September 30, 1981

Funding Level: $37,690

Funding Source: U.S. Department of Energy, Richland Operations Office

PROJECT SUMMARY

Project Title: Study of Coupled Energy and Mass Transport in Geologic Media

Principal Investigator: Stuart Childs

Organization:

Department of Soil Science
Oregon State University
Corvalis, OR 97331
(503) 754-2441

Project Goals: Examine the physical principles of energy and mass transport in geologic media, and identify soil and environmental conditions or parameters influencing the efficiency of aquifer thermal energy storage.

Project Status: A preliminary interpretive report and annotated bibliography of key references on energy and mass transport have been completed. The following observations can be made based on information gathered for this study:

1) Mechanisms of heat and water flow change markedly in the transition from water table to atmosphere. Under saturated conditions, heat transfer is dominantly conduction and free convection and flow is exclusively in the liquid phase. Under unsaturated conditions, heat transfer is by conduction or convection but both sensible and latent heat transfer occur and flow is reduced but can be in either liquid or vapor phase. Near the soil surface, vapor phase transport is important for both heat and water transport.

2) The coefficients in the heat and water flow equations are temperature dependent. For ATES applications, the magnitude of heat and water flow may increase dramatically as a result of increased thermal and hydraulic diffusivities.

3) Sizeable fluxes of both heat and water to the atmosphere can be expected where thermal storage is attempted in shallow ground-water systems.

4) The physics of heat and water exchange are poorly understood where sizeable water vapor and latent heat fluxes occur.

5) Techniques to quantify resistance to heat and mass transfer between soil surface and atmosphere are not well developed.

6) Prediction of temperature effects on the coefficients of the flow equations can provide acceptable estimates, but measurements of these characteristics for specific soils are required.

The final project deliverable for Phase I including both the preliminary report and the results of the parametric study will be completed in July.

Contract Number: DE-AC06-76RLO 1830, Subcontract B-97620-A-O

Contract Period: July 1, 1980 through July 31, 1981

Funding Level: $43,660

Funding Source: U.S. Department of Energy through Pacific Northwest Laboratory

PROJECT SUMMARY

Project Title: Nonaquifer STES Concepts

Principal Investigator: Donald E. Blahnik

Organization:
Pacific Northwest Laboratory
P.O. Box 999
Richland, WA 99352

Project Goals: Survey, evaluate and select nonaquifer thermal energy storage concepts for seasonal applications. Recommend further research and development that can lead to utilization of promising concepts.

Project Status: A formal report, "PNL-3625, "Preliminary Survey and Evaluation of Nonaquifer Thermal Energy Storage Concepts for Seasonal Storage" was completed and issued in December 1980. Since then emphasis has been placed on the promising STES concepts recommended in the report which include: (1) Pond, lake, earth, cavern, abandoned mines, rock and water tank storage for sensible heating and cooling, (2) ice and compacted snow for latent cooling, and (3) sulphuric acid/water heat pump for thermochemical heating and cooling.

Literature has continued to be gathered for the nonaquifer portion of the STES library. There is a tremendous amount of literature available because the results of research studies and experiments are coming to fruition. Review and evaluation of the literature indicates that our initial criteria and selection of promising concepts was practicable.

Currently the literature is being used to make a coarse preliminary evaluation of the promising nonaquifer STES concepts. The concept evaluation includes costs, thermal efficiencies, likely markets, advantages and disadvantages, development needs and overall potentials for use.

A task plan for the development of promising concepts is being formulated and it should be completed by the end of this fiscal year. The plan will be used to guide research through FY 1985.

NONAQUIFER STES CONCEPTS

Donald E. Blahnik
Pacific Northwest Laboratory
Richland, WA 99352

ABSTRACT

A preliminary evaluation of promising Seasonal Thermal Energy Storage (STES) concepts is under way at PNL. The Thermal Energy Storage (TES) concepts being evaluated include pond, lake, cavern, tank, earth, rock, and ice storage. All these concepts appear to be technically feasible and have potential to become economically feasible for particular markets and sites. Additional research and development on each concept is needed to establish design criteria, reduce costs, and eliminate uncertainties that stand in the way of implementation. Probably the most important need is for reliable, low-cost insulation and lining methods.

INTRODUCTION

The main purpose of the nonaquifer STES task is to survey, evaluate, and select potential nonaquifer concepts for seasonal use. The initial survey and evaluation indicated that in general the promising STES concepts use temperatures less than 95°C, low-cost storage media (water and rock), construction with earth, good insulation and leak-tightness, and economies of large scale. The initial concept recommendations that fell into that category included pond, lake, cavern, tank, earth, rock and ice thermal storage. Although the entire range of TES concepts is periodically reviewed and evaluated, those seven potential STES concepts have received special emphasis this past year. This paper provides a preliminary assessment of those concepts.

DISCUSSION

This section briefly discusses each of the concepts now being evaluated. These are general concepts that can have many specific variations due to the wide range of site characteristics, climates, markets, developments, alternative designs, and other factors that need to be considered. The literature presents an almost endless number of ideas and variations for thermal energy storage.

Pond STES

Ponds engineered to be leak-tight and well insulated provide a viable STES concept. Ponds must be specially designed for each site. Fig. 1 shows a basic pond.

The basic pond is a depression scooped out of the earth, and the excavated earth provides an embankment that increases the pond capacity. The sides and bottom are covered with an impermeable liner to contain the water. The top of the pond is covered with insulation and in some cases the sides and bottom will also be insulated. The pond cover also reduces thermal losses due to convection and evaporation of the water. This type of pond is constructed where the land is level.

Alternative pond designs where less excavation is required include a dammed-up natural valley or abandoned open-pit mines. Ponds filled with rocks can serve as artifical aquifers. Ponds can be made in rock by blasting the rock and using the rock with water in situ. Pond covers can be covered with a solar collector system to provide an energy source. A solar pond over a conventional thermal energy storage pond separated by an insulated membrane may have promise as a hybrid concept.

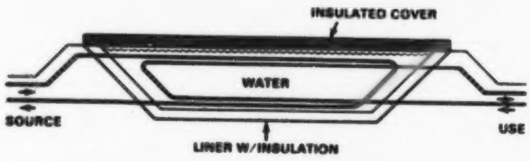

Fig. 1. Pond STES

Pond technology has been well established by many years of constructing municipal ponds, cooling ponds, etc. One of the principal needs for pond STES is to develop a low-cost liner that will last more than 20 years at up to 100°C. The main area of concern for the liner is to have adequate shear strength on sloping regions of the pond. Lining materials which are sprayed on rock or mixed with soil should be investigated. Development of insulation that can be placed in direct contact with soil or water without absorbing moisture is also needed. A method to seal or integrally line the insulation might reduce the requirement for a separate liner. Technology advancements that reduce pond construction costs would be helpful.

A large number of sites are available for constructing ponds. The market size required for heating or cooling would be predominantly in the 100- to 10,000-home equivalent range.

The cost of a pond storage unit can vary substantially between sites. A pond in dry, stable soil will be less expensive because of lower insulation and drainage system costs. A pond that requires full insulation will be most expensive. The cost of a pond that is constructed in a leak-tight open-pit mine would be very low because no excavation or liner would be necessary, and perhaps, insulation cost would be low. The lining and insulation usually make up a large portion of pond storage costs, and if they can be reduced or eliminated, large savings would result.

Lake STES

The lake STES concepts vary from small natural lakes to large dam reservoirs and to portions of large lakes or oceans. Studied concepts have included lakes serving a small community and upwards to a city exceeding 1,000,000 people.

The basic lake STES concept is shown in Fig. 2. The concept comprises an insulated floating cover with breakwater and insulated side panels that are anchored to the bottom. Bottom barriers might be used to stabilize the store thermocline(s). A solar collector system can be added to the floating cover, as with pond storage. The lake store should be sheltered from wind, ice, and wave action. Lake storage is also site specific, but some of the construction materials could be standardized, for example, the floating cover and side panels. Potential hybrid systems include a lake coupled with rocks, thin-walled tanks, and underwater reservoirs.

Lake STES promises very low costs and very large capacities. Lakes have the advantage of not requiring excavation, and construction using modular assemblies can be rapid and simple. Despite its attractiveness, lake storage research has been limited to scoping studies, and no sizable development has commenced. Development of an insulation system that will not absorb moisture is very important to maintain good thermal effectiveness.

Sites for lake storage are likely to be limited because of environmental reasons, regulatory and alternative use priorities. Sites at or near power plants, and where the distance to a large consumer is within 100 km, would be attractive. Power plants are a good thermal energy source because there are a large number of them in existence already, and there is a need to market waste heat. Future plants would have increased justification if they operated as both an electric and thermal generation facility (dams, nuclear, coal plants, and others). The earliest projects may be most attractive where electricity and fuel prices are high.

Swedish studies indicate that lake storage has the potential to be the lowest-cost STES method. Coupled with heat pumps, lake storage capacity is tremendous.

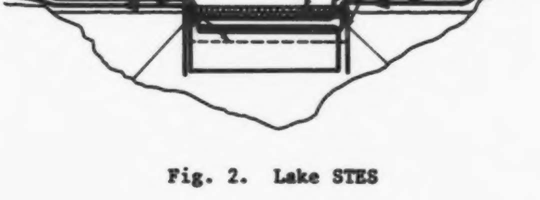

Fig. 2. Lake STES

Cavern STES

An example of a cavern store is shown in Fig. 3. Caverns can be natural or mined out of hard rock, salt, and other minerals. The caverns can use in situ blasted rock to reduce excavation costs. An abandoned near-surface mine with a height-to-width ratio of about one, relatively easy to seal, which can be piped through existing shafts and simply needs filling with water, is a perfect cavern. A perfect cavern store would be even more economical than a perfect aquifer store.

Caverns have been used to store warm oil (to 55°C) in Sweden with volumes of up to two million cubic meters at a single site. A 35,000-m^3 development cavern for storing hot water is currently under construction there. Development work is under way to determine chemical effects at higher temperatures, effects of thermal cycling, and the stability of temperature gradients. Insulation might be developed to reduce some of these operating effects. Development of low-cost lining methods for caverns would reduce the economic and technical risks in using this concept.

Caverns are site limited to materials that are compatible with hot water and gradual thermal cycling. Caverns should serve sites needing a heating capacity equivalent of 100 to 10,000 homes. Some uninsulated caverns may need a heat pump booster because the temperature of the heat is reduced during storage.

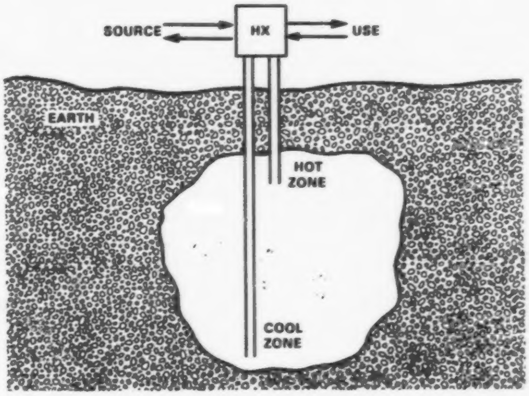

Fig. 3. Cavern STES

Tank STES

A tank can take many forms. A schematic of an insulated tank is shown in Fig. 4. A tank can be located above ground or can be completely buried. The most common tanks considered for TES applications are round and constructed of steel or concrete. For large tanks, concrete is usually more economical. Tanks required for STES must be large and will usually be constructed onsite. Very huge tank stores can be constructed as a gravity dam to a size limited only by the site and design requirements. Tanks can be lined if necessary. Tanks must be well insulated to be used on a seasonal basis. Multiple tanks and tank barriers can be used to give better thermal efficiencies. Tanks may someday be used to contain phase-change and thermochemical TES for seasonal uses.

Tank technology is well established and results in a relatively low technical risk. Additional development is needed for lining materials. Development of a sealed insulation that can be placed inside of the tank would also be beneficial. Structural foam insulation which can take some or perhaps all of the loads would reduce costs of tank construction. Low-cost, double-walled tanks also might be a beneficial development.

Tanks can be installed virtually anywhere where the earth is stable. The exception would be where an environmental (e.g., height above ground) or safety concern would prevent construction.

Tanks do not appear to be economic where a single annual thermal inventory turnover is involved. When multiple annual inventory turnovers occur, such as with solar energy or continuous energy sources (e.g., waste heat from industrial plant), a tank may be economical. If thermal fuel costs continue to rise more rapidly than construction costs, a tank store may become viable for a single annual inventory turnover.

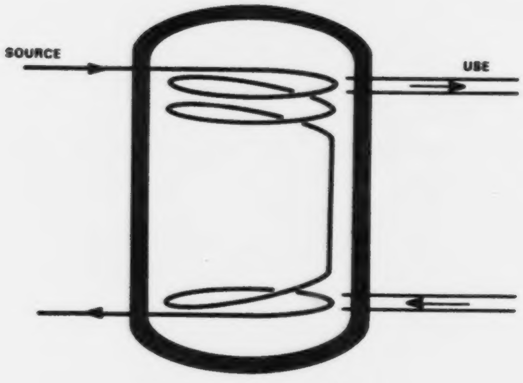

Fig. 4. Insulated Tank STES

Conventional tanks appear best suited to serve markets the size of 50 to 500 homes. However, large reinforced concrete gravity dam-type tanks appear to be competitive with a market of more than 10,000 homes and should be looked at more closely. Another tank concept in which small tanks are stored in a large, high-density, insulated warehouse should also be investigated.

The thermal effectiveness of large tanks (>100 homes) is excellent. Tanks can provide a precise thermal gradient by using a height-to-diameter ratio exceeding one. However, use of taller tanks will reduce the volume-to-surface ratio and thus offset some of the thermal efficiency gains made with taller tanks.

Earth STES

A method of using earth STES is shown in Fig. 5. The heat exchange concept can take many forms such as with coils, horizontal or vertical pipe, or plates. Vertical pipes and plates can be installed without excavation at some sites. Wet earth or dry earth STES can be used with clay, soil, sand, gravel, and other onsite materials. Earth storage can be combined with other storage such as pond and tank. It can be placed in covered piles (e.g., sand, overburden, excavated soil). Like all of the other types of storage, this concept can take on many variations in design.

Earth storage technology is in the process of being developed in several countries including the U.S. The largest test demonstration is a 85,000-m^3 clay STES facility in Sweden. Most of the stores have low temperatures and some systems require heat pumps to upgrade the heat for usefulness.

There are a large number of sites for use of this technology. For uninsulated stores the market served starts at about 50 homes and extends to perhaps 1,000 homes. For insulated and wet earth stores, the market could extend down to a one-home basis for do-it-yourselfers when coupled with solar heat and/or perhaps a heat pump. Farms could utilize low-temperature heat (40-50°F) for animal shelters) and thus use the earth source heat itself.

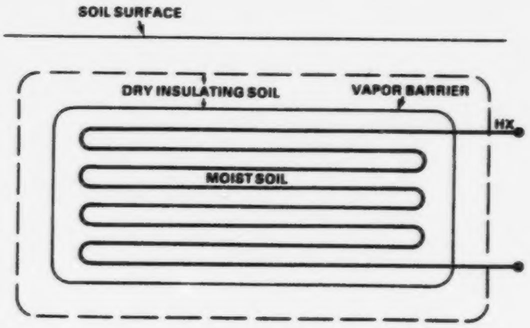

Fig. 5. Earth STES

The cost of earth stores varies over a wide range because of variations in the site materials (stability, wet and dry, amount of excavation required, and others) and the different degree to which they must be sealed and insulated. The lowest-cost systems will probably be installed with little or no excavation and coupling with heat pumps.

The thermal effectiveness can vary substantially. Water-saturated earth stores with good insulation can operate close to water tank performance. On the other extreme, very dry earth results in slow heat recovery at much lower temperatures and may require a temperature boost with heat pumps to be useful.

Rock STES

A schematic showing how rock in situ can be used for STES is shown in Fig. 6. Rock can be used in other forms such as underground and surface blasted rock, surface piles, trenches, etc. It can also be coupled with water in some of those forms.

Rock STES in the U.S. has been limited to paper studies. The Swedes, again probably have the most development experience in this area. They are especially interested in the deep rock store shown in Fig. 6. They have built and operated a 10,000-m^3 demonstration facility of this type. Cheaper drilling methods and improved lining technology would benefit this concept. Although the literature indicates that rock thermal cycling fracturing is a concern, it may not be as much in STES applications where only one inventory turnover occurs annually.

Rock storage should serve markets in the 100- to 1,500-home equivalent size range. The sites for use of this technology are somewhat limited to where the host rock is relatively impermeable, unfractured, and compatible with hot water.

The cost for rock well storage is very low. Rock well storage is particularly advantageous where source temperatures are low or at the other extreme where source temperatures are high over long periods of time.

Where source temperatures are low or where temperatures will degrade substantially, a heat pump system will be necessary to upgrade the heat quality. For large systems the rock will insulate well, enabling good thermal recoveries although usually at a lower temperature.

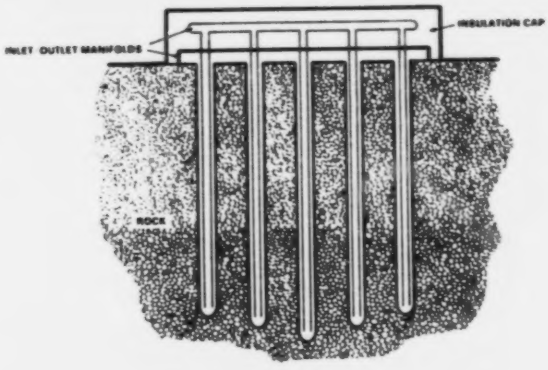

Fig. 6. Rock STES

Ice STES

Ice can be generated through the use of heat pumps and/or by winter outdoor chill. Since heat pump-augmented systems such as ACES and CASE are dealt with in other Department of Energy programs, they will not be included in this discussion. Use of outdoor chill will be covered here, and an example of an ice STES concept is given in Fig. 7. Ice concepts include ice formed in brine tanks through outside heat exchangers, heat pipe ice bins, flooded trays and ice bins, snow-making sprinklers, water sprayed on refrigerated drums, ice harvested from ponds and lakes, and others.

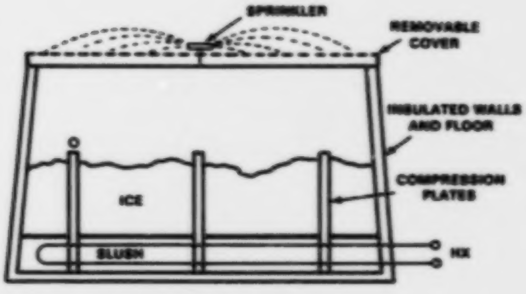

*OPTIONS - PIPE OVER FINS, FANS, ETC.

Fig. 7. Ice STES

The development of ice storage is currently being done mostly in the U.S. and Canada. Concepts using heat pipes with a tank, brine cooling tank, snow-making machines with a pond, and a flooded ice bin hold promise. The main development needs are to optimize the ice production and harvesting methods and to provide low-cost insulation and heat exchange systems.

Ice storage can be used for STES where the winter months stay below 25°F most of the time. Ice can be formed at up to 35°F through sprinkling in air and through radiation from shallow water trays. Ice storage is promising for markets as small as a single home up to perhaps 10,000 homes. The main use area will be in regions where winters get adequately cold and significant air conditioning is required during summer months.

Ice has the advantage of a large heat of fusion (144 Btu/lb) and thus can provide cooling at a steady temperature. Ice near 100% theoretical density requires a smaller amount of storage volume than water systems. Also, ice can be piled high so that only the lower portion, where there is water, requires leak tightness and structural strength. With good insulation the ice store can be very thermally efficient and deliver water at a steady level of coolness.

Hybrid STES

Many of the technologies and concepts can be combined to perform at an optimum level for the total system (energy source/store/use). Some of the hybrid systems have been mentioned in the discussions of the STES technologies. There are too many possibilities for hybrid TES to even summarize them in this paper.

One system that, along with ice STES, might be used for as small as single-home units is the combination of solar energy with tank or ponds. Most other STES systems require at least 50- to 100-home equivalents to become thermally and economically effective. An example of a combined solar pond/conventional pond is shown in Fig. 8. A variation would be to include tray collectors mounted on tank roofs with a high-temperature section for absorptive air conditioning. This type of concept is probably economical already for do-it-yourselfers in regions that allow an adequate number of annual inventory turnovers. Most crucial to achieving a market for 1 to 50 homes is the development of low-cost insulation/liner materials and low-cost construction such as has occurred in the swimming pool industry.

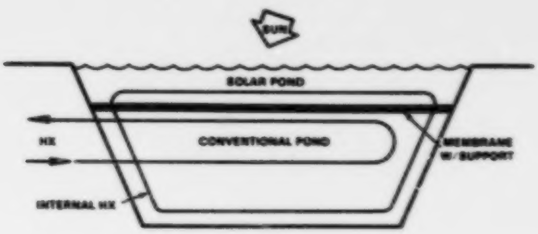

Fig. 8. Hybrid Solar/Conventional Pond STES

Heat Pump

Use of the heat pump can be valuable in improving the performance of STES systems. The effective capacity of TES systems can be nearly doubled by the use of heat pumps. The heat pumps can take advantage of heat from the earth source as well. One study in Britain used a heat pump to provide a STES pond with the source heat from a river and another heat pump to upgrade the temperature of pond heat distributed to the user. Heat pumps can make STES systems more flexible as in the CASE and ACES systems. The use of heat pumps is very important to the future of STES concepts.

Annual Thermal Inventory Turnover Rate

In the literature, concepts which require anywhere from one to one hundred inventory turnovers of heat per year have been called seasonal storage. In reality, seasonal storage should fall more in the range of one to twenty turnovers at most. Stores which collect almost all of their heat in less than two months will probably have only a single annual turnover. Stores which collect a large portion of their heat in three months but continue to draw heat over another six months at a lesser rate (e.g., solar source) can have inventories that turn over two or three times. An almost constant source of energy, such as waste heat from a power or industrial plant, will result in inventory turnover from four to twenty times per year.

More frequent inventory turnover usually can justify a more expensive storage system. Fig. 9 shows roughly how increased storage costs can be justified by more frequent inventory turnovers when compared to output from fuel oil burned at 65% efficiency. This is why tank storage, although more costly, is likely to find application in STES. Systems such as tank, cavern, pond, and lake storage have the capability of having many inventory turnovers annually because they can be efficiently charged and discharged at the same time. Future STES cost studies should exploit this fact.

As research comes to fruition, phase change and thermochemical TES concepts should also be examined for use in STES where multiple annual inventories are allowed.

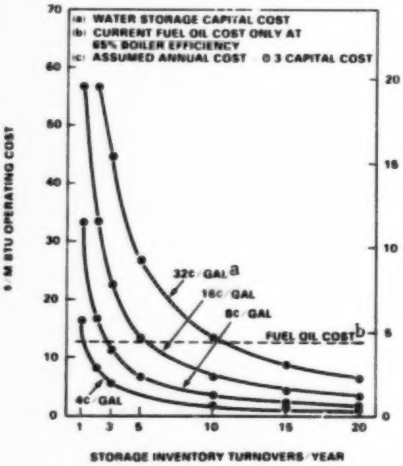

Fig. 9. Rough Thermal Energy Cost Rates as a Function of Storage Capital Cost and Annual Storage Inventory Turnover Rate

CONCLUSIONS AND RECOMMENDATIONS

A rough comparison of the selected STES concepts is provided in Table 1. The table compares the concepts on a common basis in the areas of development status, capital cost, thermal effectiveness, site availability, market size requirements, safety and environmental, and potential for future exploitation. All of the concepts have fair-to-good potential based upon this preliminary general evaluation. Except for tank storage, the concepts must be justified using site-specific studies.

Table 1. Rough Relative Comparison of Promising STES Concepts(a)

Subject of Comparison	Pond(b)	Lake(b)	Cavern(b)	Tank(b)	Earth	Rock Wells	Ice
• State of Technology Development	2	4	3	1	2-3	3	2
• Capital Cost (Store only, $/M Btu)							
<50	4	2	4(c)	X(d)	4	3	2-3
50-100	2	1	3(c)	4(d)	2	1	1
100-200	1	1	1	2(d)	1	1	1
>200	1	1	1	1	1	1	1
• Thermal Effectiveness(e) (>100 homes)							
>90% Heat Recovery Potential	1	1	1	1	1	1	1
Quality of Heat Discharged	1	1	2(f)	1	3	3	1
• Site Availability	2	3	3-4	1	1-2	3	2-3
• Market Size Required (homes)							
<100(k)	3	4	4	4(g)	3	3	2
100-1,000	1	2	1	3(g)	2	2	1
1,000-10,000	1	1	1	X	2	2	1
10,000-100,000	1	1	2	X(h)	X	X	3
>100,000	X	1	X	X(h)	X	X	X
• Safety and Environmental	2-3	2-4	2-3	1-3(i)	2	1-2	1-2
• Overall Potential(j)	2?	2?	2-3?	2?	2?	2?	1-2?

Relative Rating: 1 = Excellent
2 = Good
3 = Fair
4 = Poor
X = Not applicable or not sure

(a) Crude assessment based upon preliminary analysis. More detailed study required. Based upon single annual inventory turnover. Increasing the inventory turnover will improve market size ratings and reduce thermal energy cost rate.

(b) Charge and discharge simultaneously. Can exceed more inventory turnover/year.

(c) Natural cover or abandoned mine could be rated 1.

(d) Gravity concrete dam-type tank would be exception at 1 or 2. Applies to store size that serve >10,000 homes.

(e) Coupled with heat pump greater recoveries and higher quality are possible.

(f) With insulation the rating is 1.

(g) Increased annual inventory turnover would improve rating.

(h) Exception, gravity dam tanks would rate 1 for >10,000 homes.

(i) Above ground tanks have higher safety and environmental impact than buried tanks.

(j) All concepts can be improved with heat pumps incorporated.

(k) Specific concepts with better ratings for 1-100 home size range are solar heating/cooling coupled to pond or tank, insulated wet earth and ice/snow cooling.

Tank storage is the most developed concept and lake storage in the least developed. Costs favor lake, rock well, and ice storage the most. All the concepts have good thermal recovery potential, although the heat is degraded somewhat in earth and rock well storage. Tank, earth, and pond stores have the best site availability. Each concept has a different market size requirement and they all start over 50 homes equivalent for cost and thermal effectiveness. Concepts which might become attractive to the 1- to 50-home market size include solar/tank, earth, and ice STES. Based on current information, the safety and environmental considerations, and overall potential for use of the concepts are very hard to assess and compare. General comparisons of the concepts are difficult because there are a large variety of designs within a concept generic category. It will be necessary to study the concept designs in more detail to improve the preciseness of the evaluation.

Storage and utilization of waste heat has tremendous potential. A single large power plant using STES could supply all the heating needs of a large city. Review of waste heat dumped into air or cooling ponds by existing power plants may turn up some immediate potential projects. STES can be utilized on smaller-scale cogeneration projects for communities and industries. STES should also be considered as part of another project (e.g., mining venture, new power plant) when practicable.

Heat pumps coupled to STES systems have tremendous potential and should always be considered in STES projects. They can extend storage capacities, reduce costs, and provide operating flexibility.

More detailed cost studies need to be performed using a consistent methodology for all concepts. Variations in conceptual designs should be assessed for cost. The costs are needed for marketing studies.

Marketing studies need to be made to determine how sites for specific STES concepts match up with current and future thermal energy sources and uses in our country. The potential markets should also be assessed as a function of regions, costs and sizes. The future market for both retrofitting and new applications should be assessed.

More research and development is needed for effective, low-cost insulation and lining materials for all of the concepts. Improvements in construction methods would also be beneficial for all the concepts. Design criteria are needed to cope with the wide range of variations (e.g., geology, climate) that occur between sites.

Concepts need to be analyzed in greater depth for their thermal effectiveness as a function of size, geometry, containment, insulation, construction materials, storage media, heat exchange methods, and surrounding geology and climate.

Site geologic stability and compatibility with the various concepts should be reviewed on a broad basis. Safety, environmental, and institutional considerations need to be reviewed.

MECHANICAL ENERGY STORAGE PROGRAM

BLANK PAGE

PROJECT SUMMARY

Project Title: Mechanical Energy Storage Technology Project

Principal Investigator: Thomas M. Barlow

Organization:
University of California
Lawrence Livermore National Laboratory (LLNL)
P.O. Box 808, L-388
Livermore, California 94550/Phone: (415) 422-8200

Project Goals: To develop, demonstrate, and evaluate mechanical-energy-storage technology for vehicular and fixed-base applications.

Project Status: The efforts of LLNL were initiated in FY 1975. These efforts initially involved the development and characterization of fiber-composite materials for use in high-performance flywheels. Late in FY 1977 the Project was expanded to include development of MEST technology for application to electric and hybrid vehicles. Heat-engine/flywheel vehicle systems and disc-type flywheel-rotor development were added in FY 1978. In FY 1980 the Project was again expanded to include responsibility for the development of flywheel-rotor and mechanical-component technology, as well as for the evaluation of fixed-based applications of flywheel systems.

The Project's FY 1981 milestones included:

- Direction and management of the 1980 Flywheel Technology Symposium.
- Documenting of selected flywheel-rotor designs for further development.
- Completion of the conceptual design for a flywheel primary-containment structure for automotive applications.
- Submission of recommendations and a preliminary design for an enlarged flywheel test facility.
- Evaluation and demonstration of the existing capability for flywheel-rotor cyclic tests.

The Project currently consists of the six tasks listed below. The estimated FY 1981 expenditure level for each task is included; efforts funded directly by the DOE are not included in the expenditures.

• Transportation Applications	$522,000
• Fixed-Base Applications	342,000
• Fiber Composite Materials Characterization	365,000
• Flywheel Rotor Technology	926,000
• Advanced Component Technology	390,000
• Project Management and DOE Support	320,000

Most of the Project's activities are carried out through subcontracts to private industry. In-house activities include technical management, materials characterization, and the development of supporting technology for flywheel rotors.

Contract No.: W-7405-Eng-48

Contract Period: Funded through FY 1981

Funding Level: $2,865,000 (budget outlay)

BLANK PAGE

DEVELOPMENT OF MECHANICAL ENERGY STORAGE (MEST) TECHNOLOGY*

Thomas M. Barlow
University of California
Lawrence Livermore National Laboratory
P. O. Box 808
Livermore, California 94550

ABSTRACT

The Mechanical Energy Storage Technology Project at the Lawrence Livermore National Laboratory exercises field technical management of the Department of Energy's flywheel technology program. This paper summarizes the objectives, approaches, structure, and principal accomplishments of the Project during FY 1981. It also summarizes efforts in international flywheel-related technology and complementary efforts in the United States.

INTRODUCTION

Background

Flywheels have been in use since ancient times and have, since the industrial revolution, become commonplace in machinery. Their primary role has been to correct, mechanically, the timing mismatch that commonly occurs in most energy-delivery systems, allowing energy sources to more effectively meet energy demands.

Present and future requirements for energy-storage technology are now more rigorous than ever before. The continually increasing cost and shortage of petroleum-based fuels has become a serious problem for the Nation, and new technologies are needed to use these fuels more efficiently and to allow for the substitution of other energy sources when practical.

As an energy-conservation concept, mechanical-energy-storage technology has several particularly attractive characteristics. One vitally important attribute is its ability to accept and deliver energy at high rates. And, in contrast to many electrochemical energy-storage methods, its energy-storage capacity is independent of delivery rate. These characteristics can be used to advantage to complement other energy-storage devices, such as the batteries in an electric vehicle, for a more effective and economical system.

Heat-engine-powered and electric vehicles (HEV and EV) are also expected to derive significant benefit from the application of flywheel technology. Fuel-economy improvements of 50 to 100% are forecast for the HEV; in this case, the benefit will be derived by recovering braking energy, by using the flywheel to meet peak power demands, and by permitting the engine to perform in its most favorable load/speed range. Electric vehicles will use the power capability of flywheels to extend battery life by reducing peak-power demands on the battery, to improve acceleration by supplementing the power available from the battery, and to increase range by allowing the battery to operate in a more favorable load regime.

The timing mismatch between energy supply and demand is readily apparent in photovoltaic and wind energy systems. While various energy-storage methods might be used to correct this mismatch, certain operating characteristics of mechanical-energy-storage systems are very promising. Among these are the systems' all-mechanical nature and the potential for simplified power-conversion hardware.

---

*This work was performed under the auspices of the U.S. Department of Energy by Lawrence Livermore National Laboratory under contract No. W-7405-Eng-48.

The saving in petroleum consumption provided by such applications of mechanical-energy-storage technology can be significant. This saving can be realized by enabling and enhancing the market penetration of alternative energy sources and by allowing petroleum to be used more effectively in conventional systems.

To realize the energy-saving and substitution potential of flywheel technology, however, we must develop fiber-composite materials, flywheel rotor designs, and energy-conversion devices. We must also establish the safety and reliability of flywheel systems and reduce their cost.

Project History

The Mechanical Energy Storage Technology (MEST) Project began in early CY 1979 when several independent efforts in flywheel R&D at the Lawrence Livermore National Laboratory (LLNL) were brought together. Subsequently, the Laboratory accepted responsibility for field technical management of the Department of Energy's (DOE's) flywheel technology efforts, and work directed by Sandia Laboratories, Albuquerque, New Mexico, was transferred to LLNL. The transition was complete by the start of FY 1980.

The Laboratory's acceptance of the field management role called for expansion of Project capabilities at LLNL. To meet the need, additional staff members were hired to plan, prepare work specifications, select and direct subcontractors, and maintain accountability for the work. An expanded capability in critical-path network analysis was also required.

Project efforts were redirected in FY 1981 to increase the emphasis on research-oriented activities. At the same time, a general budget recision reduced Project funding. Further reductions in funding are expected in 1982. Plans are currently underway to transfer Project responsibility to Oak Ridge National Laboratory, where it will be integrated with other activities related to energy storage.

PROJECT OBJECTIVES AND APPROACHES

Objectives

The objectives of the MEST Project are to develop, demonstrate, and evaluate mechanical-energy-storage technology for vehicular and fixed-base applications. The management and technical approaches to meeting these objectives are outlined below.

Approaches

The principal actions included in the management approach are:
- To develop a multiyear plan and determine priorities.
- To provide an operating structure and identify interrelationships within the Project and with related work elsewhere.
- To establish a system of controls and accountability.
- To promote and develop industry participation in all phases of the Project.
- To disseminate information on a broad scale.

The principal actions of the technical approach, which can be summarized similarly, are:
- To identify R & D needs.
- To assess the applicability of MES technology.
- To carry out analytical and experimental efforts.
- To validate laboratory-scale results through proof-of-concept tests.
- To conduct limited-scale engineering tests in cooperation with end-use organizations.
- To emphasize technology transfer in all phases of R&D.

PROJECT STRUCTURE

Organization

The MEST Project consists of five technical tasks arranged into two primary areas of responsibility--applications and technology base, as shown in Fig. 1. Applications covers efforts to develop and evaluate MEST for transportation and fixed-based systems, while technology base addresses research in fiber-composite materials, flywheel rotors and containment, and mechanical components. Analytical studies include design studies and evaluations of MEST's technical and economic potential for energy saving and substitution.

Task Interactions

Figure 2 shows the interactions and "products" of the five technical tasks. Task requirements, in terms of cost and performance, were developed through applications analysis and then became the criteria for technology development. The net results of the Project were a system-level evaluation of the technology and establishment of a technology base for general use.

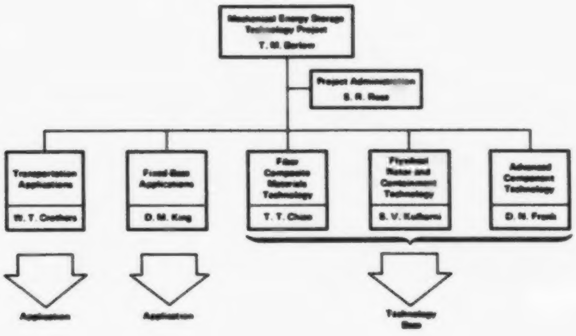
Mechanical Energy Storage Technology Project
T. M. Barlow
Project Administration
S. R. Ross
Transportation Applications
W. T. Crothers
Fixed-Base Applications
D. M. Kay
Fiber Composite Materials Technology
T. T. Chiao
Flywheel Rotor and Containment Technology
S. V. Kulkarni
Advanced Component Technology
D. N. Frank
Applications
Application
Technology Base

Figure 1. MEST Project Structure

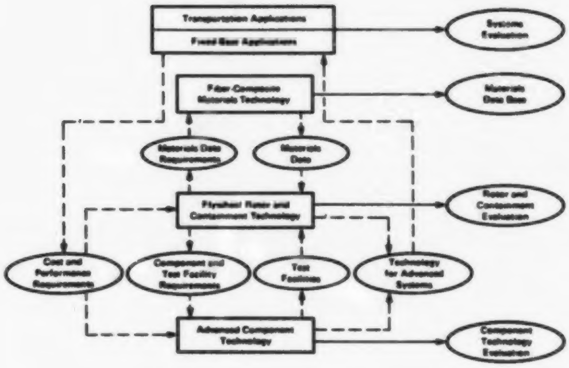
Transportation Applications
Fixed-Base Applications
Systems Evaluation
Fiber-Composite Materials Technology
Materials Data Base
Materials Data Requirements
Materials Data
Flywheel Rotor and Containment Technology
Rotor and Containment Evaluation
Cost and Performance Requirements
Component and Test Facility Requirements
Test Facilities
Technology for Advanced Systems
Advanced Component Technology
Component Technology Evaluation

Figure 2. Task Interactions Within the MEST Project

Subcontract Activities

Project activities are carried out primarily through subcontracts to private industry and universities. In FY 1981, the MEST Project undertook 45 individual R&D activities, exclusive of its technical management function. Of these, 29 were subcontracted to private industry and 13 to universities or related laboratories, one was performed by Los Alamos National Laboratory, and two were done at LLNL. Most of the major subcontracts will be described separately as part of the 1981 Annual Contractors' Review; additional subcontractors and their respective areas of R&D are listed in Table 1.

Table 1. Subcontracted R&D efforts not described in the 1981 Annual Contractors' Review.

Subcontractor	Area of R&D effort
Garrett-AiResearch	10-kWh flywheel energy-storage system
	Rim-type rotor fabrication
University of Minnesota	Cellulosic flywheel
Dyna East	Delamination analysis
VPI and SU[a]	Spectrum load fatigue
Purdue University	Time-dependent fatigue
Boeing Vertol	S2-glass composite fatigue tests
General Electric-Space Division	Kevlar-29 composite fatigue tests
General Electric	Disc-type rotor design/fabrication
William Brobeck & Associates	Multidisc rotor analysis
Ewald Corporation	Rotor-fabrication processes
Owens-Corning/Lord Corporation	Molded-rotor fabrication
Rocketdyne	Rotor testing
Applied Physics Laboratory	Rotor testing
	Test-facility design/development
Ifield Engineering	Hydrostatic CVT modification
Shirley Software Systems	PERT program modification
La Posada Resort Hotel	Support to 1980 Flywheel Technology Symposium

[a] Virginia Polytechnic Institute and State University.

PRINCIPAL PROJECT ACCOMPLISHMENTS--FY 1981

The MEST Project completed most of its activities in FY 1981, but several will continue into FY 1982. The following is a brief summary of the Project's principal accomplishments; it includes accomplishments described separately in the 1981 Annual Contractors' Review, as well as those that were not presented because of time constraints.

- Eaton Corporation, in consultation with the University of Wisconsin, proceeded with the analysis and design of a propulsion system for the heat-engine/flywheel vehicle.

- Lincoln Laboratory (Massachusetts Institute of Technology) completed testing of the one-tenth-scale, flywheel-energy-storage system.

- Garrett-AiResearch was awarded a subcontract to develop a 10-kWh flywheel-energy-storage system; cutbacks in funding and a redirection of Project efforts caused early cancellation.

- The Charles Stark Draper Laboratory assessed the potential of flywheel energy storage for several fixed-based applications and for metropolitan-area taxi fleets. Los Alamos National Laboratory conducted an in-depth analysis of the New York taxi-fleet application.

- Subcontracts were placed with several universities in support of the Project's research into fiber-composite materials technology. Washington University will establish an engineering data base for selected composites; Virginia Polytechnic Institute will study the effect of spectrum loading on fatigue life; and Purdue will investigate cycle-rate effects. Dyna-East, a minority-owned firm, will conduct an analysis on the delamination of composite rotors.

- An evaluation panel selected two rotor configurations for further testing: the Garrett-AiResearch multirim design (for its energy-density characteristics) and the General Electric/LLNL disc-type design (for its low cost potential). The AVCO bidirectional weave will be tested to determine its current and potential performance.

- The University of Oklahoma neared completion of its rotor-dynamics design guide, which will provide information in a format useful to engineers and designers.

- Rotor-fabrication development efforts proceeded on two fronts. Owens-Corning, in conjunction with Lord Corporation, worked on the molded disc with circumferential overwrap; and Ewald Corporation pursued studies relevant to the two selected rotor configurations noted above.

- Columbus Laboratory, Battelle Memorial Institute, began a cost study of rotor and containment systems. The study will identify both dominant cost centers and predicted rotor costs.

- Rotor spin tests were completed by Union Carbide's Y-12 facility, APL, and Rocketdyne. All prototype designs, except AVCO's, have now been tested. The fatigue-test capability of the Y-12 facility was assessed and demonstrated.

- Flywheel containment configurations were established by General Electric and AVCO; experimental prototype containment rings were included in some rotor tests at Y-12.

- Plans and preliminary cost estimates for a 50-kWh flywheel test facility were established.

- Ifield's hydrostatic, continuously-variable transmission (CVT) was modified to incorporate performance characteristics appropriate to a heat-engine/flywheel vehicle.

- Ifield and the University of Wisconsin, using the Ifield transmision, studied the potential of hydraulic-accumulator energy storage for vehicles.

- Over 120 representatives from 10 nations attended the 1980 Flywheel Technology Symposium.

The Project's annual report for CY 1980[1] describes many of these accomplishments in detail.

OTHER U.S. AND INTERNATIONAL DEVELOPMENT EFFORTS

Flywheel technology is being developed in a number of countries, with funding provided by both government and the private sector. The Department of Transportation, in addition to DOE's Energy Storage Program in the United States, is sponsoring two projects for the development of a flywheel-powered trolley bus. Plans for the work, which is contracted to Garrett-AiResearch and General Electric, currently call for a laboratory evaluation of the propulsion system.

The Department of Energy, through its mining technology research program, is also sponsoring development of a flywheel-powered, mine shuttle car. Analyses indicate that improved operating performance and enhanced safety will result. FMC is the prime contractor, and Rocketdyne is responsible for development of the flywheel energy-storage unit.

Through active participation in technical societies and international meetings, the MEST Project staff has been able to establish and maintain contact with a number of European organizations active in flywheel research and development. The efforts of several of these organizations were described in the proceedings of the 1980 Flywheel Technology Symposium.[2] Those efforts and others are summarized below.

- MAN-Neue Technologie of Germany is developing a diesel/flywheel propulsion system for buses that features a steel, disc-type flywheel rotor and hydrostatic transmission (CVT). A second effort uses a hydraulic accumulator for energy storage.

- Volvo has also developed a diesel/flywheel bus with hydrostatic transmission and has tested two prototypes. The flywheel, which is made of steel, was housed in a small trailer in the first and incorporated into the bus in the second. Volvo has also evaluated a heat-engine/flywheel passenger vehicle, but we are not aware of any active development effort.

- A third bus configuration is under development by Fiat of Italy. The flywheel, which is of the bare, wound-filament type, will use either steel wire or Kevlar fibers; both hydromechanical and electric transmissions are being considered.

- Aerospatiale of France has developed an emergency power system and has accepted a contract to supply units to France's telephone company. A second-generation unit, with increased energy-storage capacity, is now under development.

- The Urban Transportation Development Corporation of Canada is developing a flywheel-powered bus, with technical support provided by the University of Ottawa. Fiber-composite flywheels are being considered.

- The Swiss and Dutch have a developing interest in fixed-base systems. Alternate energy sources (other than petroleum) are of interest, and energy storage is seen as means of making these resources more viable.

- The flywheel/electric vehicle is being studied in the United Kingdom. The British have successfully employed electric vehicles for urban deliveries and see flywheels as a means of improving performance and economics, thus permitting more-widespread use of electric vehicles. A mechanical CVT, the Perbury drive, is incorporated into a system under test at the University of Sussex.

SUMMARY

Considerable progress has been made in flywheel technology since the current Department of Energy program was initiated in 1975, including the indentification of applications and the establishment of performance and economic criteria. However, despite the significant achievements in flywheel energy storage, the economics of operation have not been established and few companies are willing to commit to full-scale commercial development, feeling the financial risk is too great.

Rotor technology has been the subject of intensive research in the United States, while the Europeans have probably concentrated more on the development of specific systems. The need for international cooperation has been heightened, however, by common interests and the reduced funding available for government-sponsored research in many countries. This need could form the basis for a cooperative R&D program to fully utilize and share the talents of researchers.

REFERENCES

1. T. M. Barlow, W. T. Crothers, T. T. Chiao, D. N. Frank, D. M. King and S. V. Kulkarni, Mechanical Energy Storage Technology Project: Annual Report for Calendar Year 1980, Lawrence Livermore National Laboratory, Livermore, Calif., UCRL-50056-80 (1981).

2. T. M. Barlow, Proceedings of the 1980 Flywheel Technology Symposium, U.S. Department of Energy, Livermore, Calif., CONF-801022 (1980).

PROJECT SUMMARY

Project Title:	A Preliminary Assessment of the Impact of Flywheel Energy Storage Technology on Taxicab Fleet Operation in a Large Metropolitan City
Principal Investigator:	Milton C. Krupka
Organization:	Los Alamos National Laboratory Analysis and Assessment Division Los Alamos, New Mexico 87545
Project Goals:	Evaluate the impact and benefits in terms of energy conservation, environmental improvement, and economics of incorporating flywheel energy storage systems into fleet vehicle operations. Specifically examine the case of taxicab fleet operations within New York City. Identify institutional barriers to implementation.
Project Status:	The project has been completed and the final report issued, LA-8722-MS, February 1981. Operational information for the study has been obtained from both regulatory and private organizations in New York City. Energy conservation, environmental, and economic impacts have been determined based on assumptions keyed to both operational data and a projected fuel economy for hybrid flywheel-internal combustion engine vehicles.
Contract Number:	LLNL order SANL 820-020, Task 7.203
Contract Period:	August 29, 1980 through October 31, 1980
Funding Level:	$15 000
Funding Source:	U.S. Department of Energy through the Lawrence Livermore National Laboratory, Mechanical Energy Storage Technology Project

ASSESSMENT OF TAXICAB FLEET OPERATION IN NEW YORK CITY

Milton C. Krupka Sydney V. Jackson
Los Alamos National Laboratory
Analysis and Assessment Division
Los Alamos, New Mexico 87545

ABSTRACT

This paper describes a preliminary assessment of the impacts resulting from incorporation of flywheel energy storage systems into automotive fleets in a large metropolitan city. Specifically, the case of taxicab fleet operation within New York City is examined.

Based upon available taxicab operational data, a levelized life-cycle cost comparison between a standard internal combustion engine vehicle in present use as a taxicab and a projected hybrid flywheel-internal combustion engine vehicle (taxicab) has been generated. Energy conservation and environmental benefits are discussed and potential institutional barriers to rapid deployment of flywheel energy storage systems are identified.

The results obtained from this study generally emphasize the value of incorporating flywheel energy storage systems into future vehicles designed for taxicab use.

INTRODUCTION

The incorporation of flywheel energy storage systems (FESS) into automotive vehicles has been under consideration for some time. Previous studies have suggested that FESS can yield substantial benefits in automotive vehicle operation, particularly for urban driving. Enhanced interest has come about due to major advancements in materials science and engineering as applied to flywheel system development.

This study presents a preliminary assessment and evaluation of the economic, energy conservation, and environmental benefits of the introduction of FESS into a standard internal combustion engine vehicle (ICEV). To further assess the impacts resulting from FESS incorporation into certain types of automotive fleets, a preliminary examination of taxicab fleet operation in a large metropolitan city, in particular New York City, was made. The taxicab transportation sector was chosen in view of certain unique operational characteristics that permit a more visible intercomparison of their vehicles with and without new energy storage systems.

AUTOMOTIVE FLEET VEHICLE MARKET AND TAXICAB SECTOR

The fleet market is especially valuable as a technological test market for new vehicle and component design because:

(a) availability of professional management and fiscal resources permits a higher degree of risk involvement;
(b) conscientious maintenance, vehicle control, and record-keeping practices exist;
(c) vehicles can be assigned to specific and well-defined missions;
(d) mileage and operational data accumulate rapidly; and
(e) there is high product visibility.

Because of the wide diversity of purpose existing within the fleet market, it is convenient to subdivide fleets into a number of sectors, one of which is the taxicab sector. In considering the purchase of vehicles within this sector, surveys have indicated that maintenance represents the primary purchase criterion with life-cycle costs and reliability close secondary criteria.

NEW YORK CITY TAXICAB OPERATION*

Characterization of taxicab operation in New York City is difficult because there are several taxi systems. The city has about 12 000 licensed taxicabs, controlled by the New York City Taxi and

---

*Information mainly obtained from the New York City Taxi and Limousine Commission, 67 Wall St., New York City, New York 10005, and the Metropolitan Taxicab Board of Trade, Inc., 24-16 Bridge Plaza South, Long Island City, New York 11101. The latter organization controls the fleet operation of about 2200 taxicabs, about 20% of those licensed.

Limousine Commission. About 60% operate as fleets and minifleets and the remainder as independent owner/drivers. There is also a substantial but indeterminate number of livery service vehicles (gypsies) operating within and without the city limits and not controlled by the Commission.

Characteristics unique to the New York City taxicab sector include: very high annual mileage accumulation (50 000-80 000 miles); relatively short vehicle lifetime (18-36 months); urban stop-go driving and significant braking; low average speed (about 7-11 mph) and low average gasoline mileage (about 10 mpg) in central business districts (CBD). Additional characteristics, operating parameters, and data used for the economic analysis is given in Ref. 1.

The characteristics of New York City taxicab operation strongly suggest that evaluations of new technologies such as FESS be conducted under New York City taxicab drive cycles in addition to the Federal urban drive cycle usually considered. The former emphasize CBD type of driving and are perhaps best characterized by extensive periods of zero velocity (engine idle or stop) and net low average speeds.

ECONOMIC ANALYSIS

A levelized life-cycle cost (LLC) methodology was used to perform the economic analysis. The advantage of LLC is that the total operating cost, including the capital investment, is characterized by a single number. A detailed discussion of LLC methodology is contained in the user's manual for the computer code (BICYCLE) used in this analysis (Ref. 2). The data used in the analysis reflect primarily that relating to fleet operation with estimates made where necessary.

Results of the analysis are shown in Fig. 1.

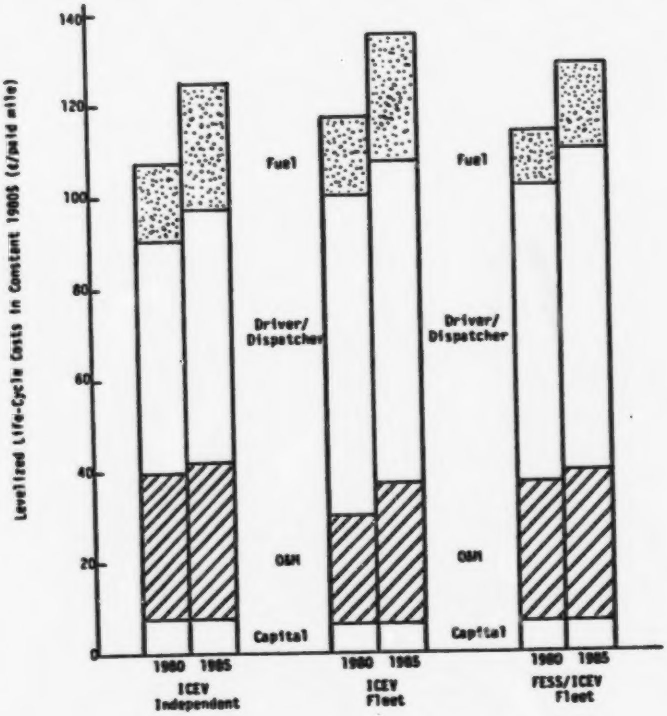

Fig. 1. Comparison of levelized life-cycle costs for three systems of taxicab operation.

Sensitivity studies were performed on selected parameters of interest. Results are shown in Figures 2-4.

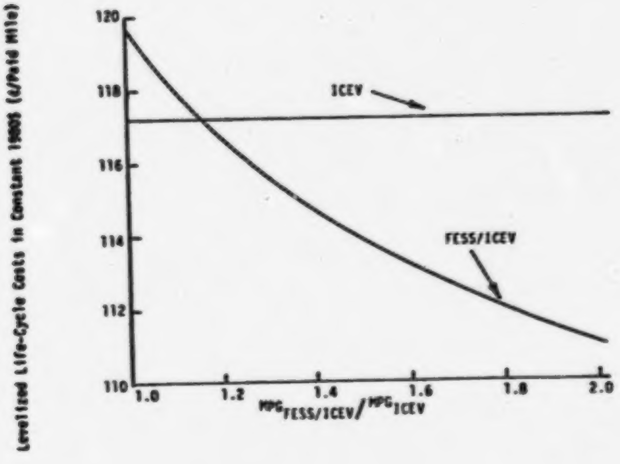

Fig. 2. Life-cycle costs (fleet operation) of taxicab ICEV and FESS/ICEV as a function of fuel economy ratio.

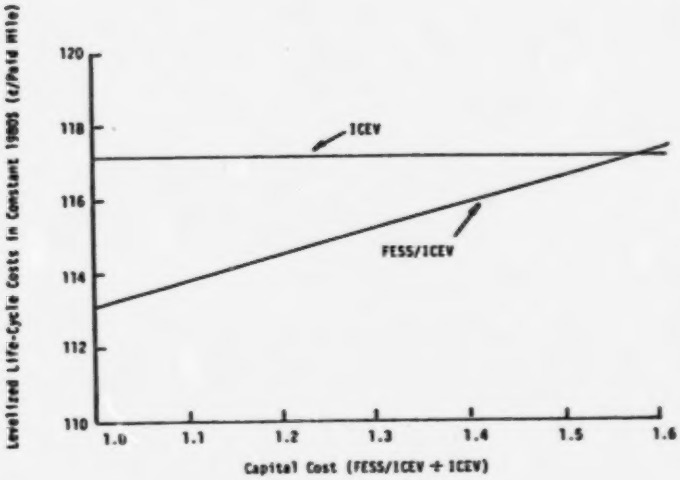

Fig. 3. Life-cycle costs (fleet operation) of taxicab ICEV and FESS/ICEV as a function of capital cost ratio.

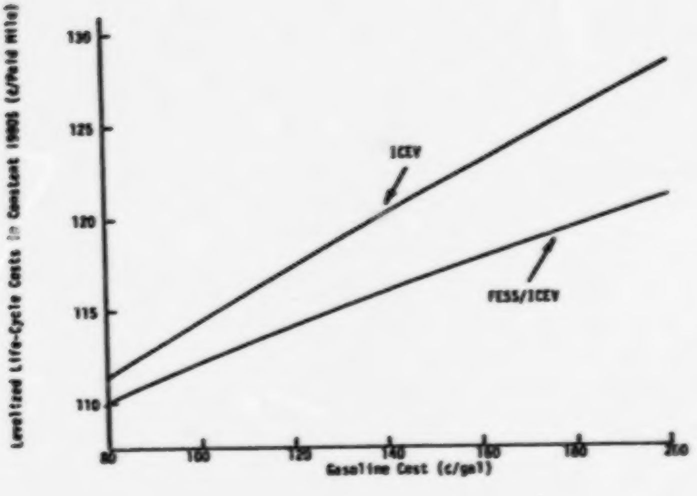

Fig. 4. Life-cycle costs (fleet operation) of taxicab ICEV and FESS/ICEV as a function of gasoline cost.

Life-cycle costs of FESS/ICEV are reduced with continued improvement in fuel economy relative to a base value 10 mpg (1.0 ratio) for the ICEV. The breakeven gasoline mileage is about 11.8 mpg. Operating costs are higher for FESS/ICEV above the breakeven point.

The life-cycle cost vs the capital cost ratio is of particular interest. It suggests that the capital costs for a FESS/ICEV could be increased as much as 58% before exceeding the ICEV life-cycle costs. This additional capital investment would be warranted to achieve projected gains in fuel economy.

The FESS/ICEV system is less costly at all values of gasoline cost shown in Fig. 4. An interpolation would demonstrate breakeven cost at about 60-65¢/gal in this study. As fuel costs increase, the FESS/ICEV becomes progessively more economical.

ENERGY CONSERVATION

The gain in fuel economy projected to come from FESS in a vehicular application is the result of not only the regenerative braking concept but also the concurrent efficient operation of an optimized engine and drive train system. This combined engineered system has been studied by several groups, including the University of Wisconsin, for a number of years (Ref. 3).

As a conservative measure, it is assumed that a 50% gain in fuel economy is realistic for vehicles in the approximate weight class of taxicabs. The savings in energy consumption by licensed taxicabs can be shown assuming the gain mentioned above. For about 12 000 taxicabs accumulating between 50 000-80 000 miles per year, the gain in fuel economy results in a savings of about 33% in fuel purchases, a savings of about 25 x 10^6 gallons per year, which at a cost of $1.20 per gallon amounts to $30 x 10^6 per year. The energy equivalent of gasoline is about 125 000 Btu per gallon, therefore, about 3.1 x10^{12} Btu per year can be conserved.

ENVIRONMENTAL CONSIDERATIONS

The introduction of flywheel technology is likely to have its most noticeable effects upon air quality (emissions) and associated health impacts, especially in urban environments.

The New York City Taxicab and Limousine Commission mandates strict emission standards. Taxicabs of years 1979 and 1980 and the future must meet emission standards equivalent to those for California.

Since there are significant savings in terms of fuel usage, environmental improvement in the form of reduced emissions is to be expected with the introduction of FESS/ICEV taxicabs.

Because New York City also regulates noise levels, any noise problems presently encountered in development should be solved before introduction into the city environment.

INSTITUTIONAL BARRIERS

A number of institutional factors that may visibly affect rapid deployment of FESS/ICEV vehicles in the taxicab market sector have been identified.

These include: the automobile industry production infrastructure as it relates to the small market for taxis; lack of maintenance and service information for the taxicab industry, which prefers relatively short downtime periods; the ownership of patent or commercial rights relating to component development by contractors using government funds; and the necessary education of regulators, insurers, and the public with regard to the safety of FESS. More positively, there is already a precedent in New York City regarding taxicab fleet technology demonstrations, diesel engine-powered taxicabs having been tested previously. Generally, regulations do not appear to be restrictive.

CONCLUSIONS

A preliminary assessment of the economic, energy conservation, and environmental impacts related to the introduction of flywheel energy storge systems (FESS) into automotive (taxicab) fleets in a large metropolitan city (New York City) has been made. The results obtained generally emphasize the value of incorporating flywheel energy storage systems into future vehicles designed for taxicab use. A large-scale demonstration test would provide a more accurate evaluation of the benefits discussed herein.

REFERENCES

1. M. C. Krupka and S. V. Jackson, "A Preliminary Assessment of the Impact of Flywheel Energy Storage Technology on Taxicab Fleet Operation in a Large Metropolitan City," LA-8722-MS (February 1981).

2. R. W. Hardie, "BICYCLE - A Computer Code for Calculating Levelized Life-Cycle Costs," LA-8493-MS (August 1980).

3. N. H. Beachley and A. A. Frank, "Flywheel Energy Management Systems for Improving the Fuel Economy of Motor Vehicles," Final report, DOT/RSPA/DPD-50/79/1 (August 1979).

PROJECT SUMMARY

Project Title:	Assessment of Flywheel System Benefits in Selected Vehicle Applications
Principal Investigator:	Lester Forrest
Organization:	The Aerospace Corporation El Segundo, California 90245
Project Goals:	Assess the value of the flywheel as a range extender or energy conservation device in passenger car applications.
Project Status:	The technical work is nearing completion. The vehicle simulation programs for the various drivetrains investigated are fully developed, verified and operational. Energy analysis results for the series configuration heat engine/flywheel drivetrain have been reported to DOE. Work is in progress on the analysis of performance for the parallel configuration heat engine/flywheel and the battery/flywheel drivetrain systems.
Contract Number:	DE-AC08-79ET26306
Contract Period:	January 1980 through July 31, 1981
Funding Level:	$199,500
Funding Source:	U.S. Department of Energy

ASSESSMENT OF FLYWHEEL SYSTEM BENEFITS IN SELECTED VEHICLE APPLICATIONS

L. H. Kubo L. Forrest
The Aerospace Corporation
El Segundo, California

ABSTRACT

The performance of vehicle systems incorporating energy storage flywheels was investigated in a recent Aerospace study for the Department of Energy. This paper presents a synopsis of the study effort and of results obtained to date. The effort involved an in-depth assessment of flywheel system benefits in two vehicle applications: a four-passenger commuter car with electric drive (flywheel range extension application) and a six-passenger family car with conventional heat engine drive (flywheel fuel conservation application). The special case of the six-passenger vehicle as used in taxicab service was also investigated. The study examined a number of possible component design/selection alternatives for flywheel rotors, continuously variable transmissions, batteries, motors, and other propulsion elements. Results of the assessment are provided for the case of a series-configuration heat engine/flywheel drivetrain as used in the passenger car and urban taxi vehicle missions.

BACKGROUND AND INTRODUCTION

Flywheels have been used for many years to conserve momentum in reciprocating machinery. Until recently, the only transportation applications were a number of buses and small mine locomotives powered by steel flywheels in conjunction with electrical motor/generator sets. These units were manufactured by the Oerlikon Engineering Company of Zurich, Switzerland during the 1950s and 1960s.

Other steel flywheel application activities include (1) a Garrett-AiResearch energy storage device installed and tested in a New York City subway car, (2) a Rocketdyne counter-rotating disc design for the U.S. Army Mobility Equipment Research and Development Center, (3) a Garrett-AiResearch flywheel for the University of Wisconsin experimental hybrid passenger vehicle, and (4) a Garrett-AiResearch flywheel used in a battery/flywheel hybrid postal jeep.

Flywheel rotors fabricated from fiber composites and materials other than steel are a relatively new development. A number of experimental rotors of this type have been built and tested with varying degrees of success by such organizations as Johns Hopkins University, Sandia Laboratories, the Lawrence Livermore Laboratory, and AiResearch. The only such system which has reached the stage of prototype testing in a vehicle is that of AiResearch, which uses an S-glass/Kevlar/epoxy composite flywheel in a regenerative power system to increase the capacity and performance of the ETV-2 electric vehicle developed under the EHV RD&D Program of DOE.

In addition to the hardware programs noted above, there have been several analytical assessments of the potential of flywheels in transportation energy conservation, including those of the Lawrence Livermore Laboratory [1], the University of Wisconsin [2], AiResearch [3], JPL [4], and The Aerospace Corporation [5,6,7]. These studies have suggested that, in certain applications, the flywheel can be used successfully to augment vehicle range or to reduce the energy consumption requirements of the vehicle prime mover. In general, these benefits accrue through the use of the flywheel to load-level the motor/battery or ICE engine system and/or to recover vehicle kinetic energy which would otherwise be dissipated in braking.

In a quantitative sense, the value of incorporating a flywheel system in an automotive vehicle will depend upon (1) the flywheel system specific energy, energy capacity, loss characteristics, weight, and volume; (2) specified goals for vehicle road performance (acceleration, passing); (3) vehicle duty cycle and trip length; and (4) the weight, volume, and efficiency characteristics of flywheel-related powertrain components. Flywheel spindown losses, for example, can have a significant impact on short-trip energy efficiency, and may demand the development of advanced seal and bearing designs, or force consideration of smaller-diameter, lower-speed rotors, along with lower-pressure atmospheres in the housing. Power-absorbing accessories in the form of vacuum pumps or oil pumps for bearing lubrication also can significantly reduce the effectiveness of a flywheel system.

Despite the hardware programs and study activities noted above, no clearly definable picture has emerged as to the specific value of a flywheel as a mileage extender (range increase) or as an energy conservation device in an automotive transportation vehicle. This is due in part to (1) the multiplicity of prime movers (heat engines, battery/motors) with which flywheels have been coupled, (2) the multiplicity of operational modes envisioned, and (3) the lack of test data or equivalent information concerning flywheel system design requirements and operating characteristics.

In a recent study by The Aerospace Corporation for the Department of Energy, the issue of flywheel benefits in automotive applications was addressed in a focused investigation of specific vehicle missions involving passenger cars and taxicabs. This paper provides a summary description of the study effort and presents results for the case of a series-configuration heat engine/flywheel drive train as used in a six-passenger family car and urban taxi. Work is in progress on parallel-configuration heat engine/flywheel and battery/flywheel powertrain systems.

APPROACH

A review of previous analytical assessments of flywheel system performance was conducted for the purpose of establishing appropriate guidelines for the present effort. In general, these past assessments cover a broad range of energy storage vehicle types and missions, and do not portray the performance of the flywheel system and its related powertrain components in detail. Freqdently the flywheel, CVT, motor/generator, and other components of the flywheel powertrain have been treated as black boxes, using single-valued efficiency characteristics to represent the average performance of the powertrain components. In particular, flywheel operational characteristics, including parasitic losses, energy requirements for spinup, and energy losses due to spindown in an extended stop interval, have not been treated in the assessment of overall system energy effectiveness.

With the benefit of the groundwork and hindsight provided by these past efforts, the present study elected to narrow its field of investigation to a relatively few powertrain and vehicle configurations, and to concentrate on the realistic definition and analysis of flywheel powertrain operating characteristics and performance effects. A major objective in this work was to identify desirable directions for future DOE flywheel research and development programs.

The study focused on two specific automotive applications in which the capabilities of flywheel-equipped vehicles were compared to their non-flywheel counterparts: a four-passenger commuter vehicle with electric drive (range extension application of the flywheel system) and a six-passenger family car with conventional heat engine drive (fuel conservation application of the flywheel system). The six-passenger vehicle was also examined with respect to its use in urban taxi service.

The study first characterized both metal and fiber composite flywheel systems in terms of size, speed, energy capacity, weight, and volume. Next, an operational analysis was performed to determine flywheel system loss characteristics for several basic flywheel system designs. In a third step, candidate propulsion powertrain configurations were selected for detailed examination and the driveline components in these configurations were characterized as to efficiency, size, and weight. In a final step, the defined vehicle/propulsion systems were analyzed using a computer simulation program to determine range extension and energy conservation effects as a function of vehicle driving cycle, vehicle use mode, battery type (range extension application), and flywheel system design. These analyses focused on the flywheel subsystem and its specific contribution to energy conservation.

VEHICLE SYSTEMS DEFINITION

Vehicle Types and Sizing

A number of baseline vehicles were used as references in determining the energy benefits of the flywheel system. Sample characteristics of the principal baseline vehicle types are shown in Table 1. The intermediate class vehicle is a front-wheel-drive (FWD) configuration that generally conforms to GM projections for the 1982 downsized A-body vehicle (present Malibu, etc.). The electric vehicle generally reflects the dimensional characteristics of current FWD subcompact vehicles, but the values exhibited are those for the Department of Energy's near-term electric vehicle, ETV-1.

The dimensional, weight, and power values displayed in Table 1 were used as inputs to the vehicle simulation program in determining the performance characteristics of the reference systems. The range, grade, and acceleration numbers shown in the table are nominal or reported values which were used as preliminary guidelines in sizing the energy storage and prime mover elements of flywheel-equipped vehicles. The principal thrust in this approach was to create flywheel vehicles capable of delivering repeatable performance comparable to their reference vehicle counterparts. With these designs established, the flywheel vehicle performance capability was varied as a study parameter to determine the effects on energy conservation.

A realistic evaluation of flywheel benefits in automotive applications must consider the effects of energy storage system weights and volumes as packaged in the automotive vehicle. These elements impact the design of the vehicle and thereby propagate a weight effect in the body and chassis. The effect is particularly large in the case of battery vehicles, where the energy storage components comprise a large fraction of total vehicle mass. Here, a weight/volume change in the energy storage system (i.e., the displacement of batteries by the flywheel, or the change from one battery system to another) may have a profound effect on vehicle curb weight.

To account for this effect, an empirical technique for estimating the weight of flywheel-equipped vehicles was developed. Basically, this technique stretches the engine and trunk compartments of the baseline vehicle as needed to accommodate the packaged density of the flywheel powertrain. Dimensions of the passenger compartment were held constant at the values representative of the respective vehicle market class. The weight of the altered body and powertrain and the propagation of weight effects on the chassis are then included in the computation of vehicle curb weight. By this means the study properly accounts for the weight difference in baseline and flywheel-equipped vehicles of comparable performance.

Table 1. Baseline Vehicle Characteristics

Vehicle	ICE Passenger Car and Urban Taxi[a] (Intermediate)	Electric Commuter Car[b] (Subcompact ~ ETV-1)
Passenger Capacity	6	4
Passenger Compartment Length, ft	6.6	6.2
Vehicle Length, ft	15.3	14.1
Vehicle Width, ft	5.7	5.5
Vehicle Height, ft	4.5	4.3
Drag Coefficient	.44	.31
Curb Weight, lb	2780	3320
Battery Weight, lb	----	1080
Engine/Motor Peak Rated Power, hp	90	41[c]
Construction	Conventional	Aluminized
Range, mi	350[d]	51[e]
Top Speed, mph	95+	60[f]
Sustained Speed on 5% Grade, mph	70	55
Acceleration Time, sec		
0-30 mph	4	9.0
0-60 mph	12	29
25-55 mph	7	17
Urban Fuel Economy, mpg[g]	25	---
Highway Fuel Ecnomy, mpg[g]	32	---
Taxi Cycle Fuel Economy, mpg[g]	14	---

[a] Auto trans/300 lb Payload/Std 4 Cyl Engine/2.53 AR
[b] Pb-acid Batteries/300 lb Payload
[c] Assumes motor specs are met
[d] Urban Cycle
[e] J227a(D) Cycle/Simulation at 100% DoD
[f] Motor Speed Limit
[g] Simulation/No AC

Drivetrain Configurations/Operating Modes

The number of potential drivetrain configurations with which the flywheel system may be coupled is extremely large. An analysis of possible designs for the heat engine/flywheel system alone identified 16 configurations involving various combinations of mechanical and electrical components in both series and parallel power flow arrangements. This study focused on two configurations for the heat engine/flywheel powertrain and one configuration for the battery/flywheel powertrain. The selection of these systems was largely based on considerations of simplicity (i.e., economic feasibility), energy effectiveness, and operational flexibility.

The selected drivetrains are shown schematically in Figures 1, 2, and 3. Figure 1 depicts a heat engine/flywheel powertrain with components arranged in a series power flow arrangement similar to that used by the University of Wisconsin in their Ford Pinto experimental vehicle. The heat engine and flywheel are linked by a speed reduction gear of fixed ratio, and the flywheel is linked to the wheels through a continuously variable transmission (CVT)[1] which operates to match flywheel rotational speed to the road speed requirement.

---

[1] As indicated in Figure 1, an advanced (wide speed ratio range) CVT design could eliminate the need for an additional gear box in the driveline. The advanced design CVT was one of several transmissions examined in the study.

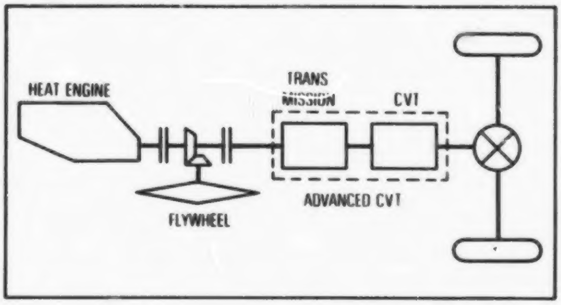

Figure 1. Heat Engine/Flywheel Drivetrain -- Series Arrangement

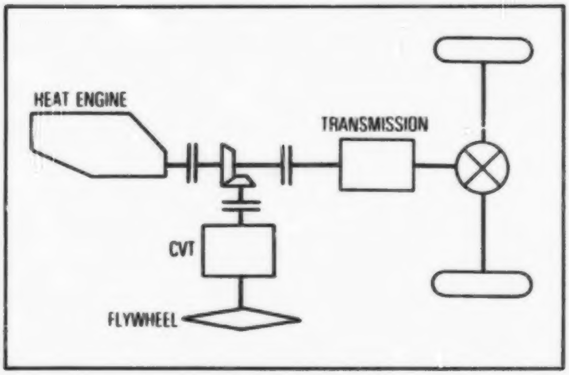

Figure 2. Heat Engine/Flywheel Drivetrain -- Parallel Arrangement

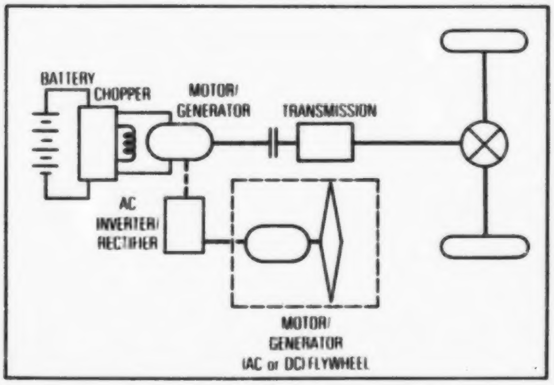

Figure 3. Battery/Flywheel Drivetrain -- Parallel Arrangement

In this configuration, the flywheel (effectively) drives the vehicle, while the heat engine operates in an on-off mode to maintain flywheel speed above a controlled lower limit (a study variable). When on, the engine operates at near wide-open-throttle, minimum BSFC (brake specific fuel consumption) conditions for maximum efficiency. Vehicle kinetic energy during deceleration is recovered by using the forward motion of the vehicle to spin up the flywheel. Beyond a controlled upper-limit flywheel speed (a study variable), conventional braking is used to slow the vehicle. Engine on-off operation in this configuration is controlled solely by the flywheel state of charge and is independent of vehicle operating mode (accel, cruise, etc.).

From the standpoint of driver perceptions, an improvement over the on-off mode of engine operation could be achieved by inserting a clutch between the flywheel and speed reducing gear shown in Figure 1. The engine could then be operated in a continuous (optimum efficiency) mode, with the flywheel engaged as required to augment engine power output or to recharge the flywheel. Flywheel engagement, however, demands a matching engine speed, and in this mode the system operates identically to the system shown in Figure 1.

Flywheel and heat engine operation can be made independent by means of the (parallel power flow) drivetrain configuration shown in Figure 2. Here the CVT is inserted between the flywheel and speed reducing gear, with other components remaining the same as in Figure 1. In this arrangement, the engine can be operated in a conventional manner (at some sacrifice in efficiency) by adjusting the CVT speed ratio to match flywheel speed with the engine/driveline output.[2] The clutches shown provide the means to (1) disengage the wheels on initial flywheel spinup, (2) disengage the engine in braking energy recovery, and (3) disengage the CVT/flywheel during highway cruise operation.

A battery/flywheel drivetrain based on a series power flow arrangement typically consists of a motor/generator, flywheel, and transmission connected in tandem, with the flywheel designed in a through-shaft configuration to provide mechanical power output to the driveline. This arrangement was examined as a potential candidate for the flywheel/battery vehicle, but was rejected in favor of the parallel configuration shown in Figure 3, which was found to provide greater latitude in the selection and investigation of alternative flywheel system designs. As indicated in the figure, the flywheel system may be a through-shaft configuration, or a vacuum-encapsulated flywheel-motor/generator unit of the types developed by GE and AiResearch under the DOE Mechanical Energy Storage Technology Program.

---

[2] Other engine operating modes are possible, including on-off.

In the system shown in Figure 3, the prime propulsion unit is a battery-powered separately excited DC motor which is mechanically linked to the vehicle wheels through an (optional) two- or three-speed transmission. The flywheel unit outputs electrical energy to augment the battery source as needed to meet peak road power demands. In this manner, the flywheel acts to load-level the battery, thereby increasing its energy capacity so as to extend vehicle range. On deceleration, vehicle kinetic energy is recovered by using the forward motion of the vehicle to operate the traction unit as a generator and the flywheel unit as a motor to spin up the flywheel. When the flywheel is fully charged, the regenerative electric energy is routed to the battery. An optional system feature would permit the flywheel to deliver spin-down energy to the battery during an extended stop interval.

Component Characteristics

Given the available data base, every effort was made to apply a uniformly detailed approach to the definition of drivetrain component operating characteristics. This was emphasized as a means to obtain realism in the simulation of vehicle performance and visibility into component improvements that would enhance the energy benefits of flywheel vehicle systems.

The components studied and characterized encompass all operating elements of the baseline vehicles ientified in Table 1 and the flywheel vehicles shown in Figures 1, 2, and 3, including several different designs of flywheel and CVT systems, AC and DC motor/generators, conventional transmissions and differentials, spark ignition engine, etc.

A prime example of the work done in the area of flywheel systems was the development of a stand-alone computer model which determines flywheel dimensional, weight, and loss characteristics based on inputs of energy storage capacity desired, rotor configuration and material, and certain flywheel system design specifications. Loss characteristics generated by this program for a flywheel system based on the AiResearch ETV-2 vehicle design are given in Figure 4, showing component loss contributions and the total loss characteristic as a function of rotor speed. The total flywheel loss curve generated by this model was used as an input to the vehicle simulation program.

The significance of the flywheel parasitic load is illustrated in part by Figure 5, which shows that in an extended vehicle stop interval an ETV-2 type flywheel system (design loss-to-energy ratio of 0.5) would decay to half speed or 25 percent energy

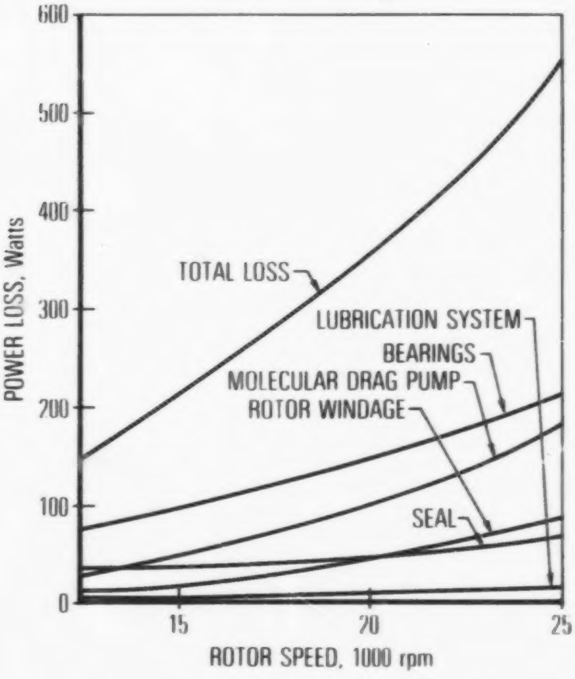

Figure 4. Parasitic Losses in ETV-2 Type Flywheel System

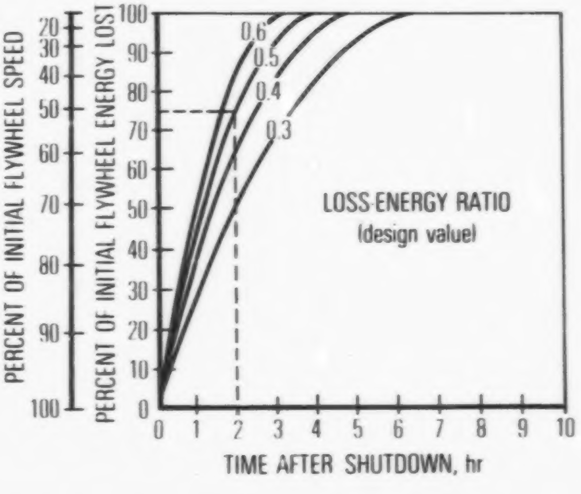

Figure 5. Energy Loss Characteristics of ETV-2 Type System as the Flywheel Spins Down

capacity in about two hours. This loss could have an adverse effect on short-trip energy efficiency for some vehicle designs and missions.

Other examples of the component characterization effort are given in Figures 6 and 7. Figure 6 is a generalized map of spark ignition engine fuel consumption characteristics, reflecting the composite performance of several modern IC engines in the displacement (rated power) range of interest to this study. Figure 7 shows the efficiency characteristics used to represent the performance of the DC separately excited motor/generator. The generalized motor parameters displayed are based on an explicit calculation of losses in a well-designed DC machine sized to the nominal requirement of a battery/flywheel powertrain.

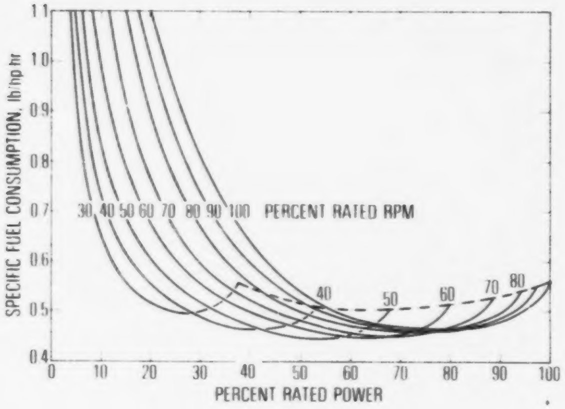

Figure 6. Spark Ignition Engine Fuel Consumption Characteristics

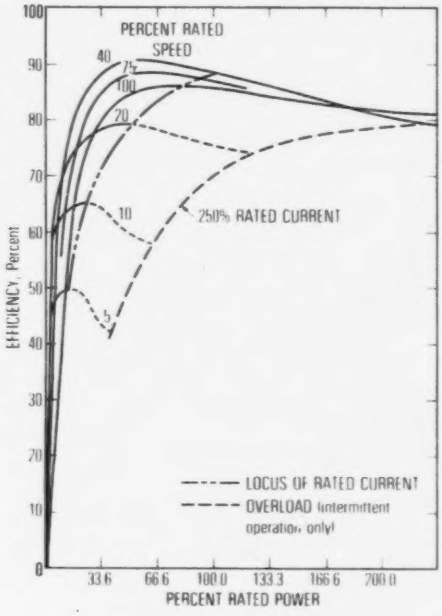

Figure 7. Efficiency Characteristics -- DC Separately Excited Motor

Energy Analysis

The focus of the energy analysis effort was a case study of the vehicle systems and missions described earlier, in which flywheel-equipped vehicles were compared with their non-flywheel counterparts (baseline systems). To accomplish this, it was necessary to develop a computer-based vehicle simulation program sufficiently detailed to accurately portray (1) the performance characteristics of powertrain components, (2) the operating interactions of vehicle subsystems, and (3) the energy flow logic associated with individual drivetrain configurations and operating strategies. As a matter of expediency, this resulted in a separate simulation for each vehicle system examined.

Beyond this, the computer operation is unremarkable. In a wheels-to-engine sequence, it determines the propulsion power required to negotiate each element of the driving cycle, and apportions this power between prime mover and storage device according to one or more selected operating strategies. The state of flywheel (and/or battery) charge is continuously tracked, along with the consumption of fuel or dissipation of battery energy. Energy flows associated with flywheel spinup and spindown, engine startup, clutch engagement, motor controller operation, and all other major component processes are accounted for.

At this time, the computer analysis work is incomplete and it is only possible to report on results obtained for the series configuration of the heat engine/flywheel powertrain. Examples of the output for this element of the study are presented in Figures 8 through 12, showing flywheel vehicle fuel economy benefits expressed as a percentage improvement over baseline vehicle performance. All data except for Figure 12 are ideal quantities in the sense that flywheel final spindown losses are neglected.[3] Figure 12 addresses the influence of the spindown loss effect.

---

[3] The vehicle simulations start with a fully charged flywheel and bring the system back up to its initial state at the end of the driving cycle.

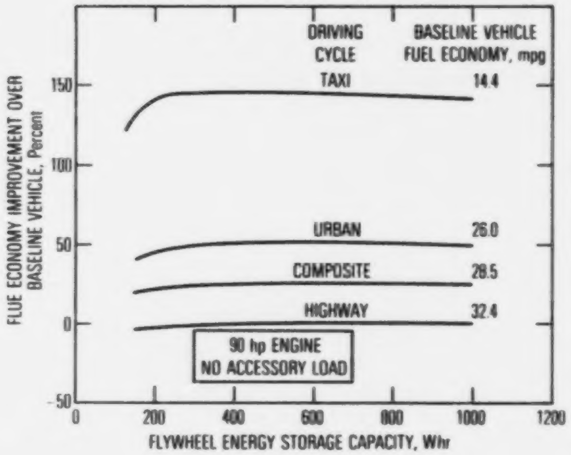

Figure 8. Driving Cycle and Storage Capacity Effects on Flywheel Vehicle Fuel Economy Benefits

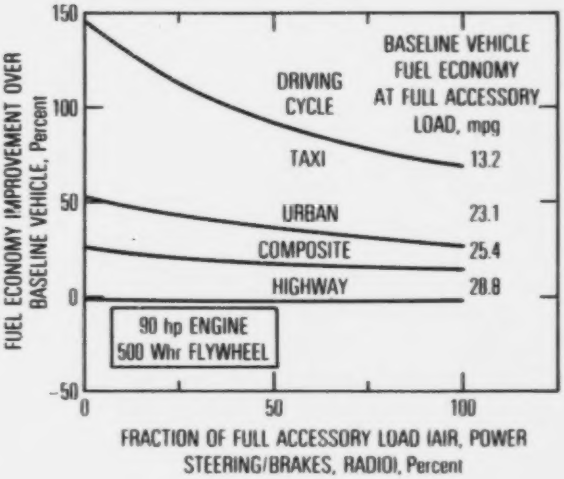

Figure 9. Accessory Load Effects on Flywheel Vehicle Fuel Economy Benefits

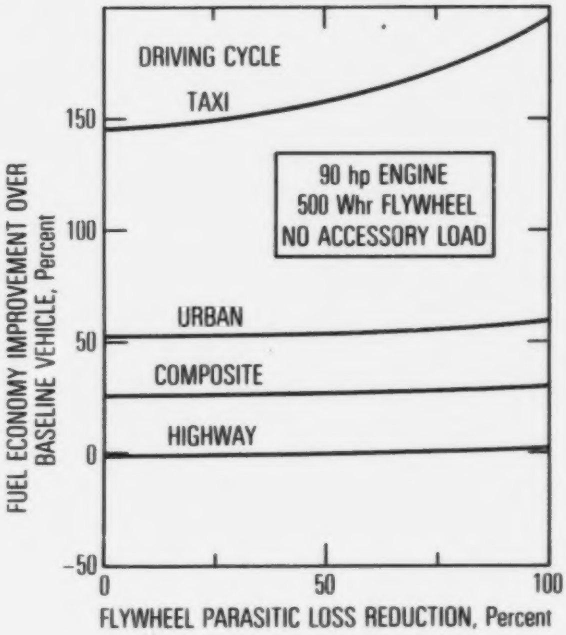

Figure 10. Flywheel Parasitic Loss Effects on Flywheel Vehicle Fuel Economy Benefits

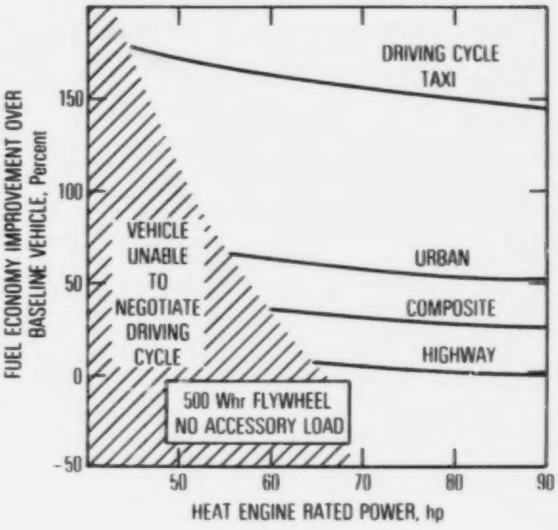

Figure 11. Heat Engine Size Effects on Flywheel Vehicle Fuel Economy Benefits

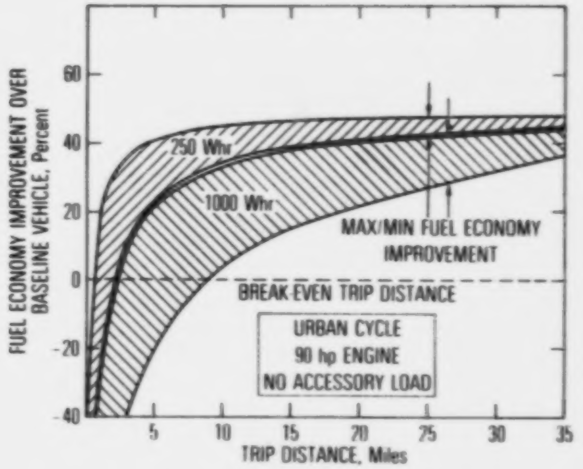

Figure 12. Rotor Spindown Loss Effects on Flywheel Vehicle Fuel Economy Benefits

In these plots, the vehicle systems represented are (1) a conventional 6-passenger car equipped as described in Table 1 (baseline), and (2) a size-equivalent heat engine/flywheel automobile with series drivetrain arrangement (Figure 1). The flywheel vehicle is here equipped with a composite-rotor flywheel system based on the AiResearch, ETV-2 vehicle, design.[4] The curb weight of the baseline vehicle is constant (2780 lbs), while the curb weight of the flywheel vehicle varies over a 225 lb range as influenced by flywheel system size (rotor energy storage capacity), heat engine size (rated power), and related vehicle weight propagation effects. The payload assumed is 300 lb (all vehicles). The passenger car mission is represented by results shown for the urban, highway, and composite driving cycles, while the urban taxi is represented by results shown for the taxi cycle.

Figure 8 shows the flywheel vehicle fuel economy improvement as influenced by driving cycle and by flywheel rotor energy storage capacity (heat engine size is fixed at 90 HP rated). The improvement is highly variable with driving cycle. It is a negative quantity for the highway cycle, where flywheel system losses constitute an energy liability, and it is greatest (approaching 150 percent) for the taxi cycle, where the potential for braking energy recovery by the flywheel is a maximum.

For the flywheel system represented (composite rotor design), the improvement characteristic is shown to be relatively insensitive to rotor energy storage capacity. This is the net result of the following disparate effects which occur as rotor energy storage capacity is increased: (1) vehicle weight increases, (2) the frequency of heat engine starts (and associated fuel consumption) decreases, (3) braking energy recovery increases, and (4) flywheel system loss increases. In general, the curves decay at the low end of the capacity range, reflecting regenerative braking saturation effects in the smallest capacity wheels investigated.

Accessory loads can reduce the fuel economy benefits of flywheel vehicles substantially, as indicated in Figure 9. Here shown is a 500 WH flywheel system operating with air conditioning, power steering, power brakes, and radio (air conditioning is the significant load element). With this equipment, the percent improvement for the taxi cycle is reduced from 146 to 70 percent. By comparison, the same accessory load in the baseline vehicle reduces fuel economy from 14.4 to 13.2, a loss of only 8 percent. This contrasting impact is due to several factors, including (1) no part of the (substantial) accessory load is recoverable through regenerative braking, (2) the flywheel accessory drive is less efficient than the heat engine accessory drive, and (3) the added accessory load tends to improve heat engine BSFC for the baseline vehicle (but not for the flywheel vehicle) and provides a source of useful work output during idle operation.

The effect of possible technological improvements which could reduce flywheel system parasitic losses (windage, bearing friction, etc.) relative to the values employed in this analysis is illustrated in Figure 10. As indicated, the influence on fuel economy improvement is negligible for all but the taxi cycle, where the benefits are significant only for highly optimistic levels of loss reduction.

A reduction of heat engine size (rated power) has the principal effect of reducing engine (and vehicle) weight, but does not significantly improve BSFC for the series configuration heat engine/flywheel vehicle, since the engine already operates in an optimum efficiency mode. To maintain performance equivalent to the baseline vehicle for road acceleration maneuvers, it may be necessary to increase the minimum storage capacity of the flywheel system, either by increasing rotor size or by operating the flywheel at higher average speed to ensure a reserve capacity.[5] Figure 11 disregards the road performance requirement and therefore displays the best fuel economy improvement that can be expected in the series heat engine/flywheel vehicle by means of engine downsizing. The shaded region in the figure identifies a zone in which the vehicle does not meet the driving cycle power requirements at one or more points. This condition could be obviated if a wider speed ratio range (advanced technology) CVT (or larger flywheel) were employed. As indicated, the improvements related to engine downsizing are modest, suggesting that the full size engine may be the preferred choice for this drivetrain design.

---

[4] Subsequent analyses will treat steel rotors and other flywheel system designs.

[5] Both tend to increase flywheel system losses.

The effect of flywheel spindown loss is incorporated in the fuel economy results presented in Figure 12, showing flywheel vehicle fuel economy improvement under urban cycle driving conditions, plotted as a function of trip length for two flywheel capacities. The data reflect a net flywheel loss defined by the difference between (1) the energy initially required to bring the flywheel up to design speed[6] and (2) the residual energy in the flywheel at trip end. Two extreme end conditions are considered for a given trip: one in which the flywheel is at the low end of its operating speed range (minimum spindown loss) and one in which the flywheel is at the high end of its operating speed range (maximum spindown loss). Actual flywheel speed at trip end will fall randomly between these limits, as represented by the shaded bands in the figure.

Figure 12 demonstrates that the true fuel economy benefit of the flywheel vehicle will vary significantly with trip length. The fuel economy improvement characteristic rises with increasing trip distance and asymptotically approaches the ideal (long distance) values reported in Figure 8 (see urban cycle results). The improvement is poor for short trips because the rotor spindown loss constitutes a large fraction of trip energy expenditure. At the limits defined by the break-even trip distance plateau, the flywheel vehicle provides no fuel economy advantage over the baseline conventional vehicle and is less fuel-efficient at distances below these values. The smaller capacity flywheel is seen to be distinctly superior with respect to the spindown loss effect. Therefore, it appears that the smallest wheel meeting the power requirements of the driving cycle and capable of absorbing cycle-available braking energy without saturation would be an ideal selection for the implementation of a practical vehicle system.

CONCLUSIONS

The series heat engine/flywheel automobile provides substantial fuel economy benefits for driving duty cycles in which the potential for braking energy recovery is large (e.g., taxi, urban cycles). The benefits appear to be essentially constant over a wide range of rotor energy storage capacities (for the case of the composite rotor flywheel design) and start to decay only when wheel capacity is reduced to the magnitude of the cycle-average recoverable energy level. Accessory loads have a much larger fuel efficiency impact on flywheel vehicles than on conventional vehicles for reasons cited in the analysis; a full accessory load including air conditioning reduces the fuel economy benefit of the flywheel vehicle by a factor of about one half.

For the ETV-2 flywheel system examined, parasitic losses constitute a relatively small part of total powertrain losses; therefore, technological advances in flywheel design alone do not appear to offer significant benefits in overall vehicle fuel economy improvement. Heat engine downsizing appears to have little effect on flywheel vehicle performance for the series configuration drivetrain. Flywheel spindown loss can have a significant effect on flywheel vehicle short-trip energy efficiency. The smaller rotors are best in this regard, as shown by the concept of break-even trip distance.

REFERENCES

1. "Energy Storage Systems for Automobile Propulsion," Lawrence Livermore Laboratory, Report No. UCRL-52303, December 15, 1977.

2. "Improved Fuel Economy in Automobiles by Use of a Flywheel Energy Management System," A. A. Frank and N. Beachley, Proc. 1975 Flywheel Technology Symposium, November 1975.

3. "Near-Term Electric Vehicle Program, Phase I Final Report," AiResearch Manufacturing Company, Report No. SAN/1213-1, August 1977.

4. "Hybrid Vehicle Potential Assessment," Jet Propulsion Laboratory, Report No. CONS-4209-T1, September 30, 1979.

5. "Current Status of Alternative Automotive Power Systems and Fuels -- Vol. IV, Electric and Hybrid Systems," The Aerospace Corporation, Report ATR-74(7353)-1, July 1974.

6. "Hybrid Vehicle Technology Constraints and Application Assessment Study," The Aerospace Corporation, Report No. DOT-TSC-OST-77-23, November 1977.

7. "Characterization and Applications Analysis of Energy Storage Systems," The Aerospace Corporation, Report No. ATR-77(7538)-1, December 1977.

---

[6] May not be needed for systems with adequate engine power.

PROJECT SUMMARY

Project Title: Heat Engine/Flywheel Vehicle Drive Design Results and Analysis, Phase I

Principal Investigator: Ilmar Kalns

Organization:
Eaton Corporation
Engineering & Research Center
P. O. Box 766
26201 Northwestern Highway
Southfield, Michigan 48037

Project Goals: Study heat engine-flywheel-CVT propulsion system concepts, propose an automated, product hardware-oriented system design and controls, performance test a suitable CVT, develop a mathematical model of the propulsion system and predict the fuel economy improvement of a passenger vehicle in city driving.

Project Status: A heat engine-flywheel-CVT drivetrain and controls for an automobile propulsion system has been conceptualized and a mathematical model has been formulated. Computer simulations of the system have been performed over the FUDC, and they indicate fuel economy improvement over a conventionally-equipped vehicle. Efficiency tests of a potentially suitable continuously variable element of the advanced transmission have been performed. Two preliminary layouts of the engine-flywheel-CVT systems have been completed and indicate compact size and suitability for installation in an X-body car.

Contract-Number: Subcontract 9515409

Contract Period: August 4, 1980, through September 30, 1981

Funding Level: $430,944

Funding Source: Department of Energy, University of California, Lawrence Livermore National Labs

HEAT ENGINE/FLYWHEEL VEHICLE DRIVE
DESIGN RESULTS AND ANALYSIS, PHASE I

I. Kalns
Eaton Corporation
P. O. Box 766
26201 Northwestern Highway
Southfield, Michigan 48037

ABSTRACT

A heat engine-flywheel-CVT drivetrain and controls for an automobile propulsion system has been conceptualized, and a mathematical model has been formulated. Computer simulations of the system have been performed over the FUDC, and they indicate fuel economy improvement over a conventionally-equipped vehicle. Efficiency tests of a potentially suitable continuously variable element of the advanced transmission have been performed. Two preliminary layouts of the engine-flywheel-CVT systems have been completed and indicate compact size and suitability for installation in an X-body car.

INTRODUCTION

Considerable research effort in the U.S. and abroad has gone into exploring the potential of flywheel energy storage for fuel economy improvements in vehicular systems. Analytical studies and some breadboard hardware developments of drivetrain systems show promise that these fuel economy improvements can be substantial.

Previous research efforts in flywheel technology have produced remarkable energy densities. However, research into the means by which the energy is transferred in and out of the flywheel has not been sufficient. Information to date indicates a CVT is required to provide control of the power flow. The problem is that the ratio range over which current-technology CVT elements deliver acceptably high efficiency is too narrow for use in an engine-flywheel propulsion system. A practical means to extend this ratio range is with discrete-ratio gearing. However, aside from increased parts count, the complexity becomes significant, as it is necessary to provide smooth, responsive energy flow through such a transmission during ratio changes in order to prevent unexpected skids or sudden accelerations. Therefore, research into a propulsion system that would properly integrate the heat engine, the flywheel, and the CVT into an efficient, safe, smoothly-functioning, economical automated system clearly represents a major technological challenge.

This presentation describes the Phase I effort, which consists of the following technical tasks: System Concept Selection, Control System Conceptualization, Evaluation of the Transmatic CVT, and Computer Simulation of the Propulsion System.

DRIVETRAIN CONCEPT SELECTION

Recognizing the critical importance of this task to the success of the program, considerable effort was put into screening more than ten different mechanical system arrangements.

Automatic control was addressed as a major consideration, in addition to the basic considerations of size, weight, and cost. It is to be recognized that the function of this system is considerably more varied and complex than that of a conventional automatic transmission-equipped drivetrain. Instead of one energy source, there are two—the engine and the flywheel. Also, unlike conventional automobiles, there are two absorbers—the flywheel and the service brakes. Depending on the operational mode of the vehicle, either one source alone or both sources together can be delivering power, or one source can be delivering while the other is absorbing. Transition from one combination to any other has to be smooth, safe, and has to be achieved with a minimum of energy-wasting slipping elements such as clutches. Similarly, in the braking mode, energy has to be channeled to either one or both of the two absorbers—the flywheel and the service brakes. The system has to be capable of switching from one to the other almost instantaneously but smoothly (like when the flywheel is fully charged) with minimum torque disturbance and with continuous, highly-responsive control of the deceleration rate—for safety and acceptable feel. For example, should this instantaneous, smooth transition not occur, one could foresee the car burning rubber under a start condition with a full flywheel charge or a violent jerk, or possibly a skid when the flywheel absorbing capability is reached by demand and the service brakes are applied.

These considerations make all schemes containing a driveline arrangement of two transmissions in series questionable, as range-shifting these transmissions would invariably involve driveline torque fluctuations. The search, therefore, focused on two promising, parallel arrangements. Both provide stepless ratio change throughout the vehicle speed range, eliminating the need for discrete-step transmissions.

The first arrangement, shown schematically in Figure 1, is mechanically simple, requiring only four clutch elements to perform all desired functions in the various vehicle operational modes. This concept recirculates power and draws it off when desired and in the amount desired; thus, excellent drivability with low system cost and comparative high reliability are achieved. However, these potential benefits are achieved only with a sacrifice in total system efficiency because of the recirculation of power. Nonetheless, a 16% improvement over the standard vehicle is projected for this system.

The second arrangement, shown schematically in Figure 2, is mechanically more complex, requiring eight clutch elements to perform all functions. Its predicted efficiency is significantly higher, as there is no power recirculation at any vehicle speed with this arrangement. The improvement in fuel economy is projected to be 35%. These improvements are conservative due to the excessive loss in the industrial Transmatic CVT hydraulic pump. Current investigation into the reduction of this excessive loss is being conducted.

Both arrangements have been carried through preliminary layout stage, Figure 3 and 4. Either package is sufficiently compact to fit in the engine compartment of an X-body car.

CONTROL SYSTEM CONCEPTUALIZATION

Four basic, driver-selected vehicle operational modes are contemplated: city driving with flywheel power, highway cruise with engine power, flywheel-fill mode, and flywheel-emptying mode. The control process in each mode will be automated in order to approach the drivability of conventional powertrains. The flywheel-fill and flywheel-emptying modes will require anticipatory action from the driver. For instance, when descending a grade at highway speeds, at which the flywheel is normally not used, the driver will have the option of switching from highway-cruise to flywheel-fill mode, thus regenerating energy into the flywheel for use in subsequent hill climb or passing another vehicle. Similarly, in anticipation of stopping the vehicle for an extended period, the driver will be able to select the flywheel emptying mode in order to minimize subsequent spin-down loss.

COMPUTER MODEL OF THE POWERTRAIN

A complete computer vehicle simulation model of the powertrain was developed in four months at Eaton's Engineering & Research Center when it became apparent that the use of the Boeing HEAVY program threatened to seriously delay the entire Phase I effort. The ERC model was first used to simulate a stock vehicle, then applied to the flywheel-CVT powertrain. The simulation method has been reviewed with University of Wisconsin and Aerospace Corporation researchers.

EVALUATION OF TRANSMATIC CVT

The mechanical design and hydraulic controls of the Van Doorne Transmatic were studied in considerable detail, as both represent critical subsystems in the powertrain. Efficiency tests in drive mode, coast mode, and during ratio changing have been completed. The results indicate efficiencies in the mid 80's to low 90's. As was previously mentioned, investigation is proceeding into the reduction of the hydraulic pump losses.

CONCLUSIONS AND RECOMMENDATIONS

The results reported are preliminary and are currently being refined for incorporation into the final report. The Phase I effort is scheduled to be concluded by September 30, 1981. On the basis of the preliminary results, further research into the energy transfer device and controls is recommended. In particular:

1. Combination, refinement, and consolidation of the computer simulations of Aerospace, University of Wisconsin, Boeing, and Eaton.

2. Incorporation of the Eifield hydraulic test results into the vehicle simulation and prediction of its efficiency and drivability.

3. Design, fabrication, and laboratory testing of the most promising concept.

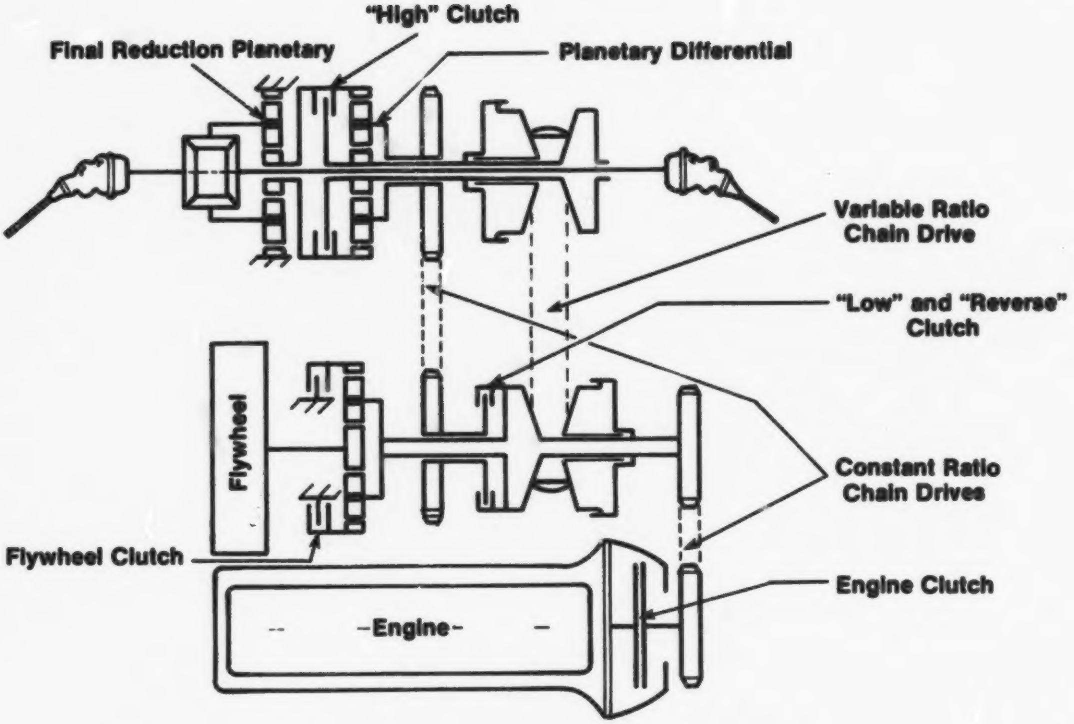
"High" Clutch
Final Reduction Planetary
Planetary Differential
Variable Ratio Chain Drive
"Low" and "Reverse" Clutch
Flywheel
Constant Ratio Chain Drives
Flywheel Clutch
Engine Clutch
–Engine–

Figure 1 **Flywheel CVT Propulsion System Recirculating Power Concept**

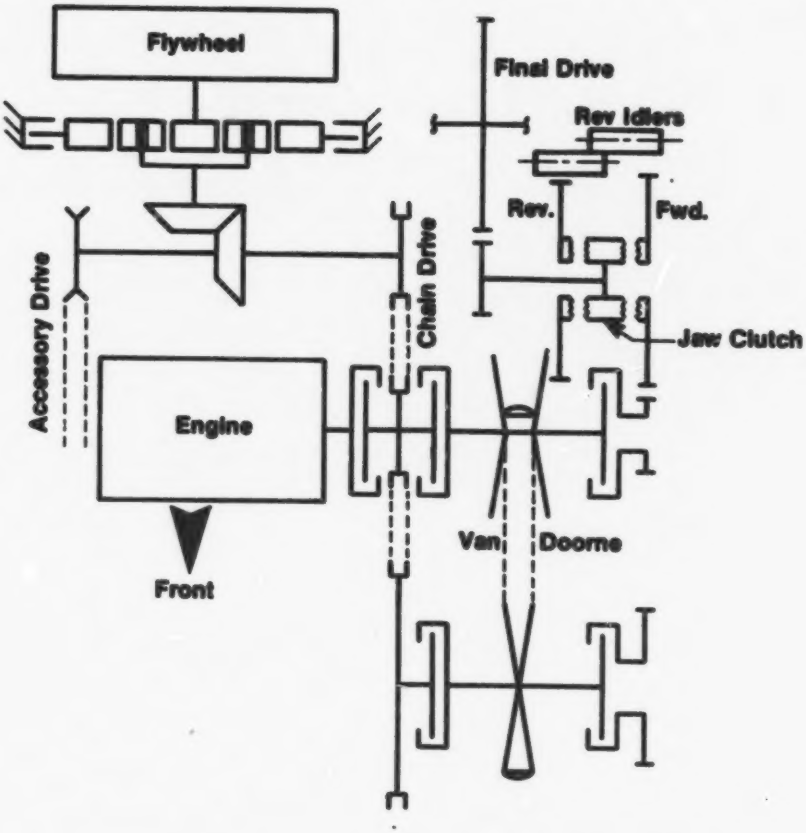
Flywheel
Final Drive
Rev Idlers
Rev.
Fwd.
Accessory Drive
Chain Drive
Jaw Clutch
Engine
Front
Van
Doorne

Figure 2 **Flywheel CVT Propulsion System Non-Recirculating Power Concept**

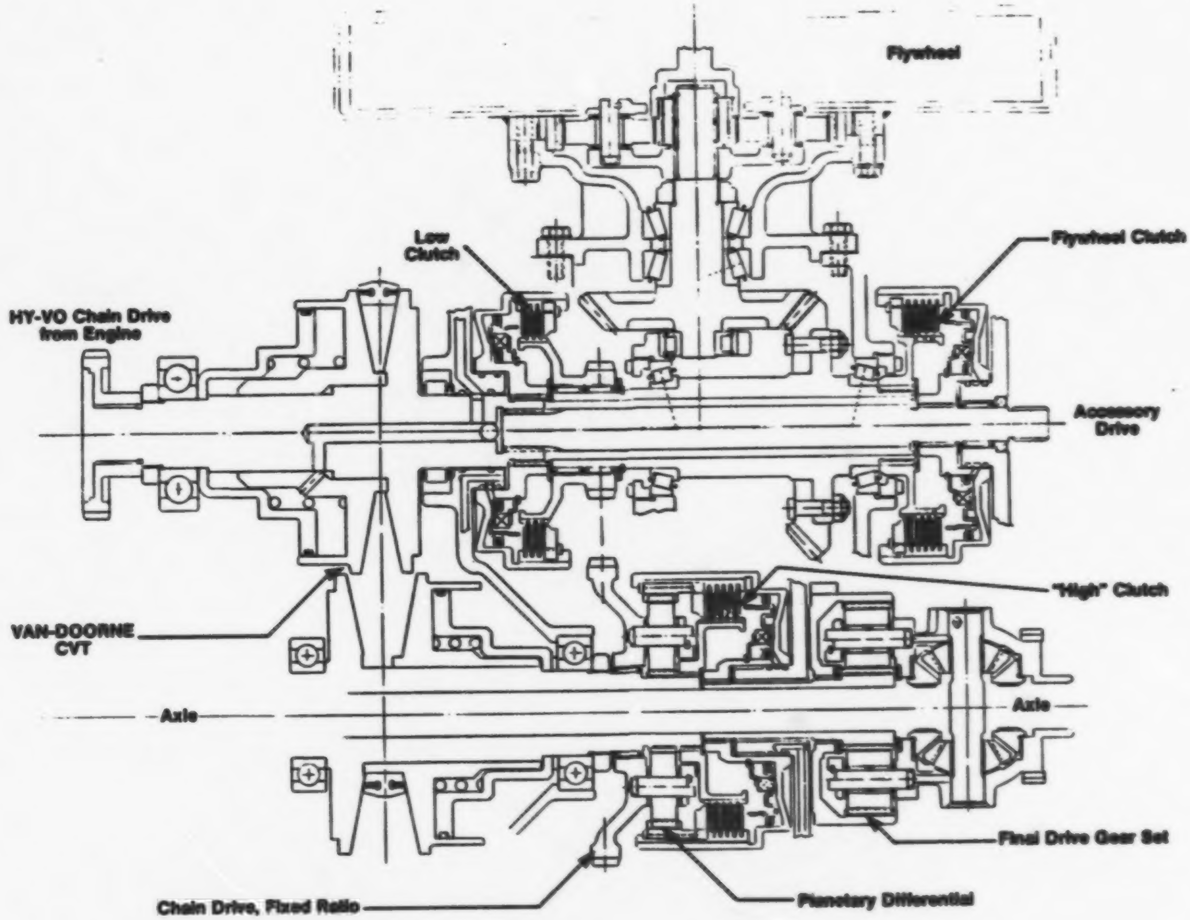
Flywheel
Low Clutch
Flywheel Clutch
HY-VO Chain Drive from Engine
Accessory Drive
"High" Clutch
VAN-DOORNE CVT
Axle
Axle
Final Drive Gear Set
Planetary Differential
Chain Drive, Fixed Ratio

Figure 3 **Preliminary Layout of the Recirculating Power Concept**

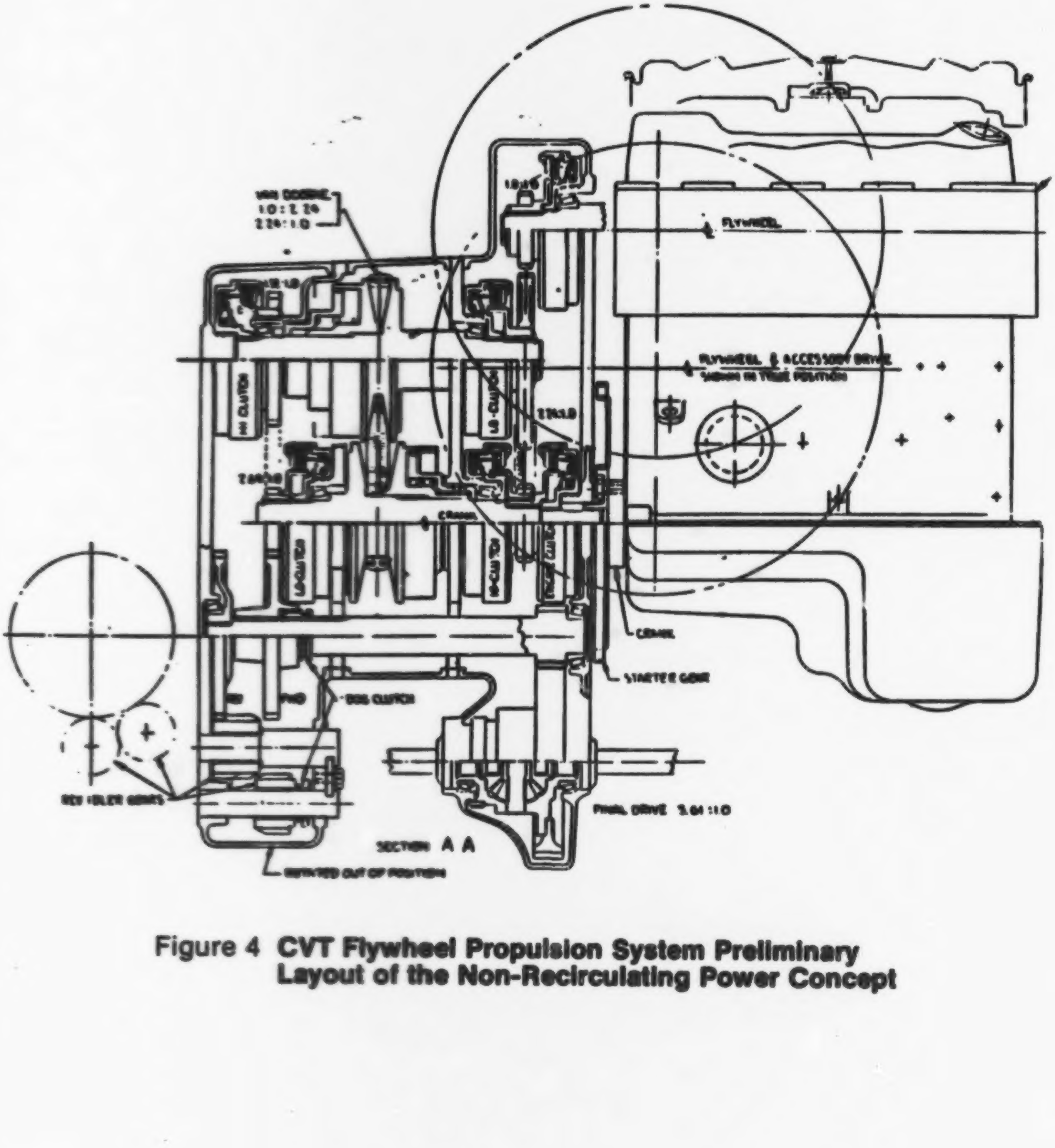
VAN DOORNE
1.0 : 2.24
2.24 : 1.0
FLYWHEEL
FLYWHEEL & ACCESSORY DRIVE
SHOWN IN TRUE POSITION
HI CLUTCH
LO CLUTCH
LO CLUTCH
HI CLUTCH
CRANK
STARTER GEAR
REV
FWD
DOG CLUTCH
REV IDLER GEARS
FINAL DRIVE 3.04 :1.0
SECTION A A
ROTATED OUT OF POSITION

Figure 4 **CVT Flywheel Propulsion System Preliminary Layout of the Non-Recirculating Power Concept**

PROJECT SUMMARY

Project Title:	Flywheel-Engine Powerplant Research and Development Studies
Principal Investigators:	Norman H. Beachley and Andrew A. Frank
Organization:	College of Engineering University of Wisconsin Madison, Wisconsin 53706
Project Goals:	Goals of this phase of the project were to (1) monitor the design of a flywheel/continuously-variable-transmission/heat-engine vehicle to be constructed by industry, (2) continue development of the continuously variable transmission (CVT) and test CVT components, (3) address the flywheel safety issue, and (4) provide a design for the control system to coordinate flywheel drive and engine-CVT drive.
Project Status:	Preliminary designs have been submitted by Eaton Corporation and Vadetec Corporation for a flywheel/heat-engine/CVT vehicle. These designs are being evaluated now for accuracy of analysis, controllability and feasibility. CVT components are being tested on a square-rig transmission tester designed and developed for testing CVT's. Results will be used to test CVT's and CVT controls. No further progress has been made on the flywheel-safety issue, since the result of our present control policy minimizes the need. Basic control principles have been proposed with operating ranges for "on-off" flywheel operation as well as continuous engine-CVT operation. Continued research will be done under sponsorship by commercial companies and other government agencies.
Contract Number:	W-7405-ENG-48, Subcontract 4492309, Amend. 3
Contract Period:	October 1, 1980, through September 30, 1981
Funding Level:	No additional funding
Funding Source:	U.S. Department of Energy through Lawrence Livermore National Laboratory

CONTROL-STRATEGY STUDY FOR A HEAT-ENGINE/FLYWHEEL/ CONTINUOUSLY-VARIABLE-TRANSMISSION VEHICLE

Andrew A. Frank Norman H. Beachley
College of Engineering
University of Wisconsin-Madison
Madison, WI 53706
(608) 263-1577

INTRODUCTION

Work began in 1973 with U.S. Department of Transportation support to greatly improve fuel economy while keeping within emission constraints. The result of a two-year study and design phase was the construction of an automobile in 1976 based upon a Ford Pinto. The vehicle was designed using a flywheel specified and purchased from Garrett Corporation AiResearch Division. The system was designed by computer simulation and projected a fuel-economy gain of 50% over a standard vehicle (reference 1). Emissions were to be at the current 1980 level. The vehicle, shown in Fig. 1, was constructed and tested both at the University of Wisconsin laboratory and the Ford Motor Company. It was found to have a 50% improvement over the standard Ford Pinto (reference 2). The mileage achieved was 32 miles per gallon on the Ford Motor Company dynamometers in Detroit.

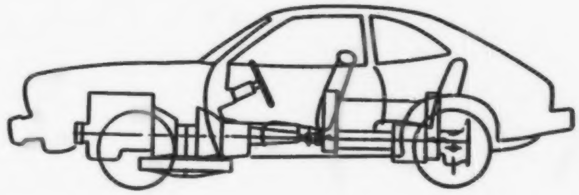

Fig. 1. Flywheel Pinto installation diagram.

In 1979, we began the design effort to construct a second-generation flywheel vehicle capable of 100% improvement in mileage over the standard-transmission automobile on the EPA city cycle. This funding was provided by the U.S. Department of Energy through Lawrence Livermore National Laboratory. The 1980 project objective was to set the design specifications for a transmission system which would be built by industry with the capability of 50 miles per gallon in a 3000-pound inertia-weight vehicle. Design areas include (1) transmission mechanical component design, (2) transmission control systems, (3) system controls and flywheel sizing studies. The objective of this report is to provide information on the last phase of our study at the University of Wisconsin, that is, the control strategy for the heat-engine/flywheel vehicle. The control strategy is interrelated with the size of the required flywheel.

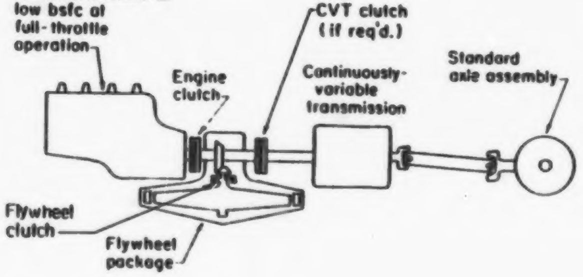
Engine calibrated for low emissions & low bsfc at full-throttle operation
CVT clutch (if req'd.)
Engine clutch
Continuously-variable transmission
Standard axle assembly
Flywheel clutch
Flywheel package

Fig. 2. Schematic diagram of a flywheel hybrid automobile.

STUDY TECHNIQUE

In order to study the control strategy for a heat-engine/flywheel vehicle, we must first design a system with a heat-engine, flywheel, and continuously variable transmission (CVT). There are a number of possible configurations which can be used for this design (reference 3). Over the past 8 to 9 years, we have evolved to a design which we feel is superior in many respects to other possible configurations. This particular configuration, shown in Fig. 2, is used for the purposes of this study. The study proceeds, however, by computer simulation. A listing of the information input to the computer-simulation program is as follows.

(1) Road load. The rolling friction of the vehicle as measured at the axle of the drive wheels is called road load. This data may be obtained by a coast-down test of a standard

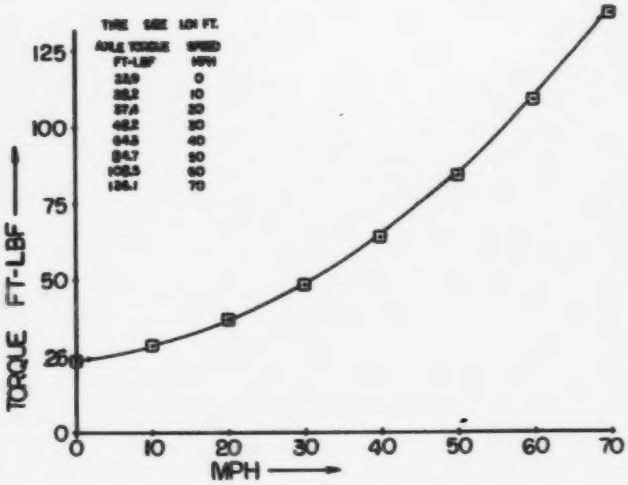

Fig. 3. Road-load standard for a 3000-lb inertia-weight vehicle.

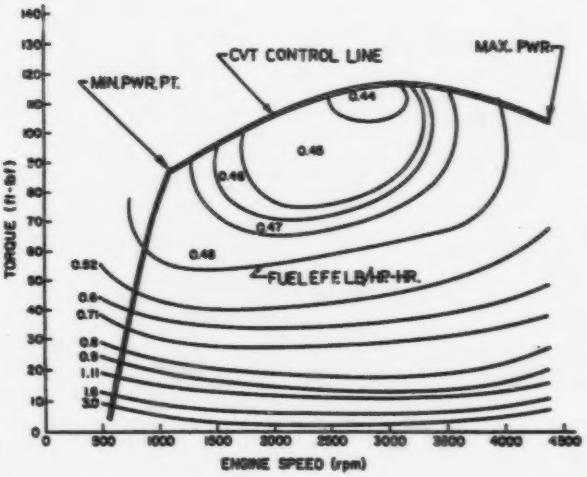

Fig. 4. CVT-engine operation line during direct drive.

vehicle, or it may be obtained by a set of rolling coefficients as determined by manufacturers for their particular vehicles. Perhaps the most important technique of obtaining this road load is to project from the EPA-city-cycle-specified load to the axle of the vehicle. The road load is given in Fig. 3. It is most important to be consistent in design on this particular figure because, obviously, a variation in the road load would greatly affect the resulting fuel economy. All researchers should use the same road load.

(2) Engine data. The engine used for this study is the Pontiac Phoenix four-cylinder engine. A map of a 1978 calibration for this engine, based on data reported by the Bartlesville Energy Technology Center in reference 4, is shown in Fig. 4. Of importance is the idle fuel-flow rate, as well as the overall fuel efficiency of this engine. Idle fuel flow for this engine is 1.5 lb/hr.

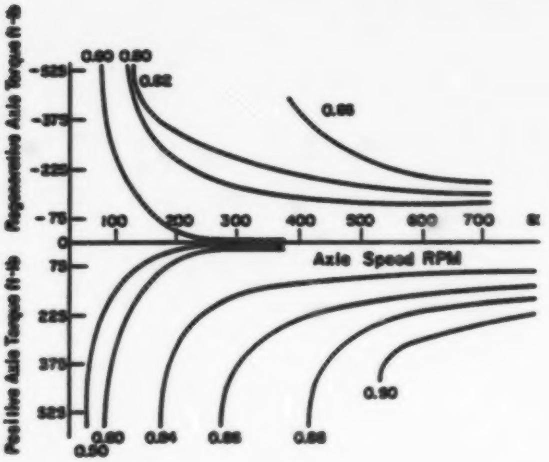

Fig. 5. Efficiency contours for a flywheel transmission with a constant 3000 rpm input.

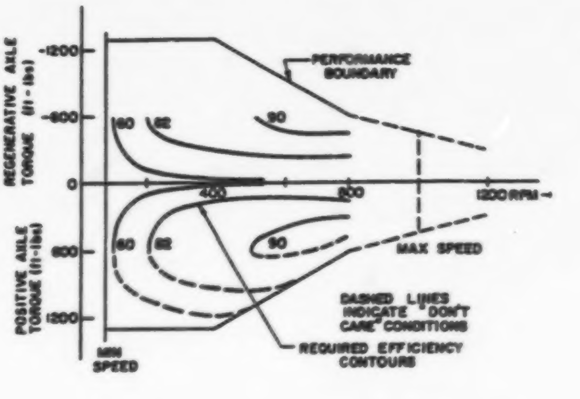

Fig. 6. Efficiency contours for a flywheel transmission vehicle and performance boundary to achieve 50 mpg at 3000 lb.

(3) Transmission-loss data. Since the major difference between the various designs is the transmission, the loss data for the transmission are the most crucial portion of this simulation. We at the University of Wisconsin on an earlier phase of this contract developed a transmission-efficiency map as a goal for each transmission to be designed for this project. This map is shown in Figs. 5 and 6. For the purposes of our simulation, we are using this transmission-efficiency map.

(4) Accessory data. At the present time, we have assumed that all accessories are included in the engine data. That is, the alternator, water pump, exhaust, etc., are part of the engine map. There is no power steering for this particular vehicle, and the losses due to a power-steering pump have not been included. Also, air conditioning is not included in this particular design.

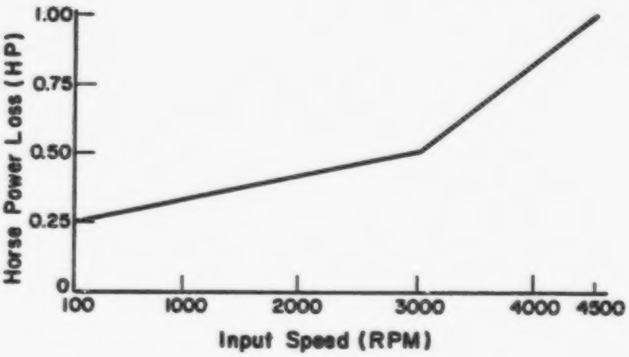

Fig. 7. Maximum permissible spin-loss requirement for flywheel CVT at the input shaft.

(5) Flywheel-loss data. Based upon the experimental flywheel Pinto, we have projected a flywheel loss of no more than 1 hp at 5000 rpm from the entire flywheel package. This loss includes the windage in the flywheel itself, the gearbox, and the clutches connected to either side of the flywheel. Thus, the flywheel system in the vehicle with the clutch open would experience a maximum loss of 1 hp at 5000 rpm, decreasing to the 1.8 power of rpm, as shown in Fig. 7. This loss correlates with the losses found experimentally in our 1976 Pinto.

COMPUTER ANALYSIS TECHNIQUE

There are two computer-analysis techniques used. The first is termed the second-by-second method. This technique uses Newton's equation of motion, i.e., $f = ma$, $v = \int a\, dt$, and $s = \int v\, dt$. The f or force is the force on the vehicle developed by the driveline acting on the wheels. We then proceed from the wheels through the driveline to the transmission and finally to the flywheel and/or engine. In this procession, we include the losses due to road load, the losses due to the final driveline, (i.e, tires and axle), and the losses through the transmission. If the flywheel is used, then the flywheel losses are also included. The losses through the transmission, driveline, and flywheel are a function of the actual torque and speed required at every point in this driveline. Flywheel losses are spin losses plus 3% of the torque transmitted. The resulting velocity is dependent on the amount of force commanded, but the amount from the engine is unknown because the losses are unknown; therefore, we have to use feedback to determine correct vehicle speed, or we have to iterate to compute implicitly

Table. 1. Axle state frequency matrix.

Velocity	0	0	7	14	21	28	35	42	50
(mph)	0	7	14	21	28	35	42	50	57
Velocity	0	0	100	200	300	400	500	600	700
(rpm)	0	100	200	300	400	500	600	700	800
Torque (ft-lbf)									
-750- -600	0	0	0	0	0	0	0	0	0
-600- -450	0	0	.07	0	0	0	0	0	0
-450- -300	0	2.12	2.70	2.56	1.02	.07	0	0	0
-300- -150	0	1.31	.15	1.39	.95	.44	.15	0	0
-150- 0	0	.80	.95	1.97	5.70	1.75	.22	.29	.44
0- 0	17.60	0	0	0	0	0	0	0	0
0- 150	0	.73	.73	3.73	17.53	7.60	.37	1.53	3.80
150- 300	0	1.17	.88	3.80	3.73	.95	.29	.58	.95
300- 450	0	.95	1.24	1.53	.44	.22	.07	.07	0
450- 600	0	1.68	1.75	.80	.07	.15	0	0	0
600- 750	0	0	0	0	0	0	0	0	0

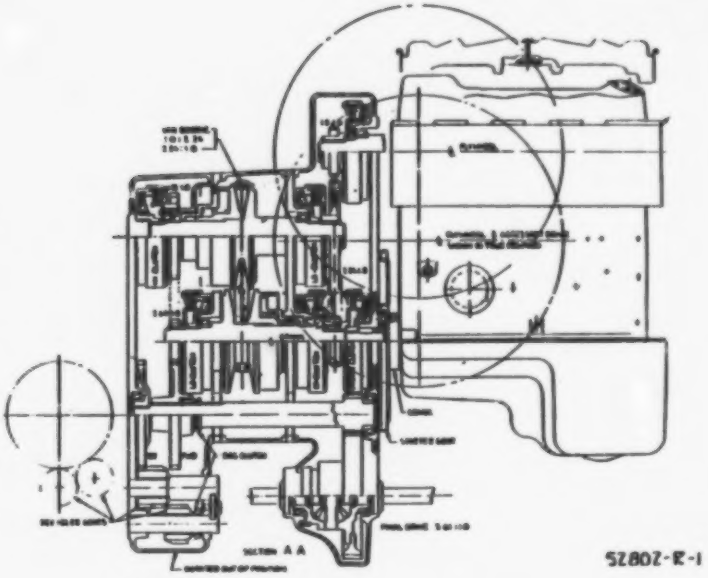

Fig. 8. Eaton-designed van Doorne 25:1 transmission.

the correct torque from the engine or flywheel.

The second method of analysis is what we term the steady-state matrix method. Here we again begin with Newton's equation of motion, $f = ma$, but now we say $a_{k'} = (v_k - v_{k-1})/2$ and $f_{k'} = ma_{k'}$ . . In this case, we begin with the required acceleration as derived from a driving cycle and then develop a time-torque-speed discrete matrix, as shown in Table 1. We consolidate some of these 1371 points for the city driving cycle into approximately 100 such points, and from this we then are able to study the losses in the system. Far less computer time is required for this technique as compared to the second-by-second method.

Both techniques are used for analysis and are checked periodically to see that the results correspond.

TRANSMISSION-COMPONENT POSSIBILITIES AND MECHANICAL REQUIREMENTS

From our developed transmission specifications stated above, one should note that the transmission maximum-power requirement is 100 hp. The torque maximum at the axle is 1250 ft-lbf, and the maximum axle speed is above 1200 rpm. There are many possible mechanical components. The first is a variable steel belt or van Doorne, the second is a hydrostatic unit, the third is a traction-drive unit, and the fourth is a slipping-clutch/torque-converter unit. These are shown in Figs. 8, 9, 10, and 11.

TRANSMISSION-CONTROL CONCEPT

For any of the transmissions described, the essential control concept is the ability to provide output-torque control. That is, the ratio of these transmissions must be set by some automatic mechanism which will provide the correct output torque as commanded by a driver. Thus, the driver accelerator pedal or brake pedal will command either a positive or a negative output torque, and the transmission ratio and ratio rate must be set in such a way that the correct output torque is developed. This concept is fundamental for the flywheel driving mode. If we have the flywheel disconnected and only the engine connected to the input of the CVT, we are still interested in the output torque. The transmission then must find the ratio which will provide that particular output torque, depending on the engine operating condition. If the engine in this mode is designated to operate along a certain torque-speed line, then the output-torque command requires a change in engine speed to provide the desired output torque. Thus, as the accelerator pedal is moved, the engine speed varies more than the engine torque. The engine operating line will be as shown in Fig. 4.

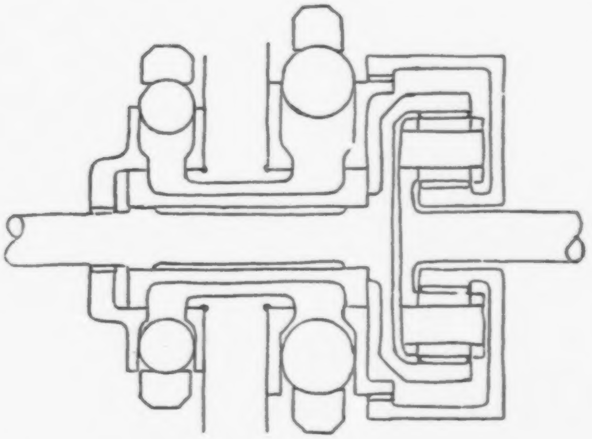

Fig. 9. Proposed hydrostatic power-split CVT configuration as a torque converter replacement for a 4-speed transmission.

If a flywheel is connected to the system, the torque ratio and ratio rate will be adjusted to provide the output torque. The

Fig. 10. Vadetec traction-drive CVT for a 3000-lb vehicle with 13.4:1 ratio range.

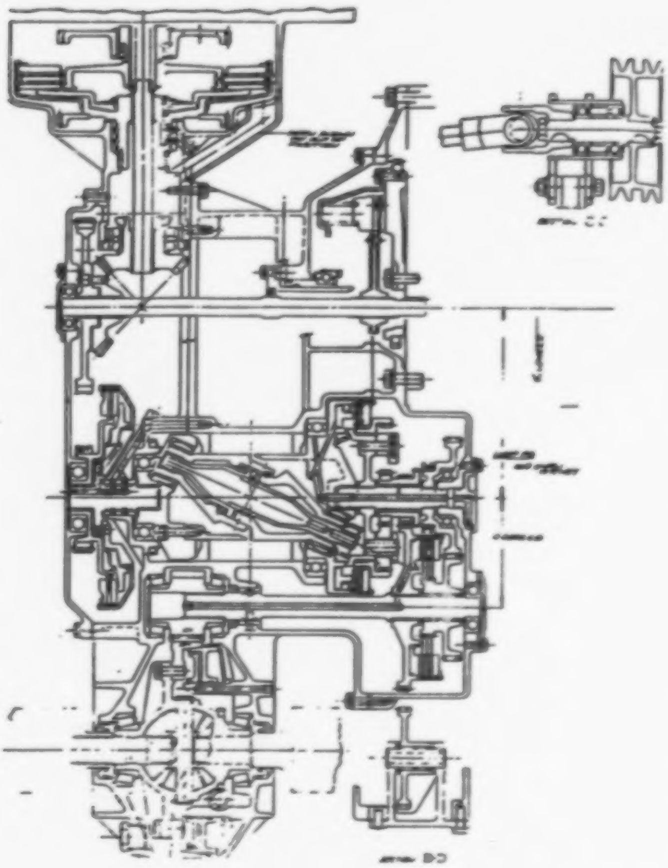

change from flywheel mode to engine mode may require a change in system gain to provide comparable response whether the system is running on the engine or the flywheel.

ENGINE CONTROLS

From our discussion of the transmission system, there are obviously two possible modes of operation, that is, engine-CVT or flywheel-CVT. The controls for the engine must be designed so that it is compatible with both modes of operation. In the flywheel mode the engine will be run "on" and "off." But when the engine is "on," it will operate over a specified torque-speed line. With the flywheel disconnected, the engine-CVT system should operate along this same line at the prescribed engine speeds and torques. However, because in the engine-CVT mode there is greater flexibility required of the engine, the engine will be allowed to go down to idle as shown in Fig. 4. Thus, the engine-operation line is selected as shown in this figure. The difference in operation is that the engine in the CVT mode is operating continuously and is operating on-off in the flywheel mode.

SYSTEM CONTROLS

From the studies made on different types of driving cycles with different average speeds, we find that if a vehicle is driving with an average speed above about 45 mph, as shown in Fig. 12, the on-off flywheel concept no longer contributes a very large percentage to the possible fuel-economy gain of an automobile. Thus, we find that the flywheel would be used most effectively in the low-speed regime of the automotive drive cycles. That is, in the city the flywheel is most useful. The reason for this is shown in Fig. 13, showing the amount of regenerative energy available as a function of average vehicle speed. Once the vehicle average speed goes above 45, it becomes justified to remove the flywheel from the system and allow the engine to operate continuously. This philosophy leads to a concept of a much smaller required flywheel. Thus, for the 3000-pound inertia-weight vehicle, we are projecting a flywheel size of approximately 0.3 hp-hr--or a flywheel less than 1/4 kw-hr. Such a flywheel size implies that a steel wheel weighing less than 60 lb would be adequate for this 3000-lb vehicle. While we could go to a composite wheel of perhaps 30 lb, the savings in weight would not necessarily

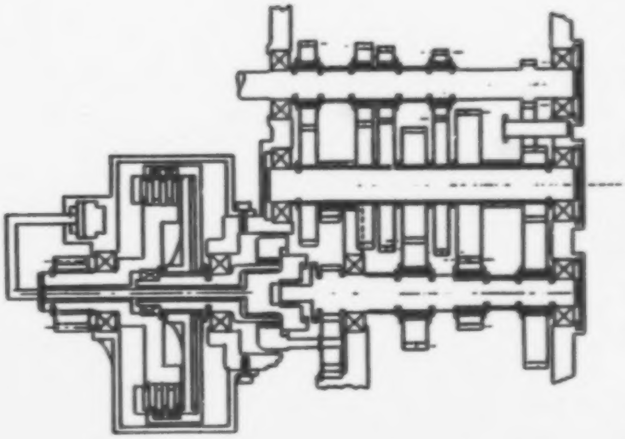

Fig. 11. Ten-speed slipping-clutch transmission.

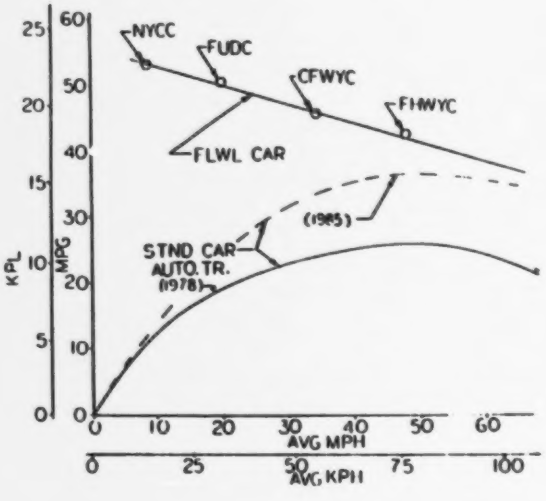

Fig. 12. Fuel economy of the flywheel energy-storage vehicle compared with a standard 3000-lb automatic-transmission car over various drive cycles.

justify the cost. The operating policy is shown in Fig. 14. This figure shows a plot of engine speed versus vehicle speed and the region of flywheel operation. The EPA city fuel economy is not affected using this control policy.

CONCLUSIONS

Feasibility of a flywheel-drive automobile has been demonstrated by an experimental vehicle which has achieved 32 mpg using a hydrostatic power-split transmission built in our laboratory at the University of Wisconsin-Madison. In the design of this transmission, we have avoided design pitfalls such as spin loss and poor transmission efficiency in the inappropriate torque-speed ranges. Thus, new projects being undertaken should be wary of such pitfalls and design their systems to avoid such problems.

Controls for the flywheel-CVT power-plant system are to be accomplished completely without the aid of a computer. Thus, hydraulic or mechanical implementations of the control system can be anticipated. We are currently designing such control systems for vehicles.

The primary control strategy being investigated is to use the flywheel system and the engine in an "on-off" mode below 45 mph. The engine would be used continuously above 45 mph, with the flywheel disconnected from the system. Thus, the flywheel would be allowed to run down if the vehicle cruises at speeds above 45 mph for a length of time. In addition, an advantage to this kind of system is that the flywheel can be smaller and also can be controlled to run at its minimum speed at high vehicle speeds. Eventually, the flywheel will slow to a complete stop if the vehicle is maintained at speeds above 45 mph. This means that the safety features of the flywheel can be reduced because the flywheel

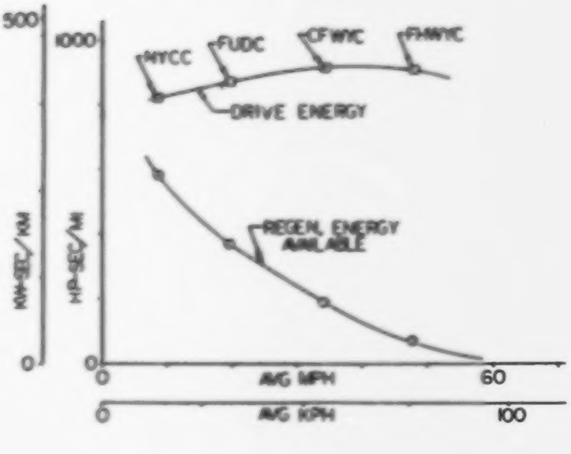

Fig. 13. Positive energy required and negative energy available for various drive cycles.

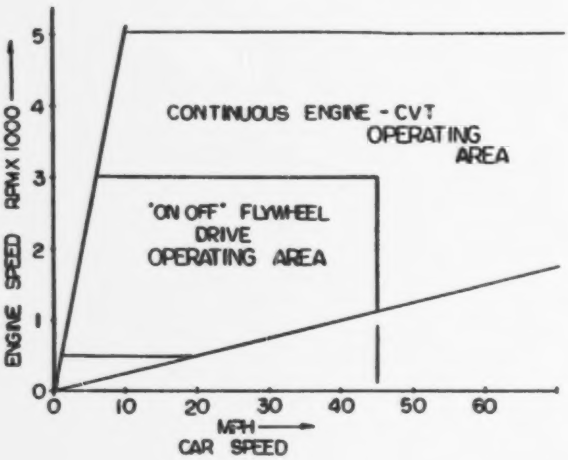

Fig. 14. Operating range of proposed flywheel-CVT transmission.

will not be spinning at high speeds at high vehicle speeds. Thus, the fear of a 60-mph crash with the flywheel at full speed will be eliminated, since this condition would not exist.

The control strategy has yielded a small flywheel for a 3000-lb vehicle. The flywheel required using this control strategy is 1/4 kw-hr. Of course, for a smaller vehicle, i.e., lower inertia weight, the flywheel size would be proportionally smaller. The mileage, however, is inversely proportional to the weight. Thus, a small 1500-lb vehicle with a 1/8-kw-hr flywheel would have an EPA mileage goal of 100 mpg. This size vehicle is being planned for production by many auto companies.

There has been some reluctance on the part of auto manufacturers to look carefully at the flywheel energy-storage techniques. This stems partially from the drastic change in the control concepts of an automobile, for example, the accelerator pedal being connected only to the transmission and not the engine, and the engine operating "on" for 30 sec and "off" for 3-5 min. It is suggested that an alternative two-phase program to further interest the auto companies be undertaken to fit in the context of energy storage. This two-phase effort would consist of a phase 1 in which an engine/continuously-variable-transmission vehicle is designed and a phase 2 in which a flywheel is added to such a vehicle. Thus, confidence would be built into the automotive companies, since the continuously-variable-transmission/engine system would not be a radical departure from the standard transmission system. In actual fact, there will be radical changes if the engine operates at its most efficient point, since the engine would not be throttled to vary output power. However, from a cursory look, the engine-CVT system is not a radical departure from the conventional engine-transmission systems today. At least the engine would operate continuously. This technique of a two-phase program may be more palatable than projecting an energy-storage vehicle from the beginning.

In both phases, however, it must be shown to the automobile companies that a control system can be implemented which is simple, controllable by anyone, and fully automatic. Further, the control system should not initially require a computer, since the cost of electronics and equipment associated with a computer can make the system noncompetitive with conventional systems. Finally, with such a transmission and such a control system, it should be shown that simplifications in the prime mover and the overall vehicle can result. It is thus recommended that this program proceed with a phase 1 to develop a continuously-variable-transmission automobile without a flywheel and that later, after such an investigation and a demonstration vehicle are completed, the flywheel be added to show the increased improvement.

REFERENCES

1. A. A. Frank, N. H. Beachley, R. W. Harter, A. P. Dietrich, K. C. Lau, "Continuously-Variable Transmission Concepts Suitable for Flywheel Hybrid Automobiles." Proceedings of the 12th Inter-Society Energy Conversion Engineering Conference, Washington, D. C., Aug. 28-Sept. 2, 1977, pp. 26-33.

2. A. A. Frank, N. H. Beachley, "Evaluation of the Flywheel Drive Concept for Passenger Vehicles" (SAE 790049). SAE 1979 Transactions, Society of Automotive Engineers, Inc., 1980, pp. 230-241.

3. A. A. Frank and N. H. Beachley, "Design Considerations for Flywheel-Transmission Automobiles" (SAE 800886). Automotive Engineering, vol. 88, 1980, pp. 77-83.

4. D. E. Koehler, W. F. Marshall, Performance Characteristics of Automotive Engines in the United States; Third Series - Report No. 4, 1978 Pontiac, 151 CID (2.5 Liters), 2V. Bartlesville Energy Technology Center, Bartlesville, OK, Feb. 1979 (prepared for U. S. Dept. of Transportation, Report No. DOT-TSC-NHTSA-79-4).

PROJECT SUMMARY

Project Title: Regenerative Braking Through Elastomeric Energy Storage

Principal Investigator: Lyle O. Hoppie

Organization:
Eaton Corporation
Engineering & Research Center
P. O. Box 766
26201 Northwestern Highway
Southfield, Michigan 48037

Project Goals: Determine the technical and economical feasibility of an elastomeric regenerative braking system (ERBS) for automotive applications.

Project Status: Phase II-B of this project was initiated in June 1980 and covers the following major tasks:

- Verify, through test and evaluation of full-size elastomeric energy storage units, the theoretical predictions which were based on previous small-scale experimental results.
- Conceive of a compact method of mechanically attaching the elastomers, followed by test and evaluation on small-scale units.
- Incorporation of the compact method of mechanical attachment into full-size units, followed by test and evaluation.
- Selection of an energy transfer device and control strategy.
- Design, fabrication, test and evaluation of a small-scale elastomeric regenerative braking system.

With regard to the full-size unit and its mechanical attachment, several fabrication-related difficulties were initially encountered, but recent results are encouraging. The small-scale system is currently being assembled for laboratory testing.

Contract-Number: University of California Subcontract 2617509

Contract Period: June 1980 - October 1981 for Phase II-B

Funding Level: $272,000 for Phase II-B

Funding Source: U. S. Department of Energy through Lawrence Livermore Laboratory

REGENERATIVE BRAKING THROUGH ELASTOMERIC ENERGY STORAGE

L. O. Hoppie and G. C. Nowell
Eaton Corporation
P. O. Box 766
26201 Northwestern Highway
Southfield, Michigan 48037

ABSTRACT

Full-size elastomers, ultimately intended as the energy storage device of an automotive regenerative braking system, have been fabricated and are currently undergoing test and evaluation. A small-scale elastomeric regenerative braking system incorporating the simplest energy transfer device yet conceived has been designed and fabricated and is presently being assembled. The system will be tested in order to measure system efficiency during transient speed conditions such that more accurate estimates of energy savings in an actual automotive application can be made. Experiments will also be carried out to see if there are any control problems requiring further research and development.

INTRODUCTION

At the previous STOR meeting, it was reported(1) that our attention was being focused on the Axially-Loaded Torsion stressing scheme, wherein isolated elastomeric rods are initially stretched and then restrained from motion in the axial direction: energy is delivered to or from the elastomer by rotating one end relative to the other. Based on previous small-scale experimental results, it was projected that the kinetic energy of an "X" car traveling at 30 mph (approximately 10^5 J) could be stored in about 1.2 ft^3 of elastomer.

A tentative design for an "X" car involving two units each initially 2' long by 7.5" diameter axially loaded such that the lengths and diameters become 8' and 3.75", respectively, was then arrived at. Subsequently, units such as shown in Figure 1 were fabricated by Teledyne-Monarch Rubber Company and are currently under test.

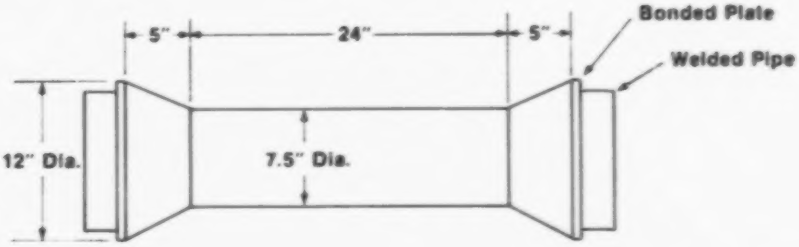

Figure 1 Dimensions of Full-Size Axially Loaded Torsion Energy Storage Units

Note the uniform section of the elastomer has the dimensions indicated above, that the ends are flared to a 12" diameter, and that steel plates are bonded onto the elastomer as a straightforward method of attachment. This attachment method was chosen for the initial full-scale tests as it was felt that bonding to such a large plate would reduce the bond stress and present no unanticipated problems. This method is impractical in an automotive application, however, because of the excessive volume required by the ends. Another objective of the current effort, therefore, is to conceive of a compact method of attachment. Experimental results obtained during the testing of the units indicated by Figure 1 are presented in the next section.

Also presented at the previous STOR meeting were results of the theoretical analyses of several devices which permit the transfer of energy between the vehicle and the elastomer. Since that time, we have designed and are currently fabricating a complete small-scale elastomeric regenerative braking system incorporating one of these energy transfer devices. The control strategy and design of this system are described in the last section.

TEST RESULTS ON FULL-SIZE UNITS

In this section, theoretical and experimental results on full-size elastomeric energy storage units are presented. Included are torque and axial load versus rotation characteristics, energy density and round-trip energy transfer efficiency, and some initial data on fatigue life and stress-relaxation.

Torque and Axial Load Characteristics

Rivlin$^{(2)}$ has considered the case of large deflections in elastomers and his theory can be applied to the Axially-Loaded Torsion stressing scheme prior to the occurrence of the first knot. His theory predicts that the torque and axial load are given by:

$$T = r_i^4 M\theta/(\lambda l_i) \qquad (1)$$

$$F_z = 2\pi r_i^2\, M(\lambda - 1/\lambda^2) - \frac{\pi}{2}\, r_i^4 M(\theta/\lambda l_i)^2 \qquad (2)$$

where r_i and l_i are the initial radius and length of a circular rod, θ is the rotational angle in radians, M is a material property having units of a modulus (force per unit area), and λ is the elongation:

$$\lambda = \frac{l_f}{l_i}, \qquad (3)$$

l_f being the final length of the rod after it is stretched. Previous curve fitting to small-scale experimental results led to the approximate empirical result:

$$\theta_{Max} = \frac{\pi}{2}\frac{l_i}{r_i}\lambda^{3/2} \qquad (4)$$

as the rotational angle at which the first knot occurs. The maximum rotational energy which can be stored prior to the occurrence of the first knot is thus given by:

$$E_{Max} = \int_0^{\theta_{Max}} T(\theta)\, d\theta \qquad (5)$$

which leads to:

$$\frac{E_{Max}}{V_{Elas}} = \frac{E_{Max}}{V_{Total}} = \frac{M}{2}\left(\frac{\pi}{2}\right)^2 \lambda^2 \qquad (6)$$

as the energy density of a nonbuckling, Axially-Loaded Torsion bar.

Some of the initial results obtained during the recent testing of a full-size unit are shown in Figure 2, where the effect of preloading the unit axially can be seen. Also indicated are the theoretical curves of Rivlin, Equations 1 and 2. For each curve in Figure 2, the rotation was reversed at the point at which buckling was about to occur and then decreased to zero. Note that for the torque curve with $\lambda = 3.0$, however, buckling did occur and the first "knot" was generated. A photograph of the unit at $\lambda = 3.0$ and an as-received unit are shown in Figure 3.

These and other data confirmed that the energy which can be stored in a nonbuckling, Axially-Loaded Torsion bar is given approximately by Equation 6, and as indicated above, the tentative design calls for the value $\lambda = 4$.

Fatigue Life, Energy Density and Efficiency

Before the unit was axially loaded to $\lambda = 4.0$, an endurance test at $\lambda = 3.0$ was initiated. During this test, the elongation was maintained at $\lambda = 3.0$ while one end was repeatedly rotated relative to the other end between 0.0 and 7.2 revolutions and back again in 15 seconds. Data for the 100,000th cycle are shown in Figure 4, where several significant features can be observed:

- The round-trip efficiency for rotational energy transfer exceeds 0.98.

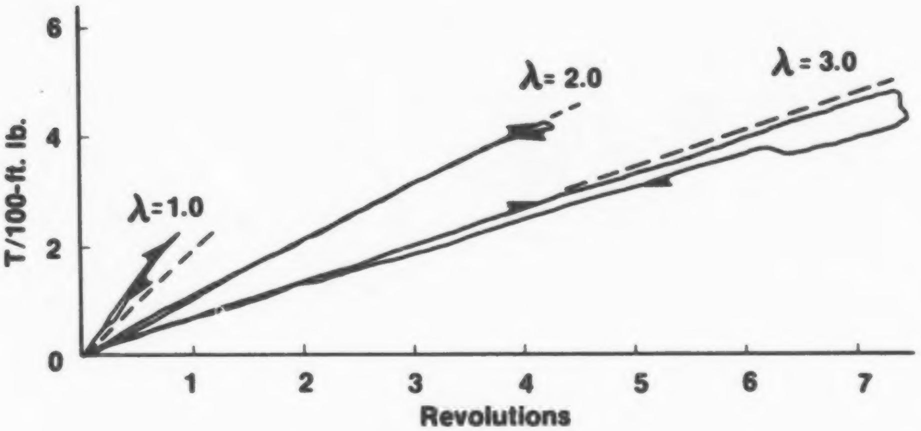

2(a) Torque Characteristics of a Full-Size Axially Loaded Torsion Energy Storage Unit with Elongation, λ, as Parameter

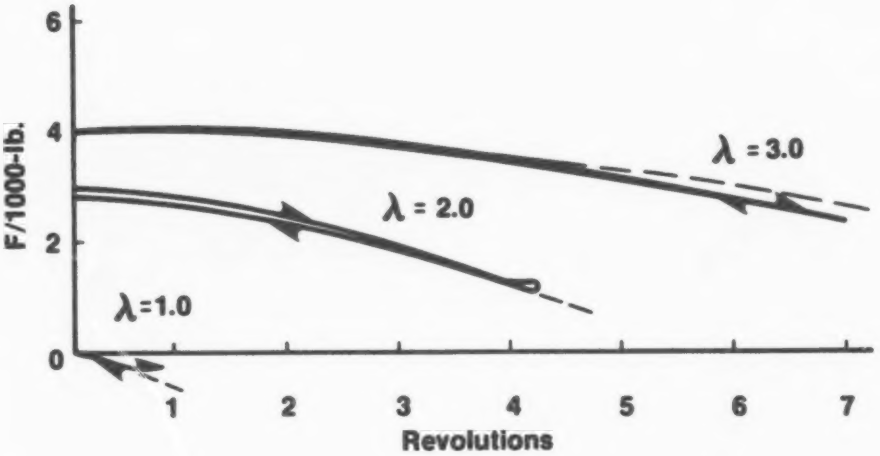

2(b) Axial Load Characteristics of a Full-Size Axially Loaded Torsion Energy Storage Unit with Elongation, λ, as Parameter

Figure 2 Initial Characteristics of a Full-Size Energy Storage Unit. Predicted Results Are Indicated by Dashed Lines.

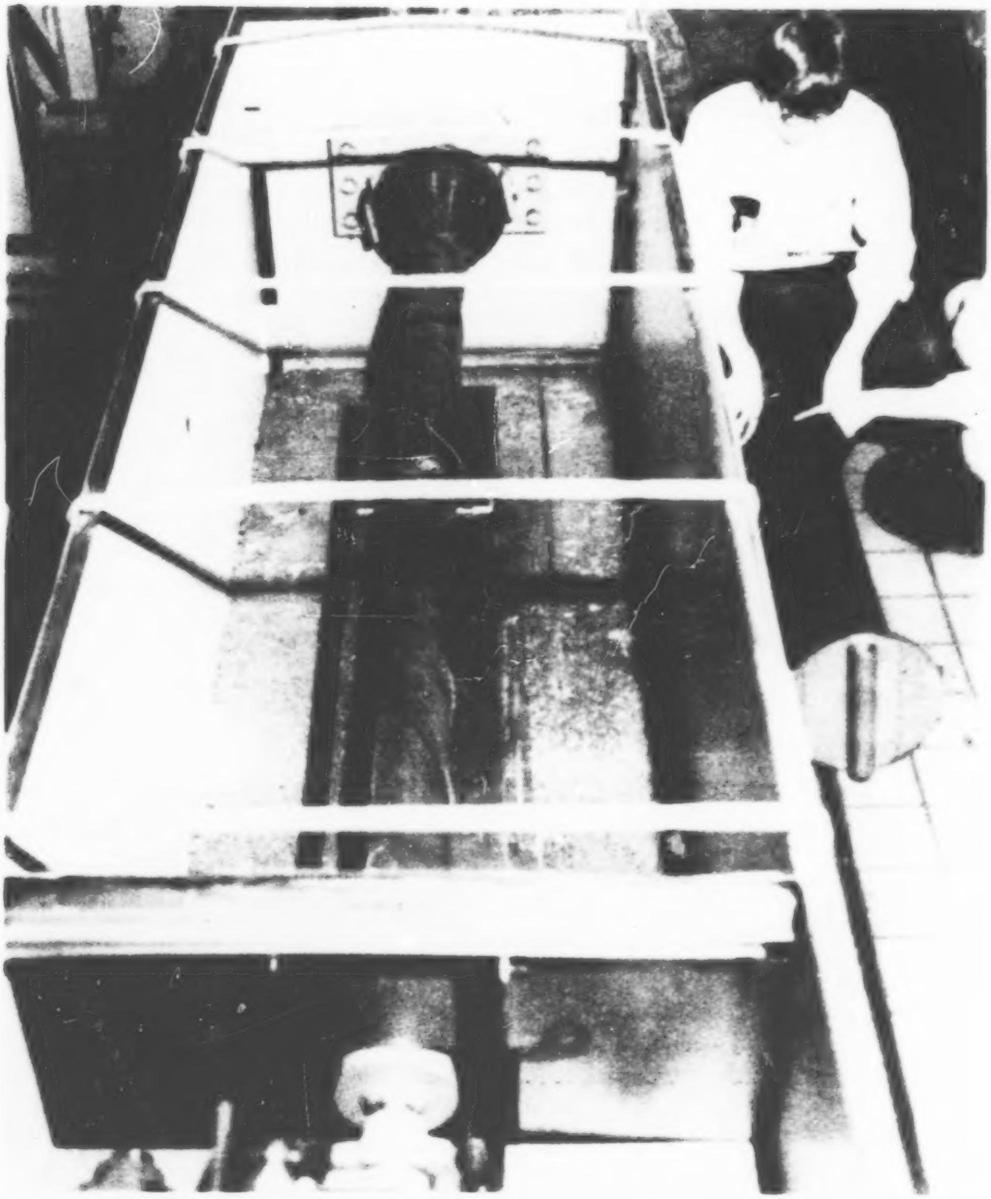

Figure 3 Full-Size Axially-Loaded Torsion Energy Storage Unit Under Test at $\lambda = 3.0$

- The axial load data shows a type of "hysteresis" even though the torque data does not. This phenomena is not understood.

- Compared to early cycles (not shown), the energy density has fallen by only about six percent, i.e., from 0.696 J/cm^3 to 0.653 J/cm^3 at cycle 100,000.

- The torque curve indicates zero torque for 0.0 $\leq$ revolutions $\leq$ 0.3, which shows that rotational set has occured. Other data, however, show that recovery does occur if zero revolutions are maintained for a few minutes.

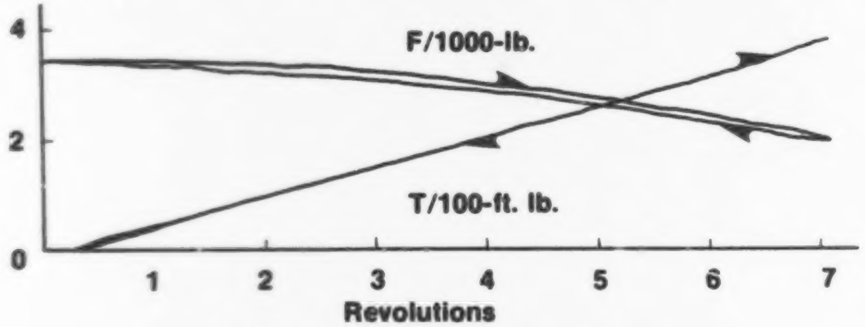

Figure 4 Characteristics of a Full-Size Axially Loaded Torsion Energy Storage Unit After 100,000 Cycles at λ =3.0

Shortly after the data shown in Figure 4 were recorded, the unit was loaded to λ = 4.0 and the endurance test was continued. Figure 5 shows the last recorded data, cycle 158,904: failure occurred at cycle 173,657. From Figure 5 it can be seen that the efficiency was 0.963 and the energy density was 1.06 J/cm^3.

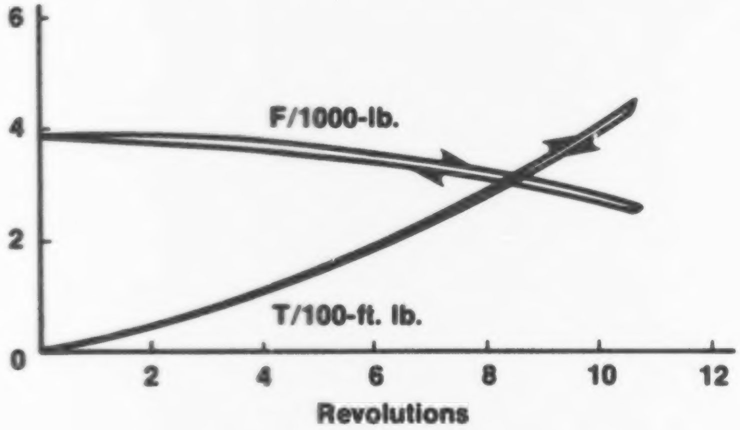

Figure 5 Characteristics of a Full-Size Axially Loaded Torsion Energy Storage Unit After 100,000 Cycles at λ=3.0 and 58,900 Additional Cycles at λ=4.0

These and other results on full-size units stressed in the Axially-Loaded Torsion scheme clearly demonstrate the following:

- Torque, axial load and energy density versus revolutions can be adequately predicted in terms of size, geometry and material properties.

- Efficiencies even higher than anticipated are achievable in full-size units at an elongation of 4.0.

- A fatigue life of 50,000 cycles (the preliminary goal) is achievable.

It must be pointed out, however, that the energy density of the aforementioned unit is only about one half that obtained on small-scale samples. This is because the modulus of the full-size unit was lower than that of the small-scale samples by about fifty percent. Consequently, Teledyne-Monarch Rubber Company altered the curing cycle of the elastomer in an attempt to correct this situation. Test results for the unit fabricated with the altered curing cycle at $\lambda = 5.0$ are shown in Figure 6. Note that the energy density was more than doubled to 2.48 J/cm^3 and that the round-trip energy transfer efficiency was 0.948. This unit, however, had a surface flaw which soon developed into a large tear after a few hundred cycles. Additional units will be tested in an attempt to determine the energy density/fatigue life trade-off.

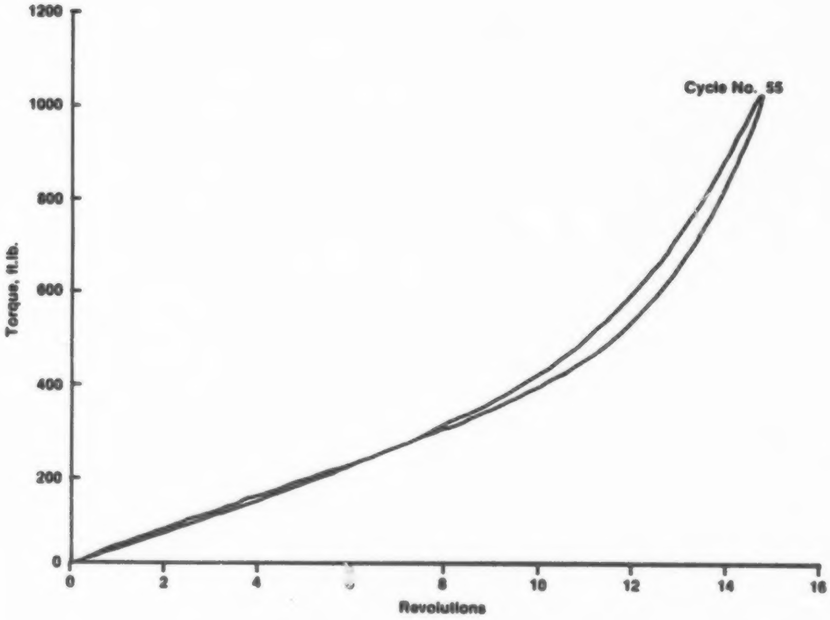

Figure 6 Torque-Rotation Characteristics of Latest Elastomeric Energy Storage Unit at $\lambda = 5.0$

Prolonged Energy Storage

During the aforementioned fatigue-life test, the dwell time at zero revolutions (zero energy storage) and maximum revolutions (maximum energy storage) was essentially zero. In order to investigate the effect prolonged energy storage as would result if a vehicle were parked with the elastomer fully charged, for example, the unit depicted in Figure 3 was restrained at the maximum energy storage condition for 50 hours immediately after cycle 100,001. Figure 7 shows the end point of this cycle, the return to zero energy after 50 hours of energy retention, and the next complete cycle. From this data it can be seen that:

- Approximately 95 percent of the energy initially delivered to the elastomer was extracted after being retained for 50 hours. The 5 percent loss is attributable to stress-relaxation.
- The next complete cycle shows unit efficiency and an energy storage capacity approximately 97 percent of the value prior to the prolonged energy storage test. This result shows that large moulded elastomers exhibit recovery, as was anticipated.

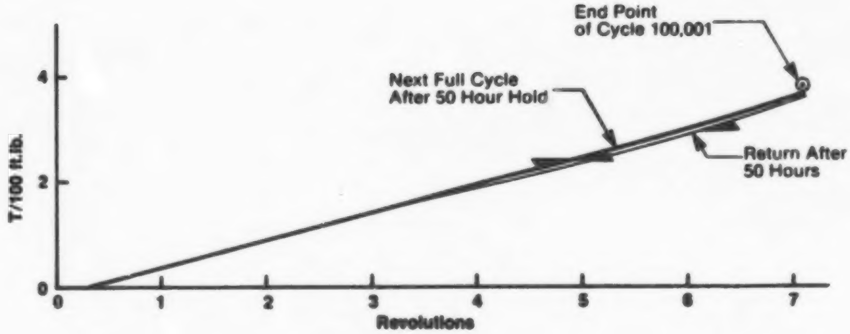

Figure 7 Torque-Rotation Characteristics During an Energy Retention Test

Long-Term Stress-Relaxation

As the endurance test was being carried out, the maximum axial load and torque were periodically recorded in order to investigate the effects of stress-relaxation on a full-size unit. Results are shown in Figure 8, wherein the open circles are data for $\lambda = 3.0$ plotted versus the number of days the unit was at $\lambda = 3.0$, and the solid circles are data for $\lambda = 4.0$ plotted versus the number of days the unit was at $\lambda = 4.0$ (NOT the cumulative number of days the unit was at $\lambda = 3.0$ and 4.0). The scatter in the axial load data, Figure 8(a), is primarily due to the Joule Effect since the temperature of the laboratory varied by ±3 kelvin as the endurance test was being carried out. It is noteworthy that as the elastomer was being cyclically stressed and relaxed, no variation in surface temperature could be detected with the bare hand.

Significantly more scatter can be seen in the torque data, Figure 8(b), primarily because the controller did not cause the unit to be rotated to the exact upper rotational limit each cycle and, to a lower extent, because of the Joule Effect. Even though there is significant scatter in these load and torque data, the following conclusions can be drawn:

- The torsional stress-relaxation rate is less than the axial load stress-relaxation rate. This phenomena is not yet understood.
- The stress-relaxation rate is not a significant function of elongation for large elongations, i.e., the rates appear to be the same for $\lambda = 4.0$ as for $\lambda = 3.0$.
- If a unit is to be "aged" prior to use at an elongation of λ_o in order to minimize any noticeable stress-relaxation effects, it must be aged at λ_o: aging at less than λ_o is not beneficial. Thus, even though the unit was "aged" for about 30 days at $\lambda = 3.0$, the aging process appears to have started over as the elongation was increased to $\lambda = 4.0$.

The long-term (a few years) effects of stress-relaxation are not yet known. If it is found that the long-term rates are not significantly larger than those indicated in Figure 8, the effect of stress-relaxation could be compensated for in the initial design by using an appropriately larger amount of elastomer.

DESIGN AND FABRICATION OF A COMPLETE SMALL-SCALE ERBS

A block diagram of the small-scale Elastomeric Regenerative Braking System (ERBS) now being fabricated is shown in Figure 9. The dc Motor and the Flywheel simulate the prime mover and inertia, respectively, of a small-scale vehicle. With this experimental facility, both the dynamical response of the "vehicle" and the round-trip energy transfer efficiency of the ERBS can be measured.

Note the Energy Storage Device consists of two elastomeric units coupled at one end by a chain and attached to the Input and Output Shafts of the Energy Transfer Device (ETD) at the other. Also note that the ETD consists of two One-Way Clutches (shown as ratchets), a Clutch, and a Brake. Operation of the ETD can be understood by observing the four possible modes of operation shown in Table I below.

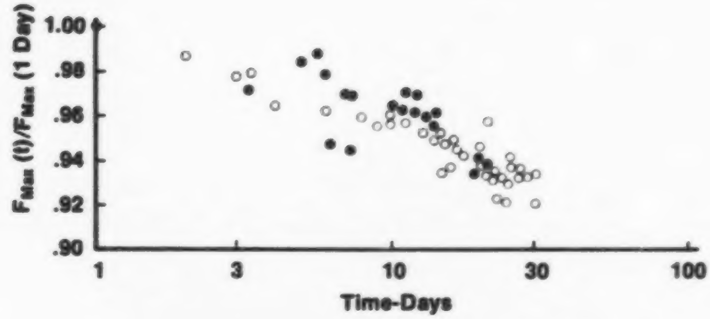

8(a) Relaxation of Maximum Axial Load for a Full-Size Axially Loaded Torsion Energy Storage Unit: ○: λ =3.0 ●: λ =4.0

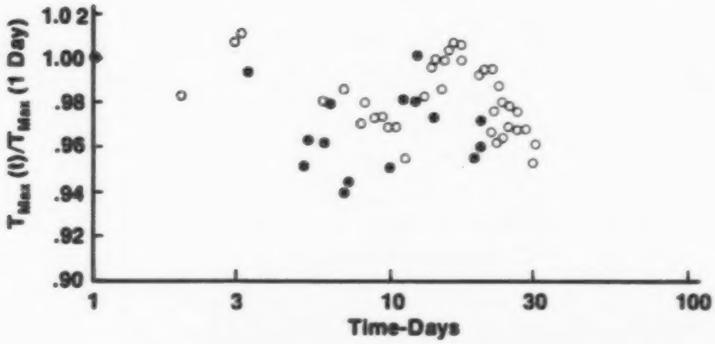

8(b) Relaxation of Maximum Torque for a Full-Size Axially Loaded Torsion Energy Storage Unit: ○: λ =3.0 ●: λ =4.0

Figure 8 Stress-Relaxation Characteristics of a Full-Size Axially Loaded Torsion Energy Storage Unit Obtained During a Fatigue Life Test

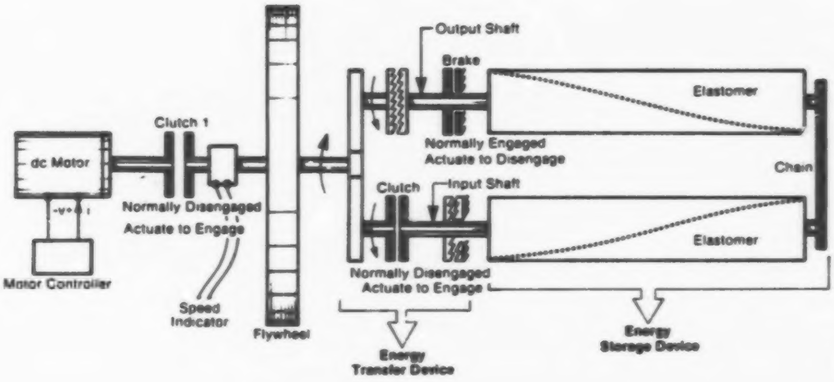
Output Shaft
Brake
Elastomer
Clutch 1
dc Motor
Normally Engaged
Actuate to Disengage
Chain
Clutch
Input Shaft
-V+
Normally Disengaged
Actuate to Engage
Elastomer
Motor Controller
Normally Disengaged
Actuate to Engage
Speed Indicator
Flywheel
Energy Transfer Device
Energy Storage Device

Figure 9 Block Diagram of ERBS

TABLE I. OPERATING MODES OF THE ETD

Mode	Clutch	Brake	Condition of Elastomer	Condition of Vehicle
1	Disengaged	Engaged	Stationary	Coasting
2	Engaged	Engaged	Absorbing Energy	Decelerating
3	Disengaged	Disengaged	Delivering Energy	Accelerating or Cruising
4	Engaged	Disengaged	Uniform Rotation	Coasting

When no torque demand signal exists, the control strategy adopted calls for Mode 1 operation, and hence the Clutch is normally disengaged and the Brake is normally engaged. Actuation of the vehicle's brake pedal will engage the Clutch, putting the ETD in Mode 2. Similarly, actuation of the vehicle's accelerator pedal will disengage the Brake, putting the ETD in Mode 3. Should the brake and accelerator pedals be actuated simultaneously, Mode 4 would result. In this case, the two elastomers would rotate uniformly about their respective shafts such that energy is neither absorbed nor delivered by the Energy Storage Device.

Notice that with this control strategy, actuation of the accelerator pedal always permits energy to flow from the elastomer, even if the vehicle is cruising. After each acceleration, therefore, the elastomer eventually arrives at the zero energy storage state and will automatically stop rotating. Hence, there is no "spin loss" during cruise conditions. Similarly, the complete system is stationary and produces no "spin loss" when the vehicle is at zero speed.

The gear ratios shown in the ETD would be chosen so that the resultant velocity-time profile of the vehicle during decelerations or accelerations would be the same as those most commonly experienced in typical driving. Higher rates of deceleration (acceleration) would be provided in a final system by supplementing the elastomer with the mechanical brakes (prime mover).

The main problem with this control strategy has to do with providing less than the nominal deceleration (acceleration) rate: presently this can be done with high efficiency only if the driver of the vehicle modulates the brake (accelerator) pedal. Whether or not the resultant ride quality would be acceptable is uncertain.

SUMMARY

Experimental results on full-size elastomeric energy storage units indicate that the preliminary goals which were set for energy density, efficiency and fatigue life can be achieved. The limited data which has been acquired on stress-relaxation is encouraging in that this phenomena does not appear to be excessive, but the long-term (a few years) effect of stress-relaxation is not yet known.

A simple Energy Transfer Device and control strategy have been conceived and designed for use in a small-scale ERBS to be dynamically tested in the laboratory. Experiments will be run to measure efficiency and to investigate controllability, but unfortunately these tests will provide very little information on the ride quality of a vehicle incorporating such a system.

REFERENCES

1. L. O. Hoppie, et al., "Regenerative Braking Through Elastomeric Energy Storage Systems, Conf-801128, pp. 328-339.

2. R. S. Rivlin, "Large Elastic Deformations of Isotropic Materials," Part VI, Phil. Trans. A, 242, pp. 173-195.

PROJECT SUMMARY

Project Title: Development of a Flywheel Energy Storage System (FESS) for a Transit Bus

Principal Investigator: L. J. Lawson

Organization: Garrett-AiResearch
Torrance, California 90509

Project Goals: Develop a full-scale engineering prototype flywheel propulsion system suitable for propelling a 40-foot transit bus between fixed or enroute electric charging stations. Install the flywheel propulsion system into a standard transit bus or trolley coach and conduct extensive vehicle tests.

Project Status: The detailed FESS design has been completed with propulsion system components currently being manufactured. All supporting analyses for the component designs have been finished with results showing adequate design margins. An accelerated life test was conducted on a full-size composite flywheel module in which the unit was shown to be capable of meeting the requirement for 23 years operational life in regular transit service. Two 16-kwh capacity composite flywheel rotors are now being fabricated using the Garrett subcircular multi-rim design which was successfully tested.

The flywheel-electric drive propulsion system has been designed to meet the requirements of the urban transit industry which will make the flywheel bus suitable for replacement of the present diesel buses and trolley coaches. By virtue of the high-capacity flywheel, the Garrett FESS bus can operate over city transit routes for distances of 5.6 to 8 km between recharges. Provision has been made to permit FESS vehicle recharging "on the run" under short sections of tangent overhead wire. In addition, the high power density of the flywheel can provide better acceleration and higher maximum speed than a diesel bus, all without dependence on petroleum fuel.

The present program plans will result in the initial demonstration of the FESS bus during the last quarter of FY1982.

Contract Number: DOT-TSC-1653

Contract Period: April 18, 1979 through May 1, 1983

Funding Level: $6,200,000

Funding Source: U.S. Departments of Transportation and Energy through Transportation Systems Center.

URBAN TRANSIT BUS PROPULSION WITH A PRACTICAL COMPOSITE FLYWHEEL

L. J. Lawson
Garrett-AiResearch
Torrance, California

ABSTRACT

The flywheel energy storage system (FESS) currently being fabricated at Garrett under the joint sponsorship of the U.S. Departments of Transportation (DOT) and Energy (DOE) will be employed as the propulsion system for full-size urban transit buses. These vehicles, when charged electrically, can then operate over urban transit routes for distances up to 8 km off-wire using energy stored in a 16-kwh capacity composite flywheel. The Garrett subcircular multi-rim composite flywheel design provides superior energy density along with an inherent high degree of safety. The resultant flywheel bus with its long range between charges and high level of acceptability for urban transit operations is expected to offer an attractive and cost-effective alternative to the present diesel bus and trolley coach.

INTRODUCTION

Over the past decade, many U.S. transit properties have indicated a need for rubber-tired transit vehicles that could provide clean, quiet, high-performance operation like the electric trolley coach, but also offer the route flexibility of the diesel bus. Such vehicles would be expected to have the advantages of low maintenance cost and long service life, which are characteristic of electric transit, without the fixed cost and maintenance burden of a continuous energy collection system. In addition to these improvements, the new vehicles could help alleviate the energy shortage because of the improved regenerative braking energy efficiency and the compatibility with electric energy rather than petroleum fuel for propulsion. The most practical means of propelling such a new class of urban transit vehicles is by use of an onboard energy storage system employing a flywheel in conjunction with an electric drive.

In reviewing the transit industry needs, it has been found that the urban transit bus offers a unique combination of characteristics that make it suitable for the demonstration of new propulsion concepts like the flywheel energy storage system (FESS). In particular, the bus is an excellent candidate for evaluating the high level of energy conservation made possible by the use of regenerative braking. First, buses are heavy vehicles that move at relatively high speeds, resulting in the availability of substantial values of kinetic energy for recuperation. Second, buses have frequent start-stop operations that increase the opportunities for energy recovery. Also, because of their size, buses are not very sensitive to the volume and weight of the new propulsion systems. In addition, reasonable control can be maintained over buses used for the demonstration of new propulsion concepts because the vehicles are generally operated over predictable routes and can be regularly inspected and serviced in the transit property maintenance facility. It is also expected that the results of the tests and demonstrations of new energy-efficient propulsion systems conducted in transit buses can be extrapolated to a wide range of vehicles from small commuter cars to large trucks and vans.

Transit operators have also stated their desire for improved vehicle productivity since the major single element of operating cost is the bus drivers' salary and fringes. Thus, buses with higher acceleration performance which can shorten journey times can reduce operating costs as well as vehicle fleet size. The high power density which is inherent in flywheels makes such improvements available.

The multiphase flywheel-propelled transit vehicle program, which is now underway under joint DOT and DOE sponsorship, is intended to expedite the deployment of new energy storage vehicles in revenue service. This will satisfy the user industry needs and at the same time demonstrate the energy economics of regenerative braking so that the concept can be applied to many other vehicle types.

Thus, the impetus for the flywheel bus demonstration program is the transit industry desire for improved vehicles and the urgent need to reduce energy consumption, particularly petroleum fuel.

PROGRAM OUTLINE

The flywheel-propelled transit bus program is divided logically into the four phases shown below with review points for assessment of technical progress and concept viability and marketability during and at the end of each phase.

Phase I - FESS Design Study (completed in 1977)

Phase II - Engineering Prototype FESS Development, Fabrication, and Test

Phase III - Revenue Service Demonstrations by Transit Properties

Phase IV - Production

PROGRAM OBJECTIVES

The overall purpose of the FESS bus program is the demonstration and ultimate production of a new class of transit vehicles that can provide improved quality transit service while conserving energy, particularly petroleum fuel. The rubber-tired transit bus is considered to be important to petroleum fuel conservation because of the increasing scarcity (and cost) of oil. Thus, as the fuel shortage and the availability of increasingly attractive public transit service cause commuters to abandon their cars, highly efficient transit vehicles that can use electric energy will be available.

FESS PROPULSION SYSTEM DESCRIPTION

The functional block diagram of the Garrett FESS is shown in Figure 1. This system is designed to operate from the fixed 600 volts dc (nominal) power available on many U.S. transit properties which operate electric rail vehicles or trolley coaches. This power is connected through an Automatic Collector system (which can be used to engage or disengage power wires automatically in response to a driver's command) to the Switchgear. Power collection can be accomplished either enroute as the vehicle is operated under a short section of tangent trolley wires or while the vehicle is standing at a passenger stop or route terminal. For the stationary case, dc power is switched to the Dual Converter (with the Traction Motor disconnected). The Dual Converter is a three-phase, full-wave phase delay rectifier which operates as an inverter during charging with load commutation provided by the overexcited synchronous homopolar inductor-type Flywheel Motor. In this mode of operation, the Flywheel Motor and Flywheel are accelerated until the fully charged condition is reached. Enroute charging of the Flywheel is accomplished by engaging the trolley wires on the run with the Automatic Collector and then operating the coach over its route while charging is accomplished. Power from the trolley wires is coupled to both the Traction Motor and Dual Converter to provide for normal vehicle performance while Flywheel charging is being accomplished. When the Flywheel is fully charged, the Automatic Collector poles may be stowed without stopping the vehicle.

FLYWHEEL PROPULSION SYSTEM

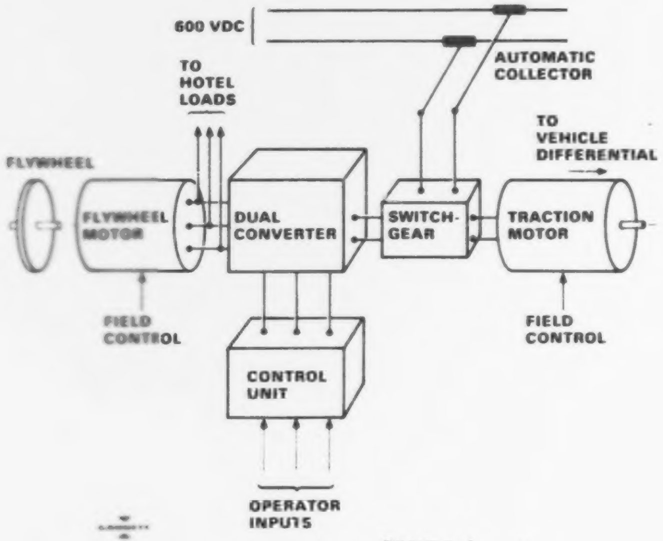

FIGURE 1

The normal route operation of the flywheel propulsion system of Figure 1 on flywheel energy is accomplished by extracting energy from the Flywheel by field control of the Flywheel Motor. This three-phase ac power is rectified by the Dual Converter and fed to the armature of the Traction Motor. During initial acceleration, the Traction Motor armature voltage is varied in proportion to vehicle speed up to the Traction Motor speed at which full armature voltage can be applied (base speed). At that point, constant armature voltage is applied, and the tractive effort is controlled by varying the field excitation of the Traction Motor. The control of the two motor fields and the conduction angles of the Dual Converter thyristors are coordinated by the Control Unit in response to the Operator Inputs.

All vehicle braking may be done electrically by the use of the Traction Motor as a generator which converts vehicle kinetic energy to dc power. The Traction Motor output is then coupled to the Dual Converter which acts to accelerate the Flywheel in the same manner as during charging. Recuperative electric braking is continued until zero speed at which point the normal bus service brake system is used to hold the vehicle. The full electric braking capability results in a substantial savings in friction brake maintenance cost as well as improved braking energy recuperation.

The operation of the flywheel coach may be continued with full route freedom until the Flywheel is discharged. Tradeoff studies have determined that the optimum flywheel speed range is about two to one, which makes available 75 percent of the stored energy for propulsion. Thus, when the Flywheel slows to half speed, the vehicle is recharged under enroute trolley wires or at a charging station.

FESS DESIGN PHILOSOPHY

In response to the demands expressed by the three principal North American bus manufacturers (General Motors, Grumman-Flxible, and Flyer Industries Limited) and the major U.S. transit properties, the Garrett FESS design philosophy emphasizes the following points:

1. Compatibility with new vehicle or retrofit installation into all of the buses now commonly in service. These include the following new vehicles:

   GM RTS II and RTS 04
   Flxible Model 870
   Flyer Models D901 and E901
   GM of Canada "New Look"

   and the following older vehicles:

   AM General Model E10240T and "New Look"
   GM "New Look"
   Flxible "New Look"
   Flyer E800 and D900

2. Installation of the maximum possible flywheel capacity into the vehicle without exceeding permissible axle and tire loads or removing passenger seats.

3. Provision of the highest available performance in the FESS vehicles (significantly in excess of present diesel buses) to improve vehicle productivity.

The implementation of this design philosophy in the Garrett Phase II Program has been possible due to the availability of improved flywheel technology using composite rather than metallic materials. As a result, it has been possible to install a relatively high-capacity flywheel (16 kwh) into a bus without compromising axle loading or passenger seating.

FLYWHEEL DESIGN

Steel Flywheels. The broad Garrett experience with flywheels of various designs and materials for transportation applications is the foremost in the U.S. as described in References 1, 2, and 3. This background was reviewed in order to determine the optimum configuration and capacity for the flywheel bus. The early Garrett flywheel experience was with steel flywheels used for rail car braking energy recuperation. This background included the only transit revenue service demonstration in the United States; i.e., the energy recuperation system on two New York Metropolitan Transportation Authority Type R-32 Subway cars in 1976 (Reference 1).

The 3.2-kwh capacity R-32 (Reference 1) and 4.5-kwh capacity ACT-1 (Reference 2) steel flywheel designs were initially considered for the FESS application. These flywheels at first appeared well-suited to the bus application since the rotors were fully contained and had been extensively tested for safety during all failure modes expected in transit service. However, the flywheel energy storage capacity for the FESS vehicle was found to be about 16 kwh in order to satisfy the transit industry requirements for 5.6 to 8 km range between charges. A 16-kwh steel flywheel assembly using the proven Garrett designs would weigh approximately 7000 lbs. This flywheel weight is incompatible with installation of the FESS into a transit bus which meets the statutory limitations on axle weights. Actually, the maximum permissible weight of the flywheel assembly itself is less than 1800 lbs. Fortunately, work has been underway at Garrett for more than a decade on the use of composite materials which provided a solution to the FESS flywheel weight dilemma.

Composite Flywheels. Recent flywheel activities at Garrett have been directed toward the development of practical composite flywheels as described in Reference 4 for vehicular applications. Here, use has been made of a technology base resulting from over 15 years of extensive experience with composite materials operating at high rotating stresses for a stationary application.

A summary of representative Garrett composite flywheel experience is shown in Table 1 where various flywheel hardware is listed along with the energy storage capacities and rotor energy densities

TABLE 1

REPRESENTATIVE COMPOSITE GARRETT FLYWHEEL EXPERIENCE

Application	Flywheel Capacity	Rotor Energy Density
IR&D	0.7 kwh	19 wh/kg
MERADCOM	2.4 kwh	53 wh/kg
Near-Term Electric Vehicle (NTEV) (References 5, 6, and 7)	1 kwh	44 wh/kg
Lawrence Livermore	0.25 kwh	40 wh/kg
Sandia	1.1 kwh	79.4 wh/kg

Flywheel failure tests reported in Reference 7 have shown that composite flywheels require only about 15 percent of the containment weight needed for metallic flywheels. On this basis, the improvement in flywheel rotor energy density for composites over steel flywheels is maintained for the complete flywheel assembly.

The composite flywheel, when compared to metallic flywheels, offers other advantages which must be considered, particularly for vehicle applications. For example, flywheel overspeed leading to catastrophic failure is always a dreaded possibility with metallic rotors but is not a serious problem with the composite flywheel in which the rim is designed to lift off the hub at 110 percent rated speed. In addition, unpredicted structural failure of a composite flywheel results in microfractures of the matrix and unraveling of the fiber which fills the housing with a fluff-like material which transfers rotor momentum to the housing at a relatively low rate. In contrast, the momentum transfer from a metallic flywheel following catastrophic failure is nearly instantaneous which requires that the flywheel assembly mounting be capable of allowing the entire flywheel unit to rotate rather than the vehicle.

Rotor Design. The FESS flywheel rotor is comprised of six axial composite rims installed on a single forged cruciform aluminum hub as shown in Figure 2. Each rim segment is a subcircular multi-rim which at zero speed has the form shown in Figure 3. At the rated speed of 16,000 rpm with a peripheral velocity of 2500 ft/sec, the rim attains a fully circular shape. At 10 percent overspeed (17,600 rpm), the rim segment increases in diameter sufficiently to lift off the hub so that no additional torque can be applied. In this way, the Garrett composite flywheel design provides inherent protection against overspeed.

The assembly of the subcircular rim is accomplished by simultaneously applying outward forces adjacent to four equidistant points on the inner rim surface to distort the rim sufficiently to permit hub insertion. When the distorting forces are removed, the rim will attempt to regain its circular shape, thereby placing the hub spokes in compression. The hub insertion fixture is shown in Figure 4.

The flywheel multi-rim segments are comprised of nine circumferential layers of composite materials with thin interlayers of teflon as shown in Figure 5. The inner layer of the rim is laid up with S2 Fiberglass/Epoxy. The next three innermost layers are then comprised of low-modulus KEVLAR 29/Epoxy while the outer five layers are made up of high-modulus KEVLAR 49/Epoxy.

Flywheel and Material Tests. To supplement data gathered on the previous composite flywheel programs, several tests have been conducted to demonstrate the integrity of the composite flywheel when operated in the FESS bus environment. These tests have provided material data and design information that have minimized the risks inherent in building full-scale flywheels.

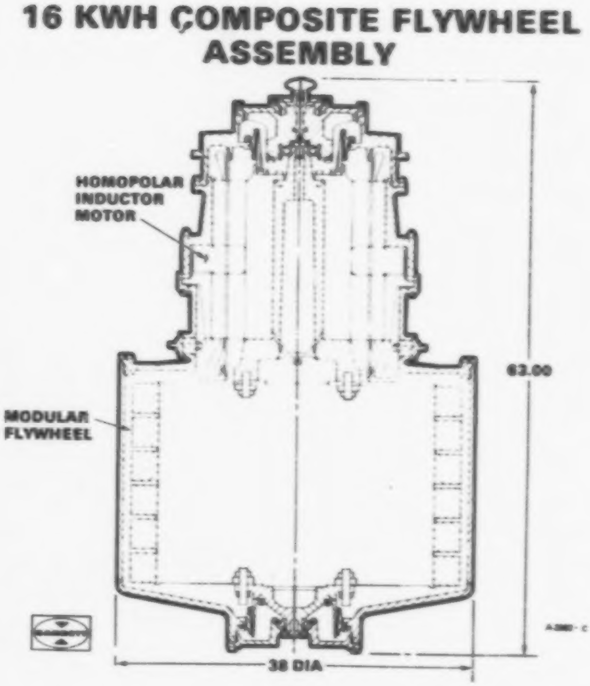
16 KWH COMPOSITE FLYWHEEL ASSEMBLY
HOMOPOLAR INDUCTOR MOTOR
MODULAR FLYWHEEL
63.00
38 DIA

Figure 2

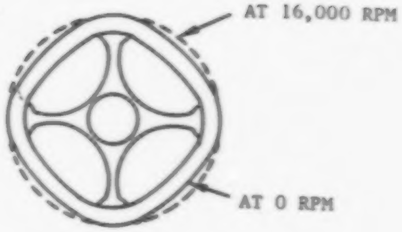
AT 16,000 RPM
AT 0 RPM

Figure 3. Flywheel Rotor Segment

Figure 4. Flywheel Hub
Insertion Fixture

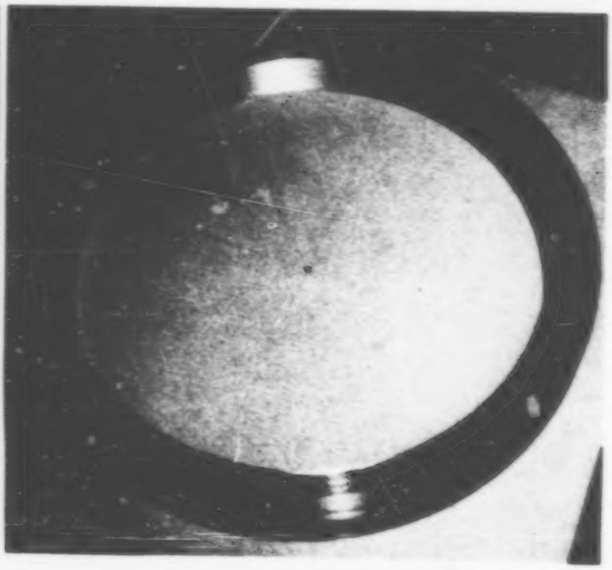

Figure 5. FESS Bus Flywheel
Rim Segment

In the first series of tests, the effects of wetting of the composite material by vacuum oil from the flywheel bearings were evaluated. Test samples were soaked in the selected vacuum oil and these samples, along with control samples, were tested for composite interlaminar shear strength. The oil did not affect the material properties of the composite.

Next, to simulate the stress cycles anticipated in 23 years of transit bus operation, a million-cycle tension fatigue test was accomplished on three test rings at a stress level corresponding to the maximum tensile strength of the flywheel rotor. After these samples successfully passed the cycle test, a burst test demonstrated that the material still had a significant residual strength.

In addition, the fabrication technique of the composite was evaluated by a microsection analysis. Several samples were sectioned and microsections were examined for voids to establish the quality of manufacture.

The final test was a module spin test on one of the six flywheel rotor elements, shown after the test in Figure 6. This test is a proof-of-design test because it subjects a full-scale rotor segment to all stresses of actual operation. Here, 638 cycles from zero to 106 percent of maximum speed were performed to achieve the equivalent of 10^6 operating cycles. At the successful conclusion of this test, the total flywheel rotor design was released for fabrication. The flywheel assemblies are expected to be completed and ready for laboratory testing during the first quarter of FY1982.

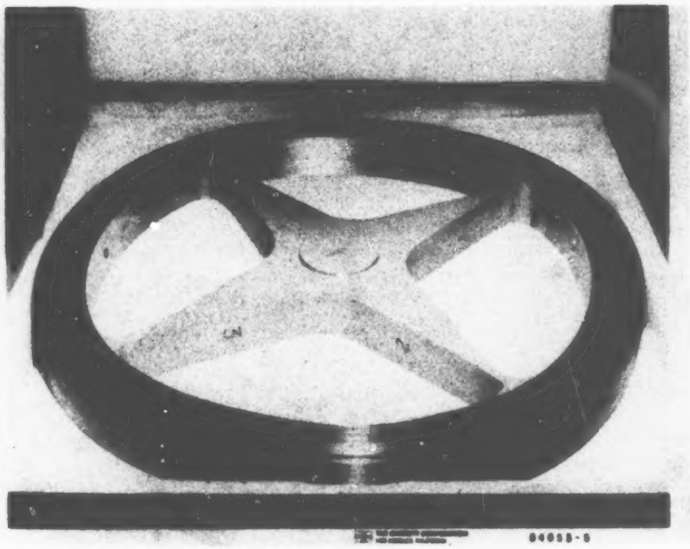

Figure 6. Flywheel Spin Test Module

VEHICLE INSTALLATION

The selected 16-kwh composite flywheel package is compatible with installation in the propulsion compartment of all currently available North American transit buses. A pictorial view of a typical installation of the flywheel unit and other system components in the coach is shown in Figure 7. After FESS laboratory tests, the prototype system will be installed into a standard transit bus for vehicle tests which will commence during the fourth quarter of FY1982.

TRANSIT OPERATORS' REACTIONS

The results of the FESS development program to date were presented by Garrett to 14 transit operators in a series of face-to-face meetings in the spring of 1981. The properties were asked for comments on the program after these presentations as well as for their reactions to the concept. A summary of these flywheel trolley coach deployment meetings along with the comments of the transit properties contacted is presented in Table 2.

CONCLUSIONS

The FESS Program being performed by Garrett will result in a prototype design which is compatible with new vehicles and retrofit installation into all buses now commonly in service. Numerous transit

ENERGY STORAGE INSTALLATION

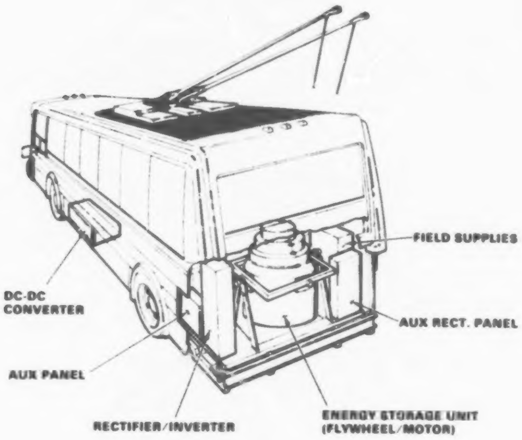
FIELD SUPPLIES
DC-DC CONVERTER
AUX RECT. PANEL
AUX PANEL
RECTIFIER/INVERTER
ENERGY STORAGE UNIT (FLYWHEEL/MOTOR)

Figure 7

TABLE 2

TRANSIT PROPERTY REACTIONS

Property, City	Support Concept	Favor Phase II Completion	Apply for 5 Vehicle Grant	Routes Identified	Phase IV Market
MUNI, San Francisco	Yes	Yes*	Yes*	Yes	900
SCRTD, Los Angeles	Yes	Yes*	No	Yes	200
LBPTC, Long Beach	Yes	Yes	Maybe	Yes	40
OCTD, Garden Grove, CA	Yes	Yes	No	No	No
SCTC, San Diego	Yes	Yes	No	Yes	50
METRO, Seattle	Yes	Yes*	Maybe	Yes	200
TRI-MET, Portland	Yes	Yes	Maybe	Yes	50
WMATA, Washington DC	Yes	Yes	No	Yes	20
MVRTA, Dayton	Yes	Yes	No	Yes	400
GCRTA, Cleveland	Yes	Yes	No	Yes	100
MBTA, Boston	Yes	Yes	Maybe	Yes	1000
CTA, Chicago	Yes	Yes	No	Yes	?
METRO, Houston	Yes	Yes	No	Yes	60
SEPTA, Philadelphia	Yes	Yes*	No	Yes	320

*Willing to provide vehicle for Phase II tests.

TOTAL 3300

properties have endorsed the design approach and its proposed method of implementation. The selection of a composite flywheel for the program was a fundamental part of the successful design approach for the following reasons:

- Composite flywheels have lower technical risk than metallic flywheels in large capacities having high-energy density
- Composite flywheels can be modular in design which can make a single rotor module design suitable for a wide range of applications
- Lower development cost for a composite flywheel than a metallic flywheel
- Greater system safety due to inherent safe failure modes of composite flywheels
- Reduced flywheel assembly weight and, therefore, greater vehicle range without exceeding permissible axle loading
- Greater growth potential of composite flywheels to nearly twice the energy density of the selected design

REFERENCES

1. Raskin, D., "Energy Storage Propulsion System for Rapid Transit Cars, Test Results, and System Evaluation," prepared for UMTA by Metropolitan Transportation Authority under Contract No. UMTA-NY-06-0006-75, October 1978.
2. "ACT-1 Advanced Concept Train Development Program, Final Report," prepared for UMTA under Contract No. DOT-UT-10007, July 1979.
3. Beachley, N. H., et al., "Experimental Evaluation of Flywheel Energy Management Automobile," Proc. 4th International Symposium on Automotive Propulsion Systems, April 1977.
4. Place, T. W., "Composite Material Flywheel for Department of Transportation Coach," Proceedings of 1980 Flywheel Technology Symposium, October 1980.
5. Rowlett, B. H., "Battery-Flywheel Power System for an Urban Automobile," NATO Proceedings of the 4th International Symposium on Automotive Propulsion Systems, Vol. 2, pp. 902-913, February 1978.
6. Satchwell, D. L. and Towgood, D. A., "High-Energy Density Composite Flywheel," Final Report prepared for Sandia Laboratories under Contract No. AT/29-1/789, February 1980.
7. Towgood, D. A., "An Advanced Vehicular Flywheel System for the ERDA Electric-Powered Passenger Vehicle," 1977 Flywheel Technology Symposium Proceedings, pp. 63-68, October 1977.

PROJECT SUMMARY

Project Title: Technical Support & Engineering Analysis for Flywheel Technical Development

Principle Investigator: David B. Eisenhaure

Organization: The Charles Stark Draper Laboratory, Inc.
555 Technology Square
Cambridge, MA 02139

Project Goals: Investigate alternative flywheel applications and determine the economic and technical goals required for flywheels to exceed their competition in these applications. Determine development requirements for these applications in light of these goals.

Project Status: The project and documentation requirements have been completed.

Major Program Reports

R-1472 Aerodynamic Heating and Windage Loss Characteristics of Flywheel Rotors
R-1474 Technical and Economic Considerations in the Design of Low Loss Flywheel Electromagnetic Bearings
R-1477 The Influence of Material Properties on Flywheel Optimization Criteria
R-1482 Development Requirements for Fixed-Base Flywheel Systems
R-1486 Utilization of Flywheel-Hybrid Drive Trains for Commercial Taxicab Fleets

Major Program Accomplishments

1. Development of Control Requirements for a Flywheel System in a PV/Grid Connected Mode
2. Determination of the Relationships Between Flywheel Losses, Flywheel Temperatures, and System Vacuum Level
3. Development of Economic and Technical Criterion for Electromagnetic Flywheel Bearing/Suspension System
4. Economic Comparison of Flywheel Storage Systems with Battery Systems
5. Economic and Technical Evaluation of Candidate Rotor Materials for Stationary Applications
6. Determination of the Effect of Storage Efficiency on Overall System Economics
7. Determination of High Payoff Storage Applications
8. Review of Prior Studies of Stationary Flywheel Systems

Contract Number: 9385809

Contract Period: October 1, 1980 through September 30, 1981

Funding Level: 198,493

Funding Source: U.S. Department of Energy through Lawrence Livermore National Laboratory

MECHANICAL ENERGY STORAGE APPLICATION STUDIES

David B. Eisenhaure, Tim E. Bliamptis, Bruce G. Johnson
The Charles Stark Draper Laboratory, Inc.
555 Technology Square
Cambridge, Massachusetts 02139

ABSTRACT

Flywheel energy storage has advantages over competing storage technologies in a number of power generation and energy conservation systems. In these systems, flywheels have several functions which include recovering waste energy, increasing system efficiency, and matching source availability with load requirements. Developments are required in most applications before the advantages of flywheels can be translated into improved storage systems. The economic criteria and technical requirements necessary for flywheels to exceed their current and near term competition are the most important factors in determining flywheel development requirements. This paper quantifies the economic criteria, technical requirements, and conservation potential for several fixed and moving base flywheel applications. The developmental requirements for these applications are identified and contrasted in light of these factors. One moving-base application examined involves the use of flywheels in urban-based taxicab fleets for engine load leveling and regenerative braking. In this vehicle application, systems developed from state-of-the-art technology allow substantial fuel savings and economic gain. One fixed-base application examined involves the use of flywheels for daily energy storage in conjunction with solar photovoltaic or wind power generation. In this application, flywheels compete functionally with battery systems. The inherent long life and the anticipated high storage efficiency of flywheels provide significant economic leverage over batteries.

INTRODUCTION

Traditionally, flywheels have been utilized for high rate, short term energy storage. The numerous applications have included punch presses, piston engines, and grain milling machines. Researchers are currently considering improved flywheels as storage elements in power generation and energy management systems. This research is often treated as a single field with unified research goals. When specific flywheel applications are considered, however, quite distinct and conflicting development requirements are seen to exist among them. This paper focuses on these distinctions in both fixed-base and moving-base "energy" applications and outlines the development requirements. These requirements are contrasted with those of high technology flywheel applications for space and military power systems.

Flywheels have a combination of attributes that is unique among storage technologies. These attributes include high power density, long life, high efficiency, and direct mechanical output. Fixed-base applications primarily exploit the long-life characteristics of flywheels and, to a lesser extent, their efficiency advantages. Moving-base applications generally have short duty cycles that take advantage of the high power capability of flywheels. Developments are required in most flywheel applications before these advantages can be translated into improved energy storage systems. Depending on the application, improvements are required in bearings, low cost rotors, high energy density rotors, continuously variable transmissions and their controls, and power converters.

The technical and economic criteria required for flywheels to exceed their current and near term competition are the most important factors in determining required flywheel developments. The competition may be prime energy sources or other storage technologies. Once the economic goals and technical requirements have been defined for a particular application, a determination must be made as to whether the base technology exists to develop components which meet these requirements. If the base technology does exist, then the required R&D must be weighed against other R&D ventures in terms of the potential to increase the supply of available energy or the potential to conserve existing energy supplies. Figure 1 outlines the general analysis and assessment process through which new flywheel technologies should be screened prior to development.

The major emphasis of CSDL's application studies has been the determination of these economic goals and technical requirements, the identification of baseline system configurations and their performance sensitivities to changes or tradeoffs in subsystem technology. Consideration was given to expected developments in science and engineering and activities in other development programs to determine recommended areas for research and development. The end result is the identification of "energy" applications where relatively little development effort would produce viable flywheel systems which improve the country's energy supply.

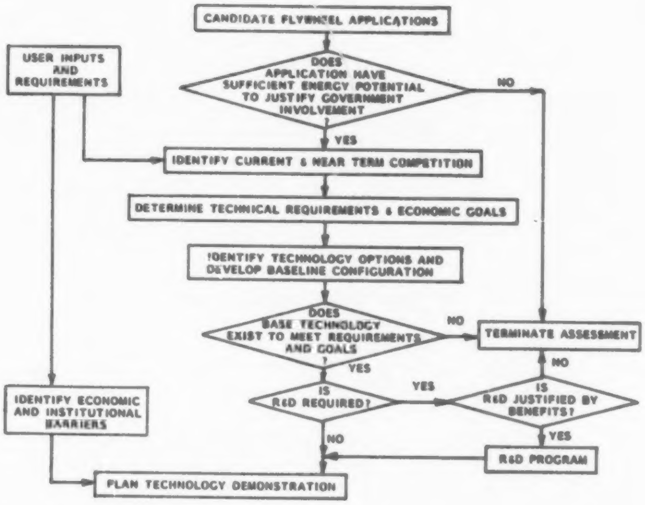
CANDIDATE FLYWHEEL APPLICATIONS
USER INPUTS AND REQUIREMENTS
DOES APPLICATION HAVE SUFFICIENT ENERGY POTENTIAL TO JUSTIFY GOVERNMENT INVOLVEMENT ?
NO
YES
IDENTIFY CURRENT & NEAR TERM COMPETITION
DETERMINE TECHNICAL REQUIREMENTS & ECONOMIC GOALS
IDENTIFY TECHNOLOGY OPTIONS AND DEVELOP BASELINE CONFIGURATION
DOES BASE TECHNOLOGY EXIST TO MEET REQUIREMENTS AND GOALS ?
NO
TERMINATE ASSESSMENT
YES
NO
IDENTIFY ECONOMIC AND INSTITUTIONAL BARRIERS
IS R&D REQUIRED?
YES
IS R&D JUSTIFIED BY BENEFITS?
NO
YES
R&D PROGRAM
PLAN TECHNOLOGY DEMONSTRATION

Figure 1. Assessment Methodology for Screening Flywheel Applications to Determine Development Requirements.

The applications reviewed are 7-day storage for remote site photovoltaic (PV) systems, 24-hour storage for both utility peak shaving and PV array or wind generation complementary storage, wayside subway storage, storage for a PV buffer in synchronous or low earth orbit satellites, taxicab fleets, and military power systems. In most of the stationary applications, the current competition is batteries. In most moving-base applications, the competition is the cost of fuel or petroleum related R&D. The flywheel economic goals and technical requirements as determined by this competition are specified by a number of parameters: cost, power, storage capacity, efficiency, cycle time, and life. With these goals and requirements in mind, baseline flywheel systems are configured for each application. The procedure used to develop baseline systems is shown in Figure 2, which is a more detailed description of the corresponding step "Identify Technological Options and Develop Baseline Configurations," in Figure 1. As can be seen, existing subsystems - rotor, bearing, vacuum, power conversion, and containment - are used to configure a preliminary system. After the relationships between the subsystems and the goals and requirements are established, system tradeoffs are performed. These tradeoffs are influenced by both existing state-of-the-art technology and possible subsystem developments and their expected costs. With these influences in mind, baseline system options are constructed. Those subsystem technological advancements which give the greatest increase in system performance, with consideration given to expected development costs, are suggested as areas of research and development.

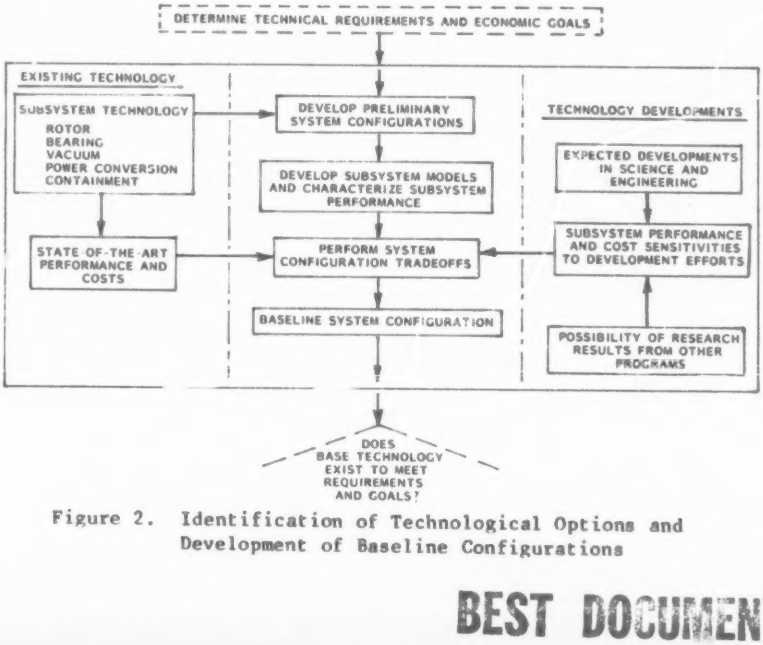
DETERMINE TECHNICAL REQUIREMENTS AND ECONOMIC GOALS
EXISTING TECHNOLOGY
SUBSYSTEM TECHNOLOGY
ROTOR
BEARING
VACUUM
POWER CONVERSION
CONTAINMENT
STATE-OF-THE-ART PERFORMANCE AND COSTS
DEVELOP PRELIMINARY SYSTEM CONFIGURATIONS
DEVELOP SUBSYSTEM MODELS AND CHARACTERIZE SUBSYSTEM PERFORMANCE
PERFORM SYSTEM CONFIGURATION TRADEOFFS
BASELINE SYSTEM CONFIGURATION
TECHNOLOGY DEVELOPMENTS
EXPECTED DEVELOPMENTS IN SCIENCE AND ENGINEERING
SUBSYSTEM PERFORMANCE AND COST SENSITIVITIES TO DEVELOPMENT EFFORTS
POSSIBILITY OF RESEARCH RESULTS FROM OTHER PROGRAMS
DOES BASE TECHNOLOGY EXIST TO MEET REQUIREMENTS AND GOALS?

Figure 2. Identification of Technological Options and Development of Baseline Configurations

FIXED BASE DAILY STORAGE CYCLE APPLICATIONS

A 24-hour storage period is common to many fixed-base flywheel applications including solar photovoltaic complementary storage and utility load leveling. In a solar photovoltaic complementary system, energy would be collected during periods of excess insolation and stored for later use. In utility load leveling applications, base power is stored during periods of low demand for use during peak demand. This is desirable since base generation plants operate at significantly higher efficiency and lower cost than peaking generation plants. In agricultural and pipeline use flywheels coupled with solar photvoltaic could displace 293×10^6 barrels of petroleum per year. In utility applications, flywheel systems could displace most or all of the approximately one billion barrels of petroleum utilized annually.

Fixed-base flywheel storage systems operating on a 24 hour duty cycle compete directly with battery energy storage systems [1]. The primary considerations in determining the relative value of flywheel rotors and batteries are the relative life and efficiency of the two approaches and battery capital costs. Flywheels have an economic advantage over batteries due to their longer life and potential for higher energy efficiency. While current and near term battery costs vary from 40 to 70 $/kWh, studies indicate that the 20 to 30 year life projected for flywheel systems dictates a competitive flywheel rotor cost goal of 100 to 150 $/kWh for systems of equal efficiency [2]. Of available flywheel materials, steel wire and high-strength steel forgings can currently meet this cost goal. High energy density composite wheels will require substantial cost reductions to meet this goal.

In daily storage applications, primary consideration must be given to system efficiency. The energy efficiency of the storage system is determined by the conversion and self-discharge losses integrated over the specific duty cycle. To be competitive with batteries, the total energy efficiency must be greater than 70%. This overall energy efficiency goal can be met with a conversion efficiency requirement of greater than 87% combined with a self-discharge rate requirement of less than 0.5%/h [1]. For 24 hour applications, however, an energy efficiency of 85% (which requires 94% conversion efficiency combined with a 0.25%/h self-discharge rate) or higher appears feasible,especially for larger systems. Increasing the energy efficiency increases the storage worth because of a decrease in required source capacity, storage capacity, and fuel consumption. At the current cost of PV arrays ($15/W), an increase in energy efficiency from 70 to 85% produces an increase in the PV storage value of 490 $/kWh.

While battery conversion efficiency can be improved upon with flywheel technology, developments are necessary to achieve the self-discharge requirement in a cost-competitive system. Self-discharge losses consist primarily of bearing and windage losses. The very low losses required in 24-hour applications make electromagnetic bearings the best choice for the bearing subsystem [3]. Aerodynamically induced self-discharge is a flywheel problem area not found in other storage technologies [4]. CSDL has performed a study which describes the effects of vacuum level, energy density, rotor storage capacity, rotor material, and rotor geometry on both self-discharge rate and rotor temperature. The vacuum level required to achieve a given level of relative windage loss decreases with increased storage capacity for geometrically similar wheels of a given material. Windage loss increases with energy density but decreases with mass density. This behavior strongly penalizes high energy density, low mass density, composite wheels in comparison to wheels.

WAYSIDE SUBWAY APPLICATIONS

Regenerative braking of subway trains reduces energy consumption. Instead of being dissipated as heat, the energy of the braking train is converted back into electricity and returned to a flywheel via the rails. The high power densities required for this application make flywheels an ideal choice.

In conservation applications, such as this one, the present value of the energy savings per unit time determines storage worth. As the cycle time becomes shorter, the competitive value of the flywheels increases because the energy savings per unit energy storage capacity increases. The subway storage system is one example of a system with short cycle times, and therefore high value for the flywheel. In this application, the flywheel competes economically with utility generated power. Rapid economic pay back has been demonstrated.

The inclusion of wayside flywheel modules in new subway systems can be justified on a purely economic basis [1]. A recent CSDL study found the payback time for a flywheel storage system included in the Massachusetts Bay Transportation Authority (Boston) subway system. The pay back period is strongly influenced by the traffic density. The highest traffic density station studied had a two-year pay back period. Wayside flywheel storage has economic advantages over competitive regeneration schemes, in particular, over on-board flywheel storage [1]. Wayside flywheel storage requires little or no development and can be engineered using available technology.

FIXED BASE REMOTE-SITE STORAGE APPLICATIONS

Applications such as remote repeater stations and relay towers use photovoltaic solar energy as their sole source of power. Since power must be available whenever required, the system must have sufficient storage to isolate it from inclement weather and load variations. In most locations storage times on the order of one week are required to assure adequate probability of service. The primary competition for flywheels in these applications are charge retention batteries. The long life of flywheels coupled with the derating required with charge retention batteries leads to competitive flywheel worth as high as 2880 $/kWh,for systems of equal efficiency. For applications where the storage cycle is on the order of a week, the self-discharge rate determines the feasibility of the storage system. In order to utilize power conversion equipment of realistic efficiency, and achieve energy efficiencies that are competitive with those of alternate storage technologies, the self-discharge rate must be on the order of 0.05% [1]. This self-discharge rate coupled with an 87% conversion efficiency would yield an energy efficiency of 70%.

As with other flywheel applications, the self-discharge rate is primarily made up of bearing and windage losses. The implementation of suspension and vacuum systems that will produce competitive flywheels, for these applications, will probably test the limits of these technologies. To achieve windage losses that are of the order required for this application, vacuum levels will have to be similar to those employed in precision laboratory equipment. The bearing loss for electromagnetic bearings of the type recommended for 24-hour storage applications is excessive for applications having long storage times. There are modifications, however, that may be made to these electromagnet designs used in the 24-hour application, that can reduce the power consumption. Alternatively, permanent magnet bearings are justifiable components for this application from a point of view of self-discharge rate. These permanent magnet materials should be of the moderate cost and energy product ceramic type such as Barium Ferrite or Strontium Ferrite.

FIXED BASE SATELLITE ENERGY STORAGE APPLICATIONS

Historically, space power systems have utilized Nickel-Cadmium (NiCd) batteries as a PV buffer in synchronous or low earth orbit satellites. The NiCd batteries are drastically derated to achieve adequate cycle life, and are being displaced by Nickel-Hydrogen batteries due to this deficiency. The specific energy density of these cells is 200 kJ/kg. Their energy efficiency is 70%, but at slow discharge rates it is significantly lower due to severe self-discharge characteristics. Life varies from 6000 cycles at 80% depth of discharge (DoD) to 30,000 cycles at 40-50% DoD. Current costs are $32,000/kWh.[1]. In very high volume production, costs are estimated at 600 to 1000 $/kWh. In addition to self-discharge problems, these batteries suffer from low volume efficiency.

With proper development, high technology flywheel systems can compete very successfully in this area on an efficiency, weight, and cost basis. These flywheel systems will incorporate high energy density composite rotors, advanced magnetic bearings, and high efficiency power conversion equipment. These flywheels may be configured for Integrated Power and Attitude Control (IPAC) [1]. In these applications, the capability of the flywheel to store both angular momentum and energy will be utilized. High energy density flywheels appear a natural candidate for this application.

MOVING BASE TAXICAB FLYWHEEL HYBRID DRIVETRAINS

The Charles Stark Draper Laboratory has recently studied a baseline flywheel-hybrid powertrain as a means of increasing taxicab fuel economy [5]. Increased fuel economy is achieved because of the flywheel's ability to recover braking energy and because the engine is allowed to operate at its maximum brake specific fuel consumption point. Taxicabs consume 1.4 x 10^9 gallons of fuel annually so total savings can be significant. Taxis are also an entry point to general automotive use where 79 x 10^9 gallons of fuel are utilized. In this application, the flywheel system competes with the cost of fuel and petroleum related R&D.

Projected fuel mileage was obtained via computer simulation as a parametric function of transmission efficiency and flywheel loss rates. Perhaps the most startling result is a projected 200 percent increase in fuel mileage for the Checker Model 12 with a regenerative flywheel-hybrid powertrain driven over the Central Business District cycle. The gains for other urban scenarios were more modest, but still substantial, showing the high potential for fuel savings in urban vehicles.

Since cycle time is on the order of minutes, relatively high self-discharge rates (50%/hr) are tolerable. Vehicle flywheels will probably run at higher pressures than their fixed-base counterparts because sophisticated vacuum technology is prohibitively expensive for automotive applications. A 10 mm Hg (1.3 kPa) vacuum seems a reasonable compromise between losses and vacuum technology. Temperature considerations dominate the design process of composite rotors at these pressure levels. Temperature effects will limit the energy densities of composite wheels to approximately 7.5 Wh/lb (60 kJ/kg). Drag losses increase with energy density and decrease with mass density, which strongly penalizes composite rotors relative to metallic rotors [4].

Efficient power conversion is the key to flywheel-hybrid vehicles. Fuel economy is a strong function of transmission efficiency, and unlike conventional automobiles, vehicle performance is limited primarily by the torque capacity of the transmission. The flywheel-hybrid vehicle requires a efficient CVT and a controller capable of controlling the flywheel, engine, and CVT while retaining conventional accelerative control [5].

HIGH-PERFORMANCE MILITARY APPLICATIONS

Many high performance military applications currently utilize NiCd or thermal batteries for high power applications. NiCd batteries are limited in their shelf life and low temperature performance. Thermal batteries are limited by their lack of testability. Flywheels offer an attractive alternative which can compete in size and weight with these batteries while offering both testability and long shelf life.

These applications require a unique technology development emphasis. Since power is available up until discharge, self-discharge losses have no effect on storage capacity. Storage losses only increase stand-by power consumption. That power consumption, however, goes directly into heating the volume allocated for the energy storage module. Therefore, heat capacity and transfer considerations establish the upper limit on losses. Power consumption is reduced by use of medium vacuum and low loss bearings. The major technical concerns are obtaining bearings capable of withstanding high accelerations and designing for extermely high reliability.

A novel system has been developed and tested for this application. A 2500 J, 500 W version of this system has been develcped at the Charles Stark Draper Laboratory [1]. This system competes in both volume and weight with competitive battery systems while requiring substantially reduced maintenance.

CONCLUSIONS

Various flywheel applications possess distinct and conflicting development requirements. The key to a successful flywheel research and development program is a thorough understanding of theapplications toward which flywheel technology developments are directed. This understanding is required to establish appropriate technical and economic goals for these developments. The establishment of these goals allows the technical alternatives to be evaluated and the development effort to be focused on the most promising of these alternatives. Emphasis should be placed on developing those technologies unique to flywheels that are unlikely to result from parallel research activities in other fields. The flywheel applications reviewed are summarized in Table 1 together with their development requirements.

Stationary Applications

Stationary applications differ primarily in their storage times, which vary from minutes to several days, with corresponding self-discharge requirements of 50 to 0.05% of full storage capacity per hour (%/h). These self-discharge requirements, coupled with the economic constraints of many "energy" applications, dictate the development requirements and options. Systems with self-discharge rate requirements on the order of 50%/h require little development effort while systems requiring self-discharge rates of 0.5%/h or less require substantial development. These self-discharge losses consist primarily of windage and bearing losses. The self-discharge requirement determines the tradeoffs between bearing losses, windage losses, rotor energy density, and capital cost that in turn determine rotor, bearing, and vacuum requirements.

Moving Base Applications

Moving-base applications have a different set of performance and efficiency requirements than do fixed-base applications. Moving base flywheels operate in a much more severe dynamic environment, which increases bearing requirements and reduces the vacuum level that can be practically employed.

APPLICATION	COMPETITION	FLYWHEEL ADVANTAGES	CRITICAL DEVELOPMENTS	ENERGY POTENTIAL
24-hr photovoltaic and utility load-leveling	Batteries	Longer life Higher efficiency	Low cost wheels $150/kWh Low cost/low loss bearings	Very high
Wayside flywheel system (subway)	On-board flywheel system	Reduces car weight Lower system cost	None required Existing technology	Modest due to limited U.S. subway system
Space power systems	Batteries (NiH_2)	High efficiency Reduced volume	High density wheels Low loss/long life bearings	None
Remote photovoltaic(7-day storage)	Batteries (high battery cost)	Long life	Extremely low losses require major developments	None-although military/commercial potential exists
Flywheel IC engine hybrid	Compressed air/elastomers	Efficiency/adaptability	CVT and related controls, bearings	Very high
Military pulse power applications	High performance batteries/capacitor banks	Testable, high reliability. Monitorable failure modes	Power conversion High density wheels	None

Table 1. Development Requirements for Various Flywheel Applications

Both of these factors increase the self-discharge rate. Therefore, promising moving-base flywheel applications have short duty cycles that take advantage of the high power characteristics of flywheels. Further differences among moving-base applications are the severity of the dynamic environment and the energy to power ratio, which may vary from fractions of a second to many minutes. In contrast to the fixed-base applications, where developments are dominated by self-discharge requirements, moving-base applications are dominated by power conversion requirements.

Overall

Significant prior research has been directed toward the development of high performance composite rotors. These rotors appear ideally suited to meeting the development requirements of high technology space and military storage applications. The development requirements of these high technology applications, however, are quite different from those of the three "energy" applications reviewed. The energy applications consisted of daily fixed-base storage, wayside subway storage, and flywheel-hybrid vehicles. In the fixed-base application, both technical and economic considerations dictate the development of modest energy density, low-cost rotors (5-10 Wh/lb (40-80 kJ/kg), < $150/kWh) and low-loss, low-cost bearings. For the flywheel-hybrid vehicle, development requirements exist for continuously variable transmissions (CVT) and related controls and high performance bearings. These areas would all benefit from a focused research effort.

REFERENCES

1. D. Eisenhaure, J. Downer. Aerodynamic Heating and Windage Loss Characteristics of Flywheel Rotors. C.S. Draper Laboratory, R-1472, June 1981.
2. D. Eisenhaure, J. Downer, T. Savarino. Technical and Economic Considerations in the Design of Low Loss Flywheel Electromagnetic Bearings. C.S. Draper Laboratory, R-1474, June 1981.
3. D. Eisenhaure, B. Johnson, R. Drescher. The Influence of Material Properties on Flywheel Optimization Criteria. C.S. Draper Laboratory, R-1477, June 1981.
4. D. Eisenhaure, J. Downer, T. Bliamptis, B. Johnson. Development Requirements for Fixed-Base Flywheel Systems. C.S. Draper Laboratory, R-1482, June 1981.
5. D. Eisenhaure, T. Bliamptis, B. Johnson, J. Downer. Utilization of Flywheel-Hybrid Drivetrains for Commercial Taxicab Fleets. C.S. Draper Laboratory, R-1486, July 1981.

PROJECT SUMMARY

Project Title: "Advanced Flywheel Storage System"

Principal Investigator: Philip O. Jarvinen

Organization:
Massachusetts Institute of Technology
Lincoln Laboratory
Energy Systems Engineering
P.O. Box 73
Lexington, Massachusetts 02173
(617) 862-5500 ext. 213

Project Goals: To develop a flywheel system to store electrical output from a solar photovoltaic array and convert it to regulated 60-Hz ac for use in residences or load centers, and to analyze its performance, worth and cost.

Project Status: An experimental measurements program was carried out on the 1/10 scale solar photovoltaic flywheel energy storage unit over the full operating range from 7,500 to 15,000 RPM to determine the system in-out electrical storage efficiency and the electrical power transfer efficiencies of its components including the maximum power point tracker, motor drive system generator and output power-conditioning systems. The flywheel test set-up contained power-conditioning hardware of both the utility-interactive inverter and stand-alone cycloconverter types. An electrical efficiency measurement accuracy of ±0.5% was achieved by using calibrated power meters and by conducting the tests in a hard vacuum of 10^{-6} torr to eliminate rotor friction drag effects and associated data corrections. In the utility-interactive mode, a round trip storage efficiency of 82% was measured for one-hour storage of the electricity before removal and a 78% efficiency was measured for a 10-hour storage time. Six thousand hours of operation have been achieved to date.

Preparations are underway to test a GFE advanced composite rotor on magnetic suspension. The GFE biannulate rim rotor which weighs 123 pounds, is 24 inches in diameter and stores 1 kWh at 15,000 RPM recently passed a 10-percent overspeed spin test to 16,500 RPM, a requirement for its installation in the vacuum test chamber. Integration of the composite rotor, magnetic suspension system and enlarged containment system is in progress at Lincoln Laboratory.

Contract Number: DOE-AC02-76ET20279

Contract Period: FY-81

Funding Level: $366K

Funding Source: U. S. Department of Energy, jointly by Divisions of Energy Storage and Photovoltaic Energy Systems

DOE/ET/20279-157

ADVANCED FLYWHEEL STORAGE SYSTEM* ** +

Philip O. Jarvinen

Massachusetts Institute of Technology
Lincoln Laboratory
P.O. Box 73
Lexington, Massachusetts 02173

ABSTRACT

This paper reports on an efficiency measurements program conducted on a 1/10-scale prototype flywheel energy storage unit employing magnetic bearings; on the design of an improved configuration for a full-scale, 20-kWh residential flywheel unit; and on an in-progress effort to test a GFE advanced composite rotor on magnetic suspension.

INTRODUCTION

At last year's review meeting, it was reported (1) that construction of a 1/10-scale prototype residential solar photovoltaic (PV) flywheel energy storage unit had been completed (Fig. 1 and Fig. 2), and that the unit had been exercised over its full operating speed range (from 7500 RPM to 15000 RPM) to verify the motor-drive electronics, magnetic bearings, motor-generator and output power-conditioning equipment of both the utility-interactive inverter and stand-alone cycloconverter types (Fig. 3 and Fig. 4). In the concept being pursued, electricity from a solar PV array on the roof of a residence or other location is stored in the flywheel during the day and then removed as needed to supply the electrical loads of the residence. The 1/10-scale prototype employs a 400-pound, 15-inch-diameter steel-rotor storage element with 1 kWh of energy storage at its maximum design speed of 15000 RPM. The 120-V, 60-Hz output power quality from the unit was shown to be excellent (1), with total harmonic distortions of only a few percent or less. Manufacturer cost studies and user-worth studies were presented which showed that flywheel energy storage systems are cost competitive with lead-acid and advanced battery storage systems in PV applications.

CP267-819

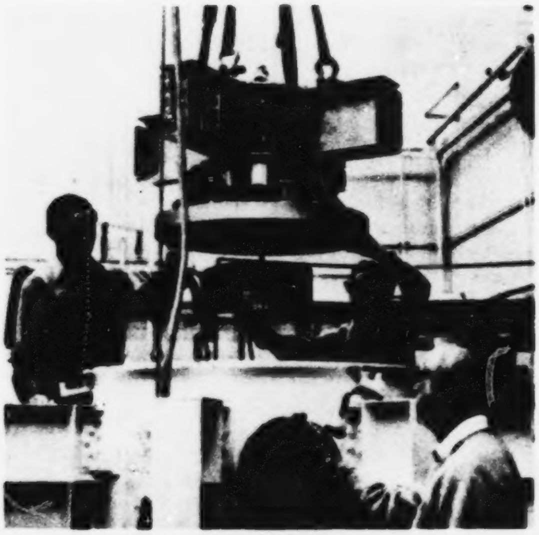

Fig. 1. Installation of the 1/10-scale prototype flywheel unit in the vacuum test chamber.

C71-1020

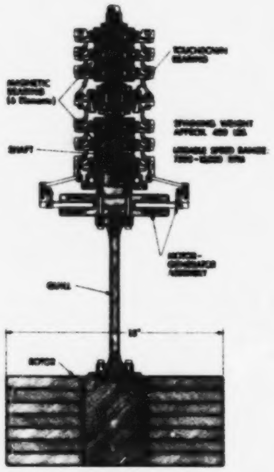

Fig. 2. 1/10-scale prototype flywheel unit.

---

* This work was sponsored by the U.S. Department of Energy.

** The U.S. Government assumes no responsibility for the work presented.

+ Progress Report for the Mechanical, Magnetic, and Undergound Energy Storage 1981 Annual Contractors' Review, Washington, DC, 24-26 August 1981.

108083-R

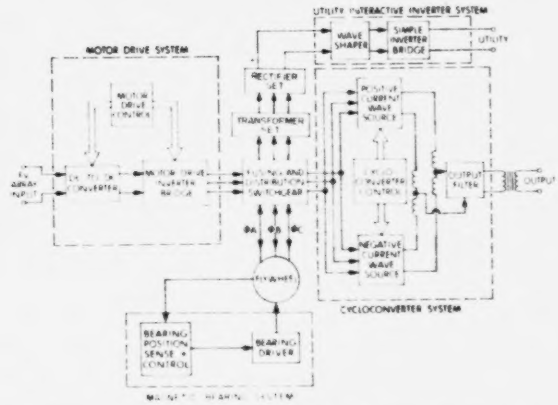
UTILITY INTERACTIVE INVERTER SYSTEM
WAVE SHAPER
SIMPLE INVERTER BRIDGE
UTILITY
MOTOR DRIVE SYSTEM
MOTOR DRIVE CONTROL
RECTIFIER SET
TRANSFORMER SET
PV ARRAY INPUT
DC TO DC CONVERTER
MOTOR DRIVE INVERTER BRIDGE
FUSING AND DISTRIBUTION SWITCHGEAR
POSITIVE CURRENT WAVE SOURCE
CYCLO CONVERTER CONTROL
NEGATIVE CURRENT WAVE SOURCE
OUTPUT FILTER
OUTPUT
ΦA
ΦB
ΦC
FLYWHEEL
CYCLOCONVERTER SYSTEM
BEARING POSITION SENSE + CONTROL
BEARING DRIVER
MAGNETIC BEARING SYSTEM

Fig. 3. Flywheel electrical test set-up.

C74-1009

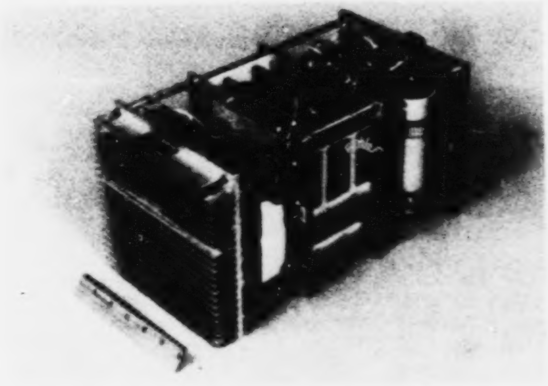

Fig. 4. 1-kW utility-interactive inverter.

During FY-81, efforts in the flywheel program have been directed to three areas: a careful measurements program to characterize the existing 1/10-scale prototype flywheel unit, design studies of a full-scale, 20-kWh solar PV residential flywheel storage unit incorporating cost reduction improvements, and the testing of a GFE advanced composite rotor on magnetic suspension. The measurement program objectives included the determination of the in-out electrical storage efficiency of the flywheel unit and the power-transfer efficiencies of its components, including the PV array maximum-power-point tracker, motor-drive electronics, motor-generator and output power conditioners. An electrical efficiency measurement accuracy of ± 0.5% was achieved by installing calibrated power meters and by conducting the tests in a hard vacuum of 10^{-6} torr to eliminate any rotor aerodynamic friction drag effects and associated data corrections. The measurement program served two functions in that it confirmed the performance credentials of the flywheel unit and provides potential commercial manufacturers with a data base for evaluating the maturity and market potential of such a storage approach.

The cost reduction efforts in the 20-kWh residential flywheel unit centered on a reduction in the number of magnetic bearing elements required to support the flywheel rotor. Analyses and experimental tests of magnetic bearings were carried out which showed that a two-element magnetic bearing unit was a viable technical solution. The change to a two-element design from the original approach which employed six elements meant a much reduced parts count and a lower magnetic bearing cost.

Preparations for testing the GFE advanced composite rotor on magnetic suspension included digital computer analyses of critical frequencies, mode shapes, excursion amplitudes and internal hysteris effects of the GFE composite flywheel and support system; the design, fabrication and assembly of a simplified two-element samarium-cobalt magnetic support system; design and construction of an enlarged containment system for the GFE rotor, and air turbine overspeed testing (spin testing) of the GFE rotor to 16500 RPMs before installation in the vacuum test chamber. The measurements program, 20-kWh residential flywheel unit design, and GFE rotor testing are discussed on the following pages.

1/10-SCALE PROTOTYPE EFFICIENCY TESTS

The physical arrangement and electrical features of the prototype flywheel test unit are described in depth in references 2 and 3 and only a brief review will be presented here. The main physical elements are the permanent magnet magnetic-bearing suspension system, the permanent magnet motor-generator, the flexible quill, the flywheel rotor, and the vacuum tank. The magnetic-bearing suspension system is supported from the walls of the vacuum chamber by stiff structural members. The motor-generator flexible quill and rotor are attached, in that order, below the suspension system. For purposes of testing, the prototype flywheel unit has been placed in an existing vacuum tank at Lincoln Laboratory, Fig. 1. The magnetic suspension system is an axially active, radially passive, attractive design with lifting forces provided by samarium-cobalt permanent magnets. An axial position feed-back control loop with auxiliary electromagnetic control is provided to ensure axial position stability.

The flywheel electrical test setup consists of four major sections: the motor-drive system, the utility-interactive inverter system, the stand-alone cycloconverter system, and the magnetic-bearing sense and control servo system, Fig. 3. The motor-drive system contains three parts: a maximum-power-point-tracking dc-to-dc converter, a motor-drive control, and a motor-drive inverter bridge. The dc-to-dc converter acts as a variable matching network or "dc transformer" to allow the PV array to operate at the maximum-power-point voltage despite the wide dynamic variations of the motor-drive bridge-input voltage. The motor-drive inverter bridge is a three-phase, six-pulse, inductor-fed, phase-controlled rectifier set operated in the inverting region. The motor-drive control circuit has two purposes. It generates gate-firing pulses and changes the bridge-commutation mode at low speeds. Variable-frequency, variable-voltage ac output power from the generator is provided directly to the stand-alone cycloconverter power converter or passed through a rectifier if it is intended for use in the utility-interactive inverter system.

When the flywheel system is used in a utility-interactive application, the inverter acts as a utility-synchronized, 60-Hz, ac-current source. The power flow from the flywheel to the utility is as follows: first the flywheel rotor/generator output voltage is rectified; next, the rectified dc is shaped into a 60-Hz, full-wave rectified current using a 20-kHz switching regulator; finally, the full-wave rectified current is "unfolded" (inverted) into a distortionless 60-Hz sine wave which is fed to the utility, Fig. 5.

108081-N

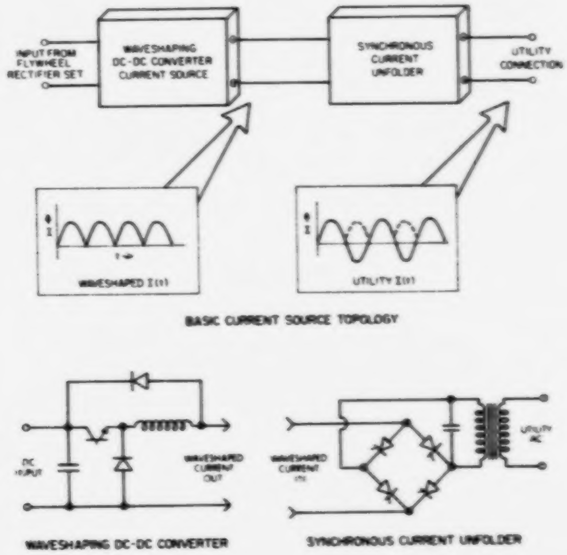

Fig. 5. Utility-interactive inverter principle.

The overall in-out electrical storage efficiency of the flywheel system was measured as were the power-transfer efficiencies of individual components and the spin-down tare losses due to effects of the magnetic bearing, mechanical damper and armature. Power-transfer efficiencies of the dc-to-dc down-converter, motor electronics and utility-interactive inverter were determined from measurements of the input power to an output power from the component, while motor generator/rectifier and cycloconverter efficiencies were determined by measuring the change in the stored energy (rotor-spin speed) for measured speed versus time with the system electrically isolated from all inputs or outputs. Examples of data taken during operation in the utility-interactive mode are presented in Figs. 6 through 9. The dc-to-dc converter efficiencies were found to range from 98 to 99.5% in the speed range from 7500 to 12000 RPM, Fig. 6. Inverter efficiencies over 90% were measured at flywheel RPMs between 9600 RPM (248 Volts) and 13300 RPM (343 Volts), Fig. 7. The spin-down tare loss was found to increase linearly with rotor speed, Fig. 8, to a maximum of only 4W at 15000 RPM. Figure 9 tabulates the component efficiencies and overall efficiencies versus spin speed. Overall in-out electrical storage efficiency of 82% was measured if electricity is stored for one hour before removal, while electricity stored for a 10-hour period before removal was recovered with a 78% in-out efficiency. A full-scale unit would do somewhat better than the 1/10-scale prototype because the tare losses would be a smaller percentage of the stored energy. Six thousand hours of operation wtih the steel rotor have been achieved to date.

C74-1287

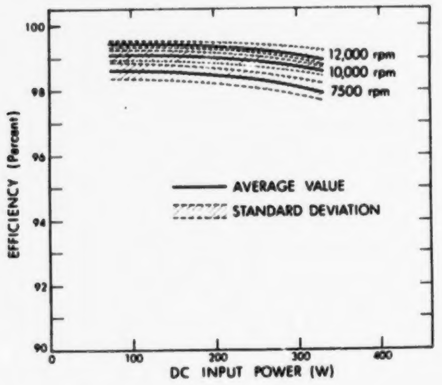

Fig. 6. DC-to-DC down-converter efficiencies.

108082-N

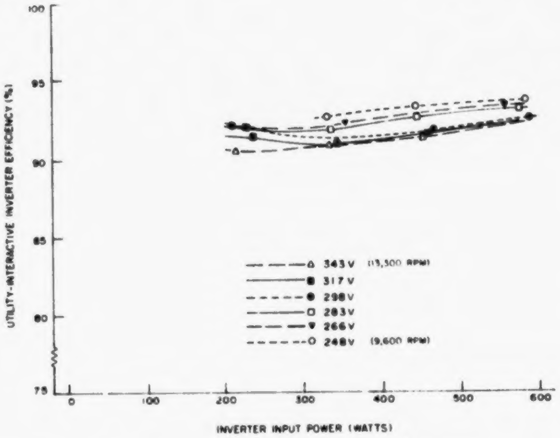

Fig. 7. Inverter operating efficiency.

C74-1214

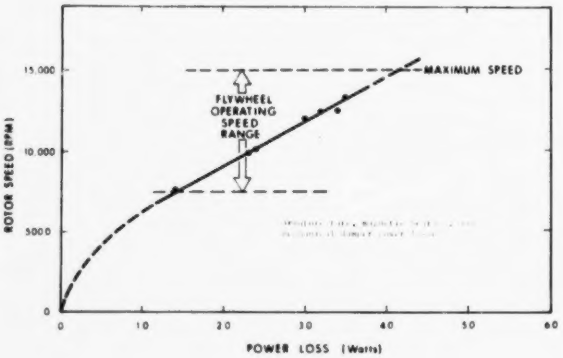

Fig. 8. Spin-down tare loss.

108123-N

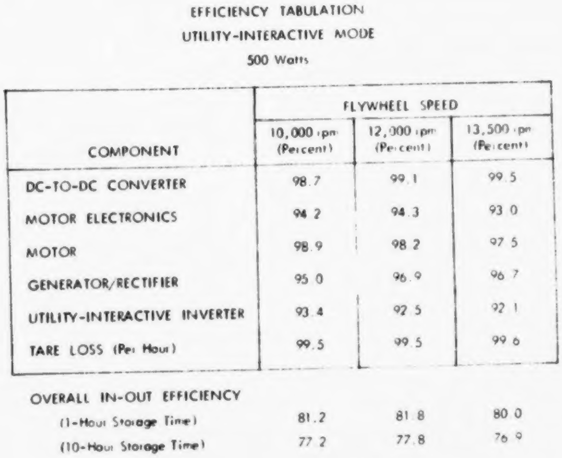
EFFICIENCY TABULATION
UTILITY-INTERACTIVE MODE
500 Watts

COMPONENT	FLYWHEEL SPEED		
	10,000 rpm (Percent)	12,000 rpm (Percent)	13,500 rpm (Percent)
DC-TO-DC CONVERTER	98.7	99.1	99.5
MOTOR ELECTRONICS	94.2	94.3	93.0
MOTOR	98.9	98.2	97.5
GENERATOR/RECTIFIER	95.0	96.9	96.7
UTILITY-INTERACTIVE INVERTER	93.4	92.5	92.1
TARE LOSS (Per Hour)	99.5	99.5	99.6
OVERALL IN-OUT EFFICIENCY			
(1-Hour Storage Time)	81.2	81.8	80.0
(10-Hour Storage Time)	77.2	77.8	76.9

Fig. 9. Efficiency tabulation utility-inverter mode: 300 watts in, 500 watts out.

FULL-SCALE, 20-kWh RESIDENTIAL FLYWHEEL SYSTEM DESIGN

Studies were performed to determine whether the number of bearing elements in the magnetic bearing system might be reduced from the six-element design originally evaluated for manufacturing costs by three industrial manufacturers (1). A reduction in the number of magnetic elements would translate into a smaller parts count and thus into a reduced cost for the bearing. A two-bearing element, magnetic-bearing suspension system was found to be a viable technical option to the original magnetic bearing and a full-scale, 20-kWh residential flywheel storage unit employing this approach was designed (Fig. 10). This flywheel unit would employ a 36-inch-diameter, 19-inch-high, 1500-pound advanced composite rotor with a maximum design speed of 15000 RPM. The overall height of the flywheel unit including the vacuum tank and support arms would be 4 feet, 8 inches and the overall width would be 3 feet, 10 inches.

TEST OF A GFE ADVANCED COMPOSITE ROTOR ON MAGNETIC SUSPENSION

A program to test a GFE advanced composite rotor on magnetic suspension is in progress at Lincoln Laboratory. The GFE rotor is a biannulate rim type with tension balance spokes and was constructed for Sandia Laboratories by William Brobeck and Associates. The rotor is 23.5 inches OD and 7.85 inches high, weighs 123 pounds (96-pound rim), and stores 1 kWh of energy at 15000 RPM, the maximum expected test speed, Fig. 11. The flywheel was originally designed for a vehicular application which differs from its present use and its maximum design speed and maximum stored energy for that application are listed as 32725 RPM and 4.95 kWh, respectively.

107566-N

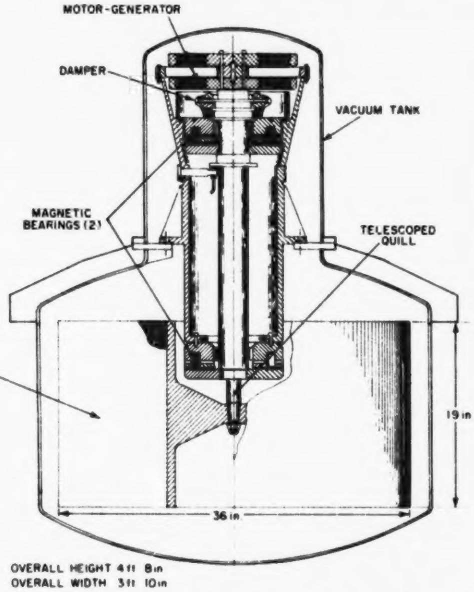

Fig. 10. 20-kWh, 6-kW residential design with a two-element magnetic bearing.

CP267-6342

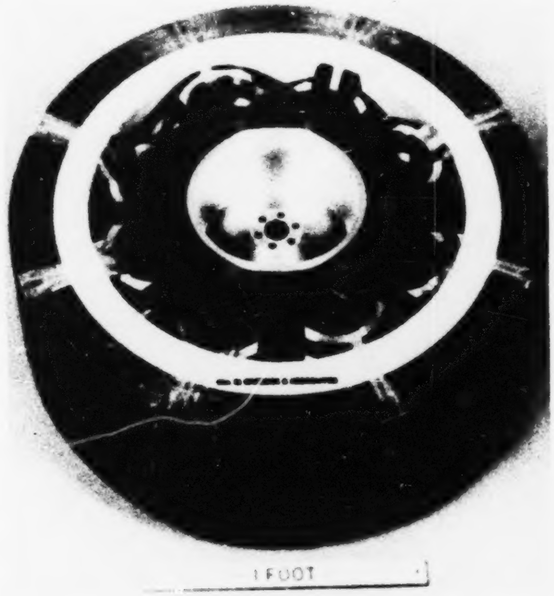

Fig. 11. GFE advanced composite rotor.

This will be the first test of an advanced composite rotor on magnetic suspension. The development of low-speed whirl modes because of internal hysterisis effects in the test of the steel flywheel on magnetic suspension, and their elimination by the addition of external damping, was previously shown (1) to be an important design consideration. The present test program will evaluate this effect with respect to an advanced composite rotor. A steel flywheel simulator with the same weight, the same moment of inertia and the same ratio of inertias as the composite rotor has been built and will be used as a tool to distinguish effects peculiar to the advanced composite rotor. A two-element magnetic bearing of the type now preferred for the full-scale residential flywheel system was designed and fabricated for the composite rotor tests. A side-by-side comparison of the original and new approaches is shown in Fig. 12 and the reduction in number of parts in the two-bearing approach is evident. The magnetic bearings for the two-bearing design are shown in Fig. 13 and a significant fraction of the parts for the magnetic bearing assembly are shown in Fig. 14. The two-element bearing configuration was selected on the basis of digital computer calculations that examined questions of static and dynamic stability, including the effects of critical mode frequencies, mode shapes, static and dynamic flywheel imbalances, and excursion amplitudes. The magnetic bearing assembly is now in the final stages of assembly. The motor-generator assembly from the original flywheel storage unit will be used without modification in the new test series.

The GFE composite rotor successfully passed a 10% overspeed test to 16500 RPM, a requirement before its installation in the vacuum test chamber. The test was conducted at Barbour Stockwell Co. in Cambridge, Massachusetts, on their air turbine driven equipment. The GFE rotor was suspended below the air turbine on a quill, Fig. 15. A six-inch ruler has been placed in the foreground to provide a scale for comparison. The spin test pit, flywheel and test control console are shown in Fig. 16. Prior to this spin test, the balance of the as-received GFE rotor was checked by E. E. Lindskog Co., Bedford, Massachusetts, and found to be unsatisfactory; a dynamic imbalance of 1/8 of a degree was measured. Using standard procedures, the GFE rotor was then balanced to 5/1000 of a degree dynamic imbalance by attaching balance weights to the inner rim surface. During the test at Barbour Stockwell Co., the GFE rotor was accelerated from stop to 16500 RPM in 35 minutes. The tests were conducted at a chamber pressure of 85 millitorr and the displacement amplitude of the quill was monitored by a probe located above the flywheel. The 10% overspeed condition was reached without incident and inspection of the flywheel after test showed no visible changes as a result of the test.

C74-1480

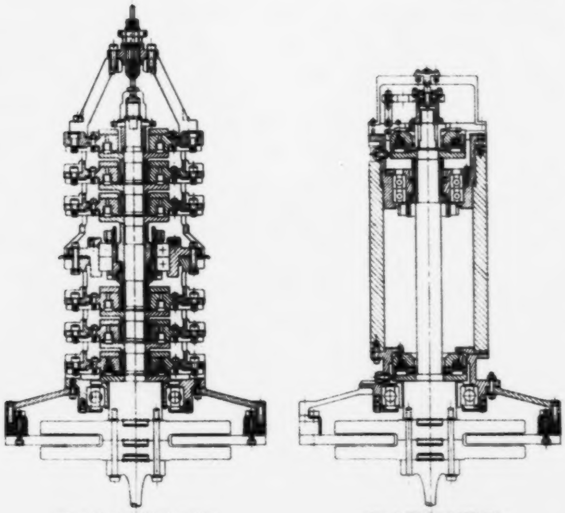

ORIGINAL 6 BEARING DESIGN

NEW 2 BEARING DESIGN

Fig. 12. Comparison of old and new magnetic bearing approaches.

CP267-6899

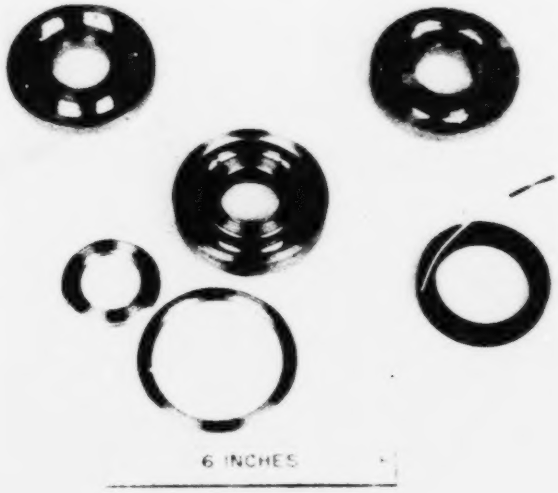

Fig. 13. Magnetic bearings for the two-element design.

CP267-6900

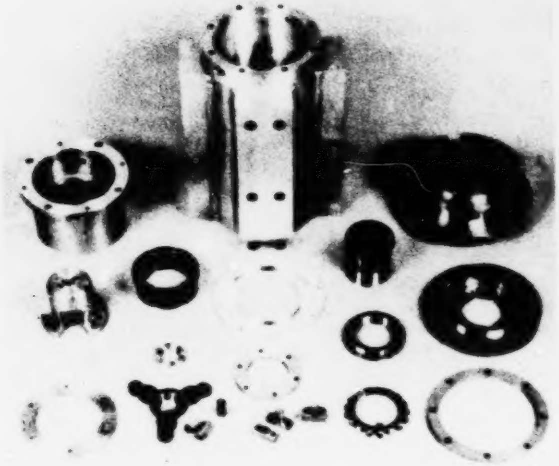

Fig. 14. Parts for the magnetic bearing assembly.

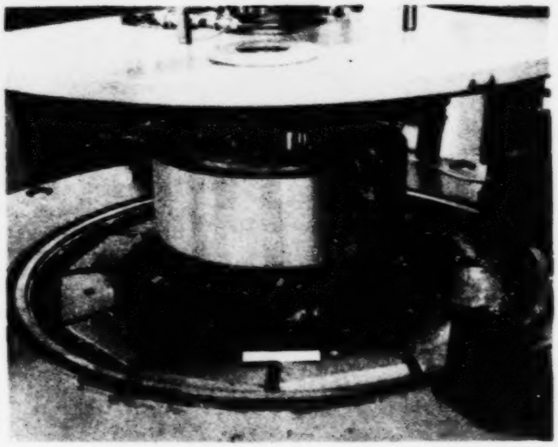

Fig. 15. Air turbine spin pit with the GFE rotor.

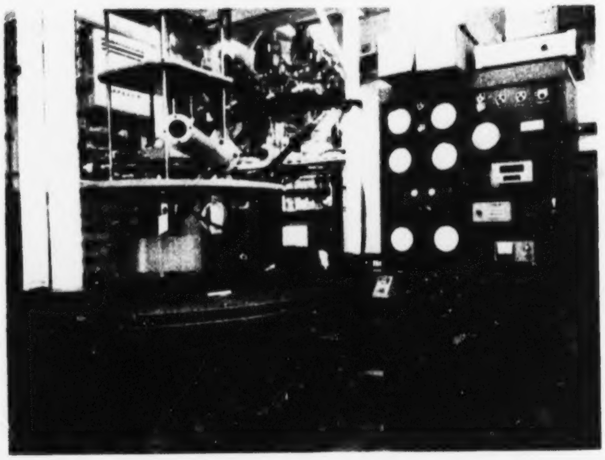

Fig. 16. GFE composite rotor overspeed test set-up.

Substantial outgassing from the GFE rotor was observed during a two-week vacuum chamber outgassing test performed at Lincoln Laboratory prior to the spin test and also during the Barbour Stockwell Co. spin tests. For example, in the laboratory tests it was observed that upon shutting the vacuum pump off, the chamber pressure would rise from 10^{-4} torr to 10^{-3} torr within about one minute and to 10^{-2} torr within about five minutes. This level of outgassing will not hinder the planned magnetic suspension tests because sufficient pumping capacity is available, but it would be critical to an in-the-field flywheel concept where long time periods are planned between maintenance vacuum pump-downs. It is recommended that more consideration be given to the selection of materials to minimize outgassing in future rotors.

Integration of the GFE rotor, magnetic bearing unit and enlarged containment system is now under way with completion of this task expected by early September. Testing of the rotors will commence immediately thereafter. The enlarged containment system was required because of the size increase from steel to composite rotor, 15 inches diameter to 24 inches diameter, respectively.

SUMMARY AND CONCLUSIONS

The in-out electrical storage efficiency of the 1/10-scale, magnetically supported flywheel unit has been measured in the utility-interactive mode to be 82% after one hour and 78% after ten hours of storage time. The magnetic-bearing unit for a full-scale system has been simplified by adopting a design that uses two-bearing elements with a much reduced parts count. Preparations are nearly complete to test a GFE advanced composite rotor on magnetic suspension. The advanced rotor has been overspeed tested to 16500 RPM without incident. The GFE composite rotor, two-element magnetic bearing and enlarged containment system are undergoing final assembly and integration.

REFERENCES

1. Jarvinen, P. O., "Photovoltaic Energy System Applications of Flywheel Technology," Mechanical, Magnetic and Underground Energy Storage 1980 Annual Contractors' Review, Washington, DC, 10-13 November 1980, DOE Conference-801128, pp. 340-345.

2. Jarvinen, P. O., Brench, B. L. and Rasmussen, N. E., "Performance Characteristics of Solar Photovoltaic Flywheel Storage Systems," 15th IEEE Photovoltaic Specialists' Conference, Orlando, FL, 11-15 May 1981.

3. Jarvinen, P. O., Brench, B. L., Hay, R. D. and Rasmussen, N. E., "Testing and Evaluation of a Solar Photovoltaic Flywheel Energy Storage System," 16th Intersociety Energy Conversion Engineering Conference, Atlanta, Georgia, 9-14 August 1981.

PROJECT SUMMARY

Project Title: Flywheel Rotor and Containment Technology Development

Principal Investigator: S. V. Kulkarni

Organization: Lawrence Livermore National Laboratory

Project Goals:

- To develop, by FY1984, an economical and practical composite flywheel having an energy density of 88 Wh/kg at failure, an operational energy density of 44 to 55 Wh/kg, and an energy storage capacity of approximately 1 kWh.
- To determine the suitability of various manufacturing processes for low-cost rotor fabrication.
- To investigate flywheel and flywheel-systems dynamics.
- To test and evaluate prototype rotors for use in transportation and stationary applications.
- To develop, by FY1984, a fail-safe, lightweight, and low-cost flywheel containment.

Project Status: The following tasks have been accomplished:

- Evaluation and selection of 1-kWh, first-generation, advanced flywheel rotor designs for subsequent development towards the DOE-established energy density goal of 88 Wh/kg at burst. (Task Milestone).
- Completion of an advanced design concept for a flywheel primary containment structure, capable of containing the failure of a 1-kWh flywheel rotor and targeted for vehicular applications (Task Milestone).
- Non-destructive inspection and burst testing of approximately twenty (20) prototype rotors, and initiation of cyclic testing.
- Completion of various activities in the areas of rotor manufacturing processes, dynamic analyses and composite materials design data generation.
- Initiation of an economic feasibility study to establish a rational costing methodology for composite rotors and containment.

Contract Number: W-7405-Eng-48

Contract Period: October 1, 1980 to September 30, 1981

Funding Level: $926,000

Funding Source: U.S. Department of Energy

FLYWHEEL ROTOR AND CONTAINMENT TECHNOLOGY DEVELOPMENT*

Satish V. Kulkarni
University of California, Lawrence Livermore National Laboratory
Livermore, CA 94550

ABSTRACT

The status of the flywheel rotor and containment technology development program during FY81 is reviewed in this paper. The specific objectives of the different activities are delineated, and progress during the present reporting period is described briefly. Because of the current emphasis in certain areas such as flywheel cost analysis, rotor dynamics, testing, and containment development, accomplishments in those areas during FY81 are reported separately.

INTRODUCTION

With the increased emphasis on energy conservation and fuel economy, the development of energy-storage devices has gained considerable momentum. These devices accomplish load leveling, power boost, and energy recovery. Flywheels are one such method of energy storage that has received increasing attention in the past few years. It has been concluded that incorporating a flywheel in a vehicle that operates predominantly in urban driving situations will result in significant fuel savings. Flywheels also have potential applications in various fixed-base application, such as wind- and solar-energy generation and utility load leveling. While the flywheel is not a new concept, the use of fiber-reinforced composite materials in a flywheel is. These materials possess high specific stiffness and strength, the latter being a direct measure of the specific energy of the flywheel rotor. The high specific strength enables fiber-reinforced composite rotors to have higher energy-storage efficiency than metallic rotors. It has also been demonstrated that fabrication costs for composite material components are lower than their metallic counterparts in many cases. In addition, failures in composites are generally less catastrophic, thus, requiring lighter containment structures.

The two primary objectives of this effort are:

- To develop an efficient, economical, and practical composite flywheel having an energy density of 88 Wh/kg (40 Wh/lb) at failure, with an operational range of 44 to 55 Wh/kg (20 to 25 Wh/lb) and an energy-storage capacity of approximately 1 kWh.

- To develop a fail-safe, lightweight, and low-cost composite containment for the flywheel.

The strategy being followed to achieve the objectives is outlined below:

- Design, develop, fabricate, and test the most promising generic rotor and containment concepts.

- Use existing technologies wherever applicable.

- Initiate effort, as needed, to support pertinent technology areas.

- Seek active participation by industry, national laboratories, and universities to (1) use expertise in an optimum fashion, (2) promote cross fertilization of ideas, and (3) create a competitive environment.

---

*This work was performed under the auspices of the U.S. Department of Energy by the Lawrence Livermore National Laboratory under contract No. W-7405-Eng-48.

The highlights of the accomplishments for this task during FY81 are:

- Completed the evaluation of prototype flywheels and identification of promising designs for further development and testing (Task Milestone).
- Evaluated the Flywheel Programs in W. Europe for DOE.
- Prepared a multi-year plan (1981-85) for Flywheel Rotor and Containment Technology Development.
- Attained highest energy density for any flywheel rotor to date (36.1 Wh/lb for the Garrett AiResearch design).
- Obtained highest energy density for a laminated composite flywheel rotor (30.5 Wh/lb for LLNL design).
- Obtained highest energy capacity for any composite flywheel (1.94 kWh for the Rocketdyne design).
- Initiated a study for the cost analysis of composite flywheels.
- Used ultrasonic and radiographic techniques at LLNL for nondestructive inspection of all prototype flywheels.
- Spin-tested to failure approximately twenty (20) prototype flywheels. Test data are the most comprehensive to date. Many failures were both repeatable and predictable. Understanding of failure modes has considerably enhanced our understanding of the containment process.
- Developed a preliminary cyclic test plan at LLNL for composite rotors for establishing relationship between short-term spin tests and long-term service performance.
- Fabricated and tested steel and aluminum/Kevlar-29 cloth containment rings for the six prototype rotors.
- Completed two competitive containment design studies.

Specific objectives and the status for different activities are discussed in the following pages.

OBJECTIVES AND STATUS OF VARIOUS ACTIVITIES

The work breakdown structure of this task consists of eight (8) major subtasks and several activity areas under each subtask. Because of the current emphasis in certain areas such as flywheel cost analysis, rotor dynamics, testing, and containment development, progress during FY81 is reported separately.

1. Technical Management, Lawrence Livermore National Laboratory (LLNL)--Technical management activities play a crucial role because of the various industry and university subcontracts and the interdisciplinary nature of this task.

Objectives:

- To identify activities and projected costs with the Task goals and the availability of funding.
- To prepare IFPs and evaluate responses.
- To evaluate technical performance and track contract schedules and milestones.

- To provide consultation to industry.
- To promote technology transfer.

Status:

- Planned, coordinated, and directed approximately twenty five (25) activities at LLNL, other national laboratories, industry, and universities.
- Evaluated the Flywheel Programs in W. Europe for DOE.
- Prepared a multi-year plan (1981-85) for Flywheel Rotor and Containment Technology Development.
- Completed the evaluation of prototype flywheels and identification of promising designs for further development and testing. Decision analysis techniques were utilized in the evaluation process (Task Milestone).

While the ultimate decision-making responsibility rested with LLNL, a Rotor Selection Committee comprised of experts from various technology/application areas was formed to facilitate the decision-making process. The committee was formed because of the need to address many different and diverse issues such as performance, costs, systems adaptability, development risks, etc.

Based on the various selection criteria and the rankings, the following recommendations were made:

- Further development and testing of (a) the Garrett multi-material multi-ring rim rotor, and (b) the constant thickness laminated disk rotor with and without a rim (LLNL and GE designs) should be continued.

Since the GE and LLNL designs are generically similar, development of these two concepts under a single activity is justifiable.

- As an option, since the Avco rotor design was ranked highly, a prototype should be fabricated and spin-tested to assess its potential.

Figure 1 illustrates the Garrett, LLNL, GE, and the proposed Avco designs.

2. Composite Laminated-Disk Rotor Technology Development (LLNL)

Objectives:

The two primary objectives are:

- To develop the technology for high-energy-density, fiber-composite flywheels based on the laminated-disc concept.
- To demonstrate a prototype of this design for a practical flywheel.

The specific tasks for FY81 are:

- To conduct stress analysis and optimization studies of laminated disk/ring type flywheels.
- To develop a cyclic test plan for rotors.
- To establish NDI procedures, and evaluate the effect of defects on rotor performance.

- To generate design data for elastomeric bond.
- To develop a biaxial stress test fixture.

Status:

- Both constant and tapered thickness S2-glass and graphite/epoxy laminated disks designed and fabricated by LLNL were spin-tested to failure at Applied Physics Laboratory (APL) and Oak Ridge Flywheel Evaluation Laboratory (ORFEL). The constant-thickness S2-glass/epoxy disk had an energy density of 30.5 Wh/lb at burst.

- Stress analysis and optimization studies were conducted for chopped fiber S2-glass/polyester sheet molding compound (SMC) molded disk/filament-wound graphite/epoxy ring hybrid rotors. The effect of ring radial thickness and cross-section shape (such as trapezoidal, exponential, etc.) on energy density was investigated. The disks were fabricated by Owens-Corning, and the rings by Lord Kinematics.

- For the rotor cyclic test plan, see "Composite Flywheel Durability and Life Expectancy: Test Program," by K. L. Reifsnider, S. V. Kulkarni, and D. M. Boyd, in this meeting.

- Ultrasonic and radiographic NDI was conducted for various prototype rotors before testing them at APL and ORFEL.

- Limited static and fatigue data in torsion were obtained for the rotor/hub elastomeric bond. The bonding technique which utilizes a urethane elastomer instead of the natural rubber/adhesive combination was developed at LLNL.

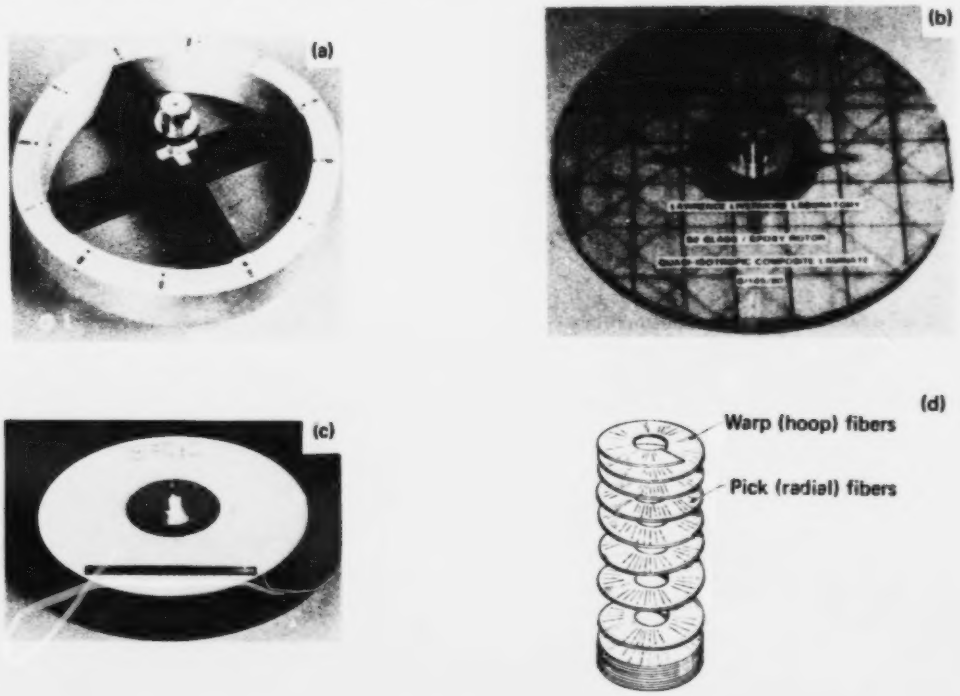

Fig. 1. Flywheel Designs Identified for Further Development and Testing. (a) Garrett Multi-Material, Multi-Ring Flywheel. (b) LLNL Disk-Type Flywheel. (c) General Electric Disk-Rim Hybrid Flywheel. (d) Avco Bidirectional Weave Flywheel Concept.

- The biaxial test fixture was fabricated and tests were performed for circular composite laminate specimens. Test results indicate that modifications to the loading and gripping mechanism will be required.

A detailed description of the LLNL activities is given in Refs. 1 and 2.

3. Advanced Rotor Concepts—Industry

a. Alpha-Ply Composite Laminated Disk/Ring Hybrid Rotor Development (GE)

Objectives:

- To design and fabricate two (2) prototype alpha-ply S2-glass/epoxy laminated disk/filament-wound graphite/epoxy hybrid flywheels.

- To perform analytical studies in the areas of disk/ring optimization, fatigue and creep effects, and hub attachment designs.

Status:

- This effort has been completed (Ref. 3).

- The design and fabrication of the two (2) prototype flywheels and the analytical studies were completed during FY81.

- Burst tests of the GE prototype flywheels at APL yielded a maximum energy density of 25.6 Wh/lb.

- One (1) prototype was fatigue-tested at ORFEL.

b. Bidirectional Weave Composite Rotor Materials Evaluation (Avco)

Objectives:

- To conduct optimization studies for the S2-glass bidirectional weave by altering the ratio of the percentages of radial and hoop fibers as a function of disk radius.

- To evaluate the potential of bidirectionally (radial and hoop) woven composite materials for flywheel application by weaving sample laminates and conducting tests to obtain the pertinent mechanical properties.

Status:

- This effort has been completed (Ref. 4).

Also see "Circular Weave Flywheel Materials Evaluation and Composite Flywheel Burst Containment," by A. Sapowith and W. Handy in this meeting.

c. Development of Metglas Flywheel—Applied Physics Laboratory (APL)

Objectives:

- To design, fabricate, and test subscale and prototype wound Metglas ribbon rotors.

Status:

- This activity is complete (Ref. 5).

- Four (4) 50-Wh and two (2) 200-Wh Metglas prototype rotors were fabricated and tested. The rotors were wound from nominal 2-mil-thick Metglas amorphous metal ribbon on a four-spoke aluminum hub. A maximum energy density of 9 Wh/lb was obtained at burst for the prototypes.

d. Advanced, 1-kWh "State-of-the-Art" Prototype Rotor Development (Garrett AiResearch)

Objectives:

- To design, fabricate, and deliver ten (10) multi-material, multi-ring prototype rotors having an energy capacity of up to 1 kWh and a maximum energy density of 40 Wh/lb at burst and an operational energy density of 20-25 Wh/lb.

Status:

- A subcontract has been placed with Garrett for design and fabrication of ten (10) prototype rotors. The development effort will involve minor design modifications of the existing graphite/epoxy hub.

e. Prototype Rotor Development for Vehicular Applications (GE)

Objectives:

- To design, fabricate, and deliver nineteen (19) laminated disk/filament-wound rim hybrid prototype rotors having performance goals consistent with vehicular application requirements.

Status:

- A subcontract has been placed with General Electric for the design and fabrication of nineteen (19) prototype flywheels.

4. Composite Rotor Manufacturing Technology Development

a. Compression-Molded Energy-Storage Flywheels (Owens-Corning)

Objectives:

- To develop chopped S2-glass/polyester SMC (sheet molding compound) having an ultimate tensile strength of 45 ksi.

- To develop the processing technology required to mold 1-in. thick SMC parts.

- To mold constant- and tapered-thickness SMC flywheels in a single step.

Status:

- This activity is complete (Ref. 6).

- Tensile strengths of up to 45 ksi (the highest to date) were obtained for chopped S2-glass/polyester SMC.

- A fabrication process was developed for molding thick SMC laminates and successfully molding 21-in.-diam, 1-in.-thick constant- and tapered-thickness disks.

- Burst tests of the SMC molded disk graphite/epoxy ring hybrid rotors at APL and ORFEL yielded an energy density of 14·7 Wh/lb at failure.

b. Fabrication of High-Performance Filament-Wound Fiber Composite Rings (Lord Kinematics)

Objectives:

- To filament-wind rings (graphite, Kevlar-49/epoxy, and hybrid) of rectangular and trapezoidal cross section for SMC molded disk/ring hybrid rotors.
- To explore the utilization of SiC whiskers as matrix reinforcement in the filament winding process.
- To assemble, by a "shrink-fit" approach, the SMC molded disk/ring hybrid rotors.

Status:

- Twelve (12) graphite/epoxy rings (21-in. i.d.) with and without SiC whisker reinforcement were filament-wound.
- Five (5) constant-thickness SMC molded disk/ring hybrid rotors were assembled by the "shrink-fit" approach. Two of these rotors have been burst-tested at APL and ORFEL.

c. Composite Flywheel Fabrication and Process Optimization (Ewald Associates)

Objectives:

- To define and optimize the compression molding technique to fabricate laminated disk/filament-wound rim flywheels in a single step.
- To fabricate and deliver six (6) flywheels for testing and evaluations.
- To fabricate ten (10) graphite/epoxy composite hubs for the Garrett prototype flywheel.

Status:

- A subcontract has been placed with Ewald Associates.

d. Composite Rotor and Containment Cost Analysis (Battelle-Columbus)

Objectives:

- To develop a costing methodology to establish the cost range as a function of rotor and containment design, materials, manufacturing process, and production quantities.

Status:

- A subcontract was placed with Battelle-Columbus Laboratories. Also see "The Approach for Manufacturing Cost/Design Trade Studies for Flywheels," by B. Noton in this meeting.

5. Investigation of Flywheel and Flywheel Systems Dynamics

a. Dynamics of Composite Material Flywheels (Univ. of Oklahoma)

Objectives:

- To perform continuum analysis of various generic composite-material flywheel rotors and a system analysis of the rotor system to obtain natural frequencies for various vibrational modes.

Status:

- This task is partially complete (Ref. 7). Also see "Design Guide for composite Material Flywheels (Dynamics)," by C. W. Bert in this meeting.

b. Dynamic Analysis of Bonded Multi-Disk Assemblies (Brobeck Associates)

Objective:

- To investigate the dynamic characteristics of bonded multiple-disk flywheel assemblies in order to understand the effects of bond thickness and radius, and aspect ratio of the assembly.

Status:

- This study has been completed (Ref. 8). Important conclusions of this analysis are: (1) transverse, torsional, and out-of-plane whirl modes exist within the operating speed range, (2) natural frequencies increase with the square root of Young's Modulus of the elastomeric bonding material.

6. Fiber-Composite Flywheel Rotor Design Data

a. Failure Analysis of Composite Laminate Flywheels (Villanova Univ.)

Objective:

- To develop a laminate-failure analysis code which incorporates bilinear stress-strain behavior, and compare failure predictions from the code with test data.

Status:

- This study has been completed (Ref. 9). A computer code called BILAM was developed. This code performs laminate-failure analysis using bilinear stress-strain approximations of the nonlinear stress-strain curves. Predictions of laminate failure stresses made with this code correlate better with experimental results.

b. Tension-Tension Fatigue Tests of Unidirectional S2-Glass/Epoxy Laminates (Boeing-Vertol)

Objectives:

- To generate fatigue design data for filament-wound unidirectional S2-glass/epoxy laminates.
- To investigate effects of frequency, stress ratio, and cyclic loading wave shape.

Status:

- This activity has been completed and a report prepared (Ref. 10). S-N curves and residual strength data have been obtained for two load ratios simulating the spin-up and spin-down deep cycles and the stop and go shallow cycles, respectively.

The following observations can be made from these data: (1) cycles to failure decrease with increasing cyclic rate, and (2) a square wave pattern significantly reduces cyclic life, as compared to a smoother sine-wave load spectrum.

c. Tension-Tension Fatigue Tests of Unidirectional Kevlar-29/Epoxy Laminates (GE)

Objectives:

- To generate fatigue design data for filament-wound unidirectional Kevlar-29/epoxy laminates.
- To investigate effects of frequency, stress ratio, and cyclic loading wave shape.

Status:

This effort has been completed and a final report written (Ref. 11). Static and limited fatigue data were obtained. Problems associated with tab failures in the specimens prevented the attainment of all the objectives.

7. Test and Evaluation of Prototype Rotors

a. Burst and Cyclic Testing of Prototype Rotors (ORFEL)

Objectives:

- Burst tests of one (1) LLNL and one (1) GE prototype rotor.
- Follow-up tests for Rocketdyne Prototype No. 1 rotor.
- Burst tests of two (2) Owens-Corning/Lord rotors.
- Fatigue tests of GE disk/ring prototype and Garrett single-rim rotors.

Status:

- This activity is partially complete. Some results of this test program are given in Table 1. See Ref. 12 and "Rotor Testing in FY81," by R. S. Steele in this meeting.

b. Spin-Testing of Prototype Rotors (APL).

Objective:

- To burst-test ten (10) prototype rotors supplied by LLNL.

Status:

- This test program has been completed (see Ref. 13). Ten (10) rotors which included the LLNL constant and tapered thickness laminated disk, GE laminated disk/ring, Owens-Corning/Lord molded disk/ring, and Brobeck designs were tested during FY81. Some of the results of the tests are tabulated in Table 1.

c. Spin-Testing of Rocketdyne RPE-10 Flywheel with Fixed Bearing Supports (Rocketdyne)

Objective:

- To perform nine spin tests of the Rocketdyne Prototype Rotor No. 2 to operating speed with a fixed bearing suspension system.

Status:

- The test has been completed (Ref. 14). The stated objective was not met because the flywheel failed at the first full speed run at 21,500 rpm. The most probable reason for the failure was the separation of the overwrap due to increase of temperature in the spin test chamber to about 260°F.

8. Development of Flywheel Containment

a. Rotor Containment Concept Development (GE)

Objective:

- To design a lightweight, fail-safe, and low-cost containment concept for generic rotor designs.

TABLE 1. Advanced Rotor Designs and Maximum Energy Densities.

	Design	Test Facility	Materials	Maximum energy density Wh/lb (kWh)
1	Garrett multi-material, multi-ring rim	ORFEL	Kevlar-49/-29/S2-glass rings/graphite hub	36.1 (1.23)
2	Brobeck multi-material rim with tension-balanced spokes	APL	S2-glass/Kevlar-49 ring, Kevlar-29 spokes, Al/Kevlar-49 hub	28.9 (0.71)
3	Rocketdyne rim with overwrap and twin-disk hub	ORFEL	Graphite/Al hub	16.4 (1.94)
4	Hercules contoured rim	ORFEL	Graphite/Al hub	17.0 (0.85)
5	GE alpha-ply laminated disk with rim	APL	S2-glass disk/graphite ring/Al hub	25.6 (0.283)
6a	LLNL tapered-thickness laminated disk	APL	Graphite/Al hub	28.4 (0.31)
6b	LLNL constant-thickness laminated disk	APL	Graphite/Al hub S2-glass/Al hub	23.00 30.5 (0.157)
7	LLNL/OC/Lord Molded disk with rim	APL	S2-glass SMC disk/graphite ring/Al hub	14.7 (0.419)
8	APL Metglas ribbon rim	APL	Metglas rim/Al hub	9.00 (0.039)

Status

- This activity has been completed (Ref. 15). Also see "Flywheel Housing Design Concept Development," by A. P. Coppa in this meeting.

Figures 2 and 3 illustrate the containment rings designed by GE for the Garrett and the LLNL tapered disk flywheels.

b. Composite Flywheel Containment Design Study (Avco)

Objective:

- To design a lightweight, fail-safe, and low-cost containment concept for generic rotor designs.

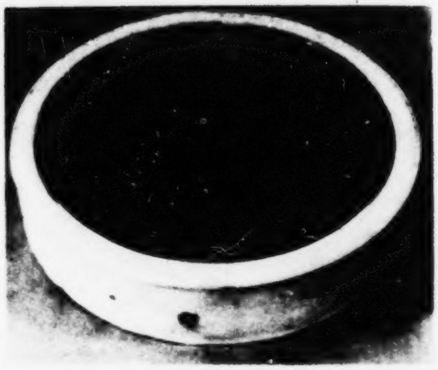

Fig. 2. Containment Ring for Garrett Rotor (aluminum liner overwrapped with dry, woven Kevlar fabric).

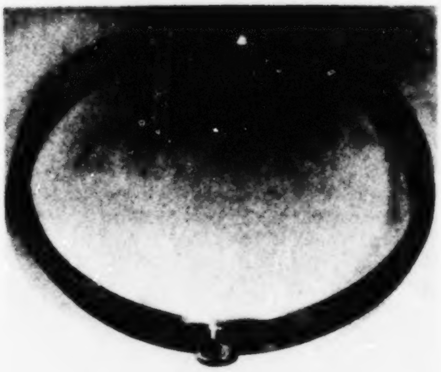

Fig. 3. Steel Containment Ring for LLNL Rotor.

Status:

- This activity has been completed (Ref. 16). Also see "Circular Weave Flywheel Materials Evaluation and Composite Flywheel Burst Containment," by A. Sapowith and W. Handy in this meeting.

CONCLUSIONS

In summary, an overview of the flywheel rotor and containment technology development effort during FY81 has been presented. That this effort encompasses a broad spectrum of technologies is obvious. Every effort is being made to use state-of-the-art techniques and advance them, if necessary, to accomplish the task objectives. The assessment is that significant progress has been made during the present reporting period and that it is indeed feasible to develop adequate rotor and containment designs suitable for both transportation and stationary applications.

REFERENCES

1. T. M. Barlow, W. T. Crothers, T. T. Chiao, D. N. Frank, D. M. King, and S. V. Kulkarni, Mechanical Energy Storage Technology Project: Annual Report for CY1980, Lawrence Livermore National Laboratory, Livermore, Calif., UCRL-50056-80 (1981).

2. B. W. Maxfield, D. M. Boyd, S. V. Kulkarni and A. J. Schwarber, Nondestructive Evaluation of Fiber Reinforced Composite Panels and Flywheels, Lawrence Livermore National Laboratory, Livermore, Calif., UCRL-84930 (1980).

3. R. P. Nimmer, General Electric, "Laminated Composite Disc Flywheel Development," final report prepared for the Lawrence Livermore National Laboratory under LLNL P.O. No. 2749309, 1981.

4. A. D. Sapowith et al, Avco, "Evaluation and Design Considerations of Woven Composite Flywheel Materials Constructions," final report prepared for the Lawrence Livermore National Laboratory under LLNL P.O. No. 6692009 and 1118701, June 1981.

5. D. W. Rabenhorse, W. O. Wilkinson, Applied Physics Laboratory, "Metglas Flywheel Feasibility Demonstration," final report prepared for the Lawrence Livermore National Laboratory under LLNL P.O. No. 7825509, 1981.

6. J. F. Kay, Owens-Corning Fiberglas, Compression Molded Energy Storage Flywheels, Lawrence Livermore National Laboratory, Livermore, Calif., UCRL-15324 (1980).

7. C. W. Bert, Univ. of Oklahoma, "Dynamic Analysis of Composite Material Flywheels - Part I System Whirling and Stability Analysis," final report prepared for the Lawrence Livermore National Laboratory under LLNL P.O. No. 6448509, 1981.

8. William M. Brobeck Associates, "Dynamic Stability of Stacked Laminated Disk Rotors," final report prepared for the Lawrence Livermore National Laboratory under LLNL P.O. No. 2602600, 1981.

9. P. V. McLaughlin, Jr., A. Dasgupta, and Y. W. Chun, Villanova University, "BILAM, A Composite Laminate Failure Analysis Code Using Bilinear Stress Strain Curves," final report prepared for the Lawrence Livermore National Laboratory under LLNL P.O. No 6448409, 1980.

10. Boeing/Vertol, "Fatigue Testing of Filament Wound Unidirectional S2-Glass/Epoxy Laminates,"final report prepared for the Lawrence Livermore National Laboratory under LLNL P.O. No. 6991805, 1981.

11. C. H. Zweben, General Electric, "Tensile and Fatigue Strength Properties of Filament Wound Unidirectional Kevlar-29/epoxy Composites," final report prepared for the Lawrence Livermore National Laboratory under LLNL P.O. No. 6624409, 1981.

12. R. S. Steele, E. F. Babelay, B. J. Sutton, Union Carbide Nuclear Division, Y-12 Plant, Oak Ridge Flywheel Evaluation Laboratory Annual Report, Oak Ridge, Tenn. (1981).

13. D. W. Rabenhorst, W. O. Wilkinson, Applied Physics Laboratory "LLNL Flywheel Spin Test Program," final report prepared for the Lawrence Livermore National Laboratory under LLNL P.O. No. 7825509, 1981.

14. Rocketdyne/Rockwell, "RPE-10 Composite Flywheel Tests," final report prepared for the Lawrence Livermore National Laboratory under LLNL P.O. No. 9519409, 1981.

15. A. P. Coppa, "Flywheel Housing Design Concept Development," final report prepared for the Lawrence Livermore National Laboratory under LLNL P.O. No. 6624409, August 1981.

16. A. D. Sapowith and W. Handy, "A Composite Flywheel Burst Containment Study," final report prepared for the Lawrence Livermore National Laboratory under LLNL P.O. No. 1121401, August 1981.

PROJECT SUMMARY

Project Title: "Cost-Driver Identification and Cost Analysis Methodology Development for Manufacturing Cost/Performance Trade-Studies on Fibrous Composite Flywheels"

Principal Investigator: Bryan R. Noton

Organization:
Battelle's Columbus Laboratories
505 King Avenue
Columbus, Ohio 43201

Project Goals: Identify operational sequences and cost-drivers in the manufacture, including inspection, of composite flywheel designs. Present qualitative cost comparisons of manufacturing processes. Develop a performance/manufacturing cost methodology, utilizing manufacturing man-hours, for comparison of selected flywheel designs.

Project Status: The manufacturing operational sequences have been specified for six composite flywheel designs. The cost-drivers (major costs) in the manufacture of the flywheels, have been identified. A methodology to conduct flywheel performance/manufacturing cost trade-studies is recommended. Industry is currently reviewing the results accomplished.

In a later phase, it is proposed that the methodology be utilized for the following concepts: Garrett multi-material, multi-ring rim; the General Electric (GE) alpha-ply, laminated disk with rim; the Lawrence Livermore National Laboratory (LLNL) tapered thickness laminated disk; and, the Avco bidirectional weave disk.

Contract Number: W-7450-ENG-48 (SANL 908-005)

Contract Period: February 1, 1981 to September 30, 1981

Funding Level: $45,000

Funding Source: Lawrence Livermore National Laboratory

APPROACH FOR MANUFACTURING COST/DESIGN TRADE-STUDIES FOR FLYWHEELS

Bryan R. Noton
Battelle's Columbus Laboratories
505 King Avenue
Columbus, Ohio

ABSTRACT

The primary objective of this program is to develop a procedure to enable credible comparisons to be made of different flywheel designs, based on both performance ratings, manufacturing and inspection cost. Development of the methodology requires identification of all steps in the manufacture and inspection of each design, cost-drivers and, ground-rules and, providing a man-hour summary. The approach to determine the recurring and non-recurring manufacturing man-hours is presented. It is expected that the methodology will be applied to flywheel designs developed by Garrett, General Electric, Avco and the Lawrence Livermore National Laboratory.

INTRODUCTION

Promising designs of flywheels for both automotive and stationary applications are in various stages of development. The designs utilize widely differing configurations and material combinations, including hybrids. It is pointed out by D. Rabenhorst, Reference 1, that among the basic criteria for materials and concept selection, is cost. It is therefore necessary to conduct trade-studies between flywheel performance, e.g., energy per unit weight and energy per unit volume, and acquisition cost. The ultimate objective is to compare the performance of the each system, i.e., flywheel and containment, with the manufacturing cost. Decision makers, i.e., management and design and manufacturing engineers require a "tool" or methodology to enable the acquisition cost to be determined.

The objective of this program is to develop a method which not only enables credible manufacturing and inspection costs to be determined in person-hours or dollars, but also, by means of designer oriented formats displaying cost-drivers, to provide guidance to conceptual and detail designers to achieve lowest cost. To realize this objective, interaction with industry is important and therefore advance information on the program has been submitted to designers and manufacturers of flywheels for critical review and to serve as the basis of discussions during visits required by Lawrence Livermore National Laboratory.

PRINCIPAL TASKS OF PROGRAM

1) To identify cost-driving designer influenced cost-elements (DICE), manufacturing and test, inspection and evaluation (TI&E) operational sequences for flywheels, including the hub and containment
2) Project cost-effectiveness criteria for flywheel systems from literature sources
3) To develop manufacturing cost/performance trade-study methodology for flywheel/containment systems
4) Develop worksheet for systems assessment and rating
5) Develop qualitative illustrations, e.g., pie and bar charts, of cost-drivers in design, manufacturing and TI&E for flywheels, including hub and containment
6) Conduct cost-analysis of selected flywheel systems to demonstrate applicability of cost/performance trade-study methodology (3 above).

Experimental flywheel rotors and containment are produced in several material types and by a variety of manufacturing processes, e.g., filament winding and MMCDM. The design and manufacturing cost-driver analysis for each design and fundamental process is therefore necessary.

The experimental nature of the composite flywheel system projects creates problems for manufacturers as, for example, the tooling utilized may not lend itself to the automated production methods eventually required. The manufacturers may not therefore have adequate knowledge of the costs of producing even experimental hardware and the production mode is considerably more complex. The early application of "Manufacturing Cost/Design Guide" (MC/DG) principles to the DOE flywheel selection is therefore important.

GROUND RULES FOR FLYWHEEL COMPOSITES

General and detailed ground rules are essential when comparing designs of any engineering system. Ground rules provide a common base to achieve understanding, consistency, uniformity and accuracy in developing the manufacturing recurring and non-recurring man-hours. Ground rules therefore promote confidence in the results of trade-studies. General and detailed ground rules are required for the following examples of categories:

GROUND RULES

General

(a) Composite Material Types

(b) Manufacturing Method

(c) Facilities

(d) Data Generation

- Recurring Costs
- Non-Recurring Costs

(e) Support Function Modifiers

Detailed

(a) Material Specifications

(b) Material Cost Trends

(c) Flywheel Engineering Drawings

(d) Manufacturing Tolerances

(e) Manufacturing Cost Methodology

COST-DRIVERS IN FIBROUS COMPOSITE MANUFACTURING

The following are examples of cost-driving operations in the manufacture of composite flywheels:

(a) Material Cost

(b) Hand Layup (slats)

(c) Close Tolerances

(d) Machining

(e) Assembly (fit-up)

(f) Curing

- Parts or
- Assembly

(g) Inspection

Cost-drivers for specific designs of flywheels are shown in Table 1. Filament-winding is a common method to fabricate flywheel components. An assessment of the man-hour distribution for the filament-winding process is shown in Table 2. The percentage labor for winding and curing will be noted.

MANUFACTURING COST METHODOLOGY

The methodology utilized has drawn upon Battelle's experience with development of a "Manufacturing Cost/Design Guide" (MC/DG) for the Air Force. The IDEF method (Integrated Computer-Aided Manufacturing Definition Method), based on structured analysis, was therefore applied. It is not possible to include illustrations showing all controls and mechanisms of the trade-study model. However, Figures 1 to 3 indicate the principle. The recurring and non-recurring costs (man-hours) are utilized in the worksheet, Table 3, to determine the total cost of the system, which includes the flywheel, suspension and containment.

TABLE 2

ASSESSMENT OF MAN-HOUR DISTRIBUTION FOR
FILAMENT WINDING MANUFACTURING PROCESS

DIRECT OPERATIONS	% TOTAL LABOR
1. Clean Mandrel	3
2. Apply Mold Release	1
3. Load Mandrel	1
4. Wind	58
5. Unload & Remove Excess Resin	2
6. Oven Cure	11
7. Extract Mandrel	4
8. Finish Trim	5
9. Deburr & Clean Up Flash	2
10. Inspect	2
11. Identify	4
12. Package or Store	2
	95%

INDIRECT OPERATIONS	% TOTAL LABOR
1. Incoming Material Inspection	1
2. Creel Loading	1
3. Resin Mixing	2
	4%

NONRECURRING OPERATIONS	% TOTAL LABOR
1. Thread Up	1/2
2. Machine Setup	1/2
	1%

CONCLUSION

Manufacturing operational sequences have been identified for 6 designs of composite flywheels. Cost-drivers in composite manufacture are reviewed. The methodology to conduct performance/manufacturing cost trade-offs is recommended based on the Air Force Integrated Computer-Aided Manufacturing (ICAM) standardized documentation system or structured analysis model. To summarize the recurring and non-recurring tooling costs, a table has been prepared. The manufacturing operational sequences, cost-drivers and methodology are under review by designers and manufacturers of flywheels in industry.

REFERENCES

1. D. W. Rabenhorst, Metals and Composites in Superflywheel Energy Storage Systems. 14th Annual Symposium of New Mexico Sections of the American Society of Mechanical Engineers and the American Society for Metals. February 28, 1974. Applied Physics Laboratory, Silver Springs, Maryland.

2. R. C. Flanagan, et. al., Evaluation and Program Recommendations for Anisotropic Material Flywheels (Road Vehicle Applications). Report No. (DSS File No.) 07SU 31155-9-6615. February 10, 1981. Department of Mechanical Engineering, University of Ottawa, Canada.

3. S. V. Kulkarni, Flywheel Rotor and Containment Technology Development Program for the U.S. Department of Energy. UCRL-84713 (Preprint), August 6, 1980, Lawrence Livermore National Laboratory, U.S. Department of Energy.

4. A. P. Coppa, C. H. Zweben and L. Miranda, Flywheel Containment Technology Assessment. UCRL-15261, July 10, 1980. Funded by U.S. Department of Energy through Lawrence Livermore National Laboratory. General Electric Company, Contractor.

5. S. V. Kulkarni, Flywheel Rotor Selection/Review Committee Meeting, Lawrence Livermore National Laboratory. Correspondence, April 27, 1981.

6. B. R. Noton, Advance Information on: Cost-Driver Identification and Cost Analysis Methodology Development for Manufacturing Cost/Performance Trade-Studies on Fibrous Composite Flywheels. June 29, 1981. Funded by U.S. Department of Energy through Lawrence Livermore National Laboratory. Battelle's Columbus Laboratory, Contractor.

TABLE 1. FLYWHEEL COST-DRIVER IDENTIFICATION

FLYWHEEL	OPERATION DESCRIPTION	REMARKS
• Garrett-AiResrearch: Multi-Material Multi-Rim Rotor Design		
- Cruciform Hub Slats (spokes)	• Hand lay-up of slats • Turning outside diameter of cruciform	• Due to number of plies and orientation requirements • Difficult to hold and machine for forced fit
- Rim Fabrication	• Filament winding • Turning inside diameter of rim	• Three materials requiring close control • Holding dimension for forced fit.
- Quill Adapter	• Machining (lathe)	• Depends on tolerance requirements
- Assembly	• Force fit and assembly	• Primarily hand operation (See General Notes A and B)
• Hercules Contoured Disk		
- Flywheel Fabrication	• Filament winding	• Filament winding labor is approximately 60% of total flywheel labor cost
- Hub Fabrication	• Machining (lathe)	• Depends on tolerance requirements for forced fit
- Hub Cap	• Machining (lathe)	• Depends on tolerance requirements for forced fit
- Assembly		• Mechanical assembly (cryogenic optional) (See General Notes A and B)
• Rocketdyne-Rockwell International Multi-Material-Rim Composite Flywheel with Twin-Disk Hub		
- Aluminum Hub Disk	• Close tolerance lathe operations	• Extensive material removal and complex part with thin sections
- Aluminum Mandrel Rim	• Close tolerance lathe operations	• Extensive material removal--thin walls
- Circumferential Rim Wrap	• Filament winding and wrapping	• Specification requires ambient curing cycles between lay-up operations
- Radial Pin		
- Assembly		• Depends on acceptance specifications (See General Notes A, B, and C)
• Brobeck: Multi-Material Rim		
- Ring	• Filament winding	• No graphite--avoids General Note B problems
- Tension Balanced Spokes	• Filament winding-cost of expansion molding die	• Sixteen (16) required per flywheel
- Hub	• Machining (lathe)	• Depends on tolerance requirements
- Hub Overwrap	• Filament winding	• Operations assume inside diameter dimension is not machined
- Hub Overwrap Assembly	• Shrink fit-cryogenic	• Tolerance requirements to provide shrink fit
- Spoke Spacers		• Simple parts, but contribute to excessive assembly costs
- Spoke Weights		• Simple parts, but contribute to excessive assembly costs
- Assembly	• Assembly of parts (part count)	• Very difficult assembly--hand work--not suitable for automation (See General Notes A and C)
• LLNL: Tapered Thickness Rotor		
- Disk	• Cost of compression molding die	• Curing cost less than autoclave, oven, etc.
- Disk	• Machining tapered surfaces	• Machining graphite/epoxy is a slow operation
- Hub	• Machining	• Depends on tolerances (See General Note B)
• General Electric: Hybrid Disk Ring Concept		
- Laminated Disk	• Machining bevel	• Close tolerance required for shrink fit
- Outer Ring	• Filament winding • Machining bevel	• Tolerances for shrink fit and machining graphite
- Hub	• Machining	• Simple part--tolerances could be cost-driver
- Assembly	• Press fit	• May require cryogenics (See General Note A)

GENERAL NOTES

A. Conventional curing processes (vacuum bag/autoclave, vacuum bag/oven, vacuum bag/hydroclave) are common cost-drivers in all composites. These processes are cost-drivers due to high energy requirements as well as hand labor costs. When co-curing is not feasible due to various temperature and pressure requirements, the curing costs escalate into a major cost-driver.

B. The use of aluminum in conjunction with, or bonded to, graphite composites is a potential source of corrosion due to possible electrolytic action between aluminum and graphite.

c. Most of the flywheels analyzed are manufactured in limited quantities on a development bases and require considerable re-design to be cost competitive.

BEST DOCUMENT AVAILABLE

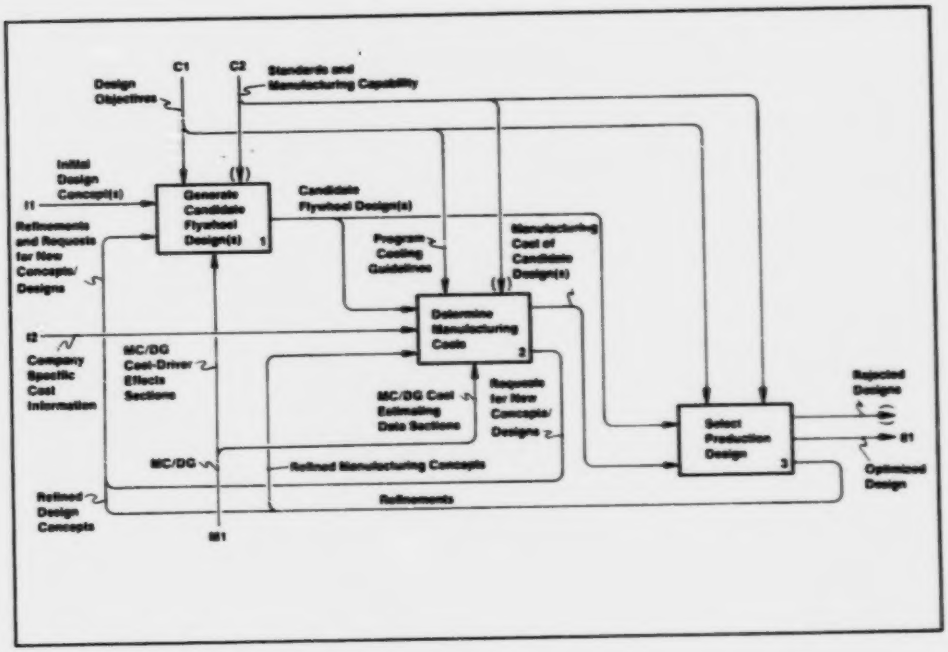
C1
C2
Design Objectives
Standards and Manufacturing Capability
Initial Design Concept(s)
I1
Generate Candidate Flywheel Design(s) 1
Candidate Flywheel Design(s)
Refinements and Requests for New Concepts/ Designs
Program Costing Guidelines
Manufacturing Cost of Candidate Design(s)
Determine Manufacturing Costs 2
I2
Company Specific Cost Information
MC/DG Cost-Driver Effects Sections
MC/DG Cost Estimating Data Sections
Requests for New Concepts/ Designs
Select Production Design 3
Rejected Designs
O1
Optimized Design
MC/DG
Refined Manufacturing Concepts
Refinements
Refined Design Concepts
M1

FIGURE 1. OVERALL VIEW OF TRADE-STUDY METHODOLOGY

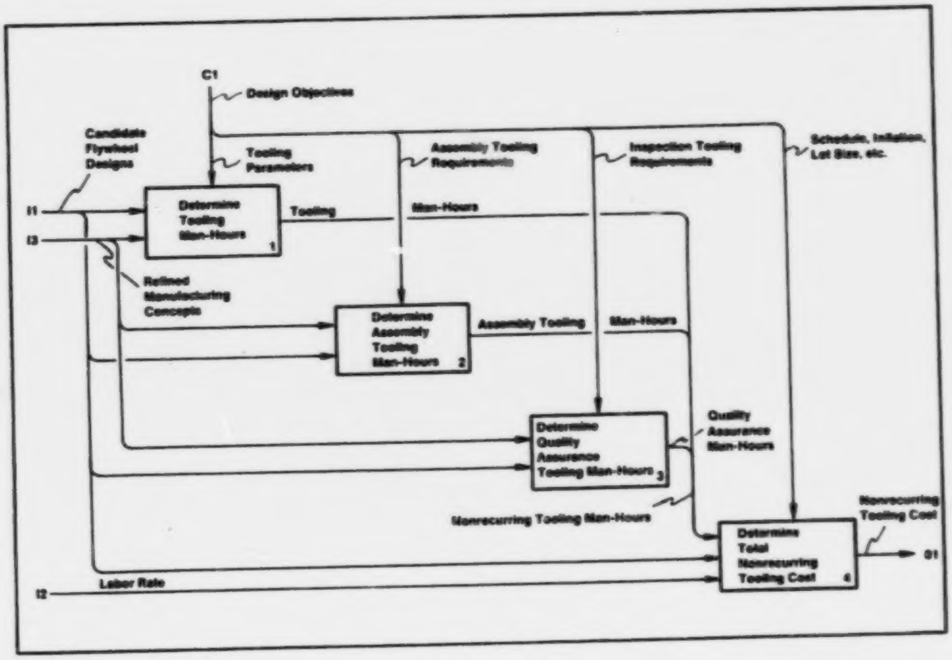
C1
Design Objectives
Candidate Flywheel Designs
Tooling Parameters
Assembly Tooling Requirements
Inspection Tooling Requirements
Schedule, Inflation, Lot Size, etc.
I1
I3
Determine Tooling Man-Hours 1
Tooling Man-Hours
Refined Manufacturing Concepts
Determine Assembly Tooling Man-Hours 2
Assembly Tooling Man-Hours
Determine Quality Assurance Tooling Man-Hours 3
Quality Assurance Man-Hours
Nonrecurring Tooling Man-Hours
Determine Total Nonrecurring Tooling Cost 4
Nonrecurring Tooling Cost
O1
Labor Rate
I2

FIGURE 2. DETERMINATION OF NON-RECURRING COSTS

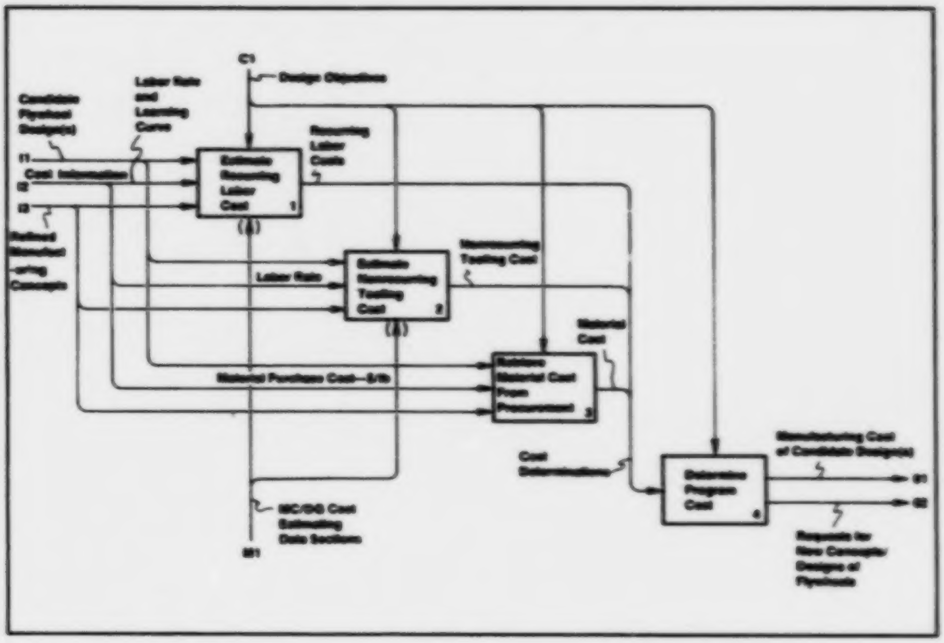
C1
Design Objectives
Candidate
Flywheel
Design(s)
Labor Rate
and
Learning
Curve
I1
Cost Information
I2
I3
Refined
Manufact-
uring
Concepts
Estimate
Recurring
Labor
Cost
1
Recurring
Labor
Costs
Estimate
Nonrecurring
Tooling
Cost
2
Labor Rate
Nonrecurring
Tooling Cost
Material
Cost
Retrieve
Material Cost
From
Procurement
3
Material Purchase Cost—$/lb
Cost
Determinations
Determine
Program
Cost
4
Manufacturing Cost
of Candidate Design(s)
O1
O2
Requests for
New Concepts/
Designs of
Flywheels
RC/DG Cost
Estimating
Data Sections
M1

FIGURE 3. DETERMINATION OF FLYWHEEL PROGRAM COST

TABLE 3. WORKSHEET FOR COST ANALYSIS OF FLYWHEEL ENERGY STORAGE SYSTEMS

FLYWHEEL DESIGN CONCEPT		RECURRING COST (RC)								NON-RECURRING COST (NRC)			PROGRAM COST		
		[illegible]								[illegible]			[illegible]		
PART NO	DESCRIPTION	LABOR REC DIG MH PT (1)	LEARNING CURVE FACTOR (2)	LABOR RATE $ MH (3)	LABOR RC $ PT (4)	MATERIAL $ PT (5)	RE-CURRING COST PT $ (6)	DESIGN QUANTITY (7)	PROGRAM RC $ (8)	NRC REC DIG MH (9)	LABOR RATE $ MH (10)	PROGRAM NRC $ (11)	PROGRAM COST $ (12)	DESIGN QUANTITY (13)	COST SYSTEM $ (14)
	FLYWHEEL														
	•														
	•														
	•														
	SUSPENSION														
	•														
	•														
	•														
	CONTAINMENT														
	•														
	•														
	•														
	TOTALS														

NOTES

BY

DATE

BEST DOCUMENT AVAILABLE

PROJECT SUMMARY

Project Title:	Design Guide for Composite-Material Flywheels (Dynamics)	
Principal Investigator:	Charles W. Bert	
Organization:	University of Oklahoma School of Aerospace, Mechanical and Nuclear Engineering Norman, Oklahoma 73019	
Project Goals:	Phase I.	Develop linear system analyses of a typical energy-storage flywheel system, including rigid flywheel rotor, flexible quill shaft, damper, and air-turbine drive. These analyses include free-whirling critical speeds and mode shapes, stability limits, and forced whirling response to flywheel mass eccentricity and initial tilt.
	Phase II.	Develop continuum dynamic analyses of three different generic configurations of composite-material flywheels.
Project Status:	Phase I.	This phase of the project has been completed, and a draft of the final report was submitted to the sponsor for comments. This draft is now being revised to incorporate the suggestions. The paper beginning on the next page is a brief summary of only some of the results obtained.
	Phase II.	Continuum dynamic analyses are in progress for these three different composite-material flywheel configurations: A. Rim type B. Disk type C. Multiple-disk type
Contract Number:	Subcontract 6448509	
Contract Period:	August 1, 1979 through August 31, 1980; no-cost time extension requested	
Funding Level:	$40,742	
Funding Source:	U.S. Department of Energy through Lawrence Livermore National Laboratory	

FLYWHEEL ROTOR DYNAMICS:
WHIRLING OF COMPOSITE-MATERIAL FLYWHEEL SYSTEMS

C.W. Bert and G. Ramanujam
University of Oklahoma
School of Aerospace, Mechanical and Nuclear Engineering
Norman, Oklahoma 73019

ABSTRACT

Linear system analyses have been developed to predict the rotor-dynamic characteristics of high-performance, advanced-composite-material flywheel systems pendulously supported in a quill-shaft configuration typical of air-turbine drives used in current flywheel spin-testing facilities. These analyses provided the following information useful to design and test engineers: critical whirling speeds and their associated mode shapes, stability limits, forced whirling response to flywheel mass eccentricity and initial tilt. The analyses have been applied to study three specific prototype flywheel systems and also to study the effects of various design parameters.

INTRODUCTION

Flywheel energy-storage systems are being developed rapidly for use in conserving petroleum-derived fuels in transportation systems ranging from small automobiles to large trolley coaches. Due to their high strength and low density, advanced filamentary composite materials have been selected for the rotor material in many of the high-performance flywheels currently under development in the United States. However, to actually achieve this higher energy-storage potential of advanced-composite flywheels, it is imperative that they be operated at much higher rotational speeds than is feasible for flywheels constructed of conventional homogeneous materials, such as metallic alloys. Unfortunately, however, the higher speed requirement has been very elusive to achieve in practice, at least partially due to rotor-dynamic problems.

Although rotor-dynamic analyses date back to the work of Rankine in 1869, most of the previous work was concerned with geometric configurations typical of steam and gas turbines, compressors, pumps, and electric motors. Rotor-dynamic analyses specifically developed for flywheel configurations date from the work of Thomson, Younger, and Gordon in 1977 (reference 1). Other linear analyses of flywheel rotor dynamics include references 2-5.

The work reported here extends the work of reference 5 in three major respects. First, it models a different air-turbine drive system which has different mechanical restraints. Second, it includes presentation of the mode shapes, information which is necessary in order to study the effectiveness of damper locations, for example. Third, it includes two different mathematical models of the system: one is a seven-degree-of-freedom lumped-parameter model, analogous to but more complicated than those in references 1-5; the other is a combined distributed- and lumped-parameter model. All of the derivations and computer documentation may be found in a forthcoming report (reference 6). Due to page limitations, only selected results are presented here. It should be mentioned that the work reported in reference 6 constitutes Phase I of a two-phase effort. Phase II, not yet completed, consists of continuum dynamic analyses of three generic configurations of composite-material flywheels.

The following sections summarize results obtained for the critical speeds and mode shapes for a system which was selected to be the baseline system in this study. This is the 58.4-cm (23-in.) diameter, 80-w-hr/kg wheel developed by Garrett AiResearch in Torrance, California, and described in detail in reference 7. The air-turbine drive data are for a 10.2-cm (4-in.) Barbour Stockwell turbine as installed at the Oak Ridge Flywheel Evaluation Laboratory, reference 8. Also results applicable to the General Electric disk-ring flywheel (reference 9) and Lawrence Livermore National Laboratory's tapered-thickness flywheel (reference 10), and parametric studies are presented.

CRITICAL WHIRLING SPEEDS AND MODE SHAPES FOR THE GARRETT SYSTEM

The seven-degree-of-freedom, lumped parameter model is shown schematically in Figure 1. The resulting Campbell diagram or "whirl map" shown in Fig. 2 is a plot of various whirling frequencies of lateral vibration versus rotational speed (Ω). At zero rotational speed, there are seven natural frequencies. However, as Ω is increased, each of these frequencies (and also their associated mode shapes) "splits" into two distinct branches, as shown in Fig. 2. The deviation between the two branches associated with a given zero-speed mode is caused by the gyroscopic tilting moments induced in the various masses which are free to tilt. The branches having the higher frequencies in each set are associated with forward whirling, i.e., the shaft is whirling in the same direction as the rotation. The branches with the lower frequencies in each set are associated with backward (or retrograde) whirling, i.e., the direction of whirling is opposite to the direction of rotation. Notice that the lower modes have the most pronounced splitting deviation. In fact, within the range of the plot (Ω up to 100,000 rpm), no splitting is discernible in the two highest frequency modes. The net effect of the gyroscopic action is to stiffen the system for forward whirling and soften it in the case of retrograde whirling.

In rotating machinery, one of the most important classes of excitation is that caused by mass eccentricity and initial tilt of the principal axes of the larger rotating masses. This is still true, although to a smaller extent, even in the case of a carefully balanced system. The frequency of this sinusoidal forcing system is the same as the rotational speed. Thus, the intersections of the dotted line labeled $\omega = \Omega$ (a straight line, since Fig. 2 is a log-log plot) with the various modal-frequency curves result in so-called first-order "critical speeds". Although all of these are potential resonances, experiments (reference 1) have shown that those associated with the forward whirling branches are more severe than those associated with the retrograde branches. Furthermore, there is considerable variation in the "severity" of the various forward-whirling critical speeds. Practical experience has shown that generally the lower-speed critical speeds are much less important than the higher-speed ones. There are two reasons for this: first, the higher the rotational speed the higher the kinetic energy in the system and the stiffer it becomes (in forward whirling). Secondly, and perhaps more importantly, it is usually much easier to accelerate sufficiently rapidly through lower-speed critical speeds than higher-speed ones. The reason for this is that typically air-turbine drives have a torque capacity that decreases as the rotational speed is increased.

Another important class of excitation may result from a combination of gravity force (only in the case of a horizontal or nearly horizontal axis of rotation) and nonaxisymmetric shaft cross section (due to either small errors in machining or the presence of a fatigue crack). This excitation has a frequency of exactly twice the rotational speed. Hence, the upper dotted line labeled $\omega = 2\Omega$ determines this excitation frequency, and the associated intersections with the various whirling branches give the second-order critical speeds (speeds read from the abscissa, Ω). All of the predicted first- and second-order critical speeds up to 100,000 rpm are listed in Table 1.

To supplement the information provided in a Campbell diagram, experience has shown that mode shapes are very helpful. In the case of a lumped-parameter system, the mode shapes depict the relative motions of the various rigid-body masses of the system. (In free whirling, as in free vibration of a nonrotating system, only relative motions, not absolute ones, can be determined.) The mode shapes predicted by the lumped-parameter-model analysis at speeds close to the lowest first-order critical speed and the second second-order critical speed are shown in Figs. 3 and 4. They were plotted by computer graphics, using simple, straight lines to connect adjacent mass-center locations. The dotted lines denote flexible shaft portions, which obviously will actually deflect in smooth curvilinear fashion. Also note that for convenience, the plots have been rotated 90°, with the turbine wheel at the left and the flywheel at the right. As would be expected at a speed (1,023 rpm) near the first-order critical speed, the most drastic mode in Fig. 3 is the first one (1F) and in this mode the main action is taking place in the lower end of the quill shaft, the damper and turbine being relatively unaffected.

It can be seen in Fig. 4, at a rotational speed of 15,849 rpm, that the damper is operative in the first, second, and fourth forward modes only. This is also true for the third second-order critical speed (41,687 rpm, not shown). In contrast, at 269 rpm (the first second-order critical), the damper is operative in only the second and fourth modes.

Although the combined model of the system has an infinite number of forward modes, each with a forward and retrograde branch, only a relatively small number of frequency curves intersect the $\omega = \Omega$ and $\omega = 2\Omega$ lines in the region up to $\Omega = 100{,}000$ rpm. The associated first- and second-order forward and retrograde critical speeds are listed in the second line of Table 1. The major difference between the two models is that in the combined model, the critical speeds are shifted into higher regions. This is especially noticeable at higher rotational speeds and higher modes (see Table 1). This trend suggests that the distributed shaft masses stiffen the system by virtue of their gyroscopic actions.

It is interesting to note that in the region covered (up to $\Omega = 100{,}000$ rpm), although this system has many second-order forward critical speeds and first-order retrograde ones, it has only one first-order forward critical speed. For this critical speed, there is good agreement among the two different models and test data obtained at Oak Ridge, as can be seen in Table 1.

PARAMETRIC STUDIES

The numerical results presented in the preceding section completely describe the free whirling response of the Garrett system (hereafter called System A), which was used as a baseline. However, to obtain data applicable to all of the existing or conceivable flywheel systems would require not only extensive computations but also a prohibitively large number of plots. Thus, in this section, the present investigators have chosen to give in tabular form the results of parametric studies in which selected parameters are varied.

In this section, two additional existing flywheel systems are studied. These are the General Electric Company's constant-thickness, alpha-ply, disk-ring-type flywheel (reference 9) and the Lawrence Livermore National Laboratory's tapered-thickness, quasi-isotropic, composite-disk-type flywheel (reference 10). These are designated hereafter simply as Systems B and C, respectively.

The importance of the first (lowest) forward critical speed of the first order was discussed previously for System A. The dynamic parameters of Systems A, B, and C are listed in Table 2 along with their first forward critical speeds of first order (Ω_{11}). In all three of the systems the second first-order forward critical speeds occur at 108,500 rpm. It was determined from mode-shape analysis (reference 6) that at 108,500 rpm, the main action takes place at the turbine end with the flywheel remaining inactive. Further, the first and second first-order forward critical speeds are so far apart that there is no coupling between them. Thus, variations in flywheel parameters do not affect the second first-order forward critical speed significantly.

The effect of varying flywheel mass on the first first-order forward critical speed is summarized in Table 3. Here, t_f, $I_{pf}/m_f t_f^2$, and I_{df}/I_{pf} are held constant at the same values as those of System A. Notice that Ω_{11} increases as the mass is reduced, like a single-degree-of-freedom spring-mass system, with $\Omega_{11}\sqrt{m_f}$ staying approximately constant.

In Table 5 the effect of I_{pf}, with m_f, I_{df}, and t_f held constant at their respective values as in System C, only the first first-order forward critical speed is listed. From the results we see that as I_{pf} is increased, the critical speed Ω_{11} also increases. That is, with the other parameters remaining the same, increasing I_{pf} produces a larger gyroscopic action on the system, thus stiffening the system in forward whirling.

What happens to the lowest first-order forward critical speed when the non-bending length (t_f) of the quill shaft is increased? The answer to this question may be seen by inspecting Table 6. Here, all the parameters are kept the same as those of System C except t_f, which is increased. The decrease in Ω_{11} is explained as follows. Increasing length t_f increases the moment arm at which the flywheel force is applied and thus, makes the system more flexible and reduces Ω_{11}. Note that the lengths of the flexible portions of the shaft sections have been held constant.

For purposes of comparison of the critical-speed characteristics of Systems B and C, all forward and retrograde critical speeds of first and second order up to 100,000 rpm are listed in Tables 7 and 8, respectively.

Although each system has three retrograde first-order critical speeds and three retrograde second-order critical speeds in the range up to 60,000 rpm, these should not cause any serious problems in spin testing. They could, however, be important in connection with decreasing speed during power-takeoff tests. Also, each system has three forward second-order critical speeds in the range up to 60,000 rpm. However, there should not be much excitation available to excite such critical speeds unless the systems were operated with the shafts horizontal instead of vertical. (We are assuming that the shaft out-of-round tolerances are reasonably close to ensure axisymmetric stiffness of the shafts.)

CONCLUSIONS

The results of the system analysis of the free whirling of three different composite-material flywheel systems installed in the spin-test facility at Oak Ridge was described. Two linear models, a lumped-parameter model and a combined lumped- and distributed-parameter model, were used for the system analysis. The air-turbine-drive wheel and turbine shaft dynamics were included in the formulation. It should be mentioned that all of the solutions were mathematically exact and no other approximations than suitable engineering assumptions were used.

For all the flywheel systems, the critical speeds predicted by the combined model were higher than those from the lumped model. Thus, the effect of the distributed mass, which was neglected in the lumped model, is to increase the apparent stiffness of the system. This effect is pronounced at larger rotational speeds and higher modes of vibration (only the lowest four modes were considered for comparison).

Parametric studies were made on the effects of various flywheel parameters (m_f, I_{pf}, I_{df}, and t_f) on the lowest first-order forward critical speeds (Ω_{11}). Decreasing m_f increased Ω_{11} with $\Omega_{11}\sqrt{m_f}$ remaining approximately a constant. When I_{pf} was increased, Ω_{11} increased also, due to the large gyroscopic action of the flywheel. It was found that Ω_{11} increased with decreasing I_{df} and that increases in t_f made the system softer (Ω_{11} decreased). In all the above cases, it was observed that there was no first-order critical speed below 100,000 rpm except the lowest one (at approximately 1,040 rpm).

REFERENCES

1. W.T. Thomson, F.C. Younger, and H.S. Gordon, Whirl Stability of the Pendulously Supported Flywheel System. ASME Journal of Applied Mechanics, Vol. 44, No. 2, June 1977, pp. 322-328.
2. C.N. McKinnou, Jr., Rotor Dynamic Analysis, Appendix B of Evaluation of Selected Drive Components for a Flywheel Powered Commuter Vehicle. Final Report, Contract EY-76-C-0301164, Phase I, June 30, 1977. LMC Corp., Contractor.
3. C.W. Bert, T.L.C. Chen, and C.A. Kocay, Critical Speeds and Natural Frequencies of Rim-Type Composite-Material Flywheels. Report SAND 78-7049, Contracts 05-8709 and 07-7843, Jan. 1979, funded by U.S. Department of Energy through Sandia National Laboratories, Albuquerque. University of Oklahoma, Contractor.
4. C.W. Bert and T.L.C. Chen, Lateral and Tilt Whirl Modes of Flexibly Mounted Flywheel Systems. Shock and Vibration Bulletin 49, Part 2, Sept. 1979, pp. 35-46.
5. T.L.C. Chen and C.W. Bert, Whirling Response and Stability of Flexibly Mounted, Ring-Type Flywheel Systems. ASME Journal of Mechanical Design, Vol. 102, No. 2, Apr. 1980, pp. 369-378.
6. C.W. Bert and G. Ramanujam, Design Guide for Composite-Material Flywheels: Rotor Dynamic Considerations, Part I - System Whirling and Stability. Final Report under revision, Subcontract 6448509, 1981, funded by U.S. Department of Energy through Lawrence Livermore National Laboratory. University of Oklahoma, Contractor.
7. D.L. Satchwell and D.A. Towgood, High-Energy-Density Composite Flywheel. Final Report SAND 79-7019, Contract 13-0293, Feb. 1980, funded by U.S. Department of Energy through Sandia National Laboratories, Albuquerque. AiResearch Manufacturing Company, Contractor.
8. R.S. Steele, Oak Ridge Flywheel Evaluation Laboratory. Mechanical and Magnetic Energy Storage 1979 Contractors' Review Meeting, Washington, DC, Aug. 19-22, 1979. U.S. Department of Energy, Publication Conf-790854, Dec. 1979, pp. 416-421.
9. R.P. Nimmer, Laminated Flywheel Disc with Filament Wound Outer Ring. Mechanical and Magnetic Energy Storage 1979 Contractors' Review Meeting, Washington, DC, Aug. 19-22, 1979. U.S. Department of Energy, Publication Conf-790854, Dec. 1979, pp. 399-406.
10. S.V. Kulkarni, Composite-Laminate Flywheel-Rotor Development Program. Mechanical and Magnetic Energy Storage 1979 Contractors' Review Meeting, Washington, DC, Aug. 19-22, 1979. U.S. Department of Energy, Publication Conf-790854, Dec. 1979, pp. 387-398.

Table 1. Critical Rotational Speeds

Order:	First ($\omega/\Omega = 1$)				Second ($\omega/\Omega = 2$)							
Mode & Branch*:	1R	1F	2R	3R	1R	1F	2R	2F	3R	3F	4R	4F
Lumped Model	301	1,027	12,450	54,480	172	269	6,615	16,020	30,530	42,510	64,400	61,300
Combined Model	304	1,038	14,140	56,120	173	271	7,516	18,100	31,400	43,390	74,000	70,050
Experimental**		1,040										

*For example, 1R denotes the first (lowest) mode, retrograde branch, while 4F denotes the fourth mode, forward branch.

**Data provided by Dr. R.S. Steele, Union Carbide Corp., Nuclear Division, Oak Ridge, TN.

Table 2. Parameters of Systems A, B, and C and Their First First-Order Forward Critical Speeds

System	m_f (lb-s^2/in)	I_{pf} (lb-in-s^2)	I_{df} (lb-in-s^2)	t_f (in)	$I_{pf}/m_f t_f^2$	I_{df}/I_{pf}	Ω_{11} (rpm)
A	0.0951	8.517	4.830	7.05	1.802	0.5671	1,038
B	0.0576	2.036	1.648	3.45	2.970	0.8094	1,907
C	0.0336	1.645	0.823	3.15	4.934	0.5003	14,230

Table 3. Effect of Flywheel Mass (m_f) on the Lowest First-Order Forward Critical Speed*

m_f (lb-s^2/in)	I_{pf} (lb-in-s^2)	I_{df} (lb-in-s^2)	Ω_{11} (rpm)	$\Omega_{11}\sqrt{m_f}$
0.0951	8.517	4.830	1,038	320
0.08	7.165	4.063	1,133	320
0.06	5.373	3.047	1,307	320
0.05	4.478	2.539	1,432	320
0.03	2.687	1,524	1,848	320

*Fixed Parameters:
$I_{pf}/m_f t_f^2 = 1.802$, $I_{df}/I_{pf} = 0.5671$, $t_f = 7.05$ in.

Table 4. Effect of Flywheel Diametral Mass Moment of Inertia (I_{df}) on the Lowest First-Order Forward Critical Speed†

I_{df} (lb-in-s^2)	I_{df}/I_{pf}	Ω_{11} (rpm)
0.823	0.5003	14,230
0.987	0.6	12,400
1.151	0.7	8,851
1.316	0.8	4,018

†Fixed Parameters:
$m_f = 0.0336$ lb-s^2/in, $I_{pf} = 1.645$ lb-in-s^2,
$t_f = 3.15$ in.

Table 5. Influence of Flywheel Polar Mass Moment of Inertia (I_{pf}) on the Lowest First-Order Critical Speed*

I_{pf} (lb-in-s^2)	$I_{pf}/m_f t_f^2$	I_{df}/I_{pf}	Ω_{11} (rpm)
1.000	3.0	0.8228	2,619
1.334	4.0	0.6171	9,358
1.645	4.934	0.5003	14,230

*Fixed Parameters:
$m_f = 0.0336$ lb-s^2/in, $I_{df} = 0.823$ lb-in-s^2,
$t_f = 3.15$ in.

Table 6. Effect of the Distance (t_f) of the Flywheel Center of Mass from the Lower End of the Quill Shaft on the Lowest First-Order Forward Critical Speed (System C)

t_f (in)	Ω_{11} (rpm)
3.15	14,230
4.0	9,817
5.0	3,143
6.0	1,752
7.05	1,280

Table 7. First- and Second-Order Critical Rotational Speeds for System B as Calculated by the Two Different Models

Order	First ($\omega/\Omega = 1$)				Second ($\omega/\Omega = 2$)							
Mode & Branch	1R	1F	2R	3R	1R	1F	2R	2F	3R	3F	4R	4F
Lumped Model	611	1,895	14,970	54,480	347	535	7,740	10,230	30,530	42,500	61,530	62,160
Combined Model	612	1,907	17,000	56,140	348	536	8,790	11,600	31,400	43,370	70,310	71,170

Table 8. Critical Rotational Speeds for System C

Order	First ($\omega/\Omega = 1$)				Second ($\omega/\Omega = 2$)						
Mode & Branch	1R	1F	2R	3R	1R	1F	2R	2F	3R	3F	4R
Lumped Model	765	12,540	18,980	54,490	452	1,000	9,814	38,640	30,540	42,580	62,010
Combined Model	766	14,230	21,530	56,160	453	1,002	11,130	41,620	31,420	44,390	70,910

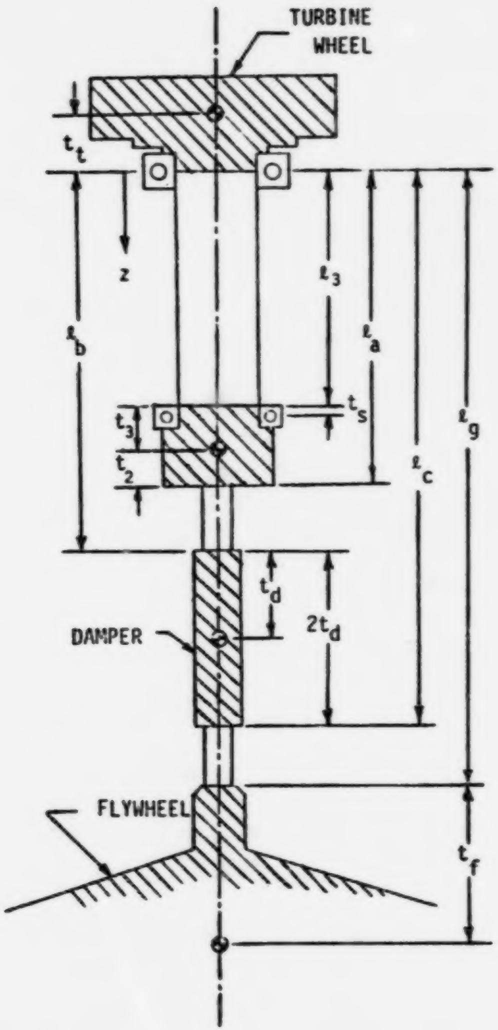
TURBINE WHEEL
t_t
z
ℓ_b
ℓ_3
ℓ_a
ℓ_c
ℓ_g
t_s
t_3
t_2
t_d
$2t_d$
DAMPER
FLYWHEEL
t_f

Fig. 1. Schematic Diagram of the Lumped-Parameter Model with Dimensions. Drawing not to Scale.

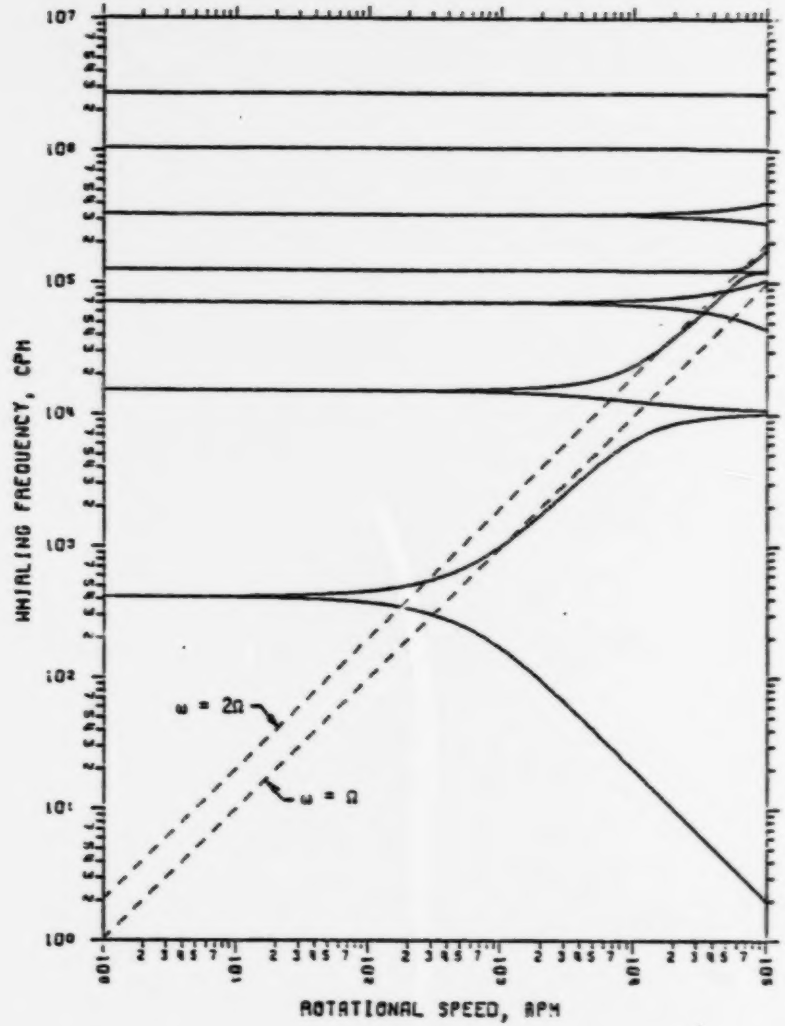

Fig. 2. Campbell Diagram for System A, as Calculated Using the Lumped-Parameter Free-Whirling Analysis.

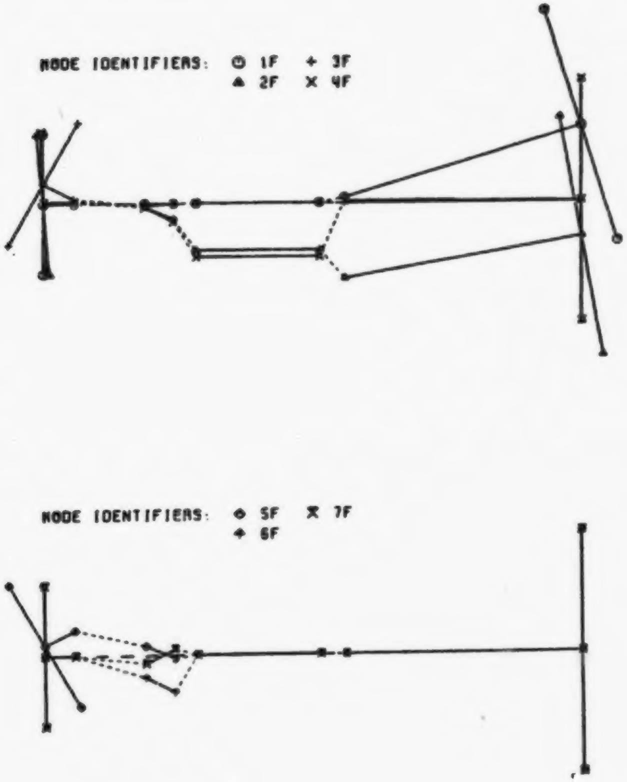

Fig. 3. Mode Shapes of the Seven Forward Branches at a Rotational Speed (1,023 rpm) near the Lowest First-Order Critical Speed, using the Lumped-Parameter Analysis.

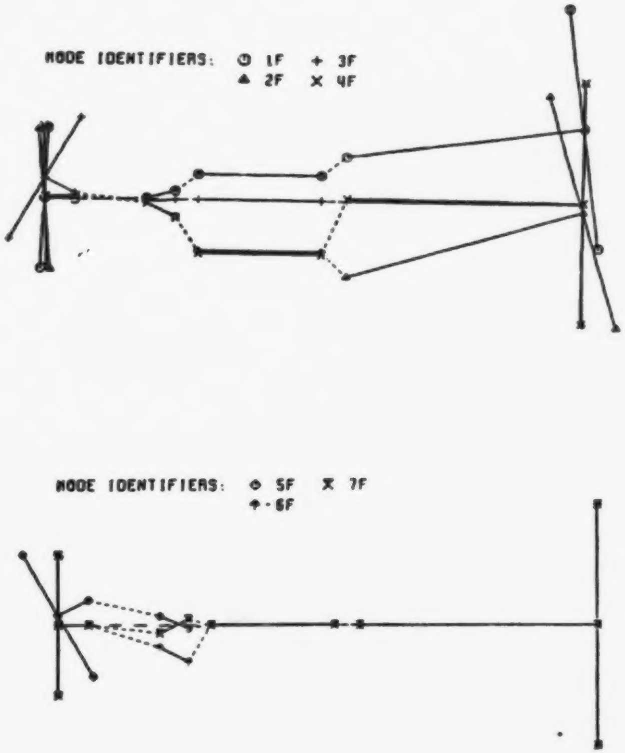

Fig. 4. Mode Shapes of the Forward Branches of the Seven Modes at 15,849 rpm, near the Second Second-Order Critical Speed, using the Lumped-Parameter Analysis.

PROJECT SUMMARY

Project Title: Composite Flywheel Durability and Life Expectancy: Test Program

Principal Investigators: K. L. Reifsnider, S. V. Kulkarni, D. M. Boyd

Organization: Lawrence Livermore National Laboratory

Project Goals: Determine the durability and life expectancy of flywheel rotors, identify critical performance and durability characteristics that control the long-term service and safety of rotors and rotor containments. Develop test procedures that can be used to economically evaluate the performance of flywheels under cyclic loading in the laboratory and to relate that information to long-term service behavior.

Project Status: Approximately half the project is complete, including the following tasks:

- A material property data base has been assembled for each major material to be used in the flywheels.
- Material property data has been characterized and modeled.
- The initial version of a generic test program has been designed.
- Some NDE characterization of all prototype composite flywheels rotors has been conducted.

Contract Number: W-7405-Eng-48

Contract Period: October 1, 1980 to September 30, 1981

Funding Level: See "Flywheel Rotor Development" by S. V. Kulkarni

Funding Source: U.S. Department of Energy

COMPOSITE FLYWHEEL DURABILITY AND LIFE EXPECTANCY: TEST PROGRAM*

K. L. Reifsnider S. V. Kulkarni D. M. Boyd
Lawrence Livermore National Laboratory
Livermore, California 94550

ABSTRACT

Under the leadership of LLNL, various industries and national laboratories have developed flywheels from composite materials that are capable of achieving significantly higher energy densities than those made from conventional metals. Recent burst tests have firmly established this fact. The only remaining major question is in regard to their durability and life expectancy. In other words, how will they perform during long-term service loading? The test program discussed in this report is being developed to answer that question.

INTRODUCTION

The four-year development effort led by LLNL and Sandia has produced several composite flywheel rotor designs that have been successfully tested at energy density levels significantly higher than those achieved by previous designs using conventional metals. Table 1 provides a summary listing of the prototype rotors developed including their maximum energy densities at burst. On the basis of those tests, and following a rigorous evaluation process based on performance, cost, safety and various manufacturing aspects, a selection was recently made of the most promising such rotors.

The state-of-the-art rotor selected was the Garrett multi-material multi-ring rim design (1b in Table 1). A photograph of that rotor appears as Fig. 1. The Garrett design seems capable of reaching the Department of Energy goal of 40 Wh/lb energy density at failure. That design is also being used in a Department of Transportation-sponsored development program conducted by Garrett AiResearch, which will result in flywheel-powered bus-trolley systems to be operational by 1983.

For vehicular applications, the designs selected were the simple disc design developed by LLNL (shown in Fig. 2) and the disc-rim hybrid design developed by General Electric Corporation (shown in Fig. 3). The evaluation process indicated that those designs would be best suited for regenerative braking in passenger vehicles, all factors considered. Criteria used for the evaluation were based on automobile (or projected) requirements.

The results of the development and evaluation program generally indicate the clear superiority of composite flywheels over other known types due to their ability to store a maximum amount of energy per unit weight.

Another important result of that program relates to safety. Composite flywheels are inherently safer than metal wheels since failure of composite rotors does not generally produce large pieces of rotor debris that can become dangerous projectiles. Failure of the composite flywheels usually produces highly fragmented, low density particles that can be easily contained.

Composite flywheels are also thought to be more durable since such materials generally perform very well (frequently better than metals) under long-term and cyclic (fatigue) loading. However, only limited experience has been gained using composite materials in high-performance structures over long periods of time, and relatively little has been postulated regarding the behavior of composite material in unfamiliar situations. Hence, it is essential that the durability and life expectancy of composite flywheels be established by carefully designed test programs. It is the general goal of this effort to design and conduct such a test program.

---

*This work was performed under the auspices of the U.S. Department of Energy by the Lawrence Livermore National Laboratory under contract No. W-7405-Eng-48.

BEST DOCUMENT AVAILABLE

TABLE 1. Advanced Composite-Rotor Designs and Maximum Energy Densities

	Design	Sponsor(s)	Materials	Maximum energy density, Wh/lb (kWh)
1a	Garrett multi-material, multi-ring rim	JPL/DOE/DOT	S2-glass/Kevlar-29 Kevlar-49/aluminum hub	24
1b	Garrett multi-material, multi-ring rim	Sandia/DOE	S2-glass/Kevlar-29 Kevlar-49/graphite hub	36.1 (1.23)
2	Brobeck multi-material rim with tension-balanced spokes	EPRI/Sandia/DOE	S2-glass/Kevlar-29 Kevlar-49 spokes Al/Kevlar-49 hub	28.9 (0.71)
3	Rocketdyne rim with overwrap and twin-disc hub	Sandia/DOE	Graphite/Al hub	16.4 (1.94)
4	Hercules contoured rim	Sandia/DOE	Graphite/Al hub	17.0 (0.85)
5a	GE alpha-ply laminated	LLNL/DOE	S2-glass/Al hub	18
5b	GE alpha-ply laminated disc with rim	LLNL/DOE	S2-glass/graphite rim/Al hub	25.6 (0.283)
6a	LLNL tapered-thickness laminated disc	DOE	Graphite/Al hub	28 (0.31)
6b	LLNL constant-thickness laminated disc	DOE	Graphite/Al hub S2-glass/Al hub	23 30.5 (0.157)

The two major parts of the program, life determination and durability determination, are outlined below. The overall objectives of the test program are:

1. To establish the durability and life expectancy of flywheel rotors under conditions, including all the essential elements of spectrum loading, that rotors are likely to sustain as an energy storage device for various applications.

2. To identify critical performance and durability characteristics potentially limiting long-term rotor use and safety and rotor containment designs currently under development.

3. To develop test techniques and hypotheses that can be used for the fatigue testing of flywheels, and to relate laboratory specimen data to rotor performance.

4. To develop test procedures that can be used to economically evaluate flywheel rotors without the expense of actual vehicle or bench tests.

Several aspects of this test program (such as dynamic effects, strongly multiaxial, nonuniform stress fields, and material-geometry-performance-cost trade-offs) are more complex and potentially more difficult than aerospace applications, which dominated our earlier

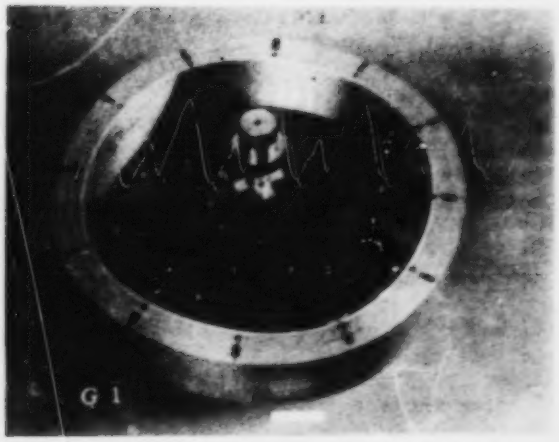

Fig. 1. Garrett Multi-material, Multi-ring Flywheel Rotor.

Fig. 2. LLNL Disc-Type Flywheel Rotor.

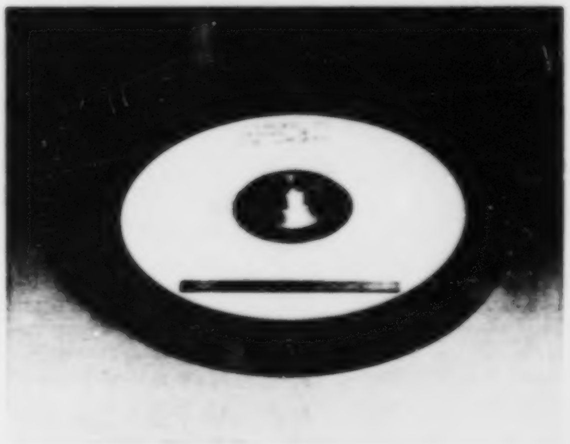

Fig. 3. General Electric Disc-Rim Hybrid Design Flywheel Rotor.

experience. The test plan includes long-term as well as short-term tests, thus taking into consideration any possible effects of time-at-load (creep-fatigue) in the observations. However, things such as spectrum loading and frequency effects are not identified in the test plan and represent an opportunity for its further development.

LIFE EXPECTANCY DETERMINATION

It is necessary to know how long a flywheel will last when it is subjected to the load history and environmental conditions expected during service. The material stresses caused by a specific loading history are determined by essentially four items, the flywheel design, the power required from the flywheel, the energy that the wheel must store, and the variations caused by energy transfer into and out of the flywheel as required by the application. While life expectancy determination depends on the specifics of each application, we take a more generic approach to the problem by attempting development of a test program that can be used for many different flywheel applications. However, for the sake of development and illustration, we consider the requirements and specifications associated with the application of the flywheel to energy storage in an automobile as the conditions for which the test will be designed.

For automobile applications, the flywheel is typically expected to provide about 0.25 kWh of stored energy when decelerated from maximum rotational speed to half speed. For present designs, this energy storage capacity will require flywheel rotational speeds of from 20-25,000 rpm. The energy density of the flywheel has less impact on vehicle performance than other factors, as long as the energy density of the flywheel system is from 2-3 Wh/lb. Flywheel power output is expected to be on the order of 90 hp. Depending upon rotational speeds and rotor design, this requirement can be expected to create torques on the order of 20 ft-lb. If energy normally lost in heat during braking is used to recharge the flywheel, the torques associated with that process might be somewhat higher than the discharging torques unless the braking torques are modified by a power-coupling device. Service variations are controlled by the experience of a "typical" driver.

We have chosen the LA4 FTP Urban Driving Cycle (UDC) to define this "typical driving experience" and have estimated that the flywheel will drive a 3,000-lb car about one mile on the average, using the 0.25 kWh of stored energy. Since the LA4 FTP UDC covers about 7.5 miles, the flywheel can be expected to be charged about 7.5 times per UDC. At the end of the UDC, the flywheel will come to rest. Since the UDC covers about 7.5 miles over about 22 minutes, the flywheel can be expected to be charged and discharged about once every three minutes. If the total service life of the flywheel is taken to correspond to 100,000 miles traveled by the automobile it propels, then the flywheel must be capable of withstanding at least 100,000 cycles of the type just described.

Figure 4 indicates the suggested test chronology. Two options are shown as "Cycle I" and "Cycle II." Cycle I is a time-controlled test and Cycle II is a torque-controlled test. For several of the current designs the two options produce quite similar test conditions. The

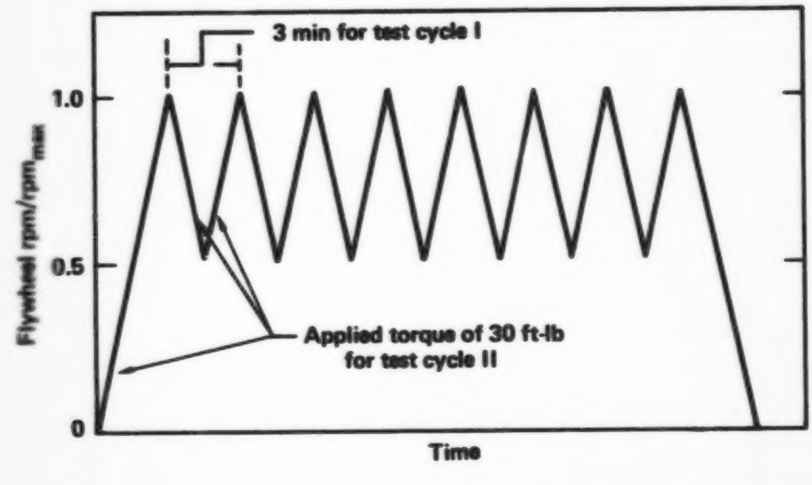

Fig. 4. Schematic Diagram of Two Suggested Test Cycles for the Simulation of an LA4 FTP Urban Driving Cycle.

controlled torque test is thought to be important in those instances when bonded hubs or other joints may be potential failure points sensitive to torque levels. The torque-related stresses in the flywheel rotors themselves are so low as to be negligible for the cases considered. The time-controlled option is thought to be of greatest importance in determining life expectancy of the flywheel rotor and the joints. It also has the advantage of controlling time-at-load in a manner coincident with expected service conditions. Both Cycle I and Cycle II testing is advised.

The design of the flywheels to be tested naturally also influences the test program. If the flywheel rotor is a simple disc made from multiaxial laminates, the dominant stress field is highly two-dimensional and nonuniform. Anisotropic laminate strength and life properties under biaxial loading are controlling. Materials for such a design are likely to be glass-epoxy or graphite-epoxy.

Another primary design type is the rim-spoke arrangement. Unidirectional material is used for the rim, which controls failure. The stress field that controls behavior is more uniform than that for the disc, and the two-dimensional aspects of the field are more easily dealt with, although transverse and interlaminar stresses do play a role in the rim-type designs. Ring fiber failure modes are to be avoided because that type of fracture is difficult to contain. Joint or spoke failures become possible issues.

A third and very successful design type is the disc-rim hybrid. For that design, all considerations previously mentioned must be weighed.

All these designs involve several different materials, including laminated, continuous-fiber glass-epoxy and graphite-epoxy, unidirectional aramid-epoxy and glass-epoxy, and chopped fiber-epoxy. The test program is being designed based on the fatigue response of those materials, as illustrated in Figs. 5 and 6. Figure 5 shows least-square approximations of the fatigue response of unidirectional Kevlar 49, graphite-epoxy and glass-epoxy and quasi-isotropic graphite-epoxy laminated material. The responses of these materials vary greatly in some cases. The unidirectional graphite-epoxy and glass-epoxy drop sharply at low life levels compared to the unidirectional aramid-epoxy or graphite-epoxy laminate. In general, the fatigue response of the aramid-epoxy material (a Kevlar 49 product) seemed to be the best. The fatigue response of unidirectional glass-epoxy and graphite-epoxy is quite similar when normalized by their static strength (average value).

The failure of the rim-type flywheel rotors is usually due to radial stresses (by design) to avoid fiber-fracture failures that are more difficult to contain. In that case, the fatigue response of unidirectional material loaded perpendicular to the fiber direction is controlling. Figure 6 shows such response for glass-epoxy (top curve) and graphite-epoxy (bottom curve). The fatigue effect is much greater than for loading in the fiber directions. It should be noted that the data shown in Figs. 5 and 6 were obtained for uniaxial loading. This is true of virtually the entire data base assembled by the authors since nothing else was available. There is a serious shortage of biaxial fatigue response (and quasistatic response) data for composite materials.

For test design purposes, the fatigue response of the materials was generalized and approximated by a straight line over the region of interest, i.e., from about 1,000-100,000 cycles. We have found that such approximations can be made with correlation coefficients of typically 0.9 or greater, with a few cases in the 0.82-0.9 range. For our test scheme such a generalization is illustrated in Fig. 7. As shown in that figure, the suggested test levels for a small number of tests are determined from the equation:

$$S/S_{ult} = 1 - \frac{n}{8}\left(1 - \frac{S_{op}}{S_{ult}}\right)\log N \qquad n = 1,3,4,5 \qquad (1)$$

where S is the total stress range, S_{ult} is the material static ultimate strength, S_{op} is the operating stress range specified by the flywheel designer, and N is the number of cycles to

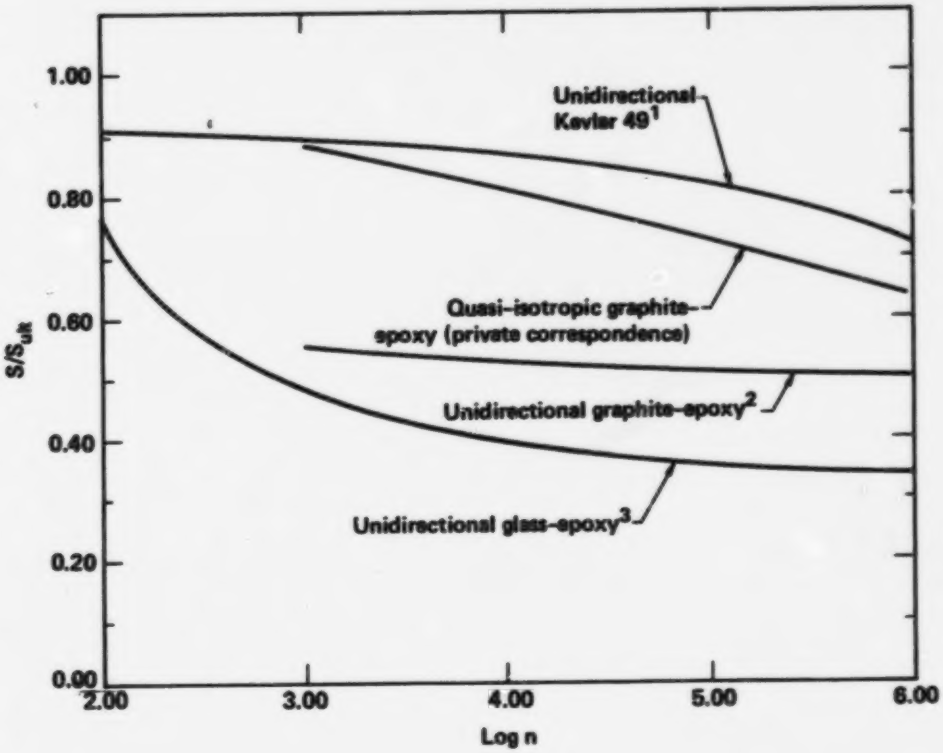

Fig. 5. Least-Squares Fit of Fatigue Data to Curves of Type S/S_{ult} at $6/N^x$ for Kevlar 49, graphite-epoxy and glass-epoxy.

failure. It is assumed that the design lifetime (including all "knockdown factors") corresponds to an actual life of about 10^8 cycles for purposes of this test design. The other stress levels correspond to estimates of life expectancy equal to

$$N = 10^5,\ 10^4 \text{ and } 10^3 \text{ cycles,}$$

so that data properly distributed over the range of interest are obtained.

The number of tests run at each level is also important since the statistical significance and reliability of conclusions drawn from the data set will be determined by the number of specimens tested compared to the spread in the data. Cost constraints may, however, limit the total number of tests. Figure 7 suggests that the number of specimens run at each level should be chosen based on a statistical analysis of the results from documents, such as ASTM E123, A Recommended Practice For Choice of Sample Size, ASTM, and A Guide for Fatigue Testing and the Statistical Analysis of Fatigue Data: (ASTM Special Technical Publication 91-A, 1963), or a variety of more recent publications.

The minimum number of specimens needing testing depends upon the accuracy desired and the risk tolerability. However, for data for which previous experience is very limited, no less than four stress levels (with at least five specimens tested at each level) are recommended as an absolute minimum. The recommended test size is commonly 50 specimens, total, according to the references just cited. It is impossible to establish the reliability, durability and safety of the flywheels without such a test series.

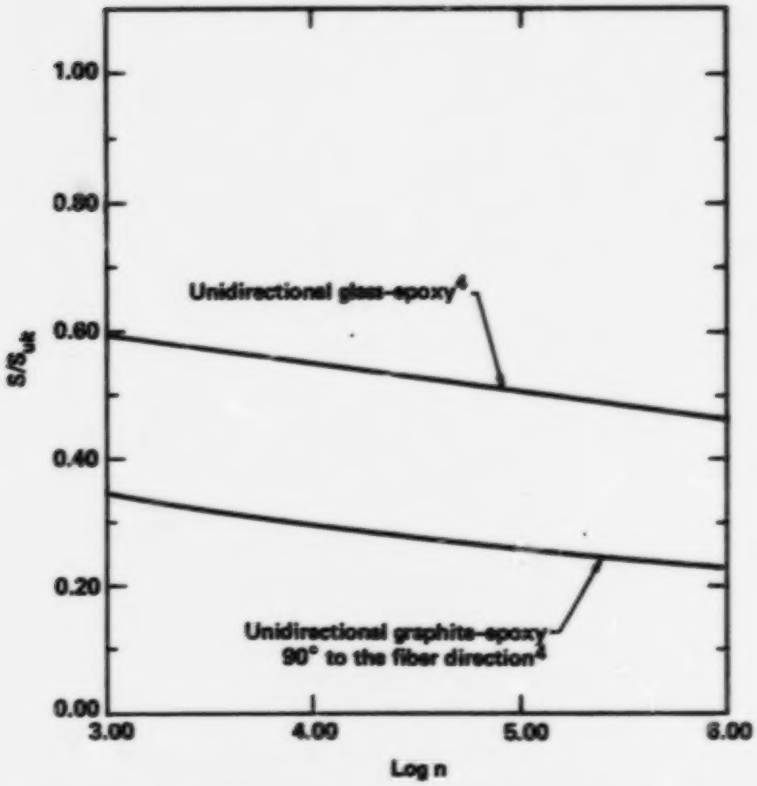

Fig. 6. Least-Squares Fit of Fatigue Data to Curve of Type S/S_{ult} at $6/N^x$ for glass-epoxy and graphite-epoxy.

A brief example will illustrate how Eq. (1) is used. Let us consider a rim-type flywheel such as the Garrett design. We assume that the designer of the wheel has specified an allowable fatigue based on a design process that considers stress multiaxiality and nonuniformity, residual stresses, joining stresses, creep strain, size effects, dynamic stress redistribution, possible failure and damage modes, material stiffness variations with time-temperature-loading, dynamic stability, optimum geometry and optimum material choices. Let us suppose that the design allowable for life is 25,000 rpm. Let us also assume that the burst tests indicate that the ultimate strength of the rotor occurs at 39,000 rpm. Since stresses in the flywheel are proportional to the square of the rotational speed,

$$\frac{S_{op}}{S_{ult}} = \left(\frac{25,000}{39,000}\right)^2 = 0.41, \qquad (2)$$

for which Eq. (1) yields

$$S/S_{ult} = 0.41,\ 0.63,\ 0.71,\ 0.78 \qquad (3)$$

for test levels.

In terms of maximum test speeds, the test levels are

$$25,000,\ 30,955,\ 32,862,\ 34,444 \text{ rpm}, \qquad (4)$$

which are intended to produce data for essentially infinite life (the design allowable situation), and 10^5, 10^4, and 10^3 cycles to failure.

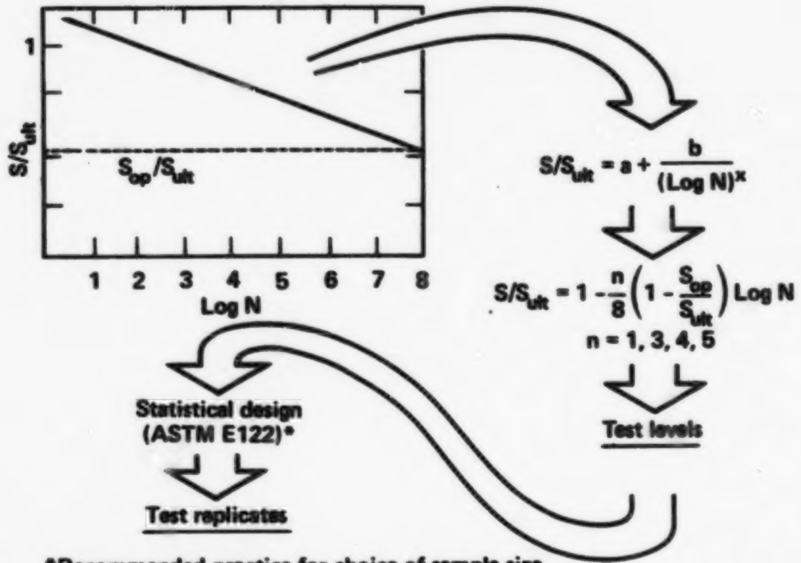
1
S/S_{ult}
S_{op}/S_{ult}
1 2 3 4 5 6 7 8
Log N
$S/S_{ult} = a + \frac{b}{(\mathrm{Log}\ N)^x}$
$S/S_{ult} = 1 - \frac{n}{8}\left(1 - \frac{S_{op}}{S_{ult}}\right) \mathrm{Log}\ N$
n = 1, 3, 4, 5
Test levels
Statistical design (ASTM E122)*
Test replicates

*Recommended practice for choice of sample size

Fig. 7. Schematic of Test Level and Replicate Determination Scheme.

Life is a binary property since a flywheel either fails or does not and not much engineering can be done with this property alone. It is also essential to establish flywheel durability, i.e., how much residual strength, stiffness and life expectancy does a flywheel have after a load history or period of service? From the material standpoint, durability can be thought of as resistance to degradation of material properties and structural integrity. If we determine only that a flywheel fails at a specific time, and we do not know why or how it failed, or what kind of damage occurred, or what the residual strength and stiffness were at various points in time before failure, we really have very little information to work with. Durability information is essential in determining reliability, safety, and serviceability and equally essential for the continued improvement of flywheel performance and safety.

Durability is usually monitored with the help of various nondestructive evaluation (NDE) techniques used to detect variations in the internal integrity of the materials. The type of NDE method and the way it is used depends primarily on the material to be tested, the geometry of the test piece (including the thickness and shape), and the type of defect or defect structure to be detected. Several useful references for this subject appear in the literature.[5-8] However, the application of NDE to flywheels made from composite materials is still in an early stage of development.

For rim-type rotors that use unidirectional, circumferentially wound material, the most common type of flaw is matrix cracking or debonding. Ultrasonic attenuation measurements are very sensitive to this type of damage but do not produce spatial information about the location of flaws. For matrix cracks that go through the thickness of the rim perpendicular to the wheel radius, x-ray radiography is likely to be effective. If widely dispersed micro-damage occurs, the elastic dynamic response of the rotor may be altered, causing a shift in the resonant frequencies of the flywheel system. This may also influence system damping.

The spokes and hub supporting the rim may also require examination. Appropriate techniques for that job will be highly dependent on the wheel design.

Disc-type flywheels present a somewhat different challenge. Present evidence suggests that matrix cracking and crazing of interior regions of the discs may influence their durability. As mentioned earlier, ultrasonic attenuation is very sensitive to this type of damage, although interpretation of absolute damage severity and residual response is difficult. Ultrasonic C-scan methods are generally not very useful for this type of damage unless a unit with gray-scale (attenuation) capabilities is available. If the disc is laminated, delamination is a possible damage mode. C-scan methods are best suited for delamination detection. Radiography is not generally sensitive to delaminations unless opaque penetrations are used. An extensive discussion of NDE techniques will be an essential part of the final test program plan. However, detection of damage or defects is only half the problem. Interpretation is the critical link between NDE and performance. For that reason, it is especially important to combine inspection and nondestructive interrogation with tests of residual strength, stiffness and life. Only then can NDE data be quantitatively significant.

Figures 8a and 8b show another aspect of NDE usefulness. Figure 8a is a radiograph of a Hercules graphite-epoxy rim-type flywheel showing low-density rings. These suggest a resin-rich region along the radial direction. Figure 8b is a video recording of the surface of that flywheel spinning at 350 rps. Circumferential cracks have formed at the position of the low density rings in the radiographs. (The radial features are painted reference marks.) Hence, initial NDE revealed a manufacturing irregularity that became the source of the rotor failure.

In general, there are many NDE techniques that can be applied to composite flywheels, including ultrasonic methods, x-ray radiography, stiffness and damping changes, acoustic emission, video-thermography and holography. Each of these methods has its strengths and weaknesses; however, the key to successful use of a method is accurate interpretation.

Fig. 8a. Axial Radiograph Showing Three Low-Density Rings (see Arrows) in The Hercules Graphite Flywheel.

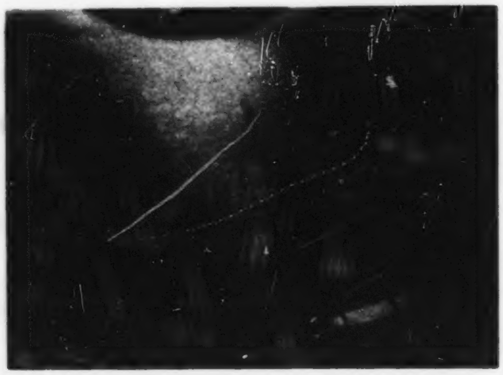

Fig. 8b. Video Recording of the Lower Flywheel Surface Spinning at 350 rps Showing Circumferential Cracks, Which Formed in the Positions Identified with Arrows in Fig. 8a.

SUMMARY

The test program presently under development will:

1. Provide information about specific and generic durability as well as life expectancy for flywheel rotors and similar composite structures.
2. Establish relationships between short-term laboratory tests and long-term service performance.
3. Develop NDE methods that can be used to monitor service-induced damage to imply residual service life, strength and safety.

In general, the test program should make a significant contribution to the continued success, development, and safety of composite flywheels. Although the test plan is being developed specifically for certain types of rotors, it is essentially a generic plan and could be used for any type of rotor with minor alterations. It should also be mentioned that the present test plan is basically different from the usual "accelerated test plan." The present plan is based on experimental observations of damage states and rates over a wide range of loading conditions. This forms the basis for mechanistic modeling from which residual strength, stiffness and life expectancy are estimated. No a-priori empirical damage rate expressions are assumed. Different models will be used for different damage and failure modes. This mechanistic approach is unique to the plan under development.

REFERENCES

1. H. T. Hahn and W. K. Chin, Environmental Effects on Mechanical Properties of a Kevlar 49/Epoxy Composite, Materials Research Laboratory Report, Washington University, St. Louis, Mo. (1980).
2. K. E. Hofer et al., Development of Engineering Data on the Mechanical and Physical Properties of Advanced Composite Materials, Technical Report AFML-TR-74-266, Air Force Materials Laboratory, Dayton, Ohio, (1975).
3. E. J. Riegner Testing and Evaluation of Composite Materials: Unidirectional Filament Wound S2-Glass, Contractors Report to Lawrence Livermore National Laboratory Subcontract No. 6991805 (1981).
4. D. F. Sims and V. H. Brogen, "Fatigue Behavior of Composites Under Different Loading Modes", Fatigue of Filamentary Composite Materials, ASTM STP 636, K. L. Reifsnider and K. N. Lauraitis, Editors (American Society for Testing and Materials 1977) pp. 185-205.
5. R. P. Nimmer, "Calendar Year 1980 Progress Summary; General Electric Hybrid Disc-Ring Composite Flywheel" (March 1980).
6. R. P. Nimmer, K. Torossian, and J. Hickey, Laminated Composite Disc Flywheel Development, Lawrence Livermore National Laboratory, Livermore, Calif., UCRL-15301 (1980).
7. K. L. Reifsnider, E. G. Henneke II, and W. W. Stinchcomb, "The Mechanics of Vibrothermography", in Mechanics of Nondestructive Testing, W. W. Stinchcomb, Ed. (Plenum Press, New York, 1980) pp. 249-276.
8. B. W. Maxfield, D. M. Boyd, S. V. Kulkarni, and A. J. Schwarber, Nondestructive Evaluation of Fiber Reinforced Composite Panels and Flywheels, Lawrence Livermore National Laboratory, Livermore, Calif., UCRL-84930 (1980).

PROJECT SUMMARY

Project Title: Oak Ridge Flywheel Evaluation Laboratory

Principal Investigator: R. S. Steele

Organization:
Union Carbide Corporation
Nuclear Division
Post Office Box Y
Oak Ridge, Tennessee 37830

Project Goals: To provide the DOE flywheel program with the ability to comprehensively evaluate high performance composite flywheels.

Project Status: Three flywheels were evaluated for ultimate speed performance and a cyclic fatigue test for a fourth flywheel is in progress.

Major findings are as follows:

1. The LLNL tapered graphite disk achieved a maximum speed of 569 rev/s and stored a maximum kinetic energy of 0.33 kWh at 56.1 Wh/kg.
2. The Owens-Corning/Lord flywheel with SMC disk and graphite ring reached a speed of 333 rev/s and a maximum stored kinetic energy of 0.36 kWh at 28 Wh/kg.
3. The General Electric Company's constant thickness, α-ply disk with graphite ring was limited to a speed of 535 rev/s by the hub attachment rather than composite material properties.

Detail test reports including balance, temperature, dimensional inspection, resonant frequency, and stability data are being prepared.

Contract Number: SANL/Requests 803-039, 903-044, and 903-091

Contract Period: October 1, 1980 through September 30, 1981

Funding Level: $368,000

Funding Source: U. S. Department of Energy through Lawrence Livermore National Laboratory

ROTOR TESTING IN FY 1981*

R. S. Steele, Jr.   E. F. Babelay, Jr.
Union Carbide Corporation, Nuclear Division
Oak Ridge, Tennessee 37830

ABSTRACT

This paper summarizes the results and observations of flywheel spin tests conducted in the Oak Ridge Flywheel Evaluation Laboratory for the Mechanical Energy Storage Technology project at the Lawrence Livermore National Laboratory (LLNL). Two types of tests are discussed. The first is an ultimate speed test similar to those performed in FY 1980. It includes ultimate speed evaluations for a tapered, quasi-isotropic, graphite composite flywheel built by LLNL, a constant thickness disk with an SMC core and circumferentially wound graphite restraining ring built by Owens-Corning Fiberglas and Lord Kinematic Corporation, and a constant thickness disk with an S-glass, α-ply layup core and circumferentially wound graphite ring built by General Electric. The second type of test is a cyclic fatigue test. A matching General Electric flywheel was used as the first test unit. Test results as well as general observations and conclusions are presented.

INTRODUCTION

The Oak Ridge Flywheel Evaluation Laboratory (ORFEL), located at the Oak Ridge Y-12 Plant, was established to comprehensively evaluate high performance composite flywheels for the Department of Energy's Flywheel Program. It is operated under a subcontract from the Mechanical Energy Storage Technology Project (MEST) at the Lawrence Livermore National Laboratory (LLNL). The FY 1981 goals included determining the ultimate speed and energy storage capability of three flywheel rotor concepts sponsored by MEST and beginning the evaluation of cyclic fatigue life characteristics of such designs.

The ultimate energy storage capacity of a flywheel rotor is often considered to be limited by material properties. In reality the limiting factor may be associated with design, fabrication, response to dynamic loading, balance characteristics, or any number of other parameters. For this reason, evaluations at ORFEL include many measures other than the magnitude of the maximum speed achieved. In this paper, we have limited the discussion to only those data which bear directly upon the final conclusions on the performance for the individual flywheels.

TAPERED DISK EVALUATION

This flywheel was designed and fabricated at the Lawrence Livermore National Laboratory.[1] It was a quasi-isotropic, graphite/epoxy layup machined to a modified Stodola taper profile. The flywheel, shown in Figure 1, was approximately 25 mm (1 in.) thick in the middle and 6 mm (0.25 in.) thick at the outer diameter of 0.6 m (24 in.). A central aluminum hub was bonded to one side of the flywheel using a polyurethane elastomer over a 76-mm (3 in.)-diameter bonding surface. The ORFEL serial number for this flyhweel was LLNL-1.

The flywheel achieved a maximum rotational speed of 569 rev/s (34,140 rpm) with a tip speed of 1072 m/s. It was storing 0.33 kWh of kinetic energy at 56.1 Wh/kg (25.5 Wh/lb). The flywheel was dynamically stable throughout this final run exhibiting neither whirl nor flexural resonant frequencies except for a resonance with the first forward whirl mode. A gradual growth to approximately 0.025 mm (0.001 in.) in the relative motion between the disk and the aluminum hub between speeds 200 to 560 rev/s was considered of little consequence.

The time domain plots of runout shown in Figure 2 demonstrate how rapidly the failure occurred. These data indicate that all sensors were destroyed within 400 μs. Since they were in different locations about the flywheel, the short time indicates a very fragmented failure mode. This was confirmed by the flaky nature of the debris seen in Figure 3 and by the fact that the hub and parts of the composite were still attached to the turbine.

---

*Work performed at the Oak Ridge Y-12 Plant which is operated for the U. S. Department of Energy by Union Carbide Corporation, Nuclear Division, under contract W-7405-eng-26.

Figure 1. Quasi-isotropic flywheel fabricated by LLNL and evaluated at ORFEL. (196585)

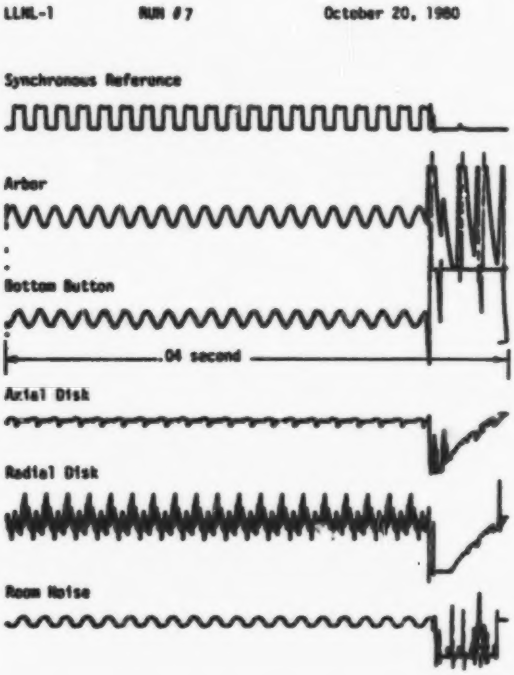

Figure 2. Time domain display of the sensor data data at the time of failure. (201753)

SMC/GRAPHITE RING FLYWHEEL EVALUATION

Flywheel OCLA was a constant thickness S-glass disk made from sheet molding compound (SMC) and was surrounded by a circumferentially wound graphite ring.[2] Figure 4 shows the unit fabricated by Owens-Corning Fiberglas and Lord Kinematic Corporation. The flywheel was approximately 25 mm (1 in.)

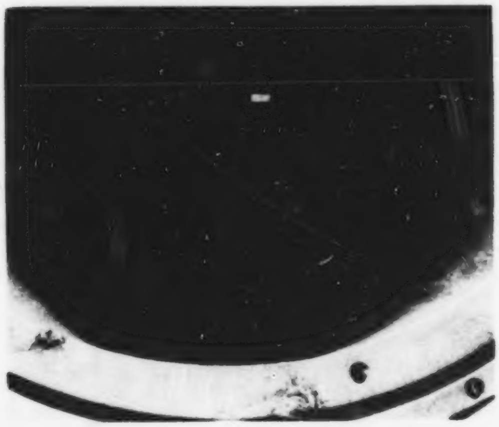

Figure 3. Failure debris in the graphite epoxy flywheel, containment and probe support structure. (196856)

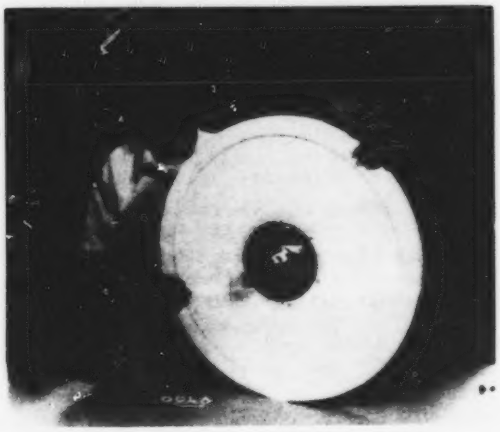

Figure 4. Flywheel fabricated by Owens-Corning Fiberglas and Lord Kinematic Corporation and evaluated at ORFEL. (198742)

thick and 0.6 m (24 in.) in diameter. The aluminum hub was bonded to the center of one side of the disk with an elastomeric bonding agent over a 152-mm (6-in.)-diameter bond area. The SMC disk does not possess the strength and thus energy storage potential of a layup-type construction because of the use of chopped fibers in a random orientation. However, this same property is responsible for the low and highly attractive cost for the unit and led to its consideration as a candidate flywheel.

The flywheel contained a rather severe imbalance in its as-received condition resulting from an assembly misalignment of the hub. Final machining of that hub brought the geometric center line to within 0.25 mm (0.01 in.). The holes used to achieve the final balance were the five 8-mm (0.3125-in.) holes in the SMC shown in Figure 5.

Flywheel OCLA achieved 333 Hz (19,980 rpm) and a peripheral speed of 644 m/s. The 12.9 kg (28.4 lb) flywheel achieved 95% of its predicted performance by storing 0.357 kWh of kinetic energy at 27.7 Wh/kg. As with flywheel LLNL-1, the failure was very sudden and catastrophic. Figure 6 shows some of the major pieces taken from the debris. A ring hoop stress failure followed by a disk breakup is the most likely failure sequence. The balancing holes did not appear to be a major factor in the failure.

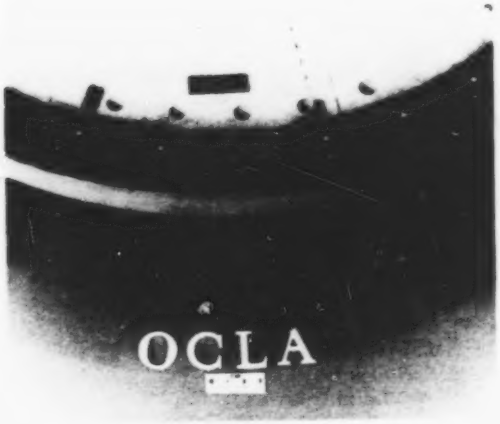

Figure 5. Balance holes drilled in the SMC portion of flywheel OCLA (198946)

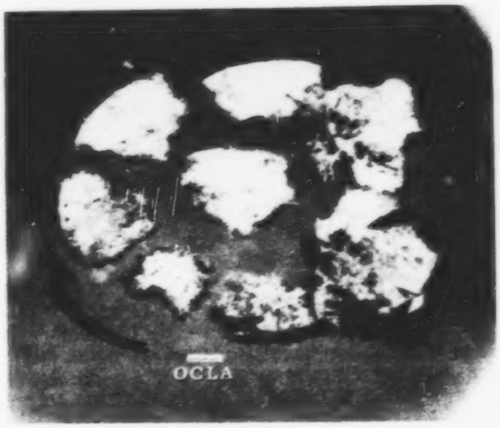

Figure 6. Major pieces from OCLA debris. (199229)

A problem was developing with a growing relative displacement between the disk and the hub. Figure 7 shows the runout plots for several flywheel surfaces at increasing speeds. This plot shows that the hub moved 0.140 mm (0.005 in.) while the disk moved only 0.37 mm (0.001 in.) between speed points at 200 and 330 rev/s. The total vectorial displacment was 0.178 mm (0.007 in.).

α-PLY LAYUP/GRAPHITE RING FLYWHEEL EVALUATION

General Electric designed and fabricated flywheel[3] GE-1 as a constant thickness, solid, circular disk of laminated, uniaxial S-glass composite sheets in an α-ply layup. The central disk was surrounded by a circumferentially wound graphite ring of the same thickness. The flywheel shown in Figure 8 was 25 mm (1 in.) thick, had a diameter of 450 mm (17.7 in.), and weighed 10 kg (22 lb). The same aluminum hub design as with flywheel OCLA was used, i.e., 152-mm (6-in.)-diameter elastomeric bonding area.

During its evaluation in ORFEL, the ultimate speed of the flywheel was limited by an instability that occurred at the first forward whirl frequency as the relative movement between the hub and the disk grew. Figure 9 shows that the runout at the arbor during Run 10 grew with increasing spin speed while the disk runout did not. This is analogous to swinging a spring-supported mass and noting the

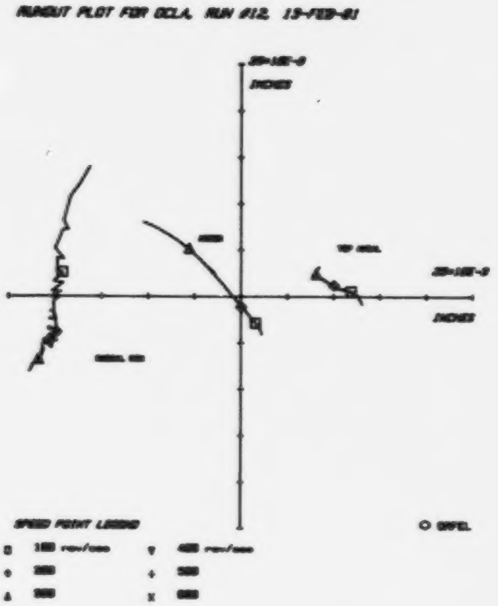

Figure 7. Runout plot for flywheel OCLA (201760)

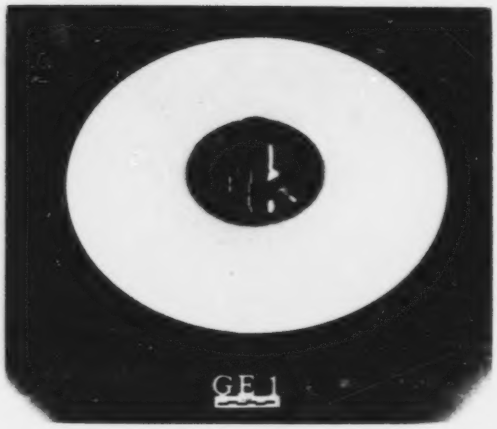

Figure 8. The General Electric flywheel evaluated at ORFEL. Top and OD surfaces have been painted white. (196365)

elongation of the spring at increasing speeds. The runs were limited by whirl which increased in amplitude with increasing speed until the facility limit for radial clearance, 0.5 mm (0.020 in.), was reached. The runout was successfully reduced by balancing the aluminum hub relative to the composite disk. Figure 10 shows the reduction in relative displacement during the final run to the maximum speed of 535 rev/s (32,000 rpm). The maximum speed was again limited by unacceptably large amplitude whirl at the first forward whirl frequency.

During the final run, a minor material sling occurred from the inside corner of the graphite ring. Some of the loose fibers are seen in Figure 11. While this sling does not appear structurally significant, it indicates that flywheels are not exempt from this troublesome characteristic of composite joints.

Since the failure expected by further increases in speed would likely be the result of a dynamic instability rather than a material limit, further testing at ORFEL was terminated.

The flywheel was subsequently tested at the Applied Physics Laboratory where it achieved 583 rev/s (35,040 rpm). At that speed it stored 0.47 kWh of energy at 45 Wh/kg (20.6 Wh/lb).

Fatigue Testing of GEB

The second type of evaluation performed this fiscal year by ORFEL was a cyclic fatigue test in which the flywheel was accelerated to a maximum speed, slowed by braking to some minimum speed, then allowed to automatically shuttle between the two points until stopped because of a scheduled inspection, some unexplained observation regarding balance, chamber pressure, appearance on video, dynamic resonances, etc., or failure. With the current control system there is no hold or delay at the upper and lower set points. Using the 4-inch air turbine in its normal configuration as the drive and brake, we are currently cycling with an overall average power of 4.7 kW (6.4 hp).

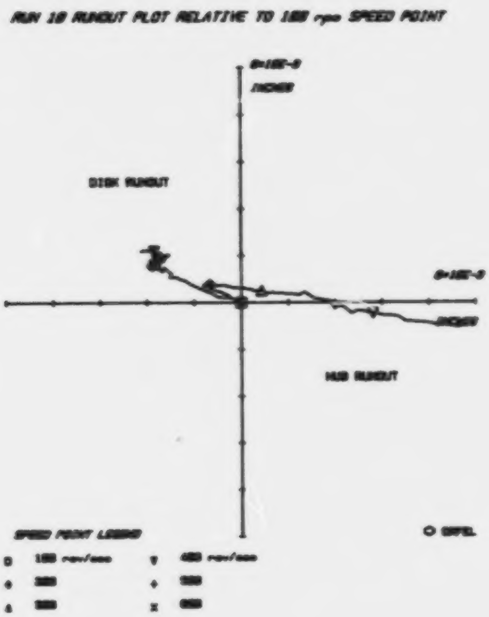

Figure 9. Runout plot for flywheel GE-1's Run #10 with runouts plotted relative to their 100 rev/s speed point. (201758)

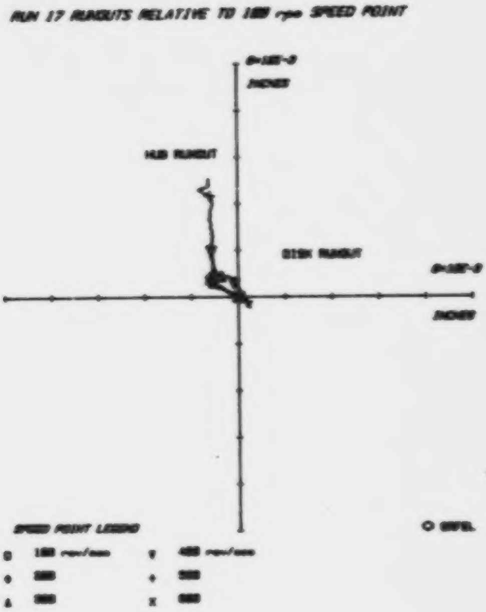

Figure 10. Runout plot for flywheel GE-1's Run #17 with runouts plotted relative to their 100 rev/s speed point (201761)

The first flywheel test unit (serial number GEB) was identical to flywheel GE-1 and suffered similar problems with the hub attachment. Figure 12 shows that during a typical cycle between 140 and 417 rev/s, the runout of the arbor shuttles between 0.20 mm (0.008 in.) and 0.30 mm (0.012 in.) on the 40-degree radius while the disk (bottom button) remains nearly stationary. Fortunately, the whirl experienced is not sufficient to terminate testing, and the flywheel has, as of June 24, 1981, cumulated over 1000 cycles.

For the first 100 cycles, the brake and drive air hoses were intentionally reversed so that the braking power was maximized by working against the drive vanes, but the overall average power was lower because the drive power was diminished. Once the ability to withstand the larger braking torque was demonstrated, the system was returned to its normal configuration. The resulting power and torque curves calculated from velocity changes are shown in Figures 13 and 14.

Two parallel studies are running concurrent with this fatigue test. The resonance frequencies of several flexural vibration modes are experimentally measured each time the flywheel is stopped for visual inspection, and ultrasonic attenuation through the thickness is measured at 49 points every 500 or so cycles. Both of these tests are studying nondestructive methods for monitoring internal damage by measuring the internal damping of the material. The results of these tests will be presented as they become available.

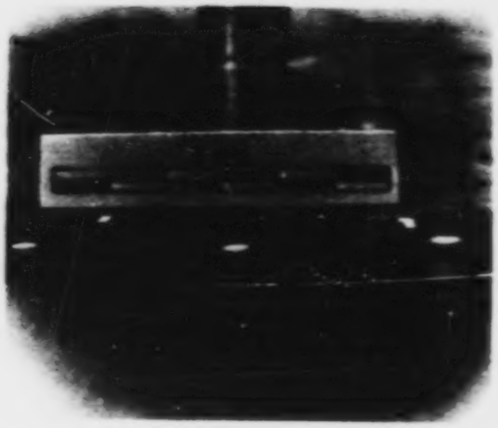

Figure 11. Fiber sling area showing loose fibers. (197963)

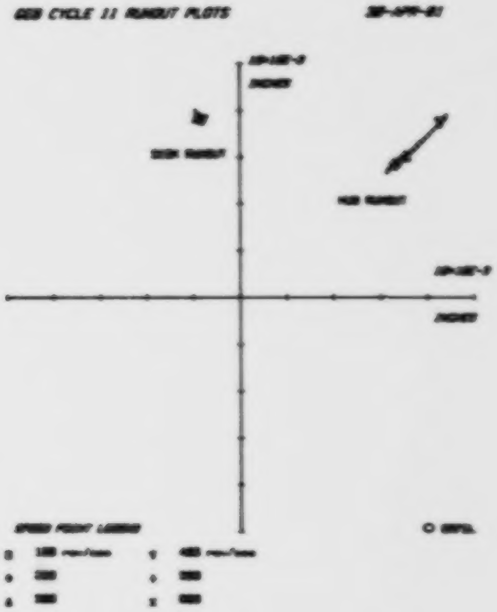

Figure 12. Typical runout plot for flywheel GEB. (201759)

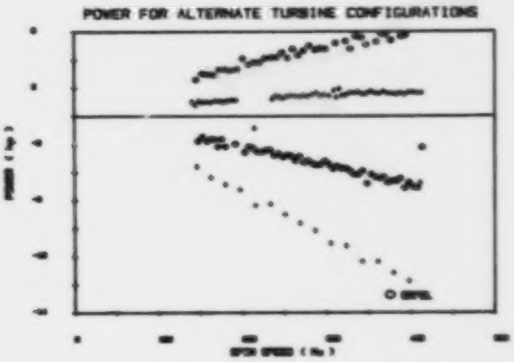

Figure 13. Measured power curves for both normal and reverse turbine configurations. (201754)

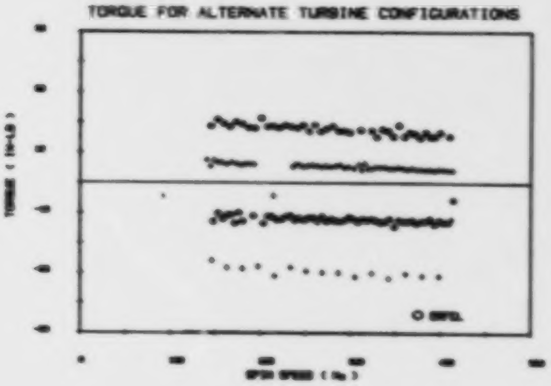

Figure 14. Measured torque curves for both normal and reverse turbine configurations. (201757)

OBSERVATIONS AND CONCLUSIONS

Balance data from the last two years[4] indicate that flywheel imbalance may be a significant problem in their successful application. Most of the flywheels evaluated by ORFEL altered their geometric center relative to their mass center with changes in speed regardless of the quality of their initi balance by an amount greater than is typically tolerated in industrial practice.[5] The actual magnitudes of the imbalance numbers are small; but since the speeds are large, the results are significant and should not be ignored.

Our experience has demonstrated that solid disks are somewhat more stable dynamically than spoke-centered circumferentially wound rims but suffer from the elastomerically bonded hubs used in the current series of flywheels. The use of large bonding areas and low modulus elastomers seem to excite a dynamic instability at high speeds where large differental growth between the disk and hub occurs and large centrifugal forces are found. The smaller bond area and higher modulus elastomer used in the LLNL flywheel was an improvement but did not eliminate the phenomenon. Observations of the failed flywheels indicate that obtaining a uniformly good bond appears difficult. This is compounded by the fact that these bond lines are very difficult to inspect for quality prior to use.

The fatigue test is required to assure the flywheel user that composite flywheels are capable of the large numbers of cycles needed in an automotive application. This test is now available. But the time required to perform the test may be too long. Some method for valid extrapolations must be developed to allow testing at higher speeds or higher temperatures in order to shorten the time required to obtain valid results.

REFERENCES

1. S. V. Kulkarni, "Flywheel Rotor and Containment Technology Development Program of the U. S. Department of Energy," 1980 Flywheel Technology Symposium, October 1980, CONF-801022, Scottsdale, Arizona.

2. J. F. Kay, "Low-Cost Compression Molded Fiber Reinforced Flywheels," Proceedings of Mechanical, Magnetic, and Underground Energy Storage 1980 Annual Contractors' Review, CONF-801128, Washington, D. C.

3. R. P. Nimmer, "The Alpha-Ply Laminated-Disc Flywheel Rotor," Proceedings of Mechanical, Magnetic, and Underground Energy Storage 1980 Annual Contractors' Review, CONF-801128, Washington, D. C.

4. R. S. Steele, Jr., E. F. Babelay, Jr., B. J. Sutton, Oak Ridge Flywheel Evaluation Laboratory Annual Report, Union Carbide Corporation, Nuclear Division, Oak Ridge Y-12 Plant, Oak Ridge, Tenn., Y-2233 (April, 1981).

5. D. Muske and B. Flores, "Balancing Criteria and their Relationship to Current American Practice, Journal of Engineering for Industry, pp 1035-1046 (November 1969).

PROJECT SUMMARY

Project Title: Mechanical Properties of Composite Materials for Flywheel Applications

Principal Investigator: H. Thomas Hahn

Organization:
Washington University
Materials Research Laboratory
St. Louis, Missouri 63130

Project Goals: (1) Characterize mechanical properties of composite materials for flywheel applications, and identify problem areas. (2) Prepare and update a design data manual for composites.

Project Status: A Kevlar 49/epoxy composite has been completely characterized and a new S-2 glass/epoxy composite is being studied. A design data manual has been prepared and will be published shortly.

The composite studied was Kevlar 49/epoxy (DER 332/Kelpoxy G293/Helox 68/Tonox 60-40) filament-wound at Lawrence Livermore National Laboratory. Five uniaxial static properties were determined at room temperature in air before and after preconditioning in vacuum at 75° C. The preconditioned specimens were tested also at 75° C. Fatigue properties in longitudinal tension were characterized at room temperature and at 75° C in vacuum after the preconditioning.

The combination of vacuum and 75° C was found to have only a negligible effect on the mechanical properties.

The design data manual contains data on the hygrothermomechanical properties of glass/epoxy, Kevlar/epoxy, graphite/epoxy, and boron/epoxy. The manual covers a total of eleven composite systems.

Contract Number: LLNL-6641009

Contract Period: September 16, 1980 through September 30, 1981

Funding Level: $89,950

Funding Source: U. S. Department of Energy through Lawrence Livermore National Laboratory

FIBER COMPOSITE MATERIALS TESTING

H. Thomas Hahn W. K. Chin
Materials Research Laboratory
Washington University
St. Louis, Missouri

ABSTRACT

The mechanical properties of a filament-wound Kevlar 49/epoxy composite have been characterized under a simulated flywheel service environment of vacuum and 75° C. The five uniaxial static properties and the fatigue properties in longitudinal tension were found to be only slightly affected by the environment. No extraneous weight loss was observed after a long-term exposure to the environment. Both macroscopic and microscopic examinations of failed specimens did not indicate any deleterious effect of the environment on the mechanical properties of the composite.

INTRODUCTION

The objective of this program was to develop design data for and investigate failure mechanisms of a Kevlar 49/epoxy composite in a simulated flywheel service environment. The composite panels were filament-wound at Lawrence Livermore National Laboratory using an epoxy DER 332/Kelpoxy G293/Helox 68/ Tonox 60-40 (77/23/65/37.3). The simulated flywheel service environment was a vacuum of ~7. x 10^{-3} torr at 75° C.

Static properties were measured under five different loadings while only the longitudinal tension properties were characterized in fatigue. Some of the specimens were preconditioned in the simulated service environment before mechanical tests. Details of specimen fabrication and test methods are described in [1]. In this paper we summarize the results obtained so far. The following abbreviations are used throughout the paper:

RT: room temperature in air

RTP: room temperature in air after preconditioning (in vacuum at 75° C)

RTV: room temperature in vacuum after preconditioning

ET: elevated temperature (= 75° C) in air

ETP: elevated temperature in air after preconditioning

ETV: elevated temperature in vacuum after preconditioning

LT, LC: longitudinal tension and compression, respectively

TT, TC: transverse tension and compression, respectively

S: shear (longitudinal)

ENVIRONMENTAL STABILITY

The total weight loss of a group of 0.5 mm thick specimens during preconditioning was found to be about 2%. The weight stabilized after 400 hours and no further weight loss was observed for up to one and a half years so far. The diffusivity through the thickness of unidirectional composites at 75° C was 4.89 x 10^{-7} mm^2/s.

The moisture content in specimens left in the laboratory environment is rather sensitive to the relative humidity. Figure 1 shows the change of weight gain with the relative humidity at room temperature. The specimens had been dried before the test started.

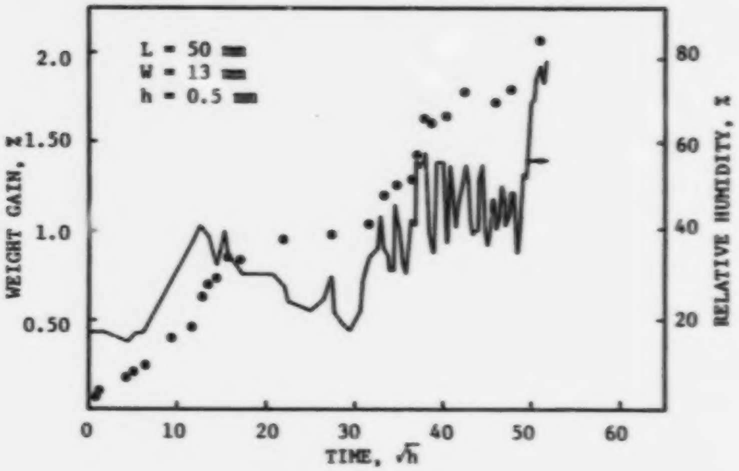

Fig. 1. Weight gain of a dried specimen subject
to the change in relative humidity at room temperature

The desorption of moisture in vacuum is accompanied by shrinkage. In laminates such shrinkage leads to higher residual tensile stress normal to fibers in constituent plies. The residual stresses can be high enough to cause matrix and interfacial failure.

Figure 2 shows the number of cracks in the 25 x 75 mm gage section of $[\pm45]_{2s}$ laminate specimens, which were used for the in-plane shear tests, as a function of the period of preconditioning. The cracks developed during the cool down of the specimens to room temperature for weight measurements. The number of cracks is seen to correlate well with the weight loss: the greater the weight loss, the more cracks there are.

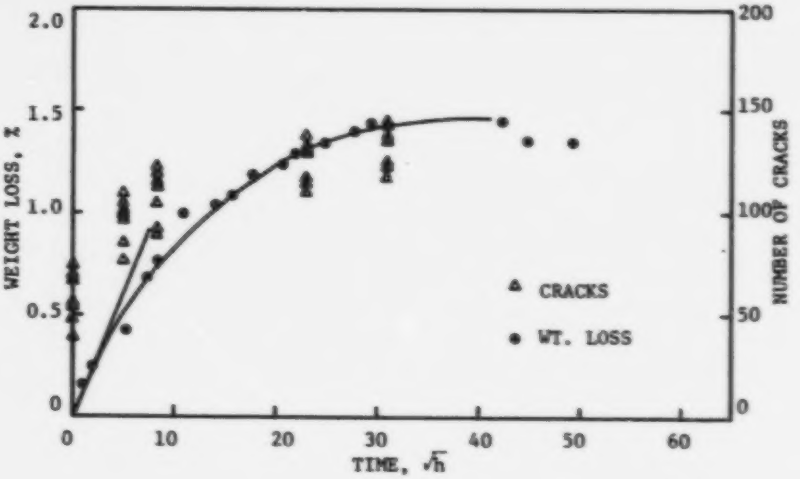

Fig. 2. Weight loss and number of cracks in $[\pm45]_{2s}$ laminates

The residual transverse stress in the constituent plies of a $[\pm45]_{2s}$ laminate can be estimated by using the laminated plate theory if the stress-free temperature is known. For the present composite we can choose the initial cure temperature of 60° C as a conservative stress-free temperature. The resulting residual stress at the room temperature of 25° C is about 15 MPa. This residual stress is substantially higher than the transverse tensile strength of the unidirectional composite. Therefore, the observed cracking of the constituent plies is not surprising.

At present the ply failure caused by residual stresses and its effect on the laminate behavior are not well understood. This problem should be investigated further to ensure an efficient and reliable application of Kevlar 49/epoxy composites.

STATIC PROPERTIES

The strength and modulus data are summarized in Tables 1 and 2, respectively. The longitudinal properties were normalized to 65 vol % of fiber. The nominal fiber volume content of panels varied from the lowest of 54% to the highest of 71%.

Table 1. Static strengths in MPa

Strength	Environment			
	RT	RTP	ET	ETP
LT	1586	1641	1621	1631
LC	243	244	--	182
TT	8.9	8.3	--	7.1
TC	67	79	--	58
S	27	23	--	24

Table 2. Modulus in GPa

Modulus	Environment			
	RT	RTP	ET	ETP
LT	77	83	75	78
LC	69	78	--	71
TT	4.7	5.0	--	4.2
TC	--	--	--	--
S	1.8	1.5	--	1.4

All specimens except at RT and ET were preconditioned at least for 45 days. In each case the period of preconditioning was long enough for the stabilization of weight loss.

On the whole, there is only a small reduction of properties at 75° C after the preconditioning. In fact, the preconditioning slightly improves the room-temperature properties except in shear. The improvements are believed to be the result of moisture having been driven out of the composite. The ply cracking observed in the $[\pm 45]_{2s}$ laminate specimens is responsible for the apparent loss of strength and modulus in shear after the preconditioning.

To ascertain the excellent retention of the LT strength at ETP, specimens of bare Kevlar 49 fiber were tested. Compared with the RT strength, there is about 11% reduction at 75° C. The corresponding change in the composite strength is rather in the opposite direction. Since the higher ET strength of the composite was suspected to have been an artifact of panel-to-panel variability, additional specimens were taken from the same panel, and five specimens each were tested at RT and 75° C, respectively. The result was a 4% reduction in strength at 75° C. Yet this retention is much smaller than that observed of the fiber. Therefore, it is concluded that the composite exhibits better strength retention than the fiber itself.

The effect of preconditioning on the RT strength of the fiber is shown in Fig. 3. Two groups of specimens were conditioned for various periods of time at 75° C: one group in an air circulating oven and the other in a vacuum oven. The strength is decreased only slightly by the exposure to such environments. Also, there is no noticeable difference between vacuum and air.

The glass transition temperature of the present epoxy is around 104° C. At 75° C the epoxy retains about 70% of the RT strength and RT modulus. The corresponding retention of the composite properties, although after the preconditioning, is much better. Furthermore, the LT strength at 100° C was found to be at least 88% of the RT value.

On the whole, the Kevlar 49 fiber does not show any sign of continued deterioration under a long-term exposure to 75° C in vacuum. The composite shows a better retention of properties at 75° C than does the epoxy.

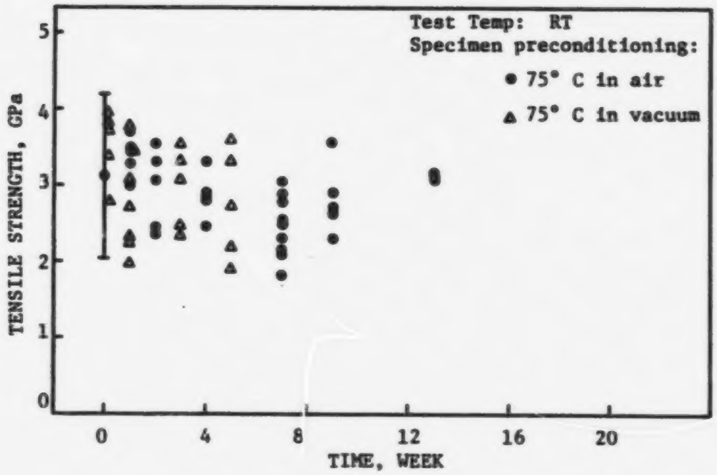

Fig. 3. Effect of preconditioning on strength of Kevlar 49 fiber

FATIGUE PROPERTIES

Longitudinal fatigue tests were run at three environments: RT, ET, and ETV. The test frequency and the stress ratio were 4 Hz and 0.1, respectively. The resulting life data were analyzed by using a two-parameter Weibull distribution of the form

$$R(N) = \exp \left[-\left(\frac{N}{N_o}\right)^{\alpha_f}\right]$$

Here R(N) is the probability of a specimen surviving N cycles. The shape parameter α_f and the characteristic life N_o were determined by the method of maximum likelihood.

The shape parameters and the characteristic lives are shown in Figs. 4 and 5, respectively. On the ordinate the maximum fatigue stress has been normalized with respect to the average ultimate tensile strength (UTS) at the respective environment. The shape parameter increases with decreasing fatigue stress except at ET. The change at ET is not monotonic. However, the shape parameters at the two lower stresses are not smaller than unity regardless of the environment. Thus, a wear-out type of failure occurs around and below 80% UTS. It is interesting to note that across this 80% UTS the slopes of the stress-logarithmic life curves also change, Fig. 5.

Additional fatigue tests were run at RTV and at 100° C. The RTV data generally fell within the scatter of RT and ETV data. A substantial reduction was observed at 100° C.

During a longitudinal tension the Kevlar 49/epoxy exhibits a strain-hardening, i. e., the tangent modulus increases about 13% with strain. Upon unloading the stress-strain relation describes a hysteresis loop, Fig. 6. Part of the residual strain is recovered with time. A similar strain-hardening behavior is observed of graphite/epoxy composites; however, there is no hysteresis loop. Thus the reorientation of internal structure responsible for strain-hardening is time dependent in Kevlar 49 fibers.

The hysteresis loop disappears with fatigue cycles, accompanied by an increase in modulus. The tangent modulus at 1% strain can increase as much as 10 to 20% at fatigue stresses of 70 and 80% UTS. The modulus decreases somewhat before the final failure.

The energy dissipation indicated by the hysteresis loop results in a temperature increase higher than observed of other composites such as graphite/epoxy and glass/epoxy. At 90% UTS the specimen surface temperature can be about 15° C higher than the room temperature. Still higher temperature increases are observed in the RTV environment because of poor heat transfer in vacuum.

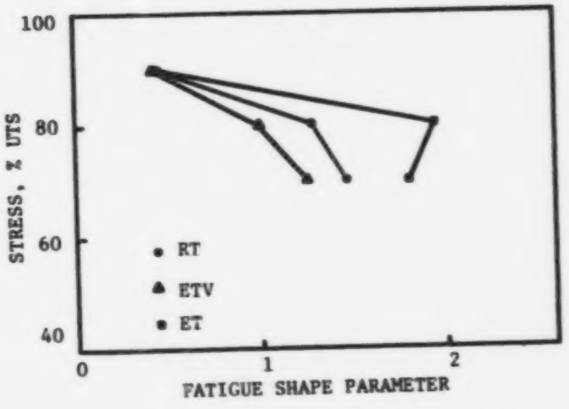

Fig. 4. Fatigue shape parameters

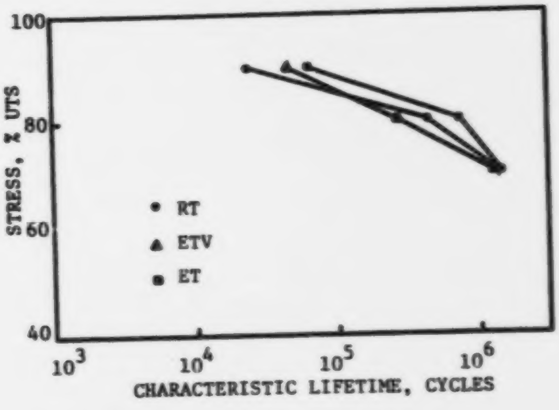

Fig. 5. Characteristic fatigue lives

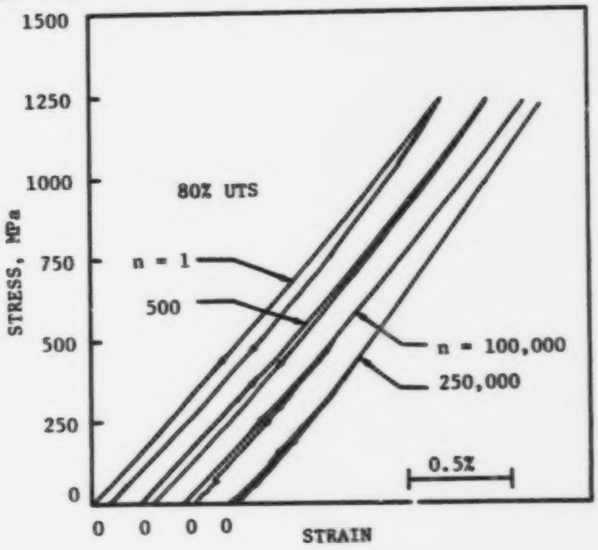

Fig. 6. Stress-strain relations during loading and unloading after fatigue. n is the number of cycles endured.

FAILURE MODES

All specimens in longitudinal tension failed in a brush-like manner regardless of the type of loading and the environment. Several longitudinal splits were initiated at the tab ends and grew into the gage section before the final failure. The longitudinal cracking was more extensive in fatigue than in static tension.

The failed specimens were examined on a scanning electron microscope (SEM). Again, no noticeable differences were found among specimens tested under different conditions. Clean fiber surfaces and the lack of matrix lacerations indicated a state of poor bonding between fibers and matrix.

The splitting of the fibers in the composite was very much similar to that of single fibers tested individually. One exception was that the fibers in the composite had part of their skin peeled off over a longer portion of their axis. The single fiber test results showed very little correlation between strength and the splitting length. Also, the period of preconditioning did not show any significant effect on the splitting length.

In transverse tension the fracture surface was normal to the loading. Clean fiber surfaces and clean fiber imprints indicated extensive interfacial failure.

Both longitudinal and transverse compression resulted in failure occurring on a plane about 45° inclined to the loading when viewed from edges. Thus the compressive failures are believed to be the result of shear failure along the failure plane.

The failure of $[\pm 45]_{2s}$ specimens for longitudinal shear was characterized by extensive cracking of plies and delamination. There were very few fiber failures. The delamination surfaces consisted of areas of bare fibers and those of fiber imprints. The bare fibers gave a shiny appearance whereas the fiber imprints were responsible for dull spots on delamination surfaces.

Some of the run-out fatigue specimens at 70% UTS were sectioned normal to the fibers and were examined on the SEM. The fibers showed very little sign of damage. The longitudinal cracks found were along the interfaces, not through the fibers.

CONCLUSIONS

The effects of the simulated flywheel service environment on the mechanical properties of a filament-wound Kevlar 49/epoxy composite have been characterized. The major findings are summarized as follows:

1. The preconditioning in vacuum at 75° C leads to an improvement in strength and modulus through moisture desorption. However, it can cause cracking of plies in multidirectional laminates. No extraneous weight loss has been observed in the preconditioning for a period of one and a half years so far. Most of the lost weight is believed to be the moisture desorbed in vacuum.

2. The composite has an excellent retention of static and fatigue properties at 75° C both in air and in vacuum. However, it suffers degradation of properties at 100° C.

3. The composite is less sensitive to the environment than the fibers and the matrix by themselves. Also, composite laminates are less susceptible to environmental degradation than composite strands because larger dimensions minimize the effect of surface degradation on bulk properties. Thus, care must be exercised in making inferences about the laminate behavior from the strard behavior.

4. The Kevlar 49 fiber shows only a small reduction in strength after a long-term exposure to 75° C in air or in vacuum. The splitting length is independent of strength and environment.

5. All specimens in longitudinal tension failed in a brush-like manner regardless of the type of loading and environment. No discernible differences were found on the SEM. Compression failures were a shear failure along the maximum shear stress plane. The run-out fatigue specimens did not show any sign of fiber splitting except for a few longitudinal cracks.

6. The composite shows both a strain hardening and a time-dependent hysteresis loop. The hysteresis loop is responsible for the temperature rise higher than observed of other composites such as graphite/epoxy and glass/epoxy.

REFERENCES

1. H. T. Hahn and W. K. Chin, Engineering Properties Determination for Composite Materials. Mechanical, Magnetic, and Underground Energy Storage 1980 Contractors' Review, Washington, D. C., November 10-13, 1980. U. S. Department of Energy.

PROJECT SUMMARY

Project Title:	Assessment of Damage and Service Potential under Spectral Loading
Co-Principal Investigators:	John C. Duke, Jr. Kenneth L. Reifsnider
Organization:	Materials Response Group Engineering Science and Mechanics Department Virginia Polytechnic Institute and State University Blacksburg, VA 24061
Project Goals:	Determine the precise nature of damage that develops during spectral fatigue loading of composite laminates. Identify the distinctive features of the fatigue damage as a function of the distinctive features of the loading spectra. Relate the distinctive features of damage for a given loading spectrum to the serviceability of the laminates.
Project Status:	The project is under way and work is in progress. A review of existing literature relating to this subject area is being conducted. A computer interactive test control and data acquisition system has been developed. Capabilities include: control of the hydraulic testing machine, acquisition of load, strain, and continuous monitoring of nondestructive testing parameters. Receipt of test panels is anticipated.
Contract Number:	W-7405-ENG-48 Subcontract 3272201
Contract Period:	March 23, 1981 through January 2, 1982
Funding Level:	$15,000
Funding Source:	U.S. Department of Energy through the University of California Lawrence Livermore National Laboratories.

FIBER COMPOSITE MATERIALS FATIGUE STUDIES

J. C. Duke, Jr., R. Stiffler and K. L. Reifsnider
Materials Response Group
Engineering Science and Mechanics Department
Virginia Polytechnic Institute and State University
Blacksburg, Virginia 24061

ABSTRACT

An experimental study to determine the precise nature of damage that develops during spectral fatigue loading of composites is under way. Distinctive features of the fatigue damage as a function of the distinctive features of the loading spectra will be identified and related to the serviceability of the quasi-isotropic laminates being considered. A computer interactive testing machine controller and data acquisition system has been developed.

INTRODUCTION

The use of composite materials continues to expand into engineering applications that require greater performance and longer durability. This is a consequence of superior engineering performance, ease in manufacturing, and (in some cases) cost effective material use or low life-cycle costs. As our understanding of the performance of composite materials develops, a new level of engineering design and application is being reached whereby engineering components are being designed from "scratch" in a way that optimizes the use of the unique properties of composite materials, rather than attempting to incorporate such materials on a replacement basis in designs that were conceived for homogeneous isotropic materials. This new level of design and application has had at least two major consequences. First, composite materials are being used more often in "primary structures," i.e. in the part or parts of components that are primarily responsible for the strength, stiffness and life of the structure. Second, the design levels of stress and life are being pushed closer to the material limits, i.e., the margin for error in anticipating the strength and life of composite materials under a given load history is necessarily decreasing. In terms of engineering performance, the durability and life of engineering components which incorporate composite materials is becoming increasingly dependent upon our ability to characterize the durability and life of those materials.

The use of composite materials in flywheels for energy storage devices is an excellent example of advanced applications. In a development program led by Lawrence Livermore National Laboratory, several flywheel designs based on the unique capabilities of composite materials were conceived, and the flywheels built and tested to failure. The highest energy storage densities ever achieved were recorded for those tests, verifying the superiority of the materials and designs. However, the durability of those components has not yet been established. Since the flywheels consist almost entirely of composite materials, and the energy storage capability depends strongly on the design levels of stress that are allowed, an understanding of the behavior of the composite materials is essential to the success (and safety) of the flywheels.

While long-term serviceability has been studied in a general way by a number of investigators, a systematic study of the relationship between the precise nature of the damage that develops during long-term fatigue loading and serviceability has not been conducted. In particular, an understanding of the specific relationships between different types of fatigue loading (including the sequence of loading) and the type of damage induced as it influences serviceability has not been established.

PHILOSOPHY

The topic of cumulative damage resulting from fatigue loading is broad and has been the subject of some earlier work by a number of investigators. However, the current information available and the current level of understanding of related response principals is inadequate to provide a solution to this problem in general, and is especially inadequate for the flywheel because of its complexity. Current engineering schemes for estimating the life of composite materials under spectrum loading are based on statistical representations of damage-rate information in a general way in order to construct "wear-out" models. These models are not based on physical mechanisms of damage known to be associated with life-limiting damage modes. Consequently, the generality of these models is extremely limited and there is no systematic or rational method of extending such models to the prediction of the life of composite materials under spectrum loading.

It is the objective of the present research program to establish the precise nature of the micro-damage that is introduced by spectral loading. The long term intention of this approach is to develop models of the damage process that can be used to anticipate durability and strength under arbitrary spectral loading histories based on sound physical understandings and measurable indications of damage that are quantitatively related to response.

APPROACH

To accomplish the program objective, extensive use of nondestructive evaluation is being made. Composite laminates supplied by the Lawrence Livermore National Laboratory are being examined as received, using ultrasonic scanning and X-ray radiography. Subsequent to this, the material is being cut into specimens for mechanical testing. Static tests are being performed on cross ply specimens in order to allow for checking of the computer interactive test facility. A discussion of the features of this system and the results of these tests are included in the next section.

Pending receipt of quasi-isotropic laminates some initialization and characterization fatigue tests at three different constant amplitudes (4 Hz and R = 0.1) will be conducted to establish the constant amplitude baseline response. Extensive examination of these specimens will be made to establish the nature of the damage development for each constant amplitude load level considered. Once the damage development is sufficiently documented for these conditions, spectral loading will be considered.

Initially, these tests will be bi-level tests, i.e., tests will be run at one of three levels used for the baseline tests for one half the number of cycles thought to correspond to the life at that stress level. Then the stress amplitude will be changed to one of the other levels used in the baseline tests and the test continued to failure. Damage development will be monitored in the same way described above for the baseline tests. Several combinations of high-low, low-high stress levels among the three levels chosen will be used. The maximum and minimum stress levels will be combined first. While comparisons with various damage "laws" (especially the linear damage rule usually associated with Miner) will be made, the major emphasis will be on identifying the differences in the development of internal damage caused by the "step-loading" process, and the relationship of this damage with the life of the specimens. Special attention will be given to the effect of load sequence, i.e., the difference caused by applying two load levels in a given sequence or in the reverse order. Residual stiffness and residual strength will also be compiled. All information will be combined to generate an understanding of the step-loading results. Based on this understanding, a preliminary philosophy concerning the effect of spectral loading will be developed. The philosophy will be used to design further investigations and will serve as the basis for the development of rudimentary modeling concepts. The philosophy will be "tested" by comparing its predictions with test results obtained at one predicted life level established by a statistically significant data set.

DAMAGE DEVELOPMENT MONITORING

Edge replication, first applied to the study of damage in composite materials in the Materials Response Laboratory at Virginia Tech, will be used to follow the damage development. Some early work demonstrating the effectiveness of this procedure is shown in Figures 1-3.[1] Figure 1 displays edge replicas of a graphite epoxy laminated specimen, $[0,\pm45,90]_s$ which was fatigued with R = 0.1 and a maximum stress of 234 MPa (34 ksi); the arrows indicate damage features (except for 2 and 4 which point out artifacts which are to be ignored). Compare to this, Figure 2 which displays replicas of a similar specimen fatigued at R = 0.1 and a maximum stress of 290 MPa (42 ksi); the arrows here indicate damage. Through the use of this technique the damage development may be monitored as is displayed in Figure 3. Results included in this graph show specimens fatigued with R = 0.1 and the maximum stresses indicated for two different quasi-isotropic laminates.

In addition to replication, changes in tensor stiffness will be monitored since they reflect in a tangible way the degradation of a material property of engineering significance. Extensive fundamental work has been done on this topic in the Materials Response Laboratory[2]. Figure 4 depicts the change in stiffness and the density of transverse cracks versus load. Figure 5 shows the theoretically predicted stiffness change as well as that observed experimentally as a function of crack density.

Whereas both edge replication and changes in tensor stiffness require interrupting the test procedure, only selected places in the deformation may be examined. To follow the progression of the damage more completely, monitoring of ultrasonic attenuation, acoustic emission and dynamic stiffness will be performed. Considerable evidence exists showing the sensitivity of both ultrasonic attenuation and acoustic emission to the distinctive features of the mechanical response of composite materials. Figure 6 shows the results of a quasi-static tension test in which both ultrasonic attenuation and acoustic emission activity exhibit a change as the material behavior becomes nonlinear[3].

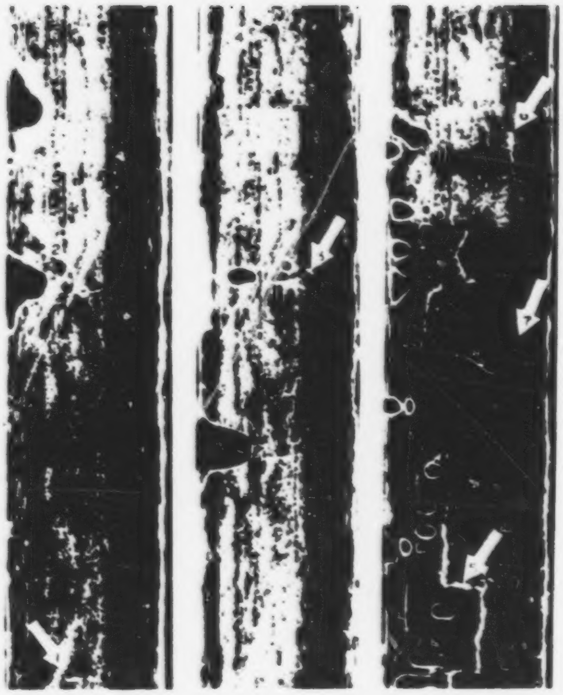

a) Static b) 50 Cycles c) 10,000 Cycles

Fig. 1. Replicas of damage in a graphite epoxy $[0,\pm45,90]_s$ laminate with R = 0.1 and a maximum stress of 234 MPa (34 ksi).[1]

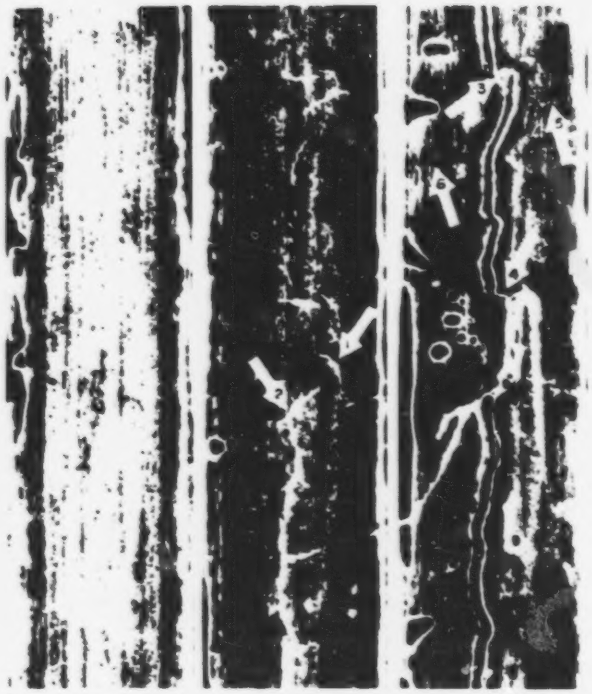

a) Static b) 50 Cycles c) 10,000 Cycles

Fig. 2. Replicas of damage in a graphite epoxy $[0,\pm45,90]_s$ laminate with R = 0.1 and a maximum stress of 290 MPa (42 ksi).[1]

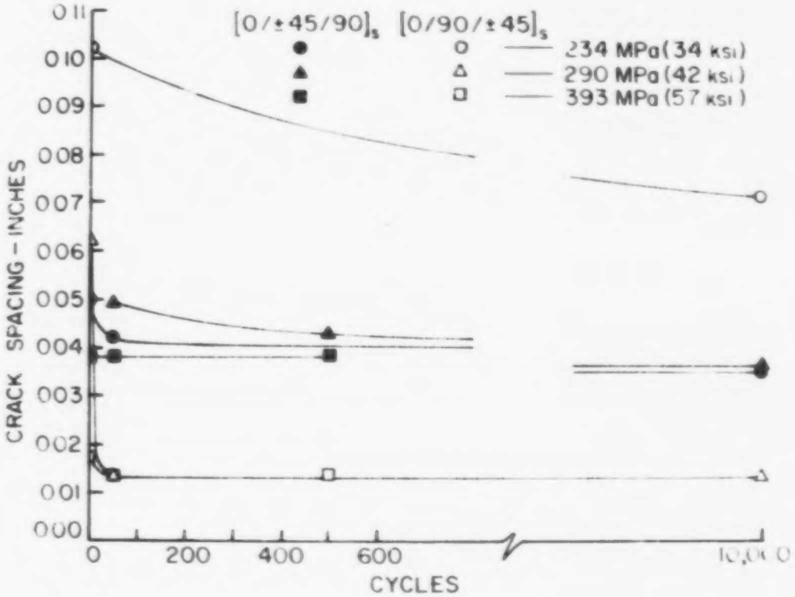

Fig. 3. Crack spacing as a function of number of cycles for two different quasi-isotropic stacking sequences. R = 0.1 and the maximum stress for each case is as shown.

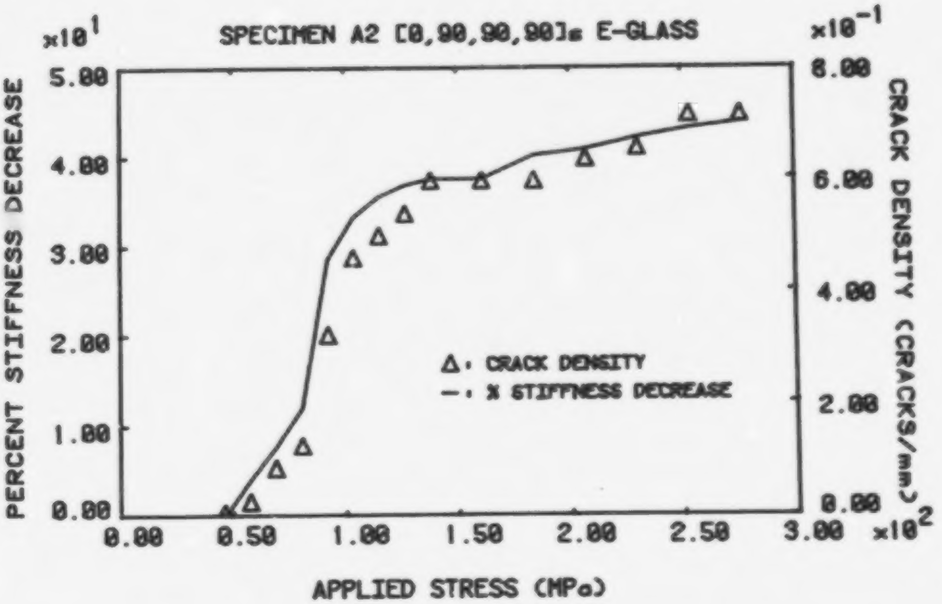

Fig. 4. Percent change in stiffness, as well as transverse crack density as a function of applied stress.[2]

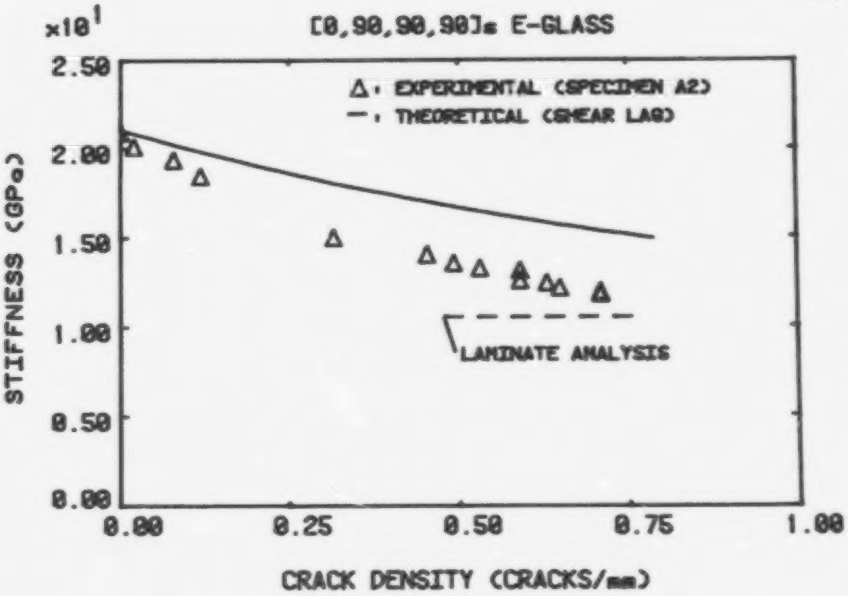

Fig. 5. Theoretical predicted and experimentally observed stiffness versus crack density.[2]

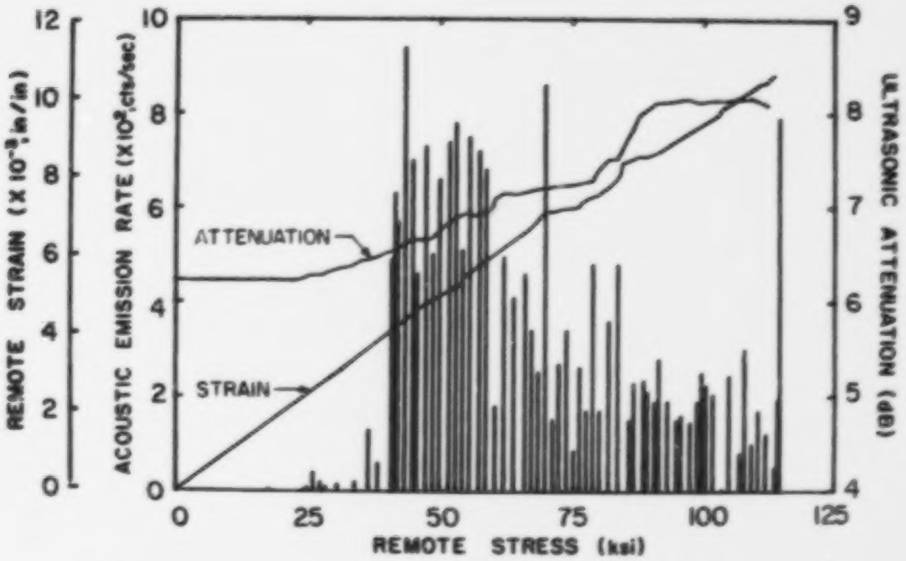

Fig. 6. Remote strain, acoustic emission rate, and ultrasonic attenuation versus the remote stress.[3]

During the fatigue tests, intervals for monitoring the acoustic emission activity, or changes in ultrasonic attenuation, will be synchronized with the cyclic loading of the specimen. This will allow these two parameters to be monitored at any desired point in the load cycle. If necessary to document the nature of the damage, tests will be terminated prior to final failure in order to allow for extensive materialography. This could involve sectioning the specimens and observing the condition using conventional optical or scanning electron microscopy.

DESCRIPTION OF TEST SYSTEM

Because of the numerous parameters being monitored during the tests and the necessity in some cases to perform calculations involving the data, a computer interactive test system has been developed. The basic system is a Z-80 S-100 microcomputer which is capable of sampling several channels of information. Load, longitudinal strain, transverse strain, acoustic emission count rate (total counts, and, or, true root mean square transducer output), and change in ultrasonic attenuation may be sampled and stored at a rate of two times a second. If desired, by utilizing a Biomation 8100 transient recorder, individual acoustic emission wave forms can be sampled, stored and processed. Periodically during the cyclic loading, load-strain data for several cycles is captured, and processed to determine the dynamic tangent and secant modulus as well as mechanical hysteresis; these processed values, collected throughout the test, are saved. Figure 7 displays the data obtained by the system during a quasi-static tension test, at a constant rate of loading of a cross ply S-2 glass epoxy laminate. For ease of comparison, each plot involves the load, although a plot of any pair is possible.

In addition to the basic system, special gating circuitry has been developed. One allows for restricting the region from which AE signals are accepted as well as provides for location of their origin. The second makes it possible to select any portion of the load cycle for monitoring. If so desired, the microcomputer can be used to operate the test machine by controlling servo actuating devices. Consequently it is possible to prescribe, within the limitations of the machine, the load rate, the strain rate, or the product of the two.

The system has been developed in order to provide an accurate means of monitoring the material's mechanical response and parameters which reflect its condition simultaneously.

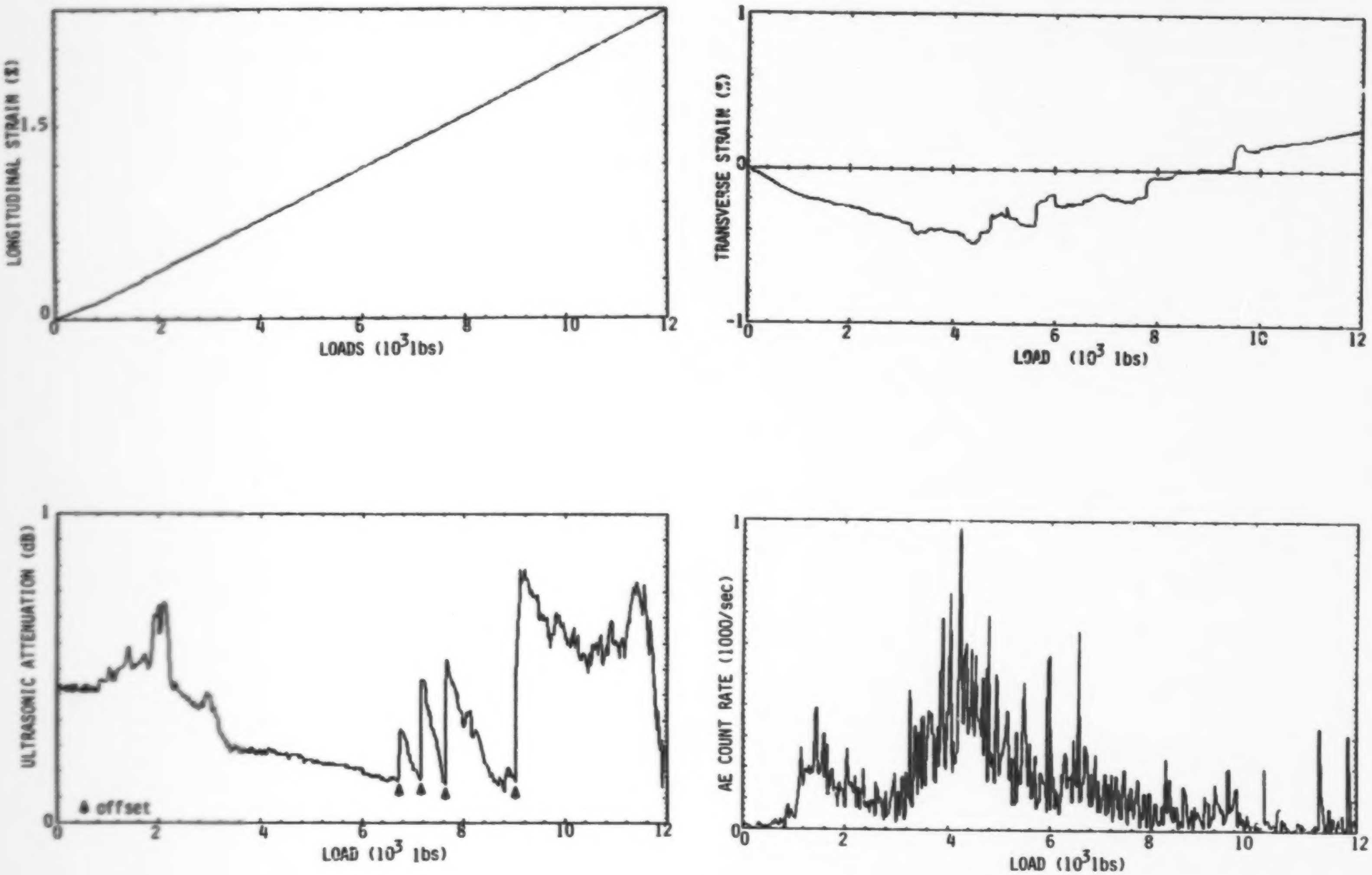

Fig. 7. Graphical output of data sampled during a quasi-static tension test of a cross ply S-2 glass epoxy specimen. For ease of comparison a) longitudinal strain, b) transverse strain, c) ultrasonic attenuation, and d) acoustic emission rate are plotted versus load.

SUMMARY

A systematic experimental program to document the precise nature of damage development during spectral fatigue loading is under way. Extensive use of nondestructive evaluation is anticipated. A computer interactive data acquisition and control system has been developed.

REFERENCES

1. D. O. Stalnaker, W. W. Stinchcomb. Load History--Edge Damage Studies in Two Quasi-Isotropic Graphite Epoxy Laminates. Composite Materials: Testing and Design (Fifth Conference). ASTM STP 674, S. W. Tsai, Ed., American Society for Testing and Materials, 1979, pp. 620-641.

2. A. Highsmith, K. L. Reifsnider. Stiffness Reduction Mechanisms in Composite Laminates. Conference on Damage in Composite Materials; Basic Mechanisms, Accumulation, Tolerance and Characterization. American Society for Testing and Materials, Bal Harbour, 1980.

3. M. N. Gibbins, W. W. Stinchcomb. Fatigue Response of Composite Laminates with Internal Flaws. Composite Materials: Testing and Design (Sixth Conference). American Society for Testing and Materials, Phoenix, 1981.

PROJECT SUMMARY

Project Title:	Long Term Creep Characteristics of Composite Flywheel Materials
Principal Investigator:	Dr. F.F. Ling
Organization:	Rensselaer Polytechnic Institute Mechanical Engineering Department Troy, New York 12181
Project Goals:	Develop a method of measuring the creep characteristics of various composite materials which are candidates for flywheel application. Manufacture test equipment and instrumentation for testing. Run long and short time tests and attempt to predict long time behavior from subsequent short term tests.
Project Status:	This project is underway with long term tests being conducted in air and vacuum. Equipment and instrumentation has been developed to accomplish the above task. Composite materials are being tested at various loads and for periods from 500 hours to 2500 hours. A determination of deformation under load, as well as plastic deformation is being conducted to show the effect that long term loading has on the candidate composite materials. In addition, duplicate tests are being run in a vacuum chamber to establish environmental effects. The tensile strength of the composite materials is being measured before and after testing and a fractographic analysis is being performed with the scanning electron microscope (SEM) to determine the failure mode or changes in failure mode due to creep.
Contract Number:	DEFG-06-81ET26504
Contract Period:	October 1, 1980 through September 30, 1981
Funding Level:	$70,000
Funding Source:	U.S. Department of Energy through The Office of Advanced Conservation Technology

LONG TERM CREEP CHARACTERISTICS OF COMPOSITE FLYWHEEL MATERIALS

F.F. Ling and S.J. Calabrese
Rensselaer Polytechnic Institute
Mechanical Engineering Department
Troy, New York 12181

ABSTRACT

A method has been developed to establish the long term creep characteristics of composite materials. The required test rigs, environmental chambers and instrumentation has been manufactured, to perform in situ deformation under load measurements on the candidate materials. A study to determine the mode of failure before and after exposure to long term deformation under load is being conducted with the aid of the Scanning Electron Microscope. Continued testing is expected to determine a confidence level for composite materials under flywheel containment environment conditions.

INTRODUCTION

At the present time, composite materials are considered to be strong candidates for the manufacture of flywheels for energy storage. However, due to the lack of available data on long term creep characteristics, it is necessary to evaluate the specific fiber/resin combination, which will be used in the flywheel. In addition, it is important to determine if the environment in the flywheel container will alter the physical properties of the composite. Hence, in order to obtain some confidence level, long term creep data must be obtained on the specific composite material in the containment environment, and at the temperature at which the flywheel will be run.

To this end, a program was initiated at RPI by the U.S. Department of Energy to obtain long term creep data on the materials which are, at the present time, the most attractive combinations for the flywheel applications. Because of the nature of the evaluation, certain problems had to be overcome that would allow a large number of long term tests to be run in vacuum, helium and air while controlling the temperature and moisture content in the environment.

PROGRAM GOALS

The program was set up to accomplish the following goals:

- Obtain creep data on the various composite material systems which would be used in a flywheel application (air).
- Obtain creep data on the same materials in vacuum and helium.
- Determine the effect of elevated temperature on the creep characteristics in air, vacuum and helium.
- Compare results to air and continue testing at various stress levels in all environments or in air depending on the results of the comparison.
- Attempt to predict long term creep characteristics from composite materials based on short term creep data.

TASKS

In order to accomplish the above goals the following tasks were performed:

a) Select specimen size and geometry
b) Design and manufacture test apparatus
c) Design and manufacture environmental chamber to accept several test rigs
d) Select a method of measuring small displacement levels due to deformation under load at elevated temperature
e) Manufacture displacement probes
f) Run preliminary tests and make necessary modifications to accomplish the above goals
g) Run tests in air and vacuum on candidate materials for the flywheel application
h) Determine the credibility of predicting long term creep characteristics from short term data.

Tasks a) through f) are complete. Task g) is in progress with specimens running at various time increments up to 3000 hours under load. Step h) will be accomplished when adequate data is available from the long term tests.

PROBLEM

There are standard ASTM test specifications for creep rupture [1] and tensile [2] which recommend a specimen configuration. Because of the length of test time and the size requirement, the standard specimen was not used. The test specimen was designed by utilizing the ASTM standard configuration with modifications which would allow for long-term testing in a closed environment.

The first problem was to design a specimen end which would not slip or deform during long-term exposure to load. Most of the grips that are used for tensile testing have a threaded end or a friction grip. However, because of the need for long-term testing it was decided that a grip with a mechanical interlock should be used that would allow the specimen to move within the grips. In addition, the in situ measurements taken would not be affected by minor changes even if slight deformation had occurred in the grips.

The specimen size was selected by the combination of the size of the environment chamber, the size of the test rig and a reasonable amount of cross-section which could be easily manufactured and deadweighted to produce the desired stress.

The final problem was to use a measurement system which would be unaffected by the length of time for the individual tests and would produce highly accurate measurements while the tests were in progress. In order to select the best arrangement, various methods were evaluated in a test rig and the one which proved to be the most reliable for long-term testing was a capacitance system.

Special probes had to be manufactured which could be used at high temperatures.

TEST APPARATUS

The objective of these experiments is to test the creep characteristics in simple tension of a number of composites at low to moderate stress levels. The test rigs had to be small enough to fit inside a test chamber of reasonable size.

With these two main constraints in mind it was decided that a configuration shown in Figure 1 would be the most appropriate test apparatus. This loading apparatus would be small enough and at the same time be able to produce the required stress level in the specimen.

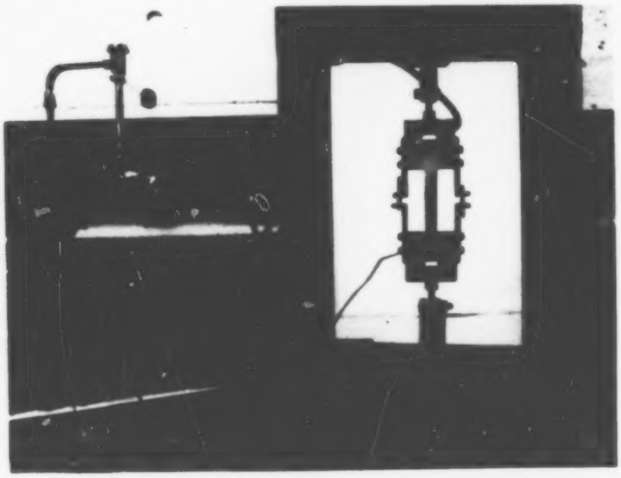

Figure 1 Test Apparatus Used to Evaluate the Creep Characteristics of Composite Materials

The most difficult problem to solve on the loading apparatus was hot to grip the specimen. With the period of testing to last about six months conventional grips would have slippage problems. With the shape and size of the specimens having been determined from Refs. [3,4], the grip configuration that was decided on (Figure 1), was such that the specimen supports itself. Initially the contact area was so small as to create bearing stress problems when loading. With the addition of wood inserts bonded to and having the same shape as the specimen, this problem was eliminated.

The specimen is kept in pure tension by the use of rod end joints which prevent out of plane loads. Torsional loads are eliminated by the use of two 1/8 inch dowels that keep the grips from rotating relative to each other (Figure 1).

ENVIRONMENTAL CHAMBER DESIGN

The environmental test chamber had to withstand a vacuum of 1×10^{-4} torr, temperature ranges from 25 to 150°C, two levels of humidity and contain air or an inert gas such as helium. The other limiting factor on the chamber design was that it had to be large enough to contain at least six test apparatuses. Six loadings on the same material and layup under the same environmental conditions were considered enough to give good repeatable data.

After careful consideration, it was decided that a box type environmental chamber had the best space utilization with the least amount of manufacturing difficulties. The primary problem with a box is that it does not withstand pressure or vacuum very well. To get around this a strong primary structure with an outer skin would provide the strength for most of the chamber.

Figure 2 shows a photograph of the test rig in the chamber. The load is applied by dead weights through a rod, hanging from the load arm and extending outside of the chamber. The temperature is controlled by quartz heaters and measured by means of a thermocouple in contact with each test specimen. Temperature is continually monitored throughout the test by means of a 12-channel recorder.

It should be noted that the chambers are used for vacuum testing and helium testing. The air tests are being sun in an atmosphere-controlled enclosure, seen in Figure 3. Since there is no need to seal the environment during the air tests there is little reason to commit a test chamber for air tests.

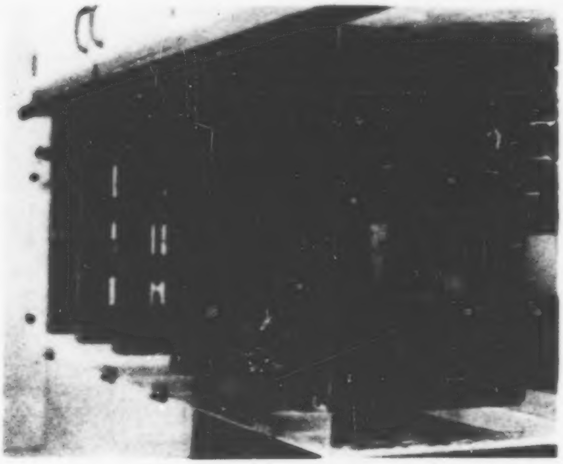

Figure 2 Photo of the Test Chamber with Two Test Rigs Seen in the Far Right Open Door

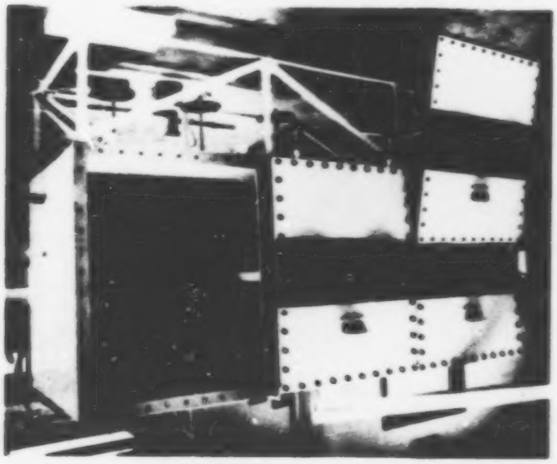

Figure 3 Atmosphere Controlled Enclosure Used to Control the Environment for Creep Tests Run in Air

The relative humidity and temperature are kept constant by means of a drying tower and water flask through which air is passed. By varying the amount of air passed through each, the enclosure is blanketed with air at the desired temperature and moisture level. The moisture content and temperature are recorded on a daily basis with the log of the displacement reading from the capacitance probes.

DISPLACEMENT MEASUREMENTS

In order to establish the best instrument system which should be used to monitor displacement under load, one test rig was set up with several representative composite materials.

After several attempts were made to measure deflection by monitoring portions of the fixture, it was found that the best method was to attach a probe to one end of the specimen and a target to the opposite end as seen in Figure 4. A micrometer head was placed on the fixture to measure gross changes in specimen length and is a rough check against the probe readings.

It was found that the system, which gave the most consistent measurements without drift, was a capacitance system. Special probes had to be manufactured which were capable of measuring long distance and at high temperatures. In addition, they were not affected by vacuum or helium. The probe design selected, allowed measurements to be taken in a range up to 1.27 mm (.050 inch) with an accuracy of four decimal places. They were also capable of temperature in excess of 200°C (392°). Figure 5 shows a typical trend of displacement (elongation) vs. time for one of the materials evaluated. Note that it took almost ten days for the specimen to slow down its elongation process and even after 50 days there still appeared to be an increase in length.

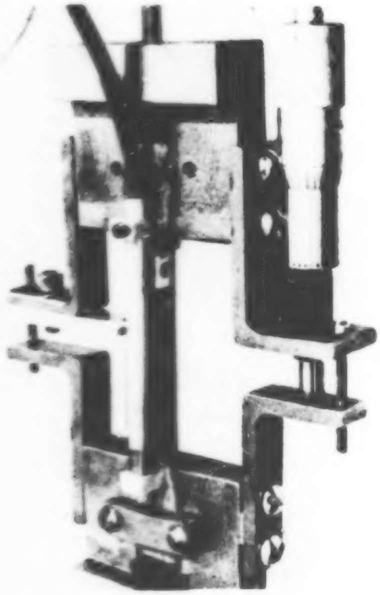

Figure 4 Specimen Arrangement to Establish Type of Displacement Monitoring System to be Used During Test

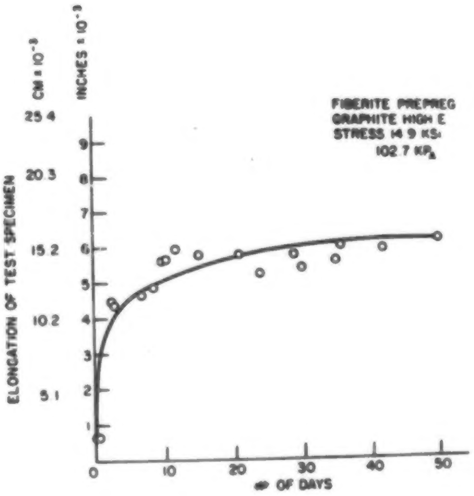

Figure 5 Typical Long Time Deformation Trend for an Epoxy Impregnated Graphite Composite Material

It should be noted that these data do not represent total elongation as a function of load, but as a function of time after the load was applied. Hence the change in specimen size is due to an increase in length under a constant load for the period of time plotted in Figure 5.

As a result of the preliminary tests it was decided that:

- Additional test rigs should be manufactured similar to those shown in Figure 4 with slight modification.
- A capacitance system with probes which would measure in a range of 1.28 mm (.050 inch) would be used to monitor displacement.

MATERIAL SELECTION

Presently there are four epoxy systems under consideration for flywheel applications [3]. They are:

A) DER 332/Jeffamine; T-403 (100/45 ratio): Low temperature application
B) DER 332/RD-2/Tonox; 60-40 (100/35/29 ratio): Medium temperature application
C) DER 332/Kelpoxy; G293/Kelpoxy; Tonox 6040 (77/23/65/34 ratio): Medium temperature application
D) CY-179/CTBN/MTHPA; 1 MI (100/5/100/1 ratio): High temperature application

The first series of tests would be run on system A with S-glass fibers. This combination was selected to complement the data already generated for the DOE flywheel program. It was decided that the fiber direction would be [0/90 ± 45], because the results would be most useful regardless of the method which would be selected to manufacture the flywheel. In the application the fiber direction would be selected depending on the anticipated stress produced in operation. Therefore the fiber direction selected would not be the optimum direction for properties but would probably be lower than that selected for the application.

TYPICAL RESULTS

The first series of creep tests are being run in the atmosphere controlled enclosure, in air, at 75°F (238°C) and the relative humidity at 8.0% ± 2.0%.

The ultimate tensile strength was found to be 126.5 MPa (25.6 ksi) and the stress applied for the testing was 41.1 MPa (5.96 ksi). Typical results are shown in Figure 6 plotted as elongation in microns/mm as a function of time. As with the original tests used to evaluate the probe, test rig arrangement, the results show a continuous increase in length for the first 120 hours. At that time, there is a leveling trend for the remainder of the time shown. The first set of readings were taken one hour after the load was applied in order to obtain consistent values. There is a continuous increase in length after the load was applied which will not allow static readings to be taken with any consistency. Hence, readings were not reported which were taken within the first hour of testing.

The change in length for the six test specimens is between 1.5 μm/mm and 3.8 μm/mm overall. When considering the gage length 76 mm, the actual percentage difference is .003%.

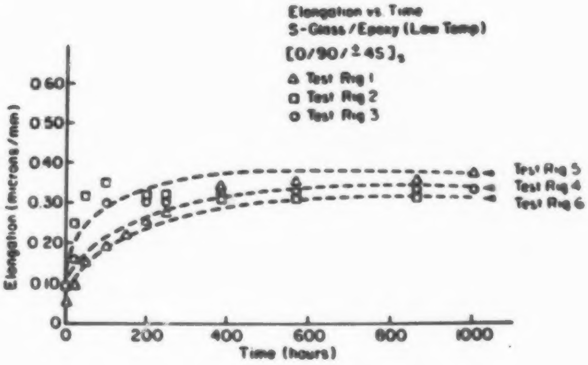

Figure 6 Effect of Time on the Deformation of Epoxy System A and S-Glass Fibers

When examining the trends in Figure 6, it is evident that the changes in length have all leveled off at between .2 and .35 μm/mm. The specimen in test rig No.6 gave the only unusual results for the first part of the test, however, it too leveled out at a value of .25 μm/mm.

At the present time a total of 12 duplicate tests were run for different lengths of time up to 3000 hours. They all fall into the same curve as seen in Figure 6. At higher stress levels, the results show a similar trend, except that the values fall in a range of between .7 and 1.4 μm/mm after 1100 hours. Tests run in vacuum at 10^{-4} torr under the same conditions do not appear to give the same results at this point but only 400 hours have been accumulated.

Before and after each set, tensile tests were run to determine the change in strength due to long time deformation under load. Each specimen is examined under the scanning electron microscope (SEM) to study the visual changes in structure.

Figures 7 and 8 show SEM photomicrographs of the material and the fibers near the fracture.

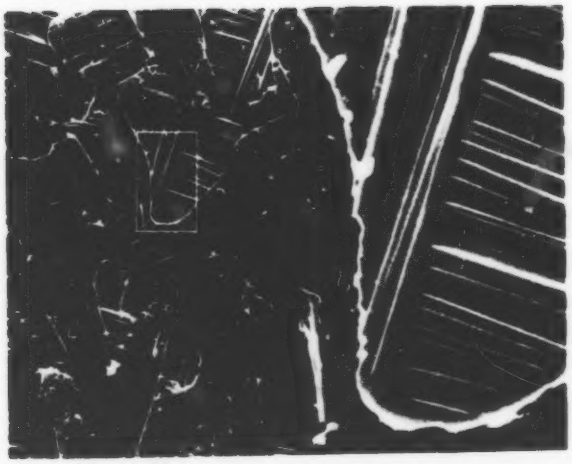

40 × mag

200 × mag

Figure 7 Typical SEM Photomicrograph of Composite Material Matrix after Exposure to Long-Term Loading

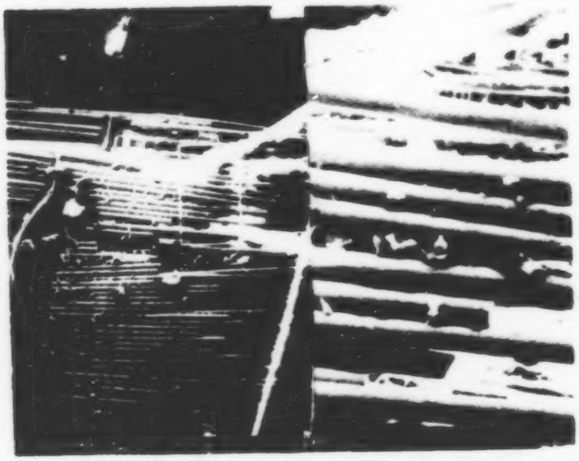

100 × mag

500 × mag

Figure 8 Typical SEM Photomicrograph of Composite Material Fibers after Exposure to Long-Term Loading

CONTINUED TESTING

At this point there does not appear to be significant difference between air and vacuum testing.

Additional tests will be performed in Helium. If neither environment shows a significant difference when compared to air, all additional tests will be performed in air at controlled temperature and relative humidity.

Hence, a family of curves will be generated for each composite system under various temperatures and in the environment which is considered important to the successful characterization of creep properties for the flywheel application.

As more long-term data is made available, attempts will be made to predict composite material characteristics for long-term loading by using short-term tests.

CONCLUSIONS

The capability to determine the long-term creep characteristics of composite materials in a flywheel environment has been developed. It is important to determine the changes in material properties for composite materials in order to establish a confidence level for a flywheel which will be subjected to long-term usage.

It may be found that additional testing can be performed in air which would eliminate the need for environment chamber testing. This could result in:

1. A considerable reduction in cost for future testing
2. Allow available data to be more meaningful for flywheel applications.

REFERENCES

1. Annual Book of ASTM Standards, D2990, 1977.
2. Annual Book of ASTM Standards, D3039, 1980.
3. Chiao, T.T., "Fiber Composite Materials Development for Flywheel Application," 1980 Flywheel Technology Symposium, co-sponsored by US DOE, ASME and ILL Conference, 801022, October 1980.

PROJECT SUMMARY

Project Title: Flywheel Housing Design-Concept Development

Principal Investigator: Anthony P. Coppa

Organization:
General Electric Company
Energy Systems Programs Department
Valley Forge Space Center
Box 8555, Philadelphia, Pa. 19101

Project Status: The project has been completed and the final report (draft) has been submitted.

A low cost flywheel housing conceptual design, which provides for containment, vacuum support, torque transfer limitation, and access for inspection and maintenance has been developed. The design is based on utilizing mass production sheet metal forming processes to obtain a rugged housing structure that is both energy and weight efficient in its performance in a flywheel system. Estimated cost of the housing for use with 0.25 kw. hr General Electric hybrid type rotors having outside diameters of 15 and 18 in. are approximately \$50 and \$58 respectively including containment ring and based on a one-year production quantity of 10^6 units. For the same rotors, estimated combined energy densities including rotor, housing, containment ring, and vehicle mounting ring are 3.82 and 3.34 whr/lb or 8.43 and 7.37 whr/lb respectively.

Containment requirements for the housing have been determined by means of a new design method that was developed under this program. The method, called the crushing fragment containment analysis has been correlated with containment test data that pertain to a variety of rotor constructions. The analysis considers rotor fragmentation as undergoing a progressive crushing process which ameliorates the loading imposed on the containment structure relative to rigid fragment actions. This has resulted in prediction of substantially reduced containment ring weights compared to previous design methods.

Important effects of fragmentation debris activity within the housing were considered in the housing design. Means were provided to inhibit the accumulation of debris in critical areas, and thereby limit to permissable levels the resulting loads that can be transmitted to the housing and vehicle.

Housing force and torque reactions that are produced by a loose rotor spinning within it were also determined. For typically small rotor running clearances, these reactions were found to be well within the housing strength capability.

Contract Number: Subcontract No. 6624409

Contract Period: September, 1980 to September, 1981

Funding Level: \$100,000

Funding Source: U.S. Department of Energy through Lawrence Livermore National Laboratory

FLYWHEEL HOUSING
DESIGN-CONCEPT DEVELOPMENT

Anthony P. Coppa
General Electric Company
Energy Systems Programs Department
Box 8555, Philadelphia, Pa. 19101

ABSTRACT

A new method for determining burst-containment requirements for composite rotors has been developed. Its important feature is the consideration of rotor fragments whose containment action is limited by their strength. This method has been applied to developing a low-cost flywheel housing that contributes to good combined housing/rotor weight and energy performance.

INTRODUCTION

Prior to commencement of the present program, containment rings were designed, fabricated, and furnished to the Union Carbide Y-12 Flywheel Evaluation Test Facility for use in prototype flywheel rotor tests (Reference 1). Four of these rings consisted of an aluminum metal liner that was overwrapped by many turns of Kevlar 29 fabric. These were designed for use with four different rotors whose major energy storage portions were of circumferentially wound construction. The remaining two rings were made of high strength low alloy steel and were applied to tests of relatively narrow, disk type rotors.

Of the six rotors tested, one burst within the containment ring, another burst at relatively low speed prior to installation of the ring, and the remaining four either failed in a non-catastrophic manner or had to be shut down before failure due to excessive vibration. As a result, little containment data were obtained. However, the efforts to design the rings for a variety of rotor constructions contributed much to the later development of containment design methods for composite rotors.

The main objective of the present program was to develop design concepts for practical, low weight and low cost vehicular flywheel housings. The program was organized into four major tasks:

Task 1 - Assessment of Flywheel Containment Tests.

Task 2 - Containment Design Method Development.

Task 3 - Design Concept Development

Task 4 - Parametric Design Assessment.

These tasks were designed with the awareness that to develop efficient flywheel housing designs, it would be necessary: (1) to improve the understanding of composite containment processes, and (2) to develop design methods that could account for the features of composite fragment action which reduce their damage potential relative to rigid, metallic fragment actions.

This paper is a summary of the final report (draft) that has been submitted (Reference 2) on Subcontract No. 6624409. The program was sponsored by the U.S. Department of Energy through the Lawrence Livermore National Laboratory; Dr. S. V. Kulkarni was the LLNL Project Engineer.

HOUSING DESIGN REQUIREMENTS

Among the requirements which the flywheel housing design must satisfy are the following:

1. Containment of Rotor Failure
    a. Rotor Burst
    b. Debris Management
    c. Limitation of Reactions Transferred to the Vehicle
    d. Loose Rotor Control

2. Vacuum Support
3. Safe Response to Vehicle Collision
4. Overall Structural Reliability
5. Noise Suppression

Of these requirements, the response of the housing to rotor burst presents the most challenge to the designer. Hence primary attention was given to developing a design methodology for composite rotor containment.

APPROACH

The approach taken was to study the results of previous burst tests of composite rotors in which measureable damage was produced in a containment structure, and then to incorporate salient features of the processes in an appropriate design analysis. Results obtained from tests performed at the Johns Hopkins Applied Physics Laboratory (APL) were found especially useful because the rotors released a substantial and defined amount of fragmentation within containment rings that were not excessively massive. The result was that the rings were substantially deformed in the more severe bursts while in the less severe ones, although not detectably deformed, they permitted deduction of an upper bound of containment process severity.

The APL tests are listed in Table 1 and involved a variety of rotor material, constructions, and failure modes. The associated test data served both to provide insight and guidance to the analysis development and as a data base against which to compare analytical predictions. The test results, however, were limited to direct burst-containment effects since the rotor housings did not have closed ends. Also, the radial clearances present were much larger than would be used in operating systems. These limitations, which are common to most available rotor burst tests, were considered throughout the analysis development effort, but did not diminish the usefulness of the data with regard to the burst-containment problem.

Table 1. Description of Flywheel Rotors Involved in the Data Correlation (Ref. 3)

Rotor Description	d_o in.	W_R lb.	KE_B kw.hr.	ω_B rpm.	Failure Mode	W_F lb.
Hybrid Rotor: FW Graphite/Epoxy Outer Ring; Laminated S-2 Glass/Epoxy Disk (General Electric)	17.68	23.3	0.459	35,040	Outer Ring Rupture	6.34
Disk Rotor: Laminated S-2 Glass/Epoxy Disk (LLNL)	15.00	5.2	0.156	49,320	Complete Disk Burst	5.2
Hybrid Rotor: FW Graphite/Epoxy Outer Ring; Molded Chopped Glass/SMC Disk (Owens Corning)	24.00	28.5	0.414	21,620	Complete Burst of Rim and Disk	28.5
Wound-Rim Rotor: FW Kevlar 49/Epoxy, Glass/Epoxy (Brobeck)	13.76	24.5	0.608	48,120	Rupture and release of 70% of Kevlar 49/Epoxy Rim	6.76
Disk Rotor: Varying Thickness, Laminated Graphite/Epoxy	24.00	11.8	0.306	34,940	Complete Disk Burst	11.8

d_o, OD, W_R, rotor weight; KE_B, energy at burst, ω_B, burst speed, W_F, fragment weight.

CRUSHING FRAGMENT CONTAINMENT ANALYSIS

In contrast to metallic fragment containment interactions which involve interface pressures that can greatly exceed bearing yield stresses, the pressures which composite fragments can produce are limited by their relatively low transverse strength. This applies to both filament wound rim as well as laminated disk rotor constructions. When the pressures induced in the fragment bulk during the containment process exceed the transverse strength, the matrix will break up, thereby releasing fibers or ribbons of fibers in filament wound construction or local crushing and delamination in laminated disk construction. Rapid heating due to high pressure, high velocity sliding along the containment surface also contributes to the break-up process. In some constructions, the fragments may already be in a highly broken state prior to impact.

Since the fragments are basically solid, as opposed to porous, bodies, such action must be accompanied by the forcible ejection of material laterally from the fragment as the remaining fragment moves radially against the containment structure. If the transverse strength is low, the fragment may continue this motion until its mass is expended. If the strength is high, however, the ejected mass will be appropriately less and a substantial portion of the original fragment will remain after its radial velocity relative to the containment surface has vanished. Such residual fragments will continue their tangential motion after this time and exert centrifugal pressures against the containment ring.

An analysis, called the crushing fragment containment analysis (CFCA) was developed to calculate the containment ring response to such a loading process and is described in detail in Reference 2. Only a brief account is given here in order to provide a basis for describing the calculated results.

The released rotor fragmentation is transferred from its original position in the intact rotor into uniformly distributed contact with the containment ring surface. From this point onward, interaction with the containment ring occurs. The interaction geometry is illustrated in Figure 1 which shows how the fragment proceeds to move into the ring. The initial state of the fragment is indicated by its bounding radii R_I and r_{iI}, thickness a_I, and centroid position r_I. The initial total, radial and angular velocities are V_o, $\dot{r}_I$, and ω_I respectively. These same quantities apply everywhere around the circumference since the fragment geometry and motion are considered to be axially symmetric. The various dashed lines indicate the trajectories of the fragment inner surface and mass center and the containment ring as time progresses. At a general instant, the fragment thickness is shown as having a centroidal radius, r, thickness, a, angular speed, ω, and total and radial speeds V and $\dot{r}$. It is noted that although V is always less than V_o, the radial speed may increase above the initial radial speed (as shown in Figure 1) for a while. The final state of the fragment is depicted by the residual thickness, a_p, at the point where its radial velocity equilibrates with that of the containment ring.

The motion of the entire fragment is therefore characterized by that of the general mass center, m, whose (variable) magnitude per unit circumference $2\pi r$ is:

$$m = 2\,\rho_F h(R-r), \tag{1}$$

where ρ_F is the distributed fragment density. The equations of motion of the fragment and containment ring are:

$$\text{Fragment:}\quad \ddot{r} + \left(\frac{\dot{R}-\dot{r}}{m}\right)\dot{m} = \frac{H^2}{r^3} - \frac{p_o h}{m} \tag{2}$$

$$\text{Ring:}\quad \ddot{R} = \frac{2\pi}{M_C}\left[(\dot{R} - \dot{r})\,\dot{m}r + p_o\,hr - \sigma_D T L_c\right] \tag{3}$$

where the single and double dots indicate first and second time derivatives respectively; $H = \omega r^2 =$ constant, p_o, fragment crushing strength; h, rotor axial length; σ_D, dynamic tensile strength of ring; T, ring thickness; and M_c and L_c, the effective mass and length of the ring. Hence, the fragment is treated as a variable mass which transfers momentum loads, $(\dot{R}-\dot{r})\dot{m}$ and pressure loads, $p_o h$ (both per unit circumference) to the containment ring. The ring resists these loads by its plastic tensile resistance, $\sigma_D T L_c$.

The initial conditions are:

$$\begin{aligned} &\text{Fragment:}\quad r(o) = r_I,\ \dot{r}(o) = V_{R_o} \\ &\text{Ring:}\quad R(o) = R_I,\ \dot{R}(o) = o \end{aligned} \tag{4}$$

During the ensuing process, the condition $\dot{r}_p = \dot{R}_p = V_{R_p}$ is reached, at which time and thereafter, the fragment is considered to be rigid. Subsequently, the fragment continues moving circumferentially at angular velocity ω_p and exerting centrifugal pressure loading on the ring:

$$p = \frac{m_p(\omega_p r_p)^2}{R_p h} \tag{5}$$

During this time the radial motion of both fragment and ring is governed by:

$$\ddot{R} = \frac{2\pi}{(m_c + M_p)}\left|p_p h r_p - \sigma_D T L_c\right| \tag{6}$$

where $M_p = 2\pi\, r_p m_p$.

BEST DOCUMENT AVAILABLE

For present purposes, equation (6) was solved assuming the bracket term to be constant. Although not necessary to do this, it is conservative and it was convenient to do so. Hence the final time at which the radial velocity ceases is:

$$t_f = t_p + \left(\frac{M_C + M_p}{2\pi}\right) \left[\frac{V_{R_p}}{\sigma_D T L_c - p_p h r_p}\right] \qquad (7)$$

and the maximum radial deflection of the ring is:

$$\Delta R_{max} = R_p - R_I + \frac{1}{2} V_{R_p} (t_f - t_p)$$

CFCA has yielded some very interesting features of containment processes of composite rotors, features which appear plausible, especially when compared to experimental evidence of fragmentation as obtained for rotors of various constructions. The following results illustrate some of these features.

Figures 2 and 3 show plots of r, $\dot{r}$, R, and $\dot{R}$ vs. time for the complete burst of a 0.25 kw.hr laminated glass/epoxy disk rotor, the principal difference being the fragment strength and ring thickness values: $p_o = 0$ and T = 0.22 in. (Figure 2) and $p_o = 12$ ksi and T = 0.35 in. (Figure 3). In each case, $\dot{r} = 3847$ in/sec. initially (which corresponds to an initial radial clearance, c = 0.25 in.) and subsequently rises to a peak value. The peak value of $\dot{r}$ is larger for $p_o = 0$ and occurs at a later time than for $p_o = 12$ ksi. Also, r approaches closer to R for $p_o = 0$ such that at the equilibration condition, $\dot{r} = \dot{R} = V_{R_p}$, the residual fragment thickness (a = 2(R-r)) is much smaller than that of the stronger fragment. This is typical of fragment behavior as revealed by CFCA. It is noted that even though $p_o = 0$, substantial deformation is produced in the ring. This, of course, is attributable to the fragment momentum loading.

Another interesting result is to show that fragments having low strength can transmit substantial deformation to the ring even when the initial radial clearance is zero. An example is illustrated in Figure 4, which pertains to the same conditions as the previous figures except $p_o = 6$ ksi, T = 0.24 in., and c = 0. Here $\dot{r}$ is initially zero (because of the zero clearance) but rises to a peak value of 4,870 in/sec. $\dot{R}$ remains at zero for the first 200 μsec. and rises thereafter to a peak value of 1,570 in/sec., almost as high for the case shown in Figure 2. The maximum ring deflection, ΔR = 0.62 in., compared to 0.60 in. (Figure 2). Since for these two cases, the ring thicknesses, T, are almost identical, it is seen that the effect of the higher fragment strength tends to be offset by the smaller clearance value.

CFCA has been successfully used to analyze the behavior of a variety of rotor configurations. When applied to the tests listed in Table 1, it permitted deduction of values of p_o for laminated glass/epoxy disk type rotors and filament wound rim type rotors of graphite/epoxy and Kevlar 49/epoxy materials. Also a procedure was devised to determine containment requirements for complete hybrid rotor bursts. Details are discussed in Reference 2.

Figure 5 shows containment weight requirements for the complete burst of a simple laminated glass/epoxy disk rotor for several ring materials, including a promising concept that uses an aluminum liner overwound by Kevlar 29 yarn. Figure 6 gives similar requirements for the complete burst of a family of General Electric hybrid disk rotors for 1/4 hard, 4130 steel rings. Requirements for the hybrid rotors include containment of the filament wound graphite/epoxy ring and the laminated glass/epoxy disk components.

Other containment considerations such as loose-rotor reactions, limitation of transferred reactions, and debris management as well as other previously listed requirements are discussed in detail in Reference 2 and have been factored into the housing design concept.

HOUSING CONCEPTUAL DESIGN DESCRIPTION

The housing conceptual design as applied to an 18 in. OD 0.25 kw.hr rotor is shown in Figure 7. It consists of two almost identical welded steel subassemblies that are bolted together, as shown in Figure 1b and 1c. Each subassembly is composed of a stamped shell with integral stiffeners, shown in plan view in Figure 1a and a cover plate. The wall thicknesses of the shell and cover plate are each 0.075 in. The containment ring is located and supported on 24 beveled ends of the convoluted stiffeners as shown in the figure. The ring will rotate relative to the housing when an applied torque exceeds the torque due to frictional resistance at the beveled supports.

The housing is mounted to the vehicle at each of its two ends. When mounted the termination of the housing subassembly on the rotor shaft end of the housing is clamped between two heavy steel members, namely the housing mounting ring and the vehicle attachment flange. At the opposite end, the housing is attached to a vehicle bracket (not shown) by means of a central support rod. These details are best seen in Figure 1c. Both of these mounts permit the entire housing to rotate relative to the vehicle when an applied torque exceeds the combined frictional resistance of the two mounts and the shear resistance of the small screws. This feature is illustrated in Figure 8, in which an applied torque, due to containment action, is indicated by the large dashed arrow and the torque delivered to the vehicle by the smaller solid and dashed arrows. Hence, the maximum torque that can be transferred to the vehicle is limited, essentially, to the combined frictional resistance of the housing mounts. Such resistance can be controlled with low friction coatings on sliding surfaces.

The housing is sealed against air leakage by three O-rings; one in the bolted closure flange, and two in the housing support ring. The bolted closure facilitates assembly, disassembly, inspection and maintenance procedures.

The housing design can accommodate a variety of containment rings and, hence, can be used to house rotors having different energy levels or fragmentation modes. Examples of efficient containment ring sections which can be produced at low cost by roll-forming are shown in Figure 9.

HOUSING PERFORMANCE AND COST

The total weight and energy density of the flywheel systems incorporating such housings and including the weights of the rotor, containment ring, and vehicle attachment ring are within the allowances that were set by the vehicle integration study. The combined system weights and energy densities, including rotor, housing, containment rings, and vehicle mounting ring for two different 0.25 Kw.hr rotor sizes are given in Table 2.

Table 2. Rotor/Housing System Performance

Performance Indices	Rotor OD, in.	
	15	18
System Weight, lb.	65.4	74.8
System Energy/Weight, whr/lb.	3.82	3.34
whr/kg.	8.43	7.37
System Energy/Volume, whr/ft^3	460	387

In all these respects, the smaller diameter rotor offers higher performance.

Cost of the housing system, based on budgetary price quotations (Reference 4) for a production rate of 10^6 units per year are (including hardened steel containment rings and tooling):

Housing for 15 in. OD, 0.25 kw. hr rotor:	$50.23
Housing for 18 in. OD, 0.25 kw. hr. rotor:	$57.61

The above estimates are based on a welded flange closure detail. The low costs result directly from the application of economical and proven mass production sheet metal forming techniques and a minimum number of component parts.

SUMMARY OF DESIGN FEATURES AND ADVANTAGES

Key features and advantages of the housing conceptual design described herein are summarized as follows:

1. Low Cost. $50.23 for 15 in. OD rotor size and $57.61 for 18 in. OD rotor size in quantities of 10^6 units/year.
2. Standard Rotor Housing. It can be used with a variety of rotors having a standard diameter but different axial lengths, energy capacity and failure modes. This is due to housing ruggedness and ability to accommodate light, moderate and heavy containment rings.
3. Torque Transfer Control. Torques applied to the containment ring and/or housing shell by containment action will cause ring and housing rotation once the housing mount friction torque is exceeded. Hence, torques that are transmitted to the vehicle are not likely to exceed the designed mount friction torque.

4. Loose Rotor Reaction Control. As shown by analysis, force and torque reactions are limited to small values by permitting the ring and housing limited rotational freedom.

5. Debris Management. Convoluted housing wall design, containment ring mounting arrangement, and enclosed annular chamber outboard of the containment ring allow initial debris to escape the vicinity of the fragmenting rotor/ring interface. Debris can move into the annular chamber or spaces between convolutions. This feature inhibits formation of "wedges" in the radial clearance space.

6. Containment Ring Expansion Freedom. The containment ring is free to expand radially during the containment process, thereby undergoing greater and more uniform plastic stretching. This requires a lower weight ring.

7. Protection Against Ring Jamming. If the ring should become bound and lose its freedom to rotate during containment, the resulting torques applied to the housing via the bound ring will be limited by the housing mount friction torque.

8. Containment Ring Cushioning. Movement of debris into the outer chamber should provide substantial isolation of the containment ring and prevent damaging metal-to-metal contacts with the housing during heavy containment action.

9. Ruggedness. Welded, double wall construction renders the housing with substantial ruggedness and abuse resistance.

10. Access to Housing Interior. Bolted closure enables routine opening and closing of the housing for maintenance, inspection and rotor replacement procedures.

11. Acceptable Weight. The housing weight is acceptable and contributes to satisfying the vehicle integration study goal of a combined housing, containment, rotor and mounting weight of 80 lb. for a 0.25 kw.hr. energy storage system.

ACKNOWLEDGEMENT

The author gratefully acknowledges the following individuals for the valuable contributions they made to this program. Dr. Satish Kulkarni, Technical Manager, Rotor and Containment Technology Task, MEST Project, Lawrence Livermore National Laboratory, Dr. Carl H. Zweben, Technical Staff Engineer and Dr. B. T. Rodini, Technical Staff Engineer, General Electric Company Space System Division, Mr. E. L. Gray, Mathematician, General Electric Company Space System Division, Dr. C. H. Marston, Manager, MHD Systems and Analysis, General Electric Company Energy Systems Programs Department, Mr. W.E. Good, Chief Engineer, Heintz Division, Kelsey-Hayes Company, Messrs. D. Rabenhorst and W. Wilkinson, respectively, Director and Test Engineer of the Johns Hopkins University Applied Physics Laboratory Flywheel Test Facility, Dr. R. S. Steele, Jr., Supervisor of the Union Carbide Corporation Y-12 Flywheel Evaluation Test Facility, Dr. R. P. Nimmer and Mr. D. Kerr of the General Electric Corporation Research and Development Center, and Mr. J. Lawson of the Garrett Corporation, AiResearch Manufacturing Company.

REFERENCES

1. Coppa, A.P., "Design of Containment Rings for Use in Tests of Six Prototype Flywheel Rotors," General Electric Company, Energy Systems Programs Department Report prepared for Lawrence Livermore Laboratory, Subcontract 6624409, February 1981.

2. Coppa, A.P., "Energy Storage Flywheel Housing Design Concept Development," General Electric Company, Report No. 81SDS4225 (Final Report; Tasks 7-11, Subcontract No. 6624409), August 1981.

3. Rabenhorst D. and Wilkinson, W., Johns Hopkins University Applied Physics Laboratory (Private Communication), February 1981.

4. Budgetary Quotation, Flywheel Housing Conceptual Design, reference P/N 1217-448, Heintz Division, Kelsey-Hayes Company, received July 16, 1981.

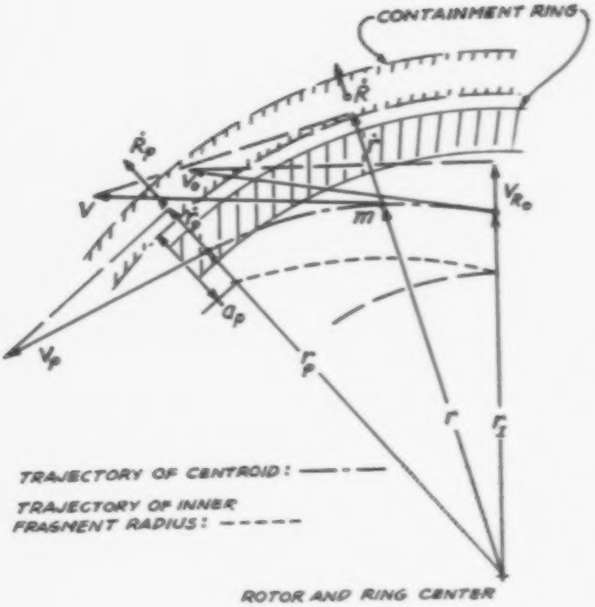
CONTAINMENT RING
$\dot{R}$
$\dot{R}_p$
$\dot{r}$
V
V_o
V_{Ro}
$\dot{r}_p$
m
a_p
V_p
r_p
r
r_i
TRAJECTORY OF CENTROID: — - —
TRAJECTORY OF INNER FRAGMENT RADIUS: - - - - -
ROTOR AND RING CENTER

Figure 1. Crushing Fragment Interaction Schematic

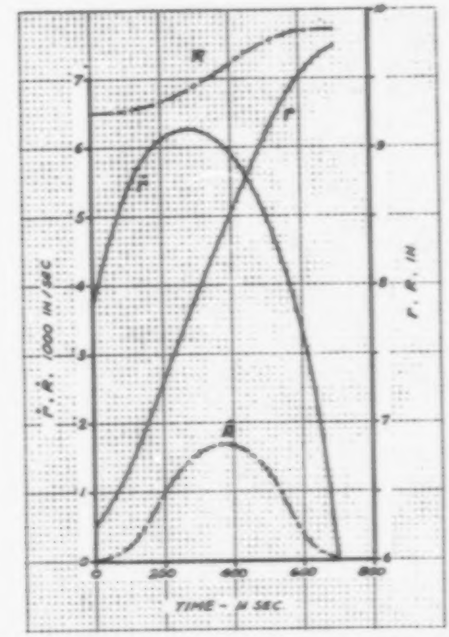

Figure 2. Calculated Fragment and Containment Ring Motions vs. Time for Complete Burst of a 0.25 kw.hr Laminated Glass/Epoxy Disk Rotor. $p_o = 0$; $\sigma_D = 158$ ksi; T=0.22 in; 1/4 Hard, 4130 Steel Ring.

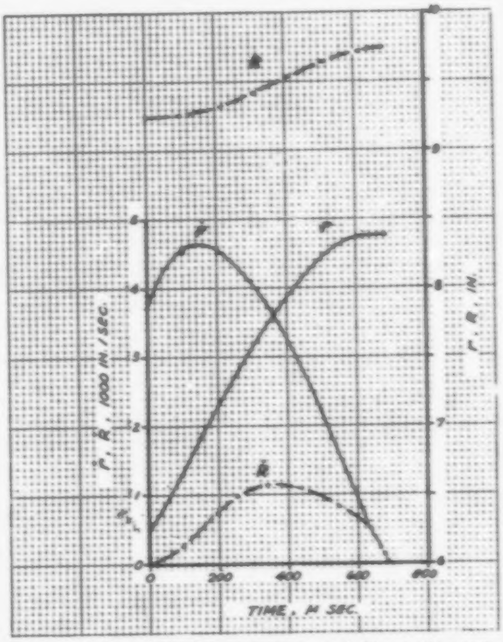

Figure 3. Calculated Fragment and Containment Ring Motions vs. Time for Complete Burst of a 0.25 kw.hr Laminated Glass/Epoxy Disk Rotor. $p_o = 12$ ksi; $\sigma_D = 158$ ksi; T = 0.35 in; 1/4 Hard, 4130 Steel Ring.

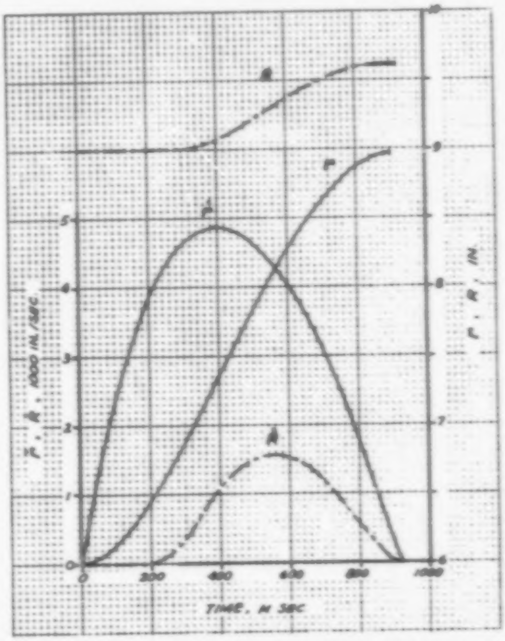

Figure 4. Calculated Fragment and Containment Ring Motions vs. Time for Complete Burst of a 0.25 kw.hr Laminated Glass/Epoxy Disk Rotor. $p_o = 6$ ksi; $\sigma_D = 158$ ksi; T = 0.24 in; 1/4 Hard 4130 Steel Ring.

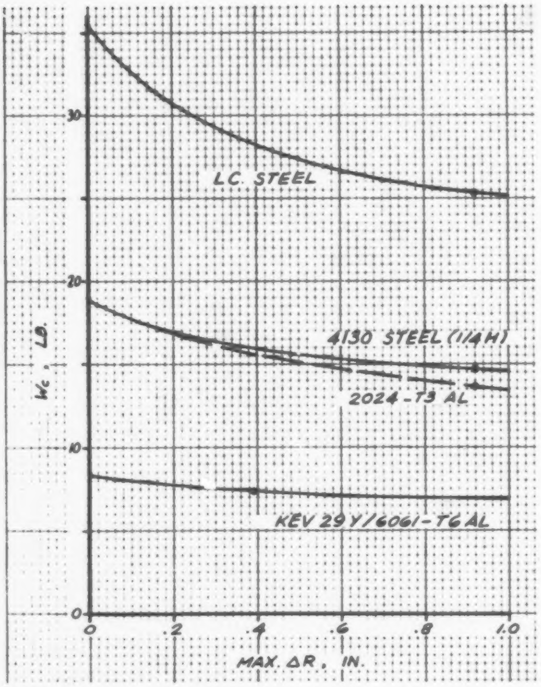

Figure 5. Containment Design Curves: W_c vs. ΔR_{max} for Complete Burst of an 18 in. OD 0.25 kw.hr GE Disk Rotor; p_{OD} = 6 ksi; for Several Containment Ring Materials

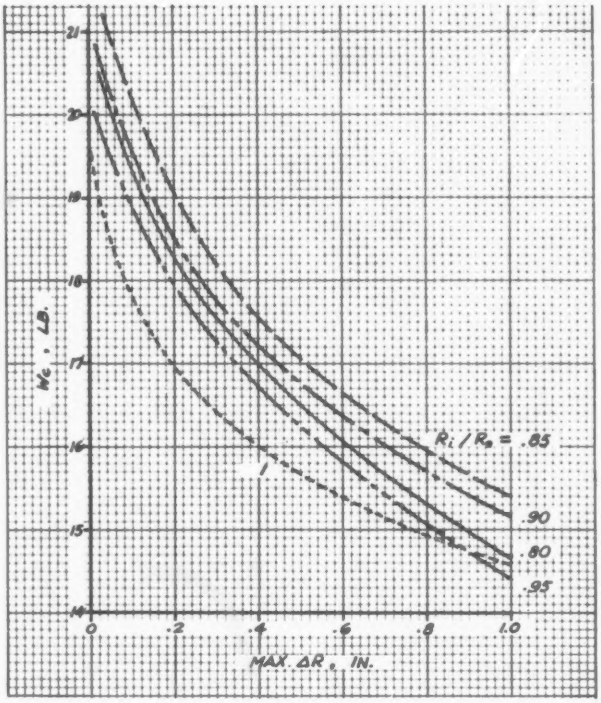

Figure 6. Containment Design Curves: W_c vs ΔR_{max} for Complete Burst of 18 in. OD, 0.25 kw.hr GE type Hybrid Rotors. p_{OR} = 20 ksi; p_{OD} = 6 ksi; σ_D = 158 ksi; ¼ Hard 4130 Steel Ring

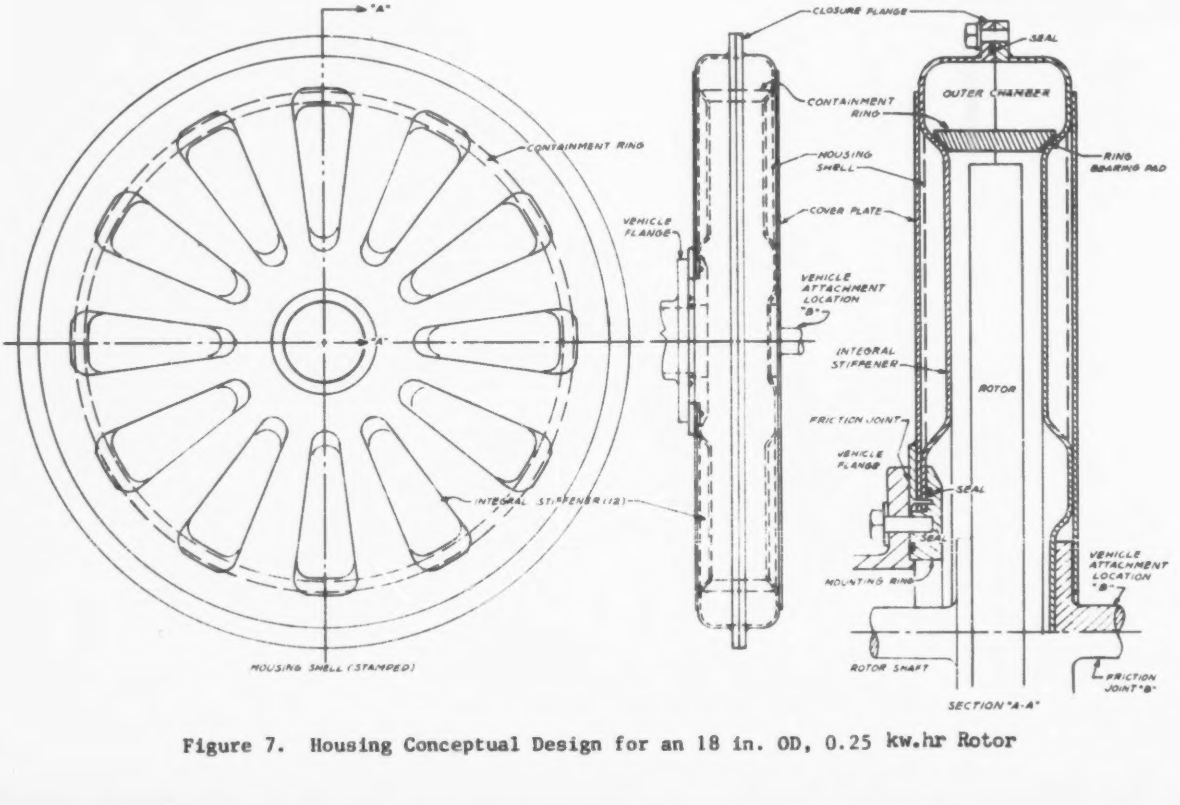
"A"
CONTAINMENT RING
"A"
INTEGRAL STIFFENER (12)
HOUSING SHELL (STAMPED)
CLOSURE FLANGE
CONTAINMENT RING
HOUSING SHELL
COVER PLATE
VEHICLE FLANGE
VEHICLE ATTACHMENT LOCATION "B"
SEAL
OUTER CHAMBER
RING BEARING PAD
INTEGRAL STIFFENER
ROTOR
FRICTION JOINT
VEHICLE FLANGE
SEAL
SEAL
MOUNTING RING
VEHICLE ATTACHMENT LOCATION "B"
ROTOR SHAFT
FRICTION JOINT "B"
SECTION "A-A"

Figure 7. Housing Conceptual Design for an 18 in. OD, 0.25 kw.hr Rotor

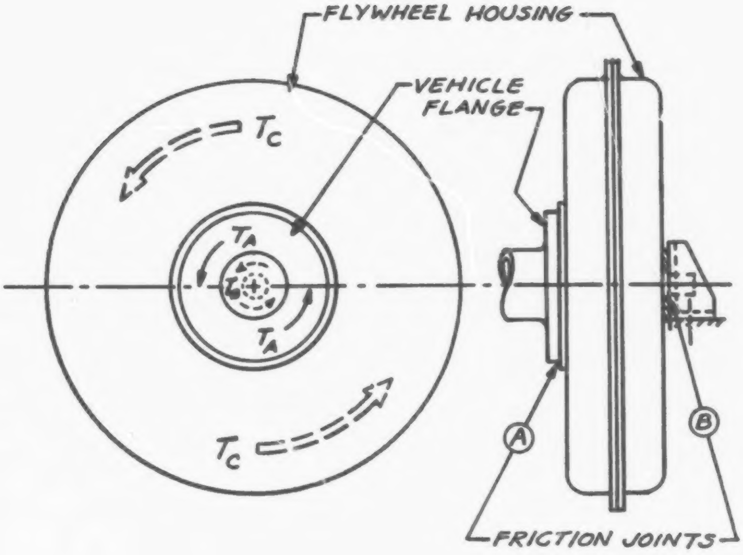
FLYWHEEL HOUSING
VEHICLE FLANGE
T_C
T_A
T_A
T_C
A
B
FRICTION JOINTS

T_C, CONTAINMENT APPLIED TORQUE

T_A, T_B, TORQUES TRANSMITTED TO VEHICLE

Figure 8. Built-In Torque Limiting Feature

PROJECT SUMMARY

Project Title:	Composite Flywheel Burst Containment
Principal Investigators:	Alan D. Sapowith, William E. Handy
Organization:	Avco Systems Division 201 Lowell Street Wilmington, Massachuetts 01887 (617) 657-2449
Project Goals:	Develop designs and design data pertaining to burst containment of composite flywheels.
Project Status:	This effort is completed. Basic design approaches and design data have been developed. Recommendations for follow-on efforts have been made.
Contract Number:	LLNL Subcontract 1121401
Contract Period:	August 1980 to August 1981
Funding Level:	$99,301
Funding Source:	U.S. Department of Energy through Lawrence Livermore Laboratories.

COMPOSITE FLYWHEEL BURST CONTAINMENT

Alan D. Sapowith
William E. Handy
Avco Systems Division
Wilmington, Massachusetts

ABSTRACT

This program develops containment designs and design data applicable to the burst containment of composite flywheels. Two approaches are discussed. The first is conventional in that it addresses containment of the linear and rotational kinetic energy of burst fragments. The second approach is unconventional in that it proposes to use initial flywheel radial growth at failure to expand into the containment ring. The resulting frictional forces stop the flywheel in seconds so that all kinetic energy is absorbed rotationally.

INTRODUCTION

This work constitutes a follow-on effort from the state-of-the-art review of burst containment conducted under LLNL subcontract 6692009. The objectives here were to develop design configurations and design data for burst containment of composite flywheels.

The flywheels considered were the three leading types of designs depicted in Fig. 1: the disk flywheel, disk with rim, and the subcircular flywheel. Designs with these configurations were scaled to 1 kWh total energy at burst. The closest actual flywheel to the 1-kWh energy level was a 34.2-lb Garrett subcircular wheel. To evaluate the several designs equitably, the same weight was applied for all designs.

Two parallel design approaches were taken. The conventional method considered the containment of flywheel burst fragments in a manner similar to that of burst containment of steel aircraft turbine blades. The second (unconventional) method considered friction braking the flywheel on its rim to achieve a slowdown before flywheel fragmentation. This method appears to offer very lightweight containment designs.

DISCUSSION

Fragmentation Containment

To apply the extensive data available pertaining to the containment of steel turbine blades, an evaluation of the penetration potential of fiberglass and steel against steel targets and containment structures was made using a computer simulation based on test data.

The MIT Jet 4c program developed under an extensive NASA study for containment analysis was used to evaluate high-velocity impact test data generated during the state-of-the-art program. The impact data were used together with varying assumed values of effective width (EW) and coefficient of restitution (e). The output for each case was peak strain and resulting fragment velocity. It was assumed that penetration would occur if the strain exceeded the allowable target strain of 10 percent and the resultant fragment velocity was positive.

Figure 2, for fiberglass, shows a typical carpet plot of values for two ballistic tests. For A, a target thickness of 0.175 in., no test penetration occurred. Thus, the range of computed values of e and EW of interest lies above the $V_A=0$ line (computed velocities are negative) and to the right of the $e_A=0.10$ line, as the 10-percent strain was not reached. For B, where test penetration did occur, only velocities below $V_B=0$ and to the left of $e_B=0.10$ are of interest. The midpoint of the boxed-in area is chosen for the mean values of e and EW.

Improved estimates of these values can be made through analyses of more GO, NO-GO test data. However, to test our results, a hypothetical steel disk was analyzed using two separate and widely different analytical approaches. The first approach used the MIT Jet 4C program and the values of e and EW derived as before, based on steel-on-steel impact tests. The computed containment thickness was 3.8 in. The second approach used Avco Lycoming's S197 containment design program, which was developed empirically through the analyses and correlation of some 25 steel turbine burst tests. This method resulted in a thickness of 3.5 in. Similarly close results for deformation were achieved for the Johns Hopkins test 80-6, as shown in Fig. 3.

Having demonstrated the validity of the estimates for e and EW for steel and fiberglass fragments, the Jet 4c program was used to modify the Lycoming program for composite flywheels. The resulting composite design curve is shown with the steel turbine design curve in Fig. 4. Here again, additional data can be used to refine this curve.

Friction Braking Containment

Figure 5 shows slowdowns detected at failure for two typical disk flywheels, one fiberglass and one Kevlar. This slowdown has been attributed to flywheel growth (only inches per second) just before fragmentation. Because this growth is as large as 8 percent, if a small gap were employed between the flywheel rim and the containment ID, friction between the two would stop the wheel in seconds. Typical stopping time versus friction is shown in Fig. 6.

To absorb the resulting thermal energy, a ring of water extended polyester (WEP) is suggested as a brake shoe. Data on this material are shown in Table 1, together with weight and operating temperature estimates.

Table 2 summarizes the calculated containment weights required for a 1-kWh burst for each of the three flywheel designs. The fragmentation weight estimates are strongly dependent on failure mode assumptions. Figure 7 shows the suggested containment design options. Steel containment rings were found to be the most cost effective.

RECOMMENDATIONS

As a result of this study, the following recommendations are made. It should be noted that most, if not all, of the recommended test data to be gathered could be obtained simultaneously on each burst test.

1. All future flywheel tests should be specially instrumented to determine whether gaseous products are released at burst and, if so, their nature. Gas temperature, pressure, and composition should be determined to properly estimate their flammability and explosive potential.

2. If hazardous gases are produced, the effects of WEP material liners inside the containment wall on gas properties should be assessed.

3. Sidewall loads at burst should be measured. This can be done by measuring peak upward loads at failure on typical spindle tests.

4. High-speed (at least 128 frames/sec) photographs of the flywheel just before and through burst should be made to determine the size of gap needed to eliminate slow growth or jamming. These data will allow one to observe whether slow growth is duplicated and the size gap needed to take advantage of it. They should also allow one to detect changes in flywheel balance.

5. If slow growth exists as is indicated, the use of WEP materials should be investigated to measure slowdown data, resultant gas compositions and character, and torque applied to the containment wall.

6. In parallel with recommendation 5, WEP compositions should be tested in high-speed clutch testing facilities for friction coefficient or braking qualities, erosion versus applied pressure, and material temperatures.

7. Coiled stainless-steel containment rings should be tested with flywheel burst tests to help determine the safety margins of the present analysis. These tests could be augmented with high-velocity impact tests that simulate the mode of failure, materials, areal density, and containment wall design of each burst test.

8. As part of any flywheel development, tests should be conducted at operational speeds with representative imbalances to demonstrate the strength of the hub/axle connection to the flywheel. These tests are similar to those conducted for aircraft turbines and should be designed to eliminate hub failure considerations.

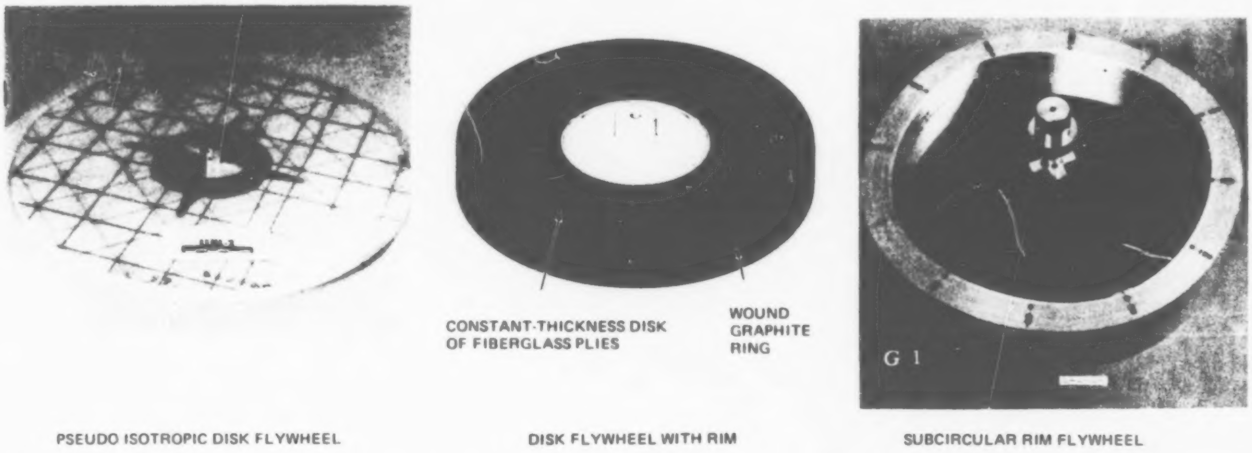
CONSTANT-THICKNESS DISK
OF FIBERGLASS PLIES
WOUND
GRAPHITE
RING
G 1
PSEUDO ISOTROPIC DISK FLYWHEEL
DISK FLYWHEEL WITH RIM
SUBCIRCULAR RIM FLYWHEEL
41 2523

Fig. 1. Composite Flywheel Design Types Evaluated for 1-kWh Burst Containment.

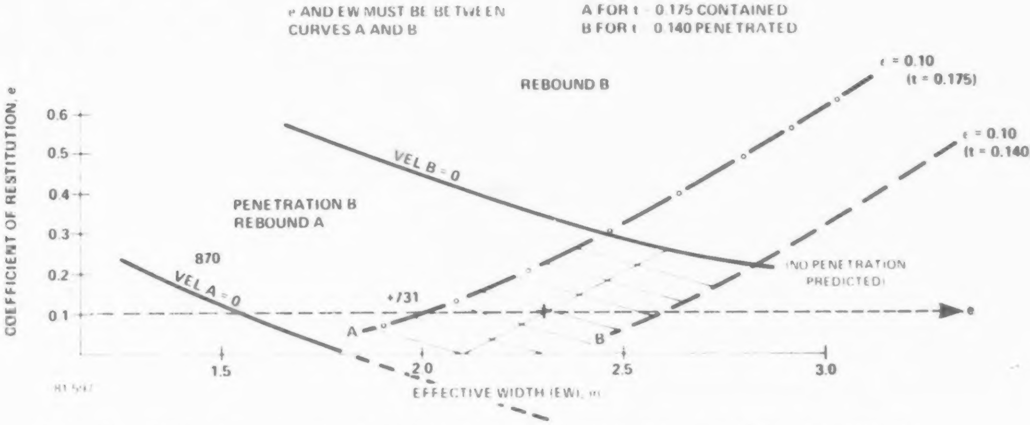

Fig. 2. Fiberglass on Steel Coefficient of Restitution and Effective Width.

CONTAINMENT RING DEFORMATION DATA

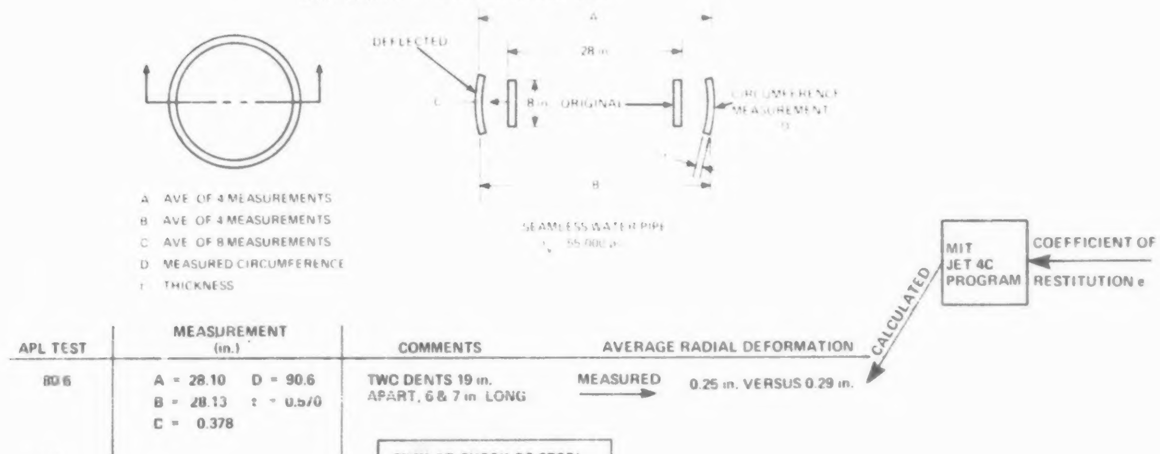
DEFLECTED
A
28 in.
C
8 in.
ORIGINAL
CIRCUMFERENCE
MEASUREMENT
D
t
B
SEAMLESS WATER PIPE
55,000 psi
MIT
JET 4C
PROGRAM
COEFFICIENT OF
RESTITUTION e
CALCULATED
MEASURED
41 2520

A AVE OF 4 MEASUREMENTS
B AVE OF 4 MEASUREMENTS
C AVE OF 8 MEASUREMENTS
D MEASURED CIRCUMFERENCE
t THICKNESS

APL TEST	MEASUREMENT (in.)	COMMENTS	AVERAGE RADIAL DEFORMATION
80.6	A = 28.10 D = 90.6 B = 28.13 t = 0.570 C = 0.378	TWO DENTS 19 in. APART, 6 & 7 in. LONG	0.25 in. VERSUS 0.29 in.

SIMILAR CHECK OF STEEL
AGAINST STEEL WITHIN 10%

Fig. 3. Check on Coefficient of Restitution.

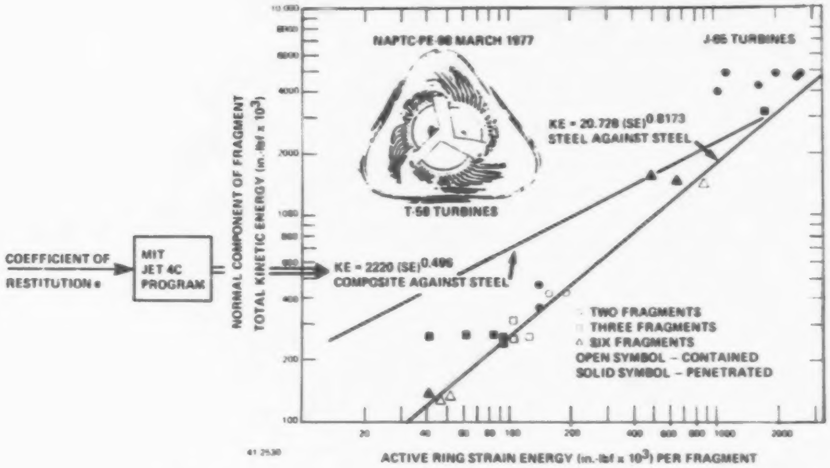

Fig. 4. Kinetic Energy Function Composite Against Steel and Steel Against Steel.

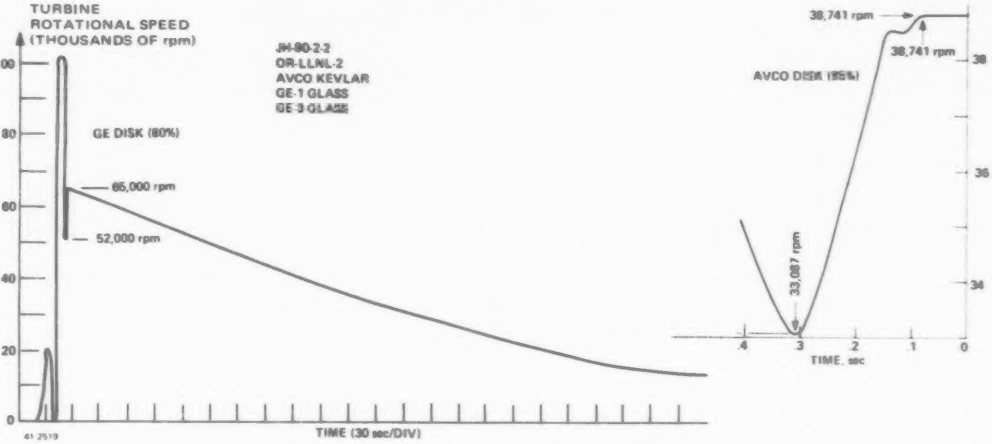

Fig. 5. Evidence of Slow Growth Failure Mode.

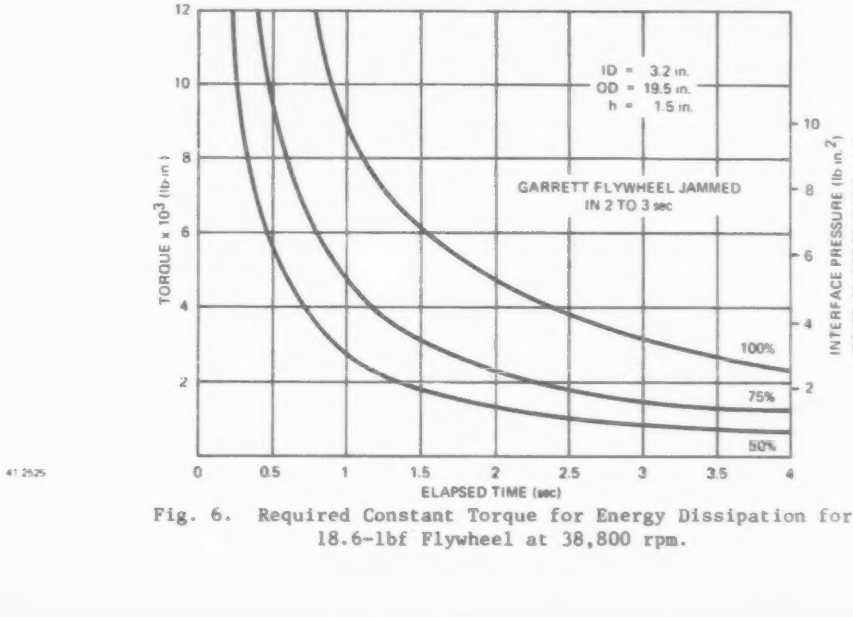

Fig. 6. Required Constant Torque for Energy Dissipation for 18.6-lbf Flywheel at 38,800 rpm.

Table 1.
Thermal Absorption Required, Water Extended
Polyester (WEP) Brake Shoe.

WEP PHYSICAL PROPERTIES (50% WATER)			
Flexural Strength		3,600 psi	
Flexural Modulus		106,000 psi	
Tensile Strength		2,600 psi	
Specific Gravity		1.09	
WEP BRAKE ESTIMATES			
WEP Composition	Weight	Thickness	Temperature
Resin/Water Vaporization	5.5 lb	0.95 in.	212°F
Fiber Reinforced Resin/ Resin Ablation + Water Vaporization	3.6 lb	0.63 in.	1000°F*

*Nonflammable, nontoxic gases produced.

Table 2.
Summary of Weight Estimates*
(1 kWh Burst, Flywheel Weight 34.25 lb).

Fragmentation Containment (No Hub Failure)	Minimum Weight (lb)	Slow Growth Weight (lb)
Disk	39	< 10
Disk with Ring	61	NA
Subcircular Rim 1/3 Outer Ring	79	< 10

*Estimate sensitive to assumed failure mode.

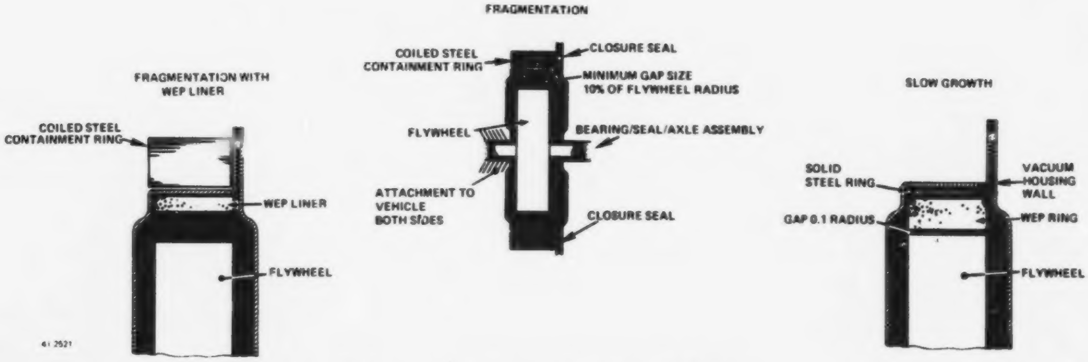
FRAGMENTATION
COILED STEEL CONTAINMENT RING
CLOSURE SEAL
MINIMUM GAP SIZE 10% OF FLYWHEEL RADIUS
FLYWHEEL
BEARING/SEAL/AXLE ASSEMBLY
ATTACHMENT TO VEHICLE BOTH SIDES
CLOSURE SEAL
FRAGMENTATION WITH WEP LINER
COILED STEEL CONTAINMENT RING
WEP LINER
FLYWHEEL
41 2521
SLOW GROWTH
SOLID STEEL RING
VACUUM HOUSING WALL
GAP 0.1 RADIUS
WEP RING
FLYWHEEL

Fig. 7. Containment Design Options.

PROJECT SUMMARY

Project Title:	Circular Weave Flywheel Materials Evaluation
Principal Investigators:	Alan D. Sapowith, William E. Handy
Organization:	Avco Systems Division 201 Lowell Street Wilmington, Massachusetts 01887 (617) 657-2449
Project Goals:	Determine for maximum energy density at burst the optimum or best mix of warp and pick fibers for Avco's bidirectional weave.
Project Status:	The materials evaluation efforts pertaining to the circular weave are completed. Follow-on efforts to build and spin-to-burst test circular weave composite flywheels are anticipated.
Contract Number:	LLNL Subcontract 1118701
Contract Period:	November 1979 to June 1981
Funding Level:	$22,444
Funding Source:	U.S. Department of Energy through Lawrence Livermore Laboratories.

CIRCULAR WEAVE FLYWHEEL MATERIALS EVALUATION

Alan D. Sapowith
William E. Handy

Avco Systems Division
Wilmington, Massachusetts

ABSTRACT

Avco's circular weave flywheel materials orient fibers in the two principal stress directions: circumferential (warp fibers) and radial (pick fibers).* Analyses and test data show an estimated specific energy density capability of this material design to be 35 to 40 Wh/lb.

NOMENCLATURE

E_R	Radial modulus, psi
E_θ	Hoop (circumferential) modulus, psi
ID	Inside diameter of the composite flywheel donut, in.
OD	Outside diameter, in.
σ	Strength, psi
ρ	Density, $lb/in.^3$
Wh/lb	Watt-hours per pound

INTRODUCTION

Avco started development of its constant stress composite flywheel in 1975 under the U.S. Army MERADCOM Contract No. DAAG-53-75-0269. This contract culminated in an instrumented burst test that achieved a specific energy at burst of 32.3 Wh/lb. The design results in a constant stress throughout the flywheel but, unlike familiar constant stress shapes, it takes the form of a right circular cylinder. Figure 1 shows the 19.5-in.-diameter flywheel tested with its strain instrumentation.

The constant stress concept employs composite fibers in the two principal stress directions: radial and circumferential. Figure 2 depicts a composite circular weave that accomplishes the same basic fiber orientations. Here the warp fibers become the circumferentials and the picks become the radials.

An initial evaluation of circular weave composite mechanical properties was conducted under LLNL subcontract 6692009. In this subcontract, additional mechanical tests and analyses were performed to identify "optimum" or best weave configurations. While the results appear quite promising, because of the limited scope of this effort it is suggested that additional improvements can, and should, be attempted. These follow-on efforts are recommended for consideration once proof-of-concept burst tests on complete circular weave flywheels have been demonstrated.

RESULTS AND CONCLUSIONS

From the first subcontract it was concluded that, for the circular weave flywheel, the optimum ratios of radial-to-hoop (circumferential) stiffnesses developed for the laminated design (alternate layers of hoops and radials) were not necessarily applicable to the circular weave design. Therefore, a range of E_R/E_θ stiffnesses was investigated, as shown in Fig. 3. The resulting stresses at failure and allowables are shown in Figs. 4, 5, and 6. It can be seen that, in each case, failure is predicted in the hoops and that, in choosing the E_R/E_θ ratio, one can move the failure point from the ID to the OD.

The flywheel strength or specific energy capacity is dependent on the specific strength, σ/ρ, of its materials. These were measured and are presented in Fig. 7. Since the hoop strength varies, for small changes in yarn count with the number of hoop yarns per inch, and since analyses show that only a minimum number of radials are needed to provide a "good" quality dry cloth, an extrapolated σ/ρ is shown in Fig. 8. This increased strength is computed as a direct ratio of hoop gain count over that tested in Fig. 7. Two notes: first, the total hoop and pick count is constant, holding density constant; second, the two test points in Fig. 7 with values of over 2400 x 10^3 in. were conservatively not included. These improved data were obtained by reducing the tensile test coupon curvatures near the gage area.

---

*Patent pending

The resulting predictions in specific energy density are shown in Table 1. Thus, the specific energy density of circular weave is estimated to be, in round numbers, 35 to 40 Wh/lb. The incorporation of a hub reduces these estimates by less than 10 percent.

It is recommended that, before conducting further optimization studies, circular weave flywheels be fabricated and burst tested as a proof-of-concept demonstration of the circular weave design.

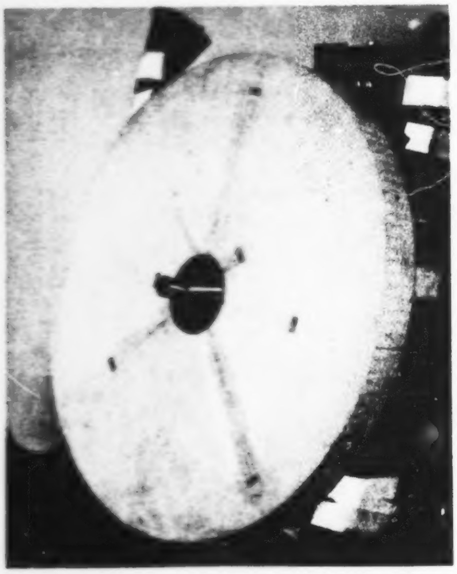

Fig. 1. Avco Laminated Design, MERADCOM Test 32.3 Wh/lb.

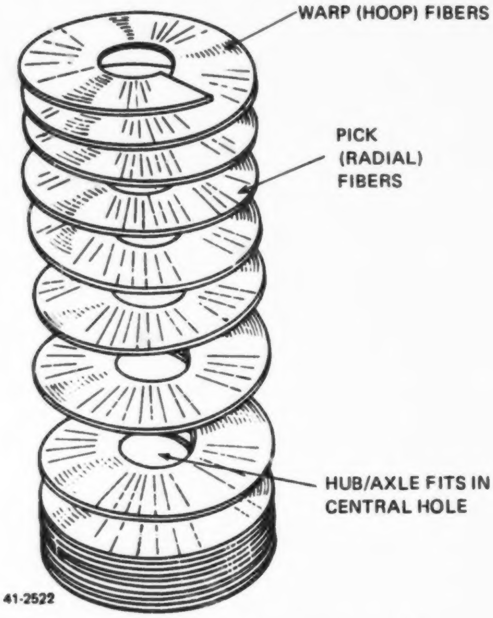

Fig. 2. Avco's Woven Flywheel Design.

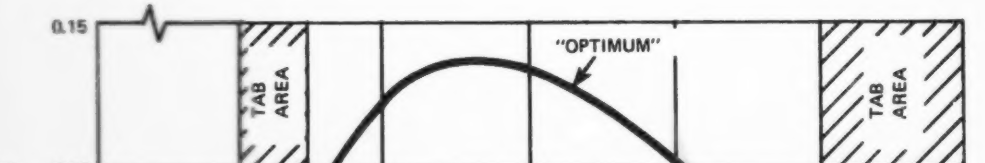

Fig. 3. Stiffness Ratios as a Function of Radius (R/R_o = 0.5).

BEST DOCUMENT AVAILABLE

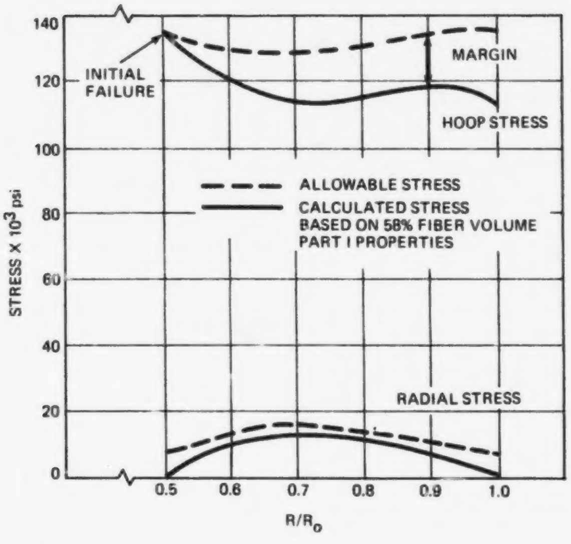

Fig. 4. Hoop and Radial Stresses at Burst for "Optimum" E_R/E_θ Ratio Shown in Fig. 3.

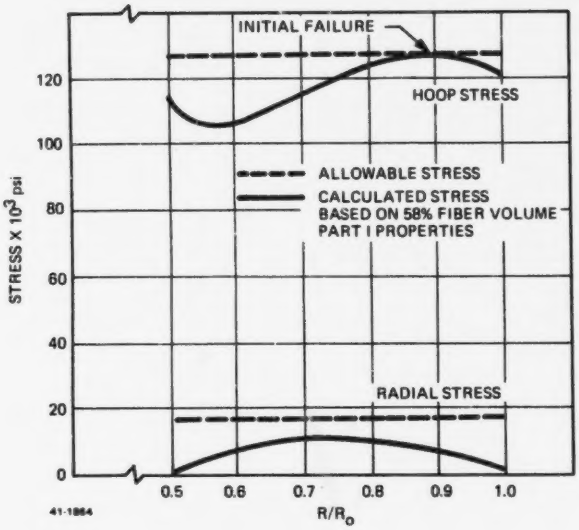

Fig. 5. Hoop and Radial Stresses for Constant E_R/E_θ Ratio = 0.057.

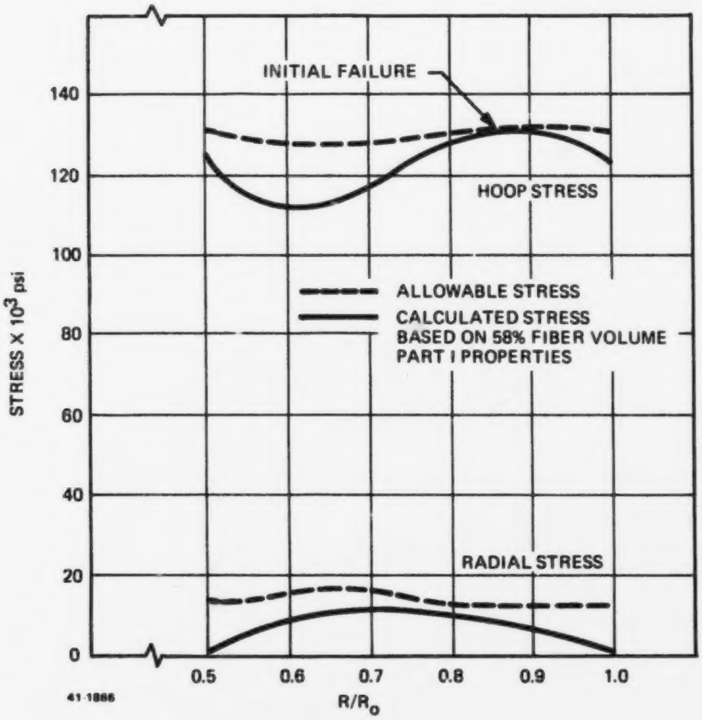

Fig. 6. Hoop and Radial Stresses for Practical Weave Pattern.

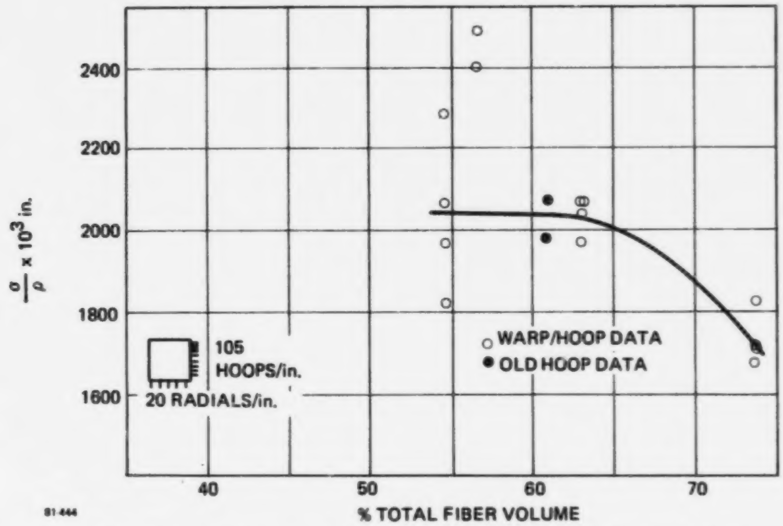

Fig. 7. As Measured Hoop Specific Strength Versus Fiber Volume, Fiberglass Circular Weave.

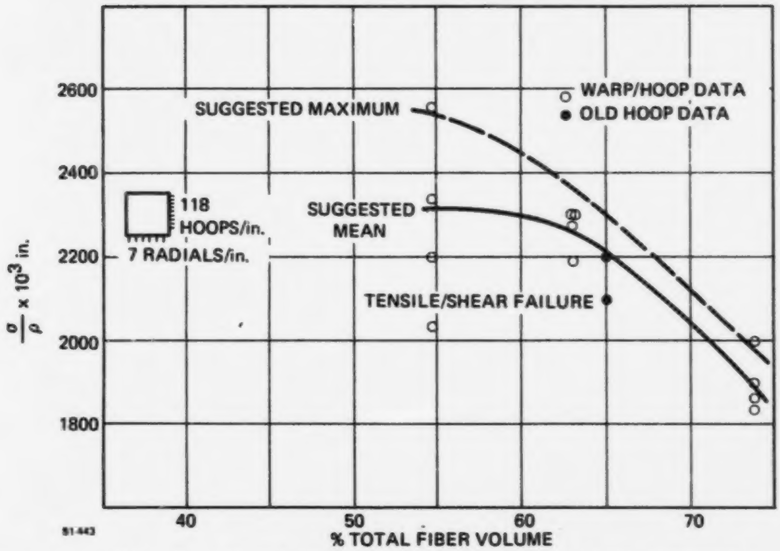

Fig. 8. Toward Optimization of Hoop Specific Strength, Fiberglass Circular Weave.

Table 1.
Energy Density Estimates Based on Test Data and Analyses.

E_R/E_θ	Mean Value		Maximum Value	
	$\sigma/\rho \times 10^6$ in.	Wh/lbf	$\sigma/\rho \times 10^6$ in.	Wh/lbf
Optimum	2.300	34.8	2.500	37.9
Constant	2.300	35.0	2.500	38.0
Practical	2.300	35.0	2.500	38.4

MECHANICAL, MAGNETIC, and UNDERGROUND ENERGY STORAGE 1981 ANNUAL CONTRACTORS' REVIEW

Washington, D.C.
August 24-26, 1981

UNITED STATES DEPARTMENT OF ENERGY
OFFICE OF ENERGY SYSTEMS RESEARCH, DIVISION OF
PHYSICAL AND CHEMICAL ENERGY STORAGE

Coordinated by Los Alamos National Laboratory
Meeting Moderator: John D. Rogers

AGENDA

SUNDAY, AUGUST 23, 1981

6:00 - 9:00 pm	Registration/Reception (Grand Ballroom, Salon A)	
9:00 - 10:00 pm	Review Committee (Rockville Suite)	

MONDAY, AUGUST 24, 1981 (Grand Ballroom, Salons A, B, & C)

7:45 - 8:30 am	Registration (Continued)	
7:45 - 8:30 am	Continental Breakfast	
8:30 - 8:45 am	Mechanical, Magnetic, and Underground Energy Storage Overview	
	Agenda, Announcements, General Information	J.D. Rogers (LANL)
	DOE Headquarters Overview	DOE Headquarter Staff
8:45 am	Compressed Air Energy Storage (CAES) Program	
8:45 - 9:05 am	CAES and UPH Program Overview and International Activities	L.D. Kannberg (PNL)
9:05 - 9:15 am	Second-Generation CAES Studies	F.R. Zaloudek (PNL) Moderator
9:15 - 9:35 am	Adiabatic CAES Using Hard Rock Caverns	M. Hobson (AAI)
9:35 - 9:55 am	CAES Equipment Evaluation	D. Chiang (ENTEC)
9:55 - 10:25 am	Thermomechanical Screening of Thermal Energy Storage Materials for CAES	D. DeCoursin (FluiDyne)
10:25 - 10:45 am	Coffee Break	

For information: MCC Associates, Inc., 8534 2nd Avenue, Silver Spring, Md. 20910 (301) 589-8130

10:45 - 11:05 am	Comparative Economics of Second Generation CAES Concepts	R.W. Reilly (PNL)
11:05 - 11:15 am	CAES Reservoir Stability Studies	T.J. Doherty (PNL) Moderator
11:15 - 11:45 am	Salt Experimental Studies for CAES	R.L. Thoms (LSU)
11:45 - 1:00 pm	Luncheon (Grand Ballroom, Salons D & E)	
1:00 - 1:30 pm	Numerical and Laboratory Studies of CAES Reservoirs in the Sykesville Gneiss	T. Brandshaug (RE/SPEC)
1:30 - 1:50 pm	Porous Media Laboratory and Numerical Studies	T.J. Doherty (PNL)
1:50 - 2:20 pm	Aquifer Field Test: Experimental Plan, Design, and Construction	J. Istvan (PB-KBB)
2:20 - 2:40 pm	Coffee Break	
2:40 pm	Magnetic Energy Storage Program	
2:40 - 3:05 pm	Magnetic Energy Storage Overview and International Activities	M.O. Hoenig (MIT)
3:05 - 3:35 pm	30 MJ Superconducting Magnetic Energy Storage for BPA Transmission Line Stabilizer	R.I. Schermer (LANL)
3:35 - 3:55 pm	30 MJ Superconducting Coil Fabrication	S. Burnett (GAC)
3:55 - 4:15 pm	Computer Automated Controls for Superconducting Magnetic Energy Storage	A.L. Criscuolo (LANL)

TUESDAY, AUGUST 25, 1981 (Grand Ballroom, Salons A, B, & C)

7:45 - 8:30 am	Continental Breakfast	
8:30 am	Seasonal Thermal Energy Storage (STES) Program	
8:30 - 9:00 am	STES Program Overview and International Activities in STES	J.E. Minor (PNL)
9:00 - 9:20 am	Aquifer Thermal Energy Storage (ATES) Demonstration Projects Bethel, Alaska Project	J.R. Raymond (PNL) Moderator
9:20 - 10:00 am	Stony Brook, New York Project	W.V. Skinner (Dames & Moore)
10:00 - 10:20 am	Coffee Break	
10:20 - 11:00 am	University of Minnesota Project	M. Walton (Univ. of Minnesota)

11:00 - 11:10 am	Seasonal Storage Technology Program	J.R. Eliason Moderator (PNL)
11:10 - 11:40 am	Nonaquifer STES Concepts	D.E. Blahnik (PNL)
11:40 - 1:00 pm	Luncheon (on your own)	
1:00 - 1:20 pm	Library Development and Survey of Reinjection Experience	C.H. Lee (MRI)
1:20 - 1:40 pm	Regional Aquifer Assessments	J.D Beemer (Century West)
1:40 - 2:00 pm	Field and Laboratory Flow Facilities	P.E. Peterson (Terra Tek)
2:00 - 2:30 pm	Mobile, Alabama Field Test Facility	J.G. Melville (Auburn Univ.)
2:30 - 2:50 pm	Coffee Break	
2:50 - 3:10 pm	ATES Simulation: State of the Art Application	J.W. Mercer (GeoTrans)
3:10 - 3:40 pm	Numerical Simulation - Site Simulation	C.F. Tsang (LBL)
3:40 - 4:00 pm	Numerical Simulation - CFEST Code Development	S. Gupta (Maddox & Assoc.)
4:00 - 4:30 pm	Economic Assessment	R.W. Reilly (PNL)
5:30 - 7:30 pm	CASH BAR - (Chevy Chase & Bethesda Suites)	
7:30 - 9:30 pm	BANQUET - (Salons A & B) The National Helium Program: Policy and Prospects	E.F. Hammel

WEDNESDAY, AUGUST 26, 1981 (Grand Ballroom, Salons A, B, & C)

8:00 am	Mechanical Energy Storage Program	
8:00 - 8:20 am	Mechanical Energy Storage Overview and International Activities	T. Barlow (LLNL)
8:20 - 8:40 am	Assessment of Taxicab Fleet Operation in New York	M. Krupka (LANL)
8:40 - 9:00 am	Mechanical Energy Storage Application Studies	L. Forrest (Aerospace Corp)
9:00 - 9:20 am	HEV/Flywheel Design Results of Analysis, Phase I	I. Kalns (Eaton Corp)
9:20 - 9:40 am	CVT/Study-Control-Strategy for HEV/Flywheel	A. Frank (Univ of Wisconsin)

9:40 - 10:00 am	Elastomeric Regenerative Braking System	L. Hoppie (Eaton Corp)
10:00 - 10:15 am	Coffee Break	
10:15 - 10:35 am	Circular Weave Flywheel Materials Evaluation and Composite Flywheel Burst Containment	A.D. Sapowith (AVCO)
10:35 - 10:55 am	Multi-Ring Composite Flywheel Assembly for FESS Trolley Coach	L. Lawson (AiResearch)
10:55 - 11:15 am	MEST Application Studies	D.B. Eisenhaure (Draper Lab)
11:15 - 11:35 am	Advanced Flywheel Storage System	P. Jarvinen (MIT)
11:35 - 12:05 pm	Flywheel Rotor Development	S.V. Kulkarni (LLNL)
12:05 - 1:15 pm	Luncheon (On Your Own)	
1:15 - 1:35 pm	Flywheel Rotor Economic Analysis	B. Noton (Battelle-Columbus)
1:35 - 1:55 pm	Flywheel Rotor Dynamics	C. Bert (Univ. of Oklahoma)
1:55 - 2:15 pm	Rotor Cyclic Test Plan	K. Reifsnider (VPI & SU/LLNL)
2:15 - 2:35 pm	Rotor Testing	R.S. Steele, Jr. (Union Carbide)
2:35 - 2:55 pm	Coffee Break	
2:55 - 3:15 pm	Fiber Composite Materials Testing	T. Hahn (Wash. Univ.)
3:15 - 3:35 pm	Fiber Composite Materials Fatigue Studies	J. Duke (VPI & SU)
3:35 - 3:55 pm	Composite Fiber Fatigue Study	S. Calabrese (RPI)
3:55 - 4:15 pm	Flywheel Containment Design	A. Coppa (GE)
4:35	Closing Remarks	J.H. Swisher (DOE)

THURSDAY, AUGUST 27, 1981 (Gaithersburg Suite)

8:30 - 10:00 am	Executive Session (Critique)
10:00 - 10:15 am	Coffee Break
10:15 - 12:00 noon	Review Committee Report and Closing

MECHANICAL, MAGNETIC, and UNDERGROUND ENERGY STORAGE 1981 ANNUAL CONTRACTORS' REVIEW

Washington, D.C.
August 24-26, 1981

LIST OF ATTENDEES

Michael Ambrosino
Ambrosino & DePinto
225 W. 34th Street, Suite 2107
New York, NY 10001

Ken Ames
Battelle-Columbus
2030 M St, NW, Suite 705
Washington, DC 20036

Joseph Asbury
Argonne National Lab
9700 S. Cass Avenue
Argonne, IL 60439

E.F. Babelay, Jr.
Union Carbide Corp/Nuclear Div
P.O. Box Y
Oak Ridge, TN 37830

Thomas Barlow
Lawrence Livermore Labs
P.O. Box 808, M/S L-209
Livermore, CA 94550

Jack D. Beemer
Century West Engineering Corporation
P.O. Box 1174
Bend, OR 97709

Michael Berger
Los Alamos National Laboratory
P.O. Box 1663
Los Alamos, NM 87545

C. Bert
Univ of Oklahoma
865 Asp Avenue
Norman, OK 73019

Ed Beyma
US Department of Energy
1000 Indep Ave., EHU Division
Washington, DC 20585

D. Blahnik
Pacific Northwest Lab
P.O. Box 999
Richland, WA 99352

C. Everett Brett
University of Alabama
Box 6282
University, AL 35486

John J. Brogan
U.S. Dept of Energy
1000 Indep Ave., RM 1G080
Washington, DC 20585

S. Burnett
Gen Atomic
P.O. Box 81608
San Diego, CA 92138

S. Calabrese
Rensselaer Polytechnic Inst.
Dept of Elect Engineering
Troy, NY 12181

David Chiang
ENTEC
451 Hungerford Dr., Suite 609
Rockville, MD 20850

Ruth Clinkscale
MCC Associates, Inc.
8534 Second Ave, Suite 400
Silver Spring, MD 20910

Robert J. Copeland
Solar Energy Research Institute
1617 Cole Blvd.
Golden, CO 80401

A. Coppa
GE Space Div
P.O. Box 8555, L9413
Philadelphia, PA 19101

Don Cornish
Lawrence Livermore Lab
P.O. Box 808 L-550
Livermore, CA 94550

A.S. Criscuolo
Los Alamos Nat Lab
MS 957, P.O. Box 999
Los Alamos, NM 87545

David DeCoursin
FluiDyne
5900 Olson Memorial Highway
Minneapolis, MN 55422

Roger Derby
Oak Ridge National Lab
P.O. Box Y, Bldg. 9204-1
Oak Ridge, TN 37830

T.J. Doherty
Pacific Northwest Lab
P.O. Box 999
Richland, WA 99352

Charles L. Driggs
Acres American Incorporated
The Clark Bldg, Suite 329
Columbia, MD 21044

J.C. Duke, Jr.
V.P.I.& State Univ
Engr Science & Mechs
Blacksburg, VA 24061

Paul J. Ebert
LLNL
U.S. Department of Energy ER-15
Wash., D.C. 20545

David B. Eisenhaure
The Charles Start Draper Lab, Inc.
555 Technology Square MS#37
Cambridge, MA 02139

J.R. Eliason
Pacific Northwest Lab
P.O. Box 999
Richland, WA 99352

Oswald C. Farquhar
Univ of Massachusetts
Dept of Geology & Geography
Amherst, MA 01003

Kurt G. Fehrle
US Department of Energy
12th & Penn Ave., NW, RM 6144
Washington, DC 20461

R.C. Flanagan
University of Ottawa
770 King Edward Ave, Col. By Hall
Ottawa, Ontario, Canada K1N 6N5

Lester Forrest
The Aerospace Corporation
P.O. Box 92957
Los Angeles, CA 90009

Arlo Fossum
RE/SPEC Inc.
P.O. Box 725, One Concourse Dr.
Rapid City, SD 57709

A. Frank
Univ of Wisconsin
1500 Johnson Drive
Madison, WI 53706

John Gahimer
US Department of Energy
1000 Indep Ave, RM 1G-080
Wash., DC 10585

B. Gallagher
15255 Watertown Plank Rd.
Elm Grove, WI 53122

Robert Giese
Argonne National Laboratory
9700 S. Cass Avenue
Argonne, IL 60439

Sumant K. Gupta
George Maddox & Associates
1301 Maple Lane
W.Richland, WA 99352

Imre Gyuk
U.S. Department of Energy
1000 Indep Ave, SW, RM 1G-080,M/S 6B-025
Washington, DC 20585

H.T. Hahn
Washington Univ
Campus Box 1087
St. Louis, MO 63130

E. F. Hammel

99 Rim Road
Los Alamos, NM 87544

R. Duncan Hay
New England Nuclear Corp.
549 Albany Street
Boston, MA 02118

Michael J. Hobson
Acres American, Inc.
The Clark Building, Suite 329
Columbia, MD 21044

Mitch O. Hoenig
Francis Bitter Natl Magnet Lab
150 Albany Street, MW 14-2219 A
Cambridge, MA 02139

L.O. Hoppie
Eaton Corp
P.O. Box 766, 26201 Nrthwst Hwy
Southfield, MI 48037

Jonathan W. Hurwitch
Battelle Columbus Lab/Wash Operations
2030 M Street, NW
Washington, DC 20036

John Istvan
PB-KBB Inc.
11999 Katy, P.O. Box 19672
Houston, TX 77024

P.A. Jarvinen
MIT/Lincoln Lab
P.O. Box 73
Lexington, MA 02173

BEST DOCUMENT AVAILABLE

Bjorn Jonsson
Swedish Embassy
600 New Hampshire Ave, NW
Wash., DC 20037

Landis Kannberg
Pacific Northwest Lab
P.O. Box 999
Richland, WA 99352

W. F. Kaufman
Ford Motor Company
20000 Rotunda Dr., RM S-1067
Dearborn, MI 49121

D. King
Lawrence Liv Natl Lab
P.O. Box 808, L-388
Livermore, CA 94550

S.V. Kulkarni
Lawrence Livermore Lab
P.O. Box 808, L-338
Livermore, CA 94550

Parker R. Lichtenstein
Owens Corning Fiberglas Corp.
Technical Center
Granville, OH 43023

Howard E. Lowitt
Energetics Incorporated
2000 Century Plaza
Columbia, MD 21055

James F. Martin
Oak Ridge Natl Lab
P.O. Box Y, Bldg 9204-1
Oak Ridge, TN 37830

Marianne B. McCarthy
MCC Associates, Inc.
8534 Second Ave., Suite 400
Silver Spring, MD 20910

J.W. Mercer
GeoTrans, Inc.
P.O. Box 2550
Reston, VA 22090

Robert T. Miller
U.S. Geological Survey, WRD
702 P.O. Bldg
St. Paul, MI 55101

A. Miyase
University of Ottawa
770 King Edward Ave
Ottawa, Ontario, Canada K1N 6N5

M. Munro
Univ of Ottawa
Dept of Mech Engr
Ottawa, Canada K1N6N5

Greg Nowell
Eaton Corporation
P.O. Box 766
Southfield, MI 48037

Ilmar Kalns
Eaton Corp - Eng & Res Center
P.O. Box 766, 26201 Northwestern Hwy.
Southfield, MI 48037

Donald L. Katz
University of Michigan
2042 East Engineering Bldg
Ann Arbor, MI 48109

Charles T. Kincaid
Pacific Northwest Lab
P.O. Box 999
Richland, WA 99352

M. Krupka
Los Alamos Nat Lab
P.O. Box 1663, MS 595
Los Alamos, NM 87545

C. H. Lee
Midwest Research Inst
425 Volker Blvd
Kansas City, MO 64110

Walter V. Loscutoff
Battelle Pacific Northwest Laboratory
Battelle Blvd., P.O. Box 999
Richland, WA 99352

Lynn Marksberry
FluiDyne Engr Corp
5900 Olson Mem. Hwy
Minneapolis, Minn 55422

Gerald T. McCarthy
MCC Associates, Inc.
8534 Second Ave, Suite 400
Silver Spring, MD 20910

J.G. Melville
Auburn Univ
Dept of Civil Engr
Auburn, Alabama 36849

Allen I. Michaels
Argonne National Lab
9700 S. Cass Avenue, Bldg 362
Argonne, IL 60439

James Minor
Pacific Northwest Lab
P.O. Box 999
Richland, WA 99352

Ronald Mueller
Argonne National Lab
9700 S. Cass Ave.
Argonne, IL 60439

B. Noton
Battelle/Columbus Labs
505 King Avenue
Columbus, OH 43201

Walter K. O'Neil
Eaton Corporation - Eng & Res Center
26201 Northwestern Hgwy, P.O. Box 766
Southfield, MI 48037

P. Eric Peterson
Terra Tek
420 Wakara Way
Salt Lake City, UT 84108

Clinton W. Phillips
Natl Bru of Stands
RM B 306 Bldg. 224/Bldg Equip Div
Wash., D.C. 20234

John R. Raymond
Pacific Northwest Labs
P.O. Box 999
Richland, WA 99352

R.W. Reilly
Pacific Northwest Lab
P.O. Box 999
Richland, WA 99352

Alan D. Roberts
Malaysian Rubber Bureau
1925 K Street, NW
Washington, DC 20006

John Rogers
Los Alamos National Lab
P.O. Box 990, M/S 464
Los Alamos, NM 87545

A.D. Sapowith
AVCO Systems
201 Lowell St
Wilmington, MA 01887

Walter J. Schaetzle
University of Alabama
P.O. Drawer ME
University, AL 35486

N.A. Schilke
GM Res Labs
GM Tech Cntr 354 RMB
Warren, MI 48090

W.V. Skinner
Dames & Moore
6 Commerce Drive
Cranford, NJ 07016

S. Strauch
US Department of Energy
Forrestal Bldg, 1000 Indep Ave. SW
Washington, DC 20585

Janet Terner
1523 Live Oak
Silver Spring, MD 20910

Stanley Trumbower
US Department of Energy
2000 M St., NW, M/S 4204
Wash., D.C. 20461

Anthony Valentino
Argonne National Lab
9700 S. Cass Avenue
Argonne, IL 60439

George F. Pezdirtz
US Department of Energy
1000 Indep, Forrestal Bldg, RM 1G080
Wash., D.C. 20585

Ari Rabl
Princeton University
Engr. Quad.
Princeton, NJ 08544

K. Reifsnider
V.P.I. & State Univ
Engr Science & Mechs
Blacksburg, VA 24061

Eberhart Reimers
US Department of Energy
Forrestal Bldg/10000 Indp Ave, SW
Wash., D.C. 20585

Wilfred J. Roesler
Johns Hopkins University
Johns Hopkins Road
Laurel, MD 20707

Stan Ruby
U.S. Department of Energy
1000 Indep. Ave, SW, RM 1G066
Washington, DC 20585

Henry A. Scarton
Rensselaer Polytech Inst
Dept of Mech Engr
Troy, NY 12181

R. I. Schermer
Los Alamos Nat Lab
MS 957, P.O. Box 1663
Los Alamos, NM 87545

Rufus W. Shivers
U.S. Department of Energy
1000 Indep Ave, CE 141
Washington, DC 20585

R.S. Steele, Jr.
Union Carbide Corp - Nuclear Div
P.O. Box Y
Oak Ridge, TN 37830

J.H. Swisher
US Department of Energy
Forrestal Bldg/1000 Indep Ave. SW
Washington, DC 20585

Robert L. Thoms
Louisiana St Univ
RM 42, Atkinson Hall
Baton Rouge, LA 70803

C.F. Tsang
Lawrence Berkeley Lab
Bldg 90, RM 1012-H, 1 Cyclotrn Rd
Berkeley CA 94720

M.S. Walton
Univ of Minnesota
319 15th Ave., SE
Minneapolis, MN 55455

Howard R. Whitman
The Charles Stark Draper Lab, Inc.
555 Technology Square
Cambridge, MA 02139

Bette M. Winer
Arthur D. Little, Inc.
Acorn Pike
Cambridge, MA 02140

F.R. Zaloudek
Pacific Northwest Lab
P.O. Box 999
Richland, WA 99352

William O. Wilkinson
Johns Hopkins APL
11100 J. Hopkins Road
Laurel, MD 20707

Thomas J. Wissing
Eaton Corporation - Eng & Res Center
P.O. Box 766, 26201 Northwestern Hgwy
Southfield, MI 48037

☆U.S. GOVERNMENT PRINTING OFFICE: 1982-361-060:2109